

Engineering Spray Freeze Dried Particles for Pulmonary Delivery of Proteins

Name: Mai Babenko

ID Number: K1455177

First Supervisor: Dr Amr Elshaer

Second Supervisor: Prof Raid G. Alany

Third Supervisor: Dr Gianpiero Calabrese

External Supervisor: Dr Waseem Kaialy

Thesis submitted for the degree of
Doctor of Philosophy

Kingston University

FACULTY OF SCIENCE, ENGINEERING AND COMPUTING

SEC Research Pharmacology, Toxicology and Pharmacy

Date of submission: 5 November 2021

Date of approval of thesis: 24 March 2022

Abstract

The thesis has focused on the development of dry powder inhaler (DPI) formulations for pulmonary delivery of antidiabetic peptide and protein drugs such as insulin and glucagon-like peptide-1(7-36) amide (GLP-1). These drugs are generally administered via subcutaneous injection that interferes with the patients' lifestyle and affects patient compliance and adherence to treatment. The primary goal of the research was to assess the value of insulin and GLP-1 DPI formulations for inhalation use in people with diabetes as an alternative treatment option to injectable antidiabetic medications. The aerosolisation performance of insulin and GLP-1 dry powders from two different types of DPI formulations; carrier free DPI formulations (drug alone) and carrier-based DPI formulations (drug and carrier) were investigated using a next generation impactor. No studies have been reported on the development of carrier free GLP-1 DPI formulations and carrier-based DPI formulations containing excipient free insulin or GLP-1 for pulmonary delivery. Particle engineering such as spray drying and spray freeze drying were employed for the drug and carrier powder preparation, respectively as a formulation strategy to optimise the properties of both drug and carrier particles (e.g., particle size, morphology). In addition, drug particles were prepared in the absence of excipients to minimise the lung safety concern. Mannitol was selected as an alternative carrier to lactose which is the most used carrier in DPI formulations but associated with chemical incompatibility with proteins. Glycine or L-leucine selected as an excipient was added to mannitol carrier to optimise carrier properties (morphology).

Spray drying demonstrated to reduce the particle size of insulin and GLP-1 powders to a suitable size range (aerodynamic diameter: $\leq 5 \mu\text{m}$) for pulmonary delivery and modified the morphologies. This resulted in high fine particle fraction (insulin FPF: $77.36\% \pm 18.01\%$, GLP-1 FPF: $90.73\% \pm 1.76\%$) showing feasible for pulmonary delivery of spray dried insulin and GLP-1 dry powders. However, spray dried drug particles for inhalation ($\leq 5 \mu\text{m}$) were naturally cohesive (high degree of drug-drug agglomeration) due to the small particles associated with high inter-particulate forces between drug particles (drug-drug cohesive forces) therefore exhibited poor powder flow and low drug delivery efficiency (total drug deposition on throat and all impactor stages) from an inhaler device (Handihaler®) (insulin delivered dose: $38.64\% \pm 3.82\%$, GLP-1 delivered dose: $32.88\% \pm 7.00\%$). Spray freeze drying produced spherical and porous carrier powders with the particle size range between $50 \mu\text{m}$ and $130 \mu\text{m}$ suitable as DPI carriers regardless of the inclusion or absence of amino acids. However, surface properties (e.g., morphology and roughness) of spray freeze dried mannitol-based carriers were dependent on the type of amino acid and its concentrations. The novel amino acid-mannitol carriers prepared by spray freeze drying were employed to improve the aerosolisation performance of DPI formulations (e.g., powder flow). Carrier-based DPI formulations containing

spray freeze dried glycine-mannitol carrier improved the powder flow of the cohesive drug particles and delivered higher drug dose from Handihaler® compared to drug particles alone in carrier free formulations (insulin delivered dose: from 38.64% ± 3.82% to over 57.0%, GLP-1 delivered dose: from 32.88% ± 7.00% to 45.92% ± 5.84%). This was attributed to the porous powders produced by spray freeze drying. Without the addition of the engineered spray freeze dried carrier to the formulation, spray dried drug particles showed poor flowability. Overall, both carrier free and carrier-based DPI formulations have shown advantages with different challenges for pulmonary administration of insulin and GLP-1. According to an online survey conducted in 2019, patients with diabetes generally accepted the idea of insulin delivery via inhalers as 73.4% of participants were willing to try insulin inhalers. National Health Service availability will have a significant influence on participants' willingness to try insulin inhalers. The successful inhaled insulin and GLP-1 products will provide an alternative treatment option for people with diabetes by reducing the burden of injection related barriers therefore improve patient compliance and adherence to antidiabetic therapy and quality of life affected by injection treatment.

Keywords: Dry powder inhaler formulation, Pulmonary drug delivery, Diabetes mellitus, Insulin, Glucagon-like peptide-1(7-36) amide, Spray drying, Spray freeze drying, Carriers, Saccharides, Mannitol, Amino acids, Glycine, Leucine, Inhaler device, Reversed-phase high performance liquid chromatography, Quantitative proton Nuclear Magnetic Resonance

Acknowledgements

I would like to thank Dr Amr Elshaer for giving me this opportunity, his support and advice throughout this research. I would also like to thank Prof Raid G. Alany and Dr Gianpiero Calabrese for providing feedback and their continuous encouragement. I would also like to extend my thanks to Dr Waseem Kaialy for his advice and feedback externally.

I am very grateful to Dr Jean-Marie R. Peron for his technical assistance on Nuclear Magnetic Resonance (NMR) data measurement and processing throughout the proton quantitative NMR method development. I would also like to extend special thanks to Richard Giddens for his assistance with Scanning Electron Microscopy imaging and Prof Peter J Foot for his assistance in generation of X-ray diffraction data.

I would like to thank all the staff, lab managers, and technicians in the Faculty of Pharmacy and Chemistry for their help during the research.

Lastly, my appreciation also goes out to my family for their patience and support over the course of the research (4 years and 2 months) including the COVID-19 pandemic started in 2020 and lockdown few times (March-July 2020, November-December 2020, January-March 2021).

Contents

Abstract	2
Acknowledgements	4
Contents	5
List of figures	12
List of tables	20
Abbreviations	25
Structure of thesis and novelty of work	28
Aim and objectives	30
Aim	30
Objectives	30
Chapter 3	30
Chapter 4	30
Chapter 5	31
Chapter 6	31
Chapter 7	31
Research output	32
The list of publications and conference	32
Chapter 1. Introduction	33
1.1. General introduction - Diabetes	33
1.1.1. Treatment of diabetes	34
1.1.2. Insulin	34
1.1.3. Glucagon-like peptide-1	41
1.1.4. Routes of insulin and GLP-1 delivery	47
1.1.4.1. Oral route	48

1.1.4.2.	Nasal route	49
1.1.4.3.	Buccal route.....	50
1.1.4.4.	Pulmonary route	51
1.2.	Instability of peptides and proteins.....	52
1.2.1.	Glass transition temperature.....	55
1.2.2.	Insulin degradation	56
Chapter 2.	Literature review	58
2.1.	Human respiratory system.....	58
2.1.1.	Mechanisms of lung clearance	60
2.1.2.	Gas flow and respiratory system resistance	61
2.1.3.	Obesity.....	61
2.2.	Pulmonary delivery.....	62
2.3.	Systemic drug delivery through pulmonary route	64
2.4.	Dry powder inhaler formulations for pulmonary delivery	69
2.4.1.	High dose dry powder inhaler formulations	70
2.4.2.	Carrier free dry powder inhaler formulations	72
2.4.2.1.	Particle engineering	73
Spray drying.....	73	
Freeze drying/Lyophilisation	81	
Spray freeze drying	82	
2.4.2.2.	Excipient free formulations	86
2.4.3.	Carrier-based dry powder inhaler formulations.....	89
2.4.3.1.	Particle engineering	95
2.5.	Dry powder inhaler devices for pulmonary delivery	97
2.5.1.	Ideal DPI devices	100
2.5.2.	Types of DPI devices.....	100
2.5.3.	Passive DPI devices	101
2.5.4.	Airflow resistance	101
2.5.5.	Available DPI devices	103
2.5.6.	Active DPI devices	104
2.5.7.	DPIs for high dose drugs	105
2.5.8.	Insulin inhalers.....	105
2.6.	Pulmonary safety of inhaled insulin	108
Chapter 3.	¹H NMR quantification of spray dried and spray freeze dried carriers in dry powder inhaler formulations	110

3.1.	Abstract	110
3.2.	Introduction	110
3.3.	Materials	112
3.4.	Method development	113
3.4.1.	Preparation of saccharide standard stock solutions	113
3.4.2.	Preparation of saccharide solutions for calibration curve	113
3.4.3.	Preparation of saccharide test sample solutions for validation	113
3.4.4.	NMR sample preparation for impaction study	114
3.4.5.	Proton NMR data measurement	114
3.4.6.	NMR data processing	114
3.4.7.	Proton NMR quantitative analysis	114
3.5.	Method validation	115
3.5.1.	Specificity	115
3.5.2.	Linearity and Range	116
3.5.3.	Accuracy	116
3.5.4.	Precision	117
3.5.5.	Limit of detection and limit of quantitation	117
3.6.	Carrier dry powders preparation by spray drying	117
3.7.	Carrier dry powders preparation by spray freeze drying	118
3.8.	Physicochemical characterisation	119
3.8.1.	Scanning electron microscopy	119
3.8.2.	Laser diffraction	119
3.8.3.	Differential scanning calorimetry	120
3.8.4.	Thermogravimetric analysis	120
3.8.5.	X-ray diffraction	120
3.9.	Impaction study	121
3.10.	Statistical analysis	122
3.11.	Results and discussion	122
3.11.1.	Method validation	122
3.11.1.1.	Specificity	124
3.11.1.2.	Linearity and range	126
3.11.1.3.	Accuracy and precision	128
3.11.1.4.	Limit of detection and limit of quantitation	129
3.11.2.	Physicochemical characterisation	130
3.11.2.1.	Scanning electron microscopy	130
3.11.2.2.	Laser diffraction	133
3.11.2.3.	Differential scanning calorimetry	134

3.11.2.4.	Thermogravimetric analysis	137
3.11.2.5.	X-ray diffraction	139
3.11.3.	Impaction study.....	141
3.12.	Conclusion	146

Chapter 4. Amino acid-mannitol dry powder inhaler formulations for improved pulmonary deposition of insulin 148

4.1.	Abstract.....	148
4.2.	Introduction	149
4.3.	Materials	150
4.4.	Method development	151
4.4.1.	Preparation of insulin standard stock solution.....	153
4.4.2.	Preparation of insulin standard solutions for calibration curve	153
4.4.3.	Preparation of insulin test sample solutions for validation	153
4.4.4.	Preparation of mobile phase	153
4.5.	Method validation	154
4.5.1.	Stability.....	154
	Insulin standard stock solution.....	154
	Insulin calibration standard solutions for short-term storage	154
	Insulin acidic aqueous solution	155
4.5.2.	Specificity	155
4.5.3.	Linearity and range	155
4.5.4.	Accuracy	155
4.5.5.	Precision	156
4.5.6.	Limit of detection and limit of quantitation	156
4.5.7.	Robustness	157
4.5.8.	System suitability	157
4.6.	Carrier dry powders preparation by spray freeze drying.....	157
4.7.	Insulin dry powders preparation	158
4.8.	Preparation of insulin dry powder inhaler formulations.....	158
4.9.	Physicochemical characterisation.....	159
4.9.1.	Scanning electron microscopy	159
4.9.2.	Laser diffraction	160
4.9.3.	Differential scanning calorimetry	160
4.9.4.	Thermogravimetric analysis	161
4.9.5.	X-ray diffraction	161
4.10.	Blend homogeneity assessment.....	161

4.11.	Impaction study	162
4.12.	Statistical analysis	163
4.13.	Results and discussion	163
4.13.1.	Method development	163
4.13.2.	Method validation.....	165
4.13.2.1.	Stability.....	165
	Insulin standard stock solution.....	165
	Insulin calibration standard solutions for short-term storage.....	166
	Insulin acidic aqueous solution for spray drying	167
4.13.2.2.	Specificity	167
4.13.2.3.	Linearity and range	168
4.13.2.4.	Accuracy and precision	170
4.13.2.5.	Limit of detection and limit of quantitation	170
4.13.2.6.	Robustness	171
4.13.2.7.	System suitability	172
4.13.3.	Physicochemical characterisation	173
4.13.3.1.	Scanning electron microscopy	173
4.13.3.2.	Laser diffraction	176
4.13.3.3.	Differential scanning calorimetry	177
4.13.3.4.	Thermogravimetric analysis	181
4.13.3.5.	X-ray diffraction	183
4.13.4.	Blend homogeneity assessment.....	186
4.13.5.	Impaction study.....	191
4.14.	Conclusion	198
Chapter 5.	Aerosolisation performance of spray dried insulin powders from amino acid-mannitol carriers	199
5.1.	Abstract.....	199
5.2.	Introduction	200
5.3.	Materials.....	201
5.4.	Carrier dry powders preparation by spray freeze drying.....	201
5.5.	Insulin dry powders preparation by spray drying	202
5.6.	Preparation of insulin dry powder inhaler formulations	203
5.7.	Physicochemical characterisation	203
5.7.1.	Scanning electron microscopy	204
5.7.2.	Differential scanning calorimetry	204
5.7.3.	Thermogravimetric analysis	204

5.8.	Blend homogeneity assessment	205
5.9.	Impaction study	205
5.10.	Insulin structural stability study	206
5.11.	Statistical analysis	207
5.12.	Results and discussion	207
5.12.1.	Physicochemical characterisation	207
5.12.1.1.	Scanning electron microscopy	207
5.12.1.2.	Differential scanning calorimetry	210
5.12.1.3.	Thermogravimetric analysis	211
5.12.2.	Blend homogeneity assessment	212
5.12.3.	Impaction study	215
5.12.4.	Insulin stability study	219
5.13.	Conclusion	223
Chapter 6. Development of spray dried GLP-1 dry powder inhaler formulations for the treatment of Type 2 diabetes		224
6.1.	Abstract	224
6.2.	Introduction	225
6.3.	Materials	226
6.4.	Method development	226
6.4.1.	Preparation of GLP-1 standard stock solution	228
6.4.2.	Preparation of GLP-1 standard solutions for calibration curve	229
6.4.3.	Preparation of GLP-1 test sample solutions for validation	229
6.4.4.	Preparation of mobile phase	229
6.5.	Method validation	229
6.5.1.	Stability	230
	GLP-1 standard stock solution	230
	GLP-1 calibration standard solutions for short-term storage	230
	GLP-1 acidic aqueous solutions	230
6.5.2.	Specificity	230
6.5.3.	Linearity and range	231
6.5.4.	Accuracy	231
6.5.5.	Precision	231
6.5.6.	Limit of detection and limit of quantitation	232
6.5.7.	Robustness	232
6.5.8.	System suitability	232
6.6.	Carrier dry powders preparation by spray freeze drying	233

6.7.	GLP-1 dry powders preparation by spray drying	233
6.8.	Preparation of GLP-1 dry powder inhaler formulations	234
6.9.	Physicochemical characterisation	235
6.9.1.	Scanning electron microscopy	235
6.9.2.	Differential scanning calorimetry	236
6.9.3.	Thermogravimetric analysis	236
6.10.	Blend homogeneity assessment	236
6.11.	Impaction study	237
6.12.	GLP-1 stability study	238
6.13.	Statistical analysis	238
6.14.	Results and discussion	239
6.14.1.	Method development	239
6.14.2.	Method validation	242
6.14.2.1.	Stability	242
	GLP-1 standard stock solution	242
	GLP-1 calibration standard solutions for short-term storage	243
	GLP-1 acidic aqueous solutions	244
6.14.2.2.	Specificity	244
6.14.2.3.	Linearity and range	247
6.14.2.4.	Accuracy and precision	248
6.14.2.5.	Limit of detection and limit of quantitation	249
6.14.2.6.	Robustness	250
6.14.2.7.	System suitability	252
6.14.3.	Physicochemical characterisation	252
6.14.3.1.	Scanning electron microscopy	252
6.14.3.2.	Differential scanning calorimetry	257
6.14.3.3.	Thermogravimetric analysis	258
6.14.4.	Blend homogeneity assessment	260
6.14.5.	Impaction study	262
6.14.6.	GLP-1 stability study	268
6.15.	Conclusion	273
Chapter 7. Perception of patients with Type 1 diabetes on insulin inhalers:		
An online survey		
7.1.	Abstract	275
7.2.	Introduction	275
7.3.	Subjects, materials, and methods	276

7.3.1. Participants.....	276
7.3.2. Questionnaire and data collection	277
7.3.3. Statistical analysis	278
7.4. Results.....	278
7.4.1. Demographics and characteristics of participants.....	278
7.4.2. Perception towards insulin inhalers.....	280
7.4.3. Factors that affect insulin inhaler acceptability	283
7.5. Discussion	286
7.6. Conclusion.....	289
Chapter 8. Conclusion	291
References.....	295
Appendix 1	315
SECTION ONE: PARTICIPANT INFORMATION	315
SECTION TWO: OPINIONS ON INJECTING INSULIN.....	316
SECTION THREE: KNOWLEDGE OF INSULIN INHALERS	317
SECTION FOUR: INSULIN INHALERS	317
SECTION FIVE: PATIENT DEMOGRAPHICS.....	321

List of figures

Figure 1: Schematic representation of human insulin structure based on Easa <i>et al.</i> (2019) with modifications. Two intermolecular disulfide bonds (cysteine (Cys) A7-B7 and A20-B19) between two polypeptide chains, A chain (21 amino acids) and B chain (30 amino acid) and one intramolecular disulfide bond in the A chain (Cys A6-A11).	35
Figure 2: A structure of glucagon-like peptide-1(7-36) amide (C ₁₄₉ H ₂₂₆ N ₄₀ O ₄₅ , Molecular weight: 3297.7 gmoL ⁻¹ , Sequence length: 30, CAS registry number: 107444-51-9). Adapted from SciFinder ⁿ Substance Results (cas.org).	42
Figure 3: The diagram of human respiratory tract with generations of airways. (Created in BioRender.com)	60
Figure 4: Schematic representation of Next Generation Impactor open view with collection cups (Stages 1-7 and MOC). MOC: micro orifice collector. (Created in BioRender.com)	66
Figure 5: Büchi Mini Spray Dryer B-290 (Büchi, 2021).	76
Figure 6: Illustration of inter-particulate adhesive forces (interactions) between drug and carrier particle surface. Created in BioRender.com based on Peng <i>et al.</i> (2016).....	91
Figure 7: Schematic illustration of drug (grey) and carrier (blue) particles mixtures based on the carrier surface roughness. A: nanoscale roughness, B: microscale roughness, C: macroscale roughness. Created in BioRender.com based on Shalash, Molokhia and Elsayed (2015).	93
Figure 8: Chemical structures of alternative carrier candidates for dry powder inhaler formulations. A: D-Mannitol, B: Sorbitol, C: Sucrose, D: Trehalose. (Created in CAS SciFinder ⁿ)	94
Figure 9: Schematic diagram of spray freeze drying process (manual process of spraying ① and freezing ②) and a picture of freeze dryer used (BenchTop Pro with Omnitronics™, SP Scientific, UK, drying process: ③) with samples in the 250 mL round bottom flasks attached.	118
Figure 10: Handihaler® inhaler fitted in the customised blue rubber mouthpiece adapter attached to the Alberta Idealised Throat placed in the next generation impactor.....	122
Figure 11: ¹ H NMR spectra of sodium benzoate with peak assignments (A), mannitol (B), sorbitol (C), and sucrose (D) in H ₂ O/D ₂ O (90:10) with the integral regions selected for quantification.	124
Figure 12: ¹ H NMR spectra multiple displays of three saccharides (mannitol, sucrose, and sorbitol) in the presence of the internal standard of sodium benzoate. TSP: Sodium 3-trimethylsilyl propionate-2,2,3,3-d ₄	125
Figure 13: ¹ H NMR spectra of saccharide alone (A: mannitol, B: sorbitol, C: sucrose) and saccharide in the presence of sodium benzoate and insulin (D, E, F).	126
Figure 14: Calibration curves for mannitol, sorbitol, and sucrose.	127
Figure 15: NMR spectra multiple displays of mannitol (A), sorbitol (B) and sucrose (C) for the calibration curves.....	127

Figure 16: Regression analysis between nominal concentration and measured concentration for mannitol, sorbitol, and sucrose.	128
Figure 17: Scanning electron microscopy (SEM) images of raw mannitol (A), spray freeze dried mannitol (B) and spray dried mannitol (C) dry powders.	131
Figure 18: SEM images of raw sucrose (before milling) (A), milled raw sucrose (B), spray freeze dried sucrose (C), spray dried sucrose (D) and raw sorbitol (E) dry powders.	133
Figure 19: Combined DSC thermograms of raw mannitol (A), spray freeze dried mannitol (B), spray dried mannitol (C), and raw sorbitol (D) dry powders.	135
Figure 20: Combined DSC thermograms of raw sucrose (A), spray freeze dried sucrose (B) and spray dried sucrose (C) dry powders.	137
Figure 21: Combined TGA curves of raw mannitol, spray freeze dried (SFD) mannitol, spray dried (SD) mannitol, and raw sorbitol dry powders.	138
Figure 22: Combined TGA curves of raw sucrose, spray freeze dried (SFD) sucrose and spray dried (SD) sucrose dry powders.	138
Figure 23: XRD patterns for raw mannitol, spray dried (SD) mannitol and spray freeze dried (SFD) mannitol dry powders.	140
Figure 24: XRD patterns for raw sucrose, spray dried (SD) sucrose, spray freeze dried (SFD) sucrose and raw sorbitol dry powders.	140
Figure 25: Particle size distribution by Next Generation Impactor (NGI) analysis at flow rate of 30 L min ⁻¹ for raw mannitol, spray dried (SD) mannitol, spray freeze dried (SFD) mannitol, raw sucrose, SD sucrose, SFD sucrose and raw sorbitol. Saccharide deposition is expressed as delivered dose (%) per NGI stage. (Data presented as mean ± standard deviation, n=3). AIT: Alberta idealised throat, MOC: Micro orifice collector.	144
Figure 26: NMR spectra multiple displays of raw mannitol (A), spray dried (SD) mannitol (B), spray freeze dried (SFD) mannitol (C), raw sucrose (D), SD sucrose (E), SFD sucrose (F) and raw sorbitol (G) for Next Generation Impactor analysis. AIT: Alberta idealised throat, MOC: Micro orifice collector.	145
Figure 27: HPLC chromatograms of insulin (insulin concentration: 54 µg mL ⁻¹ and 108 µg mL ⁻¹) at a retention time of around 4.9 mins with two UV wavelengths: 215nm (A,B) and 214nm (C,D).	164
Figure 28: HPLC chromatograms for freshly prepared (within 3 hours) insulin stock solution (1 mg mL ⁻¹) (A), insulin stock solution stored at room temperature for 7 days (B) and at 4°C for 10 days (C).	166

Figure 29: HPLC chromatograms for mobile phases (31.5:68.5 (%v/v) mixture of acetonitrile with 0.1% trifluoroacetic acid (TFA) and distilled water with 0.1% TFA) at a retention time of 2-3 minutes and raw insulin ($810 \mu\text{g mL}^{-1}$) dissolved in phosphate buffered saline (PBS) solution (pH 7.4) at a retention time of around 5 mins (A), spray dried (SD) insulin ($1000 \mu\text{g mL}^{-1}$) dissolved in PBS solution (pH 7.4) (B), raw insulin ($980 \mu\text{g mL}^{-1}$) dissolved in 0.1% acetic acid with 1M NaOH aqueous solution (pH 3.5) (C), SD insulin ($78 \mu\text{g mL}^{-1}$) in the presence of spray freeze dried (SFD) 10% glycine-mannitol carrier (D), SD insulin ($73 \mu\text{g mL}^{-1}$) in the presence of SFD 5% leucine-mannitol carrier (E), mobile phase A: acetonitrile with 0.1% TFA (F), mobile phase B: distilled water with 0.1% TFA (G), PBS solution (pH 7.4) (H), 0.1% acetic acid with 1M NaOH aqueous solution (pH 3.5) (I), raw mannitol dissolved in distilled water (1 mg mL^{-1}) (J), raw glycine dissolved in distilled water (1 mg mL^{-1}) (K), raw leucine dissolved in distilled water (0.43 mg mL^{-1}) (L).168

Figure 30: Calibration curve for human insulin in the concentration range of $2.7 \mu\text{g mL}^{-1}$ to $108.0 \mu\text{g mL}^{-1}$ (n=3).169

Figure 31: HPLC chromatograms for the calibration curve of human insulin in the concentration range from $2.7 \mu\text{g mL}^{-1}$ (bottom) to $108.0 \mu\text{g mL}^{-1}$ (top). Average retention time: $5.07 \text{ mins} \pm 0.03 \text{ mins}$, asymmetry factor: 1.00 ± 0.02 , tailing factor: 1.00 ± 0.02 , and efficiency of chromatography peak: 2392.91.169

Figure 32: HPLC chromatograms for insulin (concentration: $108 \mu\text{g mL}^{-1}$) at different flow rates: 1.0 mL min^{-1} (A), 0.9 mL min^{-1} (B) and 1.1 mL min^{-1} (C). (Area: t-test, $p < 0.05$ between 1.0 mL min^{-1} and 0.9 mL min^{-1} , between 1.0 mL min^{-1} and 1.1 mL min^{-1}).172

Figure 33: Scanning electron microscopy (SEM) images of raw human insulin before grinding (A) and ground raw human insulin (B).174

Figure 34: SEM images of spray freeze dried (SFD) mannitol (A), glycine (B), SFD 5% glycine-mannitol (C), SFD 10% glycine-mannitol (D), SFD 15% glycine-mannitol (E), leucine (F), SFD 5% leucine-mannitol (G), SFD 10% leucine-mannitol (H) and SFD 15% leucine-mannitol (I).176

Figure 35: Combined DSC thermograms of glycine and spray freeze dried (SFD) mannitol carriers with **glycine** (5%, 10% and 15%). A: Glycine, B: SFD 5% glycine-mannitol carrier (SFD5GM), C: SFD 10% glycine-mannitol carrier (SFD10GM), D: SFD 15% glycine-mannitol carrier (SFD15GM) and E: SFD mannitol.178

Figure 36: Combined DSC thermograms of leucine and spray freeze dried (SFD) mannitol carriers with **leucine** (5%, 10% and 15%). A: Leucine, B: SFD 5% leucine-mannitol carrier (SFD5LM), C: SFD 10% leucine-mannitol carrier (SFD10LM), D: SFD 15% leucine-mannitol carrier (SFD15LM) and E: SFD mannitol.180

Figure 37: Combined TGA curves of glycine and spray freeze dried (SFD) mannitol carriers with **glycine** (5%, 10% and 15%). A: Glycine, B: SFD 5% glycine-mannitol (SFD5GM), C: SFD 10% glycine-mannitol (SFD10GM) and D: SFD 15% glycine-mannitol (SFD15GM).181

Figure 38: Combined TGA curves of leucine and spray freeze dried (SFD) mannitol carriers with **leucine** (5%, 10% and 15%). A: Leucine, B: SFD 5% leucine-mannitol (SFD5LM), C: SFD 10% leucine-mannitol (SFD10LM) and D: SFD 15% leucine-mannitol (SFD15LM).182

Figure 39: X-ray diffraction patterns for glycine and spray freeze dried (SFD) mannitol carriers with and without **glycine** (5%, 10% and 15%). SFD5GM: SFD 5% glycine-mannitol, SFD10GM: SFD 10% glycine-mannitol, SFD15GM: SFD 15% glycine-mannitol. * indicates diffraction peak at 9.7° of 2 θ . 184

Figure 40: X-ray diffraction patterns for leucine and spray freeze dried (SFD) mannitol carriers with and without **leucine** (5%, 10% and 15%). SFD5LM: SFD 5% leucine-mannitol, SFD10LM: SFD 10% leucine-mannitol, SFD15LM: SFD 15% leucine-mannitol. ** indicates diffraction peak at 6.3° of 2 θ . * indicates diffraction peak at 9.7° of 2 θ185

Figure 41: The content uniformity of insulin with coefficient of variation and mannitol in dry powder inhaler (DPI) formulations. IMB: insulin and SFD mannitol blend, I5GMB: insulin and SFD 5% glycine-mannitol blend, I10GMB: insulin and SFD 10% glycine-mannitol blend, I15GMB: insulin and SFD 15% glycine-mannitol blend, I5LMB: insulin and SFD 5% leucine-mannitol blend, I10LMB: insulin and SFD 10% leucine-mannitol blend and I15LMB: insulin and SFD 15% leucine-mannitol blend. (Data presented as mean (three positions) \pm standard deviation, n=3).188

Figure 42: SEM images of insulin and spray freeze dried (SFD) mannitol blend (IMB)(A), insulin and SFD 5% glycine-mannitol blend (I5GMB)(B), insulin and SFD 10% glycine-mannitol blend (I10GMB)(C), insulin and SFD 15% glycine-mannitol blend (I15GMB)(D), insulin and SFD 5% leucine-mannitol blend (I5LMB)(E), insulin and SFD 10% leucine-mannitol blend (I10LMB)(F) and insulin and SFD 15% leucine-mannitol blend (I15LMB)(G). Red circle(s) indicate insulin particles.190

Figure 43: ^1H NMR spectra of mannitol from three different positions of seven insulin DPI formulations in the blending container. A: Insulin and spray freeze dried (SFD) mannitol blend (IMB), B: insulin and SFD 5% glycine-mannitol blend (I5GMB), C: insulin and SFD 10% glycine-mannitol blend (I10GMB), D: insulin and SFD 15% glycine-mannitol blend (I15GMB), E: insulin and SFD 5% leucine-mannitol blend (I5LMB), F: insulin and SFD 10% leucine-mannitol blend (I10LMB) and insulin and G: SFD 15% leucine-mannitol blend (I15LMB). Dashed boxes with *, **, *** indicate peaks of the internal standard (sodium benzoate), mannitol, chemical shift reference (sodium 3-trimethylsilyl propionate-2,2,3,3-d₄, TSP), respectively.191

Figure 44: Next Generation Impactor (NGI) deposition profiles of DPI formulation containing spray freeze dried (SFD) mannitol carrier (blue) and insulin (red) at flow rate of 30 L min⁻¹. Deposition is expressed as delivered dose (%) per NGI stage (Data presented as mean \pm standard deviation, n=3). AIT: Alberta idealised throat, MOC: Micro orifice collector.192

Figure 45: ^1H NMR spectra of spray freeze dried (SFD) mannitol deposition profile from IMB formulation (insulin and SFD mannitol carrier blend) studied by Next Generation Impactor. AIT: Alberta idealised throat, MOC: Micro orifice collector. Dash boxes indicate mannitol peaks. Asterisks * and ** indicate peaks of the internal standard (sodium benzoate) and chemical shift reference (sodium 3-trimethylsilyl propionate-2,2,3,3-d₄, TSP), respectively.....193

Figure 46: Next Generation Impactor (NGI) deposition profiles of each dry powder inhaler formulation aerosolised from Handihaler® at flow rate of 30 L min⁻¹. Deposition is expressed as delivered dose (%) per NGI stage (Data presented as mean \pm standard deviation, n=3). AIT: Alberta idealised throat, MOC: Micro orifice collector. IMB: insulin and SFD mannitol blend, I5GMB: insulin and SFD 5% glycine-mannitol blend, I10GMB: insulin and SFD 10% glycine-mannitol blend, I15GMB: insulin and SFD 15% glycine-mannitol blend.....195

Figure 47: Next Generation Impactor (NGI) deposition profiles of each dry powder inhaler formulation aerosolised from Handihaler® at flow rate of 30 L min ⁻¹ . Deposition is expressed as delivered dose (%) per NGI stage (Data presented as mean ± standard deviation, n=3). AIT: Alberta idealised throat, MOC: Micro orifice collector. IMB: insulin and SFD mannitol blend, I5LMB: insulin and SFD 5% leucine-mannitol blend, I10LMB: insulin and SFD 10% leucine-mannitol blend and I15LMB: insulin and SFD 15% leucine-mannitol blend.	196
Figure 48: Insulin delivered dose (%) and fine particle fraction (FPF% ≤5.0 µm) for seven dry powder inhaler (DPI) formulations. IMB: insulin and SFD mannitol blend, I5GMB: insulin and SFD 5% glycine-mannitol blend, I10GMB: insulin and SFD 10% glycine-mannitol blend, I15GMB: insulin and SFD 15% glycine-mannitol blend, I5LMB: insulin and SFD 5% leucine-mannitol blend, I10LMB: insulin and SFD 10% leucine-mannitol blend and I15LMB: insulin and SFD 15% leucine-mannitol blend.....	197
Figure 49: Scanning electron microscopy images of raw human insulin (A), spray dried (SD) insulin (B), SD insulin and spray freeze dried (SFD) mannitol blend (SDIMB)(C,D), SD insulin and SFD 10% glycine-mannitol blend (SDI10GMB) (E,F) and SD insulin and SFD 5% leucine-mannitol blend (SDI5LMB) (G,H) dry powders.....	210
Figure 50: Combined DSC thermograms of raw human insulin (A, black) and spray dried insulin (B, red) dry powders.	211
Figure 51: Combined TGA curves of raw human insulin (A, black) and spray dried insulin (B, red) dry powders.	212
Figure 52: The content uniformity for insulin with coefficient of variation and mannitol in dry powder inhaler (DPI) formulations (n=3). (Data presented as mean (three positions) ± standard deviation, n=3). SDIMB: Spray dried (SD) insulin and spray freeze dried (SFD) mannitol blend, SDI10GMB: SD insulin and SFD 10% glycine-mannitol blend and SDI5LMB: SD insulin and SFD 5% leucine-mannitol blend.	214
Figure 53: ¹ H NMR spectra of mannitol from three different positions of three carrier-based dry powder inhaler formulations in the blending container. SDIMB: spray dried (SD) insulin and spray freeze dried (SFD) mannitol carrier blend (A), SDI10GMB: SD insulin and SFD10% glycine-mannitol carrier blend (B), and SDI5LMB: SD insulin and SFD 5% leucine-mannitol carrier blend (C). Dashed boxes with *, **, *** indicate peaks of the internal standard (sodium benzoate), mannitol, chemical shift reference (sodium 3-trimethylsilyl propionate-2,2,3,3-d ₄ , TSP), respectively.....	215
Figure 54: Next Generation Impactor (NGI) deposition profiles of spray dried (SD) insulin powders in dry powder inhaler formulations aerosolised from Handihaler® at flow rate of 30 L min ⁻¹ . Insulin deposition is expressed as delivered dose (%) per NGI stage. (Data presented as mean ± standard deviation, n=3). AIT: Alberta idealised throat, MOC: Micro orifice collector. SDI: SD insulin, SDIMB: SD insulin and spray freeze dried (SFD) mannitol blend, SDI10GMB: SD insulin and SFD 10% glycine-mannitol blend and SDI5LMB: SD insulin and SFD 5% leucine-mannitol blend.	218
Figure 55: FTIR spectra of raw human insulin powder stored at -20°C (A) and freshly prepared spray dried insulin powder (B). %T: Transmittance.	221
Figure 56: FTIR spectra of raw human insulin powder stored at -20°C (A), freshly prepared spray dried (SD) insulin powder (B) and SD insulin powder stored at room temperature for 8 days (C), 25 days (D), 95 days (E), 151 days (F) and 165 days (G), 11 months (H) and 12 months (I). %T: Transmittance.	222

Figure 57: Insulin content determined by RP-HPLC. Spray dried insulin powder was stored at room temperature for up to 361 days (12 months). (Data presented as mean \pm standard deviation, n=3).

.....222

Figure 58: HPLC chromatograms for GLP-1 dissolved in distilled water (GLP-1 concentration A: 80 $\mu\text{g mL}^{-1}$ and B: 120 $\mu\text{g mL}^{-1}$) with two different compositions of mobile phase A: acetonitrile with 0.1% TFA (red) or acetonitrile alone (blue). (Area and height: t-test, $p>0.05$).240

Figure 59: HPLC chromatograms for GLP-1 stock solution (GLP-1 concentration: 1020 $\mu\text{g mL}^{-1}$) at a retention time of 3.7 mins with two detection wavelengths: 215 nm (A) and 220 nm (B).241

Figure 60: HPLC chromatograms for freshly prepared GLP-1 stock solution (GLP-1 concentration: 1 mg mL^{-1}) (A), GLP-1 stock solution stored at room temperature for 10 days (B) and 13 days (C) and stored at 4°C for 18 days (D). GLP-1 retention time: around 3.8 minutes.243

Figure 61: HPLC chromatograms for mobile phases (41:59 (%v/v) mixture of acetonitrile with 0.1% trifluoroacetic acid (TFA) and distilled water with 0.1% TFA) at a retention time of 2-3 mins and raw GLP-1 (1 mg mL^{-1}) dissolved in distilled water at a retention time of 3.8 mins (A), raw GLP-1 (1 mg mL^{-1}) dissolved in 0.1% acetic acid with 1M NaOH aqueous solution (pH 3.5) (B), spray dried (SD) GLP-1 powder prepared from 0.1% acetic acid with 1M NaOH dissolved in distilled water (0.9 mg mL^{-1}) (C), raw GLP-1 (1 mg mL^{-1}) dissolved in 0.1% acetic acid with 35% NH_4OH aqueous solution (pH 3.5) (D), SD GLP-1 powder prepared from 0.1% acetic acid with 35% NH_4OH dissolved in distilled water (1 mg mL^{-1}) (E), raw GLP-1 (600 $\mu\text{g mL}^{-1}$) dissolved in a mixture of glycine (300 $\mu\text{g mL}^{-1}$) and mannitol (300 $\mu\text{g mL}^{-1}$) aqueous solution (F), mobile phase A: acetonitrile with 0.1% TFA (G), mobile phase B: distilled water with 0.1% TFA (H), distilled water (I), 0.1% acetic acid with 1M NaOH aqueous solution (pH 3.5) (J), 0.1% acetic acid with 35% NH_4OH aqueous solution (pH 3.5) (K), raw mannitol (1 mg mL^{-1}) dissolved in distilled water (L), raw glycine (1 mg mL^{-1}) dissolved in distilled water (M).247

Figure 62: Calibration curve for GLP-1 in the concentration range of 2.0 $\mu\text{g mL}^{-1}$ to 140.0 $\mu\text{g mL}^{-1}$ (n=3).248

Figure 63: HPLC chromatograms for GLP-1 calibration curve in the concentration range from 2.0 μg (bottom) to 140.0 μg (top) mL^{-1} . Average retention time: 3.81 ± 0.004 min, asymmetry factor: 1.06 ± 0.03 , tailing factor: 1.08 ± 0.04 and efficiency of chromatography: 3061.79.248

Figure 64: HPLC chromatograms for GLP-1 dissolved in distilled water (GLP-1 concentration: 80 $\mu\text{g mL}^{-1}$ and 120 $\mu\text{g mL}^{-1}$) with two different flow rates (1.0 mL min^{-1} and 0.9 mL min^{-1}). A: 80 $\mu\text{g mL}^{-1}$ at 1.0 mL min^{-1} , B: 80 $\mu\text{g mL}^{-1}$ at 0.9 mL min^{-1} , C: 120 $\mu\text{g mL}^{-1}$ at 1.0 mL min^{-1} , and D: 120 $\mu\text{g mL}^{-1}$ at 0.9 mL min^{-1} . (Area and height: t-test, $p>0.05$).251

Figure 65: HPLC chromatograms for GLP-1 dissolved in distilled water (GLP-1 concentration: 40 $\mu\text{g mL}^{-1}$ (left), 80 $\mu\text{g mL}^{-1}$ (middle), 120 $\mu\text{g mL}^{-1}$ (right)) at a retention time of around 3.8 mins with two different HPLC systems (HPLC#4 and HPLC#5). (Area and height: t-test, $p>0.05$).251

Figure 66: Scanning electron microscopy (SEM) images of raw GLP-1 powder as received (A), spray dried (SD) GLP-1 powder produced from acetic acid with 1M NaOH (B), SD GLP-1 powder produced from acetic acid with 35% NH_4OH (C).255

Figure 67: SEM images of spray freeze dried (SFD) 10% glycine-mannitol carrier powder (sieved 90-125 μm) (A,B) and spray dried GLP-1 powder produced from acetic acid with 35% NH_4OH blended with SFD 10% glycine-mannitol carrier powder (C,D). Yellow boxes indicate SEM images with 2 μm scale bar. Yellow circles indicate SD GLP-1 particles fitting into the void spaces between indentations.

.....256

Figure 68: SEM images of raw mannitol powder (sieved 90-125 μm) (A,B) and spray dried GLP-1 powder produced from acetic acid with 35% NH_4OH blended with raw mannitol carrier powder (C,D). Yellow boxes indicate SEM images with 2 μm scale bar.257

Figure 69: Combined DSC thermograms of raw GLP-1 (A), SDGLP(NaOH): spray dried (SD) GLP-1 prepared from acetic acid with 1M NaOH (B), and SDGLP(NH_4OH): SD GLP-1 prepared from acetic acid with 35% NH_4OH (C).258

Figure 70: Combined TGA curves of raw GLP-1 (A), spray dried (SD) GLP-1 powder prepared from acetic acid with 1M NaOH (SDGLP(NaOH)) (B), and SD GLP-1 powder prepared from acetic acid with 35% NH_4OH (SDGLP(NH_4OH)) (C).260

Figure 71: ^1H NMR spectra of mannitol from three different positions of carrier-based DPI formulations in the blending container. SDG10GMB: Spray dried (SD) GLP-1 (SDGLP(NH_4OH)) blended with spray freeze dried 10% glycine-mannitol carrier (A) and SDGRMB: SDGLP(NH_4OH) blended with raw mannitol carrier (B). Dashed boxes indicate peaks of the internal standard (sodium benzoate), mannitol, chemical shift reference (sodium 3-trimethylsilyl propionate-2,2,3,3-d $_4$, TSP).262

Figure 72: Next Generation Impactor (NGI) deposition profiles of SD GLP-1 in four different dry powder inhaler formulations aerosolised from Handihaler[®] at flow rate of 30 L min^{-1} . GLP-1 deposition is expressed as delivered dose (%) per NGI stage (Data presented as mean \pm standard deviation, n=3). AIT: Alberta idealised throat, MOC: Micro orifice collector. SDGLP(NaOH): spray dried (SD) GLP-1 prepared from acetic acid with 1M NaOH, SDGLP(NH_4OH): SD GLP-1 prepared from acetic acid with 35% NH_4OH , SDG10GMB: SDGLP(NH_4OH) blended with SFD 10% glycine-mannitol carrier and SDGRMB: SDGLP(NH_4OH) blended with raw mannitol carrier.267

Figure 73: FTIR spectra of raw GLP-1 powder (as received) stored at 4 $^\circ\text{C}$ (A), SDGLP(NaOH): freshly prepared spray dried (SD) GLP-1 from acetic acid with 1M NaOH (B) and SDGLP(NH_4OH): freshly prepared SD GLP-1 from 0.1% acetic acid with 35% NH_4OH (C). %T: Transmittance.270

Figure 74: FTIR spectra of raw GLP-1 powder stored at 4 $^\circ\text{C}$ (A) and raw human insulin powder stored at -20 $^\circ\text{C}$ (B) for comparison. %T: Transmittance.270

Figure 75: FTIR spectra of freshly prepared spray dried GLP-1 powder of SDGLP(NaOH) from 0.1% acetic acid with 1M NaOH (top, blue), SDGLP(NaOH) powder stored at room temperature for 48 hours, 3 days, 6 days, 13 days, 27 days, 41 days, 62 days, 76 days, and 209 days (7 months, bottom, red). %T: Transmittance.....271

Figure 76: FTIR spectra of freshly prepared spray dried GLP-1 powder of SDGLP(NH_4OH) from 0.1% acetic acid with 35% NH_4OH (top, blue), SDGLP(NH_4OH) powder stored at room temperature for 24 hours, 48 hours, 5 days, 19 days, 33 days, 54 days, 68 days, and 203 days (7 months, bottom, red). %T: Transmittance.272

Figure 77: GLP-1 content determined by RP-HPLC. (A) SDGLP(NaOH): Spray dried (SD) GLP-1 powder produced from 0.1% acetic acid with 1M NaOH stored at room temperature for up to 209 days (7 months). (B) SDGLP(NH₄OH): SD GLP-1 powder produced from 0.1% acetic acid with 35% NH₄OH stored at room temperature for up to 203 days (7 months). (Data presented as mean \pm standard deviation, n=4).....273

Figure 78: Participants' knowledge and understanding level of insulin inhalers (n=375) (A), participants' willingness to try insulin inhalers (n=312) (B), participants' willingness to try insulin inhalers based on information status about insulin inhalers (n=233) (p=0.635) (C), participants' willingness to try insulin inhalers based on their level of knowledge and understanding of insulin inhalers (n=312) (p=0.154) (D).....281

Figure 79: Reasons not to use insulin inhalers (n=390) (A), features of insulin inhalers rated on a scale from 1 (not important) to 10 (very important) (B), participants' preferences for different inhalers rated on a scale from 1 (least preferred) to 10 (highly preferred) (C), male and female preferred inhalers based on a scale between 7 (preferred) and 10 (highly preferred) (D).283

Figure 80: Participants' willingness to try insulin inhalers in accordance to age group (n=309) (p=0.001) (A), participants' insulin inhaler acceptability if available on the NHS based on their self-rated compliance level towards current insulin treatment (n=312) (p<0.0005) (B), participants' insulin inhaler acceptability if available on the NHS based on their current insulin treatment satisfaction level (n=312) (p<0.0005) (C), participants' insulin inhaler acceptability if available on the NHS based on the duration of insulin use (n=312) (p=0.001) (D), participants' interest in insulin inhalers based on the duration of insulin use (n=375) (p=0.01) (E), participants' willingness to try insulin inhalers based on participants' perception (inhalers versus injections) (n=310) (p<0.0005) (F).285

List of tables

Table 1: The list of currently available insulin preparations (injections) in the UK (2021) (BNF, 2021).	37
Table 2: Current available GLP-1 receptor agonists (GLP-1RAs) and insulin and GLP-1RA combination products in the UK for subcutaneous use or oral administration for the treatment of Type 2 diabetes mellitus (T2DM) (BNF, 2021). t_{max} : Time reached for maximum plasma concentration. T1DM: Type 1 diabetes mellitus.....	44
Table 3: Particle size (aerodynamic diameter, μm), region of particle deposition in the respiratory tract and mechanism for particle deposition based on the aerodynamic diameter.	68
Table 4: Compositions of sample preparation. TSP: sodium 3-trimethylsilyl propionate-2,2,3,3-d ₄ . D ₂ O: deuterium oxide.	116
Table 5: Accuracy (relative error %), intra-day precision (three replicates per concentration on the same day) and inter-day precision (9 replicates per concentration over 3 days) at three different concentrations for the ¹ H qNMR method. Data presented as mean with standard deviation (SDv), relative standard deviation (RSD%) and relative error%.	129
Table 6: Linear correlation coefficient (R^2), regression equation, limit of detection (LOD) and limit of quantitation (LOQ).	130
Table 7: Particle size volume diameters (μm) at 10% (Dv10), 50% (Dv50) and 90% (Dv90) of particle size distribution for raw saccharides (mannitol, sucrose, and sorbitol), spray freeze dried (SFD) mannitol and sucrose, and spray dried (SD) mannitol and sucrose dry powders. VMD: volume mean diameter.....	134
Table 8: DSC results for raw mannitol, spray freeze dried (SFD) mannitol, spray dried (SD) mannitol and raw sorbitol dry powders.....	135
Table 9: DSC Results for raw sucrose, spray freeze dried (SFD) sucrose and spray dried (SD) sucrose dry powders.	136
Table 10: Delivered dose (%), fine particle fraction (FPF% $\leq 5.0 \mu\text{m}$), mass median aerodynamic diameter (MMAD) and geometric standard deviation (GSD) of raw mannitol, spray dried (SD) mannitol, spray freeze dried (SFD) mannitol, raw sucrose, SD sucrose, SFD sucrose and raw sorbitol dry powders determined by Next Generation Impactor analysis at flow rate of 30 L min ⁻¹ . (Data presented as mean \pm standard deviation, n=3).	143
Table 11: Cumulative fraction (%) of raw mannitol, spray freeze dried (SFD) mannitol, spray dried (SD) mannitol, raw sucrose, SFD sucrose, SD sucrose, and raw sorbitol deposited on Next Generation Impactor (NGI) stages (1-7). Cumulative fraction per NGI stage was calculated by the Copley Inhaler Testing Data Analysis software based on summation of the cumulative mass collected on NGI stages (1-7 and MOC, Alberta idealised throat is not included). (Data presented as mean, n=3).	146
Table 12: The optimal chromatography conditions and instrument used for method development and validation. TFA: trifluoroacetic acid.....	152

Table 13: Compositions of aqueous solutions (15% w/v total solid content) to prepare spray freeze dried (SFD) mannitol (M) carriers with and without glycine (G) or leucine (L) at three different concentrations (5%, 10% and 15% of mannitol). SFD5GM: SFD 5% glycine-mannitol, SFD5LM: SFD 5% leucine-mannitol, SFD10GM: SFD 10% glycine-mannitol, SFD10LM: SFD 10% leucine-mannitol, SFD15GM: SFD 15% glycine-mannitol, SFD15LM: SFD 15% leucine-mannitol.....	158
Table 14: Seven insulin dry powder inhaler (DPI) formulations prepared by blending ground insulin dry powders with spray freeze dried (SFD) mannitol-based carriers.....	159
Table 15: Comparison of recovery (%) using two wavelengths of 215 nm and 214 nm (insulin concentration: 54.0 $\mu\text{g mL}^{-1}$ and 108.0 $\mu\text{g mL}^{-1}$). Data presented as mean \pm standard deviation. RSD: relative standard deviation.....	164
Table 16: Stability study on insulin standard stock solution (1 mg mL^{-1}) stored at room temperature for 7 days and at 4°C for 10 days (Data presented as mean (%) \pm standard deviation, n=4-6).	165
Table 17: Stability study on insulin calibration standard solutions stored at room temperature and 4°C for up to 72 hours (Data presented as mean (%) \pm standard deviation, n=3).	166
Table 18: Accuracy (relative error %), intra-day precision (six replicates per concentration on the same day) and inter-day precision (12 or 18 replicates per concentration over 2 or 3 days) at three different concentrations for the RP-HPLC method. Data presented as mean \pm standard deviation (SDv). RSD: relative standard deviation.....	170
Table 19: Linear correlation coefficient (R^2), regression equation, limit of detection (LOD) and limit of quantitation (LOQ).....	171
Table 20: Results of robustness study. Data presented as mean \pm standard deviation. RSD: relative standard deviation.....	172
Table 21: Results of system suitability study (n=6). SDv: standard deviation, RSD: relative standard deviation.	173
Table 22: Particle size volume diameters (μm) at 10% (Dv10), 50% (Dv50) and 90% (Dv90) of particle size distribution for spray freeze dried (SFD) mannitol with and without 5%, 10% and 15% glycine (G) or leucine (L) powders. SFD5GM: SFD 5% glycine-mannitol, SFD10GM: SFD 10% glycine-mannitol, SFD15GM: SFD 15% glycine-mannitol, SFD5LM: SFD 5% leucine-mannitol, SFD10LM: SFD 10% leucine-mannitol, SFD15LM: SFD 15% leucine-mannitol. VMD: volume mean diameter.	177
Table 23: DSC thermal analysis results. Onset temperature and enthalpy for glycine, leucine and spray freeze dried (SFD) mannitol carriers with glycine or leucine (5%, 10% and 15%). SFD5GM: SFD 5% glycine-mannitol, SFD10GM: SFD 10% glycine-mannitol, SFD15GM: SFD 15% glycine-mannitol, SFD5LM: SFD 5% leucine-mannitol, SFD10LM: SFD 10% leucine-mannitol, SFD15LM: SFD 15% leucine-mannitol.....	180

Table 24: Insulin delivered dose (%), fine particle fraction (FPF% $\leq 5.0 \mu\text{m}$), mass median aerodynamic diameter (MMAD) and geometric standard deviation (GSD) determined by Next Generation Impactor analysis at flow rate of 30 L min^{-1} for seven dry powder inhaler (DPI) formulations (Data presented as mean \pm standard deviation, $n=3$). IMB: insulin and SFD mannitol blend, I5GMB: insulin and SFD 5% glycine-mannitol blend, I10GMB: insulin and SFD 10% glycine-mannitol blend, I15GMB: insulin and SFD 15% glycine-mannitol blend, I5LMB: insulin and SFD 5% leucine-mannitol blend, I10LMB: insulin and SFD 10% leucine-mannitol blend and I15LMB: insulin and SFD 15% leucine-mannitol blend.....	197
Table 25: Compositions of aqueous solutions (15% w/v total solid content) to prepare spray freeze dried (SFD) mannitol carriers with and without 10% glycine or 5% leucine. SFD5LM: SFD 5% leucine-mannitol, SFD10GM: SFD 10% glycine-mannitol.....	202
Table 26: Carrier free insulin formulation (SDI) and carrier-based dry powder inhaler (DPI) formulations (SDIMB, SDI10GMB, SDI5LMB) prepared by blending spray dried (SD) insulin dry powders with spray freeze dried (SFD) mannitol-based carriers.	203
Table 27: Insulin delivered dose (%), fine particle fraction (FPF% $\leq 5.0 \mu\text{m}$), mass median aerodynamic diameter (MMAD) and geometric standard deviation (GSD) determined by Next Generation Impactor analysis at flow rate of 30 L min^{-1} for dry powder inhaler (DPI) formulations (Data presented as mean \pm standard deviation, $n=3$). SDI: spray dried (SD) insulin, SDIMB: SD insulin and spray freeze dried (SFD) mannitol blend, SDI10GMB: SD insulin and SFD 10% glycine-mannitol blend and SDI5LMB: SD insulin and SFD 5% leucine-mannitol blend.....	218
Table 28: The optimal chromatography conditions and instrument used for method development and validation. TFA: trifluoroacetic acid.....	228
Table 29: Compositions of acidic aqueous solutions used to prepare spray dried (SD) GLP-1 dry powders. SDGLP(NaOH): SD GLP-1 powder prepared from acetic acid with 1M sodium hydroxide (NaOH), SDGLP(NH ₄ OH): SD GLP-1 powder prepared from acetic acid with 35% ammonium hydroxide (NH ₄ OH).	234
Table 30: Carrier free dry powder inhaler (DPI) formulations: SDGLP(NaOH): spray dried (SD) GLP-1 powder produced from acetic acid with 1M NaOH and SDGLP(NH ₄ OH): SD GLP-1 powder produced from acetic acid with 35% NH ₄ OH. Carrier-based DPI formulations: SDG10GMB: SDGLP(NH ₄ OH) blended with spray freeze dried (SFD) 10% glycine-mannitol carrier and SDGRMB: SDGLP(NH ₄ OH) blended with raw mannitol carrier.....	235
Table 31: Recovery, retention time, height, and asymmetry and tailing factors for GLP-1 solutions ($80 \mu\text{g mL}^{-1}$ and $120 \mu\text{g mL}^{-1}$) using two different compositions of mobile phase A: acetonitrile with 0.1% trifluoroacetic acid (TFA) and acetonitrile alone (Data presented as mean \pm standard deviation). RSD: relative standard deviation.....	240
Table 32: Comparison of asymmetry and tailing factors for GLP-1 ($80 \mu\text{g mL}^{-1}$ and $120 \mu\text{g mL}^{-1}$) between two different columns: C8 (4.6 x 250 mm, $5 \mu\text{m}$) and C18 (4.6 x 250 mm, $4 \mu\text{m}$) (Data presented as mean \pm standard deviation). RSD: relative standard deviation.....	241
Table 33: Stability study on GLP-1 standard stock solution (1 mg mL^{-1}) stored at room temperature for up to 13 days and at 4°C for up to 18 days (Data presented as mean (%) \pm standard deviation, $n=3$).	242

Table 34: Stability study on short-term storage of GLP-1 calibration standard solutions stored at room temperature for 24 hours (Data presented as mean \pm standard deviation, n=3).	243
Table 35: Stability study on GLP-1 (1 mg mL ⁻¹) dissolved in acidic aqueous solution (0.1% acetic acid with 1M NaOH, pH 3.5 or 0.1% acetic acid with 35% NH ₄ OH, pH 3.5) stored at room temperature and at 4°C for up to 7 days (Data presented as mean (%) \pm standard deviation, n=3).	244
Table 36: Accuracy (relative error %), intra-day precision (six replicates per concentration on the same day) and inter-day precision (18 replicates per concentration over 3 days) at five different concentrations for RP-HPLC method. Data presented as mean with standard deviation (SDv). RSD: relative standard deviation.	249
Table 37: Linear correlation coefficient (R ²), regression equation, limit of detection (LOD) and limit of quantitation (LOQ).	249
Table 38: Results of robustness study. Data presented as mean. SDv: standard deviation, RSD: relative standard deviation.	250
Table 39: Results of system suitability study (Data presented as mean, n=6). SDv: standard deviation, RSD: relative standard deviation.	252
Table 40: The content uniformity (%) with coefficient of variation for GLP-1 and mannitol in carrier-based dry powder inhaler (DPI) formulations (data presented as mean (%) \pm standard deviation, n=3 per position). SDG10GMB: Spray dried (SD) GLP-1 (SDGLP(NH ₄ OH)) blended with spray freeze dried 10% glycine-mannitol carrier and SDGRMB: SDGLP(NH ₄ OH) blended with raw mannitol carrier.	261
Table 41: GLP-1 delivered dose (%), fine particle fraction (FPF% \leq 5.0 μ m), mass median aerodynamic diameter (MMAD) and geometric standard deviation (GSD) determined by Next Generation Impactor study with Handihaler [®] at flow rate of 30 L min ⁻¹ for dry powder inhaler (DPI) formulations (Data presented as mean \pm standard deviation, n=3). SDGLP(NaOH): spray dried (SD) GLP-1 prepared from acetic acid with 1M NaOH, SDGLP(NH ₄ OH): SD GLP-1 prepared from acetic acid with 35% NH ₄ OH, SDG10GMB: SDGLP(NH ₄ OH) blended with SFD 10% glycine-mannitol carrier and SDGRMB: SDGLP(NH ₄ OH) blended with raw mannitol carrier.	267
Table 42: Demographics of participants with Type 1 diabetics (n=309, excluded incomplete responses (n=81) for gender, age, and ethnic background questions).	279
Table 43: Factors affecting and not affecting insulin inhaler acceptability.	285

Abbreviations

A21	A21 desamido insulin
AFM	Atomic Force Microscopy
AIT	Alberta Idealised Throat
ANOVA	Analysis of Variance
As	asymmetry factor
Asn	asparagine
AUC	area under the curve or area under the plasma concentration time curve
BMI	body mass index
C _{max}	maximum plasma concentration
COPD	chronic obstructive pulmonary disease
COVID-19	coronavirus disease 2019
Cys	cysteine
CV	coefficient of variation
d _{aer}	aerodynamic diameter
DM	Diabetes Mellitus
DPI	dry powder inhaler
DPP-4	dipeptidyl peptidase-4
DSC	Differential Scanning Calorimetry
Dv10, Dv50, Dv90	volumetric diameter (µm), where 10%, 50%, 90% of particles are smaller
D ₂ O	deuterium oxide
EMA	European Medicines Agency
FD	freeze drying / freeze dried
FDA	Food and Drug Administration
FDKP	fumaryl diketopiperazine
FEV ₁	forced expiratory volume in one second
FTIR	Fourier Transform Infrared Spectroscopy
FPF	fine particle fraction
FRC	functional residual capacity
GI	gastrointestinal
GLP-1	glucagon-like peptide-1 / glucagon-like peptide-1(7-36) amide
GLP-1R	glucagon-like peptide-1 receptor
GLP-1RA	glucagon-like peptide-1 receptor agonist
GP	general practitioner
GRAS	generally recognized as safe
GSD	geometric standard deviation
GSK	GlaxoSmithKline
¹ H	proton
¹ H NMR	proton Nuclear Magnetic Resonance
¹ H qNMR	proton quantitative Nuclear Magnetic Resonance, quantitative analysis using proton Nuclear Magnetic Resonance
HCP	healthcare provider
hr	hour
HbA1c	glycated haemoglobin A1C
HCl	hydrochloric acid
HMWP	high molecular weight protein
HPLC	High Performance Liquid Chromatography
HPMC	Hydroxypropyl Methyl Cellulose / Hypromellose

HSD	honestly significant difference
H ₂ O	water
ICDD	International Centre for Diffraction Data
ICH	the International Council for Harmonisation of Technical Requirements for Pharmaceuticals for Human Use
IU	international unit
kV	kilovolt
LOD	limit of detection
LOQ	limit of quantitation
µg	microgram
mg	milligram
mins	minutes
M	molar concentration, mol L ⁻¹
mM	millimolar
MMAD	mass median aerodynamic diameter
MOC	micro orifice collector
ms	millisecond, 1 second = 1000 millisecond
MW	molecular weight
NaOH	sodium hydroxide
NH ₄ OH	ammonium hydroxide
NMR	Nuclear Magnetic Resonance
NPH	Neutral Protamine Hagedorn
NGI	Next Generation Impactor
PBS	phosphate buffered saline
Ph.Eur.	European Pharmacopoeia
PIONEER	Peptide Innovation for Early Diabetes Treatment
pMDI	pressurised meter dose inhaler
rDNA	recombinant deoxyribonucleic acid
RG	receiver gain
RP-HPLC	Reversed-Phase High Performance Liquid Chromatography
RH	relative humidity
RSD%	relative standard deviation
SC	subcutaneous
SD	spray drying / spray dried
SDv	standard deviation
SEC	Size Exclusion Chromatography
SEM	Scanning Electron Microscopy
SFD	spray freeze drying / spray freeze dried
SGLT-2	sodium glucose cotransporter 2
S/N	signal to noise ratio
T1DM	Type 1 diabetes mellitus
T2DM	Type 2 diabetes mellitus
Tf	tailing factor
TFA	trifluoroacetic acid
Tg	glass transition temperature
TGA	Thermogravimetric Analysis
t _{max}	time reached for maximum/peak plasma concentration
TSP	sodium 3-trimethylsilyl propionate-2,2,3,3-d ₄
UK	United Kingdom
US	The United States

USP	United States Pharmacopoeia
UV	ultraviolet
vs.	versus
VMD	volume mean diameter
WHO	the World Health Organization
XRD	X-ray diffraction

Structure of thesis and novelty of work

An overview of the research on particle engineering for pulmonary delivery of peptide and protein drugs is described in the thesis titled "Engineering spray freeze dried particles for pulmonary delivery of proteins". The main text comprises eight Chapters with the last being a conclusion (Chapter 8). The thesis contains some novelty of work that have not been studied before. Chapter 1 provides a general introduction about diabetes. This includes the types of diabetes, current available treatments for diabetes and non-injection route candidates for antidiabetic drug delivery (i.e., insulin and glucagon-like peptide-1 (GLP-1)). Chapter 2 provides a literature review of pulmonary delivery (as an alternative route to subcutaneous drug delivery), human respiratory system, dry powder inhaler (DPI) formulations, particle engineering for improved pulmonary drug delivery and types of DPI devices. Chapter 2 also includes a summary of pulmonary safety of inhaled insulin. The review focuses on current approaches for the development of high dose DPI formulations that could apply for pulmonary delivery of peptide and protein drugs. Chapters 3-7 provide the research findings including an online survey (Chapter 7) that have been analysed and interpreted. All these chapters contain abstract, introduction, materials, methodology, results, and discussion and close with conclusion. Chapter 3 presents the process of the method development using proton Nuclear Magnetic Resonance (^1H NMR) spectroscopy for quantification of saccharide carriers (mannitol, sorbitol, and sucrose) employed in DPI formulations. Chapter 3 also includes characterisation of the saccharide carriers prepared by spray drying and spray freeze drying and assesses lung deposition patterns of carriers *in vitro* via impaction studies. Quantitative NMR techniques have been employed in various areas (e.g., pharmaceuticals, natural products, metabolites, and agriculture industry), however, it has not been applied for the deposition study of saccharides in pulmonary formulations. Therefore, an analytical method using ^1H NMR spectroscopy for quantitative analysis of saccharide contents in DPI formulations was developed and this led to publication (See **Research output**). Chapter 4 assesses how amino acids (glycine or L-leucine) added as excipient to spray freeze dried (SFD) mannitol carrier affect the aerosolisation performance of DPI formulations containing human insulin. The research of Chapter 4 was inspired by the properties of dry powders prepared by spray freeze drying that are large porous spherical particles and advantageous as aerodynamic properties. Such powders can enhance the aerosolisation performance therefore suitable for pulmonary drug delivery. So far, spray freeze drying has not been employed for carrier particle engineering for pulmonary delivery of peptides and proteins. There is no evidence in the literature of the effects of amino acids on the aerosolisation performance of DPI formulations containing insulin and SFD mannitol-based carriers. Chapter 5 is the sequence study of Chapter 4 and describes the aerosolisation performance of DPI formulations containing excipient free human insulin powder

prepared by spray drying and optimal SFD amino acid-mannitol carriers selected based on the results of Chapter 4. Chapter 5 includes novelty work on the aerosolisation performance of carrier-based DPI formulations containing spray dried insulin powder in the absence of excipients and SFD mannitol-based carriers. The addition of the SFD carrier to the formulations was to address the poor flowability of cohesive drug particles and enhance the aerosolisation performance of DPI formulations containing spray dried insulin. Previous published studies with insulin have focused on carrier free DPI formulation where insulin was incorporated in excipients to enhance insulin delivery via the lungs or excipient free insulin without the inclusion of carrier. Therefore carrier-based DPI formulations have not been studied before. Similarly, to Chapter 5, Chapter 6 describes the aerosolisation performance of two types of DPI formulations; carrier free DPI formulations containing spray dried GLP-1 alone and carrier-based DPI formulations containing spray dried GLP-1 blended with two different mannitol-based carriers for pulmonary delivery of GLP-1. Two carriers employed were SFD 10% glycine-mannitol carrier (engineered carrier) selected based on the results of Chapter 4 and Chapter 5 and raw mannitol carrier (non-engineered carrier). This was the first study focusing on the development of excipient free GLP-1 DPI formulations for inhaled therapy in Type 2 diabetes and accepted for publication in International Journal of Pharmaceutics in February 2022 (See **Research output**). Chapter 7 assesses insulin inhaler acceptability by people with Type 1 diabetes via a large-scale online survey (309 participants), which has not been performed before. Only a small-scale study consisting of four questions and 26 participants with diabetes was previously conducted over the phone by Diabetes UK in 2006. Chapter 8 is the final chapter that summarises the conclusions based on the research conducted within the thesis and concludes with suggestions for further research.

Aim and objectives

The thesis has focused on the development of DPI formulations for pulmonary delivery of antidiabetic peptide and protein drugs such as insulin and glucagon-like peptide-1(7-36) amide (GLP-1). These drugs are generally administered via subcutaneous injection that interferes with the patients' lifestyle and affects patient compliance and adherence to treatment. The primary goal of the research was to assess the value of insulin and GLP-1 DPI formulations for inhalation use in people with diabetes (GLP-1 for Type 2 diabetes) as an alternative treatment option to injectable antidiabetic medications. To achieve the primary goal, the research was divided into five main objectives which refer to as Chapters 3 to 7. Chapter 3 and Chapter 4 focused on studying carriers and Chapter 5 and Chapter 6 focused on studying formulation performance containing insulin or GLP-1. Chapter 7 was about the analysis of the online survey data.

Aim

To see if insulin and GLP-1 DPI formulations for pulmonary delivery are feasible as an alternative treatment option to injections for people with diabetes

Objectives

Chapter 3

- To develop a proton NMR quantification method for carriers used in DPI formulations
- To assess *in vitro* lung deposition pattern of three selected saccharide carriers (mannitol, sorbitol, and sucrose) prepared by spray drying and spray freeze drying

Chapter 4

- To develop an analytical method using Reversed-Phase High Performance Liquid Chromatography (RP-HPLC) for determination of insulin content in DPI formulations
- To develop optimal mannitol-based carrier powders with and without amino acids (glycine or L-leucine) using spray freeze drying for enhanced pulmonary delivery of insulin and characterise their morphology, particle size distribution, thermal behaviour, moisture content, and crystallinity
- To assess how amino acids (glycine or L-leucine) added as excipient to SFD mannitol carrier affect the aerosolisation performance of carrier-based DPI formulations containing human insulin

Chapter 5

- To develop DPI formulations containing excipient free insulin powder prepared by spray drying and amino acid-mannitol carriers prepared by spray freeze drying and investigate the aerosolisation performance of spray dried insulin DPI formulations

Chapter 6

- To develop an analytical method using RP-HPLC for determination of GLP-1 content in DPI formulations
- To develop two types of DPI formulations; carrier free DPI formulations containing GLP-1 alone (no excipients) prepared by spray drying and carrier-based DPI formulations containing spray dried GLP-1 powder blended with 10% glycine-mannitol carrier prepared by spray freeze drying (engineered carrier) or raw mannitol carrier (non-engineered carrier) for pulmonary delivery of GLP-1 and assess the aerosolisation performance of both DPI formulations
- To investigate the effect of engineered carrier (SFD 10% glycine-mannitol carrier) and non-engineered carrier (raw mannitol carrier) on the aerosolisation performance of spray dried GLP-1 powders

Chapter 7

- To explore the perception of people with Type 1 diabetes mellitus on insulin inhalers and assess insulin inhaler acceptability via an online survey

Research output

Three publications (one review and two research articles) are made available during my PhD (See the list below). The title of the review published in August 2020 is "The impact of natural and synthetic polymers in formulating micro and nanoparticles for antidiabetic drugs" (Current Drug Delivery). The research article titled "Development of drug alone and carrier-based GLP-1 dry powder inhaler formulations" was recently accepted for publication in International Journal of Pharmaceutics in February 2022. This research article is based on the results of Chapter 6. The title of the other research article published in March 2019 is "¹H NMR quantification of spray dried and spray freeze-dried saccharide carriers in dry powder inhaler formulations" (International Journal of Pharmaceutics). This research article is based on the results of Chapter 3.

I also presented a poster that contained the results of Chapter 5 at Royal Society of Chemistry Conference/Symposium on Synthesis and Drug Discovery held at Kingston University, London on the 1st of November 2019.

The list of publications and conference

Babenko, Mai, Alany, Raid G., Calabrese, Gianpiero, Kaialy, Waseem and ElShaer, Amr (2022) "Development of drug alone and carrier-based GLP-1 dry powder inhaler formulations". International journal of pharmaceutics, vol.617, pp. 121601.

Al-Hashimi, Nihad, **Babenko, Mai**, Saaed, Maria, Kargar, Negeen and ElShaer, Amr (2021) "The impact of natural and synthetic polymers in formulating micro and nanoparticles for antidiabetic drugs". Current Drug Delivery, 18(3), pp. 271-288. ISSN (print) 1567-2018
The authors contributed equally.

Babenko, Mai, Peron, Jean-Marie R., Kaialy, Waseem, Calabrese, Gianpiero, Alany, Raid G. and ElShaer, Amr (2019) "¹H NMR quantification of spray dried and spray freeze-dried saccharide carriers in dry powder inhaler formulations". International Journal of Pharmaceutics, 564, pp. 318-328. ISSN (print) 0378-5173

Royal Society of Chemistry Conference/Symposium on Synthesis and Drug Discovery held at Kingston University, London on the 1st of November 2019.

Chapter 1. Introduction

1.1. General introduction - Diabetes

Diabetes mellitus (diabetes, DM) is a metabolic disease that causes hyperglycaemia (high blood glucose) associated with long-term effects of diabetes and complications (e.g., retinopathy leading to blindness, nephropathy/kidney failure and cardiovascular disease) (Hu, Jia, 2019, Lin et al., 2019, World Health Organization, 2019). Also, it has been found that diabetes is associated with increased risk of death from coronavirus disease 2019 (COVID-19) caused by severe acute respiratory syndrome coronavirus 2 (SARS-CoV-2) (Holman et al., 2020, World Health Organization, 2021a). According to the recent study published by Holman *et al.* (2020), mortality in weekly death registrations for people with diabetes increased during the beginning of COVID-19 pandemic (the first 19 weeks of 2020) compared to the corresponding weeks in the previous 3 years (2017-2019, Type 1 DM: increased by 50.9% and Type 2 DM: increased by 64.3%) (Holman et al., 2020). The types of diabetes are classified by the World Health Organisation (WHO) classification system (2019) for diabetes and include 2 major types of Type 1 diabetes mellitus (T1DM) and Type 2 diabetes mellitus (T2DM), other specific types (e.g., monogenetic diabetes, endocrine disorders, infection related diabetes, etc.), hyperglycaemia first detected during pregnancy (e.g., diabetes mellitus in pregnancy and gestational diabetes mellitus) and new types of diabetes (i.e., hybrid forms of diabetes and unclassified diabetes) (World Health Organization, 2019). The diagnostic criteria for diabetes, based on the WHO guidelines (published in 2006 and 2011), are fasting plasma glucose concentration ≥ 7.0 mmol/L (126 mg/dl), plasma glucose concentration 2 hour after oral glucose load (75 g) ≥ 11.1 mmol/L (200 mg/dl), random blood glucose concentration ≥ 11.1 mmol/L (200 mg/dl), or the use of glycated haemoglobin A1C (HbA1c) value $\geq 6.5\%$ (48 mmol/mol) in the presence of signs and symptoms of diabetes (e.g., polyuria and polydipsia) (World Health Organization, 2019, Diabetes, 2021a).

The number of people with diabetes is increasing worldwide over time (from 108 million in 1980 to 422 million in 2014) (World Health Organization, 2021b). In the United Kingdom (UK), the number of people with diabetes is currently more than 4.9 million and is predicted to increase to 5.5 million within 10 years (by 2030) (Diabetes, 2020b). There are currently 13.6 million people at high risk of T2DM and 850 thousand people living with T2DM yet to be diagnosed (Diabetes, 2020). Around 90% of people have T2DM resulting from insulin secretion deficiency and/or the development of insulin resistance where the body is not responding effectively to insulin (dysfunction of pancreatic β cells)

whereas around 8% of people are living with T1DM resulting from little or deficiency of insulin production due to the autoimmune destruction of the β cells of islet of Langerhans in the pancreas where the body is not able to produce insulin (destruction of pancreatic β cells) (Holt, Kumar, 2015, Lin et al., 2019, World Health Organization, 2021, Diabetes, 2020, World Health Organization, 2019). About 2 % of people with diabetes have rare types of diabetes (e.g., different types of monogenic diabetes caused by a single gene mutation, cystic fibrosis related diabetes, etc.)(Diabetes, 2020).

1.1.1. Treatment of diabetes

The main treatment for people with T1DM to control hyperglycaemia is insulin therapy administered via the parenteral route (e.g., subcutaneous (SC) route/injection) whereas people with T2DM associated with obesity start with changes in diet and lifestyle (e.g., healthy eating/healthy and balanced diet and increase physical activity) along with oral antidiabetic medications (e.g., tablets) for the management of T2DM (Hu, Jia, 2019). Currently, several types of oral antidiabetic drugs in T2DM treatment are available: mainly biguanides (e.g., metformin, first line treatment for T2DM), thiazolidinediones (e.g., pioglitazone) both to improve insulin sensitivity, sulfonylureas (e.g. first generation: tolbutamide, second generation: gliclazide), glinides (e.g., repaglinide) to stimulate insulin secretion, sodium glucose cotransporter 2 (SGLT-2) inhibitors (e.g., dapagliflozin) to block glucose re-absorption in the kidney and promote glucose excretion in urine therefore lower high blood glucose levels (reduce hyperglycaemia) and dipeptidyl peptidase-4 (DPP-4) inhibitors to increase insulin secretion (Hu, Jia, 2019, Pinho et al., 2019, Al-Hashimi et al., 2020). In addition to those oral medications, oral glucagon-like peptide-1 (GLP-1) receptor agonist (GLP-1RA; semaglutide) was newly approved in April 2020 for the treatment of T2DM and is marketed as Rybelsus® by Novo Nordisk Limited (emc, 2020q, BNF, 2021f). Injectable GLP-1RAs (administered by SC injection) are also available as the T2DM treatment to increase insulin secretion (BNF, 2021, BNF, 2021i). As Type 2 diabetes progress, people with T2DM fail or are no longer able to achieve good glycaemic control with lifestyle changes and oral antidiabetic medications therefore insulin therapy will be required (Holt, Kumar, 2015, Hu, Jia, 2019).

1.1.2. Insulin

Insulin is a 51 amino acid protein (insulin considered to be a large peptide or small protein) hormone secreted by the β cells of islet of Langerhans in the pancreas and regulates blood glucose levels by stimulating cells (e.g., liver, muscle, adipose tissue) to take up glucose from the blood (Patton,

Byron, 2007, Weiss, Steiner & Philipson, 2014, Lin et al., 2019). The structure of insulin contains two intermolecular disulfide bonds (cysteine (Cys) A7-B7 and A20-B19) between two polypeptide chains, A chain (21 amino acids) and B chain (30 amino acid) and one intramolecular disulfide bond in the A chain (Cys A6-A11) (Figure 1) (Piccirilli et al., 2013, Vanea et al., 2014, Weiss, Steiner & Philipson, 2014). Both chains linked together by two disulfide bonds (Cys A7-B7 and A20-B19) stabilise the structure (Piccirilli et al., 2013, Vanea et al., 2014, Weiss, Steiner & Philipson, 2014).

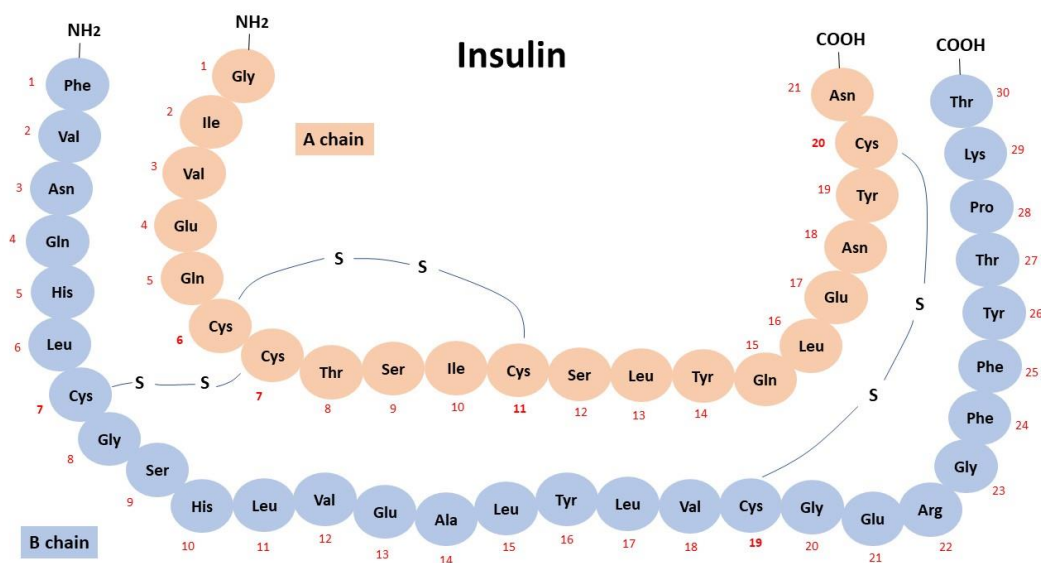


Figure 1: Schematic representation of human insulin structure based on Easa *et al.* (2019) with modifications. Two intermolecular disulfide bonds (cysteine (Cys) A7-B7 and A20-B19) between two polypeptide chains, A chain (21 amino acids) and B chain (30 amino acid) and one intramolecular disulfide bond in the A chain (Cys A6-A11).

The types of insulin available in clinical practice in the UK are human insulin, human insulin analogues and animal insulin (BNF, 2021c). Human insulins are biosynthetic human insulins produced by recombinant DNA (rDNA) technology (insert generic information of human insulin into bacteria, *Escherichia coli* or into yeast, *Saccharomyces cerevisiae*) to obtain biologically active human insulin, the same amino acid sequence as endogenous human insulin for therapeutic use in human (Sandow et al., 2015, BNF, 2021). Human insulin analogues are modified forms (modified amino acid sequence) of human insulins produced with different kinetic profiles (e.g., an extended/prolonged

duration of action or faster absorption and onset of action) (Sandow et al., 2015, BNF, 2021). Animal insulins (i.e., porcine insulin) extracted from animal sources (e.g., pancreas tissues) are available for patients who wish to continue with porcine insulin products (Sandow et al., 2015, Diabetes, 2017, BNF, 2021). In the UK, animal insulin sourced from bovine (i.e., Hypurin® Bovine insulin) was discontinued by the company, Wochhardt UK in 2017 due to a global supply issue (Diabetes, 2017). Also, different types of insulin products are available based on its time of action and generally classified into three groups of insulin: short-acting (including rapid-acting insulins), intermediate-acting and long-acting insulins (BNF, 2021). In addition to these three groups, premixed insulins, which are combinations of two different acting insulins consisting of short-acting insulin and intermediate-acting insulin prepared together in fixed ratios, are available in vials or pens (Clipper F et al., 2019). Table 1 shows the list of current available insulin preparations (injections) in the UK (BNF, 2021). Each type of insulin products has different onset of action, peak of effect and duration of action. Rapid-acting insulins analogues (e.g., insulin aspart: NovoRapid® and insulin lispro: Humalog®) provide fast onset of action within 10-20 mins with short duration of action (2-6 hours) after injections (e.g., SC administration). Fiasp® (insulin aspart) developed by Novo Nordisk Limited (January 2017) exhibited a faster initial absorption of insulin when compared to NovoRapid® also developed by Novo Nordisk Limited (September 1999) (European Medicines Agency, 2020c). These rapid-acting insulins are taken within 15 minutes before a meal or following a meal to manage mealtime blood glucose levels (minimise hyperglycaemia during a meal, minimise the sudden rise in blood glucose) (Clipper F et al., 2019). Short-acting insulins (e.g., insulin soluble human: Actrapid® and Humulin S®) taken 30 mins before meals also cover insulin requirements for meals eaten (Clipper F et al., 2019). In contrast, long-acting (basal) insulin analogues (e.g., insulin glargine: Lantus® and insulin detemir: Levemir®) are given daily or twice daily to cover daily insulin needs (Sandow et al., 2015, Clipper F et al., 2019). For example, Tresiba® (insulin degludec) developed by Novo Nordisk Limited (January 2013) exhibit a flat and stable glucose lowering effect between 0-24 hours with a duration of action up to 42 hours (emc, 2020s). Neutral Protamine Hagedorn (NPH) insulin (known as isophane insulin), which is the first synthetic human insulin using rDNA technology, belong to intermediate-acting insulin (human insulin dissolved in protamine and zinc buffer to prolong the duration of action) with the duration of action between 11-24 hours (e.g., Humulin® I and Insulatard®) (Table 1) (Clipper F et al., 2019, BNF, 2021). Three human insulin products by Sanofi (Insuman® Comb 15 (cartridge), Insuman® Comb 25 (vial) and Insuman® Basal (vial)) were recently discontinued in the UK in May-June 2020 due to non-safety related issues (limited capacity at manufacturing site) (Diabetes, 2020a). The aims of diabetes treatment using insulin therapy are to achieve optimal levels of blood glucose as close to the natural insulin secretion in healthy people

(e.g., people without diabetes) as possible and avoid undesirable side effects such as hypoglycaemia and weight gain which are the most common side effect of insulin therapy (Al-Tabakha, Moawia, 2015, Yu et al., 2018, BNF, 2021). The treatment should also reduce the risk of long-term complications (e.g., micro/macrovascular complications). The treatment requirement for glycaemic control varies from patient to patient therefore the dosage of insulin should correspond to the needs of each patient and be adjusted as necessary based on the blood glucose concentrations regularly tested (BNF, 2021).

Table 1: The list of currently available insulin preparations (injections) in the UK (2021) (BNF, 2021). Isophane human insulin known as Neutral Protamine Hagedorn.

Source of insulin preparation	Name of insulin (Brand name)	Unit available	Administration timing	Onset of action (Time to reach blood stream)	Peak of effect (Time when most effective, t_{max})	Duration of action	Reference(s)
Rapid-acting insulin							
Analogues	Insulin aspart* ¹ (NovoRapid®)	Vial Cartridge Pre-filled pen	Immediately before meals or when necessary shortly after meals	10-20 mins	1-3 hours	3-5 hours	(European Medicines Agency, 2020e)
	Insulin lispro* ² (Humalog®)	Vial Cartridge Pre-filled pen	Shortly before meals or when necessary soon after meals	15 mins	30-70 mins	2-5 hours	(European Medicines Agency, 2020d)
	Insulin glulisine* ² (Apidra®)	Vial Cartridge Pre-filled pen	Immediately (0-15 mins) before meals or when necessary shortly after meals	10-20 mins	1-2 hours	6 hours	(European Medicines Agency, 2020b)
	Insulin aspart* ¹ (Fiasp®)	Vial Cartridge Pre-filled pen	Immediately (up to 2 mins) before meals or when necessary shortly (up to 20 mins) after meals	4-5 mins after administration (5 mins earlier than	1-3 hours	Shorter than NovoRapid®	(European Medicines Agency, 2020)

				NovoRapid®)			
Short-acting insulin / Regular insulin							
Human	Insulin soluble human* ¹ (Actrapid®)	Vial Cartridge Pre-filled pen	Within 30 mins before meals	30 mins	1.5-3.5 hours	7-8 hours	(European Medicines Agency, 2020a)
	Insulin soluble human* ² (Humulin® S)	Vial Cartridge	before meals	30 mins	2-4 hours	6-8 hours	(emc, 2020e)
	Insulin soluble human* ² (Insuman® Rapid)	Cartridge	15-20 mins before meals	30 mins	1-4 hours	7-9 hours	(emc, 2020m)
Porcine	Crystalline insulin porcine & Neutral insulin porcine solution (Hypurin® Porcine Neutral)	Vial Cartridge		30-60 mins	3-4 hours	6-8 hours	(emc, 2020h)
Intermediate-acting insulin							
Human	Isophane human insulin* ² (Humulin® I)	Vial Cartridge Pre-filled pen	Twice daily (before breakfast and before dinner)	2-4 hours	4-8 hours	14-16 hours	(emc, 2020d)
	Isophane human insulin* ¹ (Insulatard®)	Vial Cartridge Pre-filled pen	Evening and/or morning injection	Within 90 mins	4-12 hours	24 hours	(emc, 2020i)
	Isophane human insulin* ² (Insuman® Basal)	Cartridge Pre-filled pen	45-60 mins before meals	60 mins	3-4 hours	11-20 hours	(emc, 2020j)
Porcine	Crystalline insulin porcine & Isophane insulin porcine suspension (Hypurin®)	Vial Cartridge	Within 2 hours	4-6 hours	6-12 hours	18-24 hours	(emc, 2020g)

	Porcine Isophane)						
Long-acting (basal) insulin							
Analogues	Insulin detemir* ¹ (Levemir®)	Cartridge Pre-filled pen	Once or twice daily at lower doses	1-4 hours	3-4 hours	Up to 24 hours depending on dose (once or twice daily)	(emc, 2020o)
	Insulin glargine* ² (Lantus®)	Vial Cartridge Pre-filled pen	Once daily at any time at the same time each day (Individually adjusted)	Vary in different individuals or within the same individual		Up to 24-26 hours	(emc, 2020n)
	Insulin glargine* ² (Abasaglar®)	Cartridge Pre-filled pen	Once daily at any time at the same time each day (Individually adjusted)	Vary in different individuals or within the same individual		Up to 24-26 hours	(emc, 2020a)
	Insulin glargine* ² (Toujeo®)	Pre-filled pen	Once daily at any time of the day preferably at the same time each day (Individually adjusted)			Up to 36 hours	(emc, 2020r)
	Insulin degludec* ¹ (Tresiba®)	Cartridge Pre-filled pen	Once daily at any time of the day preferably at the same time each day (Individually adjusted)		Flat and stable glucose lowering effect between 0-24 hours	Up to 42 hours	(emc, 2020)
Pre-mixed insulin (A mixture of rapid/short-acting insulin and intermediate-acting insulin)							
Analogues	Soluble insulin aspart (30%)* ¹ and protamine crystallised insulin aspart (70%)* ¹ suspension (NovoMix® 30)	Penfill in cartridge Pre-filled pen	Twice daily at breakfast and dinner or once daily at dinner or three times a day at meals	10-20 mins (Rapid onset of action allows administration within 10	1-4 hours	24 hours	(emc, 2020p)

				mins of the meal)			
	A mixture of insulin lispro* ² solution (25%) and insulin lispro* ² protamine suspension (75%) (Humalog® Mix 25™ and Mix 50)	Vial Cartridge Pre-filled pen	Shortly (0-15 mins) before meals	15 mins (Rapid onset of action allows administration within 15 mins of the meal)	30-70 mins	Up to 22 hours (Depending on dose, site of injection, blood supply, temperature and physical activity)	(emc, 2020b)
Human	Biphasic isophane insulin human* ² suspension consisting of dissolved insulin (25%/50%) and crystalline protamine insulin (75%/50%) (Insuman® Comb 25/50)	Cartridge Pre-filled disposable injection (pen)	30-45 mins before meals (Comb 25) / 20-30 mins before meals (Comb 50)	30-60 mins (Comb 25) / 30 mins (Comb 50)	2-4 hours (Comb 25) / 1.5-4 hours (Comb 50)	12-19 hours (Comb 25) / 12-16 hours (Comb 50)	(emc, 2020k) (emc, 2020l)
	Premixed suspension of soluble human insulin (30%) and isophane insulin human* ² (70%) (Humulin® M3/Mixture 3, Humulin® M3 KwikPen/Mixture 3)	Vial Pre-filled pen		Vary in different individuals or within the same individual		Up to 22 hours (Depending on dose, site of injection temperature and physical activity of the patient)	(emc, 2020c)
Porcine	Isophane insulin porcine and crystalline insulin	Vial Cartridge		Within 2 hours	4-12 hours	Up to 24 hours	(emc, 2020f)

	porcine soluble (Hypurin® Porcine 30/70 Mix)						
--	--	--	--	--	--	--	--

*¹ denotes that insulin is produced in *Saccharomyces cerevisiae* by recombinant DNA technology.

*² denotes that insulin is produced in *Escherichia coli* by recombinant DNA technology.

1.1.3. Glucagon-like peptide-1

GLP-1 is an endogenous incretin hormone produced in intestinal L-cells and secreted in two biologically active forms: GLP-1(7-36) amide (predominant secreted form of GLP-1, Figure 2) and GLP-1(7-37) in response to elevated blood glucose levels (e.g., nutrient/food intake) and bind to GLP-1 receptors (GLP-1Rs) present in pancreas (pancreatic β cells) and other tissues (e.g., gastrointestinal tract, brain, heart, and kidney) to exert antidiabetic effects advantageous for people with T2DM (Vahl et al., 2003, Yu et al., 2018, Pinho et al., 2019). When glucose levels are high, GLP-1 stimulates insulin secretion from pancreatic β -cells in a glucose dependent manner and inhibit glucagon secretion from α -cells in the pancreas therefore reduce blood glucose levels (Yu et al., 2018, Hu, Jia, 2019, Pinho et al., 2019, Cowart, 2020). When glucose levels are normal, the effect of insulin secretion is negligible which reduces the risk of hypoglycaemia that frequently results from insulin therapy (Zheng et al., 2011, Yu et al., 2018). GLP-1 also shows other advantageous antidiabetic effects for people with T2DM such as slow gastric emptying, low appetite and reduce energy/food intake therefore promoting weight control (e.g., weight loss) (Ismail, Csóka, 2017, Yu et al., 2018, Hu, Jia, 2019, Pinho et al., 2019). This makes GLP-1 a desirable drug for the treatment of T2DM associated with obesity (Pinho et al., 2019). As described in Section 1.1.2 insulin therapy is associated with side effects such as hypoglycaemia and weight gain (Yu et al., 2018).

The number of people with obesity are increasing in the world with the accelerated rate of obesity prevalence; the estimated global prevalence of obesity has doubled between 1980 and 2017 (Lumb, Thomas, 2020). Obesity is now considered to be a global epidemic disease and increases the risk of developing T2DM (obesity is known to be a risk factor for T2DM), which is associated with the leading causes of obesity related deaths (Holt, Kumar, 2015, Lumb, Thomas, 2020). Obesity is one of the major health care problems in the UK as almost 63% of adults in England are overweight (body mass index (BMI): 25.0-29.9) or obese (BMI: over 30) (Department of Health and Social Care, 2020, Public Health England, 2020). BMI, which is calculated by the subject's weight in kilograms divided by

their height in meters squared, is commonly used to quantify obesity, and define clinical obesity severity (Lumb, Thomas, 2020). The number of people who are obese (BMI >30, aged over 16) in England had almost doubled from 6.9 million in 1997 to 13 million in 2017 and is expected to double within 20 years (Diabetes, 2019). With the increase of overweight and obese people, more people are progressing to T2DM (Holt, Kumar, 2015, Hu, Jia, 2019). Also, it has been found that people who are overweight or obese thus higher BMI are at higher risk of hospitalisation, serious illness and death from coronavirus, COVID-19 (Department of Health and Social Care, 2020). A recent study published by Holman *et al.* (2020) looked at risk factors for COVID-19 related mortality in people with diabetes (both T1DM and T2DM) and found elevated HbA1c levels and obesity (high BMI) increased the risk of death from COVID-19 (Holman et al., 2020). COVID-19 related mortality was significantly higher in people with diabetes having BMI of above 30.0 kg/m² (T1DM) or 35.0 kg/m² (T2DM) when compared with people having BMI of 25.0-29.9 kg/m² (COVID-19 related mortality for T1DM: BMI ≥40 (p<0.0001) >35.0-39.9 (p=0.0028) >30.0-34.9 (p=0.0059) and T2DM: BMI ≥40 >35.0-39.9, P<0.0001) (Holman et al., 2020). Further, the data showed that between 26 February 2020 and 11 May 2020, more people diagnosed with T2DM registered in England died from COVID-19 (0.37%, 10,525 died out of 2,874,020 population diagnosed with T2DM registered in England) than people diagnosed with T1DM registered in England (0.18%, 464 died out of 264,390 population diagnosed with T1DM registered in England) (Holman et al., 2020). Among people with T2DM, they had a higher risk of COVID-19 related death with increasing HbA1c levels (COVID-19 related mortality: HbA1c ≥10.0% (86 mmol/mol) >9.0-9.9% (75-85 mmol/mol) >7.6-8.9% (59-74 mmol/mol) >6.5-7.0% (48-53 mmol/mol), p>0.0001) (Holman et al., 2020). Therefore, people with T2DM would be likely to face COVID-19 related death as the levels of BMI and HbA1c elevate (Holman et al., 2020). These findings show the necessity to manage T2DM (glycaemic control along with healthy lifestyle) and reduce the risk of developing complications.

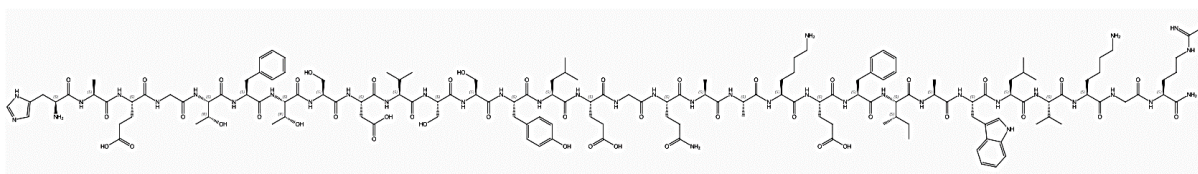


Figure 2: A structure of glucagon-like peptide-1(7-36) amide (C₁₄₉H₂₂₆N₄₀O₄₅, Molecular weight: 3297.7 gmoL⁻¹, Sequence length: 30, CAS registry number: 107444-51-9). Adapted from SciFinderⁿ Substance Results (cas.org).

Though, the endogenous GLP-1 incretin hormone has a very short half-life with less than 2 minutes due to the enzymatic degradation by DPP-4. This results in the rapid deactivation of the GLP-1 thus limiting GLP-1 clinical applications (Ismail, Csóka, 2017, Yu et al., 2018). Therefore, GLP-1RAs that are resistant to DPP-4 enzymatic action, selectively bind to and activate the GLP-1 receptors have been developed as therapeutic peptide products for the treatment of T2DM (Yu et al., 2018, Pinho et al., 2019). Currently, seven approved GLP-1RAs products (one oral and six injection dosage forms) are available as therapeutic peptides in the UK for the treatment of T2DM (GLP-1RAs should not be used in patients with T1DM) (Table 2) (BNF, 2021, BNF, 2021, Diabetes, 2021b). GLP-1RAs in injection dosage forms are self-administered by SC injection. GLP-1RAs are classified into two types based on the duration of the receptor activation: short-acting (first approved GLP-1RA injection and twice daily exenatide injection marketed as Byetta[®] by Astra Zeneca and once daily lixisenatide injection marketed as Lyxumia[®] by Sanofi-Aventis) and long-acting (once daily liraglutide injection marketed as Victoza[®] by Novo Nordisk, once weekly exenatide injection marketed as Bydureon[®] by Astra Zeneca, once weekly dulaglutide injection marketed as Trulicity[®] by Eli Lilly, once weekly semaglutide injection marketed as Ozempic[®] by Novo Nordisk Limited and once daily semaglutide tablet marketed as Rybelsus[®] by Novo Nordisk Limited) (Table 2) (Ismail, Csóka, 2017, Nuffer, Guesnier & Trujillo, 2018, Yu et al., 2018, Brayden et al., 2020, BNF, 2021, BNF, 2021). Rybelsus[®] (oral semaglutide tablets 3mg/7mg/14mg) is the first approved and orally available GLP-1RA product in the UK for the treatment of T2DM (Section 1.1.1)(BNF, 2021) and is not recommended as first line treatment for T2DM treatment (Novo Nordisk, 2021). In addition, a combination of insulin and GLP-1RA formulated together in a single injection are available to treat T2DM for SC use in the UK: insulin degludec and liraglutide combination marketed as once daily Xultophy[®] by Novo Nordisk and insulin glargine and lixisenatide combination marketed as once daily Suliqua[®] by Sanofi (Table 2) (BNF, 2021). Insulin and GLP-1RA both regulate blood glucose levels. Insulin controls blood glucose levels on fasting whereas GLP-1RA controls blood glucose levels on postprandial by stimulating the β cells in pancreas to promote insulin secretion (Yu et al., 2018). These combination therapies (insulin and GLP-1RA) have shown to provide better glycaemic control (achieve lower reduction in HbA1c) with weight control (weight loss, lower risk of weight gain) and reduced risk of hypoglycaemia when compared to insulin therapy alone (Nuffer, Guesnier & Trujillo, 2018, Yu et al., 2018). Therefore, such combination therapy might be preferable or advantageous for some patients and this can lead to improved adherence to treatment (McCarty, Olenik & McCarty, 2019, Nuffer, Guesnier & Trujillo, 2018).

Table 2: Current available GLP-1 receptor agonists (GLP-1RAs) and insulin and GLP-1RA combination products in the UK for subcutaneous use or oral administration for the treatment of Type 2 diabetes mellitus (T2DM) (BNF, 2021). t_{max} : Time reached for maximum plasma concentration. T1DM: Type 1 diabetes mellitus.

Active ingredient (Type of GLP-1RA)	Product name / Marketing authorisation holder (Date of first authorisation)	Pharmaceutical form / Administration	Pharmacodynamics	Pharmacokinetics	Reference (s)
Exenatide (Short-acting, Immediate release)	Byetta® (synthetic form of exendin-4, 39-amino acid peptide incretin isolated from Glyla monster saliva) / AstraZeneca (20 November 2006)	Solution for injection / Twice daily (Administered at any time within 60 mins before morning and evening meal, not administered after a meal)	- Improve glycaemic control (through immediate and sustained effects of lowering both postprandial and fasting blood glucose concentrations) - Suppress glucagon secretion - Slow gastric empty - Reduce body weight	t_{max} : 2 hours Half-life: 2.4 hours (Pharmacokinetics characteristics of exenatide are independent of the dose)	- (Yu et al., 2018) - (Pinho et al., 2019) - (European Medicines Agency, 2021b)
Lixisenatide (Short-acting)	Lyxumia® (exendin-4 structure based and 50% amino acid sequence homology to human GLP-1 / Sanofi-aventis (1 February 2013)	Solution for injection / Once daily	- Improve glycaemic control (through immediate and sustained effects of lowering both postprandial and fasting blood glucose concentrations) - Suppress glucagon secretion - Slow gastric emptying - Reduce body weight	t_{max} : 1-3.5 hours Half-life: 3 hours	- (Nuffer, Guesnier & Trujillo, 2018) - (Pinho et al., 2019) - (European Medicines Agency, 2021c)
Liraglutide*¹ (Long-acting)	Victoza® (97% sequence homology to human GLP-1 that binds to and activates the GLP-1 receptor) / Novo Nordisk (30 June 2009)	Solution for injection / Once daily at any time preferably around the same time of the day (independent of meals)	- Improve glycaemic control by lowering postprandial and fasting blood glucose concentrations - Slow gastric emptying - Reduce body weight and body fat mass	t_{max} : 8-12 hours Half-life: 13 hours Absolute bioavailability: approximately 55%	- (European Medicines Agency, 2021f)

			<ul style="list-style-type: none"> - Reduce hunger - Lower energy intake 		
Exenatide (Long-acting, Prolonged release)	Bydureon® (Exenatide encapsulated in poly (D,L-lactide co-glycolide) polymer microsphere formulations for extended release) / AstraZeneca (17 June 2011)	Powder and solvent for prolonged-release suspension for injection / Once weekly on the same day each week	<ul style="list-style-type: none"> - Improve glycaemic control by lowering postprandial and fasting blood glucose concentrations - Suppress glucagon secretion - Slow gastric emptying - Reduce body weight 	Mean clearance of exenatide: 9L/hr (Pharmacokinetics characteristics of exenatide are independent of the dose)	<ul style="list-style-type: none"> - (Yu et al., 2018) - (European Medicines Agency, 2021a)
Dulaglutide (Long-acting)	Trulicity® (90% homologous to native human GLP-1(7-37)) / Eli Lilly (21 November 2014)	Solution for injection / Once weekly at any time of day with or without meals	<ul style="list-style-type: none"> - Improve glycaemic control by lowering fasting, pre-meal, and postprandial glucose concentrations - Suppress glucagon secretion - Slow gastric empty - Reduce body weight 	t _{max} : 48 hours Half-life: 4.7-5 days	- (European Medicines Agency, 2021e)
Semaglutide*¹ (Long-acting)	Ozempic® (94% sequence homology to human GLP-1 that binds to and activates the GLP-1 receptor) / Novo Nordisk (8 February 2018)	Solution for injection / Once weekly at any time of the day with or without meals	<ul style="list-style-type: none"> - Reduce blood glucose level in a glucose dependent manner by stimulating insulin secretion and lowering glucagon secretion - Delay gastric emptying - Reduce body weight and body fat mass - Reduce appetite - Lower energy intake 	t _{max} : 1-3 days Half-life: 1 week	- (European Medicines Agency, 2021d)
Semaglutide*¹ (Long-acting)	Rybelsus® (94% sequence homology to human GLP-1 that binds to and activates the GLP-1	Tablet / Once daily taken on an empty stomach at any time of the day at least 30 mins before eating or drinking	<ul style="list-style-type: none"> - Reduce blood glucose in a glucose dependent manner - Delay gastric emptying - Reduce body weight and body fat mass 	t _{max} : 1 hour Half-life: 1 week Absolute oral bioavailability: 0.4-1% (variable absorption)	<ul style="list-style-type: none"> - (emc, 2020) - (BNF, 2021) - (Brayden et al., 2020)

	receptor) / Novo Nordisk (3 April 2020)		- Reduce appetite - Lower energy intake	between subjects)	
Insulin degludec*¹ (basal insulin) and Liraglutide*¹ (Insulin and GLP-1RA combination product) (Long-acting)	Xultophy® / Novo Nordisk (18 September 2014)	Solution for injection / Once daily at any time of the day with or without meals preferably at the same time of the day	- Similar pharmacodynamics profiles compared with its individual, insulin degludec and liraglutide <u>Insulin degludec:</u> - Lower glucose levels by facilitating glucose uptake and inhibiting glucose output from the liver <u>Liraglutide:</u> - Improve glycaemic control by lowering fasting plasma glucose levels and postprandial glucose levels after all meals - Delay gastric emptying - Reduce body weight and body fat mass	- Similar pharmacokinetics profiles compared with its individual, insulin degludec and liraglutide Half-life: 25 hours for insulin degludec and 13 hours for liraglutide	- (European Medicines Agency, 2020g)
Insulin glargine*² (basal insulin) and Lixisenatide (Insulin and GLP-1RA combination product) (Long-acting)	Suliqua® / Sanofi- aventis (11 January 2017)	Solution for injection / Once daily within 1 hour before a meal	<u>Insulin glargine:</u> - Target fasting plasma glucose - Lower blood glucose by stimulating glucose uptake and inhibiting hepatic glucose production <u>Lixisenatide:</u> - Target postprandial glucose - Stimulate insulin secretion from beta cells in the pancreas when blood glucose is increased - Suppress glucagon secretion	t _{max} in patients with T1DM: 2.5-3.0 hours for lixisenatide Half-life: 3 hours for lixisenatide	- (European Medicines Agency, 2020f)

			- Slow gastric emptying		
--	--	--	-------------------------	--	--

*1 denotes that GLP-1 analogue is produced in *Saccharomyces cerevisiae* by recombinant DNA technology.

*2 denotes that insulin or GLP-1 analogue is produced in *Escherichia coli* by recombinant DNA technology.

1.1.4. Routes of insulin and GLP-1 delivery

Antidiabetic peptide and protein drugs such as insulin (protein) and GLP-1 (peptide, less than 50 amino acids) are generally administered via SC route as oral delivery of peptides and proteins are limited by acidic/low pH environment and rapid enzymatic degradation in the gastrointestinal (GI) tract, elimination in the liver (first pass metabolism), low permeability across the intestinal epithelium cells for large molecular weight of biologics (peptide/protein drugs, macromolecules) and low oral bioavailability (Ismail, Csóka, 2017, Hu, Jia, 2019, Brayden et al., 2020). However, SC administration of drugs interferes with the patients' lifestyle due to inconvenience and discomfort associated with injections. Diabetes is a chronic disease and insulin therapy is a complex regimen that requires multiple daily insulin injections (e.g., short or rapid-acting insulin for the management of mealtime blood glucose levels and long-acting insulin for daily insulin needs therefore two to three times per day to control hyperglycaemia, Table 1) and is associated with undesirable side effects (e.g., hypoglycaemia and weight gain, Section 1.1.2) (Holt, Kumar, 2015, Clipper F et al., 2019, Hu, Jia, 2019, Lin et al., 2019). All these affect patient compliance and adherence to antidiabetic therapy (Farsaei et al., 2014, Heinemann, Parkin, 2018, Lin et al., 2019). According to a cross-sectional study conducted by Farsaei *et al.* (2014) to assess the barriers to insulin injection in patients with both T1DM (n=251) and T2DM (n=257), factors influencing patient adherence to insulin injection therapy were mainly related to the injection itself (Farsaei et al., 2014). These included time consuming (T1DM: 92.8%, T2DM: 87.5%), syringe based regimen (T1DM: 90.8%, T2DM: 91.1% versus (vs.) pen based regimen: T1DM: 9.2%, T2DM: 8.9%), difficulty of injection (T1DM: 90.8%, T2DM: 84.0%), injection site pain (T1DM: 70.1%, T2DM: 73.4%), the number of daily injection (e.g., ≥ 2 injections, T1DM: 59.4%, T2DM: 70.4%), and lack instructions for injection (T1DM: 60.6%, T2DM: 59.9%). In addition, adverse event related factors such as fear of hypoglycaemia (T1DM: 78.9%, T2DM: 87.2%) (Farsaei et al., 2014).

Poor patient compliance and adherence to antidiabetic therapy can result in poor glycaemic control leading to low quality of life, increased risk of long-term complications and mortality (Heinemann,

Parkin, 2018, Guerci et al., 2019, Hu, Jia, 2019, Lin et al., 2019). Further, many people with T2DM are reluctant to start insulin therapy due to inconvenience (e.g., multiple daily insulin injections to control hyperglycaemia, restrictions on daily life) and concerns about adverse events (e.g., hypoglycaemia and weight gain) (Santos Cavaiola, Edelman, 2014, Kim, E., Plosker, 2015). Healthcare professionals are also concerned about the safety and ability of patients to comply with insulin injection therapy and reluctant to start insulin therapy in their patients with T2DM (Escalada et al., 2016). Delaying the therapy initiation by healthcare providers (HCPs) also lead to glycaemic control failure and a risk of complications (Escalada et al., 2016). Escalada *et al.* (2016) conducted a survey targeted at HCPs (e.g., general practitioners (GPs) n=112, endocrinologists n=80) and looked at how they initiated insulin therapy in their patients with T2DM and identified the reasons for the delay of insulin therapy initiation (Escalada et al., 2016). The results showed that HCPs waited 3-6 months to start insulin therapy (GPs: 46.4%, endocrinologists: 31.3%) and confirmed HbA1c levels twice (GPs: 71.4%, endocrinologists: 58.8%) before starting insulin therapy (Escalada et al., 2016). HCPs are concerned that the risk of hypoglycaemia associated with insulin therapy (89.5%) and patients' fear of needles (64.1%) are barriers to start insulin therapy although GPs and endocrinologists considered insulin as effective therapy (GPs: 47.3%, endocrinologists: 66.3%) and basal insulin therapy was not difficult (GPs: 72.3%, endocrinologists: 91.2%) (Escalada et al., 2016). They were also concerned about patients' social life (GPs: 34%, endocrinologists: 30.1%) and time-consuming consultations for insulin therapy (GPs: 39.2%, endocrinologists: 45.1%) as barriers to start insulin therefore causing a delay in insulin therapy (Escalada et al., 2016). To reduce the burden of injectable medications for patients and healthcare providers' perspectives and therefore improve patient compliance and adherence to therapy of diabetes, alternative routes of drug administration to injection, non-invasive drug delivery systems (i.e., non-injection routes of drug delivery) such as oral, nasal, buccal and pulmonary routes, have been investigated for delivery of peptide and protein drugs (Santos Cavaiola, Edelman, 2014, Ismail, Csóka, 2017).

1.1.4.1. Oral route

Oral route is generally the most common and preferable route for drug administration as it is convenient; however, bioavailability is low for oral delivery of peptides and proteins (Ismail, Csóka, 2017, Hu, Jia, 2019). Although many research efforts have been made in the development of oral insulin delivery systems none have made it to the market yet (Ismail, Csóka, 2017, Hu, Jia, 2019). On the other hand, oral GLP-1RA has become available now. Rybelsus® which is the first orally available GLP-1RA (semaglutide) in the UK for the treatment of T2DM (BNF, 2021) is formulated with an absorption enhancer (sodium N-[8-(2-hydroxybenzoyl)amino] caprylate, or salcaprozate sodium, C8

derivative) to promote absorption through the intestinal epithelium and improve bioavailability (Brayden et al., 2020). Ten Phase 3 clinical trials called the PIONEER (Peptide InnOVation for Early diabEtes tReatment) programs sponsored by Novo Nordisk (semaglutide's manufacture) were conducted to assess the efficacy and safety of oral semaglutide (Rybelsus®) in patients with T2DM (Brayden et al., 2020, Cowart, 2020). In PIONEER 4, the efficacy of oral semaglutide was compared to injectable liraglutide GLP-1RA or placebo in patients with T2DM on metformin with SGLT-2 inhibitor or metformin alone (Novo Nordisk, 2020). Oral semaglutide and SC liraglutide both exhibited similar HbA1c reductions (HbA1c reduction: -1.2% to -1.1%) and oral semaglutide was superior to placebo (HbA1c reduction: -1.2% to -0.1%, $p < 0.0001$ for superiority). Oral semaglutide demonstrated greater reduction in body weight compared to both SC liraglutide (oral semaglutide vs. SC liraglutide: -4.4 kg to -3.2 kg, $p = 0.0003$ for superiority) and placebo (oral semaglutide vs. placebo: -4.4 kg to -0.6 kg $p < 0.0001$ for superiority) (Anderson, Beutel & Trujillo, 2020, Novo Nordisk, 2020, Powell, Piszczatoski & Taylor, 2020). Oral semaglutide offers a comparable alternative to GLP-1RAs injections and an attractive option for patients with T2DM who would like to avoid injections (Anderson, Beutel & Trujillo, 2020). However, oral semaglutide exhibited 0.4-1% absolute oral bioavailability with high variability in absorption between patients (emc, 2020, Anderson, Beutel & Trujillo, 2020, Brayden et al., 2020, Powell, Piszczatoski & Taylor, 2020). This indicates that 99% of semaglutide was lost before entering the systemic circulation (Anderson, Beutel & Trujillo, 2020, Brayden et al., 2020, Powell, Piszczatoski & Taylor, 2020). This resulted in a higher dose requirement for the oral formulation compared to injectable semaglutide (Anderson, Beutel & Trujillo, 2020). Oral semaglutide 14 mg once daily is comparable to SC semaglutide 0.5 mg once weekly due to the high pharmacokinetics variability of oral semaglutide (BNF, 2021). In switching from SC semaglutide 0.5 mg weekly to oral semaglutide, patient should start on semaglutide 7 mg or 14 mg (Anderson, Beutel & Trujillo, 2020).

1.1.4.2. Nasal route

The nasal drug delivery system (drug delivery via intranasal route/the nasal mucosa) is an attractive option for non-invasive route of drug delivery as it is easily accessible, has a large surface area (150 cm²) for absorption and low first pass hepatic metabolism (Leary et al., 2008, Lin et al., 2019). However, it is associated with limitations: variability in absorption and poor bioavailability as physical conditions of nasal passages and the nasal cycle vary therefore influence the absorption. The nasal mucosa is the barrier to drug absorption (Leary et al., 2008, Lin et al., 2019). Nasulin™ (Bentley Pharmaceuticals Inc., United States (US)), which consisted of regular human recombinant insulin dissolved in sterile water and main excipient (absorption enhancer) of cyclopentadecalactone (CPE-215) from plants (*Angelica archangelica*), was a nasal spray formulation designed for intranasal

administration of insulin (Leary et al., 2008). According to pharmacokinetics and pharmacodynamics studies for Nasulin™ in healthy male volunteers (age: 22.7 years \pm 2.8 years, BMI: 25.49 \pm 1.79) in a fasted state (25 international units (IU) insulin dose administered/sprayed), the intranasal formulation showed pharmacodynamics effects (decrease in plasma glucose levels) and demonstrated a rapid absorption (t_{max} : 15 mins) compared to SC regular insulin (Humulin® S, 4 IU insulin dose administered) that showed slower absorption (t_{max} : 70 mins) (Leary et al., 2008). Bioavailability of Nasulin™ was 10-20% relative to SC insulin (Leary et al., 2008). Nevertheless, phase 2 clinical trial for Nasulin™ (NCT00850161, intranasal insulin and its effect on postprandial metabolism in comparison to SC insulin aspart) was withdrawn for business related purposes (CPEX Pharmaceuticals Inc., 2016). Furthermore, human nasal cavity can hold only limited fluid volume (e.g., 200 μ L per nostril) therefore the amount of formulation delivered via intranasal route is limited as single intranasal administration (not suitable for high drug dose formulations) (Lin et al., 2019).

1.1.4.3. Buccal route

The buccal drug delivery system (drug delivery via the buccal mucosa) has advantages such as easy administration, large surface area (100-200 cm²) for absorption and avoidance of first pass metabolism (Heinemann, Jacques, 2009). However, the buccal delivery system is associated with poor penetration of drugs and great variability in drug permeability due to variable saliva secretion and flow and different thickness of oral mucosa area (e.g., thin sublingual area, thick cheek mucosa) resulting in variable absorption (Heinemann, Jacques, 2009). Oral-Lyn™ developed by Generex Biotechnology Corporation, Canada for prandial insulin therapy (T1DM and T2DM), which is not available in the UK, is a liquid insulin formulation for buccal delivery of insulin (Heinemann, Jacques, 2009). The formulation consists of human regular insulin (400 U of insulin in 28 mL) and using a propellant spray device similar to an asthma inhaler device to deliver insulin into the mouth (Heinemann, Jacques, 2009). Oral-Lyn™ exhibited rapid absorption (t_{max} : 23 mins) compared to SC regular human insulin (t_{max} : 83 mins) in healthy subjects however the relative bioavailability was about 2.6% (Heinemann, Jacques, 2009). Oral-Lyn™ claimed to deliver 10 U of insulin each puff with 10% absorption rate. This indicates that 1 U of insulin was delivered to blood circulation per one puff of 10 U insulin contained therefore require 10 puffs to meet the dose requirement (Heinemann, Jacques, 2009). This suggests that buccal delivery requires multiple applications which can be considered as time consuming for patients or require high drug dose loading in the formulations to achieve therapeutic effects. Over 95% of insulin would be swallowed by the patients and the drug is degraded in the stomach (Heinemann, Jacques, 2009). This might also affect the cost of manufacturing (Heinemann, Jacques, 2009). For example, NovoRapid® contains 1000 units per vial

(10 mL), therefore, 1 mL solution contains 100 units insulin aspart equivalent to 3.5 mg (European Medicines Agency, 2020). Insulin requirements in adults are usually between 0.5 and 1.0 unit per kg per day (European Medicines Agency, 2020). Insulin daily dose would be up to 100 units (3.5 mg) if patients weigh 100 kg.

1.1.4.4. Pulmonary route

So far, two inhaled insulin products, Exubera® (Pfizer Limited) and Afrezza® (Mannkind Corporation) have reached the market. Exubera® was the first inhaled insulin dry powder product approved by the U.S. Food and Drug Administration (FDA) and the European Medicines Agency (EMA) in 2006; it was licensed for the therapeutic indications of T1DM and T2DM (Al-Tabakha, 2015). However, it was withdrawn from the market only one year after the FDA approval due to unexpected low product sales attributed to several factors such as design of the inhaler device, poor acceptability from patients and physicians, safety concern (Al-Tabakha, 2015). Exubera® was composed of recombinant human insulin (rDNA origin with *Escherichia coli*) and exhibited rapid absorption (onset time: 10-20 mins, t_{max} : 38-78 mins) comparable to SC rapid-acting insulin analogue (e.g., insulin lispro, onset time: 15-30 mins, t_{max} : 30-90 mins) and faster than regular human insulin (onset time: 30 mins, t_{max} : 48-120 mins) in patients with T1DM and T2DM (Al-Tabakha, 2015). Exubera® was also effective in glycaemic control in patients with diabetes. Exubera® demonstrated comparable HbA1c reductions to insulin lispro in patients with T2DM (HbA1c reduction, Exubera®: -1.4% and insulin lispro: -1.6%) (Al-Tabakha, 2015). The relative bioavailability (Exubera® vs. regular human insulin) was between 8 and 11% (Al-Tabakha, 2015). Currently, Afrezza® approved by FDA in 2014 is available in the US as a rapid-acting inhaled insulin product for the therapeutic indications of T1DM and T2DM and intended to cover the mealtime insulin requirements (Sang M. Chung, Manoj Khurana, 2013, Al-Tabakha, 2015). Afrezza® is composed of recombinant human insulin (rDNA origin) and fumaryl diketopiperazine (FDKP) as an inert excipient (Technosphere™ drug carrier system) and demonstrated a fast onset of action comparable to SC insulin lispro (rapid-acting insulin analogue) and faster absorption (t_{max} : 12-15 mins) than SC insulin lispro (onset time: 15-30 mins, t_{max} : 30-90 mins) in T1DM patients (Sang M. Chung, Manoj Khurana, 2013, Al-Tabakha, 2015, Kim, Plosker, 2015). Afrezza® demonstrated significantly greater HbA1c reductions when compared with inhaled placebo in T2DM patients (HbA1c reduction, Afrezza®: -0.82% and placebo: -0.42%, $p < 0.0001$) (Al-Tabakha, 2015, Kim, Plosker, 2015). Significantly higher percentage of T2DM patients who received Afrezza® achieved HbA1c goals of $\leq 6.5\%$ (Afrezza®: 15.9% vs. placebo: 4.2%, $p < 0.01$) and $\leq 7\%$ (Afrezza®: 37.7% vs. placebo: 19.0%, $p = 0.0005$) than patients received inhaled placebo (Al-Tabakha, 2015, Kim, Plosker, 2015). The bioavailability was about 33% relative to SC insulin lispro (Sang M.

Chung, Manoj Khurana, 2013) or 21%-30% relative to SC regular insulin (Al-Tabakha, 2015). In addition to insulin, Qian *et al.* (2009) conducted a pharmacokinetics study of inhaled GLP-1RA powder (BMS-686117, molecular weight (MW): 1528.7 g mol⁻¹) in Male Sprague-Dawley rats and it demonstrated a faster absorption (t_{max} : 0.3-0.7 hr, dose: 1 mg kg⁻¹) when administered intratracheally to the lung in rats compared with SC administration of BMS-686117 (t_{max} : 1.2 hr, dose: 0.08 mg kg⁻¹) (Qian et al., 2009). Also, inhaled BMS-686117 exhibited 45% bioavailability relative to SC administration of BMS-686117 indicating the feasibility of pulmonary delivery of the GLP-1RA (Qian et al., 2009).

All these findings show that the lungs can provide rapid absorption comparable to SC injection and higher bioavailability than other non-invasive routes of delivery (oral, nasal, and buccal routes). In addition, pulmonary drug delivery avoids the hepatic first pass metabolism that oral delivery experiences (Nokhodchi, Martin, 2015, Lin et al., 2019). The lungs are known to be permeable to peptides and proteins (i.e., insulin)(Patton, Byron, 2007). The lung epithelium has shown to be permeable to both lipophilic drugs (absorbed across the pulmonary epithelium via transcellular pathway) and hydrophilic drugs (absorbed via paracellular pathways between epithelial cells in the lung) (Patton, Byron, 2007, Nokhodchi, Martin, 2015, Lin et al., 2019). Insulin, classified as hydrophilic drug (MW: 5808 Da, 5.8 kDa) has been reported to be permeable to the alveolar epithelium membrane and absorbed through paracellular pathway in the lungs (Patton, Byron, 2007, Nokhodchi, Martin, 2015).

In summary, non-invasive alternative routes such as oral, nasal and buccal routes have shown drug penetration issues (poor permeability for macromolecules) and poor bioavailability that require absorption enhancers in the formulations, in turn raise safety issues or require high drug loading whereas the lung epithelium is naturally permeable to peptide and protein drugs and pulmonary route has shown feasible for peptide and protein drugs delivery with higher bioavailability in comparison to other non-invasive routes (bioavailability: pulmonary route 10-45% vs. oral, nasal and buccal routes 0.4-20%). This suggests that pulmonary drug delivery offer advantages in the treatment of diabetes over oral or other non-invasive or parenteral administration.

1.2. Instability of peptides and proteins

The development of peptide and protein based formulations (biopharmaceuticals) in a solid state is a challenge as peptides and proteins are generally not stable for long. Characteristics of formulations/products can change over time and easily degrade when exposed to stresses (e.g., heat, high/cold temperature, moisture, extreme pH) during manufacturing process and storage therefore affecting storage stability, shelf life, safety and efficacy (Banga, 2015, Mensink et al., 2017, Emami, Vatanara, Park et al., 2018). In general, shelf life at room temperature for 1.5-2 years is ideal (Banga, 2015). Liquid-based formulations require cold chain storage conditions (e.g., refrigerated storage) that might increase the cost of maintenance and are inconvenient (Mensink et al., 2017).

Proteins are polypeptide chains consisting of different amino acids linked together through peptide bonds and have four different levels of protein structure (primary, secondary, tertiary and quaternary) and usually in a three-dimensional structure (globular proteins) (Elliott, Elliott, 2001). When polypeptide chains are arranged and folded, they are referred to as native proteins (folded form of polypeptide chains) and hydrophilic as hydrophilic (polar) groups are outside and in contact with water while hydrophobic groups are folded inside/buried within the protein, out of contact with water (Elliott, Elliott, 2001, Mensink et al., 2017). The native protein is held together by weak noncovalent bonds such as ionic bonds, hydrogen bonds and van der Waals forces/attractions (Elliott, Elliott, 2001). Ionic bonds occur due to electrostatic attraction between two charged groups that are close to each other (e.g., -COO^- and -NH_3^+). Hydrogen bonds are due to electrostatic attractions between atoms of polar molecules (weak positive and negative charge separation). Van der Waals forces/attraction are a group of weak interactions between closely positioned atoms (between nonpolar molecules that cannot form ionic bonds or hydrogen bonds) and occur between any two atoms, which must be positioned close together (Elliott, Elliott, 2001).

Peptides and proteins undergo degradation that can result in a change or loss of biological activity and the main mechanism of protein degradation can be either physical degradation (changes in noncovalent interaction, changes in secondary, tertiary, or quaternary structure of proteins) or chemical degradation (changes in covalent bonds). Physical degradation includes denaturation, aggregation, precipitation, or adsorption to surfaces whereas chemical degradation include oxidation, hydrolysis, deamidation (producing new carboxylic acid group), and Maillard Browning reaction (Depreter, Pilcer & Amighi, 2013, Banga, 2015, Mensink et al., 2017). The most common physical degradation is denaturation which is the process of unfolding the three-dimensional protein structure within the native protein conformation, the structure conversion from native proteins (soluble, folded form of the polypeptide chain) to the unfolded form of proteins where the polypeptide chain is randomly arranged (insoluble, folded form of the polypeptide chain is

destroyed) and hydrophobic groups of proteins are exposed on the outside of the protein structure (Elliott, Elliott, 2001, Mensink et al., 2017). Denaturation may be reversible or irreversible and is a partial or total disruption of secondary, tertiary, and quaternary structure of proteins usually caused by thermal stress (heat) and extreme pH (Depreter, Pilcer & Amighi, 2013, Banga, 2015). Protein denaturation is more likely to occur when proteins are in the liquid state (exposing hydrophobic parts to water) rather than in the solid state (Mensink et al., 2017). For a stable protein in a globular shape in an aqueous state, hydrophilic groups must be on the outside and in contact with water (Elliott, Elliott, 2001). Therefore, peptide and protein drugs in solid dosage forms are more stable than liquid-based formulations (Emami et al., 2018, Ziaee et al., 2019). When unfolding (denaturation) the polypeptide chain within the native protein conformation, the hydrophobic groups of the protein are exposed on the outside of the protein structure, free to interact with surfaces therefore increasing surface interaction that leads to adsorption and aggregations (Banga, 2015, Mensink et al., 2017). Protein aggregations can result in the increase of molecular weight of proteins and the formation of higher molecular weight proteins (HMWP), such as dimers, or higher forms and some aggregated proteins can lose biological activity or influence immunogenicity (Banga, 2015). Insulin in solution may exist as a mixture of monomer, dimer, hexamer, or higher states depending on many factors such as concentration (monomer at low concentration: $0.6 \mu\text{g mL}^{-1}$, dimer at higher concentration), pH, and temperature (Banga, 2015).

Chemical degradations are usually induced by the presence of moisture content or exposed to atmospheric air and temperature variations during storage and covalent aggregation is the predominant degradation mechanism in the solid state (Mensink et al., 2017). Covalent aggregations occur through intermolecular thiol disulfide exchange in proteins that contain cysteine residues and disulfide bonds to form a new intermolecular disulfide bond and frequently associated with loss of activity (Depreter, Pilcer & Amighi, 2013). Oxidation is also a major protein degradation mechanism and involve the formation of disulfide bridges via oxidation of amino acids such as cysteine to change the conformation of proteins during long-term storage (Depreter, Pilcer & Amighi, 2013, Banga, 2015). This results in protein aggregation and affects immunogenicity due to the change of protein conformation (Banga, 2015). Hydrolysis of peptide bonds in proteins are usually induced by extreme pH (e.g., acid) and cause the breakdown of the peptide bond into individual amino acids or peptides (e.g., peptide bonds at aspartate (Asp)-proline (Pro) or threonine (Thr)-serine (Ser) for insulin crystalline suspension are usually susceptible to hydrolysis) and result in degradation (Banga, 2015). Deamidation is a common chemical degradation that involves a hydrolysis reaction and occurs at the side chain amide on asparagine (Asn) or glutamine (Gln) residues to produce free

carboxylic acids (Depreter, Pilcer & Amighi, 2013, Banga, 2015). These resultant acids might have a significant impact on protein structure and bioactivity (Depreter, Pilcer & Amighi, 2013, Banga, 2015). In addition, proteins tend to react with reducing sugars (e.g., lactose and glucose) via Maillard reaction between aldehyde or ketone groups in reducing sugars and amino groups (e.g., lysine, arginine, asparagine or glutamine side chain in proteins) at high temperatures resulting in chemical degradation (Depreter, Pilcer & Amighi, 2013). Sugars (e.g., non-reducing sugars) are frequently used to stabilise proteins (Depreter, Pilcer & Amighi, 2013).

1.2.1. Glass transition temperature

Chemical degradation (e.g., covalent aggregation, deamidation and oxidation) is usually accelerated as a function of time and/or storage conditions associated with humidity because water acts as a plasticiser and reduces the glass transition temperature (T_g) therefore affecting chemical stability in amorphous solids (Weers, Miller, 2015, Mensink et al., 2017, Ziaee et al., 2019). T_g is defined as the temperature at which a transition from a disordered glassy state associated with low molecule mobility to a rubbery state where molecule mobility increases and crystallisation occurs in amorphous materials (Weers, Miller, 2015, Mensink et al., 2017, Ziaee et al., 2019). T_g is used to characterise amorphous materials (e.g., proteins) and provide an indication for changes in molecular mobility which can lead to undesirable physical and chemical changes (Weers, Miller, 2015, Mensink et al., 2017, Ziaee et al., 2019). Molecule mobility is generally high at temperature above T_g where molecules can aggregate also crystallisation occurs (Banga, 2015, Weers, Miller, 2015). Molecular mobility increases with decreasing T_g and crystallisation occurs when the storage temperature is higher than T_g (Weers, Miller, 2015, Mensink et al., 2017, Ziaee et al., 2019). The presence of moisture content (water content) in dry powders affects protein stability in the dry state and can undergo aggregation as water reduces T_g and molecular mobility increases (Ziaee et al., 2019). This influences physical stability and also can affect bioavailability (Banga, 2015, Weers, Miller, 2015, Mensink et al., 2017). Molecule mobility is limited and low tendency to crystallisation when protein molecules are in a glass state (Weers, Miller, 2015). Therefore, formulations with high T_g , above the storage condition are ideal to avoid an increase in molecule mobility (molecule mobility is low in glassy state, below T_g) and crystallisation (low tendency to crystallise below T_g) therefore enhancing storage stability (Weers, Miller, 2015, Mensink et al., 2017, Ziaee et al., 2019).

Differential scanning calorimetry (DSC), which is the most widely used technique for thermal analysis in the pharmaceutical field (Craig, Reading, 2006), monitors the changes of phase transition as a

function of temperature or time and determines the temperature and energy/heat flow associated with thermal events such as T_g , crystallisation, melting point, and decomposition reactions (Craig, Reading, 2006). DSC provides advantages such as simple measurement, the use of small sample sizes (~ 10 mg), and wide temperature ranges available (e.g., -120°C to 600°C) (Craig, Reading, 2006). In the DSC experiment, a sample of interest in a sample crucible (pan) and a reference pan, which is usually empty, are placed symmetrically within a temperature-controlled furnace (within the same furnace) heated at a controlled rate (e.g., 5°C min^{-1} to $40^\circ\text{C min}^{-1}$) to provide identical heat paths from the furnace to the sample and reference (Craig, Reading, 2006). Both pans are subjected to the same temperature profile; the only difference between them is the presence of the sample in one of the crucibles that allow direct comparisons between the sample and reference (Craig, Reading, 2006). DSC measures the temperature difference between the sample and reference as a result of the thermal event therefore the difference in heat flow released or absorbed by the sample relative to the reference as a function of temperature (Craig, Reading, 2006, Pansare, Patel, 2016). Another technique, X-ray diffraction, is also frequently used to assess crystallinity and identify amorphous and crystalline phases present in a material (Shetty et al., 2020). Moisture content is usually determined using Thermogravimetric analysis (TGA) which is simple to use and more convenient and accurate to perform than other alternative laboratory methods such as Karl Fischer analysis (Craig, Reading, 2006). TGA measures mass changes (water content, weight loss determination) upon heating as a function of temperature or time and is usually performed along with DSC analysis (Craig, Reading, 2006).

1.2.2. Insulin degradation

Insulin is a well characterised substance and insulin degradation studies (measurement of degradation products) performed by a few authors are available in literatures (Strickley, Anderson, 1997, Oliva, Fariña & Llabrés, 2000, Sadrzadeh et al., 2010). Thermal stress is a major stress for proteins and the degradation rates for the formation of degradation products increase with temperature (Sadrzadeh et al., 2010, Mensink et al., 2017). Sadrzadeh *et al.* (2010) studied the effect of temperature on stability of Exubera[®] which was amorphous (Sadrzadeh et al., 2010). Exubera[®] insulin powders were exposed to the extreme temperature range of 60°C to 120°C (non-normal conditions) for up to 72 hours to obtain insulin degradation products and the stability of insulin powders at high temperatures (60 - 120°C) over time (up to 72 hours) was evaluated (Sadrzadeh et al., 2010). Sadrzadeh *et al.* (2010) identified two major thermally induced degradants in insulin powders of Exubera[®]: A21 desamido insulin (A21) and HMWP (Sadrzadeh et al., 2010). A21 was

produced via intramolecular hydrolysis of amino acid side chains (e.g., hydrolysis of asparagine terminal carboxyl group at position 21 of insulin A chain to form aspartic acid) (Strickley, Anderson, 1997, Sadrzadeh et al., 2010). The formation of HMWP was the result of intermolecular reaction between insulin and neighbouring insulin to form insulin dimers (Strickley, Anderson, 1997, Sadrzadeh et al., 2010). HMWP was the predominant degradation product over A21 in the insulin powders due to the presence of relatively low water content (2.0% w/w) for A21 formation to the higher concentration of neighbouring reactive amino acids (B chain amine groups) for HMWP formation (Sadrzadeh et al., 2010). The content of these insulin degradation products (i.e., A21 and HMWP) are usually determined/quantitated by chromatographic techniques such as high performance liquid chromatography for A21 and size exclusion chromatography (SEC) for HMWP (Banga, 2015). SEC separates proteins based on their molecular size (Ståhl et al., 2002, Banga, 2015).

Chapter 2. Literature review

2.1. Human respiratory system

Understanding the anatomy and physiology of the human respiratory tract is important for pulmonary drug delivery. There are significant anatomical and physiological variations within subjects who have different airway geometry and inhalation profiles (e.g., inspiratory flow rate, lung volume, tidal volume) due to many factors (e.g., subject body size, age, sex, obesity, health conditions, lung disease and pathological conditions) (Nokhodchi, Martin, 2015, Lumb, Thomas, 2020). These variabilities affect pulmonary drug delivery efficiency and drug deposition in the lungs (deposition generally means drug particles are deposited in the respiratory tract after inhalation) resulting in inconsistent drug delivery to the lungs and poor DPI formulation performance therefore therapeutic efficacy (Depreter, Pilcer & Amighi, 2013, Nahar et al., 2013, Ung et al., 2014, Berkenfeld, Lamprecht & McConville, 2015, Nokhodchi, Martin, 2015).

Lung volumes vary with people and there are variations in static lung volumes (the amount of gas in the lung while no airflow) including total lung capacity, tidal volume, residual volume, and functional residual capacity (FRC) (Lumb, Thomas, 2020). Total lung capacity is the volume of air/gas held in the lung after a maximal inhalation/inspiration (Lumb, Thomas, 2020). Tidal volume is the volume of air breathed in into the lung during a normal breath/inhalation and residual volume is the volume of air remaining in the lung after a maximal exhalation (Lumb, Thomas, 2020). FRC is the lung volume at the end of normal expiration (after a normal expiration) (Lumb, Thomas, 2020). The human respiratory tract is anatomically labelled into two regions: upper respiratory tract (outside thorax/chest) and lower respiratory tract (within thorax between the neck and abdomen containing the heart and lungs) (Patwa, Shah, 2015). Upper respiratory tract is responsible for conducting air into the larynx and filtering large-inhaled particles and starts at mouth, nose followed by pharynx (throat) and larynx (produce sound waves). Lower respiratory tract, which is responsible for gas exchange in the lungs, is composed of trachea, bronchi, bronchioles, and alveoli (alveolar ducts (small tubes) and alveolar sacs) (Figure 3) (Nokhodchi, Martin, 2015, Patwa, Shah, 2015, Lumb, Thomas, 2020). The airways (air passages) in the lungs are highly branched and the branching pattern of the human tracheobronchial tree is frequently described using successive generations (generation 0 -> generation 23, numbered by Weibel) of airways in the respiratory tract starting at trachea (generation 0) and terminating in alveolar sacs (generation 23) (Figure 3) (Lumb, Thomas, 2020). Trachea with generation 0 (mean diameter: 18 mm) divides into two main branches of

bronchi (generation 1, mean diameter: 12 mm) leading to individual lungs (Lumb, Thomas, 2020). Each bronchi continues to divide into lobar bronchi (generation 2->3, mean diameter: 8->5 mm), segmental bronchi (generation 4, mean diameter: 4 mm), and further divide into small bronchi (generation 5->11, mean diameter: 3->1 mm) to reach bronchioles, terminal bronchioles (generation 12->14, mean diameter: 1->0.7 mm) (Lumb, Thomas, 2020). The air passages starting from trachea to terminal bronchioles with about 14 airway generations are referred to as conducting airways (central regions) responsible for elimination of inhaled particles and chemicals (Aulton, Taylor, 2013, Lumb, Thomas, 2020). At each generation, the internal diameter of the airways gets narrower from 18 mm (trachea) to 0.7 mm (terminal bronchioles) with increasing generations (0->14) and the velocity of gas flow decreases with increasing the number of air passages (the number of air passages: 1->16 000, trachea-> terminal bronchioles) (Lumb, Thomas, 2020). Respiratory airways (peripheral regions) where the conducting zone ends, start from respiratory bronchioles (generation 15->18, mean diameter: 0.4 mm) with no significant change in the internal diameter of respiratory bronchioles and the number of alveoli gradually increases and gas exchange takes place (Aulton, Taylor, 2013, Lumb, Thomas, 2020). Then the terminal respiratory bronchioles (generation 15-18) enter alveolar ducts (generation 19->22, mean diameter: 0.3 mm) and the air passages terminate in alveolar sacs with final generation 23 (mean diameter: 0.2 mm) (Figure 3)(Lumb, Thomas, 2020). These air passages that have alveoli are described as acinar airways and a human lung holds about 30 000 acini and each pulmonary acinus (diameter: around 3.5 mm) contain more than 10 000 alveoli (Lumb, Thomas, 2020). The mean total number of alveoli estimated in adult is about 400 million (ranging from 270 to 790 million depending on the height of the subject and total lung volume) (Lumb, Thomas, 2020). The mean diameter of a single alveolus is 0.2 mm and the total surface area of the alveoli is around 130 m² at resting lung volume/FRC (Lumb, Thomas, 2020). The advantages of pulmonary delivery for systemic applications (systemic drug absorption) are the large surface area of the alveoli (around 130 m²), thin (0.1-0.2 µm) alveolar epithelial cells, extensive vascularisation in the alveolar region and avoid hepatic first pass metabolism allowing rapid systemic drug absorption, fast onset of pharmacological action comparable to injections and high bioavailability (Nokhodchi, Martin, 2015, Peng et al., 2016, Lin et al., 2019).

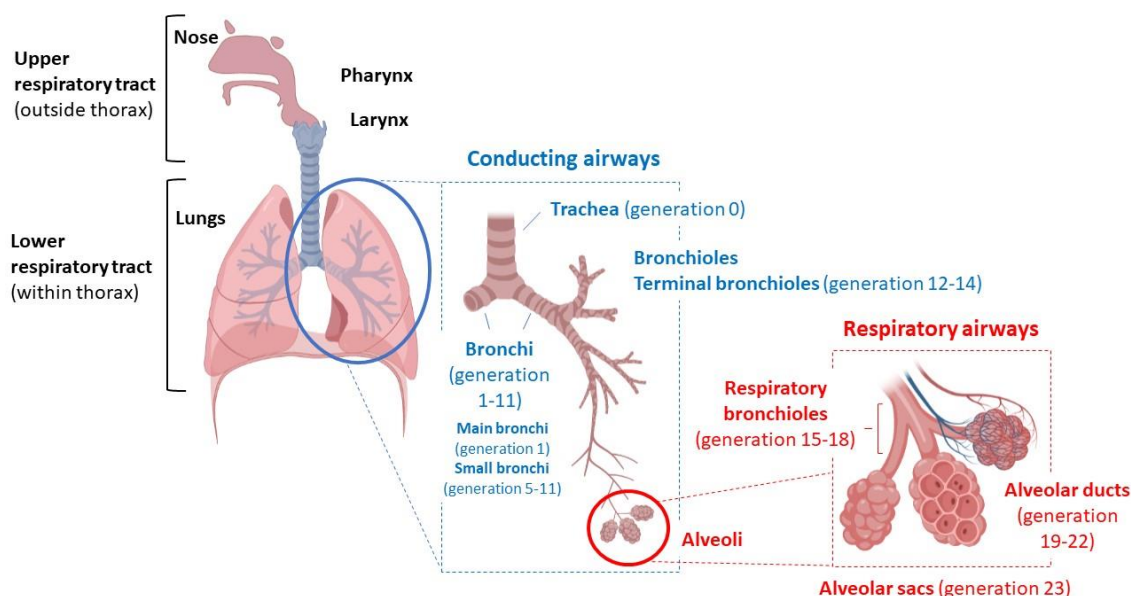


Figure 3: The diagram of human respiratory tract with generations of airways. (Created in BioRender.com)

2.1.1. Mechanisms of lung clearance

Multiple clearance mechanisms such as mucociliary clearance, alveolar macrophages, enzymatic degradation, and mechanical clearance are involved in the lungs after inhalation of therapeutic drugs to clear the drug particles that have reached the lungs (Nokhodchi, Martin, 2015, Weers, Miller, 2015, Kukut Hatipoglu, Hickey & Garcia-Contreras, 2018). Mucociliary clearance takes place within 24 hours to eliminate inhaled drug particles deposited in the conducting airways (e.g., trachea and bronchi), which restrict drug delivery to the lungs therefore affect drug delivery efficiency (Nokhodchi, Martin, 2015, Kukut Hatipoglu, Hickey & Garcia-Contreras, 2018). Alveolar macrophages in the alveolar regions remove the therapeutic drug targeted for systemic drug absorption which affect therapeutic efficacy (Nokhodchi, Martin, 2015, Kukut Hatipoglu, Hickey & Garcia-Contreras, 2018). Compared to the GI tract, less enzymatic activities occur in the lungs yet inhaled therapeutic drugs are still susceptible to enzymatic degradation and metabolism takes place in the lungs (Nokhodchi, Martin, 2015, Weers, Miller, 2015). Inhaled therapeutic drugs also can be cleared by mechanical clearance such as coughing, sneezing, or swallowing when the drugs are deposited in upper respiratory tract (Nokhodchi, Martin, 2015, Weers, Miller, 2015, Kukut Hatipoglu, Hickey & Garcia-Contreras, 2018). All these multiple clearance mechanisms facilitate the drug particles clearance from the lungs and affect the efficiency of systemic drug delivery via pulmonary route, bioavailability, and therapeutic efficacy (Nokhodchi, Martin, 2015, Weers, Miller, 2015).

2.1.2. Gas flow and respiratory system resistance

In pulmonary airways, the nature of gas flow/air flow (gas flows from a region of high pressure to lower pressure region) such as turbulent flow, laminar flow, or a mixture of the two flows is present according to the diameter of airways (Lumb, Thomas, 2020). Turbulent flow is associated with high friction forces (the flow pattern is irregular, friction between gas and airway wall is significant) and is predominantly present in conducting airways, the larger (upper) airways (e.g., the first 10 generations, high flow rate) while laminar flow is associated with little friction (theoretically it is stationary, resistance from friction between gas and airway wall is negligible) and is more likely to dominate in smaller (lower) airways (low flow rate), the region of the lungs where gas exchange occurs (e.g., after generation 15) (Lumb, Thomas, 2020). The velocity of gas decreases as the number of airways increases and mean airway diameter decreases thus gas flow velocity in smaller airways is low (Lumb, Thomas, 2020). In addition, respiratory system resistance is present resulting from a combination of both airway resistance and tissue resistance (Lumb, Thomas, 2020). Airway resistance is resistance to air flow in the airways (frictional resistance in the airways during inspiration and expiration, gas flow into the lungs and out of the lungs) whereas tissue resistance is resistance caused by the tissue deformation of lung and chest wall with breathing (Lumb, Thomas, 2020). Resistance to air/gas flow is defined as a change in pressure per flow rate; the ratio between the pressure gradient (difference) across the airways (unit: kilopascals (kPa) or centimetres of water (cmH₂O)) and flow rate (unit: L.min⁻¹) and expressed as kPa or cmH₂O per litre per minute (kPa.L⁻¹.min or cmH₂O.L⁻¹.min) (Lumb, Thomas, 2020).

2.1.3. Obesity

Obesity contributes to the change of respiratory system (e.g., changes in lung volume and airway resistance) causing reduced tidal volume, dyspnoea (difficult breathing), frequent airway closure or increasing the risk of developing obstructive airway disease (e.g., chronic obstructive pulmonary disease, COPD) due to physiological changes (the thickness of the chest wall relative to the size of the lungs, the mass of the chest wall) in people with obesity (Lumb, Thomas, 2020). The chest wall thickness and abdominal mass increase with obesity. This compresses the chest cavity (increased pleural pressure because of increased weight of the chest wall) that reduces lung volumes (e.g., FRC) and increases airway resistance therefore require increased work of breathing (Lumb, Thomas, 2020).

2.2. Pulmonary delivery

Pulmonary delivery is a non-invasive route of drug administration by inhalation and is predominantly used to deliver drugs (active pharmaceutical ingredients) in dry powder inhaler (DPI) formulations directly to the target site in the respiratory system/the lungs for local treatment of respiratory disease, such as asthma, COPD, and cystic fibrosis (Nokhodchi, Martin, 2015). In addition to these treatments, various antimicrobial or antibiotics drugs in DPI formulations for pulmonary delivery have also been developed for local treatment of respiratory infections (mainly due to *Pseudomonas aeruginosa*) to reduce delivery doses with higher concentration of drugs achieved in the lungs compared to oral antibiotics treatments thus lower systemic side effects and improve therapeutic efficacy (Ambrus et al., 2018, Sibum et al., 2018). Current available oral antibiotics treatments require high dose administration associated with side effects (Ambrus et al., 2018, Sibum et al., 2018). Few inhalation treatments (inhalation powders) for pulmonary infections in patients with cystic fibrosis are currently available in the UK including: tobramycin marketed as TOBI® Podhaler® for the treatment of chronic pulmonary *Pseudomonas aeruginosa* infection in patients with cystic fibrosis (emc, 2019e, BNF, 2021h), colistimethate sodium marketed as Colobreathe® for the management of chronic pulmonary *Pseudomonas aeruginosa* infection in patients with cystic fibrosis (BNF, 2021a, emc, 2021), and mannitol marketed as Bronchitol® for the treatment of cystic fibrosis as an add-on therapy to standard care (emc, 2019a, BNF, 2021d).

To deliver drugs as powders directly to the lungs, inhaler devices are required to generate aerosols for pulmonary drug delivery (Wilson, Luft & DeSimone, 2018). In pharmacy, aerosols are defined as solid particles or liquid droplets with small size dispersed in air (Aulton, Taylor, 2013). There are three main types of inhaler devices available for drug administration into the lungs: nebuliser, pressurised meter dose inhalers (pMDIs) both used for liquid-based formulations, and DPIs for solid based (dry powders) formulations (Depreter, Pilcer & Amighi, 2013, Peng et al., 2016, Wilson, Luft & DeSimone, 2018). Nebulisers, which comprise liquid-based formulations, convert drug solutions or suspensions into fine aerosol droplets to be inhaled by patients and deliver large volumes of drug solutions/suspensions during normal breathing (Aulton, Taylor, 2013, Peng et al., 2016, Sibum et al., 2018). However, nebulisers require long inhalation/administration time (e.g., over 2 minutes) associated with low delivery efficiency (low reproducibility and accuracy of administered doses) (Peng et al., 2016, Sibum et al., 2018). In addition, nebulisers are usually not portable (e.g., large)

and require maintenance (e.g., cleaning after each use) thus they are normally used in hospitals (Peng et al., 2016, Sibum et al., 2018). pMDIs, which also contain liquid-based formulations, deliver a specific drug dose per puff with the use of propellants (e.g., liquefied gases, hydrofluoroalkane, non-polar) to generate the aerosol for inhalation (Aulton, Taylor, 2013, Liang et al., 2020). In general, peptides and proteins considered to be hydrophilic are poorly soluble in non-polar propellants (Liang et al., 2020). pMDIs are portable and store up to 200 doses (Aulton, Taylor, 2013) and commonly designed to deliver small amounts of drugs (e.g., μg range, 6-500 μg) therefore they are not suitable when higher amounts of drugs doses (e.g., mg range) are required to be delivered (Scherließ, Etschmann, 2018, Sibum et al., 2018). DPIs can omit limitations associated with nebulisers and pMDIs. DPIs are portable, easy to handle and use which can lead to high patient compliance, and propellant free as DPIs usually use patient inspiratory flow thus propellant is not required to generate aerosol (Peng et al., 2016, Lavorini, Pistolesi & Usmani, 2017, Kadota et al., 2019). In addition, DPIs are used for dry powders (solid dosage forms) formulations that offer better formulation stability as drugs in solid dosage forms are more stable compared to liquid-based formulations and cold chain is usually not required for transport and storage (Chapter 1.2)(Peng et al., 2016, Elsayed, Shalash, 2018, Sibum et al., 2018). DPIs also can be used to deliver higher amounts of drugs (high dose formulations) (Scherließ, Etschmann, 2018, Sibum et al., 2018). Overall, among these three types of delivery devices, DPIs offer advantages over the other two systems (nebuliser and pMDIs) (Peng et al., 2016, Elsayed, Shalash, 2018, Sibum et al., 2018).

Pulmonary drug delivery is an attractive route of drug administration alternative to parenteral route, which is the most common route of administration for therapeutic peptide and protein drugs such as insulin and GLP-1RA for the treatment of diabetes (Chapter 1.1.4) (Ismail, Csóka, 2017, Wilson, Luft & DeSimone, 2018). Although oral route is generally the most common and preferable route for drug administration oral delivery of peptides and proteins results in rapid enzymatic degradation in the GI tract, first pass metabolism, and low oral bioavailability (Chapter 1.1.4) (Ismail, Csóka, 2017, Hu, Jia, 2019, Brayden et al., 2020). Parenteral administration is associated with limitations (e.g., inconvenience and discomfort due to injections) and poor patient compliance and adherence to the injection therapy (Chapter 1.1.4) (Ismail, Csóka, 2017, Hu, Jia, 2019, Lin et al., 2019). Also, proteins undergo physicochemical degradation facilitated by water in liquid-based formulations (Chapter 1.2)(Wilson, Luft & DeSimone, 2018). Therefore, to address injection related barriers and improve patient compliance for the treatment of diabetes, the lungs as a route for systemic delivery of therapeutic peptide and protein drugs have been explored as an alternative non-invasive route to

parenteral route and the lungs offer several advantages (Section 2.1) (Nokhodchi, Martin, 2015, Lin et al., 2019).

2.3. Systemic drug delivery through pulmonary route

For pulmonary drug delivery for systemic applications, inhaled therapeutic drugs (e.g., peptides and proteins) need to cross the alveolar epithelium in the lungs to enter the blood circulation for systemic therapeutic effect (Lin et al., 2019, Liang et al., 2020). The sufficient dose of the therapeutic drug aerosolised should be delivered through a DPI device to the deep lung regions where systemic absorption takes place due to the presence of alveoli having a large surface area ($\sim 130 \text{ m}^2$) and thin epithelium ($0.2 \text{ }\mu\text{m}$) compared to conducting airways associated with low epithelial permeability due to smaller surface area ($\sim 2 \text{ m}^2$), thick epithelium (trachea: $50\text{-}60 \text{ }\mu\text{m}$) and reduced blood supply (Section 2.1)(Nokhodchi, Martin, 2015, Liang et al., 2020). The deposition of inhaled therapeutic drugs occurs throughout the airways (different regions of respiratory tracts). The site of aerosolised drug particles deposition in different respiratory tract regions and efficiency of drug delivery to the lungs are dependent on an aerodynamic diameter of the drug particles that consequently determine therapeutic efficacy (Nokhodchi, Martin, 2015, Chen, L. et al., 2016). The aerodynamic diameter can be calculated by *Equation 1*:

$$d_{aer} = d_{geo} \sqrt{\left(\frac{Pp}{PoX}\right)} \quad \text{Equation 1}$$

where d_{aer} is aerodynamic diameter, d_{geo} is geometric (physical) diameter, Pp is particle density (includes internal and external voids), Po is the unit density (i.e., 1 g cm^{-3}), and X is the shape factor (e.g., 1.0 indicates an ideal spherical shape) (Vehring, 2007, Aulton, Taylor, 2013, Nokhodchi, Martin, 2015, Chen et al., 2016). The aerodynamic diameter which is the most critical physicochemical property of drug aerosol particles for inhalation, is defined as the physical diameter of a unit density sphere particle which settles through air with the settling velocity equal to the measured particle of interest (Vehring, 2007, Aulton, Taylor, 2013, Nokhodchi, Martin, 2015). *Equation 1* indicates that particle size, density and morphology/shape of the particle influence the aerodynamic diameter (Chen et al., 2016, Peng et al., 2016). Aerodynamic diameter is generally determined *in vitro* by impaction techniques such as next generation impactor (NGI) (Ung et al., 2014, Nokhodchi, Martin, 2015). NGI, which is an accepted apparatus by the United States Pharmacopoeia (USP) and European Pharmacopoeia (Ph.Eur.) for characterisation of DPI formulations, has seven stages (1-7) followed by

a micro orifice collector (MOC, terminal filter) (Figure 4) and they are arranged in descending order of cut-off aerodynamic diameters that separate the largest particles first (large particles impact onto the collection stage) and pass through the smaller particles to the next NGI stage at a pre-set airflow rate and determine particle size distribution *in vitro* (drug mass quantified against the particle sizes) (Aulton, Taylor, 2013, D'Addio et al., 2013, Nokhodchi, Martin, 2015). NGI can be performed at a different air flow rate setting between 15 L min⁻¹ and 100 L min⁻¹ where air and aerosol are drawn through the device at a pre-set flow rate (Aulton, Taylor, 2013). Particles collected from the low impactor stages (e.g., between 3 and 5) with less than or equal to 5.0 µm aerodynamic diameter generally represent the respirable-sized drug dose reaching the lungs, whereas particles deposited in the higher impactor stages (e.g., throat and stage 1) represent the oropharyngeal deposition in the oropharynx region (mouth, throat) (Nokhodchi, Martin, 2015). The aerosolisation performance of DPI formulations is generally assessed experimentally based on the values of mass median aerodynamic diameter (MMAD) determined along with geometric standard deviation (GSD), fine particle dose (FPD) and fine particle fraction (FPF%) (Nokhodchi, Martin, 2015). The aerodynamic diameter is also expressed as MMAD when aerodynamic particle size distribution data is reported (Nokhodchi, Martin, 2015, Weers, Miller, 2015). MMAD is defined as the aerodynamic diameter at which 50% of total particles by mass (the size of 50% of the particles are larger or smaller than the stated size) and reported as 50% cumulative percentage undersize distribution (below mean diameter of size fraction) of deposited inhaled particles mass collected from all the stages of the impactor (Aulton, Taylor, 2013, Shalash, Molokhia & Elsayed, 2015, Yeung et al., 2019, Ferdynand, Nokhodchi, 2020). GSD is expressed as a degree of the aerodynamic particle size distribution around the MMAD (Nokhodchi, Martin, 2015). FPD is defined as the amount of the delivered drug dose with less than or equal to 5.0 µm aerodynamic diameter. FPF (%) is defined as the mass fraction of the delivered drug dose with less than or equal to 5.0 µm aerodynamic diameter and used to characterise the *in vitro* lung deposition and efficiency of DPI formulations for pulmonary delivery (e.g., consistency in drug delivery) (Nokhodchi, Martin, 2015, Zhang et al., 2018). These parameters for aerosolisation performance are usually calculated by data analysis software (i.e., Copley Inhaler Testing Data Analysis Software Wibu)(Yeung et al., 2019).

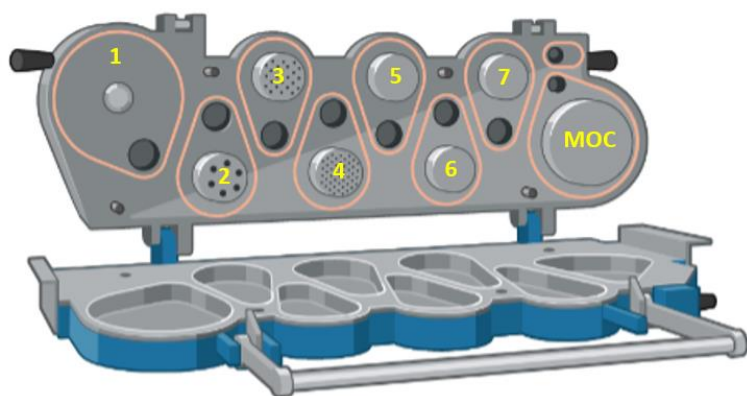


Figure 4: Schematic representation of Next Generation Impactor open view with collection cups (Stages 1-7 and MOC). MOC: micro orifice collector. (Created in BioRender.com)

To be effective for pulmonary drug delivery, the aerodynamic diameter of the drug particles for inhalation should be between 1 μm and 5 μm to reach the lungs and the aerosolised/inhaled drug particles need to deposit in the desired deep lung regions for systemic applications (Nokhodchi, Martin, 2015, Sibum et al., 2018). There are three main mechanisms involved in the deposition of aerosolised drug particles in the respiratory tracts: inertial impaction, gravitational sedimentation, and diffusion based on the aerodynamic diameter (Table 3) (Aulton, Taylor, 2013, Nokhodchi, Martin, 2015, Peng et al., 2016). Inertial impaction is the common mechanism responsible for the deposition of drug particles with the aerodynamic diameter greater than 5 μm in upper airways (large conducting airway) where turbulent flow is predominantly present and the airflow velocity is high (Section 2.1)(Table 3) (Depreter, Pilcer & Amighi, 2013, Nokhodchi, Martin, 2015). There is a change in direction of airflow (air stream) in the throat or where a bifurcation starts in the airways (Aulton, Taylor, 2013). Particles having an aerodynamic diameter greater than 5 μm is associated with high velocity within the air stream not following the inspired airstream and will impact on the wall of the bifurcated/branched airways and deposit there (large drug particles are not able to reach the lungs for deposition) (Aulton, Taylor, 2013, Nokhodchi, Martin, 2015, Peng et al., 2016). This results in early drug deposition in oropharyngeal and trachea-bronchial regions (i.e., loss of drug for systemic applications, drug deposition in the lower respiratory airways not achieved) where systemic absorption is low due to the small surface area affecting therapeutic efficacy (Nokhodchi, Martin, 2015, Peng et al., 2016). In addition, large particles ($d_{\text{aer}} > 10 \mu\text{m}$) or particles deposited in the upper airway (mouth, pharynx, larynx, large conducting airways) are rapidly removed by mucociliary clearance within 24 hours along with coughing followed by swallowing (the drug is degraded in GI tract) therefore limiting the drug deposition in the lower respiratory airways (Section 2.1.1) (Aulton,

Taylor, 2013, Depreter, Pilcer & Amighi, 2013, Nokhodchi, Martin, 2015). The drug particles with the aerodynamic diameter between 0.5/1 μm and 5 μm deposit via the sedimentation mechanism in respiratory airways (respiratory bronchioles to alveolar regions) where the airflow (air stream) velocity decreases thus avoid impaction deposition mechanism (Table 3) (Aulton, Taylor, 2013, Depreter, Pilcer & Amighi, 2013, Nokhodchi, Martin, 2015). The drug particles in the aerodynamic diameter range of 3 μm to 5 μm tend to deposit in the tracheal and bronchial regions (small conducting airways) whereas drug particles having the aerodynamic diameter smaller than 3 μm are likely to deposit in the alveolar region desirable for systemic absorption (Table 3) (Nokhodchi, Martin, 2015). The drug particles with the aerodynamic diameter less than 0.5 μm deposit via diffusion and Brownian motion (Brownian diffusion) in small respiratory airways and alveolar regions where the airflow is slow and particles deposit upon contact with the wall of the airways (collision of small particles, Brownian motion) (Aulton, Taylor, 2013, Nokhodchi, Martin, 2015, Lee, Kim & Park, 2018). Diffusion is the predominant deposition mechanism for particles with aerodynamic diameter smaller than 0.5 μm and inhaled particles collide in the respiratory tract and move down to airways' wall for deposition (Aulton, Taylor, 2013, Nokhodchi, Martin, 2015). Otherwise, such fine drug particles ($d_{\text{aer}}: <0.5\text{-}1.0 \mu\text{m}$) might be exhaled out quickly during normal tidal breathing as they might be too large for deposition by Brownian diffusion or too small for sedimentation deposition mechanism and they tend to stay airborne not depositing in the lungs (Table 3) (Aulton, Taylor, 2013, Depreter, Pilcer & Amighi, 2013, Nokhodchi, Martin, 2015). In addition, the particles with the aerodynamic diameter between 1 μm and 2 μm are likely to be cleared from the airways by alveolar macrophages affecting therapeutic efficacy (Nokhodchi, Martin, 2015, Liang et al., 2020). To target the desired deep lung regions (i.e., alveolar regions) for systemic drug absorption, the optimal aerodynamic diameter would be between 2 μm and 3 μm (Depreter, Pilcer & Amighi, 2013). For a comparison of Afrezza[®] (current available inhaled insulin product in the US) with Exubera[®] (withdrawn inhaled insulin product), the MMAD for Afrezza[®] is reported to be between 2.0 μm and 2.5 μm and exhibited rapid absorption (t_{max} : 12-15 mins) and the bioavailability was about 30% relative to SC regular insulin (Al-Tabakha, 2015, Goldberg, Wong, 2015) whereas Exubera[®] (MMAD: about 3 μm) showed slower absorption (t_{max} : 38-78 mins) and lower bioavailability (about 10% relative to SC regular insulin) (Chapter 1.1.4) (Depreter, Pilcer & Amighi, 2013, Al-Tabakha, 2015). This suggests that Afrezza[®] with small MMAD led to sufficient insulin dose delivery to deep lung regions (alveolar regions) and achieved rapid absorption and higher bioavailability (Depreter, Pilcer & Amighi, 2013). Optimised drug deposition in the lungs can be achieved by controlling the MMAD to minimise oropharyngeal deposition and targeting specific desired regions of the lungs with monodisperse size distribution (e.g., low GSD) (Yang, Chan & Chan, 2014, Nokhodchi, Martin, 2015,

Weers, Miller, 2015). To enhance therapeutic effect for DPI formulations drug deposition in the lungs should be maximised while minimising oropharyngeal deposition (Yang, Chan & Chan, 2014, Weers, Miller, 2015). Macrophage clearance should be avoided as absorption of the inhaled drug particles intended for pulmonary systemic application need to take place through the pulmonary epithelium in the alveolar region to achieve systemic bioavailability (Depreter, Pilcer & Amighi, 2013).

Table 3: Particle size (aerodynamic diameter, μm), region of particle deposition in the respiratory tract and mechanism for particle deposition based on the aerodynamic diameter.

Aerodynamic diameter (μm)	Particle deposition region	Particle deposition mechanism	
> 10	- Oropharyngeal regions (e.g., Mouth, throat/pharynx)	Inertial impaction	- Mucociliary clearance - Coughing followed by swallowing
> 5	- Upper respiratory tract - Large conducting airways (Oropharyngeal and trachea-bronchial regions)	Inertial impaction	- Low drug absorption - Mucociliary clearance (Prevent the drug particles from entering the lungs) - Affect drug delivery efficiency
1-5	- Lower respiratory tract (Lower trachea, bronchi, bronchiole, and alveoli)	Sedimentation	- Required size for drug deposition in the lungs - Particles reach the lungs - Systemic application
3-5	- Small conducting airways (Trachea-bronchial regions) - Respiratory airways (Respiratory bronchioles to alveolar region)	Sedimentation	- Systemic application
< 3	- Respiratory airways (Respiratory bronchioles to alveolar region) - Alveolar region	Sedimentation	- Desirable deposition site for systemic absorption
2-3	Alveolar region	Sedimentation	- Optimal aerodynamic diameter for alveolar deposition and rapid systemic absorption
1-2	Alveolar region	Sedimentation	- Alveolar macrophages - Affect bioavailability and therapeutic efficacy

< 0.5-1	<ul style="list-style-type: none"> - Small airways - Alveolar region 	Diffusion Brownian motion or Exhaled	<ul style="list-style-type: none"> - Low drug deposition - Low drug delivery efficiency
-------------------	--	---	---

2.4. Dry powder inhaler formulations for pulmonary delivery

DPIs are inhaler devices to deliver drugs in dry powder dosage form to the lungs and consist of DPI formulations that are generally composed of drug particles ($d_{aer} \leq 5 \mu\text{m}$) and carrier particles (particle size: 50-200 μm) (i.e., carrier-based DPI formulations) (Elsayed, Shalash, 2018, Faulhammer et al., 2018). In carrier-based DPI formulations, drug particles and carrier particles are prepared as adhesive mixtures (drug-carrier blends/mixtures) where the drug particles are adhered to the surface of the carrier via particle interactions, inter-particulate adhesive forces (drug-carrier adhesive forces) during the mixing/blending process. Upon inhalation the drug is detached from the carrier and delivered directly to the target site of drug action in the lungs to achieve therapeutic effect (Brunaugh, Smyth, 2018, Sibum et al., 2018, Yeung et al., 2018). Such carrier-based DPI formulations are commonly used for the treatment of asthma (e.g., salbutamol sulfate: selective beta 2 adrenergic receptor agonist, 100-200 μg salbutamol per inhalation, fluticasone furoate and vilanterol trifenate: long-acting beta 2 agonist, 184 μg fluticasone furoate and 22 μg vilanterol trifenate per inhalation) (BNF, 2021e, BNF, 2021b) and COPD (e.g., tiotropium: long-acting muscarinic receptor antagonist, 18 μg tiotropium per capsule) (Brunaugh, Smyth, 2018, Scherließ, Etschmann, 2018, BNF, 2021g, emc, 2019d).

Pulmonary drug delivery via DPIs is challenging due to the respirable-sized drug particles ($d_{aer} \leq 5 \mu\text{m}$) associated with large particle surface area and high surface energy (decreased particle size results in increased particle surface area and surface energy) where high inter-particulate forces are involved between drug particles (drug-drug cohesive forces) therefore naturally cohesive particles (Nokhodchi, Martin, 2015, Peng et al., 2016, Brunaugh, Smyth, 2018, Yeung et al., 2018). The high drug-drug cohesive forces caused by the small particle size of drug particles for pulmonary delivery generally include van der Waals, electrostatic and capillary forces (Weers, Miller, 2015, Peng et al., 2016, Brunaugh, Smyth, 2018, Sibum et al., 2018, Yeung et al., 2018). These forces can lead to a high degree of drug-drug particle agglomeration that have a significant effect on flowability and dispersion of the drug particles/drug deagglomeration (i.e., to break up particle agglomerates into individual particle upon inhalation with a DPI device) during inhalation therefore affect the efficiency

of aerosolised drug delivery to the lungs and aerosolisation performance of the drug particles (e.g., poor flowability and poor dispersion of the drug particles, poor deagglomeration) (Weers, Miller, 2015, Peng et al., 2016, Brunaugh, Smyth, 2018, Faulhammer et al., 2018, Sibum et al., 2018, Yeung et al., 2018). Also, adhesion forces between drug particles and the surface of the inhaler device (drug-device adhesive forces) are present where drug particles adhere to the wall of the inhaler device affecting aerosolisation performance (e.g., decreased powder flow, high powder retention in the inhaler) (Sibum et al., 2018, Yeung et al., 2018). Therefore, to address such issues of cohesive drug powder properties, carrier powders (particle size: 50-200 μm) are added to the DPI formulation as a means of delivering the drug to the lungs to improve powder flow properties; flowability of the cohesive particles and particle dispersion during inhalation, also used as a bulking agent to aid powder handling (Peng et al., 2016, Faulhammer et al., 2018, Scherließ, Etschmann, 2018, Yeung et al., 2018). Lactose monohydrate is usually used as a carrier for the purposes (Scherließ, Etschmann, 2018). For carrier-based DPI formulations for local treatment of respiratory disease, the dose requirement is low within the microgram (μg) range (low dose DPI formulations) (Brunaugh, Smyth, 2018, Scherließ, Etschmann, 2018, Yeung et al., 2018). The drug to carrier ratio of 1:67.5 w/w are known to be typical for drug-carrier mixtures with the drug concentrations of 0.1-2% (Scherließ, Etschmann, 2018) or 0.1-4% (Sibum et al., 2018). The total mass of drug-carrier mixtures dispersed by marketed inhaler devices is usually in the range of 10 mg to 25 mg (Sibum et al., 2018). At higher concentration of drug for carrier-based DPI formulations, multiple layers of the drug particles on the carrier surface and drug particle agglomerates will be formed due to the limited surface area of the carrier (Scherließ, Etschmann, 2018, Sibum et al., 2018). This adversely affects the mechanical powder stability (e.g., powder handling and dosing) thus homogeneity of drug content, dose delivery consistency (uniform drug delivery into the lungs), and dose reproducibility (Scherließ, Etschmann, 2018, Sibum et al., 2018). Consequently, the drug content should be limited to maximum 2.5 mg in 25 mg total mass of adhesive mixtures (e.g., 5-10% of drug dose) in the formulations that still meet content uniformity and stability (Sibum et al., 2018).

2.4.1. High dose dry powder inhaler formulations

High dose drug delivery via the lungs using DPIs have gained growing interest for the treatment of local pulmonary infections (e.g., tuberculosis, pneumonia) and for the management of systemic conditions (e.g., diabetes) and viral infections (e.g., influenza) and DPI formulations for the delivery of high drug doses to the lungs (i.e., high dose DPI formulations) have been developed for these conditions (Lau, Young & Traini, 2017, Brunaugh, Smyth, 2018, Yeung et al., 2018). These treatment

conditions require higher concentration of the drug (e.g., mg range) compared to the common formulations used for asthma and COPD (e.g., μg range, referred to as low dose DPI formulations, Section 2.4) (Brunaugh, Smyth, 2018, Scherließ, Etschmann, 2018, Yeung et al., 2018). For the local treatments due to low potency drugs or low bioavailability high dose of drugs should be delivered directly to the infected area to exert therapeutic effect whereas for the systemic applications, high dose of drugs is required as the lungs are used as a route to the systemic circulation to treat systemic conditions (Lau, Young & Traini, 2017, Brunaugh, Smyth, 2018, Scherließ, Etschmann, 2018, Yeung et al., 2018). For example, TOBI® Podhaler® contains 28 mg tobramycin per capsule administered using Podhaler® inhaler (emc, 2019). Colobreathe® contain 125 mg of colistimethate sodium each capsule administered using Turbospin® inhaler (emc, 2021). Exubera® (withdrawn inhaled insulin product) consisted of 1 mg or 3 mg dose of insulin per blister (fill mass of 1.7 mg or 5.1 mg powder, respectively) and Afrezza® contains 0.35 mg (4 unit), 0.7 mg (8 unit) or 1 mg insulin (12 unit) per cartridge (Al-Tabakha, 2015, Ferrati et al., 2018). Zanamivir inhalation powder marketed as Relenza® for the treatment of influenza contains 5 mg zanamivir per blister (emc, 2019c). Bronchitol® contains 40 mg mannitol per capsule (emc, 2019). All these formulations are considered as high dose DPI formulations and represent that high dose drug delivery via the lungs seem feasible and benefit patients (Das, Stewart & Tucker, 2018).

There are two main types of high dose DPI formulations: carrier free DPI formulations and carrier-based DPI formulations (Faulhammer et al., 2018, Lechanteur, Evrard, 2020). Carrier free DPI formulations are composed of drug ($d_{\text{aer}}: \leq 5 \mu\text{m}$) generally incorporated in excipients (drug is co-formulated with excipients, no carrier) or drug alone ($d_{\text{aer}}: \leq 5 \mu\text{m}$) without excipients and carrier (i.e., excipient free DPI formulations) (Brunaugh, Smyth, 2018, Yeung et al., 2018). Carrier-based DPI formulations are composed of drug powder ($d_{\text{aer}}: \leq 5 \mu\text{m}$) and carrier powder (particle size: 50-200 μm) prepared by blending both powders together to produce drug-carrier blends/adhesive mixture where the drug particles are adhered to the surface of the carrier during mixing and inter-particulate adhesive forces (drug-carrier adhesive forces) exist (Section 2.4) (Sibum et al., 2018, Yeung et al., 2018). Upon inhalation the drug is detached from the carrier when inter-particulate forces (drug-drug cohesive and drug-carrier adhesive forces) are overcome and delivered to the lungs (Yeung et al., 2018). Carrier free DPI formulations (without the addition of carrier to the formulations) skip the blending process as carrier is not added to the formulation (drug is already incorporated in excipients or excipient free) thus omitting blend homogeneity issues and drug-carrier detachment process upon inhalation which are associated with carrier-based DPI formulations (Lechanteur, Evrard, 2020). However, without the addition of carrier to the formulations (i.e., carrier free DPI

formulations) drug particles for inhalation are cohesive with poor flowability (Section 2.4)(Brunaugh, Smyth, 2018). Carrier-based DPI formulations address the issues of poor powder flow properties and dispersion, however, face challenges to deliver high dose dry powders via DPI devices as the addition of carrier increases the total powder mass of adhesive mixtures to be inhaled (Scherließ, Etschmann, 2018, Yeung et al., 2018). For the development of high dose DPI formulations, the use or amount of excipients should be reduced as it is generally impractical to deliver high amount of powders via DPI devices (Scherließ, Etschmann, 2018). High dose DPI formulations require high drug loading with reduced use of excipients (Scherließ, Etschmann, 2018). Otherwise, it will require multiple administration/inhalations to achieve therapeutic effect which is a burden for patients and affect patient adherence to therapy (Sibum et al., 2018). In addition, inhaling large powder mass might cause drug depositions in mouth and throat, thus irritation and cough (Brunaugh, Smyth, 2018, Sibum et al., 2018, Yeung et al., 2018). Therefore, the drug content should be limited to 5-10% (e.g., maximum 2.5 mg in 25 mg total mass of adhesive mixtures) in carrier-based DPI formulations (Section 2.4) (Sibum et al., 2018). It is reasonable that the pulmonary delivery of powders should be limited to 100-200 mg per day (Brunaugh, Smyth, 2018).

Both carrier free and carrier-based DPI formulations have advantages with different challenges for pulmonary administration of high dose drugs. Therefore, various formulation approaches such as particle engineering for different particle preparations have been applied to overcome the challenges associated with each formulation and develop both types of high dose DPI formulations for peptide and protein drugs (Brunaugh, Smyth, 2018, Yeung et al., 2018, Scherließ, Etschmann, 2018, Lechanteur, Evrard, 2020). Peptide/protein-based DPI formulations require good powder flow properties (e.g., flowability and dispersibility) with no or limited moisture content while maintaining their stability of protein molecules and biological activity (Banga, 2015, Yeung et al., 2018, Ziaee et al., 2019). Insulin has been investigated most in the development of DPI formulations for pulmonary delivery of antidiabetic drugs (Depreter, Pilcer & Amighi, 2013).

2.4.2. Carrier free dry powder inhaler formulations

Carrier free DPI formulations are prepared without the addition of carriers which can reduce the total powder mass (bulkiness) to be inhaled by the patient thus the delivery of high loading drug dose to the lungs becomes feasible (Healy et al., 2014, Brunaugh, Smyth, 2018, Yeung et al., 2018). A common approach to develop carrier free formulations is to reduce cohesive forces present between the drug particles and improve powder flowability and particle dispersion (Healy et al.,

2014, Yeung et al., 2018). This usually involves particle engineering such as spray drying, freeze drying and spray freeze drying that have been used as a formulation strategy to optimise the properties of drug particles (e.g., particle size, morphology) and improve aerosolisation performance of the drug particles (e.g., flowability, dispersion, lung deposition of drug particles) (Brunaugh, Smyth, 2018, Yeung et al., 2018).

2.4.2.1. Particle engineering

Spray drying

Spray drying has been used to produce dry powders of peptide and protein drugs (e.g., insulin) for pulmonary delivery as an alternative to parenteral formulations and improve storage stability (avoid cold chain storage conditions) (Mensink et al., 2017, Emami et al., 2018, Ziaee et al., 2019). Spray drying is a drying technique and a laboratory scale spray dryer (i.e., Büchi Mini Spray Dryer B-290, Figure 5) is usually used for research and consists of four main parts to perform spray drying process: namely drying chamber, atomiser/nozzle, aspirator and cyclone (Ziaee et al., 2019). The process of spray drying involves few steps: atomisation of feed solution or suspension by a gas stream (e.g., compressed air used for aqueous solutions or inert gas such as nitrogen used for organic solvents) to produce small droplets, water/solvent removal, formation of dried particles and drying. All these steps are operated as a single step process in the spray dryer to perform particle formation and drying simultaneously (drying time: a fraction of a second, the whole process in the dryer: only a few seconds) (Aulton, Taylor, 2013, Emami et al., 2018, Ziaee et al., 2019). In spray drying, drying air is sucked by aspirator at the pre-set aspirator airflow rate (i.e., drying airflow rate) and heated to the pre-set inlet temperature (i.e., temperature of heated drying air) (Ziaee et al., 2019). The hot dry air then flows into the chamber in the presence of airflow pattern selected: co-current, counter-current, or mixed flow direction (Ziaee et al., 2019). In co-current flow pattern, feedstock flows in the same direction as the flow of hot drying air where hot air is introduced through the top of the chamber to the bottom (Ziaee et al., 2019). This flow pattern is suitable for heat sensitive materials (e.g., biopharmaceuticals) as droplets move from the top to the bottom in the chamber where the final stage of drying process takes place and droplets are in contact with lower outlet temperature, which is the temperature of the drying hot air generated in the final stage of drying process, compared to other flow patterns (Ziaee et al., 2019). In counter-current flow pattern, feedstock and drying gas flow in opposite direction in the chamber where droplets are in contact with higher outlet temperature than co-current flow at the bottom of the chamber during the last stage of drying process (Ziaee et al., 2019). This flow pattern is not suitable for heat sensitive materials but provide

higher drying efficiency (Ziaee et al., 2019). In mixed flow pattern both co-current and counter-current airflows are present in the chamber and feedstock flows counter-current or co-current while hot airflow is co-current (Ziaee et al., 2019). The mixed flows offer flexibility for drying materials with different thermal stability (Ziaee et al., 2019).

Feed solution or suspension is pumped into an atomiser/a nozzle at the pre-set feed flow rate (pump, feed rate is the mass of both solvent and solid content entering the drying chamber per time) and atomised by drying air (i.e., nozzle spray flow rate, the amount of air needed to spray feedstock) into the chamber to form small droplets of water/solvent and solute (Ziaee et al., 2019). The atomised droplets are in contact with hot drying air in the chamber with the flow pattern selected (co-current flow or counter-current direction or mixed flow direction) and rapid solvent evaporation takes place to remove solvent/water from the atomised droplets and produce dried particles from the remaining solute droplets (Walters et al., 2014, Ziaee et al., 2019). The produced dried particles are then separated to a cyclone from the hot air stream at the end of the drying chamber before entering the cyclone which is the last stage of drying process (Ziaee et al., 2019). The temperature of the hot air (i.e., outlet temperature) in the final stage of drying process is the results of the combination of parameter settings (e.g., inlet temperature, aspirator flow rate (drying air flow rate), feed flow rate, concentration of the feed to be sprayed) (Walters et al., 2014, Ziaee et al., 2019). Then the final dry powders, which usually have uniform particle size and shape, are collected (Aulton, Taylor, 2013, Walters et al., 2014, Ziaee et al., 2019). Due to the use of high temperature required for drying, spray drying generates thermal stresses on peptide and protein drugs during the process of atomisation and drying (dehydration) where peptide and protein drugs are exposed to hot air stream with high temperature and air-liquid interfaces (the surface of the droplets) thus hydrophobic regions are exposed to the non-aqueous surface. This can cause denaturation (Haj-Ahmad et al., 2013, Ziaee et al., 2019). Also, water molecules required for hydrogen bonds to stabilise the secondary structure are removed which can change secondary structure of proteins (Ziaee et al., 2019). These stresses (high temperature, contact with hot air, exposed to air-liquid interfaces, dehydration) can lead to thermal degradation that have a significant effect on stability of peptide and protein drugs (Walters et al., 2014, Mensink et al., 2017, Emami et al., 2018, Ziaee et al., 2019).

Such thermal stresses on peptide and protein drugs can be controlled and minimised by optimising process parameters for drying such as inlet/outlet temperature, aspirator airflow rate (drying airflow rate) and feed flow rate as well as other parameters such as solute concentration (Walters et al., 2014, Ziaee et al., 2019). Stabilising the structure of proteins during manufacturing and storage is

important for biological activity of proteins (Haj-Ahmad et al., 2013). To avoid thermal degradation while producing dry powders with limited moisture content, outlet temperature should be kept as low as possible (Ziaee et al., 2019). Outlet temperature, which is the temperature of the air generated at the end of the drying chamber, depends on the parameter settings (e.g., inlet temperature, aspirator/drying airflow rate, feed flow rate, feed solute concentration) and is a critical factor for spray drying thermolabile biopharmaceuticals (Ståhl et al., 2002, Ziaee et al., 2019). Thermal degradation can take place when outlet temperature is high therefore low outlet temperature should be used to reduce the thermal stress (Ziaee et al., 2019). However, with the use of low outlet temperature sufficient thermal energy might not be generated to dry the particles therefore produce powders in the presence of residual moisture content that affect shelf life (lead to shorter shelf life) (Ziaee et al., 2019).

Ståhl *et al.* (2002) studied the effect of various processing parameters (e.g., feed flow rate, nozzle gas flow rate (nozzle spray flow rate), inlet air temperature and aspirator capacity (i.e., drying gas flow rate)) on the degradation of human insulin powder prepared by spray drying (insulin feedstock concentration: 5 mg mL⁻¹ dissolved in distilled water with hydrochloric acid (0.1M HCl) and sodium hydroxide (1M NaOH), final pH 7.4) for inhalation and demonstrated that the formation of insulin degradation products (i.e., A21, HMWP) in spray dried (SD) insulin powder was dependent on outlet temperature resulted from the combination of the parameter setting (i.e., inlet temperature, aspirator flow rate, feed flow rate) (Ståhl et al., 2002). The content of degradation products (i.e., A21 and HMWP) was influenced by spray drying processing settings related to thermal conditions (temperature) (Ståhl et al., 2002). Increasing inlet air temperature and aspirator airflow rate increased the formation of A21 and HMWP due to increased heat energy supply (Ståhl et al., 2002). Increased HMWP content was correlated to decreased moisture content as powders with low moisture content were produced with the use of high outlet air temperature that increased the degradation (Ståhl et al., 2002). To avoid insulin degradation, outlet temperature should be controlled and kept below 120°C where degradation was minor (A21: 0.42%, HPMW: <0.77%) and the optimal outlet temperature was found to be 61°C ± 4°C (Ståhl et al., 2002). Low outlet temperature was achieved by increasing feed flow rate as more liquid needed to be evaporated (Ståhl et al., 2002). Also, Ståhl *et al.* (2002) demonstrated that spray drying of human insulin with optimised processing parameters settings (i.e., inlet air temperature 100°C, feed flow rate: 300 mL hr⁻¹, nozzle gas flow rate: 550 L hr⁻¹, aspirator setting: 100% generated outlet air temperature: 61°C ± 4°C) produced particles in the suitable size range (mass median diameter: 2.9 µm ± 0.4 µm) for pulmonary delivery with minimised degradation (HMWP: 0.3% ± 0.1%, A21: 0.3% ± 0.05%) (Ståhl et

al., 2002). However, this setting reduced the drying capacity that resulted in the final powder product with high moisture content (moisture content measured by TGA: $3.9\% \pm 0.5\%$) (Ståhl et al., 2002). Increasing inlet temperature and drying air flow rate/aspirator capacity can decrease moisture content due to the increased heat energy supply that allow efficient drying (Ståhl et al., 2002). Overall, spray drying can produce stable insulin powders with limited degradation products when processing parameters (i.e., outlet air temperature $<120^{\circ}\text{C}$) were controlled (Ståhl et al., 2002). In addition, the process of spray drying is short (e.g., rapid evaporation) thus proteins exposed to heat/high temperature is short (Aulton, Taylor, 2013, Emami et al., 2018).



Figure 5: Büchi Mini Spray Dryer B-290 (Büchi, 2021).

Addition of excipients

In addition to the control of processing parameters to prepare stable dry powders of peptide and protein drugs, excipients (e.g., saccharides/sugars and amino acids) are often needed to physiochemically stabilise them (Ziaee et al., 2019). Also, the inclusion of excipients in the

formulations improve the aerosolisation performance (e.g., powder flowability, dispersion) by modifying physicochemical properties of particles such as particle size and distribution, and morphology which are critical to control and have a significant effect on powder flowability and aerosolisation performance of drug particles (dry powder delivery efficiency) (Walters et al., 2014, Nokhodchi, Martin, 2015, Ziaee et al., 2019). These particle properties (particle size and distribution, and morphology) are frequently characterised using particle size analysis methods such as Scanning Electron Microscopy (SEM, microscope method) and laser diffraction (laser light scattering) (Aulton, Taylor, 2013). SEM is an electron microscope to produce images (3-dimensional image) of particles (e.g., raw and engineered particles) and is commonly used to characterise particle morphology and surface properties (roughness) of the formulations along with particle size in diameter (size range of analysis: 0.1-500 μm particle diameter) (Aulton, Taylor, 2013, Nokhodchi, Martin, 2015). SEM is also used to distinguish the mixtures of different particles (e.g., drug-carrier adhesive mixtures) with different particle sizes, between small particles (e.g., drug) and large particles (e.g., carrier) (Nokhodchi, Martin, 2015). Laser diffraction is a widely used technique for the measurement of geometric particle size distribution of dry powders (size range of analysis: 1-1000 μm particle diameter) (Aulton, Taylor, 2013, Nokhodchi, Martin, 2015).

Proteins generally form hydrogen bonds with water molecules to be stable at molecular levels in solution however during the process of spray drying water is removed resulting in unstable forms of proteins (Emami et al., 2018, Ziaee et al., 2019). Therefore, sugars with hydroxyl groups (e.g., mannitol, sorbitol, sucrose, trehalose) are often used to make hydrogen bonds with proteins by replacing the hydrogen bonds between the protein and water during the process of drying (water removal) (i.e., water replacement theory) to protect and stabilise the structure of the proteins (Depreter, Pilcer & Amighi, 2013, Ziaee et al., 2019). Mannitol, sorbitol (both polyols), sucrose and trehalose, which are non-reducing sugars, tend to avoid chemical incompatibility with proteins (e.g., Maillard reaction) (Depreter, Pilcer & Amighi, 2013, Rahimpour, Kouhsoltani & Hamishehkar, 2014). Also, mannitol, sorbitol and sucrose are generally recognized as safe (GRAS) substances listed by the FDA database (U.S. Food & Drug Administration, 2020) that can be used in the inhalation field (Kaialy, Waseem, Nokhodchi, 2016). In contrast, reducing sugars such as lactose undergo Maillard reaction that leads to chemical degradation therefore they may not be selected as excipients for proteins-based formulations (Depreter, Pilcer & Amighi, 2013, Rahimpour, Kouhsoltani & Hamishehkar, 2014, Weers, Miller, 2015). In addition, amino acids (e.g., leucine, glycine, alanine), which are endogenous substances, are frequently studied as excipients to enhance DPI formulation performance by altering morphology or surface roughness to optimise inter-particulate forces (Sou

et al., 2011, Healy et al., 2014, Rahimpour, Kouhsoltani & Hamishehkar, 2014, Chen et al., 2016, Sou et al., 2016). Glycine has been used as buffering agent in the previously marketed inhaled insulin product: Exubera[®] (Al-Tabakha, 2015, Ferrati et al., 2018).

Exubera[®]

Inhaled insulin product of Exubera[®] (withdrawn) was produced by spray drying. In Exubera[®] formulation, recombinant insulin (60%) was incorporated in excipients: sodium citrate (buffering/stabilising agent), mannitol (stabilising/bulking agent), glycine (buffering agent for pH control to provide SD insulin powder stability at room temperature, to solubilise insulin in feed solution), and sodium hydroxide (pH adjustment, pH 7.2-7.4) and all excipients were used to stabilise insulin (Sadrzadeh et al., 2010, Al-Tabakha, 2015, Weers, Miller, 2015). Exubera[®] produced by spray drying exhibited uniform particle size of insulin particles (MMAD: 3 μm) suitable for drug delivery to the deep lung regions and showed consistent drug delivery (Sadrzadeh et al., 2010, Al-Tabakha, 2015, Yeung et al., 2018). This was attributed to the morphology of Exubera[®] powder which was wrinkled, raisin like appearance produced by spray drying and had external voids on particles with a folded shell (Vehring, 2007). The wrinkled insulin particles with corrugated surface roughness minimised the contact area between particles therefore reduced inter-particulate forces (cohesive forces) that assisted particle dispersion and enhanced the aerosolisation performance (Vehring, 2007, Weers, Miller, 2015). In addition, spray drying conditions (e.g., inlet temperature: 181°C and outlet temperature: 87°C) were controlled to limit moisture content in the dry powders below 2% (w/w) (Sadrzadeh et al., 2010). The secondary structure or the biological activity of insulin were not disrupted by the process of spray drying which usually cause stress to proteins (Sadrzadeh, Glembourtt & Stevenson, 2007). Furthermore, insulin co-formulated with excipients (i.e., mannitol and glycine) produced amorphous powders with high Tg (e.g., 78-95°C or 115°C depending on moisture content, 78-95°C when there was moisture content in powders or 115 °C when powders were completely dry) that enhanced insulin storage stability and provided 2-year shelf life at room temperature (Vehring, 2007, Weers, Miller, 2015). Insulin stability was optimised by selecting excipients to produce amorphous powders with high Tg where molecular mobility is limited (Sadrzadeh et al., 2010). Protein molecules in a glass state have limited molecule mobility with reduced risk of crystallisation therefore can enhance storage stability (Weers, Miller, 2015, Ziaee et al., 2019). For DPI formulations containing amorphous drugs, they are generally hygroscopic therefore powders absorbed moisture during storage or the presence of moisture in dry powders can reduce Tg and undergo aggregation as molecular mobility increase as Tg decrease (Chapter 1.2.1) (Banga, 2015, Weers, Miller, 2015). High molecule mobility at temperature above Tg can

increase powder/particle stickiness that affect particle size and aerosol performance (Weers, Miller, 2015). Also, crystallisation of the drug can occur therefore affect bioavailability (Weers, Miller, 2015). Consequently, all this affects formulation stability (Banga, 2015, Weers, Miller, 2015). Therefore, formulations with high Tg above the storage condition is ideal to avoid an increase in molecule mobility and crystallisation (Chapter 1.2.1) (Weers, Miller, 2015). Spray drying of insulin formulated with excipients (i.e., Exubera®) produced dry powders with good powder flow due to the particle surface roughness (wrinkled surface particles) and storage stability due to high Tg also low moisture content (below 2% w/w) in the dry powders (Vehring, 2007, Sadrzadeh et al., 2010).

Effect of excipients on spray dried insulin

There are some studies focused on the incorporation of excipients into insulin to prepare inhaled insulin powders using spray drying and enhance the aerosolisation performance of SD inhaled insulin powders (Razavi Rohani, Abnous & Tafaghodi, 2014, Kuehl et al., 2014). For example, Razavi Rohani, Abnous and Tafaghodi (2014) tried to use different combination of excipients (e.g., mannitol, sodium citrate and L-alanine or sodium alginate) to prepare SD insulin powders for improved aerosolisation performance (drug deposition in the deep lung regions) and formulation stability (Razavi Rohani, Abnous & Tafaghodi, 2014). Mannitol was selected as a main excipient to substitute water molecules and stabilise the protein molecule (i.e., water replacement theory) and other excipients were used to limit mannitol crystallisation by lowering the mannitol content in the formulation or by direct molecular interactions between the excipients and mannitol to inhibit the mannitol crystallisation (Razavi Rohani, Abnous & Tafaghodi, 2014, Ziaee et al., 2019). Mannitol has a low Tg (11°C) that tends to recrystallise and may lead to protein denaturation during drying process (Sou et al., 2016, Shetty et al., 2020). Crystallisation of excipients undergo phase separation therefore lose the interaction between excipients and the protein at molecular levels that adversely affect the stability of protein (Razavi Rohani, Abnous & Tafaghodi, 2014). Razavi Rohani, Abnous and Tafaghodi (2014) prepared SD insulin powders (MMAD: 2.1-4.6 µm, FPF: 46-81%) suitable for systemic pulmonary delivery of insulin (Razavi Rohani, Abnous & Tafaghodi, 2014). However, the nature of formulation ingredients (e.g., type of excipients) had an impact on powder properties (e.g., morphology, moisture content) therefore influenced aerosolisation performance: one combination of excipients provided optimal powder properties and aerosolisation performance but high moisture content while other excipient combination exhibited low moisture content but poor aerosolisation performance (Razavi Rohani, Abnous & Tafaghodi, 2014). Another study by Sou *et al.* (2016) also explored various excipients: mannitol (polyol), trehalose (disaccharide) and small molecules of amino acids (leucine and glycine) and sodium citrate to design a multi-component formulation

platform with higher T_g than storage conditions suitable for the incorporation of biopharmaceuticals (e.g., peptides and proteins) using spray drying (Sou et al., 2016). Sou *et al.* (2016) selected trehalose due to a high T_g (117°C) that tends to be amorphous after spray drying (Sou et al., 2016). Leucine was selected as a particle formation agent to assist the production of multi-component particles with the protective shell on the particle surface (Sou et al., 2016). Sou *et al.* (2016) also found that spray drying of different combination of excipients produce different properties of SD particles (e.g., crystallinity/solid state properties, morphology) that affected the performance of drug delivery (Sou et al., 2016).

Kuehl *et al.* (2014) performed pharmacokinetics study in beagle dogs to study the aerosolisation performance of SD insulin powders produced from feedstock containing human insulin (70% by weight of final solids) incorporated in dextran (30%, Dextran T10, polymer) used as a novel excipient (instead of mannitol) and compared to Exubera™ (Kuehl et al., 2014). Dextran was used as it is a GRAS substance and has high T_g that is less hygroscopic relative to mannitol (Kuehl et al., 2014). SD insulin-dextran particles exhibited corrugated particles similar to Exubera™ and generated smaller MMAD (2.8 µm) than Exubera™ (3.4 µm) (Kuehl et al., 2014). DSC analysis for SD insulin-dextran formulation and Exubera™ exposed to relative humidity (RH) of 50% showed that SD insulin-dextran formulation had higher T_g (50°C) than Exubera™ (10°C) indicating that SD insulin-dextran formulation was less susceptible to water absorption therefore less hygroscopic than Exubera™ (Kuehl et al., 2014). This was associated with higher molecular weight of dextran, high T_g and less hygroscopic compared to mannitol (Kuehl et al., 2014). Therefore, with the use of dextran physical stability of DPI formulations could be improved during storage (Kuehl et al., 2014). The results of pharmacokinetics study showed all similar between SD insulin-dextran formulation (C_{max}: 126 ± 24 µU/mL) and Exubera™ (C_{max}: 121 ± 21 µU/mL). However, SD insulin-dextran formulation demonstrated slightly higher plasma insulin concentration between 35 minutes and 90 minutes in comparison to Exubera™. This was attributed to the smaller MMAD (2.8 µm) of SD insulin-dextran formulation than Exubera™ (3.4 µm) that improved the drug deposition in the deep lung regions (Kuehl et al., 2014).

GLP-1 receptor agonist

In addition to insulin, few studies have focused on the development of GLP-1 based powders intended for pulmonary delivery (Qian et al., 2009, Kim, H. et al., 2011). GLP-1 is associated with advantages such as weight loss and low risk of hypoglycaemia compared to insulin therapy (Chapter 1.1.3) (Zheng et al., 2011, Yu et al., 2018). Qian *et al.* (2009) used spray drying to prepare GLP-1RA dry powder (BMS-686117, 11 amino acid GLP-1 receptor agonist, MW: 1528.7 g mol⁻¹) in the

presence of mannitol or trehalose intended for inhalation and conducted a pharmacokinetics study in Male Sprague-Dawley rats (Chapter 1.1.4.4) (Qian et al., 2009). Qian *et al.* (2009) selected mannitol and trehalose as excipients because these are commonly used non-reducing sugars in the formulation development for inhalation and avoid poor chemical compatibility with BMS-686117. The drug to excipient ratio used was 20:80 (w/w, BMS-686117: mannitol) or 80:20 (w/w, BMS-686117: trehalose) (Qian et al., 2009). Spray drying reduced the particle size (SD GLP-1RA particle size: 2-10 μm) and modified particle morphology (spherical) that improved powder flow property in comparison to as-received BMS-686117 powder (particle size: 2-100 μm , morphology: irregular flakes associated with poor flow property) (Qian et al., 2009). The animal study showed that SD GLP-1RA (SD BMS-686117) administered intratracheally to the lung in the rats had faster absorption (t_{max} : 0.3-0.7 hr, dose: 1 mg kg^{-1}) compared to SC administration of BMS-686117 (t_{max} : 1.2 hr, dose: 0.08 mg kg^{-1}) and exhibited high bioavailability (45%) relative to SC administration (Chapter 1.1.4.4)(Qian et al., 2009).

Freeze drying/Lyophilisation

Freeze drying (lyophilisation) is a type of drying method and usually used to dry heat sensitive materials (e.g., biological products; vaccines, antibiotics) (Aulton, Taylor, 2013). It has also been used to prepare powder biopharmaceutical formulations including inhaled insulin product, Afrezza® (Emami et al., 2018, Ziaee et al., 2019). The theory of freeze drying is based on three separate phases (solid, liquid and vapour) of water system (Aulton, Taylor, 2013). The process of freeze drying involves freezing of feed liquid solution or suspension to form ice crystals (feed samples are frozen) at low temperature (freezing process, state of matter: from liquid to solid) and then frozen water in samples is removed by sublimation using a vacuum (to drop the pressure below the triple point of the sample for sublimation) where ice crystals directly transform from its solid state to water vapour (gas phase) without going through the liquid phase (drying process, state of matter: from solid to vapour) (Aulton, Taylor, 2013, Ishwarya, Anandharamakrishnan & Stapley, 2015). The sublimation (drying process) takes place only when a temperature is below the triple point of the material/sample where all three phases (solid, liquid and vapour) coexist and pressure is not above the triple point pressure during the drying process (pressure above the triple point prevent sublimation) and the vapour generated must be removed (Aulton, Taylor, 2013). Due to the presence of solutes in feedstock, freezing temperature must be well below (typically below -18°C) the normal freezing temperature for pure water (Aulton, Taylor, 2013). Sublimation of ice crystals lead to the formation of porous structured particles (Ishwarya, Anandharamakrishnan & Stapley, 2015). Protein stability can be improved by removing water as water induce molecule mobility

(Chapter 1.2.1)(Emami et al., 2018). In freeze drying, the drying process is generally long (time consuming) with the use of high vacuum (high power/energy consumption) which can increase the operational cost (Ishwarya, Anandharamakrishnan & Stapley, 2015, Ziaee et al., 2019). Freeze drying usually limits to control particle properties such as particle size and distribution and morphology resulting in the formation of non-uniform particle size and shape therefore less frequently applied in the preparation of drug particles compared to spray drying that can control such properties (Ziaee et al., 2019).

Afrezza®

Afrezza® is a dry powder formulation of recombinant human insulin (18% w/w) with excipients of FDKP and polysorbate 80 produced by freeze drying (Al-Tabakha, 2015, Quarta et al., 2020). In Afrezza® insulin was adsorbed electrostatically onto the FDKP, which is used as the particle matrix to carry insulin to the lungs, and then freeze dried (FD) to produce particles with the aerodynamic diameter of 2.0-2.5 µm for pulmonary delivery (Al-Tabakha, 2015). Upon inhalation, insulin adsorbed onto FDKP immediately dissolve at the neutral pH in the alveolar regions (FDKP has high solubility at neutral physiological pH) where rapid insulin absorption (t_{max} : 12-15 mins) takes place and enter the systemic circulation while the FDKP which has no biological activity is excreted in the urine without metabolism (Al-Tabakha, 2015, Goldberg, Wong, 2015). In terms of storage conditions, Afrezza® requires to be stored refrigerated at 2-8°C when it is not used, however, it should be stored at room temperature for 10 minutes before use (MannKind Corporation, 2015).

Spray freeze drying

Spray freeze drying (SFD) is a relatively new drying technique (Vishali et al., 2019) yet it has been used to prepare porous powders to enhance aerosolisation performance of DPI formulations for pulmonary delivery of therapeutic peptide and protein drugs including insulin (Bi et al., 2008, Amorij et al., 2007, Pilcer, Amighi, 2010, Wanning, Süverkrüp & Lamprecht, 2015, Adali et al., 2020, Shetty et al., 2020). SFD is a combination of spray drying and freeze drying techniques and involves mainly three steps: atomisation of feedstock, rapid freezing and drying by ice sublimation (Ishwarya, Anandharamakrishnan & Stapley, 2015, Emami et al., 2018, Vishali et al., 2019). In the process of SFD, liquid solution, or suspension can be directly sprayed into liquid cryogenic medium (e.g., liquid nitrogen) where intense atomisation takes place as a spray nozzle is placed below the surface of the cryogenic medium (spray freezing into liquid: SFL) or sprayed into vapour over liquid cryogenic medium where a spray nozzle is placed above the surface of the liquid cryogenic medium therefore

atomisation takes place in the cryogenic vapour phase (spray freezing into vapour over liquid: SFV/L) (Ishwarya, Anandharamakrishnan & Stapley, 2015, Adali et al., 2020). The liquid cryogenic medium can be stirred to prevent the frozen particles clumping (Ishwarya, Anandharamakrishnan & Stapley, 2015, Adali et al., 2020). In the SFL process, liquid feedstock is atomised (broken up) into small droplets within the liquid cryogenic medium and freeze instantaneously due to the low temperature of the cryogenic medium (e.g., liquid nitrogen: -196°C) thus rapid freezing is achieved (Ishwarya, Anandharamakrishnan & Stapley, 2015). Frozen particles are then lyophilised to produce dry powders (Ishwarya, Anandharamakrishnan & Stapley, 2015). In the SFV/L process, during atomisation of feedstock the atomised droplets start to freeze while reaching to the liquid cryogenic medium and form frozen particles upon contact with the liquid cryogenic medium (Ishwarya, Anandharamakrishnan & Stapley, 2015, Adali et al., 2020). The frozen particles are then subjected to freeze drying process, transferred to a freeze dryer to remove the excess cryogenic medium and solvent to produce dry powders (Ishwarya, Anandharamakrishnan & Stapley, 2015, Adali et al., 2020). SFL process tend to produce smaller (micronised) droplets in the liquid medium due to the higher viscosity and density of liquid compared to gas when spraying into a gas phase (Ishwarya, Anandharamakrishnan & Stapley, 2015, Vishali et al., 2019, Adali et al., 2020).

The process of SFD generates various stresses (e.g., cold temperature, freezing stress, shear forces at air-water/liquid interface, and drying (dehydration) stress) that influence structure and functional stability of peptides and proteins (Walters et al., 2014, Emami, Vatanara, Najafabadi et al., 2018). Peptides and proteins exposed to shear forces at air-water/liquid interface during atomisation may cause protein adsorption, unfolding and aggregation. They are also exposed to very low temperature that protein denaturation may occur leading to protein degradation and loss of biological activity (Pilcer, Amighi, 2010, Walters et al., 2014, Emami et al., 2018, Adali et al., 2020, Shetty et al., 2020). This requires excipients to protect peptides and proteins (Emami et al., 2018). Therefore, suitable excipients of cryoprotectant (to overcome these stresses generated during SFD, protect proteins during freezing and improve protein stability) and/or lyoprotectant (to stabilise proteins and protect from degradation (e.g., denaturation) during and after freeze drying) such as sugars (e.g., mannitol, sucrose, trehalose) and amino acids (e.g., leucine, glycine) are usually added to protein feedstock prior to the SFD process. They maintain the structural stability (via water replacement and hydrogen bond formation) and provide the protection of drug structural integrity against the stresses generated during spray freeze drying (Walters et al., 2014, Emami et al., 2018, Emami et al., 2018, Vishali et al., 2019, Adali et al., 2020, Shetty et al., 2020, Mutukuri et al., 2021). For example, Emami *et al.* (2018) prepared SFD powders composed of immunoglobulin G (antibody model), trehalose and/or amino acid (leucine or glycine) as excipients to study the effects of the excipients on the

physicochemical stability of immunoglobulin G (Emami et al., 2018). Emami *et al.* (2018) found that a combination of trehalose used as a lyoprotectant and hydrophobic amino acid (leucine) or non-polar (glycine) amino acid as a stabilising agent resulted in stable SFD immunoglobulin G formulations during storage at 40°C and 75% RH for 2 months (Emami et al., 2018).

SFD offers advantages over freeze drying technique due to the rapid freezing step that prevents or minimises drug-excipient solutes phase separation in the feed solution therefore the drug can be embedded in the excipients before drug-excipient solute phase separation takes place. Also, there is no time for molecule rearrangement which results in the formation of amorphous particles before crystallisation of excipients/drugs takes place (Ishwarya, Anandharamakrishnan & Stapley, 2015, Emami et al., 2018, Adali et al., 2020). SFD also maintains stability of peptides and proteins due to rapid freezing step that minimises the exposure to air-water interface thus may prevent from denaturation or aggregation during atomisation (Wanning, Süverkrüp & Lamprecht, 2015). For the powder preparation for pulmonary delivery, SFD is also more favourable than freeze drying (Wanning, Süverkrüp & Lamprecht, 2015, Shetty et al., 2020). The properties of SFD particles such as particle size and surface morphology can be optimised by changing process parameters for atomisation and freeze drying (e.g., atomisation flow rate, feed flow rate) and/or chemical composition and concentration of the feedstock to produce powders with desired flowability (Adali et al., 2020, Shetty et al., 2020). Chemical composition/excipients and concentration of feedstock (solid content) have an influence on the surface morphology of SFD particles (Wanning, Süverkrüp & Lamprecht, 2015, Adali et al., 2020). Lowering concentration of feed solution (less solid content) produce SFD powders with higher porosity thus influence density (Wanning, Süverkrüp & Lamprecht, 2015). Very low solid concentration produces fragile powders that easily break into fragments due to high porosity (Wanning, Süverkrüp & Lamprecht, 2015).

SFD generally produces spherical and porous structure particles with high surface area (due to pores on the surface), which result from ice crystal formation during freezing step followed by sublimation in the freeze drying step, and relatively large particle size (geometric diameter, greater than 5 µm) compared to the particles produced by spray drying (Ishwarya, Anandharamakrishnan & Stapley, 2015). Such large porous spherical particles have become favourable as aerodynamic properties due to improved dispersibility, desired inter-particulate forces, and enhanced aerosolisation performance therefore suitable for pulmonary drug delivery (Wanning, Süverkrüp & Lamprecht, 2015, Weers, Miller, 2015, Ogienko et al., 2017). For large porous particles with large geometric diameter (d_{geo} : 5-30 µm) and low density (Pp : <0.1-0.4 g cm⁻³), aerodynamic diameter still represents

below 5 μm (i.e., porous particles have smaller aerodynamic diameter compared to dense particles according to *Equation 1* in Section 2.3) (Weers, Miller, 2015, Ogienko et al., 2017, Brunaugh, Smyth, 2018). The large geometric particle diameter associated with decreased surface area is less tendency to aggregate compared to smaller particles due to reduced contact area between particles (cohesive forces) and within the inhaler (adhesive forces) therefore lower inter-particulate forces (cohesive forces and adhesive forces) that promote powder dispersibility, powder emission/release from the inhaler and enhance the aerosolisation performance while particles with small aerodynamic diameter facilitate drug deposition in the lungs (improve lung deposition) (Aulton, Taylor, 2013, Wanning, Süverkrüp & Lamprecht, 2015, Ogienko et al., 2017, Brunaugh, Smyth, 2018).

Furthermore, porous particles with large geometric size deposited in the lungs could avoid macrophage (too large to be cleared by alveolar macrophages) which improve bioavailability (Aulton, Taylor, 2013, Brunaugh, Smyth, 2018). Ogienko *et al.* (2017) used SFD with the SFL process to develop DPI formulations containing a model drug of salbutamol or budesonide and glycine added as an excipient for enhanced aerosolisation performance (Ogienko et al., 2017). Glycine was used to prevent powder aggregation and improve dispersibility and flow properties of powders (Ogienko et al., 2017). SFD powders prepared by the SFL process were porous and spherical with particle diameter of 30-70 μm and exhibited good aerosolisation performance (FPF: 67.0% \pm 1.3%, inhaler device used: CDM Haler[®] at 60 L min⁻¹) despite being large particles (Ogienko et al., 2017).

GLP-1 receptor agonist

Spray freeze drying has not been employed in the development of insulin-based DPI formulations; however, it was used to develop GLP-1(7-36) amide (1% w/w) dry powders in the presence of leucine and trehalose (99% w/w, leucine: trehalose =75:25) for inhalation (Sanketkumar, Amit, December 2015). Leucine and trehalose were used as cryoprotectants to reduce the risk of GLP-1 denaturation during spray freeze drying. Leucine was also used as an aerosolisation enhancer (Sanketkumar, Amit, December 2015). GLP-1(7-36) amide powders prepared by SFD with the SFL process were highly porous with low density (0.03 g/mL) and demonstrated good aerodynamic performance (MMAD: 3.68 μm \pm 0.01 μm , FPF: 60.49% \pm 0.47%, inhaler device used: Rotahaler[®] by Cipla Ltd, India, flow rate: 60 L min⁻¹) suitable for pulmonary delivery (Sanketkumar, Amit, December 2015).

Few other studies have explored SFD to design DPI formulations with improved lung deposition (improve FPF) (Okuda et al., 2015, Otake et al., 2016). Okuda *et al.* (2015) used SFD with the SFL

process to prepare mannitol powder with the addition of leucine (75 µg) and investigated the powder dispersibility for the development of pulmonary gene delivery system. Leucine was added as a dispersion enhancer (Okuda et al., 2015). SFD powders prepared by the SFL process exhibited spherical and porous powders with small MMAD (1-3 µm) and demonstrated that the addition of leucine to mannitol improved the powder release from the capsule and inhaler device (Jethaler® at a flow rate of 28.3 L min⁻¹, powder released from the device: 97.8% ± 0.9%) and FPF (62.3% ± 3.0%) compared to SFD mannitol alone (MMAD: 15.6 µm ± 2.5 µm, powder released from the device: 74.3% ± 19.2%, FPF: 6.8% ± 1.3%) indicating enhanced powder dispersibility and improved possibility of lung drug deposition (Okuda et al., 2015). The results were explained by the porous powders along with the role of leucine as a dispersion enhancer that covered the surface of the droplets during atomisation of feed solution due to its low solubility in water and contributed to reduce the inter-particulate forces (cohesive and adhesive forces) (Okuda et al., 2015). Thus, the aerosolisation performance can be improved by introducing a particle coating using leucine. Another study by Otake *et al.* (2016) also used SFD with the SFL process to prepare spherical and porous particles of mannitol (141 mg) and leucine (5%, 7.5 mg) based powders containing sodium fluorescein (1.5 mg, “model drug”, used as a label for the quantification of the powders) (total mass: 150 mg) with improved lung deposition and flow rate independent (Otake et al., 2016). Otake et al. (2016) demonstrated that SFD leucine (5%) containing mannitol powders improved the aerosolisation performance with flow rate independent (5-53 L min⁻¹). The results were attributed to the morphology of spherical and porous particles prepared using the SFL process and reduced MMAD (MMAD: 2.43 µm ± 0.29 µm) by the addition of 5% leucine compared to MMAD without leucine (MMAD: 7.03 µm ± 0.99 µm). Also, the presence of leucine in SFD powders resulted in decreased adhesion forces consequently increased dispersibility (Otake et al., 2016). All studies using SFD have shown that SFD produce porous particles with high FPF favourable for pulmonary delivery.

2.4.2.2. Excipient free formulations

All these aforementioned studies or inhaled products were focused on the addition of excipients to insulin or GLP-1 to improve the aerosolisation performance or exploring various excipients suitable for pulmonary delivery of biopharmaceuticals (Kuehl et al., 2014, Razavi Rohani, Abnous & Tafaghodi, 2014, Sou et al., 2016, Sanketkumar, Amit, December 2015). However, due to the lung safety concern, the use of excipients in DPI formulations should be minimised (Balducci et al., 2014, Zhang et al., 2020). Therefore, excipient free formulations (e.g., insulin) have been investigated using

spray drying (Balducci et al., 2014, Quarta et al., 2020). Balducci *et al.* (2014) prepared SD bovine insulin dry powders without the inclusion of excipients for inhalation and studied *in vitro* aerosolisation performance of SD insulin powders (Balducci et al., 2014). Insulin stability test in terms of the content of degradation products (e.g., A21, HMWP) was also performed (Balducci et al., 2014).

SD insulin powders were produced from two different acidic aqueous solutions (total solid: 1% w/v): acetic acid with NaOH (1N) (pH 3.1) or acetic acid with ammonium hydroxide (10% w/w NH₄OH) (pH 3.6) and SD insulin powders produced from both feed solutions exhibited wrinkled/shrivelled shaped particles with high delivered dose (89-91%) and high FPF (>65%) under the process parameter setting (outlet temperature: 40-60°C based on inlet temperature: 120°C, drying air flow rate: 600 L hr⁻¹, aspiration: 35 m³ hr⁻¹, solution feed rate: 3.5 mL min⁻¹) (Balducci et al., 2014). However, NH₄OH based feed solution produced more deeply shrivelled particles with smaller MMAD (1.79 µm ± 0.18 µm) and higher FPF (83.6% ± 4.7%) presenting lower drug depositions in throat than powders prepared from acidic solution with NaOH that generated large MMAD (3.21 µm ± 0.11 µm) and low FPF (65.5% ± 3.0%) (Balducci et al., 2014). This was attributed to the use of volatile NH₄OH in feed solution that had an effect on the evaporation rate during spray drying and influenced particle morphology and size (Balducci et al., 2014). The stability studies showed that the content of degradants was within the required limits (below 5% for A21 and below 2% for HMWP) at 25°C (RH: 60%) for 3 months (Balducci et al., 2014). Balducci *et al.* (2014) demonstrated that excipient free insulin powder suitable for inhalation can be prepared from insulin acidic solution in NH₄OH using spray drying and provide stability at room temperature (Balducci et al., 2014). In the following study recently reported by Quarta et al. (2020), the excipient free SD insulin powder based on the study by Balducci *et al.* (2014) was further investigated in terms of pharmacokinetics and pharmacodynamics profiles of SD insulin powder (10 IU/kg) using male Wistar rats and compared with Afrezza® (10 IU/kg) (Quarta et al., 2020). Also, storage stability study on excipient free SD insulin powders, which were filled in HPMC extra dry capsules (size 3, Quali-V®-I, Spain), sealed in blisters and stored at room temperature (25°C, RH: 60%) for up to six months, was performed in terms of degradation products contents (e.g., A21 and HMWP) (Quarta et al., 2020). The SD insulin powders studied by Quarta *et al.* (2020) contained human insulin instead of bovine insulin used by Balducci *et al.* (2014) and provided good aerosolisation performance (MMAD: 0.9 µm and FPF: 91.5%) (Quarta et al., 2020). The animal study showed that SD insulin powders administered intratracheally demonstrated a faster absorption of insulin (t_{max}: 15 mins, C_{max}: 4.9 ± 1.5 mU/ml) compared to Afrezza® (t_{max}: 30 mins, C_{max}: 1.8 ± 0.37 mU/ml) (p<0.01). This was attributed to the small MMAD (0.9 µm) of excipient free SD insulin powders that led to deep lung deposition (high FPF: 91.5%) therefore enhanced

absorption while Afrezza® had larger MMAD (3.1-3.2 µm) and lower FPF (68-71%) (Quarta et al., 2020). In addition to the small MMAD, SD insulin powder in the absence of excipients would be associated with rapid dissolution therefore achieved rapid absorption rate (Quarta et al., 2020). Afrezza® uses an excipient of FDKP (insulin is adsorbed onto FDKP) that would affect the dissolution time (Quarta et al., 2020). SD insulin powders exhibited glycaemic control in rats that lowered plasma glucose levels (prevented the raise of glycaemia) after glucose administration (Quarta et al., 2020). Similar glycaemic control was also observed in Afrezza® (Quarta et al., 2020). The stability test on SD insulin powders filled in extra dry HPMC capsules and sealed in blisters showed that the content of degradation products (e.g., A21 and HMWP) was within the required limits (below 5% for A21 and below 2% for HMWP) at 25°C for six months (Quarta et al., 2020). This could avoid cold chain storage conditions when patients received their medication (Quarta et al., 2020).

In another study, Ung *et al.* (2016) also prepared SD insulin dry powders without excipients for inhalation and studied *in vitro* aerosolisation performance of SD insulin powders (Ung et al., 2016). Ung *et al.* (2016) tried to adjust the composition of insulin feedstock for spray drying by adding fraction of ethanol (e.g., 5% w/w) to water to optimise particle properties (e.g., particle size, morphology and interparticle interactions) of SD insulin powders and avoid early drug deposition in mouth and throat therefore increase drug delivery to the lungs (Ung et al., 2016). Feed solution (total solid: 0.75% w/v) for spray drying was prepared by dissolving human insulin powder alone in water or water with the addition of ethanol fraction (5% w/w) and the pH of the feed solutions was adjusted to 7.5-7.9 with sodium hydroxide (Ung et al., 2016). SD insulin powders prepared from water-ethanol solution exhibited wrinkled shape particles/corrugated particles, which was similar to the morphology of Exubera®, lowered interparticle cohesive forces due to the surface property (surface roughness) of the particles (corrugated particles with asperities on the surface) and exhibited suitable MMAD (1.7-2.0 µm) for pulmonary delivery (Ung et al., 2016). This resulted in lower drug deposition in mouth and throat (i.e., Alberta Idealised Throat, designed for adult human upper respiratory tract geometry) therefore achieved high FPF (82-85%, inhaler device used: blister-based Simoon™ inhaler with high resistance by Novartis Pharmaceuticals Corp, flow rate: 33 L min⁻¹) (Ung et al., 2016). The addition of ethanol to water influences physicochemical properties of solvent systems (e.g., increase viscosity, decrease insulin solubility, and low surface tension in the presence of ethanol) that affect the particle formation during spray drying (e.g., atomisation, drying/solvent evaporation) therefore influence particle properties of SD powders (morphology and interparticle interactions) (Ung et al., 2016). Improved drug deposition in the lungs therefore enhanced aerosolisation performance of excipient free SD powder formulations can be achieved by changing

the feedstock composition for spray drying to modulate particle properties (Ung et al., 2016). All these studies have shown that using spray drying to prepare excipient free insulin powders for inhalation is feasible and can produce powders with small MMAD and high FPF and minimise drug deposition in the mouth and throat therefore improve aerosolisation performance (pulmonary drug deposition) (Balducci et al., 2014, Quarta et al., 2020, Ung et al., 2016). For systemic application, drug deposition in the deep lung regions is critical (Ung et al., 2016).

2.4.3. Carrier-based dry powder inhaler formulations

Carrier-based DPI formulations are composed of drug powder (d_{aer} : 1-5 μm) and carrier powder (particle size: 50-200 μm) (Section 2.4.1)(Faulhammer et al., 2018, Lechanteur, Evrard, 2020). Carriers are used to address the cohesive properties of the drug particles (d_{aer} : 1-5 μm); to improve flowability of the drug particles and dispersion (Section 2.4) (Peng et al., 2016, Yeung et al., 2018). Carrier-based DPI formulations are prepared as adhesive mixtures (drug-carrier blends/mixtures) where inter-particulate adhesive forces (drug-carrier adhesive forces) exist between drug and carrier (Section 2.4) such as van der Waals, electrostatic, interlocking, and capillary forces (Figure 6) (Peng et al., 2016, Yeung et al., 2018). These adhesive forces facilitate the stability of the drug-carrier mixtures (Nokhodchi, Martin, 2015). Van der Waals forces are predominantly present as physical interactions between the drug and carrier particles when humidity is controlled and electrostatic force is associated with different surface charges between two materials (e.g., drug and carrier particle surfaces) (Peng et al., 2016). Interlocking force is derived from the drug fitting into the asperities of the carrier surface when drug particles contact with the carrier surface roughness (Peng et al., 2016). Capillary forces are introduced from environmental conditions such as moisture (Peng et al., 2016, Elsayed, Shalash, 2018). These drug-carrier adhesive forces have a significant effect on the process of drug particle detachment from the carrier surfaces (drug-carrier detachment) and consequently affect the efficiency of pulmonary drug delivery (i.e., drug deposition in the lungs, FPF) and overall aerosolisation performance of DPI formulations (Nokhodchi, Martin, 2015, Peng et al., 2016, Brunaugh, Smyth, 2018). The process of drug-carrier detachment is also influenced by dispersion forces generated in a DPI device during inhalation such as shear and friction forces (particle-inhaler wall friction) responsible for deagglomeration of cohesive particles (agglomerates), drag or lift forces (particles slide or roll on the surface before detachment), and inertial forces (particle-particle collision and particle-inhaler wall collisions) to aid the drug particle detachment from the carrier surface (Kaialy, Waseem, Nokhodchi, 2013, Nokhodchi, Martin, 2015, Weers, Miller, 2015, Elsayed, Shalash, 2018). Therefore, aerosolisation performance of carrier-based DPI

formulations (drug particle inhalation performance) is based on the balance between inter-particulate forces (cohesive and adhesive forces) and dispersion forces (e.g., shear forces, drag and lift forces, inertial forces) during inhalation (Kaialy, Nokhodchi, 2013, Elsayed, Shalash, 2018).

For drug delivery to the lungs from carrier-based DPI formulations, mainly four phases are involved in the drug deposition in the respiratory tracts (Zhang et al., 2018). Upon inhalation, the formulation of drug-carrier mixture is fluidised (fluidisation process: air is entered into the powder formulation to create shear force and turbulence to fluidise powder mass and form fluidlike gas-particle dispersion, powder bed) and dispersed (Weers, Miller, 2015, Lavorini, Pistolesi & Usmani, 2017, Zhang et al., 2018). Then, the drug-carrier mixture (the drug transported by carrier) passes through the oropharynx region where drug-carrier adhesive mixture collide with the surface of the respiratory tract by inertial impaction; large carrier particles impacted on the surface of the upper way regions are cleared (particles with $>10\ \mu\text{m}$ deposit by inertial impaction) and drug particles detach from the carrier particles and further move into the lower airways (Lavorini, Pistolesi & Usmani, 2017, Zhang et al., 2018). In the lower airways, drug particles detach from carrier particles by airflow moving to the lungs and drug particles deposit in the deep lung regions by sedimentation while the carrier particles get stuck on the narrow bronchioles and cleared by swallowing (Zhang et al., 2018). Carrier particles are designed not to reach the lungs, therefore, only the drug particles detached from the surface of the carrier particles during inhalation should be delivered to the desired deep lung regions (Peng et al., 2016).

However, drug deposition in the desired deep lung regions is a challenge due to inter-particulate forces involved between drug and carrier particles (drug-carrier adhesive force) (Nokhodchi, Martin, 2015, Peng et al., 2016). Poor drug detachment from the carrier surface (insufficient drug-carrier dispersion) due to strong adhesive forces can cause high drug deposition as drug-carrier mixture in oropharyngeal regions, which limit the drug deposition in the lower respiratory airways and negatively impact the delivery efficiency of the aerosolised drug to the lungs (i.e., low FPF) (Yeung et al., 2018, Zhang et al., 2018). To reach the deep lung regions for systemic drug absorption the drug particles delivered by carriers need to detach from the surface of the carrier particles by overcoming inter-particulate adhesive forces and minimising early drug deposition in the oropharynx region (oropharyngeal deposition) (Nokhodchi, Martin, 2015, Peng et al., 2016, Weers, Miller, 2015, Zhang et al., 2018).

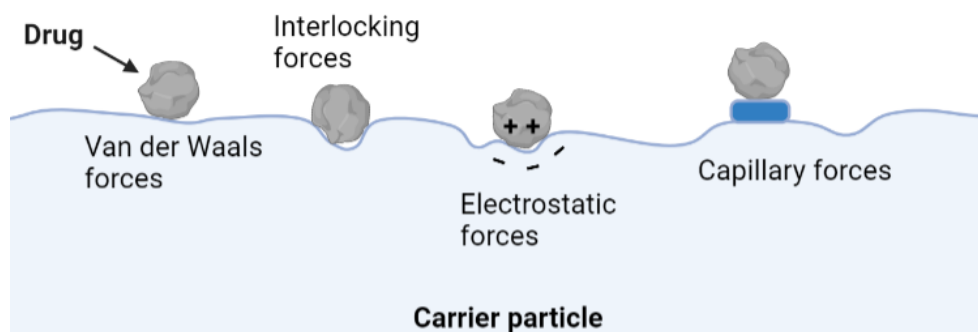


Figure 6: Illustration of inter-particulate adhesive forces (interactions) between drug and carrier particle surface. Created in BioRender.com based on Peng *et al.* (2016).

The contact area between the surface of the drug and carrier particles is dependent on surface morphology influencing inter-particulate forces of attraction and surface roughness affecting drug adherence to and detachment from the carrier surface, therefore having a significant impact on the aerosolisation performance of DPI formulations (Nokhodchi, Martin, 2015, Weers, Miller, 2015, Peng *et al.*, 2016). Surface roughness for carriers is usually described based on the scale of surface irregularities (i.e., asperities, pores, discontinuities) relative to the size of drug particles (Nokhodchi, Martin, 2015, Peng *et al.*, 2016, Elsayed, Shalash, 2018). Studies reporting on the effect of surface morphology/roughness on drug aerosolisation performance are contradictory, where different surface properties alter the surface contact area of drug to carrier adhesion leading to different drug dispersibility (Nokhodchi, Martin, 2015, Shalash, Molokhia & Elsayed, 2015, Peng *et al.*, 2016). Generally, carrier surfaces with large scale irregularities/asperities that are larger than the drug particle size (macroscale roughness, Figure 7C) are associated with strong adhesive forces due to the large drug-carrier contact area where the drug particles can fit into the asperities (Nokhodchi, Martin, 2015, Shalash, Molokhia & Elsayed, 2015, Elsayed, Shalash, 2018). The carrier surface with macroroughness provide shelter for drug particles from drag and lift forces during inhalation therefore have a negative effect on drug dispersion and drug detachment from carriers (e.g., poor drug detachment from carriers) (Shalash, Molokhia & Elsayed, 2015, Elsayed, Shalash, 2018). This requires strong dispersion forces (e.g., drag and impaction) within DPI devices during aerosolisation to overcome inter-particulate forces to fluidise powders (Shalash, Molokhia & Elsayed, 2015). In contrast, carrier surfaces with smaller scale asperities that are smaller than the drug particle size (nanoscale roughness, Figure 7A) are favourable for the drug-carrier adhesion as the contact area is smaller and associated with weaker adhesive forces that lead to increased drug detachment from

carriers and high FPF (Nokhodchi, Martin, 2015, Shalash, Molokhia & Elsayed, 2015, Peng et al., 2016).

Shalash, Molokhia and Elsayed (2015) studied the effects of carrier surface properties (surface roughness with pore size in diameter) on aerosolisation performance of carrier-based DPI formulations containing fluticasone propionate as a model drug and each of eight different raw carrier materials selected (e.g., mannitol, sucrose, lactose, etc) (Shalash, Molokhia & Elsayed, 2015). Shalash, Molokhia and Elsayed (2015) demonstrated that the carrier pore size influenced the aerosolisation performance of drug-carrier dry powder mixtures with variable FPF values depending on pore size (FPF_{< 4.46 μm}: 2.8-16.0%, inhaler device used: Aerolizer® at 60 L min⁻¹) (Shalash, Molokhia & Elsayed, 2015). Carriers with nanoscale pores (<1.00 μm, pores smaller than drug particles) had a positive influence on the performance due to a reduction of the carrier contact area therefore inter-particulate adhesion forces (Shalash, Molokhia & Elsayed, 2015). In contrast, carriers with macroscale pores (>8.06 μm, pores larger than drug particles) had a negative effect on the performance as macropores shield drug particles from forces (e.g., drag and lift) during aerosolisation thus affected drug dispersion (Shalash, Molokhia & Elsayed, 2015). Carriers with microscale pores surface (surface roughness) similar to the size of drug particles (e.g., 1.00-8.06 μm, irregularities/pore size similar to drug particle size, Figure 7B) showed a positive effect more on during mixing process than during aerosolisation (Shalash, Molokhia & Elsayed, 2015). Microscale pores/roughness were associated with increased effective contact area between drug and carrier that provided shelter for drug particles from drag forces during mixing and adequate adhesive forces with effective frictional and press-on forces. This had a positive effect on the drug adhesion to the carrier surfaces during mixing and deagglomeration of cohesive drug particles during inhalation that resulted in sufficient drug-carrier detachment and improved aerosolisation performance (Shalash, Molokhia & Elsayed, 2015). Shear and friction forces also known as press-on forces generated during mixing, which increase with the duration of mixing, are the forces to press the drug particles on the carrier particles and responsible for drug particle distribution over the carrier surface during mixing therefore have an influence on a degree of blend homogeneity (Kaialy, Nokhodchi, 2013, Nokhodchi, Martin, 2015, Shalash, Molokhia & Elsayed, 2015, Elsayed, Shalash, 2018).

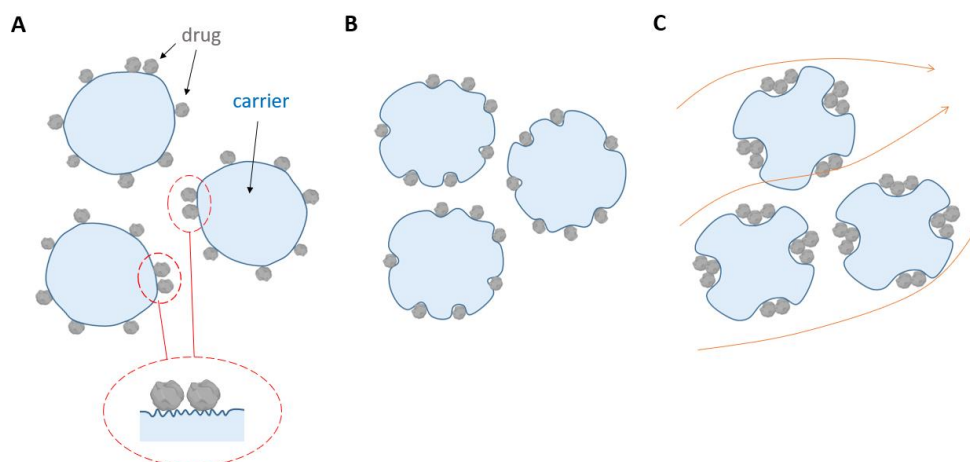


Figure 7: Schematic illustration of drug (grey) and carrier (blue) particles mixtures based on the carrier surface roughness. A: nanoscale roughness, B: microscale roughness, C: macroscale roughness. Created in BioRender.com based on Shalash, Molokhia and Elsayed (2015).

In the development of carrier-based DPI formulations, relatively small amounts of drugs (<10%) are used in DPI formulations, therefore, the overall DPI performance is generally dependent on the carrier material selections and properties of carriers such as morphology and surface roughness that determine the deposition pattern of the aerosolised therapeutic drug particles in the respiratory tracts (Nokhodchi, Martin, 2015, Peng et al., 2016). Lactose is the most used carrier in commercially available DPI formulations (Nokhodchi, Martin, 2015, Zhang et al., 2020). However, lactose may not be the carrier of choice for peptides/proteins as it is a reducing sugar associated with chemical incompatibility (e.g., Maillard reactions, Section 2.4.2.1) (Rahimpour, Kouhsoltani & Hamishehkar, 2014, Zhang et al., 2020). Non-reducing sugars such as mannitol, sorbitol, sucrose, and trehalose (Figure 8) that are not associated with Maillard reaction have been previously investigated as alternative carrier candidates in the development of DPI formulations for therapeutic peptide and protein drugs (Rahimpour, Kouhsoltani & Hamishehkar, 2014, Shalash, Molokhia & Elsayed, 2015). Among them mannitol has been most frequently studied as an alternative carrier to lactose as it is non-reducing sugar, GRAS substance provided by FDA database (U.S. Food & Drug Administration, 2020)(Section 2.4.2.1) and was used in the previously marketed inhaled insulin product, Exubera® as a bulking agent and stabiliser (Al-Tabakha, 2015) therefore commercially established excipient (Rahimpour, Kouhsoltani & Hamishehkar, 2014, Weers, Miller, 2015, Hertel, Birk & Scherließ, 2020). Besides, mannitol inhalation powder products are currently available in the UK, such as Osmohale® for the assessment of respiratory conditions (e.g., asthma) (emc, 2019b) and Bronchitol® for the

treatment of cystic fibrosis (emc, 2019, European Medicines Agency, 2022). Thus mannitol is an attractive carrier candidate for DPI formulations.

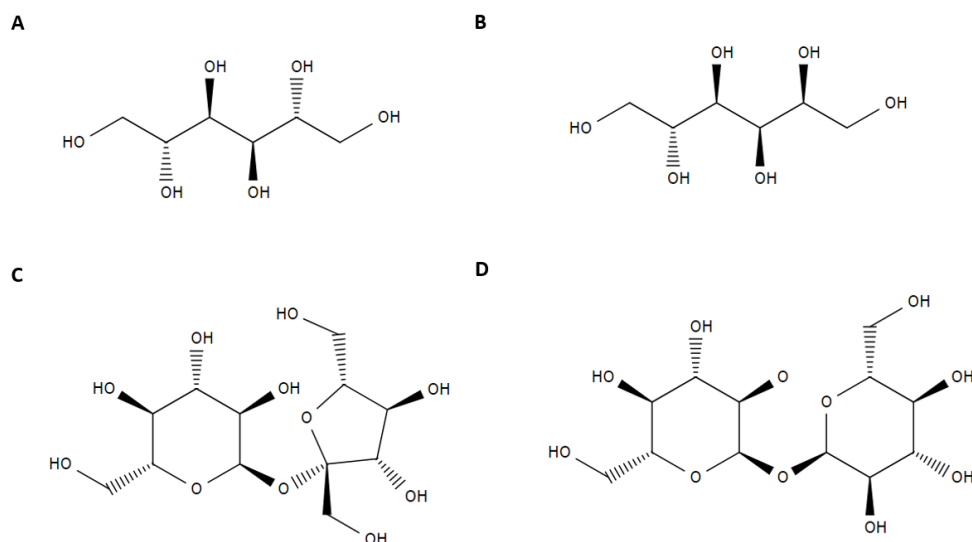


Figure 8: Chemical structures of alternative carrier candidates for dry powder inhaler formulations. A: D-Mannitol, B: Sorbitol, C: Sucrose, D: Trehalose. (Created in CAS SciFinderⁿ)

To enhance drug delivery efficiency from carrier-based DPI formulations therefore FPF, these inter-particulate forces need to be optimised (Yeung et al., 2018). Compared to low dose DPI formulations (e.g., drug dose requirement is within μg range, drug concentrations: 0.1-4%)(Section 2.4), high dose DPI formulations (drug dose in mg range, drug concentrations: 5-10%) contain greater number of fine drug particles associated with increased cohesive-adhesive forces (inter-particulate forces) leading to higher tendency of particle agglomeration and poor drug detachment from carriers (Sibum et al., 2018, Yeung et al., 2018). Also, the addition of carrier to a formulation increases the total powder mass (Yeung et al., 2018). This requires higher energy (e.g., inspiratory air) to overcome the forces to aerosolise the formulation powders for efficient deagglomeration and dispersion thus achieve efficient aerosolisation (Peng et al., 2016, Yeung et al., 2018). High airflow velocity promotes greater drug-carrier detachment (Peng et al., 2016, Yeung et al., 2018). Particle engineering such as spray drying, freeze drying and spray freeze drying have been used as a formulation strategy to optimise inter-particulate forces by modifying morphology or surface roughness of carrier particles and improve aerosolisation performance of drug particles from DPI

formulations (Nokhodchi, Martin, 2015). Using engineered carriers offer advantages as therapeutic peptide and protein drugs can be delivered by loading the drug particles on the engineered carriers (Mehta, 2018). Therefore, some studies have focused on carrier particle engineering and characterising carrier properties.

2.4.3.1. Particle engineering

In order to optimise the delivery of inhaled drugs using DPIs, various particle engineering approaches including spray drying, freeze drying, and spray freeze drying were explored and the addition of excipients to manipulate the properties of the carrier. Peng *et al.* (2017) and Zhang *et al.* (2018) both focused on the modification of mannitol carrier surface roughness through particle engineering such as spray drying to enhance the efficiency of drug deposition and aerosolisation performance of DPI formulations containing budesonide (Peng *et al.*, 2017, Zhang *et al.*, 2018). Feed solutions (solid concentration: 2.5% w/v) for spray drying were prepared by dissolving mannitol with ammonium carbonate used as a pore forming agent in water to produce porous and hollow mannitol powders with nano scale asperities (Peng *et al.*, 2017). Pharmacokinetics profiles were studied in Sprague Dawley rats for the feasibility of using SD porous mannitol carrier on pulmonary drug delivery efficiency (drug deposition in the lungs) and compared with SD non-porous spherical mannitol carrier prepared without using the pore forming agent (ammonium carbonate) (Peng *et al.*, 2017). SD mannitol carriers prepared with the use of ammonium carbonate exhibited nanoporous particles (mean pore size: 6 nm) with particle size of 5 μm and demonstrated better aerosolisation performance (FPF: between $33.29\% \pm 2.24\%$ and $56.75\% \pm 1.54\%$, inhaler device used: single dose inhaler Turbospin™ (PH&T, Italy) at airflow rate of 60 L min^{-1}) and higher budesonide concentration in the lungs (C_{max} : $149.94 \pm 15.27 \mu\text{g/g}$) when compared to DPI formulation containing SD non-porous spherical mannitol carrier with smooth surface (FPF: $20.30\% \pm 1.42\%$, $p < 0.05$, C_{max} : $75.29 \pm 10.83 \mu\text{g/g}$) (Peng *et al.*, 2017, Zhang *et al.*, 2018). Their results were attributed to the nanoscale porous structures that reduced the contact area between drug and carrier and consequently lowered inter-particulate adhesive forces. This facilitated drug-carrier detachment resulting in improved lung depositions (Peng *et al.*, 2017, Zhang *et al.*, 2018). Particle engineering of carriers using spray drying has enhanced aerosolisation performance of DPI formulations by modifying surface roughness (reduced inter-particulate forces between drug and carrier particles) (Peng *et al.*, 2017, Zhang *et al.*, 2018).

Kaialy and Nokhodchi (2013) used freeze drying to modify the morphology of mannitol carrier and studied the aerosolisation performance of DPI formulations containing salbutamol sulphate as a model drug and mannitol as a carrier (Kaialy, Nokhodchi, 2013). Three different types of mannitol carriers: namely commercial mannitol, SD mannitol or FD mannitol were used to compare aerosolisation performance of salbutamol sulphate DPI formulation (Kaialy, Nokhodchi, 2013). DPI formulation with FD mannitol carrier demonstrated higher FPF (FPF: $46.9\% \pm 3.6\%$, inhaler device used: Aerolizer® at flow rate of 92 L min^{-1}) compared to the formulations using commercial mannitol (FPF: $16.8\% \pm 1.3\%$) or SD mannitol carrier (FPF: $24.0\% \pm 2.7\%$), indicating the improved aerosolisation performance when freeze drying was used for mannitol carrier preparation (Kaialy, Nokhodchi, 2013). The results were attributed to different morphology (shape irregularity) and surface roughness of mannitol carriers associated with different inter-particulate forces therefore affected particle depositions in the respiratory airways and aerosolisation performance of DPI formulations (Kaialy, Nokhodchi, 2013). FD mannitol exhibited the smallest nanoscale roughness (8.7 nm) associated with low drug-carrier contact area and reduced drug-carrier adhesive forces therefore exhibited easier drug-carrier particles detachment than drug particles attached to commercial mannitol (roughness: 220 nm) or SD mannitol (roughness: 157 nm) carriers (Kaialy, Nokhodchi, 2013). However, FD mannitol carrier exhibited variable particle size, shapes and FPF (Kaialy, Nokhodchi, 2013).

The inclusion of the carrier in the formulations overcomes the issues of poor flow properties of the drug powders (flowability and dispersion) therefore improve powder flow, however, face challenges to deliver high dose dry powders via DPIs due to the increased total mass of adhesive mixtures/powders to be inhaled (Section 2.4.1) (Scherließ, Etschmann, 2018, Yeung et al., 2018). The amount of powders to be inhaled is limited by the energy provided by the patient's inhalation effort (Brunaugh, Smyth, 2018). As the drug dose increases more drug particles are available to deliver to the lungs, however, the aerosolisation performance tend to decrease (not all particles reach the lungs) with increasing doses due to increased cohesive-adhesive forces resulting in poor drug detachment and high drug deposition in the oropharynx (Section 2.4.3)(Yeung et al., 2018). This causes irritation of the upper airways resulting in undesirable adverse events (e.g., cough and bronchospasms) although they are generally reported to be mild to moderate (Yeung et al., 2018). Therefore, to facilitate drug-carrier detachment and improve aerosolisation performance of DPI formulations, some studies focused on the addition of hydrophobic amino acids (e.g., leucine) to the carriers to optimise inter-particulate adhesive forces by introducing a particle coating (Nokhodchi, Martin, 2015, Kaialy, Nokhodchi, 2016, Otake et al., 2016).

Kaialy and Nokhodchi (2016) prepared FD mannitol carrier and mixed it with leucine to improve aerosolisation performance of DPI formulation containing budesonide and compared the aerosolisation performance to DPI formulation with FD mannitol carrier prepared without leucine (Kaialy, Nokhodchi, 2016). The addition of leucine to FD mannitol carrier exhibited a higher FPF (FPF: $34.6\% \pm 1.9\%$, inhaler device used: Aerolizer® at flow rate of 92 L min^{-1}) compared to the formulation using FD mannitol carrier without leucine (FPF: $28.6\% \pm 1.2\%$) (Kaialy, Nokhodchi, 2016). The results were attributed to the morphology of porous FD mannitol particles that reduced the drug-carrier contact area and the addition of leucine assisted the reduction of drug-carrier adhesive forces (Kaialy, Nokhodchi, 2016). Leucine showed an anti-adhesive effect that reduced the drug-carrier adhesive forces, hence facilitated the drug particle detachment from FD mannitol carrier and improved drug aerosolisation performance (Kaialy, Nokhodchi, 2016).

Since spray freeze drying is a relatively new drying technique (Vishali et al., 2019), it has not been applied on carrier particle engineering yet. However, it has been explored to develop SFD drug powders to improve lung deposition and enhance formulation performance as the properties of SFD porous powders are advantageous for inhalation (see Section 2.4.2.1)(Wanning, Süverkrüp & Lamprecht, 2015).

2.5. Dry powder inhaler devices for pulmonary delivery

DPIs are devices used to deliver dry powder formulations of therapeutic drugs via pulmonary route for local or systemic applications (Islam, Gladki, 2008). When patients inhale through the DPI devices, air is introduced into DPI formulations (fluidisation) to fluidise the powder formulations where the particles formed by inter-particulate forces (cohesive and adhesive forces) are deagglomerated (broken up) into individual particles (deagglomeration process) and drug particles are dispersed into the patients' lungs (for carrier free DPI formulations) or drug particles are detached from the carrier surface by overcoming adhesive forces and delivered to the lungs (for carrier-based DPI formulations) (Islam, Gladki, 2008, Son, McConville, 2008, Weers, Miller, 2015, Lavorini, Pistolesi & Usmani, 2017, Yeung et al., 2018, Levy et al., 2019).

The efficiency of pulmonary drug delivery via DPI devices depends not only on the properties of DPI formulation components (e.g., particle size, morphology, powder flow of drug-excipient

incorporated particles or drug particles for carrier free formulations and drug and carrier particles properties for carrier-based DPI formulations), but also on the choice of DPI device (design, performance) together with patient factors (e.g., lung anatomy and physiology, health condition, disease states, age etc.) and patients' inhalation profiles (e.g., inspiratory flow rate, tidal volume, lung volume) (Healy et al., 2014, Yang, Chan & Chan, 2014, Nokhodchi, Martin, 2015, Yeung et al., 2018). Patient factors with variable inhalation profiles lead to variability in drug delivery efficiency and drug deposition in the lungs (inconsistent drug delivery to the lungs) that affect DPI formulation performance therefore therapeutic effect of the inhaled drug (Section 2.1) (Islam, Gladki, 2008, Healy et al., 2014, Berkenfeld, Lamprecht & McConville, 2015).

DPI devices used for DPI formulations have a significant effect on drug delivery efficiency and pulmonary drug deposition due to different device designs (Yang, Chan & Chan, 2014, Nokhodchi, Martin, 2015, Leung et al., 2016, Yeung et al., 2018). DPI devices generally consist of multiple components such as air inlet and outlet, mouthpiece, drug holder/dosing chamber (e.g., to hold dry powder formulation) and rotating impellers, grid/mesh, or cyclone designed to generate forces (e.g., swirling, turbulence, and particle-particle collisions) for drug particle deagglomeration and dispersion (Islam, Gladki, 2008, Islam, Cleary, 2012, Leung et al., 2016, Yeung et al., 2018). All these different designs have a significant effect on fluidisation and dispersion of DPI formulations and consequently affect drug delivery efficiency, aerosolisation performance of DPI formulations and therapeutic effect (Islam, Gladki, 2008, Islam, Cleary, 2012, Leung et al., 2016, Yeung et al., 2018). In addition, the design of devices affects the aerosol performance of carrier free and carrier-based DPI formulations differently (Leung et al., 2016). Leung *et al.* (2016) studied the effect of the inhaler design using Aerolizer® with original mesh/grid design manufactured by Plastiap S.p.A. (Italy) and Aerolizer® with modified designed grid structure (cross-grid, bigger void space, open grid structure) on the aerosol performance between carrier free (salbutamol sulphate alone, particle size: $1.22 \mu\text{m} \pm 0.18 \mu\text{m}$) and carrier-based (salbutamol sulphate and lactose carrier, particle size: $57.65 \mu\text{m} \pm 1.2 \mu\text{m}$) DPI formulations with three different drug to carrier mass ratios (drug to carrier weight ratio: 1:5, 1:10 and 1:100, $10.0 \pm 1 \text{ mg per capsule}$)(Leung et al., 2016). Aerolizer® with original grid design exhibited lower FPF at flow rate of 100 L min^{-1} for carrier-based DPI formulations (FPF: $31.8\% \pm 0.7\%$, $32.1\% \pm 0.7\%$, $12.9\% \pm 1.0\%$ for 1:5, 1:10 and 1:100 carrier-based DPI formulation, respectively) than carrier free formulation had high FPF (FPF: $47.5\% \pm 3.8\%$) (Leung et al., 2016). Using Aerolizer® with modified grid design resulted in a significant further decrease in the FPF values for both carrier free (FPF: $47.5\% \pm 3.8\% \rightarrow 36.8\% \pm 1.2\%$, $p < 0.01$) and 1:5 and 1:10 carrier-based formulations (FPF: $31.8\% \pm 0.7\% \rightarrow 20.9\% \pm 2.6\%$ for 1:5 carrier-based, $32.1\% \pm 0.7\% \rightarrow 21.9\% \pm 1.5\%$ for 1:10 carrier-based

formulations, $p < 0.05$) compared to the FPF values obtained from Aerolizer® with original grid design (Leung et al., 2016). The results were attributed to the modified grid design that generated more swirling flow within the mouthpiece thus increased the impaction between the powder and mouthpiece and caused the powder retention in the mouthpiece resulting in lower FPF values (Leung et al., 2016). However, the inhaler device (Aerolizer®) with two different grid designs had no influence on FPF values when drug to carrier ratio was 1:100 (FPF: $12.9\% \pm 1.0\%$ for original grid and $12.1\% \pm 1.3\%$ for cross grid, $p > 0.05$) and showed poor aerosol performance (lowest FPF) (Leung et al., 2016). The ratio of drug to carrier in carrier-based DPI formulations also had an influence on drug delivery efficiency, drug deposition patterns, aerosolisation performance of DPI formulations (Leung et al., 2016). 1:100 carrier-based DPI formulation contained low drug content therefore high carrier content where the surface of the carrier was not fully covered with drug particles due to high carrier content and low free drug particles available and strong drug-carrier adhesion forces were present (Leung et al., 2016). Therefore, particle collisions with the mouthpiece and airflow turbulence were not strong enough to deagglomerate the drug particles from the carrier surface thus low powder dispersion that resulted in deposition as drug-carrier mixtures in NGI Stage 1 (low FPF) (Leung et al., 2016). On the other hand, 1:5 and 1:10 DPI formulations contained less carrier content thus more drug content relative to lactose carrier where the surface of the carrier was covered with multi layers of drug particles and more free drug particles or particle agglomerates available for aerosolisation that resulted in higher FPF values (Leung et al., 2016). Such free drug particles or particle agglomerates were associated with better dispersion as drug particles were not attached to the lactose carrier surface and freely available (Leung et al., 2016). However, this adversely affects the mechanical powder stability (e.g., powder handling and dosing) and dose delivery consistency (uniform drug delivery into the lungs) as drug-carrier adhesive forces are to stabilise the drug-carrier mixtures (Chapter 2.4) (Kaialy, Waseem, 2016, Sibum et al., 2018, Scherließ, Etschmann, 2018). The efficiency of drug delivery to the lungs (drug deposition in the lungs) and aerosol performance for carrier-based DPI formulations exhibited more complex as different drug to carrier mass ratio (different drug and carrier contents in the formulations) was associated with different inter-particulate forces (adhesive forces) affecting drug particle detachment from the carrier surface therefore the fraction of the particles reached the lungs (lung drug deposition). Aerosol performance was dependent on the drug to carrier mass ratio associated with different inter-particulate forces (adhesive forces) (Leung et al., 2016).

Therefore, in the development of DPI formulations the design of inhaler devices and type of DPI formulations (i.e., carrier free and carrier-based) along with patients' factors, all should be carefully considered together for efficient drug delivery to the lungs, enhanced aerosolisation performance of

DPI formulations and therapeutic effect (Islam, Gladki, 2008, Yang, Chan & Chan, 2014, Nokhodchi, Martin, 2015, Yeung et al., 2018). The optimised DPI formulations can be achieved by developing DPI formulations together with developing new devices (Berkenfeld, Lamprecht & McConville, 2015).

2.5.1. Ideal DPI devices

The ideal DPI devices should be simple and easy to use and carry, promote sufficient energy to aerosolise (fluidise, deagglomerate and disperse) the powder formulation during inhalation and deliver consistent and accurate drug dose to the lungs efficiently and reproducibly over a wide range of inspiratory flow rate or regardless of patient's inhalation flow, therefore maximise the drug delivery efficiency to the lungs with low dose variability and therapeutic effect of the inhaled drug. In addition, the devices should be cost effective (Islam, Gladki, 2008, Healy et al., 2014, Berkenfeld, Lamprecht & McConville, 2015, Nokhodchi, Martin, 2015, Weers, Miller, 2015, Levy et al., 2019). DPI devices should be designed based on the type of DPI formulations (Berkenfeld, Lamprecht & McConville, 2015). It is also important to design DPI devices from patient's perspective for improved patient compliance and adherence to therapy that is associated with better treatment outcomes (Son, McConville, 2008, Berkenfeld, Lamprecht & McConville, 2015, Levy et al., 2019). For example, Exubera[®] used a large device with complicated mechanism for actuation (Son, McConville, 2008) that resulted in poor patient acceptability, poor sales and withdrawn from the market (Chapter 1.1.4). Patient's perspective (e.g., time consuming for preparation for inhalation) was one of the reasons for the product withdrawal (Ziaee et al., 2019). Additionally, certain delivery device features such as dose counters/ indicators incorporated into the device should ideally be considered in the development of new DPI devices for improved patient compliance (Son, McConville, 2008).

2.5.2. Types of DPI devices

There are two types of DPI devices based on the mechanism of powder dispersion: passive devices (breath actuated devices) and active devices (Yang, Chan & Chan, 2014). Passive DPI devices use patient's inspiratory airflow as energy source to generate forces (e.g., fluid shear forces, airflow turbulence, inertial, impaction forces/frictional forces for particle-particle or particle device collisions) for powder fluidisation, deagglomeration and dispersion thus the device performance is dependent on patient's inspiratory effort. On the other hand, active DPI devices use an energy source (e.g., compressed gas) incorporated in the device to fluidise and disperse the powder

formulations thus less dependent on patient's inspiration airflow (inspiratory airflow rate independent) and associated with precise dose and reproducible aerosols delivery (Islam, Gladki, 2008, Islam, Cleary, 2012, Yang, Chan & Chan, 2014, Berkenfeld, Lamprecht & McConville, 2015, Nokhodchi, Martin, 2015). However, the design of active devices is complicated (for example, Exubera[®] used compressed air for insulin powder dispersion) and more expensive to produce compared to passive devices therefore passive DPI devices are more commonly used compared to active DPI devices (Islam, Cleary, 2012, Nokhodchi, Martin, 2015).

2.5.3. Passive DPI devices

Passive (breath actuated) DPI devices rely on patient's inspiratory airflow rate; the energy required for deagglomeration and dispersion is generated by patient's inspiratory effort, therefore drug deposition in the lungs is also dependent on patient's inspiratory effort (Berkenfeld, Lamprecht & McConville, 2015, Nokhodchi, Martin, 2015). This affects the delivery efficiency due to variability in patient's inhalation force/effort that leads to inconsistent lung drug delivery (Berkenfeld, Lamprecht & McConville, 2015, Nokhodchi, Martin, 2015). To deliver the drug to the lungs using passive DPI devices, patients should be able to generate sufficient airflow requirement through DPI devices for deagglomeration and dispersion. Insufficient inspiratory flow can result in incomplete deagglomeration process thus low drug particles deposition in the lungs (Islam, Cleary, 2012, Levy et al., 2019). Therefore, to aerosolise the powders for therapeutic effect, passive DPIs devices require forceful inhalation by the patients to generate sufficient airflow through the DPI devices to prevent incomplete deagglomeration process and low drug deposition in the lungs. Passive DPIs devices should be able to deliver consistent drug dose to the lungs (Islam, Gladki, 2008, Healy et al., 2014, Lavorini, Pistolesi & Usmani, 2017, Levy et al., 2019).

2.5.4. Airflow resistance

DPI devices have device specific airflow resistance (resistance to inhaled airflow) in the range from low resistance (e.g., Spinhaler[®] by Fisons/Sanofi-Aventis, Aerolizer[®] by Novartis), medium (e.g., Novolizer[®] by Novartis, Diskus[®] and Ellipta[®] by GlaxoSmithKline (GSK), Nexthaler[®] by Chiesi) to high resistance (e.g., Handihaler[®] by Boehringer-Ingelheim, Turbohaler[®] (Turbuhaler[®] under FDA approval) by AstraZeneca, Easyhaler[®] by Orion Pharma, Nexthaler[®] by Chiesi, Dreamboat by Mannkind Corp) that require different inspiratory effort from patients (device specific inhalation

flow rate) for efficient powder deagglomeration and dispersion (Islam, Cleary, 2012, Healy et al., 2014, Berkenfeld, Lamprecht & McConville, 2015, Nokhodchi, Martin, 2015, Haidl et al., 2016, Lavorini, Pistolesi & Usmani, 2017, Clark, Weers & Dhand, 2019, Levy et al., 2019). Inhaler's airflow resistance is measured as "the square root of the pressure drop across the device divided by the flow rate through the device" (Healy et al., 2014, Lavorini, Pistolesi & Usmani, 2017). The inspiratory flow rate (unit: Liters per minute, L min⁻¹) through a DPI is inversely proportional to inhaler resistance and is proportional to the pressure drop (unit: kilopascal, kPa) that the patient produces across the device (e.g., standardised pressure drop of 4kPa across the device recommended by European and US pharmacopoeia for *in vitro* characterisation of DPI products) (Aulton, Taylor, 2013, Yang, Chan & Chan, 2014, Clark, Weers & Dhand, 2019, Levy et al., 2019). The pressure drop, which patients generate maximum during inspiration (maximum inspiratory mouth pressure) are dependent on respiratory muscle strength that vary with age and gender (Clark, Weers & Dhand, 2019). To aerosolise the powders with high delivery efficiency to the lungs, DPIs with low resistance (e.g., Spinhaler[®], Aerolizer[®]) require high inspiratory flow above 90 L min⁻¹, between 50-60 L min⁻¹ for DPIs with medium resistance, and high resistance DPIs (e.g., Handihaler[®]) require below 50 L min⁻¹ of inspiratory flow (Healy et al., 2014, Nokhodchi, Martin, 2015, Lavorini, Pistolesi & Usmani, 2017). The inspiratory flow achieved through high resistance DPIs is low (Clark, Weers & Dhand, 2019). Studies have shown that 30 L min⁻¹ of inspiratory flow rate is sufficient for successful inhalation for various DPIs (e.g., Easyhaler[®], Handihaler[®] and Ellipta[®]) used by patients in a broad age range from children to elderly and disease states (e.g., asthma, COPD) (Levy et al., 2019). Patients also can produce a minimum pressure drop of around 1 kPa (~10 cmH₂O) across some DPI inhaler devices (e.g., Handihaler[®], Easyhaler[®], Turbohaler[®]/Turbuhaler[®], Diskus[®]) which are found to be sufficient for pulmonary deposition and patients should receive a necessary drug dose (Clark, Weers & Dhand, 2019). The pressure drop is similar when patients inhale faster through low resistance DPIs and patients inhale slower through high resistance DPIs (Clark, Weers & Dhand, 2019). DPIs with higher resistance is often advantageous as the devices easily achieve high pressure drop (less inhalation effort required for patients thus less dependent of disease conditions) and generate more turbulent flow thus more energy available to effectively deagglomerate the powders and achieve optimal performance (Hoppentocht et al., 2014, Levy et al., 2019). However, compared to low resistance DPIs, high resistance DPIs (Handihaler[®], Easyhaler[®], Turbohaler[®]/Turbuhaler[®]) tend to generate and accumulate higher levels of electrostatic charge within the device due to higher energy input involved (e.g., high pressure, shear, turbulent airflow, friction forces (sliding, rolling or impaction)) during aerosolisation that have an influence on the drug deposition (e.g., low drug delivery efficiency) (Kaialy, 2016).

2.5.5. Available DPI devices

There is a wide range of DPI devices available from various manufactures on the market and the types of currently marketed DPI devices based on the design of dosing chambers (holding dry powder formulations) are generally single-unit dose (e.g., capsule, blister), multi-unit dose (e.g., pre-metered unit dose in capsule, blister or cartridge) and multi-dose reservoir based inhalers (multiple dose stored in a device reservoir, device metered) (Yang, Chan & Chan, 2014, Berkenfeld, Lamprecht & McConville, 2015, Lavorini, Pistolesi & Usmani, 2017). Single-unit dose DPI devices (passive inhalers) (e.g., Spinhaler[®] by Fisons, UK /Sanofi-Aventis, Rotahaler[®] by GSK, Handihaler[®], Aerolizer[®]), which are usually referred to as the first generation DPIs, are a common type of inhalers and require the patient to place a capsule or blister containing an individual drug dose (drug powder formulation) into the inhaler device before each use (Islam, Gladki, 2008, Haidl et al., 2016, Lavorini, Pistolesi & Usmani, 2017). The capsule inserted within the device is punctured before inhalation either by sliding (Spinhaler[®]) or pressing (Handihaler[®], Aerolizer[®]), or opened by rotating (Rotahaler[®]) to prepare the drug dose for powder fluidisation (Islam, Gladki, 2008, Islam, Cleary, 2012). DPI devices with multi-unit dose and multi-dose reservoir are referred to as second generation DPIs (Islam, Gladki, 2008). Multi-unit dose DPI devices (e.g., Aerohaler[®] by Boehringer-Ingelheim, Diskhaler[®], Diskus[®], Ellipta[®] by GSK) contain multi-unit/multi-individual doses pre-filled and packaged in capsules (e.g., Aerohaler[®] hold up to 6 capsules) or blisters (e.g., Diskhaler[®] with four to eight blisters, Diskus[®] with 60 doses on a coiled foil blister strip, Ellipta[®] with strip design) and deliver individual dose powder to the lungs (Islam, Gladki, 2008, Islam, Cleary, 2012, Yang, Chan & Chan, 2014, Haidl et al., 2016, Lavorini, Pistolesi & Usmani, 2017, Yeung et al., 2018). Multi-dose reservoir based inhalers (e.g., Turbohaler[®], Easyhaler[®], Novolizer[®], Nexthaler[®]) have a powder reservoir storage incorporated within the device to hold bulk dry powder formulations for multiple dose delivery (e.g., 200 doses for Turbohaler[®], replaceable cartridge with up to 200 doses for Novolizer[®], 120 doses for Nexthaler[®]) and use a dose measuring system to meter a single dose from the powder reservoir and deliver the single dose per actuation (Islam, Gladki, 2008, Islam, Cleary, 2012, Hoppentocht et al., 2014, Yang, Chan & Chan, 2014, Lavorini, Pistolesi & Usmani, 2017, Yeung et al., 2018).

All these types of DPIs have limitations and advantages. Single dose inhalers require a capsule or blister loading by the patient each time before inhalation and multi-unit DPIs (e.g., blister-based devices) face challenges with manufacturing process such as packing/filling the powder accurately into blisters or foil units which require special equipment (Islam, Gladki, 2008, Islam, Cleary, 2012,

Yang, Chan & Chan, 2014). However, single, or multi-unit dose DPI devices offer dose consistency and moisture protection thus storage stability as pre-metered doses are individually packed in capsules or blisters (Islam, Gladki, 2008, Islam, Cleary, 2012, Yang, Chan & Chan, 2014). Capsule-based DPIs can offer flexibility in terms of delivery dose as low or high amount (e.g., 28 mg tobramycin drug per capsule for TOBI[®] Podhaler[®] (emc, 2019)) of DPI formulations can be filled in capsules by changing the capsule size (Faulhammer et al., 2018, Yeung et al., 2018). Multi-dose reservoir devices are associated with low dose uniformity (reproducibility) as powders are metered and delivered from bulk formulations stored in the device for multiple doses and powders are susceptible to environmental factors (e.g., moisture) affecting aerosolisation performance (e.g., low FPF) (Islam, Gladki, 2008, Islam, Cleary, 2012, Yang, Chan & Chan, 2014). However, the design of multi-dose reservoir devices is simple thus less expensive to produce than blister-based devices and multi-dose reservoir inhalers can hold bulk formulations that might be an attractive device option for high dose formulations (Son, McConville, 2008, Yeung et al., 2019). Though, reservoir-based DPI devices might not be suitable for formulations with lower mechanical instability such as high dose DPI formulations (adhesive mixtures with high drug content) and formulations associated with hygroscopic and poor flow powder properties (Hoppentocht et al., 2014). For example, when DPIs are subjected to violent movements such as vibration or shaking (e.g., running) or dropping the device, drug-carrier mixtures might be de-aggregated/broken up within the device reservoir that might influence the flow properties and dose consistency (Hoppentocht et al., 2014, Sibum et al., 2018). Thus, single dose based DPIs could be a better choice for high dose DPI formulations (Sibum et al., 2018).

2.5.6. Active DPI devices

Active devices, which are referred to as the third generation DPIs, rely on energy source system (e.g., compressed air) incorporated within the device to generate forces and aerosolise the powder formulations, therefore, less dependent on patient's inspiration airflow (Islam, Gladki, 2008, Islam, Cleary, 2012, Yang, Chan & Chan, 2014). Active devices with built-in energy source are designed to achieve efficient drug delivery with low requirement of patient inspiratory force or independent of patient's inhalation profile therefore address the limitation associated with passive devices (inconsistent drug delivery to the lungs due to variability in patient's inhalation profiles) (Son, McConville, 2008, Islam, Cleary, 2012). Active device has previously been used in Exubera[®] which used compressed air for insulin powder dispersion (Islam, Cleary, 2012). Due to the cost concern, active devices are generally not desirable for high dose DPI formulations (Sibum et al., 2018).

2.5.7. DPIs for high dose drugs

For high dose DPI formulations (drug dose in mg range, drug concentrations: 5-10%, Section 2.4.1), the design of DPI devices should be suitable for delivering high dose dry powders efficiently to the patients also should be able to disperse large amounts of dry powders per actuation (avoid multiple inhalations) for patient's perspective (e.g., improve adherence) (Scherließ, Etschmann, 2018, Yeung et al., 2018). The current inhalation devices are generally not designed to deliver such large amounts of dry powder formulations (Scherließ, Etschmann, 2018). For examples, TOBI® Podhaler® (Novartis) (four capsules of 28 mg tobramycin twice daily)(emc, 2019) and Bronchitol® (Pharmaxis) (up to ten capsules of 40 mg mannitol twice daily)(emc, 2019), which both are capsule-based inhalation devices, require multiple inhalations (multiple capsules to be inhaled) to achieve therapeutic effect (Scherließ, Etschmann, 2018, Sibum et al., 2018). The tobramycin formulation (TOBI® Podhaler®) was optimised based on the TOBI® Podhaler® inhaler device (low resistance) available (Healy et al., 2014) by using particle engineering (i.e., spray drying) to produce highly dispersible tobramycin-excipient powders (Sibum et al., 2018). Spray drying produced hollow and porous spheroidal shape of tobramycin particles with small aerodynamic diameter (MMAD: < 4µm) that reduced cohesive forces between particles therefore less particle agglomeration (Yeung et al., 2018). These powder properties achieved high lung delivery efficiency (~60% of nominal dose delivered to the lungs) thus allowed high dose pulmonary delivery (total mass of 55 mg including excipients per capsule) (Geller, Weers & Heuerding, 2011, Sibum et al., 2018, Yeung et al., 2018). The inhaled tobramycin product would be more efficient and accepted if the design of the inhaler was adapted to the tobramycin formulation rather than the formulation adapting to the inhaler device already available (e.g., inhaler could be designed to have a strong dispersion system, therefore minimise the use of excipients for dispersion and avoid multiple inhalations or less number of inhalations to improve patient compliance and adherence to therapy) (Sibum et al., 2018). The successful formulation development for high drug dose can be achieved when the design of devices is optimised based on the DPI formulations. Nevertheless, effective high drug dose delivery to the lungs can be achieved by good relationship between the design of DPI formulations and of devices.

2.5.8. Insulin inhalers

Since pulmonary delivery of peptide and protein drugs offer many advantages (e.g., non-invasive drug delivery, large surface area for absorption, high permeability through a thin membrane, higher bioavailability compared to other non-invasive routes; oral, nasal and buccal) described in Chapter 1.1.4 and Section 2.1, several companies have worked on the development of insulin inhalation systems (insulin inhalers, as an alternative to SC insulin) to improve insulin therapy with better treatment outcomes (Rosenstock et al., 2007). In addition to Exubera[®], few other inhaler devices by different companies for insulin delivery (e.g., AIR[™] by Eli Lilly in partnership with Alkermes) had been in various stages of development in the past (Patton, Bukar & Eldon, 2004, Rosenstock et al., 2007, Al-Tabakha, M. M., Arida, 2008, Son, McConville, 2008, Nuffer, Trujillo & Ellis, 2015). However, they terminated their product development before reaching the market and shortly after the withdrawal of Exubera[®] (Easa et al., 2019). Only Afrezza[®] inhaler for insulin delivery is currently available on the market.

Exubera[®]

Inhaler device used for Exubera[®] (Nektar Therapeutics in partnership with Pfizer) was large (30 cm length when extended for inhalation) with cleaning required and had complicated mechanism for actuation that resulted in poor patient acceptability (Al-Tabakha, 2015). The device was an active device with compressed air as an energy source for insulin powder dispersion and the powder aerosolisation performance was flow rate independent in the range of 5 L min⁻¹ to 56 L min⁻¹ (Son, McConville, 2008, Islam, Cleary, 2012, Healy et al., 2014). Insulin dry powder formulation was filled in single dose blister packs and each blister contained a 1 mg (equivalent to ~3U) or 3 mg (equivalent to ~8U) dose of insulin (Rosenstock et al., 2007). Exubera[®] required a blister insertion into the device by the patient and the patient set up the inhaler device to compress air that introduced air into a clear spacer type chamber and dispersed the insulin powder formulation as unit dose into the chamber for inhalation (Rosenstock et al., 2007, Son, McConville, 2008, Healy et al., 2014). The use of the clear chamber allowed patients to visualise the dose administration upon inhalation (Healy et al., 2014). The energy generated by the device was used to draw the insulin powder (Exubera[®] formulation) from the blister pack to the chamber therefore not intended for the process of drug-carrier detachment as carrier was not contained in Exubera[®] (Son, McConville, 2008).

AIR[®]

AIR[®] inhaler device was a small (hand-held size) and simple capsule-based breath actuated device designed to deliver insulin particles (d_{aer} : 1-5 μm) incorporated in excipients (e.g., dipalmitoyl

phosphatidylcholine, a natural component of lung surfactant) (Rosenstock et al., 2007, Son, McConville, 2008). Insulin powder formulation was prefilled in capsules to deliver insulin doses equivalent to SC short-acting insulin lispro (dose equivalencies between AIR[®] and insulin lispro: 2.6 mg to 6U, 5.2 mg to 12U and 7.8 mg to 18U) (Rosenstock et al., 2007). AIR[®] inhaler device also required the patient to place a capsule into the device and puncture the capsule before inhalation (Rosenstock et al., 2007). Insulin powders were dispersed by the capsule spin motion with the inhaled airflow during inhalation (Rosenstock et al., 2007, Son, McConville, 2008). AIR[®] device having a medium resistance to inspiratory flow demonstrated high insulin lung deposition (51% of total emitted dose) in the inspiratory flow rate range of 12 L min⁻¹ to 86 L min⁻¹ (inspiratory flow independent) due to the optimised particle properties (powders associated with less tendency of agglomeration thus high dispersibility and small aerodynamic diameter for deep lung deposition) (Rosenstock et al., 2007, Son, McConville, 2008). In clinical trials (in healthy subjects) AIR[®] insulin exhibited rapid absorption (t_{max} : ~45 mins) comparable to SC insulin lispro (Rosenstock et al., 2007). In patients with T1DM, postprandial glycaemic control was comparable to SC insulin lispro (Rosenstock et al., 2007). AIR[®] insulin had 8% bioavailability relative to insulin lispro (Rosenstock et al., 2007). The patient perspective of insulin therapy with the use of the AIR[®] device was positive as the inhaler device was easy to use, ease of dosing, and comfortable using (Rosenstock et al., 2007). However, the development of the AIR[®] insulin delivery system was terminated by the company, Eli Lilly due to increased uncertainties in the regulatory environment (new potential product vs. existing medical therapies) not a result of safety concern of the product (Eli Lilly, 2008).

MedTone[®]/Gen2 inhaler/Afrezza[®] inhaler

MedTone[®] (MannKind group) later switched to Dreamboat but frequently referred to as Gen2 inhaler is a single dose breath actuated device specifically designed for the current available inhaled insulin product, Afrezza[®] (Son, McConville, 2008, Nuffer, Trujillo & Ellis, 2015). Gen2 inhaler, which is designed to reduce the device cost, is a small (palm size) and disposable device (discard after 15 days of use and replace with a new inhaler device (MannKind Corporation, 2015)) and use plastic cartridges for single use containing insulin powders (e.g., 4 unit cartridge: 0.35 mg insulin, 8 unit cartridge: 0.7 mg insulin and 12 unit cartridge: 1 mg insulin) (Rosenstock et al., 2007, MannKind Corporation, 2015, Nuffer, Trujillo & Ellis, 2015). For high doses (e.g., 24 units), a combination of different cartridges (e.g., 4 unit, 8 unit and 12 unit cartridges), multiple cartridges can be used (MannKind Corporation, 2015, Heinemann, Parkin, 2018). Afrezza[®] inhaler requires the patient to insert a cartridge into the device before inhalation (single inhalation per cartridge) (MannKind Corporation, 2015). Since the device is breath actuated based the amount of insulin delivered to the

lung is influenced by patient factors (MannKind Corporation, 2015). Afrezza® offers advantages over Exubera® in terms of the design of the inhaler device that is small (portable size) with ease of use, low maintenance/no cleaning and uses conventional international units dosing systems that encourage physicians and patients' preferences. Exubera® did not use such dosing systems (Al-Tabakha, 2015, Goldberg, Wong, 2015, Kim, Plosker, 2015, Heinemann, Parkin, 2018). Successful inhalable insulin products can be highly dependent on patients and physicians' acceptance (Al-Tabakha, 2015).

2.6. Pulmonary safety of inhaled insulin

The long-term use of Exubera® and Afrezza® both have raised concerns about possible effects of insulin inhalers on lung function and pulmonary safety (e.g., a risk of lung cancer) and the lung safety concern was one of the number of reasons for the Exubera® product withdrawal (Al-Tabakha, 2015, McGill et al., 2020). In Exubera® clinical programs, the numbers of diagnosed lung cancer cases were reported to be six, five cases among Exubera® users and one case among comparator group (patients were on other diabetes treatments, non Exubera® user) (Gatto et al., 2019). To investigate whether T1DM (14.7%) or T2DM (85.3%) patients treated with Exubera® (Exubera group, n=3875, mean age: 54.8 years ± 12.1 years, mean BMI: 31.0 ± 6.1 kg/m²) died from primary lung cancer within 2 years of trial enrolment at higher rate than patients with T1DM (15.6%) or T2DM (84.4%) on other diabetes treatments, injected insulin or oral diabetes medication (comparator group, non Exubera® users, n=3564, mean age: 54.7 years ± 12.6 years, mean BMI: 31.0 ± 6.0 kg/m²), follow-up study for Exubera® (FUSE) sponsored by Pfizer was conducted (Pfizer, 2012, Gatto et al., 2019). FUSE was an observational follow-up study of patients previously enrolled in Exubera® controlled clinical trials (the duration of 2 year prospective follow up) and 7439 participants were enrolled (Pfizer, 2012, Gatto et al., 2019). FUSE started in 2008 when Exubera® was no longer on the market (Gatto et al., 2019). There were eight primary lung cancer related mortality reported; six in Exubera® group (0.2%, n=6/3875) and two in comparator group (0.1%, n=2/3564) (Gatto et al., 2019). Exubera® group exhibited a few more patients developed lung cancer within 2 years of trial enrolment (0.2%, n=6/3875) than comparator group (0.1%, n=2/3564) (Pfizer, 2012, Gatto et al., 2019). Therefore, the higher risk of lung cancer related mortality associated with Exubera® was found but the number of patients developed lung cancer was small and those patients who developed lung cancer had a history of smoking (Pfizer, 2012, Gatto et al., 2019). The FUSE data also showed that the number of all-cause mortality was 76 (2.0%, n= 76/3875) in Exubera® group whereas 87 (2.4%, n=87/3564) died

of any cause in comparator group (Gatto et al., 2019). Exubera® did not lead to a higher rate of all-cause deaths compared to patients on other diabetes treatments (Gatto et al., 2019).

For Afrezza® (Technosphere insulin), two cases (n=2/3287 patients treated with Afrezza®) of lung cancer associated with heavy smoking history were reported in two clinical trials with Afrezza® and after the trial completion (longer than 2 years after completion of Afrezza® treatment) two additional cases of lung cancer in non-smoker patients who used Afrezza® were reported (Mannkind Corporation, 2020, McGill et al., 2020). The data available are not sufficient to determine whether Afrezza® has an effect on lung cancer (Mannkind Corporation, 2020). It is not clear whether the inhaled insulin products are associated with a risk of lung cancer; a history of smoking could be a risk factor of lung cancer or other factors such as obesity (Depreter, Pilcer & Amighi, 2013, Balducci et al., 2014, Al-Tabakha, 2015). For lung function test (i.e., forced expiratory volume in one second, FEV₁), patients treated with Afrezza® exhibited a greater (but small) decline (FEV₁: -0.08 ~ -0.13 L) in pulmonary function (FEV₁) compared to patients in comparator group (placebo, Technosphere inhalation powder without insulin, FEV₁: -0.04 L) (Mannkind Corporation, 2020, McGill et al., 2020). People with diabetes are associated with obesity (higher BMI) and obesity is strongly associated with reductions in FEV₁ (an inverse relationship between BMI and FEV₁) (Lumb, Thomas, 2020). Due to physiological changes (increased mass of the chest wall), obesity decreases pulmonary function and increases the risk of airway closure or developing respiratory diseases (Section 2.1.3) (Lumb, Thomas, 2020, McGill et al., 2020).

In addition, insufficient drug delivery to the deep lung regions results in oropharyngeal deposition, which might cause irritation leading to cough or bronchospasms (Al-Tabakha, 2015, Yeung et al., 2018). However, DPI formulations are likely associated with cough as a response to irritation and an expected side effect of dry powder formulations (Al-Tabakha, 2015, McGill et al., 2020). For Afrezza®, cough occurred within 10 min of inhalation which was generally mild and reduced over time (McGill et al., 2020). The excipient used in Afrezza® was found to be associated with cough (McGill et al., 2020). This can be prevented by minimising the number and amount of excipients used in DPI formulations (Balducci et al., 2014, Al-Tabakha, 2015).

Chapter 3. ¹H NMR quantification of spray dried and spray freeze dried carriers in dry powder inhaler formulations

3.1. Abstract

Quantitative analysis using proton nuclear magnetic resonance (¹H qNMR) has been employed in various areas (pharmaceutical analysis, vaccines, natural products, metabolites, and agriculture industry). However, it is not routinely used in the quantification of saccharides in dry powder inhaler (DPI) formulations. The aim of this study was to develop a ¹H NMR method for the quantification of saccharides employed in DPI formulations. Dry powders as DPI carriers were prepared by spray drying (SD) and spray freeze drying (SFD) using three saccharides: namely mannitol, sorbitol, and sucrose. The calibration curves constructed for all three saccharides demonstrated linearity with R² value of 1. The ¹H qNMR method produced accurate (relative error %: 0.18-3.70) and precise data with high repeatability (RSD%: 0.52-3.13) in the concentration range of 1.35-21.64 mM for mannitol, 1.35-21.62 mM for sorbitol, and 0.73-23.31 mM for sucrose. The ¹H qNMR method also demonstrated high sensitivity with low limit of detection (mannitol and sorbitol: 0.06 mM, sucrose: 0.05 mM) and limit of quantitation (mannitol: 0.18 mM, sorbitol: 0.17 mM, sucrose: 0.14 mM). Pulmonary deposition via impaction experiments of the three saccharides was quantified using the developed method. It was found that mannitol (68.99%) and sucrose (66.62%) carrier powders prepared by SFD exhibited better delivered dose (total saccharide deposition in throat and all impactor stages) than SD mannitol (49.03%) and SD sucrose (57.70%) (p< 0.05). The developed ¹H qNMR method can be routinely used to assess pulmonary deposition in impaction experiments of saccharides employed as carriers in DPI formulations.

Keywords: Quantitative NMR, Saccharides, Dry powder inhaler formulation, Lung deposition, Spray drying, Spray freeze drying

3.2. Introduction

In the development of carrier-based DPI formulations, relatively small amounts of drugs (<10%) are used in DPI formulations, therefore, the overall DPI performance is generally dependent on the

carrier material selections and properties of carriers such as particle size and distribution, morphology and surface roughness that have a significant effect on the efficiency of pulmonary drug delivery and drug deposition in the lungs (Chapter 2.4.3) (Nokhodchi, Martin, 2015, Peng et al., 2016). The deposition pattern of carriers in the respiratory tract is an important aspect of the formulation process during the development phase. Carrier particles used in DPI formulations are designed not to reach the lungs and cleared by swallowing (Peng et al., 2016). Therefore, only the drug particles detached from the carriers during inhalation should be delivered to the deep lung regions (Chapter 2.4.3)(Peng et al., 2016). Due to the safety concern and insufficient toxicology data, the amount of carriers/excipients used in DPI formulations should be minimised to reduce adverse effects (e.g., cough) (Balducci et al., 2014, Santos Cavaiola, Edelman, 2014, Al-Tabakha, 2015, Peng et al., 2016).

Many analytical methods such as high performance liquid chromatography (HPLC), ultraviolet (UV) spectroscopy and gas chromatography (GC) have been employed to quantify saccharides (Schmid et al., 2016, Chiara Pietrogrande et al., 2017). D'Addio *et al.* (2013) reported the quantification of mannitol deposition via the NGI studies using HPLC with a refractive index detector (D'Addio et al., 2013). However, with these analytical methods, routine quantitative analysis of saccharide in the DPI formulation development can be limited due to the lack of chromophores in saccharides (Coombes et al., 2014, Schmid et al., 2016). Gas chromatography and UV spectroscopy involve several steps such as derivatisation to volatilise the compounds for GC and to convert saccharides to UV detectable saccharides (Schmid et al., 2016, Chiara Pietrogrande et al., 2017). These methods are regarded as time-consuming. Although derivatisation steps are not required for HPLC, HPLC is associated with low detection sensitivity due to the lack of chromophores on sugars where specialised (and sometimes expensive) detectors are required (Chiara Pietrogrande et al., 2017). On the contrary, ^1H qNMR offers advantages, such as relatively short analysis time and simple sample preparation (simple sample dissolution in a suitable NMR solvent) due to no derivatisation steps involved, and simultaneous analysis of multiple analytes with one internal standard (Holzgrabe, 2010, Bharti, Roy, 2012, Pauli et al., 2012, Hou et al., 2014, Simmler et al., 2014, Chiara Pietrogrande et al., 2017). ^1H qNMR measurements are also reproducible with high accuracy and precision (Bharti, Roy, 2012, Pauli et al., 2012, Sterling et al., 2013, Yamazaki, Takatsu, 2014, Schievano, Tonoli & Rastrelli, 2017, Wallmeier et al., 2017). ^1H qNMR represents the direct proportional relationship between the intensity of the signal and the number of protons that gives rise to that signal in the proton NMR spectrum (Holzgrabe, 2010, Richards, Hollerton, 2011, Bharti, Roy, 2012, Günther, 2013, Simmler et al., 2014, Coombes et al., 2014, Hou et al., 2014, Yamazaki, Takatsu, 2014).

Therefore, ^1H qNMR is usually performed by comparing the integrated signals of the compound of interest with the signals of the internal standard where its structure and purity are known (Pauli et al., 2012, Simmler et al., 2014, Yamazaki, Takatsu, 2014) and have been employed in various areas. Quantification of saccharides (glucose, sucrose and fructose) in Açai raw materials using the absolute intensity qNMR method has been reported by Sterling *et al.* (2013) who demonstrated the accuracy and precision of the method (Sterling et al., 2013). Quantification of avermectin B_{1a} (macrolide antibiotic) in agriculture industry reported by Hou *et al.* (2014) showed no significant difference between HPLC and ^1H qNMR quantitation results (Hou et al., 2014). A dissolution study using ^1H NMR with water suppression reported by Coombes *et al.* (2014) demonstrated to quantify the mixture of three active drug substances (acetoaminophen, guaifenesin and phenylephrine hydrochloride) and excipient (lactose) in oral immediate-release tablets with sufficient sensitivity in the low concentrations ($6\ \mu\text{g mL}^{-1}$ as maximum concentration) (Coombes et al., 2014). Identification and quantitation of sugars excipients (mannitol, sucrose, trehalose, and lactose) in freeze-dried vaccines using Total Correlation Spectroscopy (TOCSY) 2D NMR techniques was reported (Duru et al., 2015). Schievano *et al.* (2017) identified and quantified 22 sugars (e.g., glucose, sucrose, and trehalose) present in honey samples using Chemical Shift Selective Filters TOCSY (CSSFs-TOCSY) (Schievano, Tonoli & Rastrelli, 2017). The CSSFs-TOCSY technique proved to be accurate and precise quantitative analytical tools with easy sample preparation (Schievano, Tonoli & Rastrelli, 2017).

Although there are many previous studies indicating the usefulness of NMR techniques, ^1H qNMR is not routinely used in the quantification of saccharides in DPI formulations. So far, no studies reported the use of ^1H qNMR to quantify the deposition of saccharides in pulmonary formulations. The aim of this study was to develop an analytical method using ^1H NMR spectroscopy for quantitative analysis of saccharide deposition pattern. Dry powders as DPI carriers were prepared by spray drying and spray freeze drying using three saccharides selected: namely mannitol, sorbitol and sucrose. Impaction studies were carried out employing a NGI with an Alberta Idealised Throat to estimate the lung deposition pattern *in vitro* for saccharide DPI formulations.

3.3. Materials

D-mannitol (mannitol, $\text{C}_6\text{H}_{14}\text{O}_6$, MW: $182.17\ \text{g mol}^{-1}$), sodium benzoate ($\text{C}_6\text{H}_5\text{CO}_2\text{Na}$, MW: $144.10\ \text{g mol}^{-1}$) and human recombinant insulin ($\text{C}_{257}\text{H}_{383}\text{N}_{65}\text{O}_{77}\text{S}_6$, MW: $5808\ \text{g mol}^{-1}$) were purchased from Sigma-Aldrich, UK. D-sorbitol (sorbitol, $\text{C}_6\text{H}_{14}\text{O}_6$, MW: $182.17\ \text{g mol}^{-1}$) was purchased from Sigma-Life

Science, UK. D-(+)-sucrose (sucrose, $C_{12}H_{22}O_{11}$, MW: 342.29 g mol⁻¹) was purchased from Acros Organics, UK. Deuterium oxide (D₂O) was purchased from Euriso-top®, UK. Sodium 3-trimethylsilyl propionate-2,2,3,3-d₄ (TSP) was purchased from Merck Sharp & Dohme Canada Limited, UK.

3.4. Method development

3.4.1. Preparation of saccharide standard stock solutions

Standard stock solutions of each of the three saccharides (mannitol, sucrose, and sorbitol) and internal standard (sodium benzoate) were prepared in distilled water at a concentration of 107.59 mM (19.60 mg mL⁻¹) for mannitol and sorbitol, 58.26 mM (19.94 mg mL⁻¹) for sucrose, and 297.14 mM (42.82 mg mL⁻¹) for sodium benzoate. Concentration of the internal standard was kept constant throughout the NMR sample solutions. The prepared saccharide stock solutions were stored at 4°C. The saccharide stock solutions were used to prepare standard solutions for the calibration curves (Section 3.4.2) and test sample solutions for method validation (Section 3.4.3).

3.4.2. Preparation of saccharide solutions for calibration curve

Standard calibration curve solutions at five or six different concentrations for the calibration curves in the concentration range of 1.35 mM to 21.64 mM for mannitol, 1.35 mM to 21.62 mM for sorbitol, and 0.73 mM to 23.31 mM for sucrose, which should include the concentration range of interest, were prepared using the saccharide standard stock solution prepared in Section 3.4.1. Five to six serial dilutions were prepared by mixing stock solution with sodium benzoate (10% v/v) used as an internal standard, deuterium oxide (D₂O, 10% v/v) used as an NMR solvent spiked with TSP as the chemical shift reference material and distilled water.

3.4.3. Preparation of saccharide test sample solutions for validation

The saccharide standard stock solution prepared for mannitol, sorbitol, and sucrose (Section 3.4.1) were used to prepare three selected levels of saccharide concentration (low, middle and high end of the calibration curve concentration range) per saccharide for method validation (Section 3.5) following the same method used for the preparation of standard calibration curve solutions (Section 3.4.2).

3.4.4. NMR sample preparation for impaction study

NGI sample solutions for ^1H qNMR were prepared by mixing D_2O in the presence of TSP, sodium benzoate and deposited powders collected with distilled water from each NGI stage (i.e., AIT, all 7 stages of the NGI impactor and MOC) all together in ratios of 1:1:8, respectively.

3.4.5. Proton NMR data measurement

All ^1H NMR measurements for standard calibration curves, validation experiments and NGI sample solutions were performed on a Bruker Avance III 600 NMR spectrometer (600.13 MHz for ^1H) (Bruker UK Limited, UK). Water suppression was achieved using the Bruker NOESY pre-saturation pulse sequence (Bruker noesyppr1d (avance-version 12/01/11) pulse program) which performs pre-saturation of the water signal during the relaxation delay and mixing time and further removes unwanted magnetisation artefacts. Acquisition parameters for all ^1H NMR spectra were set as follows: mixing time 10 millisecond (ms), number of scans 64, data points 64K acquired for 12KHz spectral width giving an acquisition time of 2.66 sec. The receiver gain (RG) was limited to a maximum value of 128. To mitigate possible differences in RG within replicates run in automation, the internal standard (sodium benzoate) was used to normalise integrals and thus alleviate integral discrepancies. In this study, sodium benzoate was selected as it was readily available, and its resonances were not influenced by the analyte's peaks or the water signal. Temperature was kept constant at 298.2K throughout the NMR measurements. All ^1H NMR measurements were performed in triplicate under the same parameters and conditions.

3.4.6. NMR data processing

All NMR data were processed using TopSpin™ software 3.5 pl7 (Bruker BioSpin GmbH, Germany). The spectra were automatically referenced to internal TSP, automatically phase corrected with manual fine tuning of the phase as required, and automatically baseline corrected (using polynomial degree 5).

3.4.7. Proton NMR quantitative analysis

All the signals for the internal standard, sodium benzoate, and each saccharide were manually integrated. One of the peaks from the internal standard was chosen as the calibrant in all the spectra. After completion of manual integration, the integral values for the saccharides were normalised using the calibrant and a calibration curve was constructed for subsequent quantitative analysis of saccharide lung deposition *in vitro*. Calibration curves for three selected saccharides were constructed by plotting the known concentration of saccharide on the x-axis against the normalised integral values of the saccharide on the y-axis. Normalised integral values were calculated using Equation 2:

$$\text{Integral Values (y-axis)} = \frac{(\text{Integral Values of Saccharide} / \text{Number of Atoms in Saccharide})}{(\text{Integral Values of Internal Standard} / \text{Number of Atoms in Internal Standard})}$$

Equation 2

3.5. Method validation

¹H qNMR method validation was carried out based on the International Council for Harmonisation of Technical Requirements for Pharmaceuticals for Human Use (ICH) guidelines (ICH, 2005). The main objective was to demonstrate that the ¹H qNMR analysis was suitable for the quantitation of the saccharide content used as a DPI carrier in DPI formulations. Validation characteristics, such as specificity, linearity, range, accuracy, and precision along with limit of detection (LOD) and limit of quantitation (LOQ) were assessed. All validation experiments were performed on the Bruker Avance III 600 NMR spectrometer (Section 3.4.5).

3.5.1. Specificity

Specificity was evaluated using ¹H NMR spectra of the three saccharides to see whether the signals of each saccharide, sodium benzoate and water were well separated from each other in all ¹H NMR spectra. In addition, saccharide analyte (mannitol, sorbitol, or sucrose) alone and saccharide in the presence of the internal standard and insulin (used as a model compound) were measured to see if there were any changes appeared in peak positions of analyte. The compositions of sample preparation are presented in Table 4.

Table 4: Compositions of sample preparation. TSP: sodium 3-trimethylsilyl propionate-2,2,3,3-d₄. D₂O: deuterium oxide.

Entry	Saccharide (mg)	Sodium benzoate (mg)	Insulin (mg)	TSP	D ₂ O (mL)	Distilled Water (mL)	Total (mL)	Fill volume* (mL)
A	Mannitol 2.0	-	-	-	1.000	-	1.000	0.650
B	Sorbitol 2.0	-	-	-	1.000	-	1.000	0.650
C	Sucrose 4.0	-	-	-	1.000	-	1.000	0.650
D	Mannitol 2.0	3.2	0.2	trace	1.025	0.075	1.100	0.750
E	Sorbitol 2.0	3.2	0.2	trace	1.025	0.075	1.100	0.750
F	Sucrose 4.0	3.2	0.2	trace	1.025	0.075	1.100	0.750

*Volume of solution in a 5 mm NMR tube.

3.5.2. Linearity and Range

The linearity of the ¹H qNMR method was evaluated by preparing the calibration curves for a series of 5-6 concentrations of selected saccharides. The concentrations ranges were 1.35-21.64 mM for mannitol, 1.35-21.62 mM for sorbitol, and 0.73-23.31 mM for sucrose. Linear regression analysis was used to evidence the direct proportional relationship between the signal intensity and the number of protons. The correlation coefficient (R²) and the regression equation (y intercept and slope of the regression line) were generated using Microsoft® Excel.

3.5.3. Accuracy

The accuracy of the ¹H qNMR method was assessed by measuring three concentrations (low, middle, and high end of the calibration curve concentration range) in three replicates. The mean, SDv and RSD% were calculated for each concentration. The accuracy of the measurements was reported as the difference (relative error%) between the measured concentration (*mc*) and nominal

concentration (nc) of each saccharide of interest, using *Equation 3* (Schievano, Tonoli & Rastrelli, 2017):

$$(mc-nc)/nc \times 100 \quad \text{Equation 3}$$

3.5.4. Precision

The intra-day precision of the developed ^1H qNMR method was assessed by calculating the standard deviation (SDv) and relative standard deviation (RSD%) of the replicated measurements (three different concentrations, three replicates per concentration on the same day). The inter-day precision of the ^1H qNMR method was assessed by replicating the same measurements under the same measurement conditions in the same laboratory each day for three days. The SDv and RSD% of the nine NMR data acquisitions per concentration were calculated.

3.5.5. Limit of detection and limit of quantitation

The LOD (the lowest amount of analyte detected in a sample but not necessarily quantitated, *Equation 4*) and LOQ (the lowest amount of analyte quantitated with suitable accuracy and precision, *Equation 5*) were calculated based on the calibration curve method using the standard deviation of the response (standard deviation of y-intercepts) and slope of the calibration curve with ICH guidelines equations (ICH, 2005). Regression analysis in Microsoft® Excel was performed at the 95% confidence level to calculate the standard deviation of the response and the slope.

$$LOD = 3.3 * \sigma / S \quad \text{Equation 4}$$

$$LOQ = 10 * \sigma / S \quad \text{Equation 5}$$

where σ is the standard deviation of the response and S is the slope of the calibration curve.

3.6. Carrier dry powders preparation by spray drying

Saccharides aqueous solutions (15% w/v) were spray dried using a Büchi Mini Spray Dryer B-290 (Büchi, Switzerland) under the optimised processing parameters: 320 mL hr⁻¹ feeding rate, nozzle

spray flow rate with compressed air between 473 L hr⁻¹ and 601 L hr⁻¹, 100% aspirator speed setting (drying gas flow rate, 35-40 m³ hr⁻¹), inlet temperature at 130°C and outlet temperature at 70°C ± 5°C. Collected spray dried (SD) saccharide dry powders (mannitol and sucrose) were immediately packed into tightly closed glass vials and stored in a desiccator over silica gel at room temperature (22°C ± 3°C).

3.7. Carrier dry powders preparation by spray freeze drying

Saccharides aqueous solutions (15% w/v) were sprayed over a cryogenic medium composed of liquid nitrogen in a 250 mL round bottom flask (Figure 9①②) (spray freezing into vapour over liquid, Chapter 2.4.2.1). The samples were freeze dried using BenchTop Pro with Omnitronics™ freeze dryer (SP Scientific, UK) for 48 hours at 55 μbar ± 5 μbar pressure and condenser temperature of -59°C ± 2°C (Figure 9③). After 48 hours, the produced spray freeze dried (SFD) carrier powders (mannitol and sucrose) were sieved using an AS200 DIGIT CA sieve shaker (Retsch, Germany) with the 250 μm sieve (BS410-1, Fisher Brand Test Sieve, UK) for up to 10 minutes at 1.5 mm amplitude to remove agglomerated particles produced during spray freeze drying and obtain uniform powder size fraction. Collected SFD powders (<250 μm) were immediately transferred into tightly closed glass vials and stored in a desiccator over silica gel at room temperature (22°C ± 3°C).

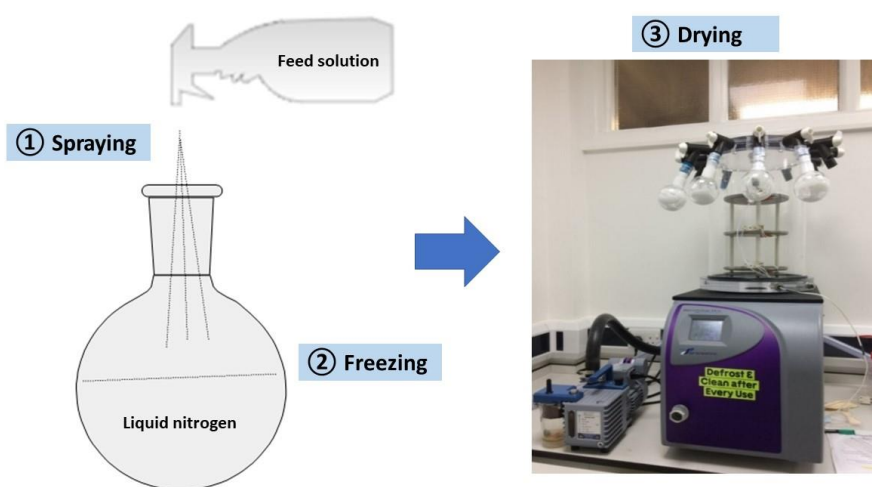


Figure 9: Schematic diagram of spray freeze drying process (manual process of spraying ① and freezing ②) and a picture of freeze dryer used (BenchTop Pro with Omnitronics™, SP Scientific, UK, drying process: ③) with samples in the 250 mL round bottom flasks attached.

3.8. Physicochemical characterisation

Saccharide carrier powders prepared by spray drying (Section 3.6) and spray freeze drying (Section 3.7) were characterised in terms of morphology, particle size distribution, thermal behaviour, moisture content and crystallinity.

3.8.1. Scanning electron microscopy

Morphology along with particle size of all three selected raw saccharides (mannitol, sucrose, and sorbitol), SD and SFD mannitol and sucrose dry powders were characterised by Scanning Electron Microscopy (SEM, ZEISS EVO®50, UK) at an acceleration voltage of 10-25 kilovolt (kV) at different magnifications. Double-sided cohesive carbon tabs were adhered to aluminium stubs and all dry powder samples were placed onto the carbon tabs. Any excess powder samples were tapped off the tabs. These samples were then coated with a palladium/gold alloy (coating thickness: around 5-8 nanometres) using a SC7640 Sputter Coater (Polaron, UK) under argon gas for 2 minutes. Multiple images of coated samples were captured for each sample.

3.8.2. Laser diffraction

Particle size distribution of all three selected raw saccharides (mannitol, sucrose, and sorbitol), SD and SFD mannitol and sucrose dry powders was measured using a HELOS/BF laser diffraction system equipped with a Rodos disperser (Sympatec GmbH, Germany) and VIBRI vibratory feeding unit (Sympatec GmbH, Germany) in the R3 measuring range from 0.5/0.9 μm to 175 μm . The trigger condition for normal measurement under the standard mode was set to start after the “channel 21” was $\geq 1.0\%$ and to stop after the optimal concentration was $\leq 1.9\%$ for 10 sec or 60 sec trigger time out. The primary pressure for the disperser was set to 1.0 bar. Sympatec WINDOX software (Sympatec GmbH, Germany) was used to calculate particle size (Dv10, Dv50 and Dv90: particle diameters below which 10%, 50% and 90% of the sample volume are equal to the measured diameters or smaller than the measured values, respectively and Dv50: the median for a volume distribution) and volume mean diameter (VMD). The width of the particle size distribution expressed as span, which is equal to $(Dv90-Dv10)/Dv50$, was calculated.

3.8.3. Differential scanning calorimetry

Thermal analysis of all three selected raw saccharides (mannitol, sucrose, and sorbitol), SD and SFD mannitol and sucrose dry powders was carried out using a DSC822e Differential Scanning Calorimetry (DSC, Mettler Toledo, Switzerland) under nitrogen gas (50 mL min^{-1}) in the temperature range from 25°C to 400°C at a heating rate of $10^\circ\text{C min}^{-1}$ or $40^\circ\text{C min}^{-1}$. The dry powder samples (2.5-4.0 mg) were placed in aluminium crucibles ($40 \mu\text{L}$) and sealed with a pierced lid on. The dry powder samples loaded pan and empty reference pan were placed on the DSC sample holder. The DSC curves were recorded at 22°C using STARe Software version 8.10 (Mettler Toledo, UK).

3.8.4. Thermogravimetric analysis

Thermogravimetric Analysis (TGA) for all three selected raw saccharides (mannitol, sucrose, and sorbitol), SD and SFD mannitol and sucrose dry powders was performed to measure moisture content using a METTLER TOLEDO® TGA/DSC1 STARe System (Mettler Toledo, Switzerland) along with DSC analysis (Section 3.8.3). The dry powder samples (4.5-12.0 mg) were loaded onto a pan ($70 \mu\text{L}$) and heated under nitrogen gas (50 mL min^{-1}) in the temperature range from 25°C to 400°C at a heating rate of $10^\circ\text{C min}^{-1}$ or $40^\circ\text{C min}^{-1}$. The TGA curves were recorded at 22°C using STARe Software version 8.10 (Mettler Toledo, UK).

3.8.5. X-ray diffraction

Crystallinity and polymorphic nature of all three selected raw saccharides (mannitol, sucrose, and sorbitol), SD and SFD mannitol and sucrose dry powders were studied using a D8 Advance X-ray diffractometer (Bruker, Germany). The dry powder samples were placed onto sample holders with the powder surface flattened and scanned from the diffraction angle of 5° to 55° or 60° at 2θ angle with a step size of $0.100^\circ \text{ sec}^{-1}$ and operated at room temperature (25°C). The X-ray diffraction (XRD) patterns were acquired using a Diffrac-Plus XRD Commander software (Bruker, Germany). The International Centre for Diffraction Data (ICDD) patterns of mannitol, sucrose, and sorbitol in the software database library were used to compare the XRD patterns of all saccharide powder samples.

3.9. Impaction study

Pulmonary deposition study for three selected raw saccharides (mannitol, sucrose, and sorbitol), SD and SFD saccharide (mannitol and sucrose) dry powders was carried out using a next generation impactor (NGI, Copley Scientific, UK) with the Alberta Idealised Throat 28028 (AIT, Copley Scientific, UK, designed for adult human upper respiratory tract geometry) (Figure 10) to determine the amount of saccharide powders deposited on AIT and all NGI stages and estimate *in vitro* lung deposition pattern of three selected saccharides (raw, SD and SFD). The NGI was equipped with a Critical Flow Controller (TPK 2000, Copley Scientific, UK) connected to a Vacuum pump (HPC5, Copley Scientific, UK). The flow rate (the airflow of the NGI) was adjusted to 30 L min^{-1} (corresponding to $<4 \text{ kPa}$ pressure drop) with the test airflow duration of 3 seconds (the time for the airflow to pass through the device, represent the duration of the patient's inspiration) using the TPK 2000 Critical Flow Controller and a Flow Meter (DFM2000, Copley Scientific, UK). The critical (sonic) flow ($P3/P2 \text{ ratio} \leq 0.5$, flow rate stability) was achieved. A leak test was performed on the NGI prior to each use. In this study, Handihaler[®] (Boehringer Ingelheim, Germany), which is a single capsule-based DPI device with high resistance, was used to deliver the content of raw, SD and SFD saccharide dry powders filled in the HPMC size 3 capsules (CAPSUGEL[®], UK) during the impaction studies. The capsule filled with saccharide dry powder was placed in the Handihaler[®] device and actuated to break the capsule prior to the NGI study. Handihaler[®] with the actuated capsule placed was then fitted in the blue mouthpiece adapter customised by Copley for the Handihaler[®] device and attached to the AIT (Figure 10) for impaction studies. The saccharide dry powders deposited on AIT and on all NGI stages (stages 1-7 and MOC) were collected by using distilled water (2 mL) and kept in glass vials at 4°C prior to ^1H qNMR analysis. Dry powders deposited on 7 stages in the NGI were based on the aerodynamic cut-off diameters of $0.541 \mu\text{m}$ (stage 7), $0.834 \mu\text{m}$ (stage 6), $1.357 \mu\text{m}$ (stage 5), $2.299 \mu\text{m}$ (stage 4), $3.988 \mu\text{m}$ (stage 3), $6.395 \mu\text{m}$ (stage 2), and $11.719 \mu\text{m}$ (stage 1) at flow rate of 30 L min^{-1} . All NGI studies were performed in triplicate at room temperature ($22^\circ\text{C} \pm 3^\circ\text{C}$). Saccharide aerosolisation performance was assessed, using Microsoft[®] Excel and Copley Inhaler Testing Data Analysis Software (CITDAS) Version 3.10 Wibu (Copley Scientific, UK) that meets the requirements of United States Pharmacopoeia (USP) and European Pharmacopoeia (Ph.Eur.), to determine the delivered dose (total saccharide deposition on AIT and all the impactor stages; 1-7 and MOC), fine particle fraction (FPF), mass median aerodynamic diameter (MMAD) and geometric standard deviation (GSD). The delivered dose (%) was determined as the ratio of the total saccharide deposition on AIT and all the NGI stages excluding the deposition in the inhaler device and capsules to the total saccharide dose delivered from the device including the deposition in the inhaler device and capsules (i.e., the mass of the saccharide filled into the capsule). In this study, FPF, MMAD and

GSD determined were based on the saccharide deposition dose. The collected saccharide dry powders were quantified using ^1H qNMR (Section 3.11.1) (Babenko et al., 2019).

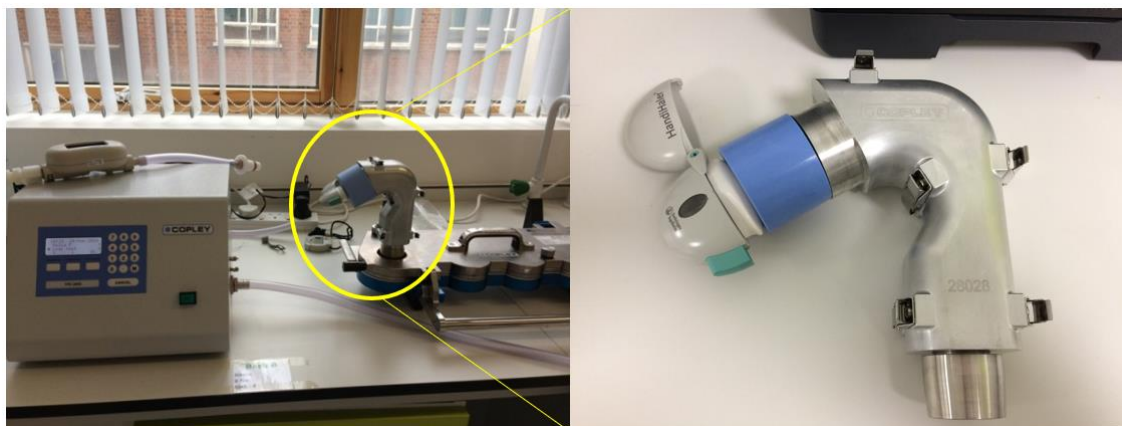


Figure 10: Handihaler® inhaler fitted in the customised blue rubber mouthpiece adapter attached to the Alberta Idealised Throat placed in the next generation impactor.

3.10. Statistical analysis

Statistical analysis was performed using Microsoft® Excel at significant level of $p < 0.05$. One-way ANOVA (Analysis of Variance) was used to compare the results (mean values) of the saccharide delivered dose (%) per stage for NGI study (Section 3.11.3).

3.11. Results and discussion

3.11.1. Method validation

Quantitative analysis using proton NMR spectroscopy (^1H qNMR) with calibration curve method was developed to quantify the content of saccharides dry powders (mannitol, sorbitol, and sucrose) used as a DPI carrier in DPI formulations. Processing parameters (e.g., signal to noise ratio, S/N) and acquisition parameters (e.g., number of scans, acquisition time and RG) were pre-optimised as these parameters affect the accuracy and precision of the measurement (Bharti, Roy, 2012). Setting RG to 128 and the number of scans to 64 allowed to achieve S/N of 250:1 or better (Holzgrabe, 2010,

Bharti, Roy, 2012). Acquisition time was 2.656 sec, and the relaxation delay was set to 4.000 sec to allow satisfactory relaxation of the protons between pulses (Holzgrabe, 2010, Lian, Roberts, 2011). Temperature, which is known to affect chemical shifts and integration (Bharti, Roy, 2012, Yamazaki, Takatsu, 2014) was kept constant at 298.2K throughout the measurements. ^1H qNMR measurements were carried out using water suppression for accurate and precise quantification of the signals of interest (Holzgrabe, 2010, Richards, Hollerton, 2011, Bharti, Roy, 2012, Coombes et al., 2014, Giraudeau, Silvestre & Akoka, 2015).

All saccharide solutions for NMR measurements were prepared by dissolving the reference compound (TSP), internal standard (sodium benzoate) and saccharide all together in distilled water and deuterated NMR solvent ($\text{H}_2\text{O}/\text{D}_2\text{O}$). All compositions were dissolved well in $\text{H}_2\text{O}/\text{D}_2\text{O}$ and each prepared NMR solution (650 μL) was transferred into a 5 mm diameter NMR tube and run by the Bruker Avance III 600 NMR spectrometer. Figure 11 shows the ^1H NMR spectra of sodium benzoate and the three saccharides (mannitol, sorbitol, and sucrose) dissolved in $\text{H}_2\text{O}/\text{D}_2\text{O}$ (90:10 v/v) with the integral regions selected for quantification. The signals of sodium benzoate were manually integrated in the range of 7.4-8.0 ppm (Figure 11A) and the signal at 7.87 ppm (Figure 11A, H_A and H_E protons) was selected as internal calibrant peak. The signals of each saccharide were manually integrated in the range of 3.6-3.9 ppm for mannitol (Figure 11B), 3.5-3.9 ppm for sorbitol (Figure 11C) and 3.4-4.3 ppm and 5.3-5.5 ppm for sucrose (Figure 11D).

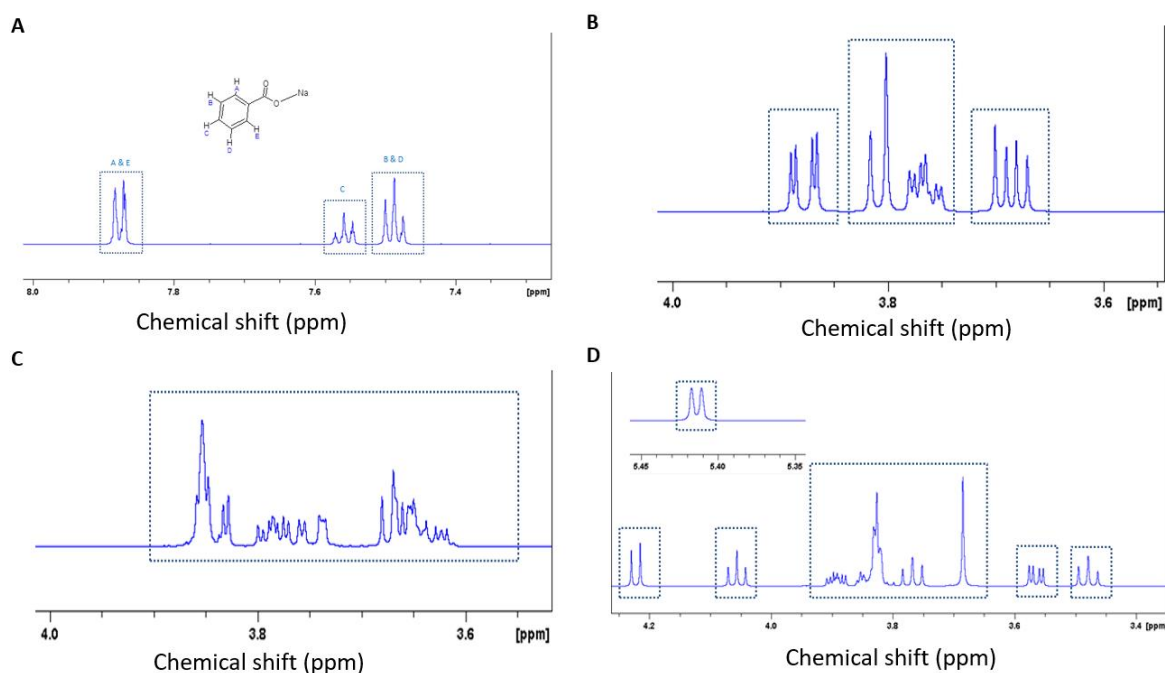


Figure 11: ^1H NMR spectra of sodium benzoate with peak assignments (A), mannitol (B), sorbitol (C), and sucrose (D) in $\text{H}_2\text{O}/\text{D}_2\text{O}$ (90:10) with the integral regions selected for quantification.

3.11.1.1. Specificity

The signals of each saccharide, sodium benzoate and water around 4.80 ppm did not overlap in any of the ^1H NMR spectra (Figure 12). There were no significant changes observed in peak positions when measured saccharide (mannitol, sorbitol, or sucrose) alone and saccharide in the presence of the internal standard and model compound (insulin) (Figure 13). Therefore, this allowed clear integration of the signals of interest.

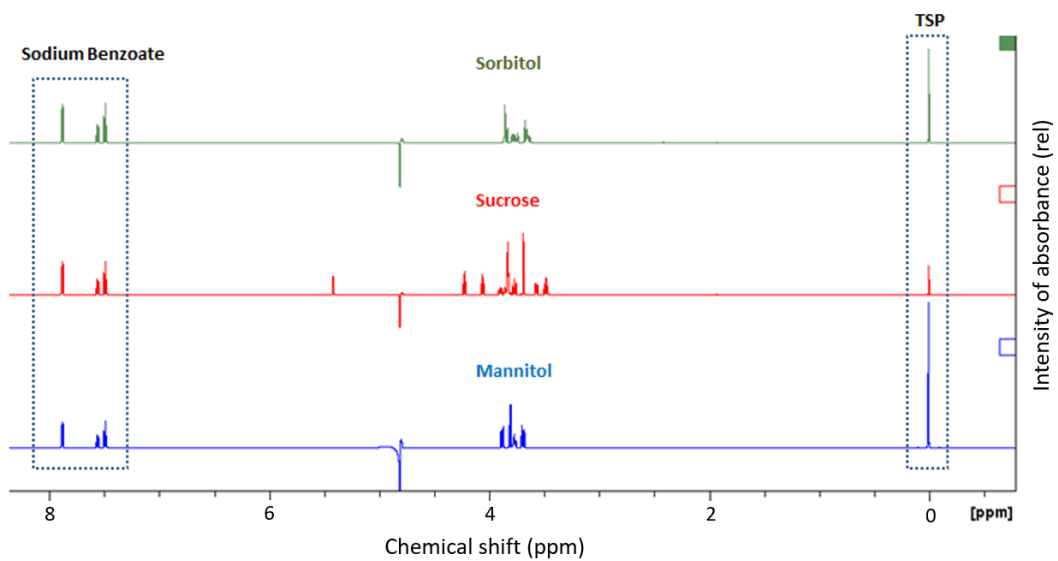
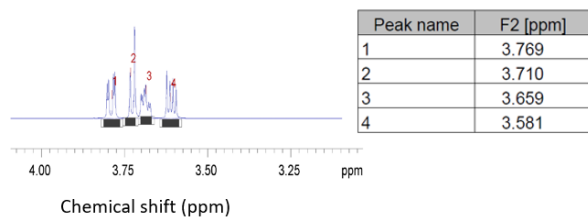
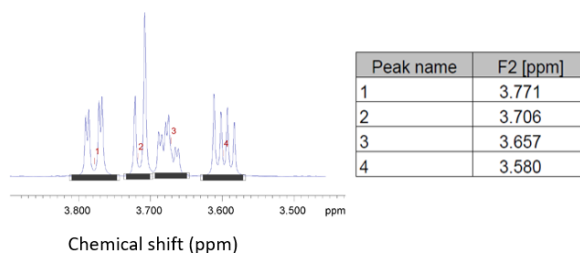


Figure 12: ¹H NMR spectra multiple displays of three saccharides (mannitol, sucrose, and sorbitol) in the presence of the internal standard of sodium benzoate. TSP: Sodium 3-trimethylsilyl propionate-2,2,3,3-d₄.

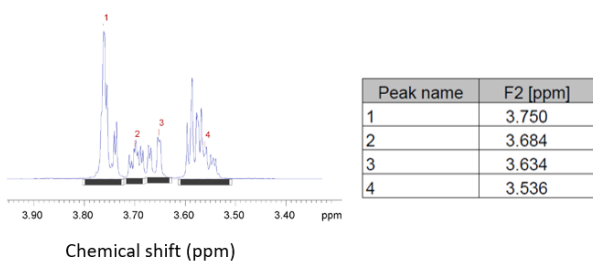
A. Mannitol alone



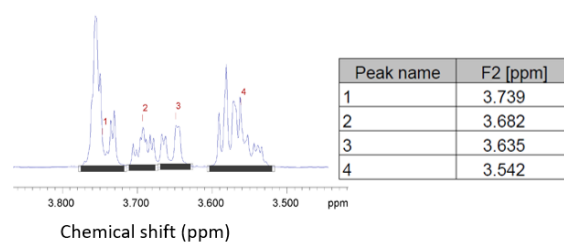
D. Mannitol in the presence of sodium benzoate and insulin



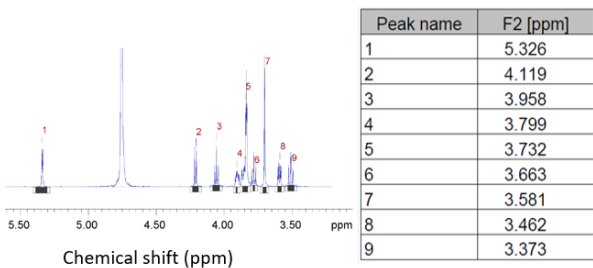
B. Sorbitol alone



E. Sorbitol in the presence of sodium benzoate and insulin



C. Sucrose alone



F. Sucrose in the presence of sodium benzoate and insulin

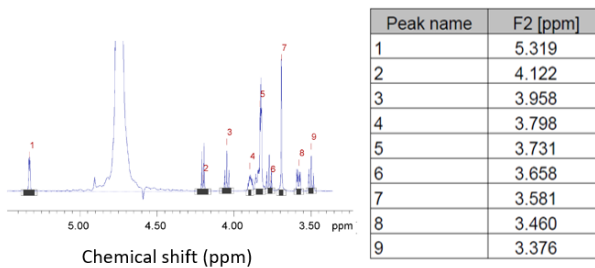


Figure 13: ^1H NMR spectra of saccharide alone (A: mannitol, B: sorbitol, C: sucrose) and saccharide in the presence of sodium benzoate and insulin (D, E, F).

3.11.1.2. Linearity and range

The calibration curves constructed for all three saccharides were linear with R^2 value of 1.0000 (Figure 14 and Table 6). NMR multiple displays for calibration curves of mannitol (Figure 15A), sorbitol (Figure 15B) and sucrose (Figure 15C) show that the integral value was proportional to concentration within the range of concentrations chosen (Figure 15). Regression analysis between nominal concentration and measured concentration for mannitol, sorbitol and sucrose for the determination of correction factors demonstrated no discrepancy as the measured concentration (y-axis) was almost as equal to the nominal concentration (x-axis) (Figure 16 and Table 6).

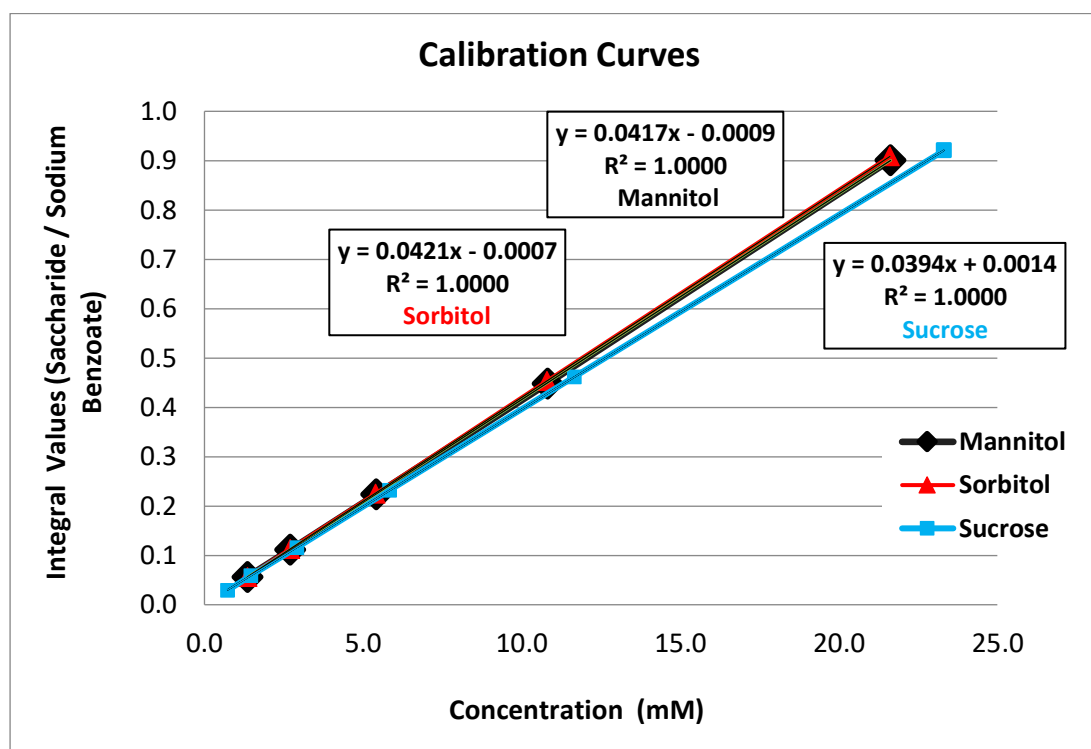


Figure 14: Calibration curves for mannitol, sorbitol, and sucrose.

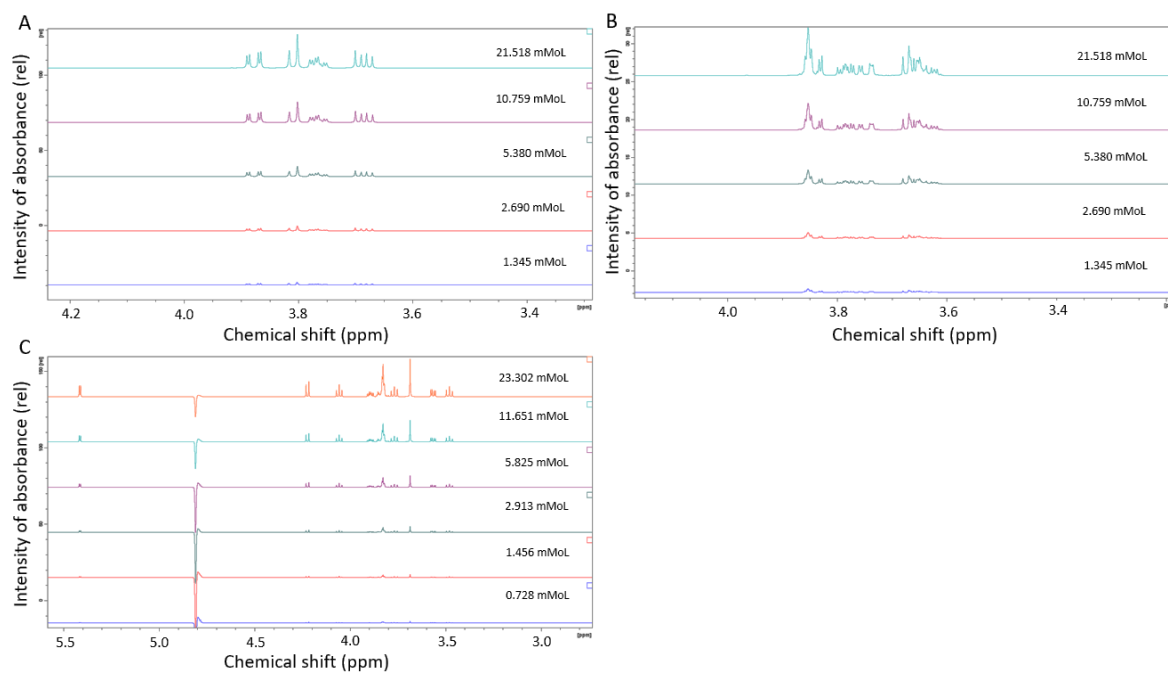


Figure 15: NMR spectra multiple displays of mannitol (A), sorbitol (B) and sucrose (C) for the calibration curves.

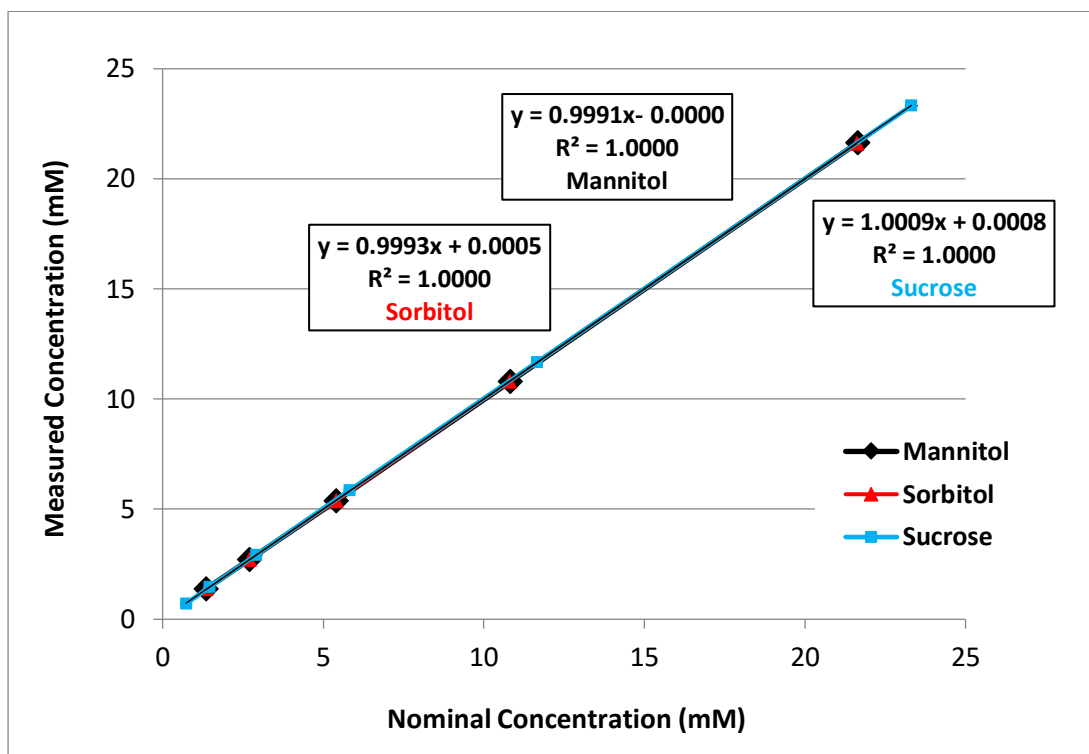


Figure 16: Regression analysis between nominal concentration and measured concentration for mannitol, sorbitol, and sucrose.

3.11.1.3. Accuracy and precision

The accuracy and precision of the ¹H qNMR method was assessed at three different concentrations. Table 5 shows that relative error (%) for mannitol, sucrose and sorbitol were all less than 3.7%. SD and RSD% values determined for the three saccharides were all below 0.39 and 3.13, respectively. These results demonstrated that the ¹H qNMR method produced accurate (relative error%: <3.7) and precise data with high repeatability (RSD%: <3.1) with linear relationship over the concentration range used.

Table 5: Accuracy (relative error %), intra-day precision (three replicates per concentration on the same day) and inter-day precision (9 replicates per concentration over 3 days) at three different concentrations for the ^1H qNMR method. Data presented as mean with standard deviation (SDv), relative standard deviation (RSD%) and relative error%.

Saccharide	Nominal concentration (mM)	Mean measured concentration (mM)	SDv	RSD (%)	Relative error (%)
Intra-day precision					
Mannitol	21.529	21.599	0.061	0.281	0.328
	5.382	5.449	0.025	0.464	1.234
	1.346	1.383	0.007	0.497	2.760
Sucrose	23.302	23.611	0.198	0.841	1.327
	5.825	5.880	0.020	0.338	0.940
	0.728	0.728	0.013	1.748	-0.054
Sorbitol	21.540	21.341	0.094	0.440	-0.924
	5.385	5.384	0.040	0.743	-0.014
	1.346	1.364	0.015	1.080	1.350
Inter-day precision					
Mannitol	21.529	21.568	0.112	0.517	0.184
	5.382	5.450	0.065	1.197	1.255
	1.346	1.395	0.011	0.789	3.697
Sucrose	23.302	23.962	0.389	1.625	2.831
	5.825	6.016	0.121	2.018	3.264
	0.728	0.741	0.023	3.126	1.755
Sorbitol	21.540	21.072	0.248	1.176	-2.173
	5.385	5.383	0.044	0.815	-0.045
	1.346	1.378	0.013	0.932	2.376

3.11.1.4. Limit of detection and limit of quantitation

The LOD and LOQ calculated for all three saccharides are presented in Table 6. The ^1H qNMR method demonstrated high sensitivity with low LOD (mannitol: 0.058 mM, sorbitol: 0.056 mM, sucrose: 0.045 mM) and low LOQ (mannitol: 0.175 mM, sorbitol: 0.168 mM, sucrose: 0.135 mM). This indicates that concentrations determined from the linear concentration range of the calibration curves were both within LOD and LOQ.

Table 6: Linear correlation coefficient (R^2), regression equation, limit of detection (LOD) and limit of quantitation (LOQ).

Saccharide	Regression equation for calibration curve	R^2	LOD (mM)	LOQ (mM)	Regression equation for correction factor
Mannitol	$y = 0.0417x - 0.0009$	1.0000	0.058	0.175	$y = 0.9991x - 0.0000$
Sorbitol	$y = 0.0421x - 0.0007$	1.0000	0.056	0.168	$y = 0.9993x + 0.0005$
Sucrose	$y = 0.0394x + 0.0014$	1.0000	0.045	0.135	$y = 1.0009x + 0.0008$

3.11.2. Physicochemical characterisation

Mannitol and sucrose dry powders were successfully prepared as DPI carriers using spray drying and spray freeze drying. Spray drying of sorbitol aqueous solution (15% v/w) failed to produce dry powders, which resulted in clear paste formation due to the use of higher inlet temperature (130°C) than sorbitol melting point (around 102°C determined by DSC, Table 8 in Section 3.11.2.3). Spray freeze drying of sorbitol aqueous solution also failed to produce sorbitol dry powders as DPI carrier resulting in collapse. This could be due to the drying process taking place at room temperature that was above glass transition temperature (T_g) of sorbitol (around 0°C, (Nezzal et al., 2009)). Due to the large particle size of raw sucrose (particle size: above 400 μm , Figure 18A) as a DPI carrier, raw sucrose was milled to reduce the particle size within the carrier particle size range. Prior to quantifying the three saccharides using ^1H qNMR, raw, SD and SFD saccharides powders were characterised using SEM (Section 3.11.2.1), laser diffraction (Section 3.11.2.2), DSC (Section 3.11.2.3), TGA (Section 3.11.2.4) and X-ray diffraction (Section 3.11.2.5). Due to the failure of producing SD and SFD sorbitol powders, only raw sorbitol powder was characterised.

3.11.2.1. Scanning electron microscopy

Different morphologies in all mannitol dry powder samples (raw, SD, SFD) were observed and both spray drying and spray freeze drying methods modified the size and surface morphology of mannitol particles (Figure 17). The SEM image of raw mannitol (Figure 17A) showed elongated particles with rather rough surface in the particle size range of 50 μm to 300 μm . SFD mannitol (Figure 17B) showed spherical and highly porous particles with large particle size ranging between 50 μm and 110 μm , which is within the suitable carrier size range (50-200 μm as described in Introduction 3.2). However, some small fragments of the porous particles were also observed and resulted in the broad particle size distribution with high span value (10.81) discussed later in Section 3.11.2.2. The SEM image of SD mannitol (Figure 17C) showed spherical particles with smooth surface in the

smaller particle size range of 2 μm to 10 μm . In comparison to SD mannitol powders, SFD mannitol powders were very fluffy.

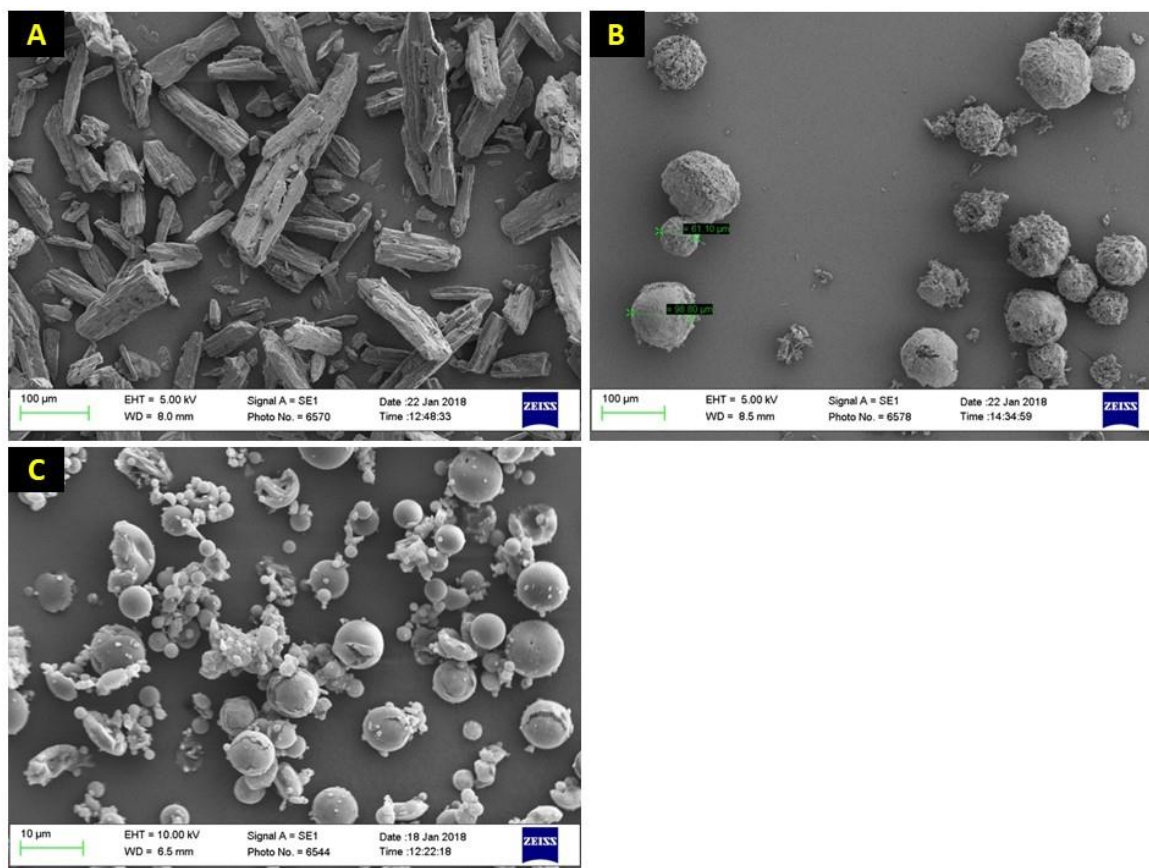
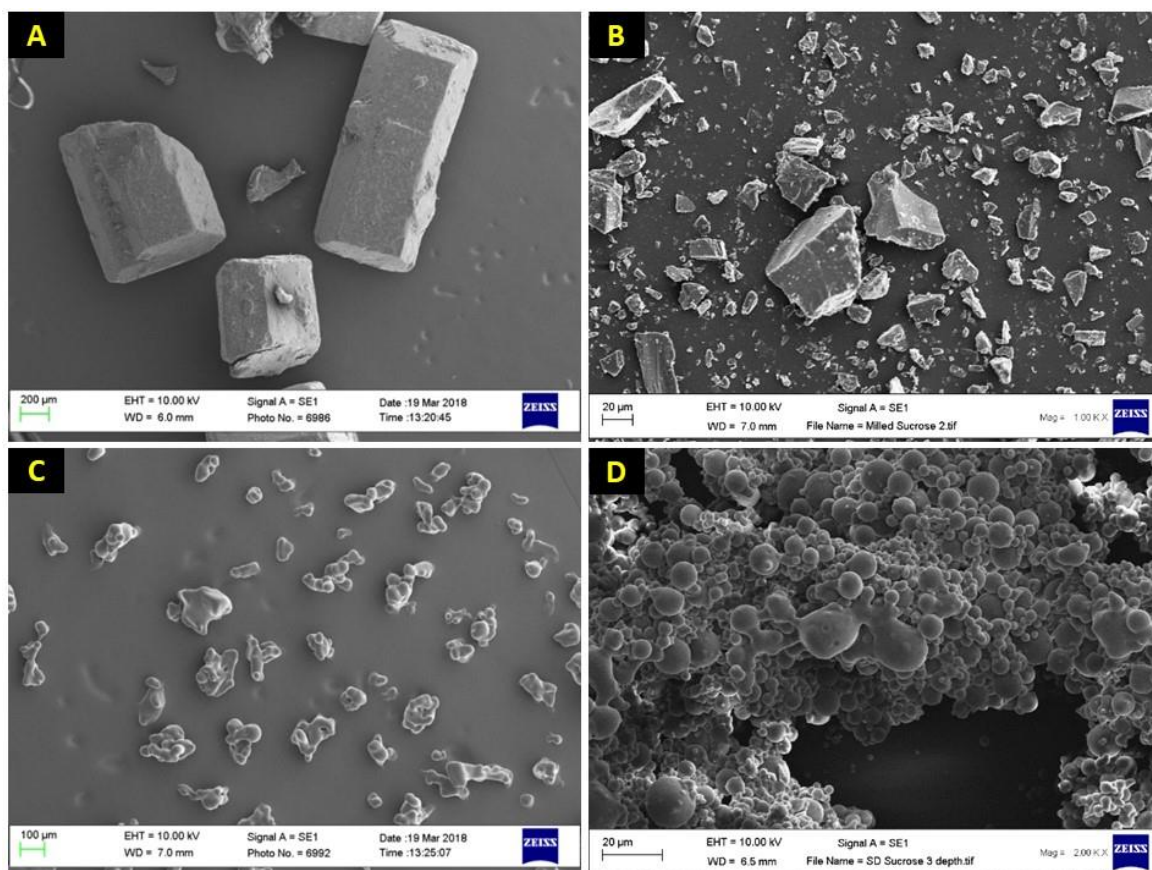


Figure 17: Scanning electron microscopy (SEM) images of raw mannitol (A), spray freeze dried mannitol (B) and spray dried mannitol (C) dry powders.

Analogously to mannitol, different morphologies in all sucrose dry powder samples were observed (Figure 18). Raw sucrose particles were elongated with large particle size above 400 μm (Figure 18A) and milled sucrose exhibited irregular shaped particles with rather rough surface in the particle size range of 4 μm to 130 μm (Figure 18B). SFD sucrose (Figure 18C) showed aggregated particles with smooth surface composed of some spherical and irregular shape particles fusing together. This was due to the aggregation occurred during the process of spraying saccharide solution over liquid nitrogen and freeze drying. SD particles also showed aggregation with smooth surface composed of spherical particles fusing together (Figure 18D). Despite the smooth surface observed for both SFD

and SD sucrose, SFD sucrose powders were rather fluffy compared to SD sucrose powders. Nonetheless, it was observed that SFD produced some spherical particles with a suitable carrier particle size range of 50 μm to 100 μm (Figure 18C) whereas SD method produced spherical particles with the smaller particle size range of 20 μm to 100 μm (Figure 18D). Raw sorbitol showed irregular particles with fibrous and rough surface in the particle size range of 15 μm to 150 μm (Figure 18E). SEM images showed various morphologies overall and the particle size for all saccharide dry powders varied with the method of dry powder preparation in the following rank order: raw > SFD > SD.



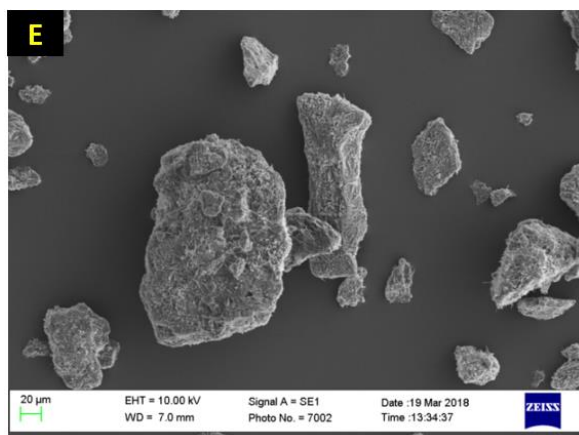


Figure 18: SEM images of raw sucrose (before milling) (A), milled raw sucrose (B), spray freeze dried sucrose (C), spray dried sucrose (D) and raw sorbitol (E) dry powders.

3.11.2.2. Laser diffraction

The particle size distribution determined by laser diffraction (Table 7) showed that raw saccharides had the largest VMD followed by SFD saccharides and SD saccharides had the smallest VMD in the following rank order: raw sorbitol > raw sucrose > raw mannitol > SFD sucrose > SFD mannitol > SD mannitol > SD sucrose. This also suggests that both SFD and SD methods modified the particle size of saccharide dry powders and supported the SEM images (Figure 17 and Figure 18). The span values were in the rank order of SFD mannitol (10.81) > SFD sucrose (3.78) > raw sucrose (2.40) > raw mannitol (2.25) > SD sucrose (2.23) > SD mannitol (2.06) > raw sorbitol (1.29) (Table 7). This represented that raw sorbitol had the narrowest size distribution with the lowest span value (1.29), whereas SFD mannitol had the highest span value of above 10 (10.81) indicating polydispersity due to the presence of some small fragments of the porous particles observed by the SEM image (Figure 17B). This might have led to the saccharide deposition in the lower NGI stages (discussed later in Section 3.11.3). SD saccharides showed narrower particle distribution with smaller span values compared to their raw and SFD saccharides. As discussed in Introduction 3.2, carrier particles used in DPI formulations should not reach the lungs and monodisperse size distribution is desirable for carriers targeting the oropharynx region as broad particle distribution would lead to variations in particle depositions.

Table 7: Particle size volume diameters (μm) at 10% (Dv10), 50% (Dv50) and 90% (Dv90) of particle size distribution for raw saccharides (mannitol, sucrose, and sorbitol), spray freeze dried (SFD) mannitol and sucrose, and spray dried (SD) mannitol and sucrose dry powders. VMD: volume mean diameter.

Saccharide	Dv10 (μm)	Dv50 (μm)	Dv90 (μm)	VMD (μm)	Span ($\text{Dv}_{90} - \text{Dv}_{10} / \text{Dv}_{50}$)
Raw mannitol	8.87	42.32	103.97	50.20	2.25
SFD mannitol	1.62	10.34	113.37	34.83	10.81
SD mannitol	1.05	4.77	10.87	5.54	2.06
Raw sucrose	4.14	48.98	121.79	56.44	2.40
SFD sucrose	2.62	25.47	99.01	40.11	3.78
SD sucrose	0.87	3.45	8.57	4.17	2.23
Raw sorbitol	17.54	107.59	156.50	94.96	1.29

3.11.2.3. Differential scanning calorimetry

The DSC curves for all mannitol dry powder samples showed a single sharp downward endothermic peak with an onset temperature range of 166°C and 168°C which corresponds to the melting point of mannitol and indicates crystalline mannitol (Figure 19 and Table 8). This is in agreement with the results reported in literatures (Kaialy, Waseem et al., 2010, Kaialy, Nokhodchi, 2013, Razavi Rohani, Abnous & Tafaghodi, 2014). However, SFD mannitol showed a small endothermic event at 154.29°C before the sharp melting point peak at 166.25°C in the DSC curve (Figure 19B and Table 8), whereas raw mannitol (Figure 19A) and SD mannitol (Figure 19C) showed no peaks appeared around 154°C. The small endothermic event for SFD mannitol would be the melting point of δ -form of mannitol where changes in forms of mannitol occurred to transform into α - or β -mannitol (Kaialy et al., 2010, Lyu et al., 2017). This indicates that SFD process produced a mixture of three crystal forms; α -, β - and δ -mannitol whereas raw mannitol and SD mannitol were a mixture of α - and β -mannitol forms present or either α -mannitol or β -mannitol form and showed no δ -mannitol form present. These DSC results were supported by the results of X-ray diffraction patterns discussed later in Section 3.11.2.5. Melting enthalpy for mannitol samples at 166-167°C was in the rank order of SD mannitol (-289.09 Jg^{-1}) > raw mannitol (-279.09 Jg^{-1}) > SFD mannitol (-257.93 Jg^{-1}) (Table 8). This suggests higher crystallinity in SD samples compared to SFD samples which agreed with XRD results (Figure 23) discussed in Section 3.11.2.5. Kaialy and Nokhodchi (2013) also reported that melting enthalpy for SD mannitol ($292.5 \text{ Jg}^{-1} \pm 4.2 \text{ Jg}^{-1}$) was higher than freeze dried (FD) mannitol ($257.0 \text{ Jg}^{-1} \pm 5.6 \text{ Jg}^{-1}$) (Kaialy, Nokhodchi, 2013). The onset temperature for decomposition was observed above 325.0°C in all mannitol dry powder samples (Figure 19). The DSC curve for raw sorbitol dry powder showed a single sharp downward endothermic peak with an onset melting temperature of 102.39°C (Figure

19D) indicating crystalline sorbitol. The onset temperature for decomposition was observed above 320.0°C in sorbitol dry powder sample (Figure 19D).

Table 8: DSC results for raw mannitol, spray freeze dried (SFD) mannitol, spray dried (SD) mannitol and raw sorbitol dry powders.

Carrier	Sample weight (mg)	Endothermic event Melting point	
		Onset temperature (°C)	Enthalpy (Jg ⁻¹)
Raw mannitol	3.90	167.60	-279.09
SFD mannitol	2.60	154.29	-4.22
		166.25	-257.93
SD mannitol	4.00	166.42	-289.09
Raw sorbitol	2.50	102.39	-129.05

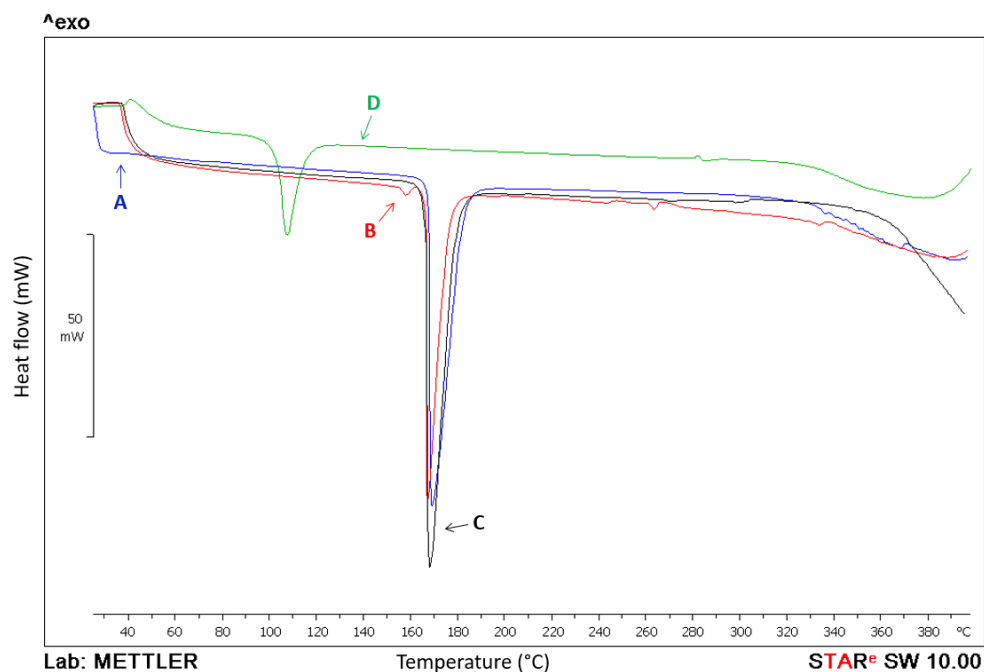


Figure 19: Combined DSC thermograms of raw mannitol (A), spray freeze dried mannitol (B), spray dried mannitol (C), and raw sorbitol (D) dry powders.

For sucrose carrier powders, raw sucrose (Figure 20A) showed a sharp endothermic peak with an onset melting temperature of 195.34°C whereas SFD sucrose (Figure 20B) and SD sucrose (Figure 20C) showed a series of three thermal transition events starting with a glass transition (35.44°C for SFD and 52.49°C for SD) followed by crystallisation (100.85°C for SFD and 99.81°C for SD) and melt (187.15°C for SFD and 183.76°C for SD) in the DSC curves (Figure 20 and Table 9). This is interpreted that raw sucrose was crystalline sucrose and sucrose dry powders produced by spray freeze drying and spray drying were amorphous sucrose. It was also found that SFD sucrose was associated with small enthalpies for crystallisation (enthalpy: 35.48 Jg⁻¹) and melt (enthalpy: -46.76 Jg⁻¹) compared to SD sucrose (crystallisation enthalpy: 59.56 Jg⁻¹, melt enthalpy: -75.22 Jg⁻¹) (Table 9) that would have had stronger solid-solid interaction. This was supported by XRD results that SD sucrose exhibited slightly higher intensity of XRD patterns compared to SFD sucrose (Figure 24) discussed in Section 3.11.2.5. The onset Tg appeared at 35.44°C for SFD sucrose was lower than the reported Tg (FD sucrose Tg: 62.0°C ± 2.6°C (Kadoya et al., 2010)). This could be due to the residual moisture content (7.5% in Figure 22 determined by TGA discussed later in Section 3.11.2.4) present in SFD sucrose that lowered the Tg. Although all sucrose samples were stored in a desiccator over silica gel, SFD sucrose absorbed moisture during storage under laboratory conditions (22°C ± 3°C) leading to a lowered Tg and facilitated crystallisation which consequently affects formulation stability (Duddu, Dal Monte, 1997, Fonte et al., 2014). The onset temperature for decomposition was observed above 240.0°C in all sucrose dry powder samples (Figure 20 and Table 9).

Table 9: DSC Results for raw sucrose, spray freeze dried (SFD) sucrose and spray dried (SD) sucrose dry powders.

	Sample weight (mg)	Glass transition (Tg)	Crystallisation		Endothermic event Melting point		Endothermic event	
		Onset temperature (°C)	Onset temperature (°C)	Enthalpy (Jg ⁻¹)	Onset temperature (°C)	Enthalpy (Jg ⁻¹)	Onset temperature (°C)	Enthalpy (Jg ⁻¹)
Raw sucrose	4.00	-	-	-	195.34	-116.75	247.67	-108.75
SFD sucrose	2.70	35.44	100.85	35.48	187.15	-46.76	243.22	-97.47
SD sucrose	2.60	52.49	99.81	59.56	183.76	-75.22	244.88	-138.97

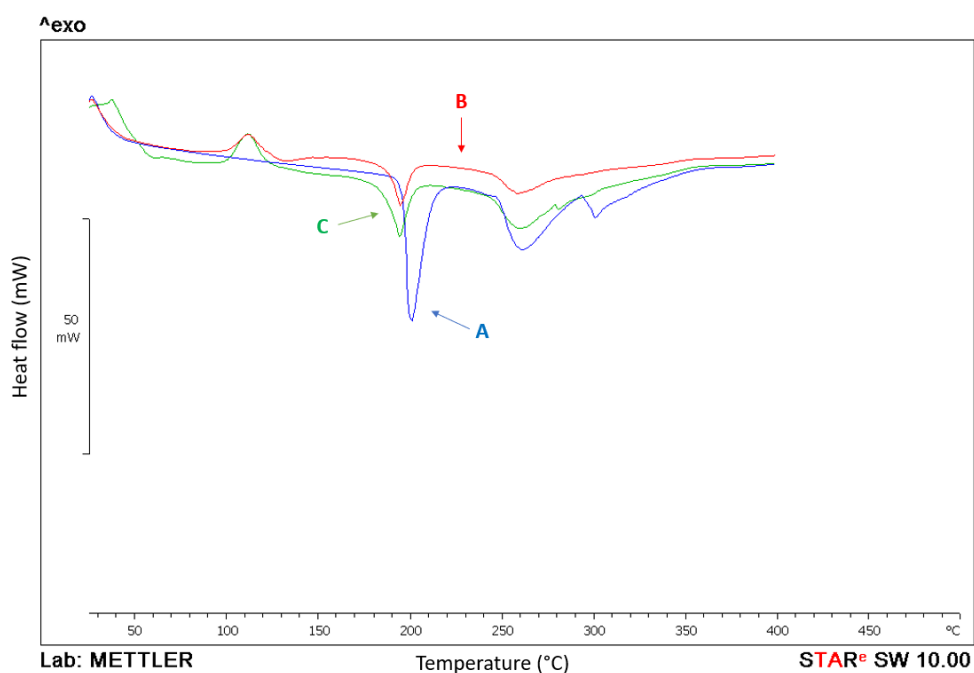


Figure 20: Combined DSC thermograms of raw sucrose (A), spray freeze dried sucrose (B) and spray dried sucrose (C) dry powders.

3.11.2.4. Thermogravimetric analysis

SFD and SD mannitol showed weight loss of 5.5% and 2.0%, respectively below 100°C (Figure 21) where water evaporation would have taken place. On the other hand, no mass change below 100°C was observed in raw mannitol (Figure 21). Figure 22 also showed that SFD and SD sucrose exhibited weight loss below 100°C (7.5% and 3.0%, respectively) whereas raw sucrose showed no mass change below 100°C. This indicates that spray freeze drying and spray drying methods produced hygroscopic saccharide formulations compared to raw saccharides (mannitol and sucrose). In contrast to the SD formulations, the higher moisture content was observed in the SFD formulations. This could be linked to the drying process which is not as efficient as spray drying that showed lower moisture content or SFD samples were easier to absorb moisture during storage or sample preparation. Raw sorbitol is considered as hygroscopic compound compared to raw mannitol and raw sucrose due to the weight loss of about 4.0% observed in the TGA result (Figure 21).

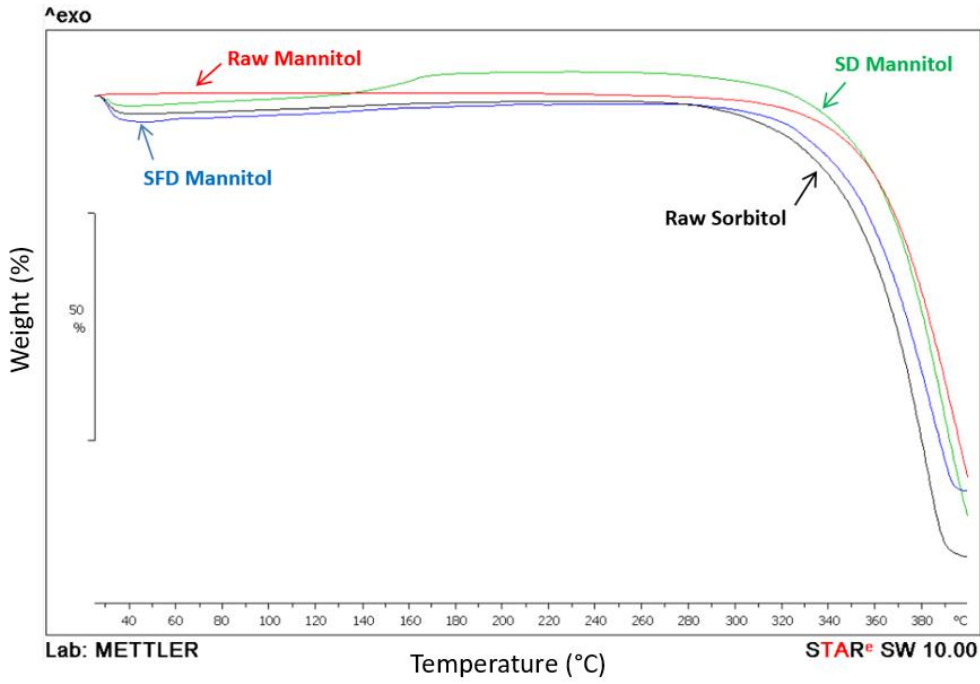


Figure 21: Combined TGA curves of raw mannitol, spray freeze dried (SFD) mannitol, spray dried (SD) mannitol, and raw sorbitol dry powders.

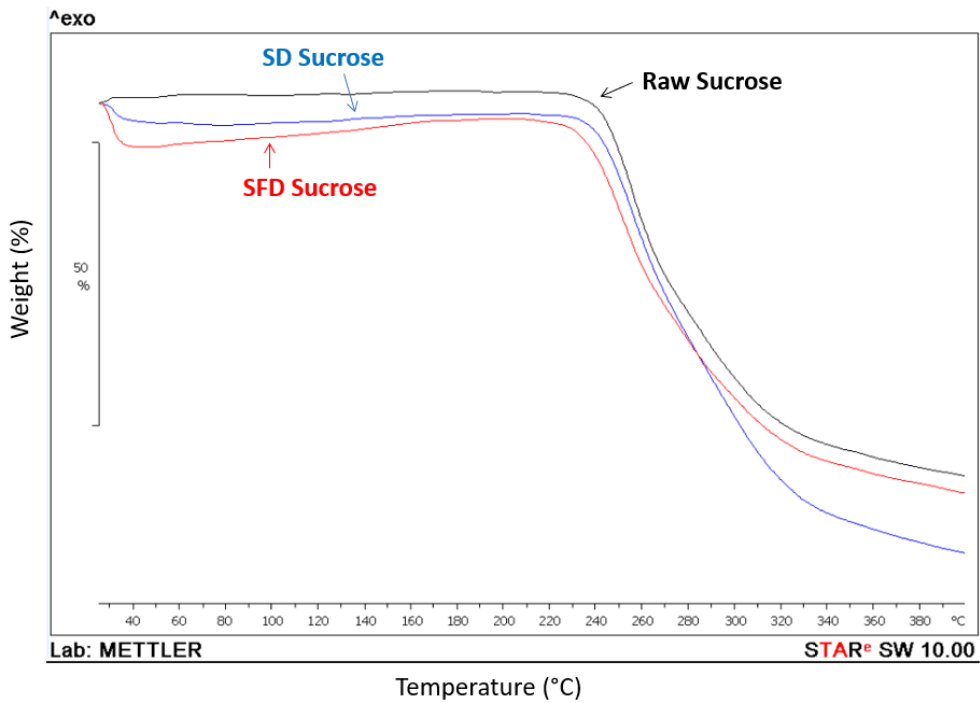


Figure 22: Combined TGA curves of raw sucrose, spray freeze dried (SFD) sucrose and spray dried (SD) sucrose dry powders.

3.11.2.5. X-ray diffraction

XRD was used to assess crystallinity and polymorphic nature of raw, SFD and SD saccharide dry powders as well as to support the DSC results (Section 3.11.2.3). The XRD patterns for all mannitol powders (raw, SFD and SD), and raw sucrose and raw sorbitol (ICDD: 27-1643) powders showed sharp diffraction peaks confirming crystalline materials (Figure 23 and Figure 24). The XRD patterns for raw mannitol showed intense peaks at 10.9°, 15.1°, 19.3°, 21.6°, 23.9°, and 29.9° of 2 θ indicating the presence of both α -mannitol (ICDD: 47-2052) and β -mannitol (ICDD: 22-1797) (Figure 23). The XRD patterns for SD mannitol showed intense peaks at 10.6°, 14.7°, 16.8°, 23.4° and 29.5° of 2 θ indicating the presence of β -mannitol and at 18.8°, 20.5° and 21.0° of 2 θ for a mixture of α -mannitol (ICDD: 22-1793) and β -mannitol (ICDD: 22-1797) (Figure 23). SFD mannitol showed diffraction peaks at 9.7 and 22.2° of 2 θ indicating the presence of δ -form of mannitol (ICDD: 22-1794) and peaks at 10.6°, 14.8°, 16.9°, 18.8°, 20.6°, 21.3°, 23.4°, and 29.6° of 2 θ were a mixture of α -mannitol (ICDD: 47-2052), β -mannitol (ICDD: 22-1797) and δ -mannitol (Figure 23). These peaks were similar to the results (SD and FD mannitol) reported by few authors (Kaialy, Waseem, Nokhodchi, 2015, Kaialy, Nokhodchi, 2016, Molina, Kaialy & Nokhodchi, 2019). These XRD patterns confirmed the DSC results discussed in Section 3.11.2.3 for the form of mannitol. Spray freeze drying produced a mixture of three mannitol forms: α -, β - and δ -mannitol and the melting point observed at 154°C (Figure 19B and Table 8) for SFD mannitol was δ -mannitol. Spray drying produced a mixture of α -mannitol and β -mannitol which agreed with the results reported in literatures (Kaialy, Nokhodchi, 2013, Lyu et al., 2017). In this study, α -mannitol was the dominated form in both raw mannitol and SFD mannitol as the peaks for β -mannitol were very weak, whereas β -mannitol was the dominated form in SD mannitol. SFD mannitol exhibited less intensity of XRD patterns (less crystallinity) compared to SD mannitol (Figure 23). This supported the DSC results (melting enthalpy for SFD mannitol was smaller than SD mannitol) (Table 8 in Section 3.11.2.3).

XRD patterns for sucrose powder samples (Figure 24) showed that raw sucrose (ICDD: 06-0142) was crystalline whereas SFD and SD produced amorphous sucrose (ICDD: 02-0119) as the broadening peaks with less intensity were observed in SFD and SD sucrose powders. This indicates that crystallinity was reduced after the process of spray freeze drying and spray drying and confirmed the DSC results that sucrose dry powders produced by SFD and SD were amorphous (Figure 20B,C in Section 3.11.2.3). However, SD sucrose exhibited slightly higher intensity of XRD patterns compared to SFD sucrose (Figure 24). This also supported the DSC results for larger enthalpies associated with SD sucrose compared to SFD sucrose (Table 9 in Section 3.11.2.3).

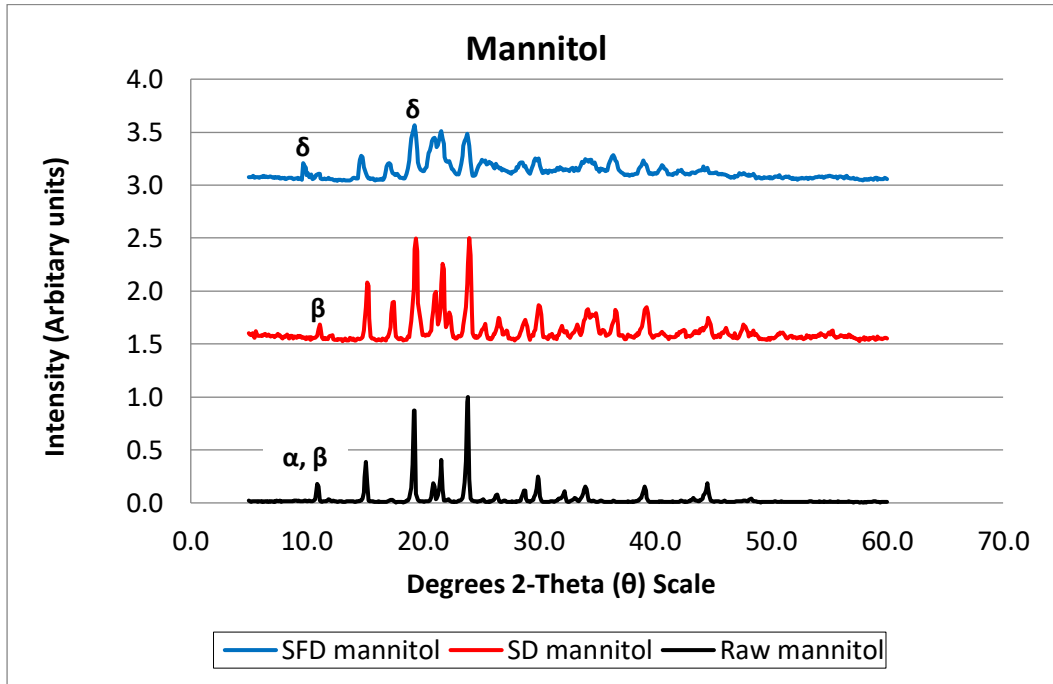


Figure 23: XRD patterns for raw mannitol, spray dried (SD) mannitol and spray freeze dried (SFD) mannitol dry powders.

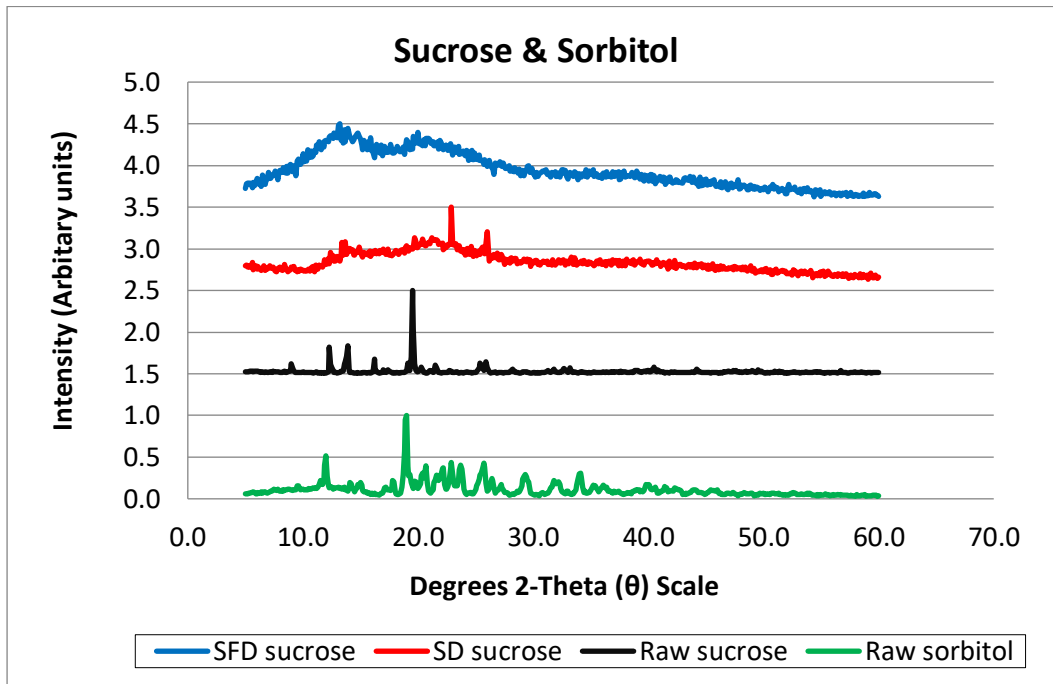


Figure 24: XRD patterns for raw sucrose, spray dried (SD) sucrose, spray freeze dried (SFD) sucrose and raw sorbitol dry powders.

3.11.3. Impaction study

Impaction study using the NGI was carried out to determine the aerodynamic particle size distribution of saccharide particles and estimate *in vitro* lung deposition profile of saccharide carriers used in DPI formulations. The amount of saccharide powders deposited on AIT and all NGI stages were quantified using the calibration curve constructed by ^1H qNMR analysis (Figure 14 in Section 3.11.1.2). The flow rate and test duration for the NGI study were adjusted based on the design of the device used (Handihaler[®]) and reported studies. The Handihaler[®] device is designed to be less dependent on the flow rate and the low flow rate allows patients with different inhalation profiles for use (Yang, Chan & Chan, 2014). Studies have shown that 30 L min^{-1} of inspiratory flow rate is sufficient for successful inhalation for Handihaler[®] and other DPIs (e.g., Easyhaler[®] and Ellipta[®]) used by patients in a broad age range from children to elderly and disease states (e.g., asthma, chronic obstructive pulmonary disease) (Levy et al., 2019). Patients also can produce a minimum pressure drop of around 1 kPa ($\sim 10\text{ cmH}_2\text{O}$) across some DPI inhaler devices including Handihaler[®] (e.g., Easyhaler[®], Turbohaler[®]/Turbuhlaer[®], Diskus[®]) which are found to be sufficient for pulmonary deposition and patients should receive a necessary drug dose (Chapter 2.5.4) (Clark, Weers & Dhand, 2019). Lindert *et al* (2014) demonstrated that the performance of Handihaler[®] was not influenced by the flow rate between at 30 L min^{-1} and 60 L min^{-1} with the inhalation volume of 1 L and deposition data was comparable to the use of low resistance Cyclohaler[®] inhaler device (drug: salbutamol, PB Pharma, Germany) (emitted dose: around 68-72% for Handihaler[®] and 59-68% for Cyclohaler[®]) (Lindert, Below & Breitzkreutz, 2014).

In this study, with the exception of SD mannitol, six saccharide carrier formulations (raw mannitol, SFD mannitol, raw sucrose, SFD sucrose, SD sucrose and raw sorbitol) with over 50% of the cumulative mass deposited on AIT and stage 1 ($11.719\text{ }\mu\text{m}$ cut-off diameter), therefore below 50% of the total mass deposited on between stage 2 ($6.395\text{ }\mu\text{m}$ cut-off diameter) and stage 7 ($0.541\text{ }\mu\text{m}$ cut-off diameter) and MOC in the NGI (Figure 25). Figure 26 also showed higher intensity of saccharides NMR peaks in AIT and stage 1 compared to the peaks between stage 2 and MOC. Therefore, MMAD was reported as NA (no available values for one side of the 50% MMAD) and consequently GSD was reported as NA (Table 10). On the other hand, SD mannitol generated MMAD ($5.78\text{ }\mu\text{m} \pm 0.35\text{ }\mu\text{m}$) (Table 10) as SD mannitol dry powders also deposited on the NGI stages between 2 and MOC (Figure 25 and Figure 26B). This could be due to the small particles prepared by spray drying ($2\text{-}10\text{ }\mu\text{m}$ by SEM Figure 17C in Section 3.11.2.1 and $5.54\text{ }\mu\text{m}$ VMD by laser diffraction in Section 3.11.2.2).

However, there was no significant difference in the deposition pattern in AIT and stage 1 (representing the oropharynx region) between all saccharide formulations (One-way ANOVA, $p > 0.05$). In contrast to the deposition pattern in AIT and stage 1, particles deposition with below $6.395 \mu\text{m}$ cut-off diameter (stage 2) was dependent on the method of dry powder preparation that represented a significant difference in deposition pattern in the lower NGI stages (One-way ANOVA, $p < 0.05$). This could be due to the various morphologies and particle size observed (Figure 17, Figure 18 in Section 3.11.2.1, and Table 7 in Section 3.11.2.2) that affected the powder deposition pattern. SD mannitol (FPF: $23.71\% \pm 3.66\%$), SFD mannitol (FPF: $11.39\% \pm 0.76\%$) and raw sucrose (FPF: $1.54\% \pm 0.44\%$) generated FPF values (Table 10) based on the saccharide deposition dose associated with high cumulative fraction between stage 3 and 5 (Table 11) where generally represents the desired deep lung regions for systemic pulmonary delivery. This presents that SD mannitol, SFD mannitol and raw sucrose dry powders would likely reach the lungs *in vivo* due to the presence of fine particles (aerodynamic diameter: $\leq 5 \mu\text{m}$) and could lead to the safety concern. SD mannitol showed higher FPF than SFD mannitol indicating that higher amounts of mannitol dry powders prepared by SD deposited on the lower NGI stages compared with mannitol dry powders prepared by SFD. Therefore, more SD dry powders would be expected to reach the lungs. Raw mannitol, SFD sucrose, SD sucrose and raw sorbitol generated no FPF values (Table 10) due to a coarse-narrow distribution that over 50% of the cumulative mass deposited on AIT and stage 1 and cumulative fraction of saccharide deposited on the lower NGI stages (2-7) was less than 1% per stage or only one stage had a cumulative fraction over 1% (i.e., 1.19% for raw mannitol) (Figure 25 and Table 11). This represents that these four different saccharide dry powders exhibited the oropharyngeal deposition in the oropharynx region, which is advantageous as DPI carriers. The delivered dose was in the order of raw sorbitol (69.93%) > SFD mannitol (68.99%) > SFD sucrose (66.62%) > SD sucrose (57.70%) > raw mannitol (57.25%) > SD mannitol (49.03%) > raw sucrose (43.35%) (Table 10). In this study, SFD mannitol and SFD sucrose with high moisture content (5.5% in Figure 21 and 7.5% in Figure 22, respectively) exhibited better delivered dose (Table 10) than SD mannitol and SD sucrose with lower moisture content (2% in Figure 21 and 3% in Figure 22, respectively). This indicated that the saccharide flowability was not dependent on the moisture content. Dry powders prepared as DPI carriers by SFD exhibited better flowability than dry powders prepared by SD. This could be due to the porous and fluffy particles produced by SFD that would have reduced inter-particulate forces between particles resulting in better fluidisation (D'Addio et al., 2013, Rahimpour, Kouhsoltani & Hamishehkar, 2014, Weers, Miller, 2015). Raw sorbitol exhibited the highest delivered dose (69.93%) among raw saccharides (57.25% for raw mannitol and 43.35% for raw sucrose) (Table 10). However,

delivered doses for all three raw saccharides are not different from each other (One-way ANOVA, $p > 0.05$).

The *in vitro* pulmonary deposition study demonstrated that SD and SFD produced saccharide dry powders with different deposition. The SFD method for saccharide dry powders preparation as DPI carriers seems to be more advantageous than spray drying method. SFD powders exhibited larger particle size suitable as DPI carriers and better powder flow (higher delivered dose) due to porous powders compared to SD powders.

Table 10: Delivered dose (%), fine particle fraction (FPF% $\leq 5.0 \mu\text{m}$), mass median aerodynamic diameter (MMAD) and geometric standard deviation (GSD) of raw mannitol, spray dried (SD) mannitol, spray freeze dried (SFD) mannitol, raw sucrose, SD sucrose, SFD sucrose and raw sorbitol dry powders determined by Next Generation Impactor analysis at flow rate of 30 L min^{-1} . (Data presented as mean \pm standard deviation, $n=3$).

Saccharide carrier formulation	Dose		Size distribution	
	Delivered dose (%)	FPF (%)	MMAD (μm)	GSD
Raw mannitol	57.25	0	NA	NA
SD mannitol	49.03	23.71 ± 3.66	5.78 ± 0.35	2.11 ± 0.08
SFD mannitol	68.99	11.39 ± 0.76	NA	NA
Raw sucrose	43.35	1.54 ± 0.44	NA	NA
SD sucrose	57.70	0	NA	NA
SFD sucrose	66.62	0	NA	NA
Raw sorbitol	69.93	0	NA	NA

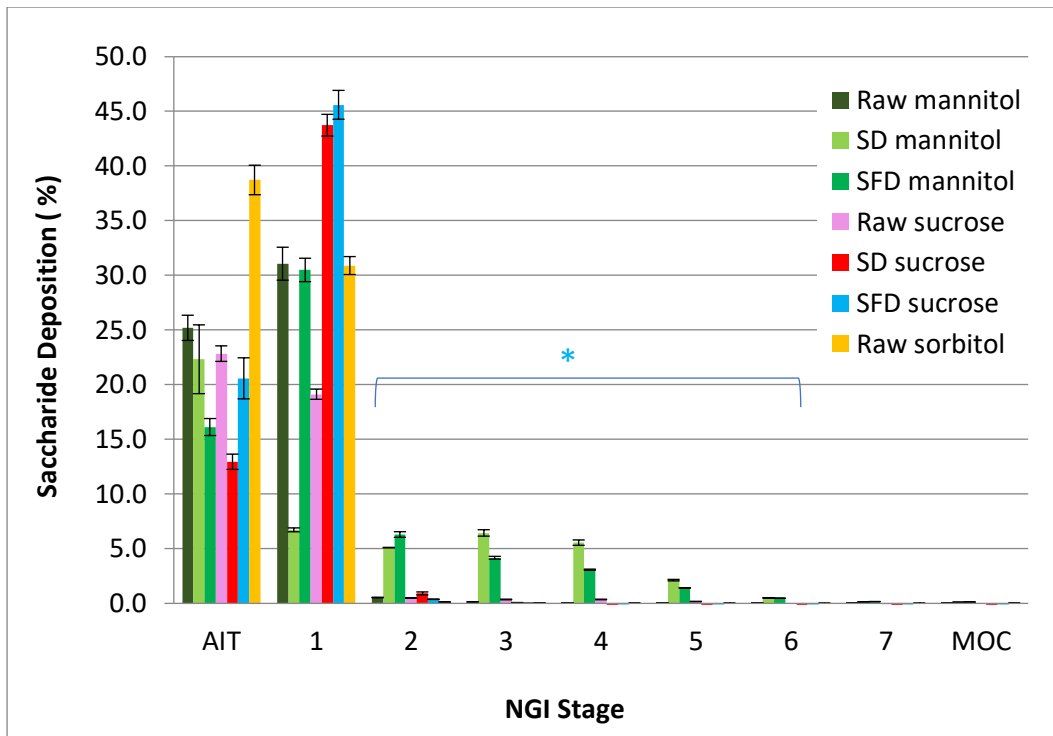


Figure 25: Particle size distribution by Next Generation Impactor (NGI) analysis at flow rate of 30 L min^{-1} for raw mannitol, spray dried (SD) mannitol, spray freeze dried (SFD) mannitol, raw sucrose, SD sucrose, SFD sucrose and raw sorbitol. Saccharide deposition is expressed as delivered dose (%) per NGI stage. (Data presented as mean \pm standard deviation, $n=3$). AIT: Alberta idealised throat, MOC: Micro orifice collector.

Asterisk (*) indicates a significant difference in saccharide deposition pattern in NGI stages 2-6 between saccharide dry powder formulations (One-way ANOVA, $p < 0.05$).

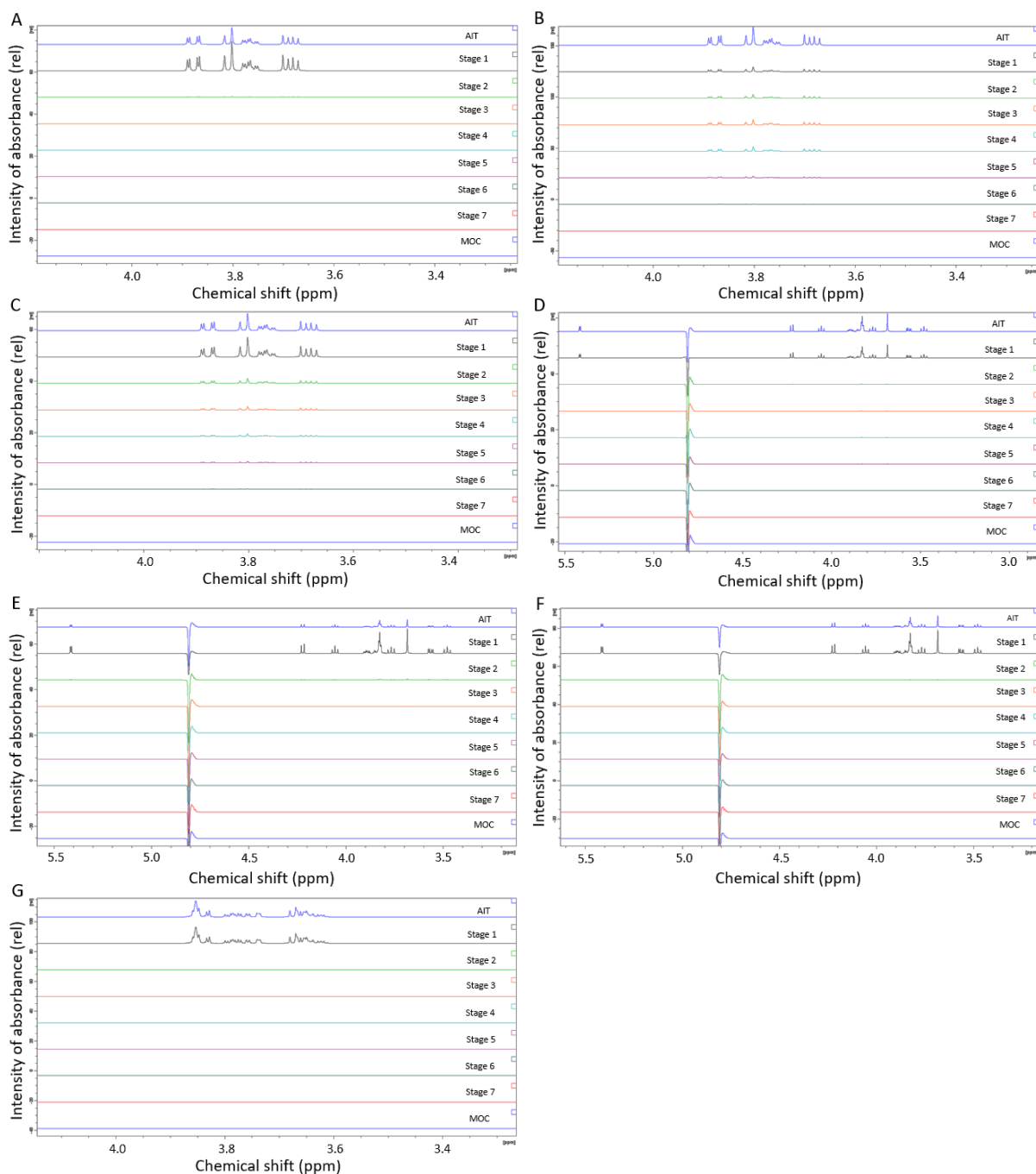


Figure 26: NMR spectra multiple displays of raw mannitol (A), spray dried (SD) mannitol (B), spray freeze dried (SFD) mannitol (C), raw sucrose (D), SD sucrose (E), SFD sucrose (F) and raw sorbitol (G) for Next Generation Impactor analysis. AIT: Alberta idealised throat, MOC: Micro orifice collector.

Table 11: Cumulative fraction (%) of raw mannitol, spray freeze dried (SFD) mannitol, spray dried (SD) mannitol, raw sucrose, SFD sucrose, SD sucrose, and raw sorbitol deposited on Next Generation Impactor (NGI) stages (1-7). Cumulative fraction per NGI stage was calculated by the Copley Inhaler Testing Data Analysis software based on summation of the cumulative mass collected on NGI stages (1-7 and MOC, Alberta idealised throat is not included). (Data presented as mean, n=3).

NGI Stage (Cut-off diameter)	Cumulative fraction (%)						
	Raw Mannitol	SFD Mannitol	SD Mannitol	Raw Sucrose	SFD Sucrose	SD Sucrose	Raw Sorbitol
1 (11.719 μm)	2.87	34.03	74.78	6.71	1.10	2.51	0.90
2 (6.395 μm)	1.19	20.40	55.65	4.34	0.16	0.34	0.51
3 (3.988 μm)	0.78	11.37	31.53	2.58	0.00	0.00	0.42
4 (2.299 μm)	0.60	4.71	10.74	0.82	0.00	0.00	0.34
5 (1.357 μm)	0.41	1.64	2.78	0.00	0.00	0.00	0.26
6 (0.834 μm)	0.25	0.63	0.88	0.00	0.00	0.00	0.17
7 (0.541 μm)	0.13	0.27	0.39	0.00	0.00	0.00	0.09

3.12. Conclusion

The ^1H qNMR method was developed to quantify saccharides employed in DPI formulations and produced accurate and precise data with high repeatability within the calibration curve concentration range. The present study demonstrated the quantification of the three saccharide DPI carriers (raw, SFD and SD) using the developed ^1H qNMR method and the lung deposition pattern *in vitro* for saccharide DPI carriers were assessed based on the amount of deposited saccharide quantified at each stage of the NGI. There was a significant difference in deposition pattern in the lower NGI stages (<6.395 μm cut-off diameter) between all saccharide formulations. These differences could be due to the various particle size and morphologies observed with the use of different methods of dry powder preparation (raw, SFD and SD) that affected the powder deposition pattern. In this study, raw mannitol, SD sucrose, SFD sucrose and raw sorbitol exhibited the oropharyngeal deposition, which is advantageous as DPI carriers whereas SD mannitol, SFD mannitol and raw sucrose dry powders would likely reach the lungs *in vivo* due to the presence of fine particles (aerodynamic diameter: $\leq 5 \mu\text{m}$). SFD mannitol showed the particle deposition both in the oropharynx region and deep lung regions for systemic pulmonary delivery due to high span value. SD

mannitol showed higher FPF than SFD mannitol. This was measured by the NGI depositions studies where ^1H qNMR showed that higher amounts of SD mannitol dry powders deposited on the lower NGI stages compared with SFD mannitol dry powders. So, it can be estimated that more SD saccharide dry powders would be expected to reach the lungs. The developed ^1H qNMR methodology can be used as an analytical method to assess pulmonary deposition in impaction experiments of saccharides employed as carriers in DPI formulations and ensure avoidance of saccharides deep deposition in lung.

Chapter 4. Amino acid-mannitol dry powder inhaler formulations for improved pulmonary deposition of insulin

4.1. Abstract

The aim of the study was to assess how amino acids (glycine or L-leucine) added as excipient to mannitol carrier affect the aerosolisation performance of dry powder inhaler (DPI) formulations containing insulin. Mannitol carriers with the inclusion of two selected amino acids (glycine or L-leucine) at three different concentrations (5%, 10% and 15% w/w) were prepared by spray freeze drying and characterised for their morphology, particle size distribution, thermal behaviour, moisture content and crystallinity. A quantitative method using a reversed-phase high performance liquid chromatography (RP-HPLC) was developed for the determination of insulin content in DPI formulations. The RP-HPLC method produced accurate (relative error%: 0.64%-4.90%) and precise data with high repeatability (relative standard deviation%: 0.63-3.97%) in the concentration range of 2.7 $\mu\text{g mL}^{-1}$ to 108.0 $\mu\text{g mL}^{-1}$ (linear calibration curve for insulin, $R^2 = 0.9999$). The limit of detection was 0.66 $\mu\text{g mL}^{-1}$ and limit of quantitation was 2.01 $\mu\text{g mL}^{-1}$. All formulated spray freeze dried (SFD) mannitol-based carriers displayed a porous spherical particle shape with the particle size ranging from 50 μm to 130 μm regardless of the inclusion or absence of amino acids. However, different surface roughness was observed in SFD carriers. All DPI formulations demonstrated significantly different insulin uniformities (One-way ANOVA, $p < 0.05$). SFD mannitol carrier without amino acid was delicate porous powder that resulted in low insulin uniformity (73.24%). It is plausible that the inclusion of amino acids (5%, 10% glycine or 5%, 15% leucine) strengthened the porous spherical structure of SFD mannitol carrier and facilitated insulin particles adhesion to the carrier surface during blending (insulin uniformity: 85-93%). SFD mannitol carrier exhibited a marked oropharyngeal deposition pattern and facilitated insulin delivery. DPI formulations with optimised aerosolisation performance were achieved when SFD 10% glycine-mannitol carrier (fine particle fraction, FPF: 15.24% \pm 12.04%) and SFD 5% leucine-mannitol carrier (FPF: 10.62% \pm 6.98%) were employed. Therefore, SFD mannitol with 10% glycine or 5% leucine can be potentially used as carriers in DPI formulations to enhance the aerosolisation performance of insulin dry powders for systemic delivery via the pulmonary route of administration.

Keywords: Spray freeze drying, Dry powder inhaler formulation, Carriers, D-mannitol, Amino acids, Insulin, Reversed-phase high performance liquid chromatography

4.2. Introduction

In order to enhance the efficiency of drug delivery from dry powder inhaler (DPI) formulations and in turn improve the fine particle fraction (FPF), various strategies such as particle engineering (e.g., spray drying, freeze drying and spray freeze drying) and the addition of amino acids, such as leucine and glycine, to the formulations have been employed in the development of DPI formulations to control the properties of carrier particles (e.g., altering the morphology or surface roughness to optimise the inter-particulate forces between drug and carrier particles) (Nokhodchi, Martin, 2015, Weers, Miller, 2015, Sou et al., 2016, Mehta, 2018, Yeung et al., 2018, Shetty et al., 2020). Li *et al.* (2016) studied the effects of leucine on moisture protection and aerosolisation performance of spray dried disodium cromoglycate (DSCG) classified as hygroscopic. The results showed that leucine had an anti-hygroscopic property as its addition to the spray dried powder formulation containing DSCG decreased the water uptake with increasing concentrations of leucine (Li et al., 2016). Also, the inclusion of a small amount of leucine (i.e., 2% w/w) improved the FPF ($71.9\% \pm 1.1\%$) compared to the spray dried DSCG alone (FPF: $57.8\% \pm 0.6\%$); this suggests leucine enhanced the DSCG aerosolisation performance (Li et al., 2016). However, no further improvement in the aerosolisation performance was observed with higher leucine concentrations of 10% and 20% (w/w) due to no further modifications of inter-particulate forces (Li et al., 2016). Glycine has been used as a buffering agent in the previously marketed inhaled insulin product: Exubera® (Al-Tabakha, 2015, Ferrati et al., 2018). This inhaled insulin product was prepared by spray drying insulin with a mixture of excipients (mannitol as stabilising/bulking agent, glycine, sodium citrate as buffering/stabilising agent, and sodium hydroxide as pH adjustment) that produced wrinkled, raisin like appearance with corrugated surface roughness of insulin particles suitable for pulmonary delivery (aerodynamic diameter: 3 μm) (Vehring, 2007, Sadrzadeh et al., 2010, Al-Tabakha, 2015). In addition, the formulation was stable at room temperature (provided 2-year shelf life) (Chapter 2.4.2.1) (Vehring, 2007, Weers, Miller, 2015). Sou *et al.* (2011; 2016) also used glycine as a morphological modifier to alter the properties of spray dried mannitol-based formulations for pulmonary delivery (Sou et al., 2011, Sou et al., 2016). Banga (2015) and Ferrati *et al.* (2018) both reported that glycine or a combination of glycine and mannitol can be used for lyophilisation to prepare the powders with elegant cake structure (Banga, 2015, Ferrati et al., 2018).

However, there is no further evidence in the literature of the effects of amino acids on the aerosolisation performance of DPI formulations containing insulin and mannitol-based carriers prepared by spray freeze drying. The aim of the study was to assess how amino acids (glycine or L-leucine) added as excipient to mannitol carrier affect the aerosolisation performance of DPI formulations containing insulin. Spray freeze drying was employed to prepare mannitol-based carriers with two selected amino acids (glycine or L-leucine) at three different concentrations (5%, 10% and 15%) for the development of carrier-based DPI formulations. The previous study (Chapter 3) demonstrated that mannitol carrier powders prepared by spray freeze drying showed better powder flowability when compared to powders prepared by spray drying (Babenko et al., 2019). In the present study, the 90-125 μm particle size fraction for carriers was selected based on the study reported by Kaialy and Nokhodchi (2015). Their study demonstrated that large freeze dried mannitol particles (90-125 μm) as a DPI carrier exhibited better flowability, lower coefficient of variation (CV%, about 2%) in the drug content (salbutamol sulphate) and higher FPF ($48.6\% \pm 1.4\%$) when compared to smaller particles of freeze dried mannitol carrier (20-45 μm , 45-63 μm or 63-90 μm) (Kaialy, Nokhodchi, 2015). The small freeze dried mannitol particles demonstrated poor flow property, higher CV% (around 4.5-7.5%) and lower FPF (around 37-46%) (Kaialy, Nokhodchi, 2015). In addition to the formulation development, a reversed-phase high performance liquid chromatography (RP-HPLC) with an isocratic elution mode for the determination of insulin content in DPI formulations was developed and validated based on the International Council for Harmonisation of Technical Requirements for Pharmaceuticals for Human Use (ICH) guidelines (ICH, 2005).

4.3. Materials

D-mannitol (mannitol), glycine ($\text{NH}_2\text{CH}_2\text{CO}_2\text{H}$, MW: 75.07 g mol⁻¹), human recombinant insulin, phosphate buffered saline tablet (PBS, 0.01M phosphate buffer, 0.0027M potassium chloride, 0.137M sodium chloride, pH 7.4) and sodium benzoate were all purchased from Sigma-Aldrich, UK. L-leucine (leucine, $(\text{CH}_3)_2\text{CHCH}_2\text{CH}(\text{NH}_2)\text{CO}_2\text{H}$, MW: 131.17 g mol⁻¹) was purchased from Sigma life science, UK. Trifluoroacetic acid (TFA, $\text{CF}_3\text{CO}_2\text{H}$, MW: 114.02 g mol⁻¹), acetonitrile ($\text{C}_2\text{H}_3\text{N}$, 41.05 g mol⁻¹), acetic acid glacial ($\text{CH}_3\text{CO}_2\text{H}$, MW: 60.05 g mol⁻¹) and sodium hydroxide pellets (NaOH, 40 g mol⁻¹) were purchased from Fisher Scientific, UK. Deuterium oxide was purchased from Euriso-top®, UK. Sodium 3-trimethylsilyl propionate-2,2,3,3-d₄ was purchased from Merck Sharp & Dohme Canada Limited, UK.

4.4. Method development

A reversed-phase high performance liquid chromatography (RP-HPLC) method with an isocratic elution mode was developed for quantitative analysis of human insulin used in DPI formulations. The method development was performed on an Agilent Technologies 1260 Infinity II high performance liquid chromatography system (HPLC, Agilent Technologies, UK) composed of a degasser (Agilent Technologies, UK), vial sampler (Agilent Technologies, UK), and UV detector (Agilent Technologies, UK). During the method development, a few different columns were tried to find a narrow and sharp symmetry peak of human insulin by changing its length or type (C18 4.6 mm internal diameter x 100 mm length, 5 μm particle size (Merck KGaA, Germany), C18 4.6 mm internal diameter x 250 mm length, 5 μm particle size (Phenomenex, UK), and C8 4.6 mm internal diameter x 250 mm length, 5 μm particle size, 130 \AA pore size (Phenomenex, UK)) from two different manufactures (Merck KGaA, Germany and Phenomenex, UK) but keeping the internal diameter (4.6 mm) and particle size (5 μm) constant. C8 column was selected over C18 columns and used as the stationary phase at room temperature for method validation (Section 4.5). The compositions of mobile phase A (organic phase) and B (aqueous phase) were acetonitrile with trifluoroacetic acid (TFA, 0.1%) and distilled water with TFA (0.1%), respectively. TFA was used to control the pH of mobile phases also used as an ion pair agent to avoid ionisation (Chen, Y. et al., 2004). Retention time, peak asymmetry factor (A_s , United States Pharmacopoeia (USP) at 10% height), tailing factor (T_f , USP at 5% height), and column efficiency (i.e., the plate number, N) for human insulin were monitored while changing the ratio of mobile phase A (acetonitrile with 0.1% TFA) and mobile phase B (distilled water with 0.1% TFA) at a constant flow rate of 1.0 mL min^{-1} in order to find a sharp peak of human insulin. The compositions of mobile phase A and B were kept the same. Peak asymmetry factor (*Equation 6*), tailing factor (*Equation 7*), and column efficiency (*Equation 8*) were calculated using the commonly used equations (Merck KGaA, 2021, Tosoh Bioscience, 2021) as follows:

Peak asymmetry factor (A_s , USP method at 10% height) was calculated using *Equation 6*:

$$A_s = b/a \quad \text{Equation 6}$$

where b is the distance from the peak midpoint to the peak tailing edge measured at 10% peak height and a is the distance from the leading (front) edge of the peak to the peak midpoint

measured at 10% of peak height. The value of 1.0 ($A_s = 1.0$) indicates a symmetrical peak. The value greater than 1 ($A_s > 1$) indicates tailing whereas less than 1 ($A_s < 1$) indicates fronting. Acceptable A_s value is generally between 0.9 and 1.2.

Tailing factor (T_f , USP method at 5% height) was calculated using *Equation 7*:

$$T_f = (a + b) / 2a \quad \text{Equation 7}$$

where a is the distance from the front edge of the peak to the peak midpoint measured at 5% of peak height and b is the distance from the peak midpoint to the peak tailing edge measured at 5% of peak height. $T_f > 1.0$ indicates tailing and $T_f < 1.0$ indicates fronting (Merck KGaA, 2021).

Column efficiency (N) was calculated using *Equation 8*:

$$N = 5.54 (t_R / w_{1/2})^2 \quad \text{Equation 8}$$

where t_R is the retention time of the analyte and $w_{1/2}$ is the width of the peak at half height.

The column temperature was maintained at room temperature. The injection volume (20 μL) was kept constant. Two similar wavelengths of 214 nm and 215 nm for human insulin detected by a UV spectroscopy (Cary UV-Vis Compact, Agilent, UK) were tested. All the development experiments were performed on the Agilent HPLC system at room temperature ($22^\circ\text{C} \pm 3^\circ\text{C}$) and the optimal conditions are summarised in Table 12. The data acquisition and chromatograms (including peak asymmetry factor, tailing factor, and column efficiency) were obtained using an Openlab ChemStation (Agilent Technologies, UK).

Table 12: The optimal chromatography conditions and instrument used for method development and validation. TFA: trifluoroacetic acid.

Instrument	Agilent Technologies 1260 Infinity II high performance liquid chromatography system (Agilent Technologies, UK)
Mobile phase A (31.5% v/v)	Acetonitrile with 0.1% TFA
Mobile phase B (68.5% v/v)	Distilled water with 0.1% TFA
Column	C8 4.6 mm x 250 mm, 5 μm particle size, 130 \AA pore size (Phenomenex, UK)
Column temperature	Room temperature

Wavelength	215 nm
Flow rate	1.0 mL min ⁻¹
Injection volume	20 µL
Elution mode	Isocratic

4.4.1. Preparation of insulin standard stock solution

Human insulin standard stock solution was prepared by dissolving raw human insulin powders in PBS solution (pH 7.4) at a concentration of 1 mg mL⁻¹. The insulin stock solution was used to prepare insulin standard solutions for the calibration curve (Section 4.4.2) and test sample solutions for method validation (Section 4.4.3). The prepared insulin stock solution was stored at 4°C.

4.4.2. Preparation of insulin standard solutions for calibration curve

Insulin standard solutions at seven different concentrations for the calibration curve in the concentration range of 2.7 µg mL⁻¹ to 108.0 µg mL⁻¹, which should cover the concentration range of interest for insulin quantification in DPI formulations, were prepared by diluting insulin standard stock solution (Section in 4.4.1) with distilled water. Insulin calibration standard solutions were used immediately after preparation.

4.4.3. Preparation of insulin test sample solutions for validation

The insulin standard stock solution prepared (Section 4.4.1) was used to prepare three selected levels of insulin concentration (low, middle and high end of the calibration curve concentration range, 5.4 µg mL⁻¹, 54.0 µg mL⁻¹ and 108.0 µg mL⁻¹) for method validation (Section 4.5) following the same method used for the preparation of standard calibration curve solutions described in Section 4.4.2.

4.4.4. Preparation of mobile phase

Mobile phase A (organic phase) was prepared by adding TFA (0.1%, v/v) to acetonitrile and mixed thoroughly (pH ~1.0). Mobile phase B (aqueous phase) was prepared by adding TFA (0.1%, v/v) to distilled water and mixed thoroughly. The final pH of the aqueous mobile phase was 2.

4.5. Method validation

Method validation was carried out based on the ICH guidelines (ICH, 2005). The main objective was to demonstrate that the developed RP-HPLC method was suitable for the quantitation of human insulin in DPI formulations. Validation characteristics, such as specificity, linearity, range, accuracy, precision, limit of detection (LOD) and limit of quantitation (LOQ) as well as robustness and system suitability were assessed. All validation experiments were performed on the Agilent HPLC system under the optimal conditions (Table 12).

4.5.1. Stability

Stability of insulin standard stock solutions (Section 4.4.1), calibration curve solutions (Section 4.4.2) and insulin acidic aqueous solutions used for spray drying (Chapter 5.5) was determined prior to the validation studies to get reliable results.

Insulin standard stock solution

Stability of insulin standard stock solution was tested to determine the acceptable time duration for sample preparation and analysis before the degradation of insulin would take place. Insulin standard stock solutions stored at room temperature ($22^{\circ}\text{C} \pm 3^{\circ}\text{C}$) and at 4°C were tested for up to 10 days after preparation. Stability was determined by comparison to freshly prepared samples and expressed as a percentage with standard deviation (SDv) and relative standard deviation (RSD%).

Insulin calibration standard solutions for short-term storage

In order to run a series of sample sets (i.e., for impaction studies) consecutively at room temperature, stability of insulin calibration standard solutions in the concentration range of $2.7 \mu\text{g mL}^{-1}$ to $108.0 \mu\text{g mL}^{-1}$ stored at room temperature and at 4°C was assessed for short-term storage period up to 72 hours (24 hr, 48 hr, and 72 hr). Stability was calculated as the ratio of the concentration of calibration standard solutions stored at room temperature or at 4°C after each storage time with respect to the concentration of freshly prepared insulin calibration standard solutions. The results were expressed as a percentage with SDv and RSD%.

Insulin acidic aqueous solution

Stability of insulin dissolved in acidic aqueous solution (0.1% acetic acid with 1M sodium hydroxide (NaOH), pH 3.5) used for spray drying (Chapter 5.5) was tested in order to determine the acceptable time duration for sample preparation before the process of spray drying and the degradation of insulin would take place.

4.5.2. Specificity

Specificity of the developed RP-HPLC method was assessed by analysing peaks of mobile phases (A: acetonitrile with 0.1% TFA and B: distilled water with 0.1% TFA), PBS solution used for dissolving human insulin powders, acidic aqueous solution (0.1% acetic acid with 1M NaOH) used for spray drying human insulin (Chapter 5) and each component of insulin DPI formulation (mannitol, glycine and leucine) to see whether those peaks were well separated from the insulin peak at a retention time of insulin (around 5.0 mins) therefore no interference in the quantification of the drug. The peak of insulin in the presence of formulation components was also measured to see if there were any changes appeared in the peak position of insulin.

4.5.3. Linearity and range

The linearity of the developed RP-HPLC method was evaluated by preparing the calibration curve for a series of seven concentrations of human insulin in the concentration range of 2.7 $\mu\text{g mL}^{-1}$ to 108.0 $\mu\text{g mL}^{-1}$. Calibration standard solution (20 μL) at each concentration was injected in triplicate. The calibration curve for human insulin was constructed by plotting the known concentration of human insulin on the x-axis against the area of the peak on the y-axis. The correlation coefficient (R^2) and the regression equation (y intercept and slope of the regression line) were computed using Microsoft® Excel. The linearity was determined by regression analysis at significant level of $p < 0.05$ in Microsoft® Excel.

4.5.4. Accuracy

The accuracy of the developed RP-HPLC method was assessed by measuring three concentrations in six replicates (each test sample solution per concentration was injected six times). The mean, SDv

and RSD% were calculated for each concentration. The accuracy of the measurements was reported as the difference (relative error %) between the measured concentration (mc) and nominal concentration (nc) of human insulin, using Equation 3 in Chapter 3.5.3:

$$(mc-nc)/nc \times 100 \quad \text{Equation 3.}$$

4.5.5. Precision

The intra-day precision of the developed RP-HPLC was assessed by calculating SDv and RSD% of the replicated measurements (three different concentrations, six replicates per concentration on the same day). The inter-day precision of the developed RP-HPLC method was assessed by replicating the same measurements under the same measurement conditions in the same laboratory each day for two to three days (six replicates per concentration). The SDv and RSD% were calculated per concentration (12 replicates per concentration over two days or 18 replicates per concentration over three days).

4.5.6. Limit of detection and limit of quantitation

The LOD (the lowest amount of insulin can be detected but not necessarily quantitated, *Equation 4* in Chapter 3.5.5) and LOQ (the lowest amount of insulin quantitated with suitable accuracy and precision, *Equation 5* in Chapter 3.5.5) were calculated based on the calibration curve method using the standard deviation of the response (standard deviation of y-intercepts) and slope of the calibration curve with the ICH guidelines equations (ICH, 2005). Regression analysis in Microsoft® Excel was performed at the 95% confidence level to calculate the standard deviation of the response and the slope.

$$\text{LOD} = 3.3 \cdot \sigma / S \quad \text{Equation 4}$$

$$\text{LOQ} = 10 \cdot \sigma / S \quad \text{Equation 5}$$

where σ is the standard deviation of the response and S is the slope of the calibration curve.

4.5.7. Robustness

The robustness of the developed RP-HPLC method was studied by slightly changing parameters of the optimal settings, such as flow rate (flow rate: $1.0 \text{ mL min}^{-1} \pm 0.1 \text{ mL min}^{-1}$) to see how the small changes would affect the results (e.g., insulin peak area where the area is directly related to the concentration). Also, a different HPLC instrument with the same manufacture and model (Agilent Technologies 1260 Infinity II) was tried under the optimal settings (Table 12). The robustness of the RP-HPLC method was assessed based on the values of recovery (%) with RSD%.

4.5.8. System suitability

The parameters for system suitability study, such as retention time, peak area, height, peak asymmetry factor (*Equation 6*), tailing factor (*Equation 7*) and theoretical plates (*Equation 8*) were assessed by analysing six replicates of human insulin solution at a concentration of $108.0 \mu\text{g mL}^{-1}$. The acceptable RSD% values of retention time, peak area and height were set to be less than or equal to 1.0% ($\leq 1.0\%$) and theoretical plates (efficiency of the column) were greater than 2000 ($N > 2000$).

4.6. Carrier dry powders preparation by spray freeze drying

Mannitol carriers with and without the inclusion of two selected amino acids (i.e., glycine or leucine) at three different concentrations (5%, 10% and 15% w/w based on mannitol content, 15 g) were prepared by spray freeze drying. The compositions of mannitol aqueous solutions (15% w/v total solid content) for spray freeze drying are listed in Table 13. Each mannitol aqueous solution was sprayed over liquid nitrogen in a round bottom flask (250 mL) and freeze dried using BenchTop Pro with Omnitronics™ freeze dryer (SP Scientific, UK) for 48 hours at $55 \mu\text{bar} \pm 5 \mu\text{bar}$ of pressure and condenser temperature of $-59^\circ\text{C} \pm 2^\circ\text{C}$. After 48 hours, spray freeze dried (SFD) carrier powders produced were sieved using a sieve shaker (Retsch, Germany) with the $90 \mu\text{m}$ and $125 \mu\text{m}$ sieves (Fisher Brand Test Sieve, UK). Collected SFD powders were immediately transferred into tightly closed glass vials and stored in a desiccator over silica gel at room temperature ($22^\circ\text{C} \pm 3^\circ\text{C}$). In this study, seven different SFD carriers (Table 13) were prepared: SFD mannitol (no amino acid), SFD 5% glycine-mannitol (SFD5GM), SFD 10% glycine-mannitol (SFD10GM), SFD 15% glycine-mannitol (SFD15GM), SFD 5% leucine-mannitol (SFD5LM), SFD 10% leucine-mannitol (SFD10LM) and

SFD 15% leucine-mannitol (SFD15LM). These SFD carrier powders (90-125 μm) were used for the development of insulin DPI formulations (Section 4.8 and Chapter 5).

Table 13: Compositions of aqueous solutions (15% w/v total solid content) to prepare spray freeze dried (SFD) mannitol (M) carriers with and without glycine (G) or leucine (L) at three different concentrations (5%, 10% and 15% of mannitol). SFD5GM: SFD 5% glycine-mannitol, SFD5LM: SFD 5% leucine-mannitol, SFD10GM: SFD 10% glycine-mannitol, SFD10LM: SFD 10% leucine-mannitol, SFD15GM: SFD 15% glycine-mannitol, SFD15LM: SFD 15% leucine-mannitol.

SFD carrier	Amino acid concentration of mannitol (% w/w)	Amino acid (leucine or glycine) (g)	Mannitol (g)	Distilled water (mL)	Total solid content (% w/v)
SFD mannitol	0	0	15.00	100	15
SFD5GM	5	0.75	14.25	100	15
SFD5LM					
SFD10GM	10	1.50	13.50	100	15
SFD10LM					
SFD15GM	15	2.25	12.75	100	15
SFD15LM					

4.7. Insulin dry powders preparation

Due to the large particle size of raw human insulin powders intended for inhalation, raw human insulin powders were ground gently using a mortar and pestle to reduce their particle size. The ground insulin powders were stored at -20°C . Raw human insulin powders with reduced particle size were used for the purpose of the pulmonary administration study *in vitro* to investigate the feasibility of using SFD mannitol-based carriers to improve insulin deposition in the lung and the DPI formulation performance.

4.8. Preparation of insulin dry powder inhaler formulations

Insulin DPI formulations (400 mg in total blends) were prepared by blending ground insulin powder (40 mg) with each SFD mannitol-based carrier (360 mg, SFD mannitol alone or SFD mannitol with 5%,

10% and 15% glycine or leucine) in ratio of 1:9 in a plastic container (2 x 9 cm) using a Turbula® system Schatz mixer (WAB, Switzerland) at a constant speed of 46 rpm for 30 min. After blending, the powder blends (400 mg in total) were stored in a desiccator over silica gel at room temperature (22°C ± 3°C) prior to the impaction study (Section 4.11). Seven insulin DPI formulations (Table 14) were prepared: insulin and SFD mannitol blend (IMB), insulin and SFD 5% glycine-mannitol blend (I5GMB), insulin and SFD 10% glycine-mannitol blend (I10GMB), insulin and SFD 15% glycine-mannitol blend (I15GMB), insulin and SFD 5% leucine-mannitol blend (I5LMB), insulin and SFD 10% leucine-mannitol blend (I10LMB) and insulin and SFD 15% leucine-mannitol blend (I15LMB). These seven DPI formulations were used for the impaction study (Section 4.11).

Table 14: Seven insulin dry powder inhaler (DPI) formulations prepared by blending ground insulin dry powders with spray freeze dried (SFD) mannitol-based carriers.

DPI formulation	Formulation component	
	Drug	Carrier
IMB	Insulin	SFD 15% mannitol
I5GMB	Insulin	SFD 5% glycine-mannitol
I10GMB	Insulin	SFD 10% glycine-mannitol
I15GMB	Insulin	SFD 15% glycine-mannitol
I5LMB	Insulin	SFD 5% leucine-mannitol
I10LMB	Insulin	SFD 10% leucine-mannitol
I15LMB	Insulin	SFD 15% leucine-mannitol

4.9. Physicochemical characterisation

Mannitol-based carriers prepared by spray freeze drying (Section 4.6) were characterised in terms of morphology (Section 4.9.1), particle size distribution (Section 4.9.2), thermal behaviour (Section 4.9.3), moisture content (Section 4.9.4) and crystallinity (Section 4.9.5).

4.9.1. Scanning electron microscopy

Morphologies along with particle size of individual materials (raw human insulin, ground human insulin, glycine, and leucine) and seven SFD carriers (SFD mannitol, SFD5GM, SFD10GM, SFD15GM, SFD5LM, SFD10LM and SFD15LM) were characterised by Scanning Electron Microscopy (SEM, ZEISS

EVO[®]50, UK) at an acceleration voltage of 10-25 kV at different magnifications. Double-sided cohesive carbon tabs were adhered to aluminium stubs and all dry powder samples were placed onto the carbon tabs. Any excess powder samples were tapped off the tabs. These samples were then coated with a palladium/gold alloy using a SC7640 Sputter Coater (Polaron, UK) under argon gas for 2 minutes. Multiple images of coated samples were captured for each sample. SEM images of seven insulin DPI formulations (ground insulin and SFD carrier blends: IMB, I5GMB, I10GMB, I15GMB, I5LMB, I10LMB, and I15LMB) after blending (Section 4.8) were also captured for the visual observation of the blends (Blend homogeneity assessment in Section 4.10) following the same method used for the individual material and SFD carriers as described above.

4.9.2. Laser diffraction

Particle size distribution of glycine and seven SFD carriers (SFD mannitol, SFD5GM, SFD10GM, SFD15GM, SFD5LM, SFD10LM and SFD15LM) was measured using a HELOS/BF laser diffraction system equipped with a Rodos disperser (Sympatec GmbH, Germany) and VIBRI vibratory feeding unit (Sympatec GmbH, Germany) in the R3 measuring range of 0.5/0.9 μm to 175 μm . The trigger condition for normal measurement under the standard mode was set to start after the “channel 21” was $\geq 1.0\%$ and to stop after the optimal concentration was $\leq 1.9\%$ for 10 sec or 60 sec trigger time out. The primary pressure for the disperser was set to 1.0 bar. Sympatec WINDOX software (Sympatec GmbH, Germany) was used to calculate particle size (Dv10, Dv50 and Dv90: particle diameters below which 10%, 50% and 90% of the total sample volume are equal to the measured diameters or smaller than the measured values, respectively and Dv50: the median for a volume distribution) and volume mean diameter (VMD). The width of the particle size distribution expressed as span, which is equal to $(Dv90-Dv10)/Dv50$, was calculated.

There was no data obtained for raw leucine due to the outside particle size measurement range (0.5/0.9 μm to 175 μm) by laser diffraction.

4.9.3. Differential scanning calorimetry

Thermal analysis of two selected amino acids (glycine and leucine) and seven SFD carriers (SFD mannitol, SFD5GM, SFD10GM, SFD15GM, SFD5LM, SFD10LM, and SFD15LM) was carried out using a DSC822e Differential Scanning Calorimetry (DSC, Mettler Toledo, Switzerland) under nitrogen gas (50 mL min^{-1}) in the temperature range from 25°C to 400°C at a heating rate of 10°C min^{-1} or 40°C min^{-1} . All dry powder samples were placed in aluminium crucibles (40 μL) and sealed with a pierced lid on.

The dry powder samples loaded pan and empty reference pan were placed on the DSC sample holder. The DSC curves were recorded at 22°C using STARe Software version 8.10 (Mettler Toledo, UK).

4.9.4. Thermogravimetric analysis

Thermogravimetric Analysis (TGA) for two selected amino acids (glycine and leucine) and six SFD carriers (SFD5GM, SFD10GM, SFD15GM, SFD5LM, SFD10LM and SFD15LM) was performed to measure moisture content using a METTLER TOLEDO TGA/DSC1 STARe System (Mettler Toledo, Switzerland) along with DSC analysis (Section 4.9.3). All dry powder samples were loaded onto a pan (70 µL) and heated under nitrogen gas (50 mL min⁻¹) in the temperature range from 25°C to 400°C. The TGA curves were recorded at 22°C using STARe Software version 8.10 (Mettler Toledo, UK). Moisture content of SFD mannitol was previously reported (Chapter 3.11.2.4) (Babenko et al., 2019).

4.9.5. X-ray diffraction

Crystallinity and polymorphic nature of two selected amino acids (glycine and leucine) and seven SFD carriers (SFD mannitol, SFD5GM, SFD10GM, SFD15GM, SFD5LM, SFD10LM and SFD15LM) were studied using a D8 Advance X-ray diffractometer (Bruker Axs, Germany). The amino acids and SFD carrier dry powder samples were placed onto sample holders with the powder surface flattened and scanned from the diffraction angle of 5° to 55° at 2θ angle with a step size of 0.100° sec⁻¹ and operated at 20°C. The X-ray diffraction (XRD) patterns were acquired using a Diffrac-Plus XRD Commander software (Bruker, Germany).

4.10. Blend homogeneity assessment

Blend homogeneity for seven carrier-based DPI formulations (IMB, I5GMB, I10GMB, I15GMB, I5LMB, I10LMB, and I15LMB) was assessed by quantifying the content of insulin and mannitol using the developed RP-HPLC method (Section 4.13.1 and 4.13.2) and proton quantitative nuclear magnetic resonance (¹H qNMR) method (Chapter 3) (Babenko et al., 2019), respectively. Blend samples (4 mg total blend; 0.4 mg insulin and 3.6 mg SFD carrier) were taken from three different positions (top, middle and bottom) of each DPI formulation in the blending container and dissolved in distilled

water (4 mL, theoretical insulin concentration: 100 $\mu\text{g mL}^{-1}$). Insulin content uniformity was determined as the ratio of the concentration of insulin to the theoretical concentration of insulin contained in the blend sample and expressed as a percentage (recovery %). Coefficient of variation (%CV or referred to as RSD%) was used as a degree of insulin content homogeneity. High %CV values indicate a low drug content homogeneity (Kaialy, Nokhodchi, 2016) and drug content is considered uniform when %CV is below 6% (Kaialy, Nokhodchi, 2015). Simultaneously, the content uniformity of mannitol in the blend sample was determined using the ^1H qNMR. All NMR data were processed using TopSpin™ software 4.1.0 (Bruker BioSpin GmbH, Germany).

4.11. Impaction study

Pulmonary deposition study for seven DPI formulations (IMB, I5GMB, I10GMB, I15GMB, I5LMB, I10LMB and I15LMB) was carried out using a next generation impactor (NGI, Copley Scientific, UK) with the Alberta Idealised Throat 28028 (AIT, Copley Scientific, UK) to determine the amount of ground insulin powders deposited on AIT and all NGI stages and estimate *in vitro* lung deposition profile of insulin. The efficiency of insulin delivery was also studied using IMB formulation (insulin and SFD mannitol carrier blend). The aerosolisation performance of insulin from DPI formulations containing SFD mannitol carriers with amino acid (glycine or leucine) was compared to DPI formulation containing SFD mannitol alone (no amino acid, IMB formulation).

The NGI was equipped with a Critical Flow Controller (TPK 2000, Copley Scientific, UK) connected to a Vacuum pump (HPC5, Copley Scientific, UK). The flow rate was adjusted to 30 L min^{-1} with the test airflow duration of 3 sec. The critical flow (P3/P2 ratio ≤ 0.5 , flow rate stability) was tested to be stable. A leak test was performed on the NGI prior to each use. Handihaler® (Boehringer Ingelheim, Germany, a single capsule inhalation device with high resistance) was used to deliver the content of ground insulin powders filled (total fill mass per capsule: 20 mg \pm 1 mg, theoretical insulin per capsule: 2 mg) in the HPMC size 3 capsules (CAPSUGEL®, UK) to the NGI. The insulin powders deposited on AIT and on all NGI stages (stages 1-7 and micro orifice collector, MOC) were collected using distilled water (2 or 3 mL) and quantified by RP-HPLC (Section 4.13.1 and 4.13.2) immediately. Insulin powders deposited on 7 stages in the NGI were based on the aerodynamic cut-off diameters of 0.541 μm (stage 7), 0.834 μm (stage 6), 1.357 μm (stage 5), 2.299 μm (stage 4), 3.988 μm (stage 3), 6.395 μm (stage 2), and 11.719 μm (stage 1) at flow rate of 30 L min^{-1} . Particles collected from the low impactor stages (e.g., between 3 and 5) with less than or equal to 5.0 μm aerodynamic diameter generally represent drug deposition required for effective systemic pulmonary delivery. All NGI studies were performed in triplicate at room temperature. Insulin aerosolisation performance was

assessed using Microsoft® Excel and Copley Inhaler Testing Data Analysis Software (CITDAS) Version 3.10 Wibu (Copley Scientific, UK) to determine the insulin delivered dose, FPF, mass median aerodynamic diameter (MMAD) and geometric standard deviation (GSD). The delivered dose (%) was determined as the ratio of the total insulin deposition on AIT and all the NGI stages excluding the deposition in the inhaler device and capsules to the total insulin dose dispersed from the device including the deposition in the inhaler device and capsules (i.e., the mass of the insulin powders filled into the capsule).

4.12. Statistical analysis

Statistical analysis was performed using SPSS® statistics software version 24.0 (IBM, UK) along with Microsoft® Excel at significant level of $p < 0.05$. One-way ANOVA (Analysis of Variance) and t-test were used to compare the mean results for data (method development and validation, and insulin content uniformity and NGI study for all DPI formulations). If the ANOVA was itself significant Post Hoc test (Tukey honestly significant difference (HSD) test) was further performed to determine which groups were different from each other (Ennos, 2012).

4.13. Results and discussion

4.13.1. Method development

The optimal chromatography conditions for insulin quantification were found as follows and presented in Table 12 (Section 4.4). Mobile phase A (organic phase) consisted of acetonitrile and TFA (0.1% v/v), whereas mobile phase B (aqueous phase) consisted of distilled water and TFA (0.1% v/v); these were used in the ratio of 31.5:68.5 (A:B, % v/v). The stationary phase was a C8 column. The elution mode was isocratic. A detection wavelength was set to 215 nm; two wavelengths of 214 nm and 215 nm for human insulin demonstrated to provide the same results (i.e., concentration recovery, t-test, $p > 0.05$) (Table 15 and Figure 27). Injection volume was 20 μL and flow rate was 1.0 mL min^{-1} . These conditions provided a symmetry peak of human insulin without tailing ($A_s: 1.00 \pm 0.02$ and $T_f: 1.00 \pm 0.02$) at a retention time of 5.07 mins ± 0.03 mins (average) and high efficiency of

chromatography peak (N: 2393) (see HPLC chromatograms for the insulin calibration curve in Figure 31).

The developed method was used for blend homogeneity assessment (Section 4.13.4 and Chapter 5.12.2), impaction studies (Section 4.13.5 and Chapter 5.12.3) and insulin stability study (Chapter 5.12.4).

Table 15: Comparison of recovery (%) using two wavelengths of 215 nm and 214 nm (insulin concentration: $54.0 \mu\text{g mL}^{-1}$ and $108.0 \mu\text{g mL}^{-1}$). Data presented as mean \pm standard deviation. RSD: relative standard deviation.

Wavelength	Nominal concentration ($\mu\text{g mL}^{-1}$)	Mean measured concentration ($\mu\text{g mL}^{-1}$)	Recovery (%)	RSD (%)
215 nm	108.0	108.59 ± 0.64	100.54 ± 0.59 (n=6)	0.59
	54.0	53.81 ± 0.66	99.65 ± 1.22 (n=7)	1.22
214 nm	108.0	112.02 ± 0.95	103.72 ± 0.88 (n=5)	0.85
	54.0	53.68 ± 0.61	99.42 ± 1.13 (n=6)	1.13

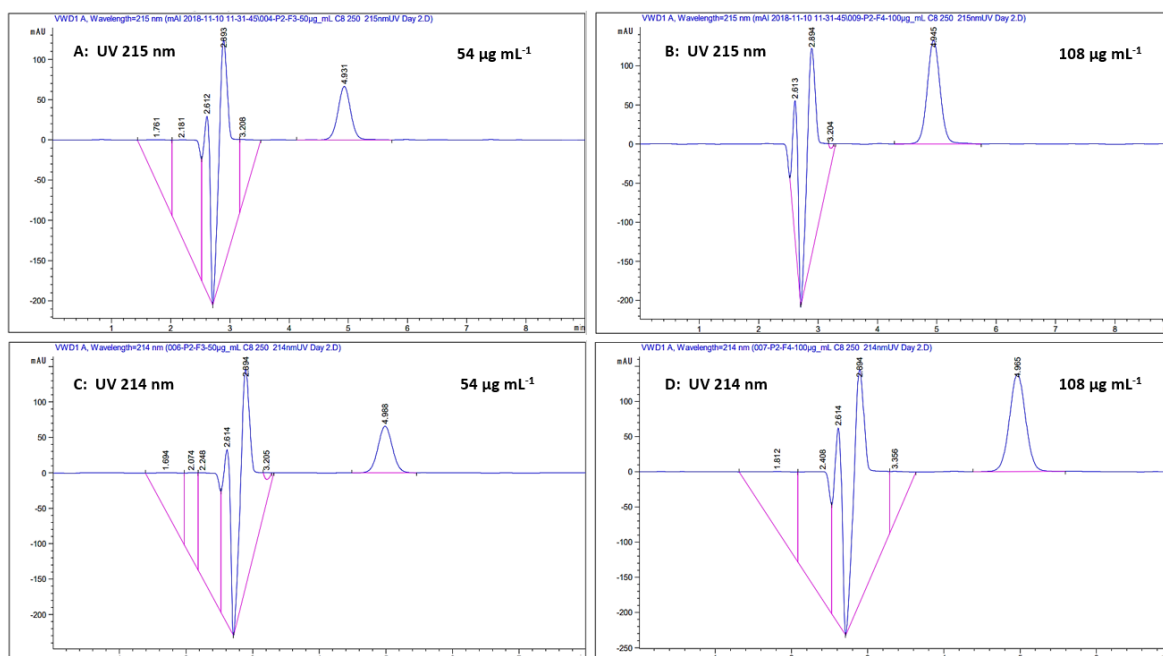


Figure 27: HPLC chromatograms of insulin (insulin concentration: $54 \mu\text{g mL}^{-1}$ and $108 \mu\text{g mL}^{-1}$) at a retention time of around 4.9 mins with two UV wavelengths: 215nm (A,B) and 214nm (C,D). Vertical axis represents area (mAU), and horizontal axis represents retention time (min).

4.13.2. Method validation

4.13.2.1. Stability

Insulin standard stock solution

Insulin stock solution (1 mg mL⁻¹) dissolved in PBS (pH 7.4) was tested to be stable for up to 74 hours when stored at room temperature and for 10 days at least when stored at 4°C (Table 16). It was observed that the stock solution stored at room temperature for 7 days generated the fluctuated base line and small peak of insulin (Figure 28).

Table 16: Stability study on insulin standard stock solution (1 mg mL⁻¹) stored at room temperature for 7 days and at 4°C for 10 days (Data presented as mean (%) ± standard deviation, n=4-6).

Insulin stock concentration (1 mg mL ⁻¹)	6hr	25hr	50hr	74hr	7 days	10 days
Room temperature	99.60 ± 0.64	99.29 ± 0.75	99.62 ± 0.40	100.70 ± 0.54	0.57±0.47	-
4°C	99.80 ± 0.63	99.65 ± 0.41	-	99.63 ± 0.41	99.64 ± 0.50	99.55 ± 0.59

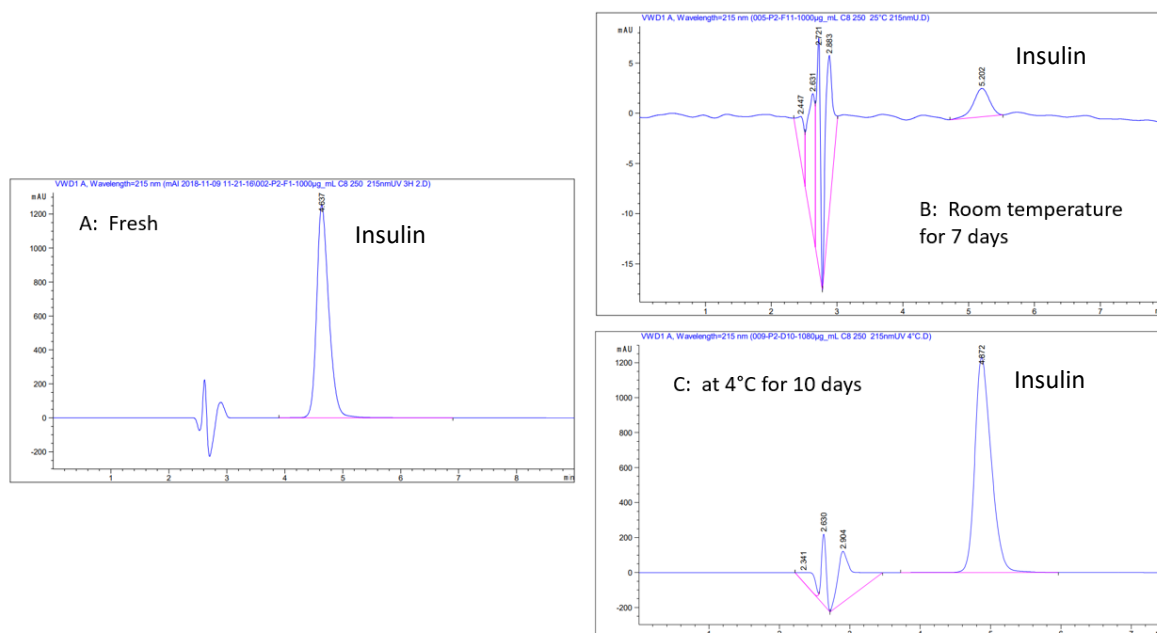


Figure 28: HPLC chromatograms for freshly prepared (within 3 hours) insulin stock solution (1 mg mL^{-1}) (A), insulin stock solution stored at room temperature for 7 days (B) and at 4°C for 10 days (C). Vertical axis represents area (mAU), and horizontal axis represents retention time (min).

Insulin calibration standard solutions for short-term storage

Insulin calibration standard solutions in the concentration range of $5.4 \text{ } \mu\text{g mL}^{-1}$ to $108.0 \text{ } \mu\text{g mL}^{-1}$ were relatively stable for up to 72 hours when stored at room temperature and at 4°C (Table 17).

However, the lowest concentration ($2.7 \text{ } \mu\text{g mL}^{-1}$) showed instability ($\leq 62\%$) when stored both at room temperature and 4°C for up to 72 hours. Therefore, it is recommended that freshly made solutions in the lower concentration range should be run immediately after sample preparation (within 24 hours) due to instability of the solutions.

Table 17: Stability study on insulin calibration standard solutions stored at room temperature and 4°C for up to 72 hours (Data presented as mean (%) \pm standard deviation, $n=3$).

Insulin concentration ($\mu\text{g/mL}$)	Room temperature			4°C		
	24h	48h	72h	24h	48h	72h
108.0	99.31 ± 0.32	98.96 ± 0.20	99.08 ± 0.37	99.76 ± 0.35	99.26 ± 0.38	98.55 ± 0.37
81.0	99.97 ± 0.12	98.94 ± 0.29	99.51 ± 0.90	100.38 ± 0.09	98.14 ± 0.34	99.62 ± 0.45

54.0	100.52 ± 0.43	98.91 ± 0.26	99.10 ± 0.34	99.77 ± 0.21	99.79 ± 0.55	99.53 ± 0.85
27.0	101.47 ± 0.37	99.27 ± 0.15	99.03 ± 0.57	98.78 ± 0.20	97.39 ± 0.31	97.93 ± 0.69
10.8	97.91 ± 0.26	98.32 ± 0.14	98.78 ± 0.19	101.40 ± 0.35	96.50 ± 0.16	99.23 ± 0.23
5.4	106.21 ± 0.15	93.76 ± 0.16	102.49 ± 0.14	87.40 ± 0.36	85.25 ± 0.24	81.83 ± 0.33
2.7	62.43 ± 0.14	53.00 ± 0.18	57.03 ± 0.05	47.21 ± 0.10	59.11 ± 0.46	57.83 ± 0.00 (n=1)

Insulin acidic aqueous solution for spray drying

Insulin acidic aqueous solution (pH 3.5) for spray drying (Chapter 5.5) was relatively stable for 24 hours when stored at room temperature ($85.84\% \pm 0.43\%$) and at 4°C ($90.06\% \pm 0.38\%$). However, freshly made aqueous solutions (within 3 hours of preparation) stored at 4°C were used for spray drying.

4.13.2.2. Specificity

All the peaks of mobile phases (A: 31.5% v/v, acetonitrile with 0.1% TFA and B: 68.5% v/v, distilled water with 0.1% TFA), PBS solution (pH 7.4), acidic aqueous solution (0.1% acetic acid with 1M NaOH, pH 3.5) and each component of insulin DPI formulation (mannitol, glycine and leucine) were well separated from the peak of insulin at the retention time of around 5 mins (Figure 29). There were no changes observed in the peak position of insulin when measured insulin in the presence of formulation components (mannitol and glycine in Figure 29D or mannitol and leucine in Figure 29E). This indicates that mobile phases and the excipients used in DPI formulations did not interfere in the analysis of human insulin. Therefore, the developed RP-HPLC method was found to be specific to measure human insulin in DPI formulation samples.

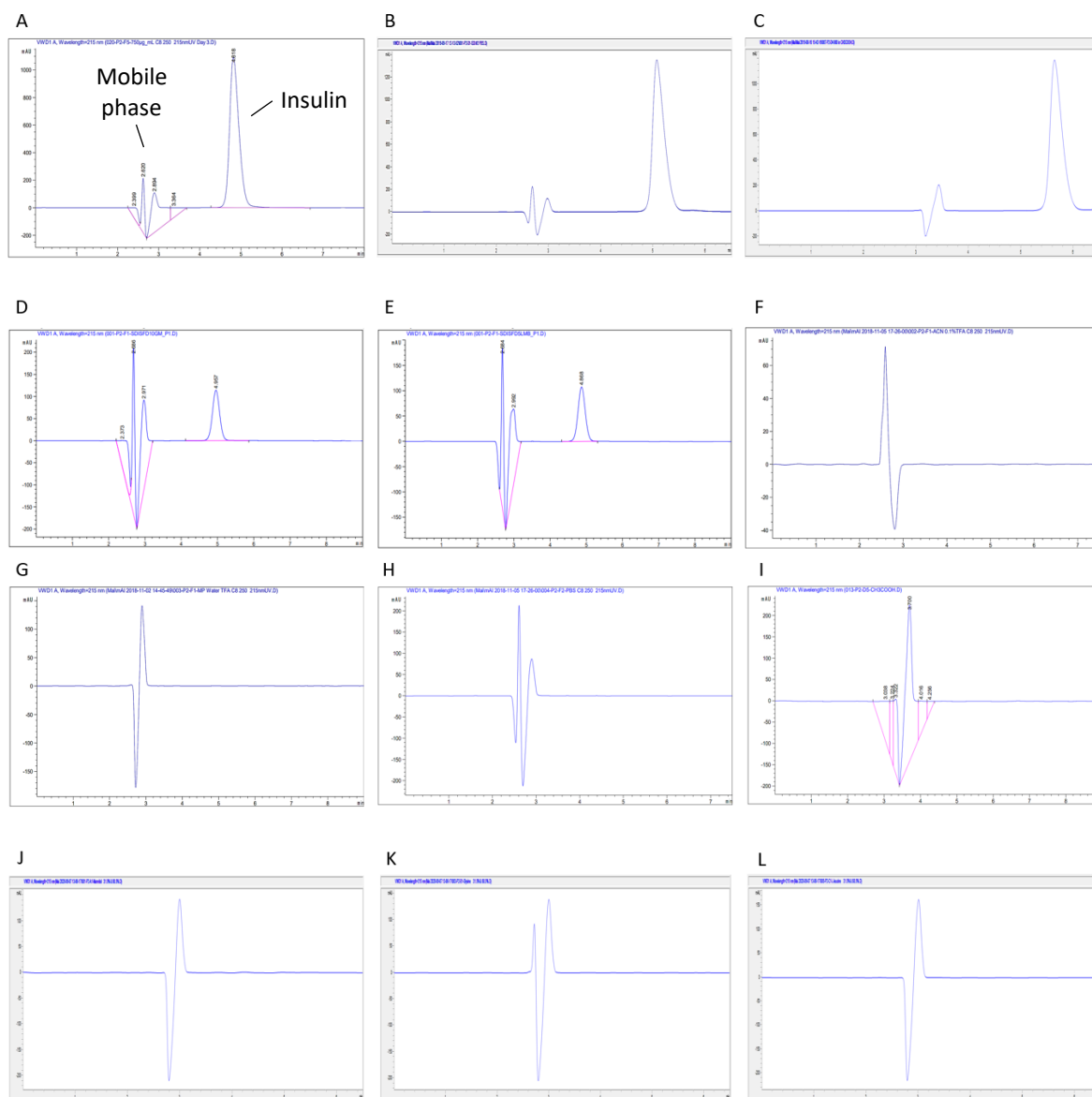


Figure 29: HPLC chromatograms for mobile phases (31.5:68.5 (%v/v) mixture of acetonitrile with 0.1% trifluoroacetic acid (TFA) and distilled water with 0.1% TFA) at a retention time of 2-3 minutes and raw insulin ($810 \mu\text{g mL}^{-1}$) dissolved in phosphate buffered saline (PBS) solution (pH 7.4) at a retention time of around 5 mins (A), spray dried (SD) insulin ($1000 \mu\text{g mL}^{-1}$) dissolved in PBS solution (pH 7.4) (B), raw insulin ($980 \mu\text{g mL}^{-1}$) dissolved in 0.1% acetic acid with 1M NaOH aqueous solution (pH 3.5) (C), SD insulin ($78 \mu\text{g mL}^{-1}$) in the presence of spray freeze dried (SFD) 10% glycine-mannitol carrier (D), SD insulin ($73 \mu\text{g mL}^{-1}$) in the presence of SFD 5% leucine-mannitol carrier (E), mobile phase A: acetonitrile with 0.1% TFA (F), mobile phase B: distilled water with 0.1% TFA (G), PBS solution (pH 7.4) (H), 0.1% acetic acid with 1M NaOH aqueous solution (pH 3.5) (I), raw mannitol dissolved in distilled water (1 mg mL^{-1}) (J), raw glycine dissolved in distilled water (1 mg mL^{-1}) (K), raw leucine dissolved in distilled water (0.43 mg mL^{-1}) (L). Vertical axis represents area (mAU), and horizontal axis represents retention time (min).

4.13.2.3. Linearity and range

The calibration curve constructed for human insulin was linear with R^2 value of 0.9999 in the concentration range of $2.7 \mu\text{g mL}^{-1}$ to $108.0 \mu\text{g mL}^{-1}$ (Figure 30). The HPLC insulin peaks for the calibration curve presented in Figure 31 show the direct proportional relationship between the area of the peak and the concentration within the concentration range selected.

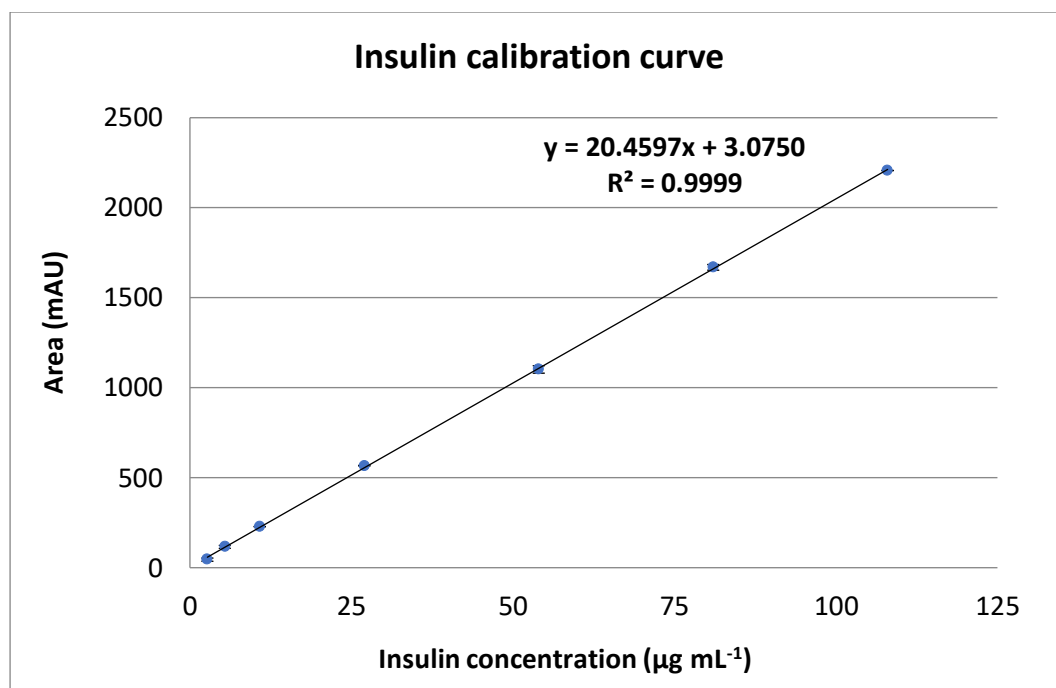


Figure 30: Calibration curve for human insulin in the concentration range of $2.7 \mu\text{g mL}^{-1}$ to $108.0 \mu\text{g mL}^{-1}$ ($n=3$).



Figure 31: HPLC chromatograms for the calibration curve of human insulin in the concentration range from $2.7 \mu\text{g mL}^{-1}$ (bottom) to $108.0 \mu\text{g mL}^{-1}$ (top). Average retention time: $5.07 \text{ mins} \pm 0.03 \text{ mins}$, asymmetry factor: 1.00 ± 0.02 , tailing factor: 1.00 ± 0.02 , and efficiency of chromatography peak: 2392.91.

Vertical axis represents area (mAU), and horizontal axis represents retention time (min).

4.13.2.4. Accuracy and precision

The accuracy and precision of the RP-HPLC method was assessed at three different concentrations. Table 18 shows that relative error (%) at three different concentrations were all below 5.0% (0.64%-4.90%). The SDv and RSD% were all below 1.0 (SDv: 0.17-1.01) and below 4.0 (RSD%: 0.63-3.97), respectively. These results demonstrated that the RP-HPLC method produced accurate (relative error%: < 5.0) and precise data with high repeatability (RSD%: <4.0) over the concentration range used.

Table 18: Accuracy (relative error %), intra-day precision (six replicates per concentration on the same day) and inter-day precision (12 or 18 replicates per concentration over 2 or 3 days) at three different concentrations for the RP-HPLC method. Data presented as mean \pm standard deviation (SDv). RSD: relative standard deviation.

Nominal insulin concentration ($\mu\text{g mL}^{-1}$)	Intra-day precision (n=6)			Inter-day precision		
	Mean measured insulin concentration ($\mu\text{g mL}^{-1}$) \pm SDv	RSD (%)	Relative error (%)	Mean measured insulin concentration ($\mu\text{g mL}^{-1}$) \pm SDv	RSD (%)	Relative error (%)
108.0	104.84 \pm 1.01	0.96	-2.93	103.97 \pm 0.66 (n=18, 3 days)	0.63 (n=18, 3 days)	-3.74 (n=18, 3 days)
54.0	51.35 \pm 0.56	1.09	-4.90	52.91 \pm 0.41 (n=18, 3 days)	0.78 (n=18, 3 days)	-2.03 (n=18, 3 days)
5.4	5.37 \pm 0.17	3.17	-0.64	5.21 \pm 0.21 (n=12, 2 days)	3.97 (n=12, 2 days)	-3.46 (n=12, 2 days)

4.13.2.5. Limit of detection and limit of quantitation

The RP-HPLC method generated low LOD ($0.66 \mu\text{g mL}^{-1}$) and LOQ ($2.01 \mu\text{g mL}^{-1}$) (Table 19) indicating high sensitivity and the concentration range of the calibration curve were both within LOD and LOQ. Insulin was quantitative with suitable accuracy and precision above the LOQ level.

Table 19: Linear correlation coefficient (R^2), regression equation, limit of detection (LOD) and limit of quantitation (LOQ).

Insulin concentration range	Calibration curve regression equation	R^2	LOD ($\mu\text{g mL}^{-1}$)	LOQ ($\mu\text{g mL}^{-1}$)
$2.7\text{-}108.0 \mu\text{g mL}^{-1}$	$y = 20.4597x + 3.0750$	0.9999	0.6637	2.0113

4.13.2.6. Robustness

The RP-HPLC method demonstrated 83-96% recovery with RSD% below 1.0% when flow rate was changed from 1.0 mL min^{-1} to 0.9 mL min^{-1} or to 1.1 mL min^{-1} (Figure 32 and Table 20) and these results were within the acceptable range of 80-120%. However, their areas were significantly different when the changes were applied (t-test, $p < 0.05$: between 1.0 mL min^{-1} and 0.9 mL min^{-1} , between 1.0 mL min^{-1} and 1.1 mL min^{-1}). The RP-HPLC method remained unaffected between instruments with the same manufacture and model under the optimal settings (recovery: 97-100% and RSD%: 0.3-3.2) (Table 20).

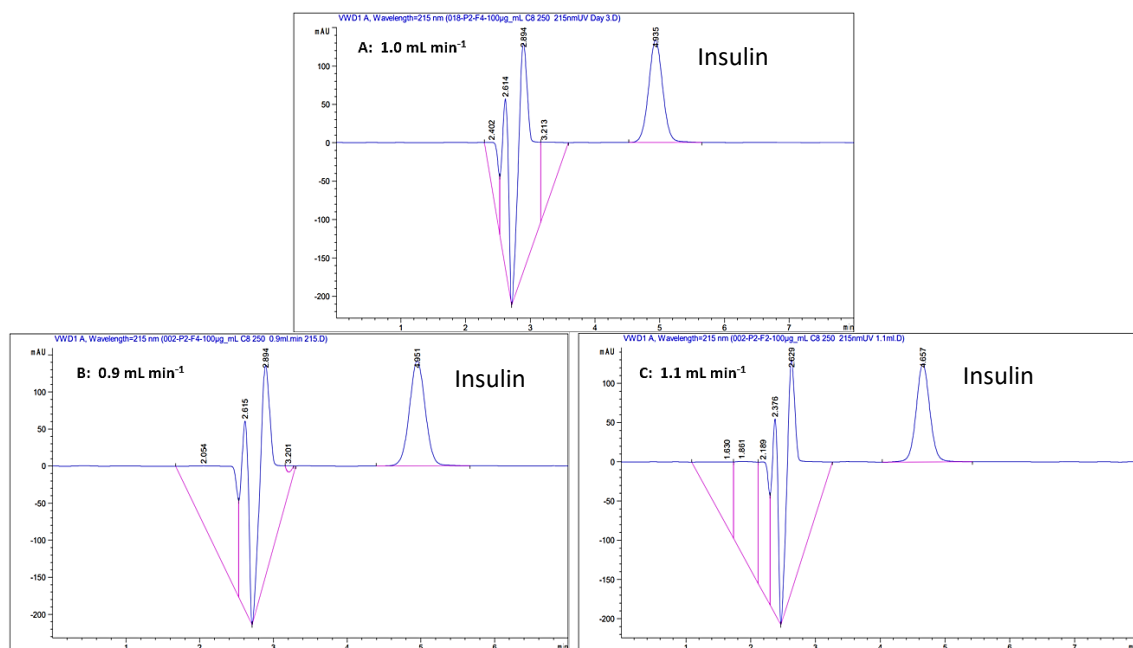


Figure 32: HPLC chromatograms for insulin (concentration: $108 \mu\text{g mL}^{-1}$) at different flow rates: 1.0 mL min^{-1} (A), 0.9 mL min^{-1} (B) and 1.1 mL min^{-1} (C). (Area: t-test, $p < 0.05$ between 1.0 mL min^{-1} and 0.9 mL min^{-1} , between 1.0 mL min^{-1} and 1.1 mL min^{-1}).

Vertical axis represents area (mAU), and horizontal axis represents retention time (min).

Table 20: Results of robustness study. Data presented as mean \pm standard deviation. RSD: relative standard deviation.

	Nominal insulin concentration ($\mu\text{g mL}^{-1}$)	Mean measured insulin concentration ($\mu\text{g mL}^{-1}$)	Recovery (%)	RSD (%)
Flow rate 0.9 mL min^{-1}	108.0	103.57 ± 0.46	95.90 ± 0.42 (n=5)	0.44
Flow rate 1.1 mL min^{-1}	108.0	89.56 ± 0.89	82.93 ± 0.82 (n=6)	0.99
Different HPLC instrument	98.0	95.34 ± 0.27	97.28 ± 0.28 (n=3)	0.29
	49.0	49.26 ± 1.56	100.54 ± 3.19 (n=3)	3.17

4.13.2.7. System suitability

RSD% values of system suitability parameters (e.g., retention time, peak area, and height) were all within 1.0% (RSD%: 0.22-0.45) and the efficiency of the column was above 2000 (N: 2379.37) (Table 21). The peak of insulin was symmetry (As: 1.04) and no tailing (Tf: 1.04). This indicated that all the

acceptable criteria for system suitability were met and all the results generated by the HPLC instrument were verified. Therefore, the developed RP-HPLC method was suitable to use for blend homogeneity assessment (Section 4.13.4 and Chapter 5.12.2), impaction studies (Section 4.13.5 and Chapter 5.12.3) and human insulin stability study (Chapter 5.12.4).

Table 21: Results of system suitability study (n=6). SDv: standard deviation, RSD: relative standard deviation.

Insulin concentration (108.0 µg mL ⁻¹)	System suitability parameter					
	Retention time (min)	Peak area (mAU)	Peak height (mAU)	Theoretical plates	Asymmetry factor	Tailing factor
Mean	4.84	2125.62	140.94	2379.37	1.04	1.04
SDv	0.01	4.66	0.64	30.91	0.01	0.01
RSD (%)	0.27	0.22	0.45	1.30	0.74	0.81

4.13.3. Physicochemical characterisation

All mannitol dry powders with and without the inclusion of two selected amino acids (5%, 10% and 15% glycine or leucine) were successfully prepared as DPI carriers using spray freeze drying (Section 4.6). Prior to the impaction study (Section 4.13.5), SFD mannitol-based carriers were characterised by SEM (Section 4.13.3.1), laser diffraction (Section 4.13.3.2), DSC (Section 4.13.3.3), TGA (Section 4.13.3.4) and X-ray diffraction (Section 4.13.3.5).

4.13.3.1. Scanning electron microscopy

The SEM images of human insulin powders in Figure 33 indicate that grinding reduced the overall particle size of raw human insulin powders, where the majority of the particle sizes were below 20 µm (Figure 33B). The SEM image of glycine (Figure 34B) showed irregular agglomerates of particles with particle size ranging between 15 µm and 150 µm. Leucine had a particle size ranging from 300 µm to 400 µm (Figure 34F) which is not suitable for DPI carrier purposes. Spray freeze drying produced spherical and porous particles with the particle size ranging from 50 µm to 130 µm (Figure 34), which is suitable (50-200 µm) as DPI carriers, regardless of the inclusion or absence of amino acids. The SEM images of SFD mannitol in the presence of glycine (Figure 34C-E) revealed spherical

particles with rough and uneven surfaces that covered mesh structures underneath. However, the surface of SFD mannitol containing 5% glycine (Figure 34C) was rather thin or flaky and porous compared to the surface of SFD mannitol containing 10% and 15% glycine (Figure 34D-E). In contrast, SFD mannitol containing leucine showed no such coating or surface layers, but spherical shapes with the mesh structures (Figure 34G-I). Reducing the concentration of leucine to 10% or 5% resulted in more crumbly looking porous particles (Figure 34G-H) compared to the particles with 15% leucine content (Figure 34I), which exhibited a pumice stone-like texture/appearance with a rough surface. It was found that using different amino acid with varying concentrations altered the morphology/surface property of SFD mannitol-based carriers where the degree of porous structured particles increased with the decrease of amino acid concentration (using higher mannitol concentration resulted in more porous and delicate particles). This might have had an influence on drug content uniformity (Section 4.13.4).

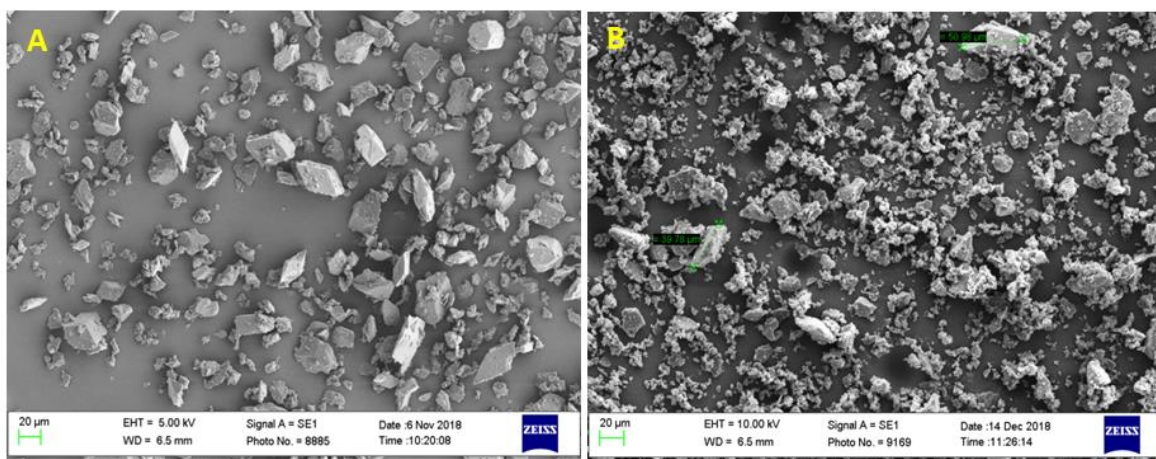
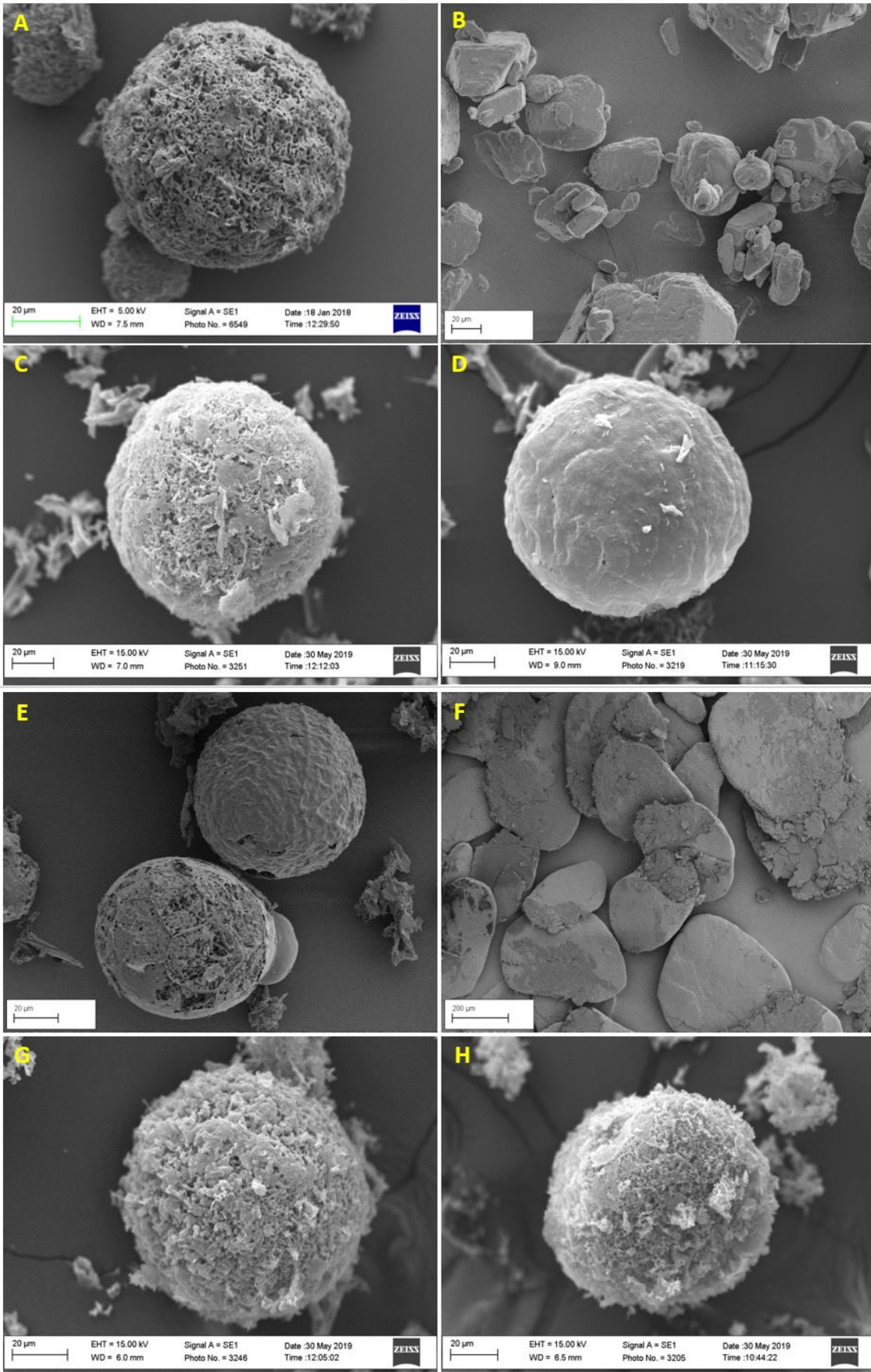


Figure 33: Scanning electron microscopy (SEM) images of raw human insulin before grinding (A) and ground raw human insulin (B).



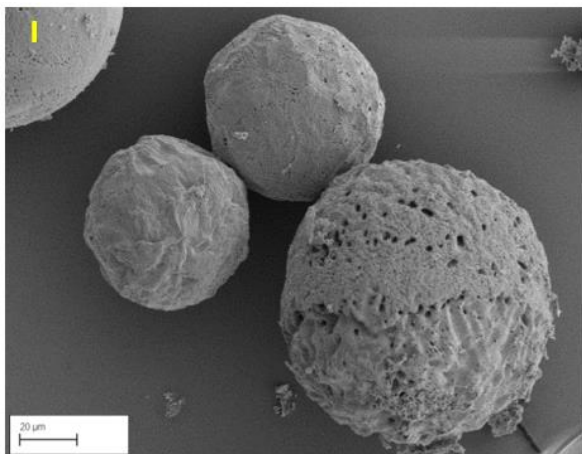


Figure 34: SEM images of spray freeze dried (SFD) mannitol (A), glycine (B), SFD 5% glycine-mannitol (C), SFD 10% glycine-mannitol (D), SFD 15% glycine-mannitol (E), leucine (F), SFD 5% leucine-mannitol (G), SFD 10% leucine-mannitol (H) and SFD 15% leucine-mannitol (I).

4.13.3.2. Laser diffraction

The results of the particle size distribution for SFD mannitol carriers with and without amino acids are presented in Table 22. Although SFD carriers with the particle size fraction of 90-125 μm were used, all SFD carriers had a smaller VMD values (below 50 μm) (Table 22). This could be due to the presence of small fragments of the porous particles observed by the SEM images (Figure 34) that would have de-aggregated during the particle size measurement. It was observed that VMD values increased with the decrease of amino acid concentration (Table 22). In comparison with SFD mannitol alone, SFD mannitol with leucine showed larger VMD values in the following rank order: SFD5LM (49.13 μm) > SFD10LM (46.69 μm) > SFD15LM (38.04 μm) > SFD mannitol (18.93 μm) (Table 22). This suggests that the inclusion of higher leucine content decreases VMD values. The span values for all SFD mannitol-based carriers were in the rank order of SFD15LM (9.32) > SFD5GM (8.47) > SFD mannitol (7.99) > SFD10GM (5.82) > SFD15GM (4.29) > SFD10LM (2.78) > SFD5LM (2.08) (Table 22). This suggests that the higher the concentration of glycine (lower mannitol concentration) the smaller the span values; conversely, the lower the concentration of leucine (higher mannitol concentration) the smaller the span values.

Table 22: Particle size volume diameters (μm) at 10% (Dv10), 50% (Dv50) and 90% (Dv90) of particle size distribution for spray freeze dried (SFD) mannitol with and without 5%, 10% and 15% glycine (G) or leucine (L) powders. SFD5GM: SFD 5% glycine-mannitol, SFD10GM: SFD 10% glycine-mannitol, SFD15GM: SFD 15% glycine-mannitol, SFD5LM: SFD 5% leucine-mannitol, SFD10LM: SFD 10% leucine-mannitol, SFD15LM: SFD 15% leucine-mannitol. VMD: volume mean diameter.

Carrier	Dv10 (μm)	Dv50 (μm)	Dv90 (μm)	VMD (μm)	Span ($Dv_{90} - Dv_{10} / Dv_{50}$)
SFD mannitol	1.31	7.33	59.71	18.93	7.99
Glycine	36.92	120.39	160.75	111.58	1.03
SFD5GM	1.56	8.15	70.61	22.65	8.47
SFD10GM	1.42	6.85	41.31	16.11	5.82
SFD15GM	1.57	7.28	32.91	13.20	4.29
Leucine	-	-	-	300-400 (SEM)	-
SFD5LM	2.38	51.08	108.67	49.13	2.08
SFD10LM	2.21	37.88	107.53	46.69	2.78
SFD15LM	1.65	11.62	109.95	38.04	9.32

4.13.3.3. Differential scanning calorimetry

The combined DSC thermograms for SFD mannitol carrier containing glycine or leucine (5%, 10% and 15%) are shown in Figure 35 and Figure 36, respectively. The onset temperature and enthalpy for glycine, leucine and SFD mannitol carriers with and without glycine or leucine are presented in Table 23. The DSC curve for SFD mannitol showed a sharp endothermic peak at the onset temperature of 166.25°C (Figure 35E and Figure 36E), which corresponds to the melting point of α - or β -mannitol and indicates crystalline. In addition, SFD mannitol showed another small endothermic event at 154.29°C before the sharp melting point peak (Figure 35E and Figure 36E). The small endothermic event would be the melting point of δ -mannitol where the δ -form of mannitol was transforming into α - and/or β -mannitol. These results were already discussed in Chapter 3.11.2.3 (Figure 19B), agreed with the works (freeze dried mannitol) (Kaialy, Nokhodchi, 2013, Kaialy, Nokhodchi, 2015) and further supported by the X-ray diffraction study previously reported in Chapter 3.11.2.5 (Figure 23). Glycine (Figure 35A) showed an endothermic peak at the onset temperature of 250.71°C with enthalpy of -943.00 Jg^{-1} (Table 23), which corresponds to the melting point of glycine. SFD mannitol with the inclusion of glycine (5%, 10% and 15%) showed endothermic peaks in the onset temperature range of 152.84°C and 157.11°C (Figure 35B-D and Table 23). This could be attributed to the melting point of α - and/or β -mannitol observed at 166.25°C in the SFD mannitol DSC curve as the X-ray diffraction study for SFD glycine-mannitol carriers showed no diffraction peak at 9.7° of 2θ indicating the absence of δ -mannitol (Figure 39*, discussed later in Section 4.13.3.5). This shows that

the formation of δ -mannitol was inhibited by the presence of glycine (the crystallisation of mannitol polymorphs was affected by the presence of glycine) (Pyne, Chatterjee & Suryanarayanan, 2003). The temperature shift could be indicated that the strong solid-solid interaction might have occurred (Molina, Kaialy & Nokhodchi, 2019) between glycine and mannitol. It was also observed that the melting enthalpies varied from 15% glycine to 5% glycine in the following rank order: SFD15GM (157.11°C , -224.46 Jg^{-1}) > SFD10GM (156.09°C , -170.90 Jg^{-1}) > SFD5GM (152.84°C , -165.72 Jg^{-1}) (Table 23). This means that the melting enthalpy increased with the increase in glycine concentration (i.e., the concentration of mannitol decreased). This could be due to the large melting enthalpy associated with glycine (-943.00 Jg^{-1}) (Table 23).

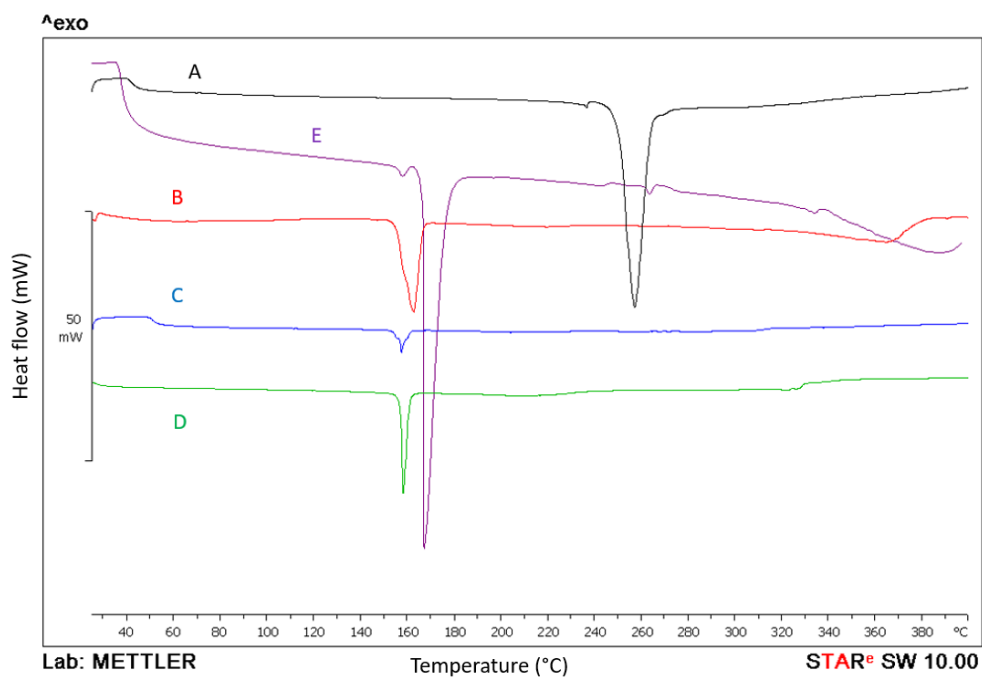


Figure 35: Combined DSC thermograms of glycine and spray freeze dried (SFD) mannitol carriers with **glycine** (5%, 10% and 15%). A: Glycine, B: SFD 5% glycine-mannitol carrier (SFD5GM), C: SFD 10% glycine-mannitol carrier (SFD10GM), D: SFD 15% glycine-mannitol carrier (SFD15GM) and E: SFD mannitol.

Leucine (Figure 36A) showed a broad endothermic peak at the onset temperature of 248.38°C with enthalpy of -82.73 Jg^{-1} (Table 23), which corresponds to the melting point of leucine. This is in agreement with the thermal characteristic of L-leucine (Li et al., 2016). SFD mannitol with the inclusion of leucine (5%, 10% and 15%) showed endothermic peaks at the onset temperature range

of 160.53°C to 164.99°C (Figure 36B-D and Table 23). This could be attributed to the melting point of α - and/or β -mannitol observed at 166.25°C with its enthalpy of -257.93 Jg^{-1} ; similar melting enthalpies were obtained for SFD mannitol containing leucine (5%, 10% and 15%) in the following rank order: SFD5LM (160.53°C, -230.82 Jg^{-1}) > SFD10LM (164.05°C, -229.53 Jg^{-1}) > SFD15LM (164.99°C, -217.95 Jg^{-1}) (Figure 36 and Table 23). This suggests that the slightly higher enthalpy was ascribed to the concentration of leucine decrease (i.e., the concentration of mannitol increase). The small melting enthalpy associated with leucine (-82.73 Jg^{-1}) (Table 23) indicates that more energy is required to melt the crystalline form of mannitol at higher mannitol concentrations. In addition, SFD mannitol carriers in the presence of 10% leucine (Figure 36C) and 15% leucine (Figure 36D) showed small endothermic and exothermic events prior to the melting. The small thermal transition events would be related to δ -mannitol transition phase where the small amounts of δ -mannitol existing in SFD mannitol with 10% and 15% leucine were transformed into α - and/or β -mannitol. Hence, the melting point of δ -mannitol followed by crystallisation. However, no such events were observed in the SFD mannitol with 5 % leucine thermogram (Figure 36B). Kim et al (1998) reported that freezing mannitol (10% w/v) slowly produced a mixture of α - and β -mannitol; on the other hand, fast freezing generated δ -mannitol (Kim, A. I., Akers & Nail, 1998). In this study, all mannitol carriers with amino acids (glycine or leucine) prepared by spray freeze drying were in the crystalline form; also, all observed endothermic peaks for SFD amino acid-mannitol carriers were in agreement with the melting point of mannitol (154.29°C for δ -mannitol and 166.25°C for α - or β -mannitol). There were no other endothermic peaks observed after 200 °C for glycine and leucine (Figure 35B-D and Figure 36B-D) indicating that the amino acids turned to be amorphous after co-spray freeze drying with mannitol.

4.13.3.4. Thermogravimetric analysis

The combined TGA curves for SFD mannitol containing glycine or leucine are shown in Figure 37 and Figure 38, respectively. The mass loss associated with the moisture content below 100°C for glycine was 2.8% (Figure 37A) and SFD15GM (Figure 37D) had the highest moisture content (6.8%) followed by SFD10GM (4.1%) (Figure 37C). However, SFD5GM showed no moisture content (Figure 37B). The weight loss for SFD mannitol on its own (no amino acid included) observed from the previous TGA study was 5.5% (Chapter 3.11.2.4)(Babenko et al., 2019). In this study, the moisture content for SFD mannitol carrier was reduced by the addition of 5% or 10% glycine to mannitol. However, the inclusion of 15% glycine increased the moisture content of SFD mannitol.

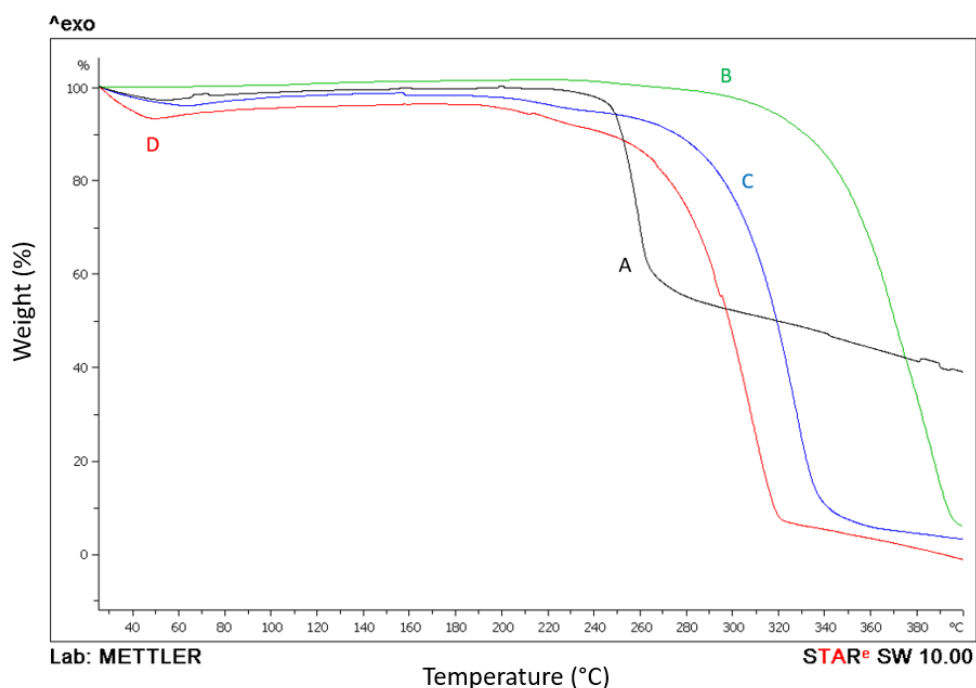


Figure 37: Combined TGA curves of glycine and spray freeze dried (SFD) mannitol carriers with **glycine** (5%, 10% and 15%). A: Glycine, B: SFD 5% glycine-mannitol (SFD5GM), C: SFD 10% glycine-mannitol (SFD10GM) and D: SFD 15% glycine-mannitol (SFD15GM).

No moisture content was detected for leucine (Figure 38A); moisture content below 100°C for SFD mannitol carriers containing leucine was in the following rank order: SFD15LM (6.0%) > SFD10LM (4.5%) > SFD5LM (3.1%) (Figure 38). This signifies that the addition of 5% or 10% leucine reduced the

moisture content of SFD mannitol alone and could be due to leucine being a rather hydrophobic amino acid that decreased moisture absorption (Sou et al., 2011, Chen et al., 2016). However, the moisture content of SFD mannitol increased with further increase in leucine content (15%). This could indicate that there was no further improvement in surface properties with the increase of leucine content. Li *et al.* (2016) studied the effect of leucine on moisture protection of spray dried powders; the authors concluded that the optimal leucine content should be achieved to protect the formulation from moisture (Li et al., 2016). In this study, the higher concentration of amino acid (15% glycine or leucine) led to hygroscopic carriers, whereas the lower concentration of amino acids (5% and 10%) produced SFD mannitol-based powders with moisture protection properties. The previous study (Chapter 3.11.2.4) (Babenko et al., 2019) revealed that moisture content did not have an impact on the SFD powder flowability; yet, the long-term stability of the DPI formulations may be affected by the presence of moisture content (Banga, 2015). Therefore, to prepare SFD amino acid-mannitol carriers with anti-hygroscopic properties, the concentration of glycine or leucine should be lower than 10%.

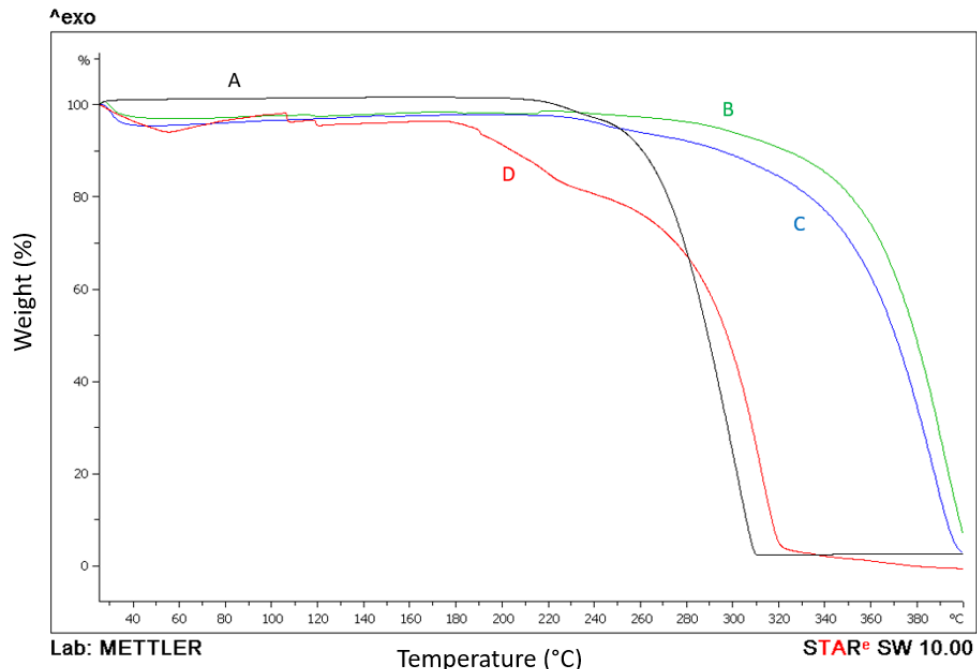


Figure 38: Combined TGA curves of leucine and spray freeze dried (SFD) mannitol carriers with **leucine** (5%, 10% and 15%). A: Leucine, B: SFD 5% leucine-mannitol (SFD5LM), C: SFD 10% leucine-mannitol (SFD10LM) and D: SFD 15% leucine-mannitol (SFD15LM).

4.13.3.5. X-ray diffraction

XRD was used in conjunction with DSC to assess crystallinity and polymorphic nature of SFD mannitol carriers with and without amino acids. Figure 39 and Figure 40 show the combined x-ray diffractograms of SFD mannitol containing glycine or leucine, respectively with the addition of SFD mannitol. All XRD patterns showed sharp diffraction peaks confirming the crystallinity of all mannitol-based carriers prepared by spray freeze drying. SFD mannitol diffractograms showed diffraction peaks at 9.7° and 22.2° of 2θ indicating the presence of δ -mannitol (ICDD: 22-1794) and peaks at 10.6° , 14.8° , 16.9° , 18.8° , 20.6° , 21.3° , 23.4° , and 29.6° of 2θ indicating a mixture of α -mannitol (ICDD: 47-2052), β -mannitol (ICDD: 22-1797) and δ -mannitol (Figure 39 and Figure 40). These results were already discussed in Chapter 3.11.2.5 and similar results were reported by few authors (Kaialy, Nokhodchi, 2015, Kaialy, Nokhodchi, 2016, Molina, Kaialy & Nokhodchi, 2019). In this study, spray freeze drying produced mannitol powders with a mixture of three crystal forms; α -, β - and δ -mannitol. However, α -mannitol was dominant in SFD mannitol (Chapter 3.11.2.5). The XRD patterns for glycine showed intense diffraction peaks at 15.1° , 19.4° , 24.3° , 28.8° , 30.2° , 35.7° and 36.5° of 2θ (ICDD: 50-2131 and 07-0718) indicating a crystalline form (Figure 39). However, these peaks were not observed when glycine (5%, 10% and 15%) was co-spray freeze dried with mannitol where it can be seen that all the XRD patterns of SFD glycine-mannitol were similar to the XRD patterns of SFD mannitol alone (Figure 39). This supports the DSC results for SFD glycine-mannitol carriers where no melting peaks were observed after 200°C (Figure 35B-D) showing that glycine turned to be amorphous after co-spray freeze drying with mannitol. There was no diffraction peak at 9.7° of 2θ for all three SFD glycine-mannitol carriers indicating the absence of δ -mannitol form (Figure 39*). The addition of glycine to mannitol inhibited the formation of δ -mannitol.

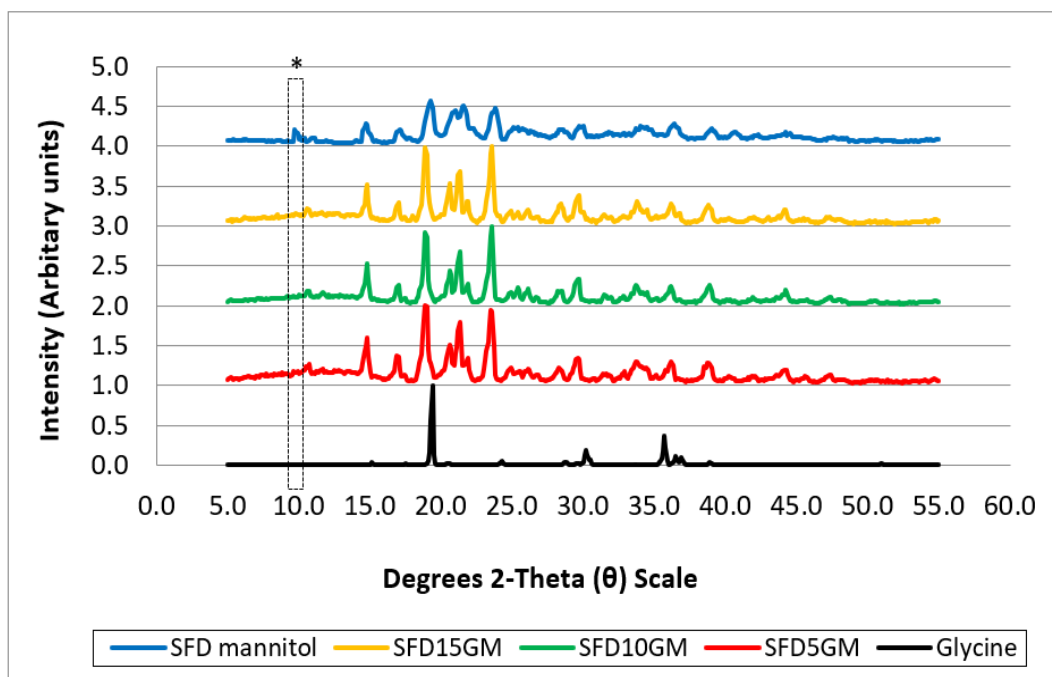


Figure 39: X-ray diffraction patterns for glycine and spray freeze dried (SFD) mannitol carriers with and without **glycine** (5%, 10% and 15%). SFD5GM: SFD 5% glycine-mannitol, SFD10GM: SFD 10% glycine-mannitol, SFD15GM: SFD 15% glycine-mannitol. * indicates diffraction peak at 9.7° of 2θ.

The XRD patterns for leucine showed sharp diffraction peaks at 6.3°, 24.0°, 30.2° and 36.5° of 2θ indicating the presence of crystalline L-leucine (ICDD: 30-1779) (Figure 40). This agreed with the XRD patterns of leucine reported by Sou *et al.* (2013). All the XRD patterns of SFD mannitol containing leucine (5%, 10% and 15%) were also similar to the SFD mannitol XRD patterns (Figure 40). This supports the DSC results for SFD leucine-mannitol carriers where no melting peaks were observed after 200°C (Figure 36B-D) showing that leucine turned to be amorphous after co-spray freeze drying with mannitol. Emami *et al.* (2018) studied thermal behaviours of formulations containing immunoglobulin G, trehalose, and different amino acids such as glycine or leucine before and after spray freeze drying (Emami *et al.*, 2018). Their XRD results showed crystallinity of the amino acids alone before spray freeze drying whereas SFD formulations showed amorphous (Emami *et al.*, 2018). In this study, all SFD leucine-mannitol carriers showed a small diffraction peak at 6.3° of 2θ indicating the presence of crystalline leucine (Figure 40**). Sou *et al.*, (2016) reported similar results when co-spray drying leucine with mannitol indicating the presence of leucine on the surface of particles (Sou *et al.*, 2016). The remaining leucine crystals might influence the particle surface properties (inter-particulate forces) and subsequently aerosolisation performance (discussed in Section 4.13.5). Also, it was observed that the intensity of the leucine peak increased with the increased its concentration

(i.e., reduced mannitol concentration) (Figure 40**). These XRD results are complementary to the DSC results where the higher leucine concentration lowered the melting enthalpy as leucine has small melting enthalpy (-82.73 Jg^{-1}) than mannitol (Table 23). SFD15LM showed another small diffraction peak at 9.7° of 2θ (Figure 40*) corresponding to δ -mannitol. This peak supports the DSC results for SFD15LM where additional small endothermic and exothermic events were observed around $151\text{-}154^\circ\text{C}$ attributed to the δ -mannitol phase transition (Figure 36D). SFD10LM also showed additional endothermic and exothermic events around $147\text{-}154^\circ\text{C}$ in the DSC curve (Figure 36C). However, no small diffraction peaks were observed at 9.7° of 2θ (Figure 40*) indicating the absence of δ -mannitol. Also, SFD5LM showed no diffraction peaks at 9.7° of 2θ (Figure 40*). Both XRD and DSC results suggest that SFD mannitol-based carriers with lower leucine content (e.g., 5%) did not allow for δ -mannitol transition phase, whereas SFD mannitol alone or in the presence of higher leucine content (e.g., 15%) generated the δ -mannitol form.

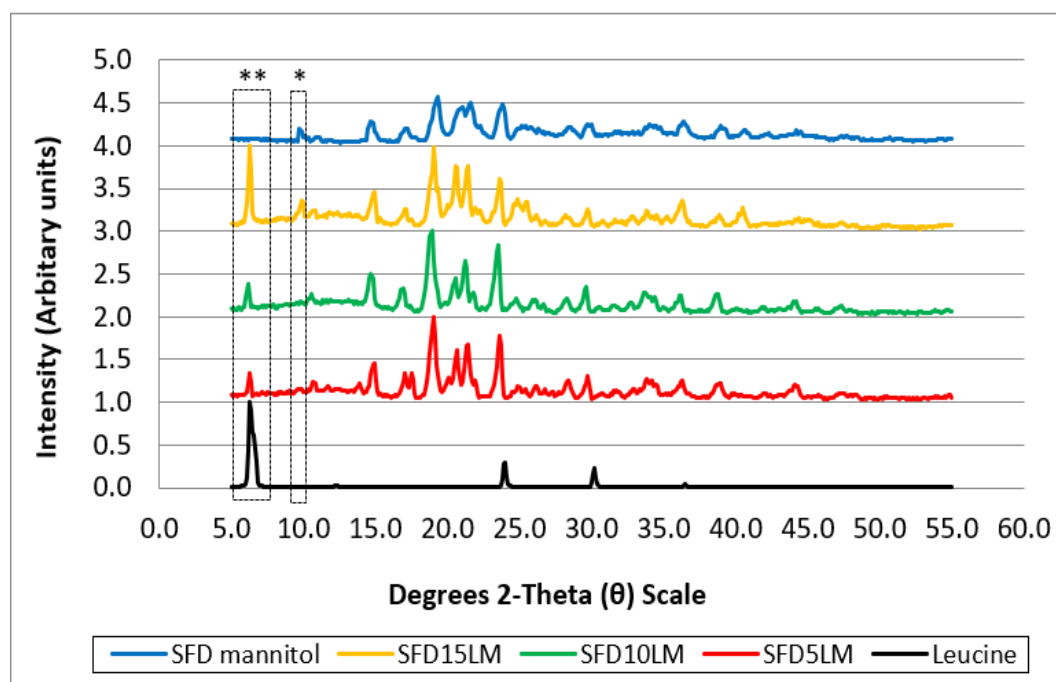


Figure 40: X-ray diffraction patterns for leucine and spray freeze dried (SFD) mannitol carriers with and without **leucine** (5%, 10% and 15%). SFD5LM: SFD 5% leucine-mannitol, SFD10LM: SFD 10% leucine-mannitol, SFD15LM: SFD 15% leucine-mannitol. ** indicates diffraction peak at 6.3° of 2θ . * indicates diffraction peak at 9.7° of 2θ .

4.13.4. Blend homogeneity assessment

All DPI formulations demonstrated significantly different insulin uniformities (One-way ANOVA, $p < 0.05$) (Figure 41). The addition of amino acids to SFD mannitol carrier did not have a significant effect on the insulin uniformity when compared to DPI formulation containing SFD mannitol alone (IMB) (Tukey HSD test, $p > 0.05$). Figure 41 shows that insulin uniformity (%) was in the following rank order: I15LMB (93.16%, %CV: 3.99) > I10GMB (86.95%, %CV: 2.42) > I5GMB (85.90%, %CV: 2.58) > I5LMB (85.82%, %CV: 1.27) > IMB (73.24%, %CV: 1.68) > I10LMB (51.49%, %CV: 3.62) > I15GMB (50.03%, %CV: 1.92). Whilst insulin content for I15LMB, I10GMB, I5GMB and I5LMB fell within the acceptable range of 85-115% of the nominal dose (British Pharmacopoeia (Yeung et al., 2019) and FDA guidelines), IMB, I10LMB and I15GMB were outside that acceptable range. Formulation I15LMB (15% leucine) had the highest %CV (3.99, Figure 41) indicating the lowest insulin content homogeneity. This could be due to the highest span value obtained from SFD15LM carrier (span: 9.32, Table 22). On the other hand, I5LMB (5% leucine) had the smallest %CV (1.27, Figure 41) indicating better insulin content homogeneity. This could be due to the smallest span value obtained from SFD5LM carrier (span: 2.08, Table 22). The content of mannitol within all DPI formulations was between 94.9% and 103.0% with low %CV (0.05-0.12) (Figure 41) indicating high degree of mannitol carrier homogeneity achieved. The intensity of mannitol NMR peaks showed similar for all formulations presenting similar mannitol concentrations quantified amongst formulations (Figure 43). However, the blending process might have affected the morphologies of some SFD mannitol-based carriers that influenced the blend homogeneity or the drug-carrier interactions during blending.

SEM image of SFD mannitol carrier before blending showed spherical particles (Figure 34A), however, after blending SFD mannitol with insulin (IMB), the majority of particles appeared scattered and irregular (less spherical) where the insulin particles were randomly distributed without adhering to the surface of SFD mannitol carriers (Figure 42A). This can be attributed to the delicate porous powders produced by spray freeze drying mannitol alone. Figure 42B and Figure 42D showed irregularly shaped particles of SFD mannitol carrier with 5% glycine (SFD5GM) and 15% glycine (SFD15GM), respectively indicating that blending affected the spherical morphologies of SFD carriers. The morphological change observed in SFD carrier with 5% glycine (SFD5GM) might have had a positive effect on the insulin content uniformity for I5GMB (85.90%, Figure 41) which was within the acceptable range. This could be due to the insulin particles fitted between the mesh structures of SFD carrier (large scale irregularities/asperities that are larger than the drug particle size, macroscale roughness) as well as insulin particles adhered to the surface of SFD carrier (small

scale asperities that are smaller than the drug particle size, nanoscale roughness, favourable for the drug-carrier adhesion and drug-carrier detachment described in Introduction 4.2) (Figure 42B). Blending also affected the carrier surface roughness as SFD 15% glycine-mannitol carrier (SFD15GM) exhibited smoother surfaces after blending (Figure 42D). The smoothed surfaces (small contact area between drug and carrier associated with weaker adhesive forces, nanoscale roughness) might have resulted in weak drug-carrier adhesive forces (poor drug adhesion to the carrier surface) affecting the drug-carrier interactions during blending. Consequently, this led to the low insulin uniformity for I15GMB (50.03%, Figure 41). Also, the hygroscopic nature of SFD15GM (moisture content: 6.8%, Figure 37) might have promoted powder aggregation leading to poor blending performance that resulted in the low insulin uniformity. However, the morphology of SFD mannitol with 10% glycine (SFD10GM) was not affected by blending as the same morphology (spherical particles) with uneven surfaces was observed before (Figure 34D) and after blending (Figure 42C). This resulted in acceptable insulin uniformity (86.95%) with relatively low %CV (2.42). It is likely that the addition of 10% glycine to SFD mannitol carrier have improved the morphology of SFD mannitol therefore produced stable and homogeneous blend of I10GMB.

SFD mannitol carriers containing leucine (5%, 10% and 15%) maintained their morphologies after blending and these SFD carrier surfaces could be associated with nanoscale roughness where irregularities/asperities were smaller scale than the drug particle size (Figure 42E-G). However, I10LMB had low insulin content uniformity (51.49%, Figure 41). This could be attributed to the presence of weak drug-carrier adhesive forces (poor drug adhesion to the carrier surface during blending) or the drug particles might have adhered to the walls of the blending container (Kaialy, Nokhodchi, 2015, Kaialy, W., 2016). In contrast, I15LMB had the highest insulin content uniformity (93.16%, Figure 41). This could be due to the spherical shapes of the SFD carrier with the rough surface observed (Figure 34I) that facilitated drug adhesion to the carrier surface (Kaialy, 2016). However, some insulin particles did not adhere to the surface of SFD carriers (Figure 42G).

In this study, different surfaces/morphologies were observed in SFD carriers which have likely influenced insulin content uniformity. It is plausible that the inclusion of the amino acids (5% or 10% glycine and 5% or 15% of leucine) supported the porous spherical structure of SFD mannitol carriers observed by SEM (Figure 34C-D, G and I) and facilitated insulin particles adhesion to the carrier surface during the blending process.

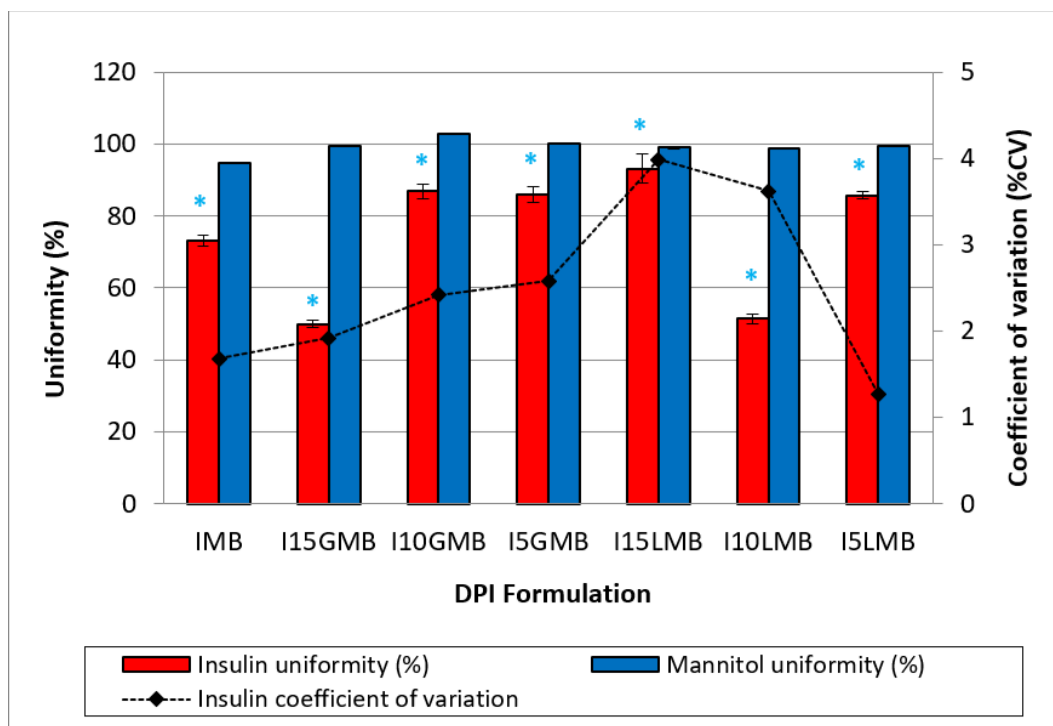


Figure 41: The content uniformity of insulin with coefficient of variation and mannitol in dry powder inhaler (DPI) formulations. IMB: insulin and SFD mannitol blend, I5GMB: insulin and SFD 5% glycine-mannitol blend, I10GMB: insulin and SFD 10% glycine-mannitol blend, I15GMB: insulin and SFD 15% glycine-mannitol blend, I5LMB: insulin and SFD 5% leucine-mannitol blend, I10LMB: insulin and SFD 10% leucine-mannitol blend and I15LMB: insulin and SFD 15% leucine-mannitol blend. (Data presented as mean (three positions) \pm standard deviation, $n=3$).

Asterisks (*) indicate significantly different insulin uniformities between DPI formulations (One-way ANOVA, $p<0.05$).

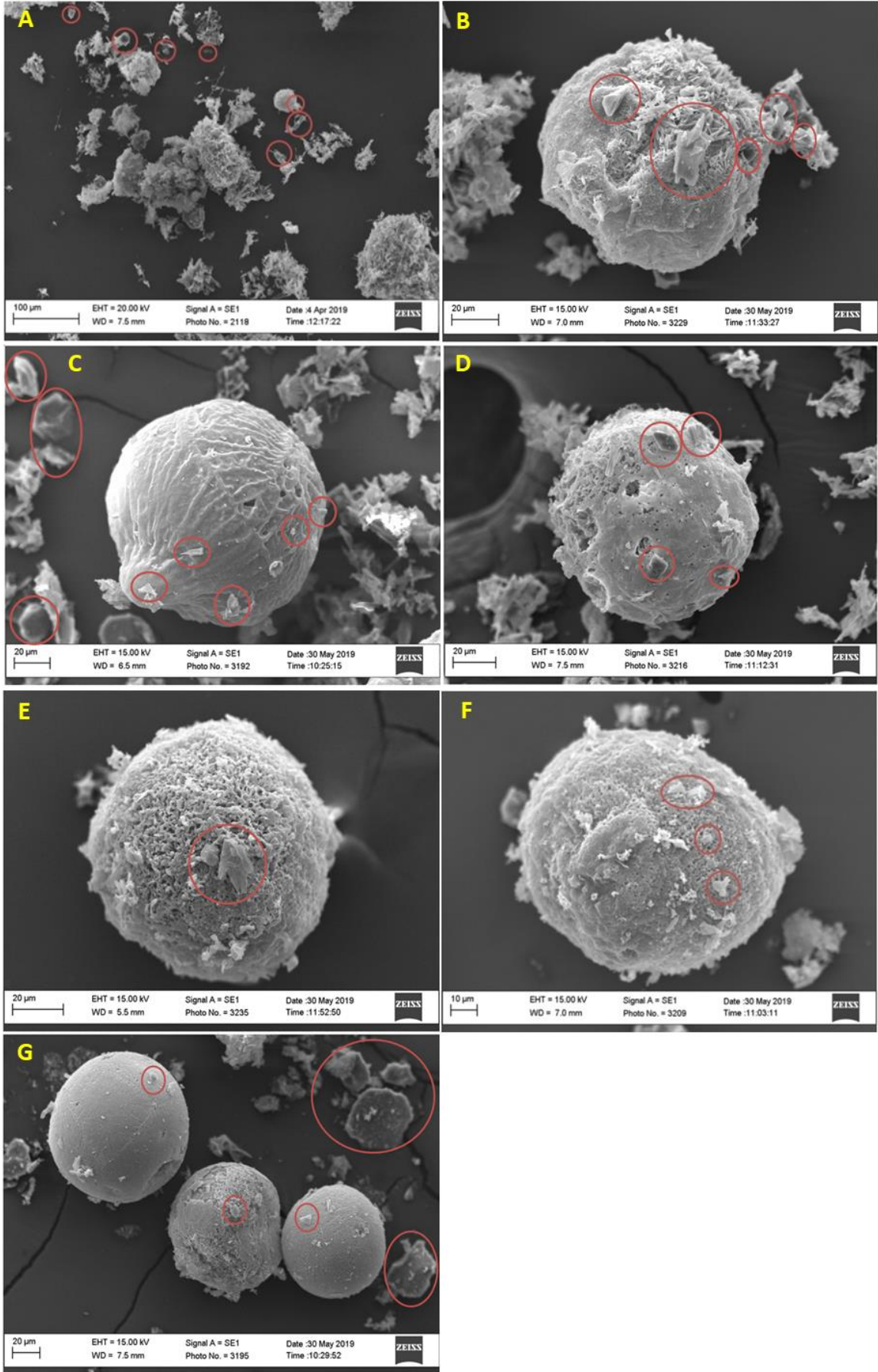
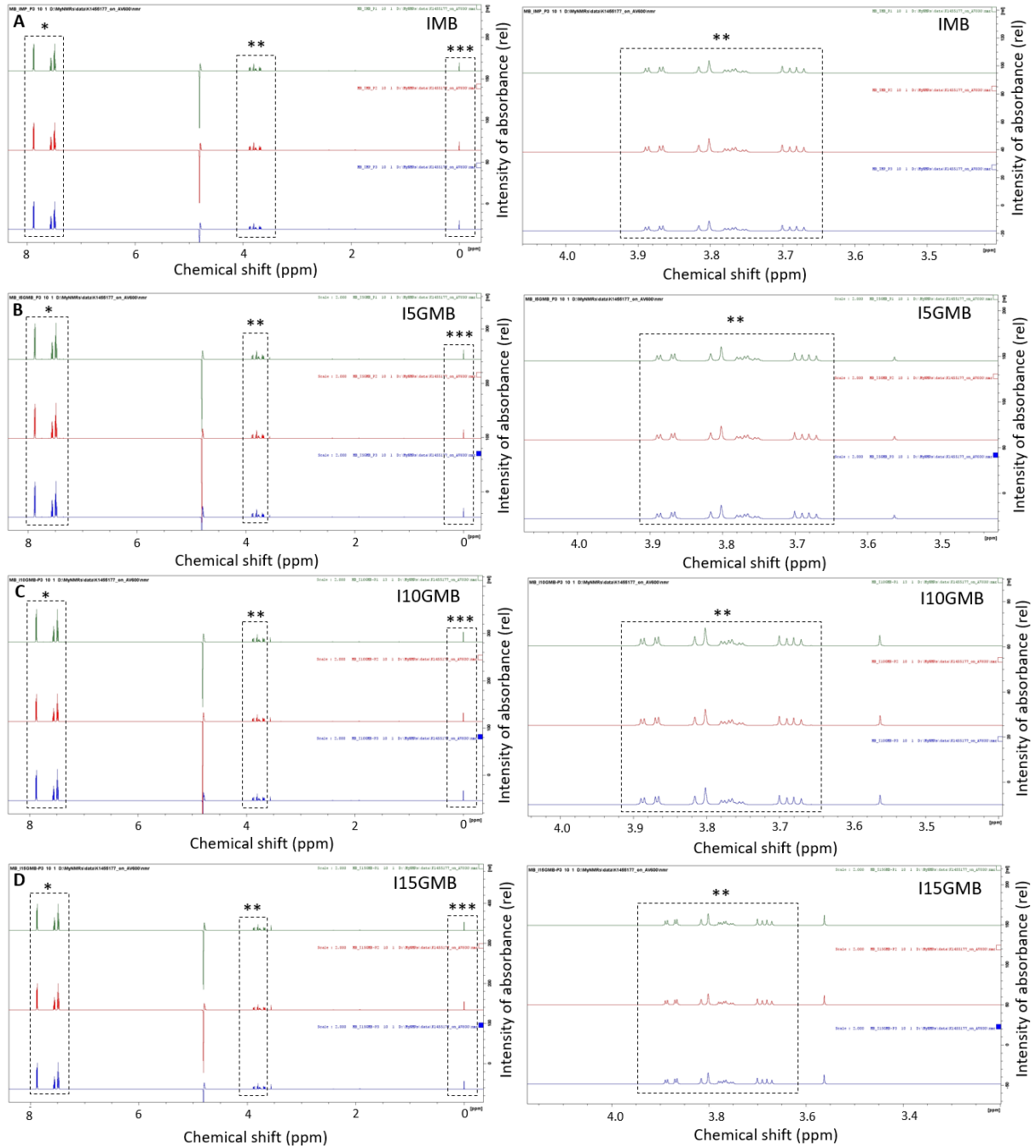


Figure 42: SEM images of insulin and spray freeze dried (SFD) mannitol blend (IMB)(A), insulin and SFD 5% glycine-mannitol blend (I5GMB)(B), insulin and SFD 10% glycine-mannitol blend (I10GMB)(C), insulin and SFD 15% glycine-mannitol blend (I15GMB)(D), insulin and SFD 5% leucine-mannitol blend (I5LMB)(E), insulin and SFD 10% leucine-mannitol blend (I10LMB)(F) and insulin and SFD 15% leucine-mannitol blend (I15LMB)(G). Red circle(s) indicate insulin particles.



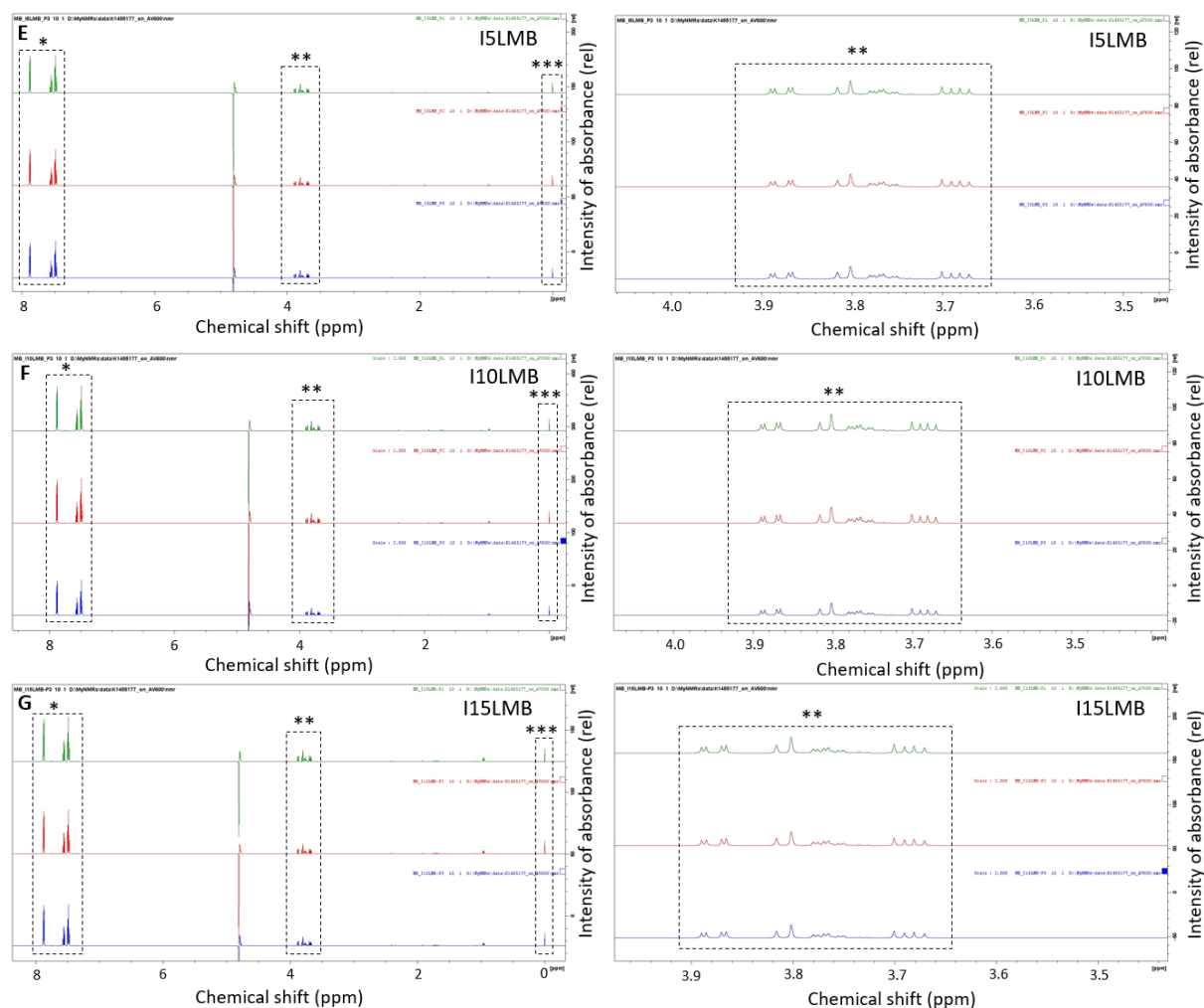


Figure 43: ^1H NMR spectra of mannitol from three different positions of seven insulin DPI formulations in the blending container. A: Insulin and spray freeze dried (SFD) mannitol blend (IMB), B: insulin and SFD 5% glycine-mannitol blend (I5GMB), C: insulin and SFD 10% glycine-mannitol blend (I10GMB), D: insulin and SFD 15% glycine-mannitol blend (I15GMB), E: insulin and SFD 5% leucine-mannitol blend (I5LMB), F: insulin and SFD 10% leucine-mannitol blend (I10LMB) and insulin and G: SFD 15% leucine-mannitol blend (I15LMB). Dashed boxes with *, **, *** indicate peaks of the internal standard (sodium benzoate), mannitol, chemical shift reference (sodium 3-trimethylsilyl propionate-2,2,3,3-d₄, TSP), respectively.

4.13.5. Impaction study

The amount of insulin (insulin deposition) and mannitol (mannitol deposition) for IMB formulation collected at each stage were quantified by the developed RP-HPLC method and the ^1H qNMR method (Chapter 3), respectively and the results are shown in Figure 44 and Figure 45. The research question asked was whether the use of SFD mannitol carrier (90-125 μm) facilitated insulin delivery from the DPI device (Handihaler[®]) and improved insulin deposition onto the lower NGI stages (e.g., between 3 and 5). These stages represent the desired deep lung regions for systemic pulmonary

delivery. Figure 44 shows that SFD mannitol carrier successfully facilitated insulin deposition in the lower NGI stages with below 3.988 μm cut-off diameter (stage 3); insulin deposition in stages 3-5 was higher in comparison to SFD mannitol deposition (t-test, $p < 0.05$). As higher SFD mannitol deposition was retrieved from the AIT and stage 1 (above 11.719 μm cut-off diameter; t-test, $p < 0.05$) (Figure 44 and Figure 45), one can postulate that the use of SFD mannitol carrier is feasible to enhance the aerosolisation performance of insulin and insulin delivery from DPI formulations.

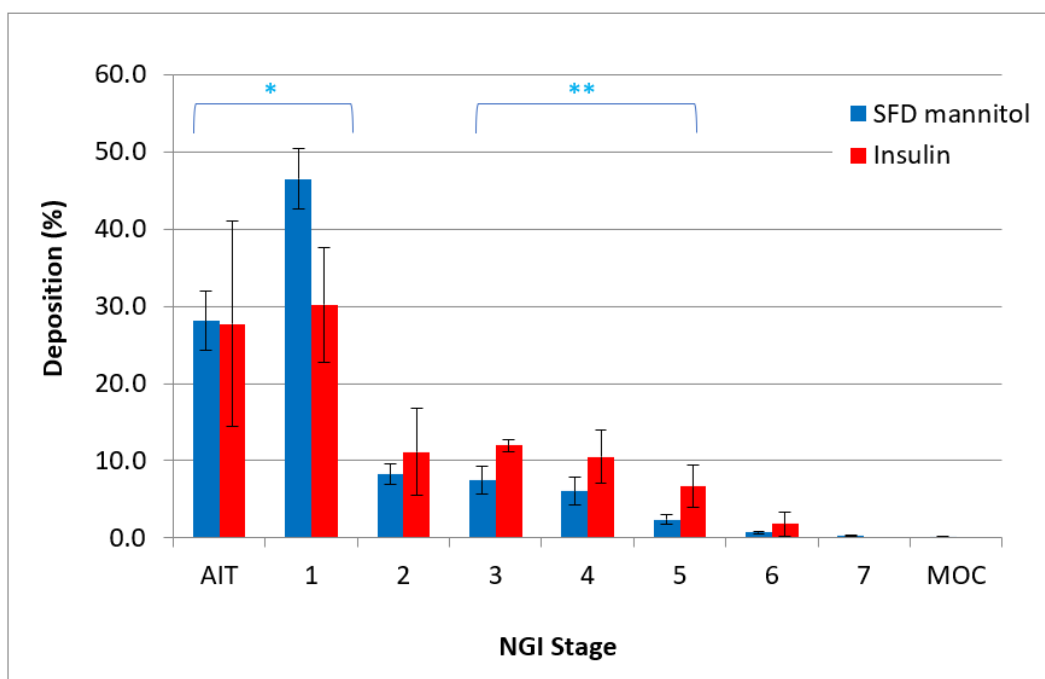


Figure 44: Next Generation Impactor (NGI) deposition profiles of DPI formulation containing spray freeze dried (SFD) mannitol carrier (blue) and insulin (red) at flow rate of 30 L min^{-1} . Deposition is expressed as delivered dose (%) per NGI stage (Data presented as mean \pm standard deviation, $n=3$). AIT: Alberta idealised throat, MOC: Micro orifice collector.

Asterisk (*) indicates statistically different between insulin deposition and mannitol deposition in AIT and stage 1 (t-test, $p < 0.05$).

Asterisks (**) indicate statistically different between insulin deposition and mannitol deposition in stages 3-5 (t-test, $p < 0.05$).

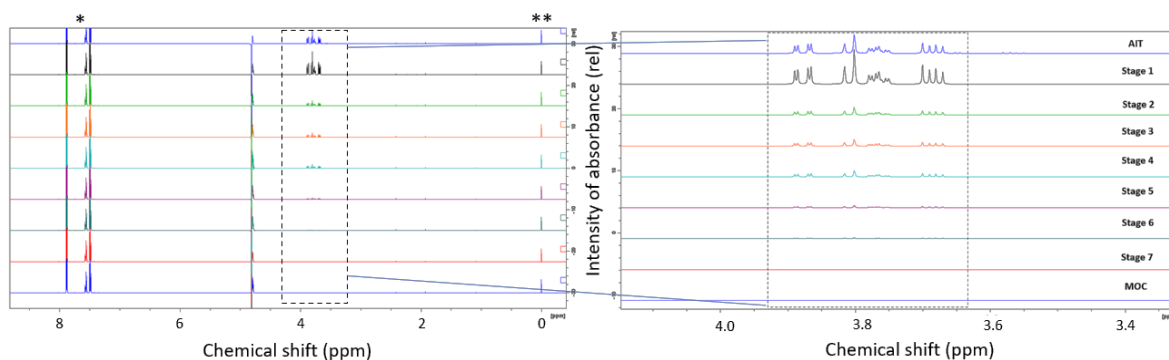


Figure 45: ^1H NMR spectra of spray freeze dried (SFD) mannitol deposition profile from IMB formulation (insulin and SFD mannitol carrier blend) studied by Next Generation Impactor. AIT: Alberta idealised throat, MOC: Micro orifice collector. Dash boxes indicate mannitol peaks. Asterisks * and ** indicate peaks of the internal standard (sodium benzoate) and chemical shift reference (sodium 3-trimethylsilyl propionate-2,2,3,3- d_4 , TSP), respectively.

The effects of the selected amino acids added to SFD mannitol carrier on the aerosolisation performance of insulin from DPI formulations were also assessed based on insulin depositions in the high impactor stages (e.g., AIT and stage 1) as well as in the lower impactor stages (e.g., between 3 and 5) for all DPI formulations; statistical analysis was performed. It was found that regardless of SFD carrier compositions (5%, 10% and 15% glycine or leucine), insulin depositions in AIT, stage 1 and stage 2 for all seven DPI formulations were not different from each other (One-way ANOVA, $p > 0.05$); whereas insulin depositions in the lower impactor stages (i.e., stages 3, 4 and 5) were significantly different from each other (One-way ANOVA, $p < 0.05$) (Figure 46 and Figure 47). This means that particle depositions between stage 3 and 5 were dependent on the formulations. This could be due to various morphologies observed in SFD carriers (Figure 34). FPF (aerodynamic diameter: $\leq 5 \mu\text{m}$) for all seven DPI formulations based on the ground insulin deposition were in the following rank order: IMB ($24.35\% \pm 7.63\%$) > I10GMB ($15.24\% \pm 12.04\%$) > I15LMB ($12.71\% \pm 3.87\%$) > I5GMB ($11.31\% \pm 6.08\%$) > I15GMB ($10.85\% \pm 3.80\%$) > I5LMB ($10.62\% \pm 6.98\%$) > I10LMB ($7.90\% \pm 5.38\%$) (Table 24). DPI formulations with higher FPF demonstrated better inhalation performance (i.e., sufficient drug detachment from SFD carriers) and higher amounts of insulin (aerodynamic diameter: $\leq 5 \mu\text{m}$) would be expected to reach the deep lung regions for systemic pulmonary application. IMB exhibited the highest FPF ($24.35\% \pm 7.63\%$) followed by I10GMB ($15.24\% \pm 12.04\%$) and I15LMB ($12.71\% \pm 3.87\%$); whereas I10LMB showed the lowest FPF ($7.90\% \pm 5.38\%$) (Table 24) presenting poor inhalation performance (i.e., insufficient drug detachment from SFD carriers). It can be explained that SFD mannitol carrier (Figure 34A) used for IMB was porous particles associated with high flowability discussed in Chapter 3 (Babenko et al., 2019) that would have improved the drug

flow and drug-carrier detachment upon aerosolisation. As for I10GMB, which is the stable mixtures prepared after blending (Section 4.13.4), the surface properties (e.g., morphology and roughness) of SFD 10% glycine-mannitol carrier (Figure 34D and Figure 42C) would have been associated with optimum inter-particulate adhesive forces. Consequently, the optimum adhesive forces would have improved the drug-carrier detachment resulting in the high FPF. I15LMB generated higher FPF in comparison to I5LMB and I10LMB. This can be indicated that insulin particles adhered to the surface of SFD 15% leucine-mannitol carrier detached more easily than insulin particles attached to SFD mannitol with lower leucine concentrations (5% and 10%). This could be linked to the XRD results that the addition of high (15%) leucine content associated with higher leucine crystallinity (Section 4.13.3.5) influenced the inter-particulate forces leading to the improved aerosolisation performance. Also, due to the highest insulin content uniformity obtained for I15LMB (93.16%, Figure 41), more drug particles were available for distribution. There were no MMAD and GSD determined (no available values for one side of the 50% MMAD) for DPI formulations in the presence of 5% glycine (I5GMB) and in the presence of leucine at all three different concentrations (I5LMB, I10LMB and I15LMB) due to the narrow distribution observed where over 50% of the cumulative mass deposited on AIT and stage 1 (Table 24, Figure 46 and Figure 47). In contrast, IMB, I10GMB and I15GMB generated MMAD in the following rank order: I15GMB ($10.94 \mu\text{m} \pm 0.81 \mu\text{m}$) > IMB ($9.30 \mu\text{m} \pm 2.19 \mu\text{m}$) > I10GMB ($7.06 \mu\text{m} \pm 0.00 \mu\text{m}$). This indicates that the MMAD values of ground insulin powders determined were not within the suitable range (MMAD: $\leq 5 \mu\text{m}$) for systemic pulmonary delivery. This could be due to the presence of some large insulin particles observed after grinding process in the SEM image (Figure 33B). Furthermore, strong drug-carrier adhesion forces might have existed in I5GMB and caused poor drug detachment from the SFD carrier. Figure 42B showed that some insulin particles were embedded between the mesh structures of SFD carriers (macroscale roughness) therefore provided shelter for insulin particles from drag and lift forces during inhalation. In this study, SFD10GM carrier demonstrated to be the most optimised SFD mannitol carrier with the use of glycine. DPI formulation (I10GMB) containing SFD10GM carrier generated the highest FPF ($15.24\% \pm 12.04\%$) and uniformity (86.95%) followed by I5GMB (FPF: $11.31\% \pm 6.08\%$ and uniformity: 85.90%) and I15GMB (uniformity: 50.03% and FPF: $10.85\% \pm 3.80\%$)(Figure 41, Figure 48 and Table 24). For DPI formulations in the presence of leucine, I15LMB formulation containing SFD15LM carrier produced the highest FPF values ($12.71\% \pm 3.87\%$, Table 24) and uniformity (93.16%, Figure 41). However, due to the concern of high moisture content (6.0%, Figure 38 in Section 4.13.3.4) and high span value (9.32, Table 22 in Section 4.13.3.2) for SFD15LM, SFD5LM carrier demonstrated to be the most optimised SFD leucine-mannitol carrier (uniformity: 85.82% and FPF: $10.62 \pm 6.98\%$)(Figure 41, Figure 48 and Table 24). SFD5LM also had the smallest span value

(2.08, Table 22 in Section 4.13.3.2) and lower moisture content (3.1%, Figure 38 in Section 4.13.3.4). SFD10GM and SFD5LM carriers along with SFD mannitol carrier (as control) can be used for further studies focusing on the aerosolisation performance of insulin dry powders within the suitable MMAD ($\leq 5 \mu\text{m}$) for systemic pulmonary drug delivery via DPI formulations.

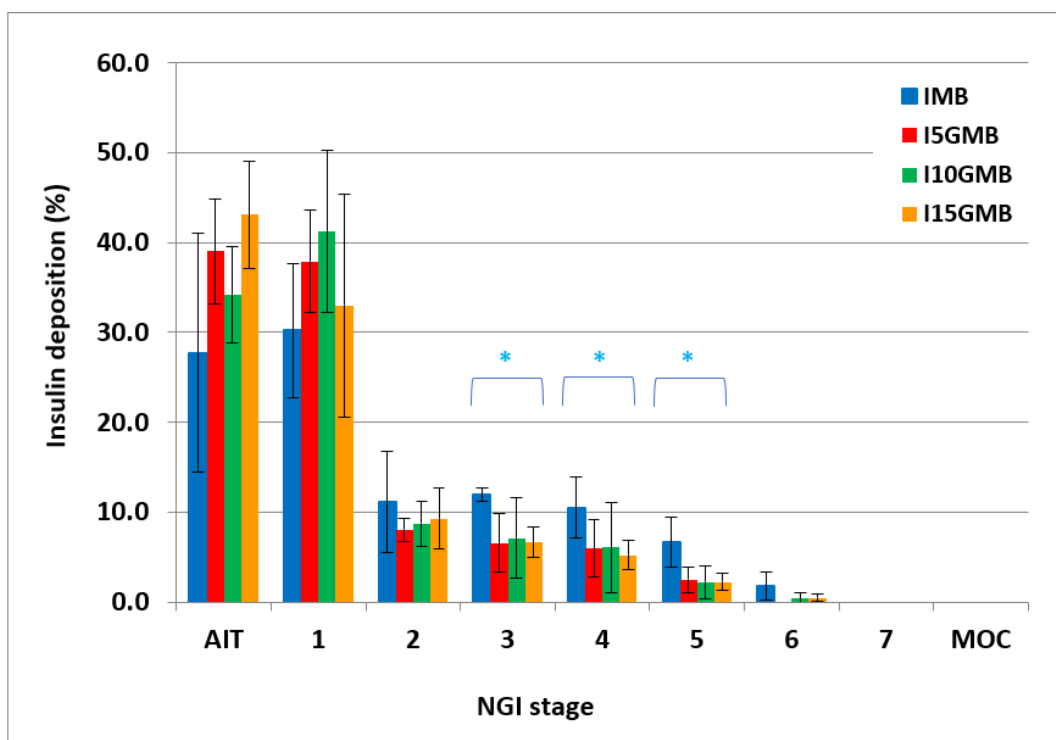


Figure 46: Next Generation Impactor (NGI) deposition profiles of each dry powder inhaler formulation aerosolised from Handihaler[®] at flow rate of 30 L min^{-1} . Deposition is expressed as delivered dose (%) per NGI stage (Data presented as mean \pm standard deviation, $n=3$). AIT: Alberta idealised throat, MOC: Micro orifice collector. IMB: insulin and SFD mannitol blend, I5GMB: insulin and SFD 5% glycine-mannitol blend, I10GMB: insulin and SFD 10% glycine-mannitol blend, I15GMB: insulin and SFD 15% glycine-mannitol blend.

Asterisks (*) indicate significantly different insulin depositions in stages 3, 4 and 5 between DPI formulations (One-way ANOVA, $p<0.05$).

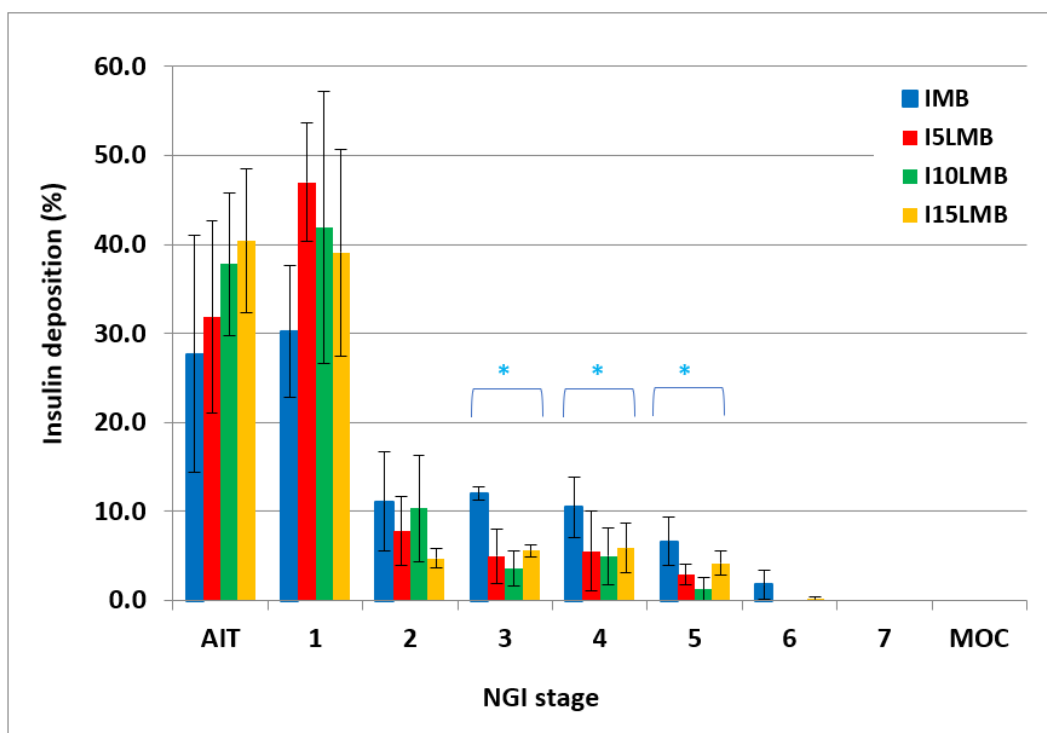


Figure 47: Next Generation Impactor (NGI) deposition profiles of each dry powder inhaler formulation aerosolised from Handihaler® at flow rate of 30 L min⁻¹. Deposition is expressed as delivered dose (%) per NGI stage (Data presented as mean ± standard deviation, n=3). AIT: Alberta idealised throat, MOC: Micro orifice collector. IMB: insulin and SFD mannitol blend, I5LMB: insulin and SFD 5% leucine-mannitol blend, I10LMB: insulin and SFD 10% leucine-mannitol blend and I15LMB: insulin and SFD 15% leucine-mannitol blend. Asterisks (*) indicate significantly different insulin depositions in stages 3, 4 and 5 between DPI formulations (One-way ANOVA, p<0.05).

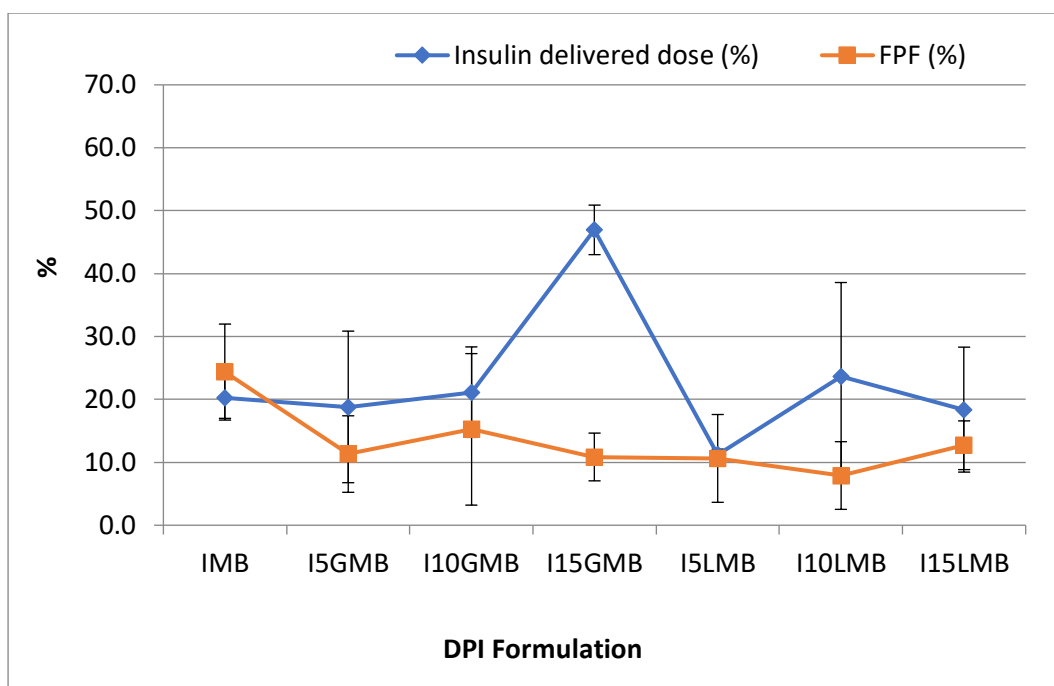


Figure 48: Insulin delivered dose (%) and fine particle fraction (FPF% $\leq 5.0 \mu\text{m}$) for seven dry powder inhaler (DPI) formulations. IMB: insulin and SFD mannitol blend, I5GMB: insulin and SFD 5% glycine-mannitol blend, I10GMB: insulin and SFD 10% glycine-mannitol blend, I15GMB: insulin and SFD 15% glycine-mannitol blend, I5LMB: insulin and SFD 5% leucine-mannitol blend, I10LMB: insulin and SFD 10% leucine-mannitol blend and I15LMB: insulin and SFD 15% leucine-mannitol blend.

Table 24: Insulin delivered dose (%), fine particle fraction (FPF% $\leq 5.0 \mu\text{m}$), mass median aerodynamic diameter (MMAD) and geometric standard deviation (GSD) determined by Next Generation Impactor analysis at flow rate of 30 L min^{-1} for seven dry powder inhaler (DPI) formulations (Data presented as mean \pm standard deviation, $n=3$). IMB: insulin and SFD mannitol blend, I5GMB: insulin and SFD 5% glycine-mannitol blend, I10GMB: insulin and SFD 10% glycine-mannitol blend, I15GMB: insulin and SFD 15% glycine-mannitol blend, I5LMB: insulin and SFD 5% leucine-mannitol blend, I10LMB: insulin and SFD 10% leucine-mannitol blend and I15LMB: insulin and SFD 15% leucine-mannitol blend.

DPI formulation	Dose		Size Distribution	
	Insulin delivered dose (%)	FPF (%)	MMAD (μm)	GSD
IMB	20.30 \pm 3.31	24.35 \pm 7.63	9.298 \pm 2.19	3.225 \pm 0.75
I15GMB	46.95 \pm 3.94	10.85 \pm 3.80	10.943 \pm 0.81	2.934 \pm 0.15
I10GMB	21.15 \pm 7.19	15.24 \pm 12.04	7.056 \pm 0.00	2.575 \pm 0.00
I5GMB	18.81 \pm 12.05	11.31 \pm 6.08	NA	NA
I15LMB	18.38 \pm 9.93	12.71 \pm 3.87	NA	NA
I10LMB	23.61 \pm 14.97	7.90 \pm 5.38	NA	NA
I5LMB	11.21 \pm 0.89	10.62 \pm 6.98	NA	NA

4.14. Conclusion

This study showed that all formulated SFD mannitol-based carriers displayed a porous spherical particle shape with the particle size ranging from 50 μm to 130 μm suitable as DPI carriers regardless of the inclusion or absence of amino acids. The use of SFD mannitol carrier facilitated insulin deposition into lower NGI stages and SFD mannitol carrier exhibited a more marked oropharyngeal deposition pattern. Surface properties (e.g., morphology and roughness) of SFD mannitol-based carriers were dependent on the type of amino acid and its concentrations. Different surface properties of SFD carriers were associated with different inter-particulate adhesive forces and affected insulin content uniformity, insulin deposition and aerosolisation performance of DPI formulations. SFD mannitol-based carriers with optimum physicochemical properties were achieved by the addition of 10% glycine or 5% leucine to mannitol and DPI formulations containing these SFD carriers demonstrated the optimised insulin aerosolisation performance. Therefore, it can be suggested for further studies that SFD mannitol with the inclusion of these might afford enhanced aerosolisation performance of insulin dry powders for systemic pulmonary delivery. The enhancement of aerosolisation performance *in vitro* could consequently have a positive influence on drug deposition profiles *in vivo* and bioavailability therefore the therapeutic efficacy of the formulation. Since insulin delivery via the pulmonary route of administration is an attractive non-invasive alternative to parenteral administration for the management of diabetes and the pulmonary route offers rapid systemic drug absorption, the development of DPI formulations using SFD carriers with optimum physicochemical properties would be a feasible approach to help patients achieve better control of blood glucose levels.

Chapter 5. Aerosolisation performance of spray dried insulin powders from amino acid-mannitol carriers

5.1. Abstract

Dry powder inhaler formulations containing insulin with and without amino acid-mannitol carriers were prepared to improve insulin aerosolisation performance. Insulin powders were spray dried (SD) whereas mannitol-based carriers with and without the inclusion of two selected amino acids (10% glycine or 5% L-leucine) were spray freeze dried (SFD). SD insulin powders were characterised in terms of morphology including size, thermal behaviour, and moisture content. The structure integrity of insulin powders before and after spray drying was tested by Fourier-transform infrared spectroscopy (FTIR) along with the developed reversed-phase high performance liquid chromatography (RP-HPLC) method. The *in vitro* drug deposition profiles were studied using a next generation impactor at a flow rate of 30 L min⁻¹.

Scanning electron microscopy imaging showed SD insulin particles were distributed on the surface of SFD carrier particles. Carrier-free SD insulin exhibited the highest fine particle fraction (FPF: 77.36% ± 18.01%) with the smallest mass median aerodynamic diameter (MMAD: 2.05 µm ± 0.69 µm) however delivered the lowest insulin dose (38.64% ± 3.82%). Carrier-based formulations improved insulin delivered dose from 38.64% ± 3.82% to over 57.0% as compared to carrier-free formulation. Formulation containing SFD 10% glycine-mannitol carrier demonstrated the best aerosolisation performance across formulations investigated in terms of insulin delivered dose (57.75% ± 4.24%), FPF (57.32% ± 6.81%) and MMAD (2.37 µm ± 0.34 µm). Insulin structural integrity was not influenced by spray drying process as FTIR spectra showed no major changes in the characteristic band positions (e.g., Amide I and Amide II) before and after spray drying and insulin content determined by RP-HPLC was 100.78% ± 0.58% within 24 hours of powder production. The use of SFD 10% glycine-mannitol carrier can improve the aerosolisation performance of formulations. This could lead to higher insulin bioavailability, which would offer a viable alternative to traditional subcutaneous injection.

Keywords: Dry powder inhaler formulation, Insulin, D-mannitol carrier, Amino acids, Spray freeze drying, Spray drying

5.2. Introduction

To date, there have not been any studies reported on the aerosolisation performance of carrier-based dry powder inhaler (DPI) formulations containing insulin. Published studies with insulin have focused on the incorporation of excipients into insulin to enhance the aerosolisation performance (Chapter 2.4.2.1) (Kuehl et al., 2014, Razavi Rohani, Abnous & Tafaghodi, 2014). This approach omits blend homogeneity issues and drug-carrier detachment upon inhalation as the drug is incorporated in excipients (Lechanteur, Evrard, 2020). However, due to the lung safety concern, the use of excipients in DPI formulations should be minimised (Balducci et al., 2014, Zhang et al., 2020). Studies on the inhalation performance of carrier-based DPI formulations have shown the advantages of the use of carriers/engineered carriers (e.g., increased fine particle fraction (FPF)) (Kaialy, Nokhodchi, 2013, Kaialy, Nokhodchi, 2016, Rashid et al., 2019). Therefore, the objective of the study was to prepare carrier particles using spray freeze drying to enhance insulin aerosolisation performance. In the previous study (Chapter 3), mannitol powders prepared by spray freeze drying were porous and spherical particles with the particle size ranging from 50 μm to 110 μm suitable as DPI carriers (Chapter 3)(Babenko et al., 2019). The impaction study showed that spray freeze dried (SFD) mannitol exhibited better delivered dose (68.99%) than spray dried (SD) mannitol (49.03%) due to the porous particles associated with better flowability (Chapter 3)(Babenko et al., 2019). The present study aimed to assess the aerosolisation performance of insulin powders prepared by spray drying for inhalation and compare it with aerosolisation in the presence of SFD mannitol-based carriers with and without amino acid (10% glycine or 5% L-leucine). SD insulin powders for inhalation were prepared in the absence of excipients to minimise the lung safety concern. To avoid heat generated degradation of insulin, outlet temperature for spray drying was controlled to be below 120°C by adjusting processing parameters (inlet temperature, aspirator capacity and feed flow rate). The pH of the feed solutions for spray drying insulin was adjusted to 3.5 using sodium hydroxide (NaOH) based on insulin stability study reported by Balducci *et al.* (2014) and insulin absorption study reported by Okumura *et al.* (1992). Okumura *et al.* (1992) studied insulin absorption from the lung in anaesthetised male Wistar rats. Recombinant human insulin (3.0 or 6.0 U/kg) in isotonic phosphate buffer solution (pH 7.0 or pH 3.0) were intratracheally administered into the exposed trachea of anaesthetised rats and relative bioavailability of insulin was calculated by comparing intratracheal administration of insulin in pH 7.0 or pH 3.0 buffer solution to subcutaneous administration of insulin (0.3 U/kg) (Okumura et al., 1992). The results showed that relative bioavailability of insulin was higher when insulin in pH 3.0 buffer solution (relative bioavailability: 41.6%) was intratracheally administered compared to insulin in pH 7.0 buffer solution (relative bioavailability: 13.1%) (Okumura

et al., 1992). SFD 10% glycine-mannitol and SFD 5% L-leucine-mannitol carriers were selected as the optimised carriers based on the preliminary experiments in Chapter 4. Mannitol was chosen as an alternative carrier to lactose. Lactose is the most used carrier in DPI formulations (Nokhodchi, Martin, 2015). However, lactose might not be the carrier of choice for proteins as it is a reducing sugar associated with chemical incompatibility (e.g., Maillard reaction) that leads to chemical degradation (Chapter 2.4.2.1) (Rahimpour, Kouhsoltani & Hamishehkar, 2014, Zhang et al., 2020). In contrast, mannitol is non-reducing sugar and generally recognized as safe substance listed by the Food and Drug Administration (FDA) database (U.S. Food & Drug Administration, 2020) that can be used in the inhalation field (Kaialy, Nokhodchi, 2016) and has been used in Exubera[®] (Al-Tabakha, 2015). Besides, mannitol inhalation powder products are currently available in the UK, such as Osmohale[®] for the assessment of respiratory conditions (e.g., asthma) (emc, 2019) and Bronchitol[®] for the treatment of cystic fibrosis (emc, 2019, European Medicines Agency, 2022). Glycine was chosen as it has been used in Exubera[®] (Al-Tabakha, 2015, Ferrati et al., 2018) and L-leucine was selected based on previously reported studies and literatures (Nokhodchi, Martin, 2015, Kaialy, Nokhodchi, 2016, Otake et al., 2016, Mehta, 2018).

5.3. Materials

D-mannitol, glycine, human recombinant insulin, phosphate buffered saline tablet and sodium benzoate were all purchased from Sigma-Aldrich, UK. L-leucine (leucine) was purchased from Sigma Life Science, UK. Trifluoroacetic acid, acetonitrile, acetic acid glacial and sodium hydroxide pellets were purchased from Fisher Scientific, UK. Deuterium oxide was purchased from Euriso-top[®], UK. Sodium 3-trimethylsilyl propionate-2,2,3,3-d₄ was purchased from Merck Sharp & Dohme Canada Limited, UK.

5.4. Carrier dry powders preparation by spray freeze drying

Mannitol carriers with and without the inclusion of two selected amino acids (10% glycine or 5% leucine, concentration % w/w based on mannitol content, 15 g) were spray freeze dried. Mannitol-based carriers with 10% glycine, or 5% leucine were selected as the optimised carriers based on the results of the preliminary study (Chapter 4). The compositions of mannitol aqueous solutions (15%

w/v total solid content) for spray freeze drying are listed in Table 25. Each mannitol aqueous solution was sprayed over liquid nitrogen in a round bottom flask (250 mL) and freeze dried using BenchTop Pro with Omnitronics™ freeze dryer (SP Scientific, UK) for 48 hours at 55 $\mu\text{bar} \pm 5 \mu\text{bar}$ of pressure and condenser temperature of $-59^\circ\text{C} \pm 2^\circ\text{C}$. After 48 hours, the produced SFD carrier powders were sieved using a sieve shaker (AS200 DIGIT CA, Retsch, Germany) with the 90 μm and 125 μm sieves (Fisher Brand Test Sieve, UK) at 1.5 mm amplitude for up to 10 minutes to obtain the particle size fraction of 90-125 μm . Collected powders (90-125 μm) were immediately transferred into tightly closed glass vials and stored in a desiccator over silica gel at room temperature ($22^\circ\text{C} \pm 3^\circ\text{C}$). In this study, three different SFD mannitol-based carriers were prepared: SFD mannitol (no amino acid), SFD 10% glycine-mannitol (SFD10GM) and 5% leucine-mannitol (SFD5LM) (Table 25).

Table 25: Compositions of aqueous solutions (15% w/v total solid content) to prepare spray freeze dried (SFD) mannitol carriers with and without 10% glycine or 5% leucine. SFD5LM: SFD 5% leucine-mannitol, SFD10GM: SFD 10% glycine-mannitol.

SFD mannitol-based carriers	Amino acid concentration of mannitol (% w/w)	Amino acid (g)	Mannitol (g)	Distilled water (mL)	Total solid content (% w/v)
SFD mannitol	0	0	15.00	100	15
SFD5LM	5	0.75 Leucine	14.25	100	15
SFD10GM	10	1.50 Glycine	13.50	100	15

5.5. Insulin dry powders preparation by spray drying

Insulin dry powders were prepared using spray drying based on the method reported by Balducci *et al.* (2014) with minor modifications. Briefly, insulin (0.1% w/v) was dissolved in acidic aqueous solution (pH 3.5) composed of acetic acid (0.1% v/v) and sodium hydroxide (1M, NaOH) at room temperature. NaOH was used to adjust the pH of the acetic acid solutions to 3.5. Insulin aqueous solution (0.1% w/v) was spray dried using a Büchi Mini Spray Dryer B-290 (Flawil, Switzerland) under standardised processing parameters: 240 mL hr^{-1} feeding rate (pump), 600 L hr^{-1} spray flow rate (nozzle spray flow rate) with compressed air, 98% aspirator speed setting (drying gas flow rate, 100% aspirator setting corresponds to 45-60 $\text{m}^3 \text{hr}^{-1}$), and inlet temperature at 119°C and these settings

resulted in outlet temperature of $60^{\circ}\text{C} \pm 2^{\circ}\text{C}$. Collected SD insulin dry powders were immediately packed into tightly closed glass vials and desiccated over silica gel at room temperature ($22^{\circ}\text{C} \pm 3^{\circ}\text{C}$).

5.6. Preparation of insulin dry powder inhaler formulations

Insulin DPI formulations were prepared by blending SD insulin powders (10 mg) with each SFD mannitol-based carrier (90 mg, SFD mannitol alone or SFD mannitol with 10% glycine or 5% leucine) in ratio of 1:9 (100 mg total) in a plastic container (2 x 9 cm) using a Turbula® system Schatz mixer (WAB, Basel, Switzerland) at a constant speed of 46 rpm for 30 minutes. The blends were then stored in a desiccator over silica gel at room temperature ($22^{\circ}\text{C} \pm 3^{\circ}\text{C}$) prior to the impaction study (Section 5.9). In this study, three carrier-based DPI formulations (Table 26) were prepared: SD insulin and SFD mannitol blend (SDIMB), SD insulin and SFD 10% glycine-mannitol blend (SDI10GMB) and SD insulin and SFD 5% leucine-mannitol blend (SDI5LMB). These DPI formulations along with carrier free SD insulin powder (SDI formulation) were used for the *in vitro* impaction study (Section 5.9 and 5.12.3).

Table 26: Carrier free insulin formulation (SDI) and carrier-based dry powder inhaler (DPI) formulations (SDIMB, SDI10GMB, SDI5LMB) prepared by blending spray dried (SD) insulin dry powders with spray freeze dried (SFD) mannitol-based carriers.

DPI formulation	Formulation Component	
	Drug	Carrier
SDI	SD insulin	-
SDIMB	SD insulin	SFD 15% mannitol
SDI10GMB	SD insulin	SFD 10% glycine and mannitol
SDI5LMB	SD insulin	SFD 5% leucine and mannitol

5.7. Physicochemical characterisation

The carrier powders prepared using spray freeze drying (Section 5.4) were previously characterised by Scanning Electron Microscopy (Chapter 4.13.3.1), laser diffraction (Chapter 4.13.3.2), Differential

Scanning Calorimetry (Chapter 4.13.3.3), Thermogravimetric Analysis (Chapter 4.13.3.4) and X-ray diffraction (Chapter 4.13.3.5) and these results were already discussed in Chapter 4.13.3.

Prior to the impaction study (Section 5.9), insulin dry powders prepared by spray drying for inhalation (Section 5.5) were characterised in terms of morphology including size (Section 5.7.1), thermal behaviour (Section 5.7.2), and moisture content (Section 5.7.3).

5.7.1. Scanning electron microscopy

Morphology along with particle size of raw human insulin, SD insulin and three carrier-based DPI formulations (SDIMB, SDI10GMB and SDI5LMB) after blending (Section 5.6) were characterised by Scanning Electron Microscopy (SEM, ZEISS EVO®50, UK) at an acceleration voltage of 10-25 kV at different magnifications. Double-sided cohesive carbon tabs were adhered to aluminium stubs and all dry powder samples were placed onto the carbon tabs. Any excess powder samples were tapped off the tabs. These samples were then coated with a palladium/gold alloy using a SC7640 Sputter Coater (Polaron, UK) under argon gas for 2 minutes. Multiple images of coated samples were captured for each sample. SEM images of three carrier-based DPI formulations were captured for the visual observation of the blends (Blend homogeneity assessment, Section 5.8).

5.7.2. Differential scanning calorimetry

Thermal analysis of raw human insulin and SD insulin powders was carried out using a DSC822e Differential Scanning Calorimetry (DSC, Mettler Toledo, Switzerland) under nitrogen gas (50 mL min^{-1}) in the temperature range from 25°C to 400°C at a heating rate of $10^\circ\text{C min}^{-1}$. The dry powder samples were placed in aluminium crucibles ($40 \mu\text{L}$) and sealed with a pierced lid on. The dry powder samples loaded pan and empty reference pan were placed on the DSC sample holder. The DSC curves were recorded at 22°C using STARe Software version 8.10 (Mettler Toledo, UK).

5.7.3. Thermogravimetric analysis

Thermogravimetric analysis (TGA) for raw human insulin and SD insulin powders was performed to measure moisture content using a METTLER TOLEDO TGA/DSC1 STARe System (Mettler Toledo, Switzerland) along with DSC analysis (Section 5.7.2). The dry powder samples were loaded onto a pan ($70 \mu\text{L}$) and heated under nitrogen gas (50 mL min^{-1}) in the temperature range from 25°C to

400°C at a heating rate of 10°C min⁻¹. The TGA curves were recorded at 22°C using STARe Software version 8.10 (Mettler Toledo, UK).

5.8. Blend homogeneity assessment

Blend homogeneity for three carrier-based DPI formulations (SDIMB, SDI10GMB, SDI5LMB) was assessed by quantifying the content of insulin (drug) and mannitol (carrier) using the developed reversed-phase high performance liquid chromatography (RP-HPLC) method (Chapter 4) and the proton quantitative nuclear magnetic resonance (¹H qNMR) method (Chapter 3) (Babenko et al., 2019), respectively.

The chromatography conditions used for insulin quantification were as follows (Chapter 4.13.1). The mobile phase was a 31.5:68.5 (%v/v) mixture of acetonitrile with 0.1% trifluoroacetic acid (TFA) and distilled water with 0.1% TFA at a flow rate of 1.0 mL min⁻¹. The stationary phase was a C8 column (4.6 mm internal diameter x 250 mm length, 5 µm particle size, 130 Å pore size, Phenomenex, UK). The elution mode was isocratic. A detection wavelength was set to 215 nm. Injection volume was 20 µL. The developed and validated RP-HPLC method produced accurate (relative error%: 0.64%-4.90%) and precise data with high repeatability (relative standard deviation, RSD%: 0.63-3.97) in the concentration range of 2.7 µg mL⁻¹ to 108.0 µg mL⁻¹ (linear calibration curve for insulin, R² = 0.9999). The limit of detection was 0.66 µg mL⁻¹ and limit of quantitation was 2.01 µg mL⁻¹ (Chapter 4.13.2). Blend samples (4 mg total blend; 0.4 mg SD insulin and 3.6 mg SFD carrier) were taken from three different positions (top, middle and bottom) of each DPI formulation in the blending container and dissolved in distilled water (4 mL, theoretical insulin concentration: 100 µg mL⁻¹). Insulin content uniformity was determined as the ratio of the calculated concentration of insulin to the theoretical concentration of insulin contained in the blend sample and expressed as a percentage. The coefficient of variation (%CV or referred to as RSD%) was used as a degree of insulin content homogeneity. High %CV values indicates a lower drug content homogeneity (Kaialy, Nokhodchi, 2016). Simultaneously, the content uniformity of mannitol in the blend sample was determined using the ¹H qNMR method. All NMR data were processed using TopSpin™ software 4.1.0 (Bruker BioSpin GmbH, Germany).

5.9. Impaction study

The aerodynamic performance of four DPI formulations (SDI, SDIMB, SDI10GMB and SDI5LMB) was assessed *in vitro* using a next generation impactor (NGI, Copley Scientific, UK) with the Alberta Idealised Throat 28028 (AIT, Copley Scientific, UK). The NGI was equipped with a Critical Flow Controller (TPK 2000, Copley Scientific, UK) connected to a Vacuum pump (HPC5, Copley Scientific, UK). The flow rate was set at 30 L min⁻¹ with the test airflow duration of 3 sec. The critical flow (P3/P2 ratio ≤ 0.5, flow rate stability) was achieved. A leak test was performed on the NGI prior to each use. In this study, Handihaler® (Boehringer Ingelheim, Germany, a single capsule inhalation device with high resistance) was used as a DPI device to deliver the content of SD insulin powders filled (total fill mass per capsule: 2.2 mg average for carrier free SD insulin and 20 mg ± 1 mg for carrier-based DPI formulations) in the HPMC size 3 capsules (CAPSUGEL®, UK) during the impaction studies. In carrier-based DPI formulations the drug content was limited to 2 mg in 20 mg total mass of adhesive mixtures (drug: carrier = 1:9) per capsule.

SD insulin powders deposited on AIT and on all NGI stages (stages 1-7 and micro orifice collector, MOC) were collected using distilled water (2 or 3 mL) and immediately quantified by RP-HPLC (Chapter 4.13.1 and 4.13.2). SD insulin powders deposited on 7 stages in the NGI were based on the aerodynamic cut-off diameters of 0.541 µm (stage 7), 0.834 µm (stage 6), 1.357 µm (stage 5), 2.299 µm (stage 4), 3.988 µm (stage 3), 6.395 µm (stage 2), and 11.719 µm (stage 1) at flow rate of 30 L min⁻¹. All NGI studies were performed in triplicate at room temperature. The aerosolisation performance of SD insulin powders were assessed using Microsoft® Excel and Copley Inhaler Testing Data Analysis Software (CITDAS) Version 3.10 Wibu (Copley Scientific, UK) to determine insulin delivered dose, FPF, mass median aerodynamic diameter (MMAD) and geometric standard deviation (GSD). The delivered dose (%) was determined as the ratio of the total SD insulin deposition on AIT and all the NGI stages excluding the deposition in the inhaler device and capsules to the total SD insulin dose delivered from the device including the deposition in the inhaler device and capsules (i.e., the mass of the insulin powders filled into the capsule). Therefore, drug loss (%) was determined as follows: 100 - delivered dose (%). The FPF defined as the mass fraction of the delivered drug dose with less than or equal to 5.0 µm aerodynamic diameter was used to characterise the aerosolisation performance of DPI formulations.

5.10. Insulin structural stability study

Preliminary stability study on insulin powders before and after spray drying and during storage (room temperature, 22°C ± 3°C) for up to 12 months was performed using Fourier-transform

infrared spectroscopy (FTIR) and the developed RP-HPLC method (Chapter 4.13.1 and 4.13.2).

Structural stability of SD insulin powders during storage was also studied using FTIR.

The FTIR spectra of raw human insulin and SD insulin powders were acquired on a Nicolet™ iS5 FTIR spectrometer (Thermo Fisher Scientific, UK) in the range of 400–4000 cm^{-1} by accumulating 16 scans with a resolution of 4 cm^{-1} at 22°C. The FTIR spectra were obtained using OMNIC™ driver version 8.2 software (Thermo Scientific, UK). The developed RP-HPLC method (Chapter 4.13.1 and 4.13.2) was used to quantify the content of human insulin in SD insulin powders.

5.11. Statistical analysis

Statistical analysis was performed using SPSS® statistics version 24.0 (IBM, UK) along with Microsoft® Excel at significant level of $p < 0.05$. One-way ANOVA (Analysis of Variance) and t-test were used to compare the mean results for data (insulin content uniformity and NGI study for all DPI formulations). If the ANOVA was itself significant Post Hoc test (Tukey honestly significant difference (HSD) test) was further performed to determine which groups were different from each other (Ennos, 2012).

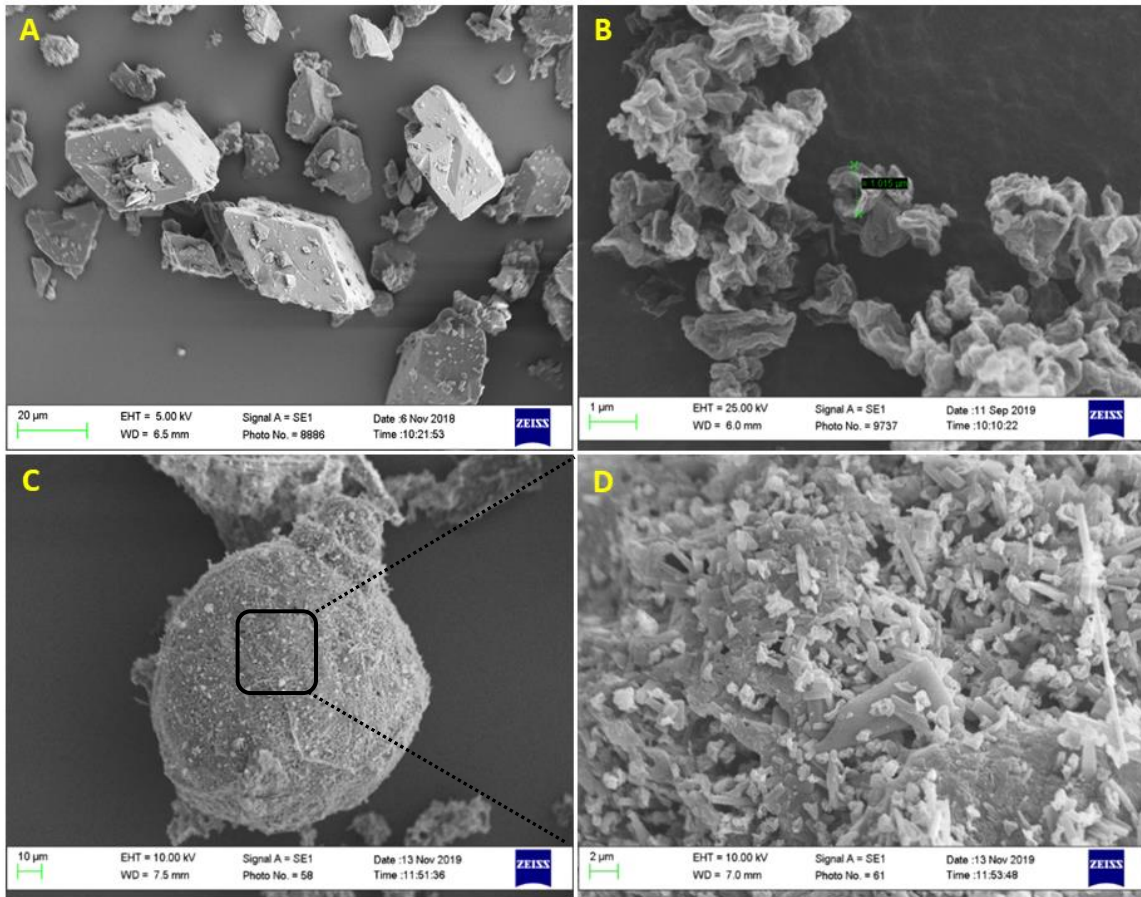
5.12. Results and discussion

5.12.1. Physicochemical characterisation

Mannitol dry powders with and without 5% leucine or 10% glycine were successfully prepared as DPI carriers using spray freeze drying (Section 5.4) and employed to improve insulin aerosolisation performance. Leucine was chosen as it has been used to enhance the aerosolisation performance of DPI formulations by altering surface property to decrease the inter-particulate forces between drug and carrier particles and improve drug-carrier detachment (Nokhodchi, Martin, 2015, Kaialy, Nokhodchi, 2016, Otake et al., 2016, Mehta, 2018). Glycine was selected as it has been used as buffering agent in Exubera® (Al-Tabakha, 2015, Ferrati et al., 2018).

5.12.1.1. Scanning electron microscopy

The SEM image of raw human insulin (Figure 49A) showed irregular particle shapes with particle size ranging from 15 μm to 40 μm , which is not within the suitable particle size range (aerodynamic diameter: $\leq 5 \mu\text{m}$) for systemic pulmonary delivery. Therefore, spray drying was employed to reduce the particle size. The SEM image of SD insulin (Figure 49B) showed wrinkled/shriveled particles in the particle size range of 1 μm to 5 μm , which is suitable for drug deposition in the lungs. It is evident that spray drying demonstrated to reduce the particle size of insulin powders to a suitable range for pulmonary delivery. The deformed/wrinkled particle shapes could be due to the rapid evaporation of the solvent upon drying, leading to such particle shrinkage (Maltesen et al., 2008, Wanning, Süverkrüp & Lamprecht, 2015, Emami et al., 2018). This morphology of SD insulin was found to be consistent with the SEM images reported by Balducci *et al.* (2014). Furthermore, Maltesen *et al.* (2008) reported that the use of low insulin concentration (5-30 mg mL^{-1}) resulted in the formation of wrinkled or folded particles (Maltesen et al., 2008). The SEM images of three DPI formulations (SDIMB, SDI10GMB and SDI5LMB) showed that all SFD mannitol-based carriers were covered with SD insulin particles as the small wrinkled/shriveled particles were seen on the surface of the carriers (Figure 49C-H). This can be an indication that the blending promoted the distribution and adhesion of SD insulin particles to the SFD carrier surfaces. Also, it was observed that SD insulin particles on the surfaces of SFD carriers were not agglomerated. This could be due to the creased shape associated with less contact areas between drug particles (Balducci et al., 2014). However, it can be seen from Figure 49D and Figure 49H that some SD insulin particles were found in the mesh structures of SFD mannitol and SFD 5% leucine-mannitol carriers. This could indicate that these SFD carrier surfaces were associated with large scale roughness that are larger than the insulin particle size (macroscale roughness), therefore large drug-carrier contact area with the presence of strong adhesive forces. This could possibly lead to poor drug detachment from carriers and affect the aerosolisation efficiency. On the other hand, the surface of SFD 10% glycine-mannitol carriers was rather continuous, but rough and uneven (Figure 49E-F). This surface property prevented drug particles from inserting inside the carrier's mesh structures. These differences in particle surface properties (e.g., morphology and surface roughness) affected the insulin content uniformity (Section 5.12.2) and aerosolisation performance of DPI formulations (Section 5.12.3).



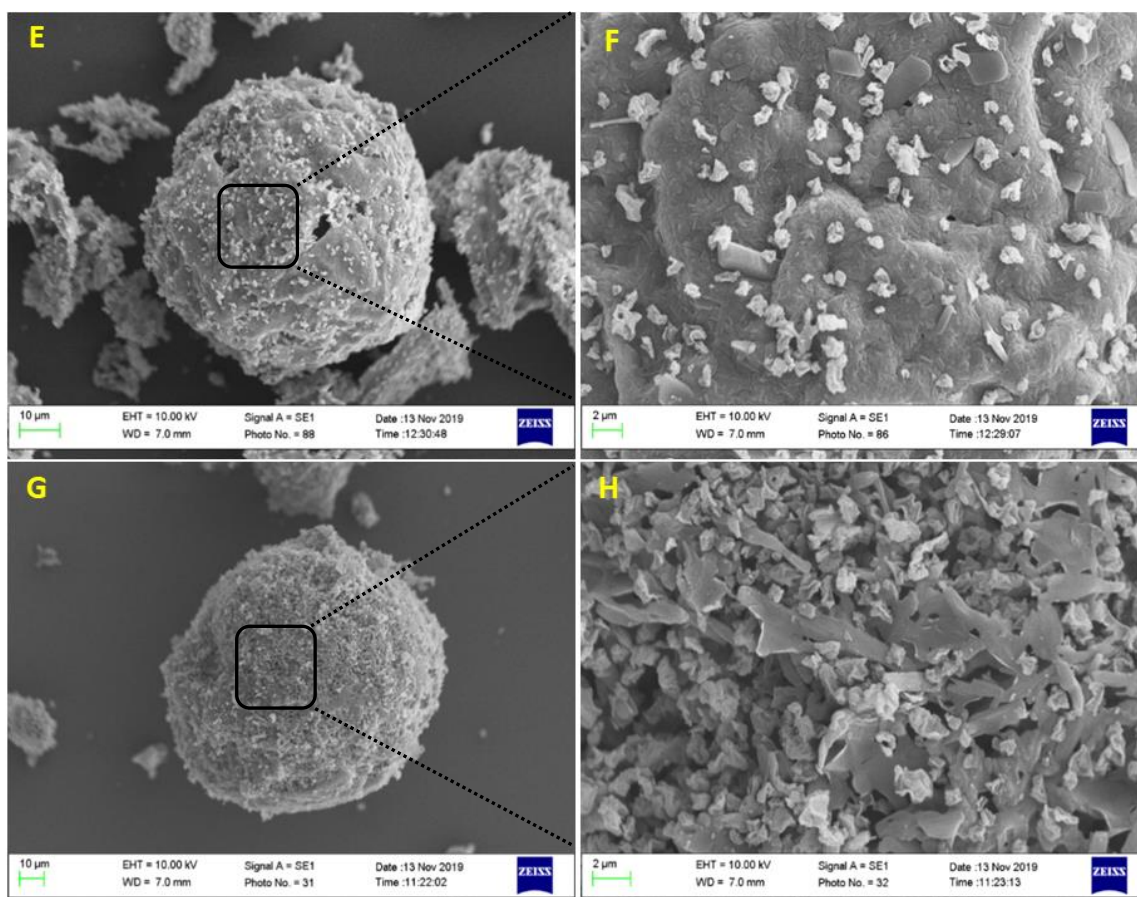


Figure 49: Scanning electron microscopy images of raw human insulin (A), spray dried (SD) insulin (B), SD insulin and spray freeze dried (SFD) mannitol blend (SDIMB)(C,D), SD insulin and SFD 10% glycine-mannitol blend (SDI10GMB) (E,F) and SD insulin and SFD 5% leucine-mannitol blend (SDI5LMB) (G,H) dry powders.

5.12.1.2. Differential scanning calorimetry

The results of DSC analysis for raw human insulin and SD insulin showed no significant sharp peaks, indicating amorphous insulin powders (Figure 50). The DSC curve for raw human insulin showed a broad endothermic peak between 40°C and 100°C, small endothermic peak around 210°C and broad exothermic peak starting at around 250°C followed by another exothermic peak starting at around 320°C (Figure 50A). The first broad endothermic peak below 100°C could be attributed to moisture loss and the second small endothermic peak around 210°C would be the onset of insulin degradation where insulin started to degrade. These results were supported by the TGA (two steps of mass loss observed below 100°C and above 200°C in Figure 51A) discussed later in Section 5.12.1.3. Also, this DSC result was similar to the insulin (human zinc-insulin) thermal transition reported by Sarmiento *et al.* (2006), however, their result did not show the small endothermic peak around 210°C and

exothermic peak above 320°C (Sarmiento et al., 2006). In comparison, the DSC curve for SD insulin showed three small and broad endothermic events starting at around 165°C, 196°C and 240°C (Figure 50B). These three events represent its decomposition. This could be attributed to the degradation of insulin occurred via the chemical or physical process influenced by the temperature conditions (Ansari et al., 2016). There is no endothermic peak observed below 100°C, which is associated with moisture loss. This indicates that spray drying successfully removed all water and produced moisture-free insulin powders. It was also observed that spray drying maintained insulin in amorphous state as all the peaks observed were small and broad.

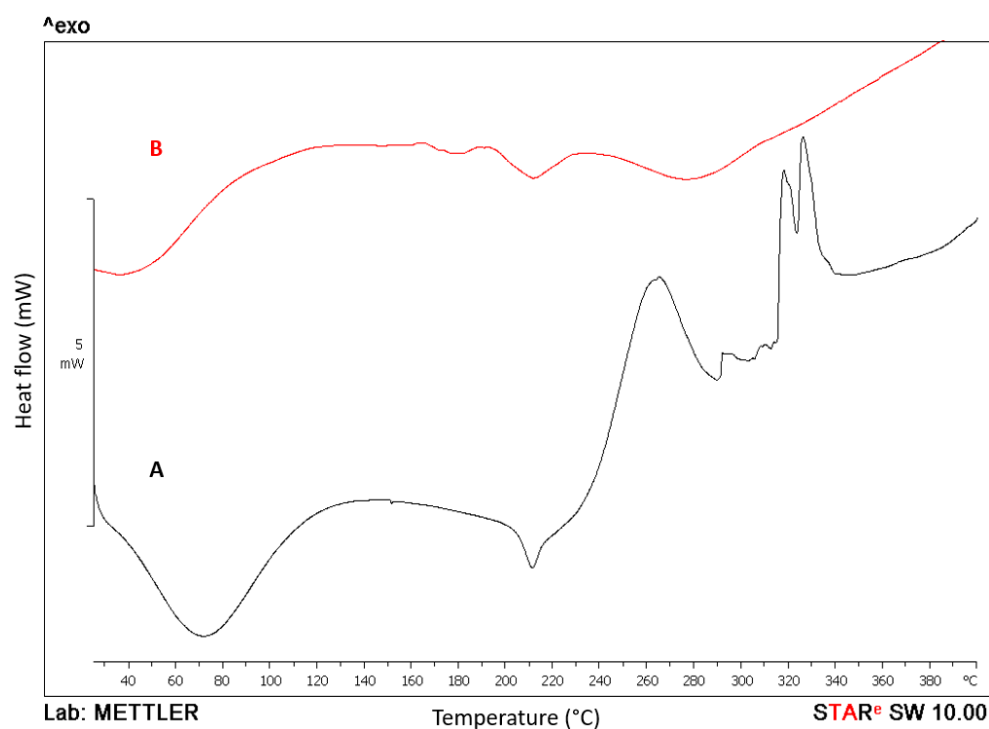


Figure 50: Combined DSC thermograms of raw human insulin (A, black) and spray dried insulin (B, red) dry powders.

5.12.1.3. Thermogravimetric analysis

The TGA curve of raw human insulin (Figure 51A) showed two steps of mass loss. The first mass loss (about 4-5%) observed in the temperature range of 50°C to 100°C was associated with moisture content. This supports the DSC curve for raw human insulin where the endothermic peak observed

under 100°C (Figure 50A) was attributed to water/moisture loss. The second mass loss (about 10%) observed between 200°C and 280°C in Figure 51A could be due to its decomposition. This also supports the DSC curve where the peaks observed above 200°C (Figure 50A) were attributed to its decomposition. On the other hand, the TGA curve for SD insulin (Figure 51B) showed three steps of mass loss starting at around 196°C (mass loss: 3%), 246°C (mass loss: 32%) and 362°C (mass loss: 5%). These mass losses can be associated with its decomposition. There were no events observed below 100°C indicating the absence of moisture content in SD insulin powders. This supports the DSC result for SD insulin (Figure 50B), where no endothermic peak was observed below 100°C. This suggests that spray drying removed all water, hence resulted in no moisture residue in SD insulin powders. This is advantageous as the presence of moisture content may affect the long-term stability of the DPI formulations (Banga, 2015).

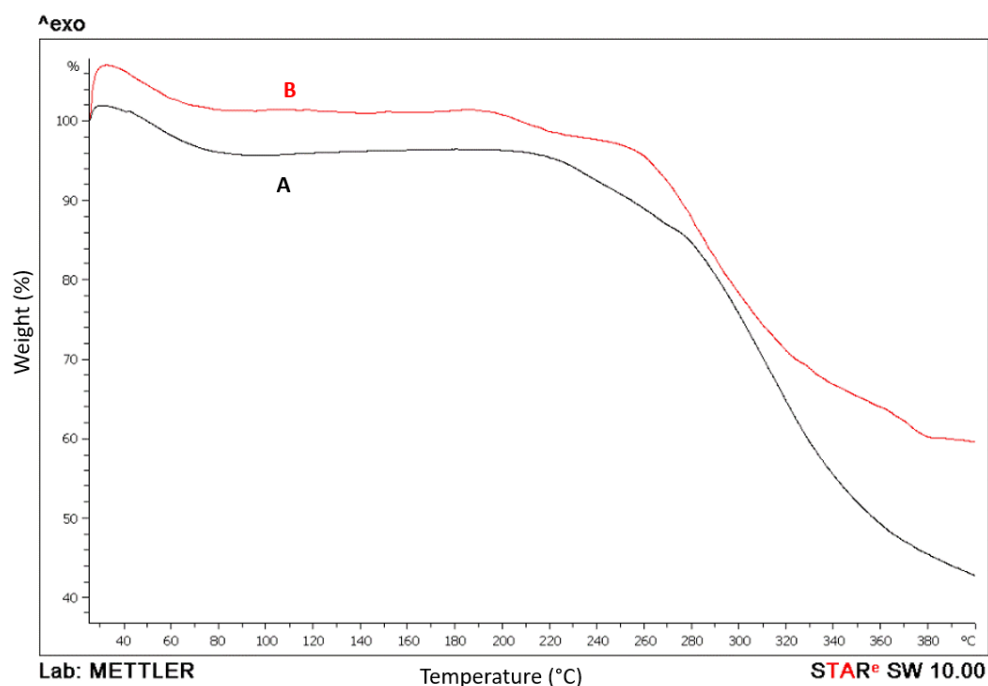


Figure 51: Combined TGA curves of raw human insulin (A, black) and spray dried insulin (B, red) dry powders.

5.12.2. Blend homogeneity assessment

The insulin content quantified by RP-HPLC and mannitol carrier content quantified by ^1H qNMR in three carrier-based DPI formulations (SDIMB, SDI10GMB and SDI5LMB) are shown in Figure 52. Figure 53 shows ^1H NMR spectra of mannitol from three different positions of DPI formulations in the blending container. Blending is an important process to prepare homogeneous mixtures consisting of drug particles and carrier particles in DPI formulations to ensure uniform drug dose distribution in the lungs (Kaialy, 2016). In this study, all DPI formulations demonstrated significantly different insulin uniformities (One-way ANOVA, $p < 0.05$). Insulin content uniformity (as %) was in the following rank order: SDI10GMB (97.60%, %CV: 0.56) > SDIMB (80.43%, %CV: 0.78) > SDI5LMB (73.20%, %CV: 0.72) with all %CV below 1.0% (0.56-0.78%) (Figure 52). The drug content for DPI formulation containing SFD 10% glycine-mannitol carrier (SDI10GMB) fell within the acceptable range of 85-115% of the nominal dose (British Pharmacopoeia Volume V Appendix XII Uniformity of Content (Yeung et al., 2019) and FDA guidelines) with good drug content homogeneity (%CV:0.56) while SDIMB and SDI5LMB were outside the acceptable range. This could be attributed to the surface of SFD mannitol (Figure 49D) and SFD 5% leucine-mannitol (Figure 49H) carriers associated with high adhesion forces where some SD insulin particles were embedded in the mesh structures of both carriers, hence, affecting drug particle distribution during blending. In comparison to SDIMB, SDI10GMB had significantly higher insulin uniformity (Tukey HSD test & t-test, $p < 0.05$), whereas the uniformity for SDI5LMB was not significantly different from SDIMB (Tukey HSD test & t-test, $p > 0.05$). This indicates that the addition of 10% glycine to SFD mannitol carrier had a positive effect on insulin content uniformity (Tukey HSD test & t-test, $p < 0.05$). However, the inclusion of 5% leucine did not have a significant effect on the insulin uniformity (Tukey HSD test & t-test, $p > 0.05$).

The mannitol content uniformity for all DPI formulations was between 91.93% and 107.97% with good mannitol carrier homogeneity (low %CV: 0.09-0.10) (Figure 52). The intensity of all mannitol peaks observed by NMR showed comparable for all formulations presenting similar mannitol concentrations were quantified amongst three DPI formulations (Figure 53). However, they demonstrated significantly different mannitol uniformities (One-way ANOVA, $p < 0.05$). Therefore, the drug (insulin) content could influence carrier (mannitol) content or vice versa and consequently affect the homogeneity of the formulation blends.

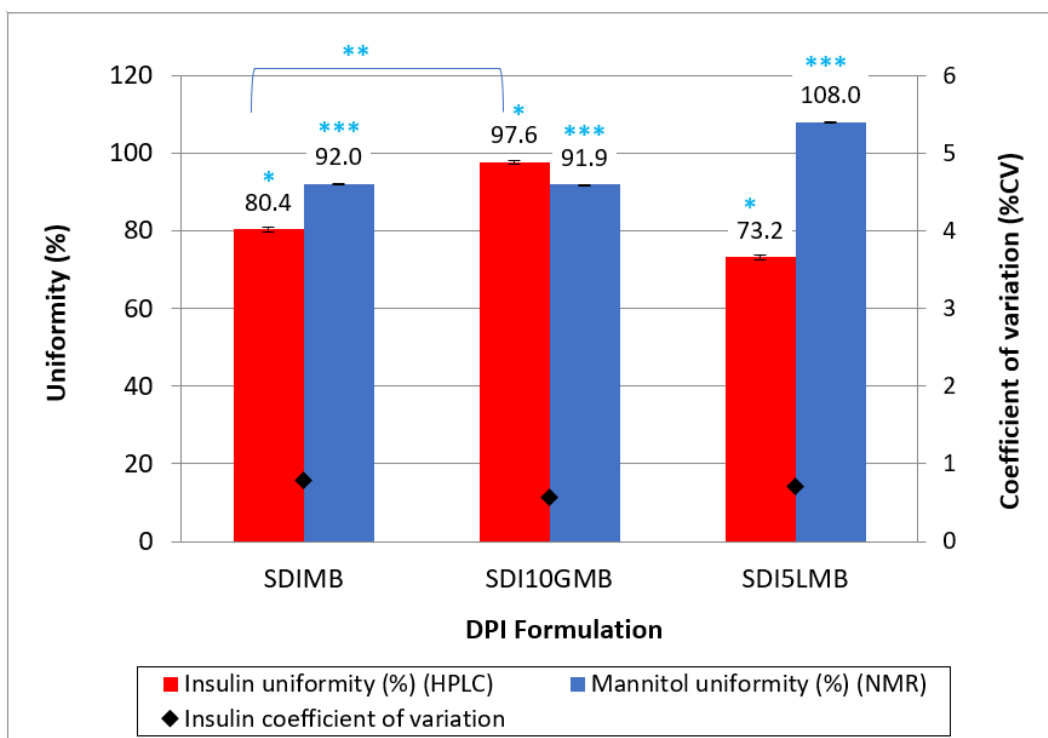


Figure 52: The content uniformity for insulin with coefficient of variation and mannitol in dry powder inhaler (DPI) formulations (n=3). (Data presented as mean (three positions) \pm standard deviation, n=3). SDIMB: Spray dried (SD) insulin and spray freeze dried (SFD) mannitol blend, SDI10GMB: SD insulin and SFD 10% glycine-mannitol blend and SDI5LMB: SD insulin and SFD 5% leucine-mannitol blend.

Asterisks (*) indicate significantly different insulin uniformities between DPI formulations (One-way ANOVA, $p < 0.05$).

Asterisks (**) indicate a statistically significant difference in insulin uniformity between SDI10GMB and SDIMB (t-test, $p < 0.05$).

Asterisks (***) indicate statistically significant differences in mannitol uniformity between DPI formulations (One-way ANOVA, $p < 0.05$).

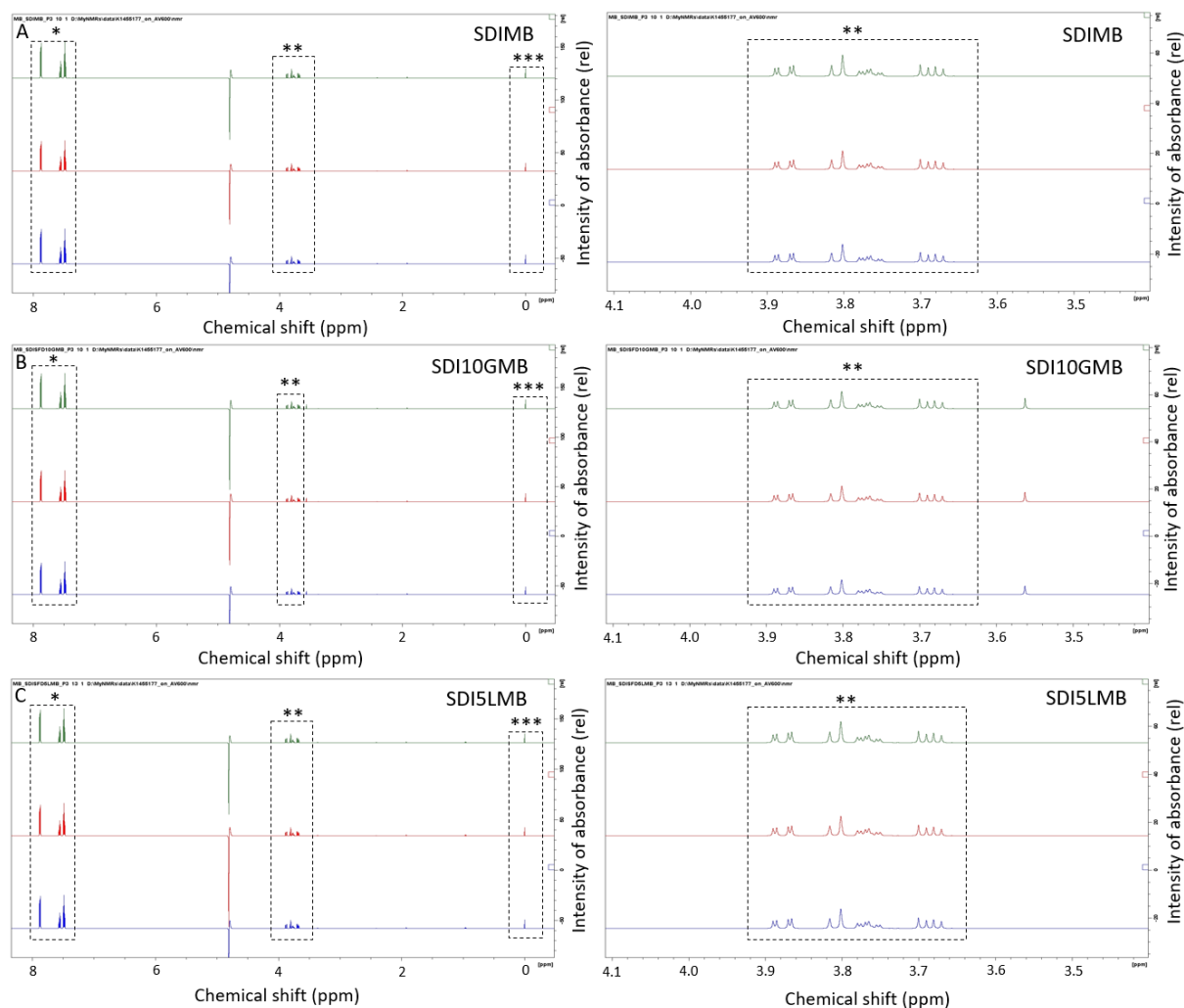


Figure 53: ^1H NMR spectra of mannitol from three different positions of three carrier-based dry powder inhaler formulations in the blending container. SDIMB: spray dried (SD) insulin and spray freeze dried (SFD) mannitol carrier blend (A), SDI10GMB: SD insulin and SFD10% glycine-mannitol carrier blend (B), and SDI5LMB: SD insulin and SFD 5% leucine-mannitol carrier blend (C). Dashed boxes with *, **, *** indicate peaks of the internal standard (sodium benzoate), mannitol, chemical shift reference (sodium 3-trimethylsilyl propionate-2,2,3,3- d_4 , TSP), respectively.

5.12.3. Impaction study

The results of insulin depositions within the NGI (Figure 54) show that all DPI formulations demonstrated significantly different insulin depositions in AIT, stages 1, 2, 3, 4, and 5 (One-way ANOVA, $p < 0.05$). This means that insulin depositions in different stages were dependent on the formulations; therefore, affected the aerosolisation performance of SD insulin powders. Table 27 shows that apart from SDI5LMB, MMAD values for SDI, SDIMB and SDI10GMB were within the suitable aerodynamic diameter range (MMAD: $\leq 5 \mu\text{m}$) for systemic pulmonary delivery in the

following rank order: SDIMB ($4.13 \mu\text{m} \pm 1.77 \mu\text{m}$) > SDI10GMB ($2.37 \mu\text{m} \pm 0.34 \mu\text{m}$) > SDI ($2.05 \mu\text{m} \pm 0.69 \mu\text{m}$). There were no MMAD and GSD determined for SDI5LMB due to the narrow distribution observed where over 50% of the cumulative mass deposited on AIT and stage 1 (>11.719 μm cut-off diameter, oropharyngeal deposition) (Figure 54 and Table 27). This resulted in generating the lowest FPF ($32.97\% \pm 2.85\%$) for SDI5LMB (Table 27). On the other hand, carrier free DPI formulation produced the highest FPF (FPF: $77.36\% \pm 18.01\%$) followed by SDI10GMB (FPF: $57.32\% \pm 6.81\%$) and SDIMB (FPF: $44.94\% \pm 8.66\%$) (One-way ANOVA, $p < 0.05$) (Table 27). The highest FPF obtained for SD insulin alone indicates that higher amounts of insulin (aerodynamic diameter: $\leq 5 \mu\text{m}$) would be expected to reach the deep lung regions for systemic drug absorption. However, despite that carrier free DPI formulation had the highest FPF, SDI had the lowest insulin delivered dose ($38.64\% \pm 3.82\%$) (Table 27). This indicates that the lowest amount of insulin powders was collected from AIT and all NGI stages therefore drug (insulin) loss was high. In contrast, carrier-based DPI formulations facilitated the delivery of insulin as higher amounts of insulin powders were dispersed from the DPI in the following rank order: SDI5LMB ($61.64\% \pm 4.97\%$) > SDIMB ($58.09\% \pm 5.49\%$) > SDI10GMB ($57.75\% \pm 4.24\%$). This showed that DPI formulations with the use of SFD carriers improved insulin delivery therefore reduced the amount of drug loss. As discussed above, SDI5LMB generated the lowest FPF, however, the addition of 5% leucine to SFD mannitol carrier enhanced the insulin delivery dose (1.6-fold increase against SD insulin alone) (Table 27). This agrees with previous studies (Kaialy, Nokhodchi, 2016, Otake et al., 2016, Li et al., 2016).

The difference in FPF values among SDIMB, SDI5LMB and SDI10GMB formulations (One-way ANOVA, $p < 0.05$) could be attributed to the different surface properties of SFD carriers associated with different adhesive forces. The carrier surface of SFD mannitol (Figure 49C-D) and SFD 5% leucine-mannitol (Figure 49G-H) with large scale roughness therefore strong inter-particulate adhesive forces might have affected negatively on drug detachment from the SFD carrier leading to lower FPF whereas the continuous, but rough and uneven surfaces of SFD 10% glycine-mannitol carrier (Figure 49E-F) would have contributed to the improvement of drug-carrier detachment resulting in high FPF. SDI10GMB exhibited significantly lower insulin deposition in stage 1 than SDIMB and SDI5LMB (Tukey HSD test, $p < 0.05$) therefore the addition of 10% glycine to SFD mannitol reduced insulin deposition in stage 1 (Figure 54). For insulin depositions in lower NGI stages (e.g., stages 3-5) where represent the desired deep lung regions for systemic pulmonary delivery, SDI10GMB had significantly higher insulin deposition than SDIMB and SDI5LMB (Tukey HSD test, $p < 0.05$) (Figure 54). This presents that insulin particles adhered to the carrier surface of SFD mannitol with 10% glycine detached more easily than insulin particles attached to SFD mannitol alone and SFD mannitol with 5% leucine. This could be interpreted that all carrier-based DPI formulations could pass through the

oropharynx region upon inhalation therefore dispersed well from the DPI device. However, DPI formulation containing SFD mannitol or SFD 5% leucine-mannitol carrier deposited as insulin-SFD carrier mixtures in AIT and stage 1 (e.g., oropharynx region). Consequently, only small amount of the drug was remained to reach the lower NGI stages resulting in low FPF. On the other hand, DPI formulation containing SFD 10% glycine-mannitol carrier minimised the early deposition of insulin-SFD carrier mixtures leading to higher amount of the drug particles available for deposition in the lower NGI stages. Further, sufficient drug-carrier detachment was achieved in the lower NGI stages resulting in high FPF.

This study demonstrated that aerosolisation performance of DPI formulations was dependent on the properties of carrier surface. DPI formulation with optimum aerosolisation performance in terms of insulin delivered dose, FPF and MMAD was achieved using SFD mannitol carrier in the presence of 10% glycine. This study suggests that it is feasible to improve the delivery efficiency of SD insulin powders and deliver insulin into the deep lung regions for systemic delivery via the pulmonary route of administration.

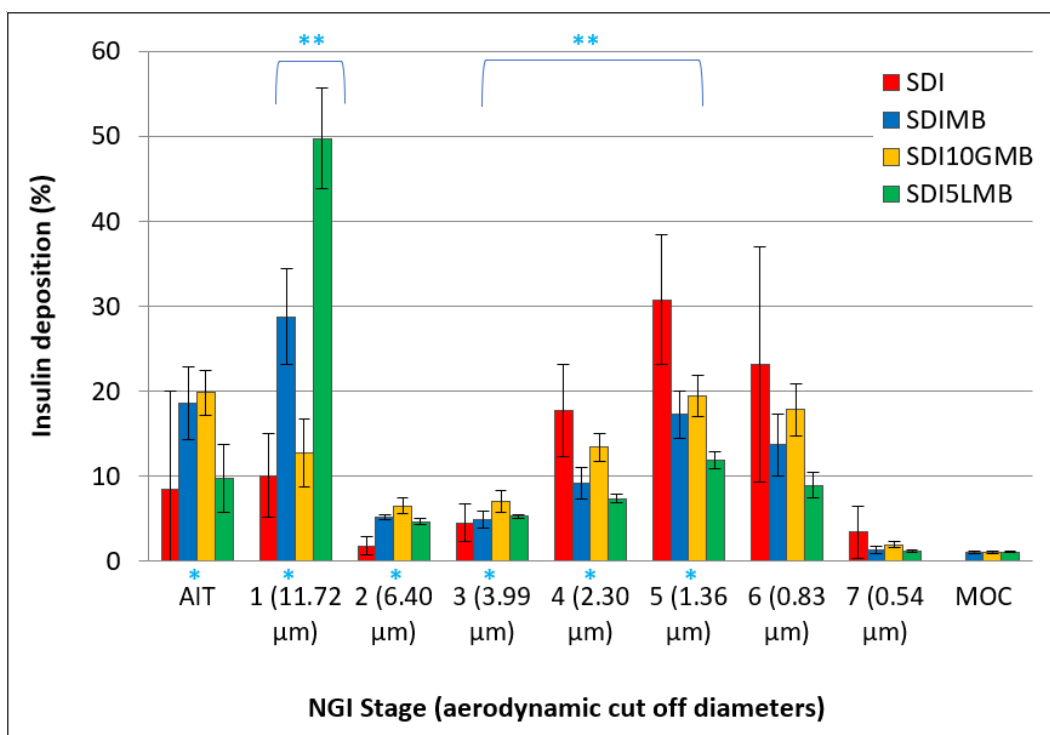


Figure 54: Next Generation Impactor (NGI) deposition profiles of spray dried (SD) insulin powders in dry powder inhaler formulations aerosolised from Handihaler® at flow rate of 30 L min⁻¹. Insulin deposition is expressed as delivered dose (%) per NGI stage. (Data presented as mean ± standard deviation, n=3). AIT: Alberta idealised throat, MOC: Micro orifice collector. SDI: SD insulin, SDIMB: SD insulin and spray freeze dried (SFD) mannitol blend, SDI10GMB: SD insulin and SFD 10% glycine-mannitol blend and SDI5LMB: SD insulin and SFD 5% leucine-mannitol blend.

Asterisks (*) indicate significantly different insulin depositions per NGI stage (i.e., AIT, stage 1,2,3,4 and 5) between DPI formulations (One-way ANOVA, p<0.05).

Asterisks (**) indicate statistically different insulin depositions in stage 1 and stages 3-5 between carrier-based DPI formulations (Tukey HSD test, p<0.05, SDI10GMB vs SDIMB or SDI5LMB).

Table 27: Insulin delivered dose (%), fine particle fraction (FPF% ≤5.0 μm), mass median aerodynamic diameter (MMAD) and geometric standard deviation (GSD) determined by Next Generation Impactor analysis at flow rate of 30 L min⁻¹ for dry powder inhaler (DPI) formulations (Data presented as mean ± standard deviation, n=3). SDI: spray dried (SD) insulin, SDIMB: SD insulin and spray freeze dried (SFD) mannitol blend, SDI10GMB: SD insulin and SFD 10% glycine-mannitol blend and SDI5LMB: SD insulin and SFD 5% leucine-mannitol blend.

DPI Formulation	Dose		Size Distribution	
	Insulin delivered dose (%)	FPF (%)*	MMAD (μm)	GSD
SDI	38.64 ± 3.82	77.36 ± 18.01	2.05 ± 0.69	2.15 ± 0.45
SDIMB	58.09 ± 5.49	44.94 ± 8.66	4.13 ± 1.77	NA
SDI10GMB	57.75 ± 4.24	57.32 ± 6.81	2.37 ± 0.34	3.49 ± 1.08
SDI5LMB	61.64 ± 4.97	32.97 ± 2.85	NA	NA

Asterisk (*) denotes statistically significant differences between DPI formulations (One-way ANOVA, p<0.05).

5.12.4. Insulin stability study

The preliminary stability study was performed to see whether SD insulin powders were stable after spray drying process and could be used for the impaction studies (also to provide information for further studies such as scale-up study). SD insulin powders were exposed to temperature variations (e.g., heating was on in winter and air conditioning was on and off in summer and direct sunlight to the powders) during 12-month storage including lockdown in March-July 2020. In general, room temperature stable formulations are ideal for inhaled products (Sadzadeh et al., 2010). Therefore, storage conditions used for insulin stability studies were room temperature (real time/real temperature conditions (ICH, 1995)) and the final products will be protected against humidity. FTIR was used to study the structure integrity (e.g., secondary structure) of human insulin in SD insulin powders whether the process of spray drying using high temperatures (inlet temperature at 119°C and outlet temperature at 60°C ± 2°C, Section 5.5) had an adverse effect on the structure of human insulin. The FTIR spectra between raw human insulin (Figure 55A) and SD insulin (Figure 55B) showed similarities as no major shift of the characteristic band positions were observed: 3290-3280 cm⁻¹ (N-H stretching vibration), 2960 cm⁻¹ (C-H stretching vibration), 1651-1645 cm⁻¹ (Amide I, carbonyl (C=O) stretching vibration of the amide groups in the protein), 1538-1515 cm⁻¹ (Amide II, N-H bending vibration and C-N stretching vibration), 1453 cm⁻¹ (C-H bending, methyl group -CH₃) and 1402-1386 cm⁻¹ (C-H bending, methyl group -CH₃) (Figure 55). These characteristic band positions observed for raw human insulin (Figure 55A) agreed with the FTIR results reported by Vanea *et al.* (2014) and Agrawal, Wakte and Shelke (2017). Amide I (1700-1600 cm⁻¹) and Amide II bands (1575-1480 cm⁻¹) are protein characteristic spectra and used for protein characterisations (Sarmiento et al., 2006, Tiernan, Byrne & Kazarian, 2020). The similarity of the FTIR spectra between raw human insulin and SD insulin powders indicates that the integrity of human insulin structure (e.g., secondary structure) was maintained after the process of spray drying despite the use of relatively high temperatures (inlet temperature at 119°C and outlet temperature at 60°C ± 2°C, Section 5.5). However, a very small absorbance difference between raw human insulin and SD insulin powders was seen (Figure 55, dashed box). The peak around 1450 cm⁻¹ for SD insulin was smaller and the peak around 1400-1380 cm⁻¹ was slightly longer (Figure 55B) when compared to the peak for raw human insulin (Figure 55A). This could be attributed to C-H bending from alkane (methyl group, 1450 cm⁻¹) and/or O-H bending from carboxylic acid (1440-1395 cm⁻¹) as SD insulin powders were produced by dissolving raw human insulin in acidic aqueous solution (0.1% acetic acid with NaOH,

pH 3.5) for spray drying. Figure 56 showed no major changes in the characteristic band positions (e.g., Amide I and Amide II) between raw human insulin and SD insulin powders stored at room temperature for up to 12 months. This suggests that human insulin retained its secondary structure integrity in SD powders stored at room temperature for up to 12 months.

The stability of insulin was also assessed by RP-HPLC and the results are shown in Figure 57. No structural changes or degradation of insulin molecule would have occurred during the process of spray drying as insulin content in SD insulin powder within 24 hours of SD powders production was $100.78 \pm 0.58 \%$ (Figure 57). SD insulin powders stored at room temperature maintained their stability for up to 4 days after the process of spray drying then dropped by over 10% within 15 days (89%, Figure 57). Further 7% drop in stability was observed at 25 day (82%, Figure 57) and then reached a plateau for about 5 months (82% at 170 days, Figure 57). After that the stability started to drop gradually (78% at 351 days and 73% at 361 days, Figure 57). Although the FTIR spectra of SD insulin powders stored at room temperature for up to 12 months showed no major changes in insulin characteristics band positions (Figure 56). This could be attributed to different sample preparations involved in FTIR (insulin sample in solid state) and RP-HPLC (insulin sample in liquid state) that might have led to structural changes in insulin during sample preparation for RP-HPLC in addition to the storage conditions (Heinemann et al., 2021).

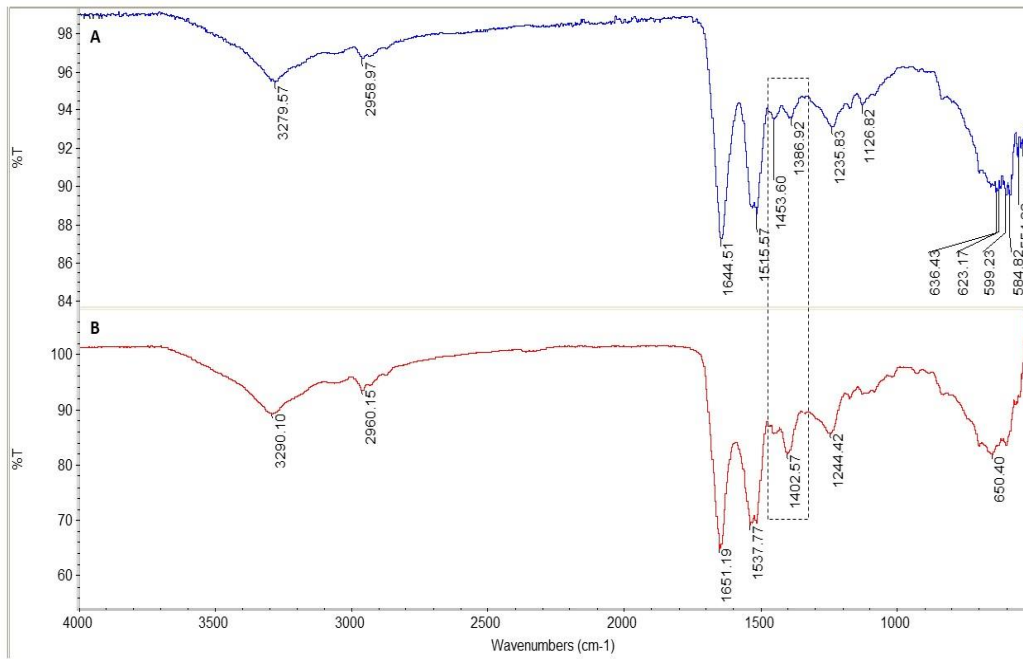


Figure 55: FTIR spectra of raw human insulin powder stored at -20°C (A) and freshly prepared spray dried insulin powder (B). %T: Transmittance.

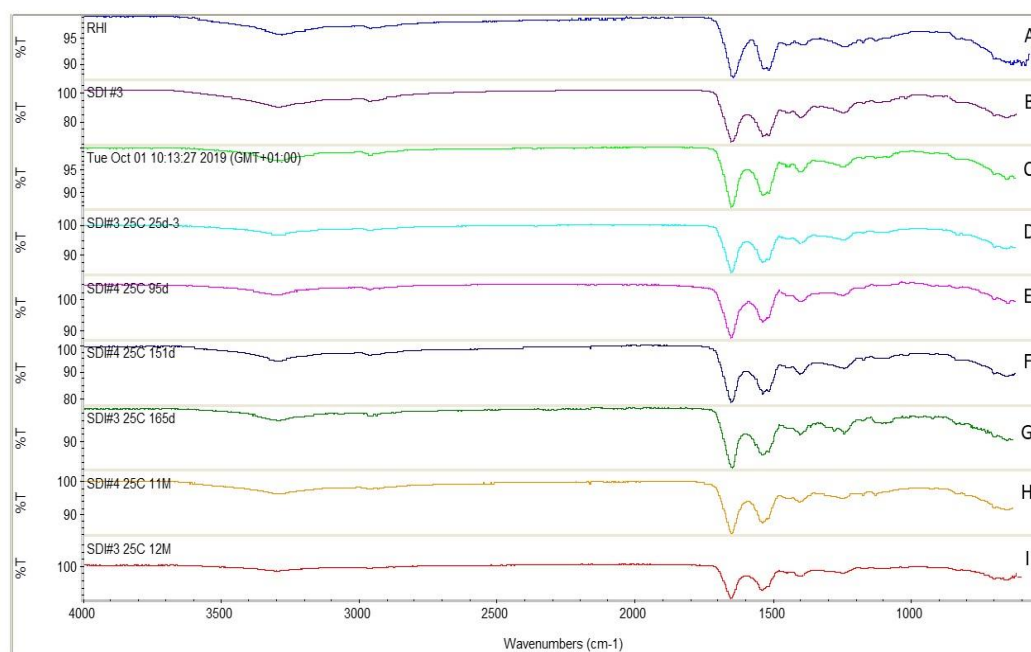


Figure 56: FTIR spectra of raw human insulin powder stored at -20°C (A), freshly prepared spray dried (SD) insulin powder (B) and SD insulin powder stored at room temperature for 8 days (C), 25 days (D), 95 days (E), 151 days (F) and 165 days (G), 11 months (H) and 12 months (I). %T: Transmittance.

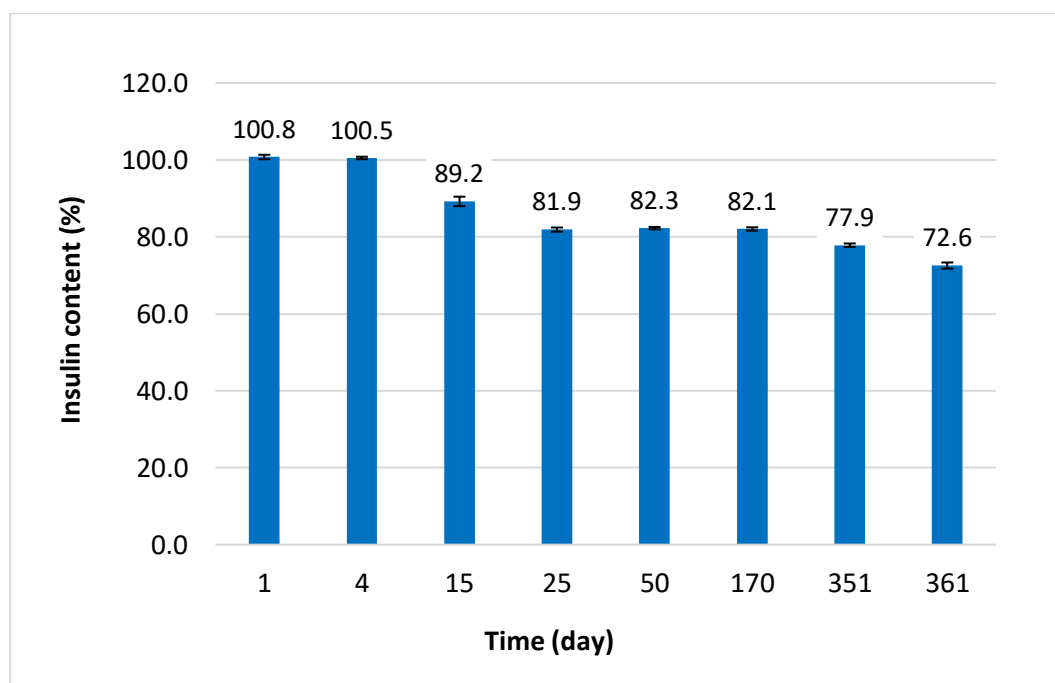


Figure 57: Insulin content determined by RP-HPLC. Spray dried insulin powder was stored at room temperature for up to 361 days (12 months). (Data presented as mean \pm standard deviation, n=3).

5.13. Conclusion

In this study, carrier free DPI formulation generated the highest FPF. However, carrier free DPI formulation delivered the lowest amount of SD insulin powders from the Handihaler®; therefore, the drug loss was high. Carrier-based DPI formulations improved insulin delivered dose as compared to carrier-free formulation. In carrier-based DPI formulations, SD insulin particles were successfully adhered to the surfaces of all SFD mannitol-based carriers. However, different surface properties (e.g., roughness) of SFD carriers significantly affected the aerosolisation performance of DPI formulations. SFD carriers with large scale roughness (i.e., SFD mannitol and SFD 5% leucine-mannitol carries) hindered from drug-carrier detachment leading to lower FPF whereas SFD carrier with the continuous and uneven surface (i.e., SFD 10% glycine-mannitol carrier) facilitated drug-carrier detachment resulting in high FPF. For the development of DPI formulations containing carriers, it is important to optimise surface properties of carriers to generate high FPF and improve pulmonary deposition. The use of SFD mannitol carrier with 10% glycine could be a feasible approach to improve the delivery efficiency of insulin by minimising drug deposition in the oropharynx region and delivering insulin into the deep lung regions for systemic delivery via the pulmonary route of administration. Consequently, this could lead to achieve higher bioavailability. Future studies should be focused on the larger scale blends of drug and carrier as all the studies performed in this study were based on the small-scale blends (micrograms). The scale-up process might affect the homogeneity of the powder mixtures therefore alter the balance of inter-particulate forces between drug and carrier within powder mixtures. Pharmacokinetics and pharmacodynamics profiles of inhaled SD insulin powders can be investigated to see if they exhibit fast absorption rate, high bioavailability, and glycaemic control (lower plasma glucose levels, prevent the raise of glycaemia) in animals (e.g., rats).

Chapter 6. Development of spray dried GLP-1 dry powder inhaler formulations for the treatment of Type 2 diabetes

6.1. Abstract

The study aimed to develop two types of dry powder inhaler (DPI) formulations containing glucagon-like peptide-1(7-36) amide (GLP-1); carrier-free (drug alone) and carrier-based DPI formulations for pulmonary delivery of GLP-1. Until now, no studies have been reported on the development of carrier free and carrier-based DPI formulations containing excipient free GLP-1 for pulmonary delivery. The aerosolisation performance of both DPI formulations was studied using a next-generation impactor at flow rate of 30 L min⁻¹. Carriers employed were either a 10% glycine-mannitol carrier prepared by spray freeze drying (engineered carrier) or raw mannitol carrier (non-engineered carrier). GLP-1 powder intended for inhalation was prepared using spray drying and characterised (morphology including size, thermal behaviour, and moisture content). A quantitative method using a reversed-phase high performance liquid chromatography (RP-HPLC) with an isocratic elution mode was also developed for the determination of GLP-1 content in DPI formulations. The structure integrity of GLP-1 powders before and after spray drying was tested by Fourier-transform infrared spectroscopy (FTIR) along with the developed RP-HPLC method.

The RP-HPLC method produced accurate (relative error%: 0.22%-4.65%) and precise data with high repeatability (relative standard deviation%: 0.67-4.50) in the concentration range of 2.0 µg mL⁻¹ to 140.0 µg mL⁻¹ (linear calibration curve for GLP-1, R² = 0.9999). The limit of detection was 0.79 µg mL⁻¹ and limit of quantitation was 2.39 µg mL⁻¹. GLP-1 structural integrity was not influenced by spray drying process as FTIR spectra showed no major changes in the characteristic band positions (e.g., Amide I and Amide II) before and after spray drying and GLP-1 content determined by RP-HPLC was 100% ± 1% within 24-48 hours of powder production.

Spray drying produced spherical particles with indented surfaces in the particle size range of 1 µm to 5 µm suitable for pulmonary delivery. Across formulations investigated, carrier free DPI formulation showed the highest fine particle fraction (FPF: 90.73% ± 1.76%) and the smallest mass median aerodynamic diameter (MMAD: 1.96 µm ± 0.07 µm), however, low GLP-1 delivered dose (32.88% ± 7.00%, total GLP-1 deposition on throat and all impactor stages). GLP-1 delivered dose was improved by the addition of engineered 10% glycine-mannitol carrier to the DPI formulation (32.88% ± 7.00% - > 45.92% ± 5.84%). This study demonstrated the advantage of using engineered porous carrier prepared by spray freeze drying over non-engineered carrier for enhanced GLP-1 powder flow. The optimised DPI formulations can be achieved by using particle engineering to prepare engineered

particles. The successful inhaled GLP-1 product will provide an alternative treatment option for people with Type 2 diabetes by eliminating the use of subcutaneous injection and improve patient compliance and adherence to treatment.

Keywords: Dry powder inhaler formulation, Glucagon-like peptide-1(7-36) amide, D-mannitol carrier, Glycine, Spray freeze drying, Spray drying

6.2. Introduction

The aims of this chapter were to develop two types of dry powder inhaler (DPI) formulations for pulmonary delivery of GLP-1, (i) carrier free DPI formulations containing glucagon-like peptide-1(7-36) amide (GLP-1) alone (no excipients) prepared by spray drying and (ii) carrier-based DPI formulations containing GLP-1 blended with two different carriers (particle size: 90-125 μm); 10% glycine-mannitol carrier prepared by spray freeze drying (engineered carrier) or raw mannitol carrier (non-engineered carrier). Until now, no studies have been published on the development of carrier free and carrier-based DPI formulations containing excipient free GLP-1 powder for pulmonary delivery. In the present study, spray dried (SD) GLP-1 powders for inhalation were prepared in the absence of excipients to minimise the lung safety concern. The pH of the feed solutions for spray drying GLP-1 was adjusted to 3.5 using sodium hydroxide (NaOH) or ammonium hydroxide (NH_4OH) based on the method of spray drying insulin (Chapter 5.5). Acidic solution with NH_4OH was tried based on the results of insulin stability study reported by Balducci *et al.* (2014). Their stability study (25°C and 60% RH) in terms of the degradation product contents of SD bovine insulin (i.e., A21 desamido insulin) showed that SD insulin powders prepared from acetic acid with NH_4OH (pH 3.6) kept the A21 degradant content within the required limit (5.0%) for up to six months at room temperature whereas SD insulin powders prepared from acetic acid with NaOH (pH 3.1) showed a shorter stability (three months) at room temperature (Balducci *et al.*, 2014). The aerosolisation performance of carrier free DPI formulations were compared with carrier-based GLP-1 DPI formulations using a next generation impactor. Both types of DPI formulations were studied to understand the effect of the carriers (engineered and non-engineered carriers) on the aerosolisation performance tested from Handihaler® DPI device. Spray freeze dried (SFD) 10% glycine-mannitol carrier was employed based on the results of preliminary experiments (Chapter 4 and Chapter 5). Chapter 4 assessed the effects of amino acids (glycine or leucine) at three different concentrations

(5%, 10% and 15% w/w) added as excipient to SFD mannitol carrier on the aerosolisation performance of DPI formulations containing raw human insulin (Chapter 4). Chapter 5 studied the aerosolisation performance of SD insulin DPI formulations where SFD 10% glycine-mannitol carrier facilitated drug powder delivery and drug-carrier detachment leading to optimum aerosolisation performance of SD insulin in terms of delivered dose ($57.75\% \pm 4.24\%$), FPF ($57.32\% \pm 6.81\%$) and MMAD ($2.37 \mu\text{m} \pm 0.34 \mu\text{m}$) (Chapter 5).

In addition, a reversed-phase high performance liquid chromatography (RP-HPLC) with an isocratic elution mode for the determination of GLP-1 content in DPI formulations was developed and validated based on the International Council for Harmonisation of Technical Requirements for Pharmaceuticals for Human Use (ICH) guidelines (ICH, 2005).

6.3. Materials

Glucagon-like peptide-1(7-36) amide (GLP-1: $\text{C}_{149}\text{H}_{226}\text{N}_{40}\text{O}_{45}$, MW: $3297.7 \text{ g mol}^{-1}$) was purchased from Henan Tianfu Chemical Co.,Ltd, China. Glycine, human recombinant insulin, mannitol, phosphate buffered saline tablet (PBS, pH 7.4), and sodium benzoate were all purchased from Sigma-Aldrich, UK. Acetic acid glacial, acetonitrile, 35% ammonia solution (NH_4OH), sodium hydroxide pellets (NaOH), trifluoroacetic acid (TFA) were all purchased from Fisher Scientific, UK. Deuterium oxide was purchased from Euriso-top[®], UK. Sodium 3-trimethylsilyl propionate-2,2,3,3-d₄ was purchased from Merck Sharp & Dohme Canada Limited, UK.

6.4. Method development

RP-HPLC method with an isocratic elution mode was developed for quantitative analysis of GLP-1 used in DPI formulations. The method development was performed on an Agilent Technologies 1260 Infinity II high performance liquid chromatography system (HPLC, Agilent Technologies, UK) composed of a degasser (Agilent Technologies, UK), vial sampler (Agilent Technologies, UK), and UV detector (Agilent Technologies, UK). During the method development, three different columns were tried to find a narrow and sharp symmetry peak of GLP-1 by changing its length, type or particle size (1: C18 4.6 mm internal diameter x 150 mm length, 4 μm particle size, 120 Å pore size, Agilent Technologies, US, 2: C18 4.6 mm internal diameter x 250 mm length, 4 μm particle size, 120 Å pore

size, Agilent Technologies, US and 3: C8 4.6 mm internal diameter x 250 mm length, 5 µm particle size, 130 Å pore size, Phenomenex, UK) from two different manufactures (Agilent Technologies, US and Phenomenex, UK) but keeping the internal diameter of 4.6 mm constant. C8 column was selected over C18 columns and used as the stationary phase at room temperature for method validation (Section 6.5). Mobile phase A (organic phase) consisted of acetonitrile and trifluoroacetic acid (TFA, 0.1% v/v), whereas mobile phase B (aqueous phase) consisted of distilled water and TFA (0.1% v/v). TFA was used to control the pH of mobile phases also used as an ion pair agent to avoid ionisation (Chen et al., 2004). Retention time, peak asymmetry factor (A_s , United States Pharmacopoeia (USP) at 10% height), tailing factor (T_f , USP at 5% height), and column efficiency (i.e., the plate number, N) for GLP-1 were monitored while changing the ratio of mobile phase A (acetonitrile with 0.1% TFA) and mobile phase B (distilled water with 0.1% TFA) at a constant flow rate of 1.0 mL min⁻¹ in order to find a sharp peak of GLP-1. Peak asymmetry factor (*Equation 6*), tailing factor (*Equation 7*), and column efficiency (*Equation 8*) were calculated using the equations (stated in Chapter 4.4) as follows:

Peak asymmetry factor (A_s , USP method at 10% height) was calculated using *Equation 6*:

$$A_s = b/a \quad \text{Equation 6}$$

where b is the distance from the peak midpoint to the peak tailing edge measured at 10% peak height and a is the distance from the leading (front) edge of the peak to the peak midpoint measured at 10% of peak height. The value of 1.0 ($A_s=1.0$) indicates a symmetrical peak. The value greater than 1 ($A_s > 1$) indicates tailing whereas less than 1 ($A_s < 1$) indicates fronting. Acceptable A_s value is generally between 0.9 and 1.2.

Tailing factor (T_f , USP method at 5% height) was calculated using *Equation 7*:

$$T_f = (a + b) / 2a \quad \text{Equation 7}$$

where a is the distance from the leading edge of the peak to the peak midpoint measured at 5% of peak height and b is the distance from the peak midpoint to the peak tailing edge measured at 5% of peak height. $T_f > 1.0$ indicates tailing and $T_f < 1.0$ indicates fronting (Merck KGaA, 2021).

Column efficiency (N) was calculated using *Equation 8*:

$$N = 5.54 (t_R / w_{1/2})^2 \quad \text{Equation 8}$$

where t_R is the retention time of the analyte and $w_{1/2}$ is the width of the peak at half height.

The column temperature was maintained at room temperature. The injection volume (20 μL) was kept constant. Two different detection wavelengths for GLP-1, 215 nm detected by a UV spectroscopy (Cary UV-Vis Compact, Agilent, UK) and 220 nm provided by the Chinese supplier (Henan Tianfu Chemical Co., Ltd) were tested. All the development experiments were performed on the Agilent HPLC system at room temperature ($22^\circ\text{C} \pm 3^\circ\text{C}$) and the optimal conditions are summarised in Table 28. The data acquisition and chromatograms (including peak asymmetry factor, tailing factor, and column efficiency) were obtained using an Openlab ChemStation (Agilent Technologies, UK).

Table 28: The optimal chromatography conditions and instrument used for method development and validation. TFA: trifluoroacetic acid.

Instrument	Agilent Technologies 1260 Infinity II high performance liquid chromatography (Agilent Technologies, UK)
Mobile phase A (41 % v/v)	Acetonitrile with 0.1% TFA
Mobile phase B (59 % v/v)	Distilled water with 0.1% TFA
Column	C8 4.6 mm x 250 mm, 5 μm particle size, 130 \AA pore size (Phenomenex, UK)
Column temperature	Room temperature
Wavelength	215 nm
Flow rate	1.0 mL min^{-1}
Injection volume	20 μL
Elution mode	Isocratic

6.4.1. Preparation of GLP-1 standard stock solution

GLP-1 standard stock solution was prepared by dissolving raw GLP-1 powders in distilled water at a concentration of 1 mg mL^{-1} . GLP-1 stock solution was used to prepare GLP-1 standard solutions for the calibration curve (Section 6.4.2) and test sample solutions for method validation (Section 6.4.3). The prepared GLP-1 stock solution was stored at 4°C .

6.4.2. Preparation of GLP-1 standard solutions for calibration curve

GLP-1 standard solutions at eleven different concentrations for the calibration curve in the concentration range of $2.0 \mu\text{g mL}^{-1}$ to $140.0 \mu\text{g mL}^{-1}$, which should cover the concentration range of interest for GLP-1 quantification in DPI formulations, were prepared at ambient conditions by diluting GLP-1 standard stock solution with distilled water. GLP-1 calibration standard solutions were run immediately after preparation.

6.4.3. Preparation of GLP-1 test sample solutions for validation

GLP-1 standard stock solution prepared at a concentration of 1 mg mL^{-1} was used to prepare five selected levels of GLP-1 concentration (low, middle and high end of the calibration curve concentration range, $5.0 \mu\text{g mL}^{-1}$, $10.0 \mu\text{g mL}^{-1}$, $40.0 \mu\text{g mL}^{-1}$, $80.0 \mu\text{g mL}^{-1}$, and $120.0 \mu\text{g mL}^{-1}$) for method validation (Section 6.5) following the same method used for the preparation of standard calibration curve solutions described in Section 6.4.2.

6.4.4. Preparation of mobile phase

Mobile phase A (organic phase) was prepared by adding TFA (0.1%, v/v) to acetonitrile and mixed thoroughly (pH ~ 1.0). Mobile phase B (aqueous phase) was prepared by adding TFA (0.1%, v/v) to distilled water and mixed thoroughly. The final pH of the aqueous mobile phase was 2.

6.5. Method validation

Method validation was carried out based on the ICH guidelines (ICH, 2005). The main objective was to demonstrate that the developed RP-HPLC method was suitable for the quantitation of GLP-1 used in DPI formulations. Validation characteristics, such as specificity, linearity, range, accuracy, precision, limit of detection (LOD) and limit of quantitation (LOQ) as well as robustness and system suitability were assessed. All validation experiments were performed on the Agilent HPLC system (Section 6.4) under the optimal conditions (Table 28).

6.5.1. Stability

Stability of GLP-1 standard stock solutions, calibration curve solutions and GLP-1 acidic aqueous solutions used for spray drying (Section 6.7) was tested prior to the validation studies in order to get reliable results.

GLP-1 standard stock solution

Stability of GLP-1 standard stock solution was tested to determine the acceptable time duration for sample preparation and analysis before the degradation of GLP-1 would take place. Stability of GLP-1 standard stock solutions stored at room temperature ($22^{\circ}\text{C} \pm 3^{\circ}\text{C}$) and at 4°C was studied for up to 13 days and 18 days, respectively after preparation. Stability was determined by comparison to freshly prepared samples and expressed as a percentage with standard deviation (SDv) and relative standard deviation (RSD%).

GLP-1 calibration standard solutions for short-term storage

In order to run a series of sample sets (i.e., for impaction studies) consecutively at room temperature, stability of GLP-1 solutions in the concentration range of $3.0 \mu\text{g mL}^{-1}$ to $120.0 \mu\text{g mL}^{-1}$ stored at room temperature was assessed for a short-term storage period (24 hours). Stability was calculated as the ratio of the calculated concentration of GLP-1 in calibration standard solutions stored at room temperature for 24 hours to the concentration of freshly prepared GLP-1 calibration standard solutions and expressed as a percentage with SDv and RSD%.

GLP-1 acidic aqueous solutions

Stability of GLP-1 dissolved in acidic aqueous solutions (0.1% acetic acid with 1M NaOH, pH 3.5 or 0.1% acetic acid with 35% NH_4OH , pH 3.5) used for spray drying (Section 6.7) was tested to determine the acceptable time duration for sample preparation before the process of spray drying and the degradation of GLP-1 would take place.

6.5.2. Specificity

Specificity of the developed RP-HPLC method was assessed by analysing peaks of mobile phases (A: acetonitrile with 0.1% TFA and B: distilled water with 0.1% TFA), distilled water used for dissolving GLP-1 powders to prepare stock solutions, acidic aqueous solutions (0.1% acetic acid with 1M NaOH and 0.1% acetic acid with 35% NH₄OH) used for spray drying GLP-1 and each component of DPI formulations (mannitol and glycine) to see whether those peaks were well separated from the GLP-1 peak at a retention time of GLP-1 (3.8 mins) therefore no interference in the quantification of the drug. The peak of GLP-1 in the presence of formulation components was also measured to see if there were any changes appeared in the peak position of GLP-1.

6.5.3. Linearity and range

The linearity of the developed RP-HPLC method was evaluated by preparing the calibration curve for eleven concentrations of GLP-1 in the concentration range of 2.0 µg mL⁻¹ to 140.0 µg mL⁻¹. Calibration standard solution (20 µL) at each concentration was injected in triplicate. The calibration curve for GLP-1 was constructed by plotting the known concentration of GLP-1 on the x-axis against the area of the peak on the y-axis. The correlation coefficient (R²) and the regression equation (y intercept and slope of the regression line) were computed using Microsoft® Excel. The linearity was determined by regression analysis at significant level of p < 0.05 in Microsoft® Excel.

6.5.4. Accuracy

The accuracy of the developed RP-HPLC method was assessed by measuring five concentrations (low, middle, and high end of the calibration curve concentration range) in six replicates (each test sample solution per concentration was injected six times). The mean, SDv and RSD% were calculated for each concentration. The accuracy of the measurements was reported as the difference (relative error %) between the measured concentration (*mc*) and nominal concentration (*nc*) of GLP-1, using *Equation 3* in Chapter 3.5.3.

$$(mc-nc)/nc \times 100 \quad \text{Equation 3}$$

6.5.5. Precision

The intra-day precision of the developed RP-HPLC was assessed by calculating SDv and RSD% of the replicated measurements (five different concentrations, six replicates per concentration on the same day). The inter-day precision of the developed RP-HPLC method was assessed by replicating the same measurements under the same measurement conditions in the same laboratory each day for three days (six replicates per concentration). The SDv and RSD% were calculated per concentration (18 replicates per concentration over three days).

6.5.6. Limit of detection and limit of quantitation

The LOD (the lowest amount of GLP-1 can be detected but not necessarily quantitated, *Equation 4*) and LOQ (the lowest amount of GLP-1 quantitated with suitable accuracy and precision, *Equation 5*) were calculated based on the calibration curve method using the standard deviation of the response (standard deviation of y-intercepts) and slope of the calibration curve with the ICH guidelines equations (ICH, 2005). Regression analysis in Microsoft® Excel was performed at the 95% confidence level to calculate the standard deviation of the response and the slope.

$$LOD = 3.3 * \sigma / S \quad \text{Equation 4}$$

$$LOQ = 10 * \sigma / S \quad \text{Equation 5}$$

where σ is the standard deviation of the response and S is the slope of the calibration curve.

6.5.7. Robustness

Robustness of the developed RP-HPLC method was assessed by slightly changing parameters of the optimal settings, such as flow rate (flow rate: 1.0 mL min⁻¹ -> 0.9 mL min⁻¹) to see how this small change would affect the results (e.g., GLP-1 peak area where the area is directly related to the concentration). Also, a different HPLC equipment with the same manufacture and model (Agilent Technologies 1260 Infinity II) was tried under the optimal settings (Table 28).

6.5.8. System suitability

The parameters for system suitability study, such as retention time, peak area, height, peak asymmetry factor (*Equation 6*), tailing factor (*Equation 7*) and theoretical plates (*Equation 8*) were assessed by analysing six replicates of GLP-1 solution at a concentration of 120.0 $\mu\text{g mL}^{-1}$. The acceptable RSD% values of retention time, peak area and height were set to be less than or equal to 1.0% ($\leq 1.0\%$) and theoretical plates were greater than 2000 ($N > 2000$).

6.6. Carrier dry powders preparation by spray freeze drying

Mannitol-based carrier with the inclusion of 10% glycine (concentration % w/w based on mannitol content, 15 g) was prepared using spray freeze drying (stated in Chapter 4.6 and Chapter 5.4). The compositions of mannitol aqueous solution (15% w/v total solid content) for spray freeze drying were glycine (1.5 g) and mannitol (13.50 g) dissolved in distilled water (100 mL). Briefly, mannitol aqueous solution was sprayed over liquid nitrogen in a round bottom flask (250 mL) and freeze dried using BenchTop Pro with Omnitronics™ freeze dryer (SP Scientific, UK) for 48 hours at 55 $\mu\text{bar} \pm 5 \mu\text{bar}$ of pressure and condenser temperature of $-59^\circ\text{C} \pm 2^\circ\text{C}$. After 48 hours, the produced SFD carrier powders were sieved using an AS200 DIGIT CA sieve shaker (Retsch, Germany) with the 90 μm and 125 μm sieves (Fisher Brand Test Sieve, UK) for up to 10 minutes at 1.5 mm amplitude to obtain the particle size fraction of 90-125 μm . Collected SFD 10% glycine-mannitol powders (particle size fraction: 90-125 μm) were immediately transferred into tightly closed glass vials and stored in a desiccator over silica gel at room temperature ($22^\circ\text{C} \pm 3^\circ\text{C}$).

6.7. GLP-1 dry powders preparation by spray drying

GLP-1 dry powders intended for inhalation were prepared by spray drying based on the method employed for spray drying insulin (Chapter 5.5) which was based on the method of spray drying insulin reported by Balducci *et al.* (2014) with minor modifications. Briefly, GLP-1 (2 mg mL^{-1}) was dissolved in acidic aqueous solution (pH 3.5) composed of acetic acid (0.1% v/v) and sodium hydroxide (1M, NaOH) or acetic acid (0.1% v/v) and 35% ammonium hydroxide (NH_4OH) at room temperature. The compositions of acidic feed solutions for spray drying are listed in Table 29. GLP-1 aqueous solution (2 mg mL^{-1}) was spray dried using a Mini Spray Dryer B-290 (Büchi, Switzerland) under standardised processing parameters: 240 mL hr^{-1} feeding rate, 600 L hr^{-1} spray flow rate with

compressed air, 98% aspirator speed setting, inlet temperature at 119°C and outlet temperature at 60°C ± 2°C. Collected SD GLP-1 dry powders (SDGLP(NaOH) and SDGLP(NH₄OH)) produced from two different acidic aqueous solutions (acetic acid with 1M NaOH or acetic acid with 35% NH₄OH) were immediately packed into tightly closed glass vials and desiccated over silica gel at room temperature (22°C ± 3°C).

Table 29: Compositions of acidic aqueous solutions used to prepare spray dried (SD) GLP-1 dry powders. SDGLP(NaOH): SD GLP-1 powder prepared from acetic acid with 1M sodium hydroxide (NaOH), SDGLP(NH₄OH): SD GLP-1 powder prepared from acetic acid with 35% ammonium hydroxide (NH₄OH).

SD GLP-1 carrier free formulation	GLP-1 (mg)	Acetic acid (μL)	1M NaOH (μL)	35% NH ₄ OH (μL)	Total in distilled water (mL)	GLP-1 concentration (mg mL ⁻¹)
SDGLP(NaOH)	100	50	50	0	50	2
SDGLP(NH ₄ OH)	200	100	0	18	100	2

6.8. Preparation of GLP-1 dry powder inhaler formulations

Carrier-based DPI formulations (100 mg total) were prepared by blending SD GLP-1 powder (SDGLP(NH₄OH), 10 mg) produced from acidic feed solution composed of 0.1% acetic acid and 35% NH₄OH with SFD 10% glycine-mannitol carrier (90 mg) or raw mannitol carrier (90 mg) in ratio of 1:9 (drug : carrier) in a plastic container (2 x 9 cm) using a low shear blender of Turbula® system Schatz (WAB, Switzerland) at a constant speed of 46 rpm for 30 minutes. The powder blends (SD GLP-1 and carrier) were stored in a desiccator over silica gel at room temperature (22°C ± 3°C) prior to the impaction study (Section 6.11).

In this study, two carrier free DPI formulations (SDGLP(NaOH): SD GLP-1 powder produced from acetic acid with 1M NaOH and SDGLP(NH₄OH): SD GLP-1 powder produced from acetic acid with 35% NH₄OH) and two carrier-based DPI formulations (SDG10GMB: SDGLP(NH₄OH) blended with SFD 10% glycine-mannitol carrier and SDGRMB: SDGLP(NH₄OH) blended with raw mannitol carrier) were prepared (Table 30). These four DPI formulations were used for the *in vitro* impaction study (Section 6.11).

Table 30: Carrier free dry powder inhaler (DPI) formulations: SDGLP(NaOH): spray dried (SD) GLP-1 powder produced from acetic acid with 1M NaOH and SDGLP(NH₄OH): SD GLP-1 powder produced from acetic acid with 35% NH₄OH. Carrier-based DPI formulations: SDG10GMB: SDGLP(NH₄OH) blended with spray freeze dried (SFD) 10% glycine-mannitol carrier and SDGRMB: SDGLP(NH₄OH) blended with raw mannitol carrier.

DPI formulation		Formulation Component	
		Drug	Carrier
Carrier free	SDGLP(NaOH)	SD GLP-1	-
	SDGLP(NH ₄ OH)	SD GLP-1	-
Carrier-based	SDG10GMB	SDGLP(NH ₄ OH)	SFD 10% glycine-mannitol (engineered carrier)
	SDGRMB	SDGLP(NH ₄ OH)	Raw mannitol (non-engineered carrier)

6.9. Physicochemical characterisation

SFD 10% glycine-mannitol carrier powder prepared (Section 6.6) were previously characterised by Scanning Electron Microscopy (Chapter 4.13.3.1), laser diffraction (Chapter 4.13.3.2), Differential Scanning Calorimetry (Chapter 4.13.3.3), Thermogravimetric Analysis (Chapter 4.13.3.4) and X-ray diffraction (Chapter 4.13.3.5) and the results were discussed in Chapter 4.13.3.

Prior to the impaction study (Section 6.11), raw GLP-1 dry powder as received and SD GLP-1 dry powders for inhalation (Section 6.7) were characterised in terms of morphology including size (Section 6.9.1), thermal behaviour (Section 6.9.2), and moisture content (Section 6.9.3).

6.9.1. Scanning electron microscopy

Morphologies along with particle size of raw GLP-1, SD GLP-1 powders (SDGLP(NaOH) and SDGLP(NH₄OH)) prepared from two different acidic aqueous solutions (acetic acid with 1M NaOH and acetic acid with 35% NH₄OH), SFD 10% glycine-mannitol (sieved 90-125 µm) and raw mannitol (sieved 90-125 µm) powders were characterised by Scanning Electron Microscopy (SEM, ZEISS EVO®50, UK) at an acceleration voltage of 10-25 kV. Double-sided cohesive carbon tabs were adhered to aluminium stubs and all dry powder samples were placed onto the carbon tabs. Any excess powder samples were tapped off the tabs. These samples were then coated with a palladium/gold alloy using a SC7640 Sputter Coater (Polaron, UK) under argon gas for 2 minutes. Multiple images of coated samples were captured for each sample. SEM images of carrier-based DPI

formulations (SDG10GMB: SDGLP(NH₄OH) blended with SFD 10% glycine-mannitol carrier and SDGRMB: SDGLP(NH₄OH) blended with raw mannitol carrier, Section 6.8) were also captured for the visual observation of the blends (Blend homogeneity assessment, Section 6.10).

6.9.2. Differential scanning calorimetry

Thermal analysis of raw GLP-1 and SD GLP-1 powders (SDGLP(NaOH) and SDGLP(NH₄OH)) was performed using a DSC822e Differential Scanning Calorimetry (DSC, Mettler Toledo, Switzerland) under nitrogen gas (50 mL min⁻¹) in the temperature range from 25°C to 400°C at a heating rate of 10°C min⁻¹. All dry powder samples were placed in aluminium crucibles (40 µL) and sealed with a pierced lid on. The dry powder samples loaded pan and empty reference pan were placed on the DSC sample holder. The DSC curves were recorded at 22°C using STARe Software version 8.10 (Mettler Toledo, UK).

6.9.3. Thermogravimetric analysis

Thermogravimetric Analysis (TGA) for raw GLP-1 and SD GLP-1 powders (SDGLP(NaOH) and SDGLP(NH₄OH)) was performed to measure moisture content using a METTLER TOLEDO® TGA/DSC1 STARe System (Mettler Toledo, Switzerland) along with DSC analysis (Section 6.9.2). All dry powder samples were loaded onto aluminium oxide crucibles (70 µL) and heated under nitrogen gas (50 mL min⁻¹) in the temperature range from 25°C to 400°C at a heating rate of 10°C min⁻¹. The TGA curves were recorded at 22°C using STARe Software version 8.10 (Mettler Toledo, UK).

6.10. Blend homogeneity assessment

After blending, the homogeneity of two carrier-based DPI formulations (SDG10GMB and SDGRMB) was assessed by quantifying the content of GLP-1 and mannitol using the developed RP-HPLC method (Section 6.14.1 and 6.14.2) and proton quantitative nuclear magnetic resonance (¹H qNMR) method (Chapter 3) (Babenko et al., 2019), respectively. Blend samples (4 mg total blend; 0.4 mg of SD GLP-1 and 3.6 mg of SFD carrier) were taken from three different positions (top, middle, and bottom) of each DPI formulation in the blending container and dissolved in distilled water (4 mL, theoretical GLP-1 concentration: 100 µg mL⁻¹). GLP-1 content uniformity was determined as the ratio of the calculated concentration of GLP-1 contained in the blend sample to the theoretical

concentration of GLP-1 and expressed as a percentage. The coefficient of variation (%CV or referred to as RSD%) was used as a degree of GLP-1 content homogeneity. High %CV values indicate a low drug content homogeneity (Kaialy, Nokhodchi, 2016) and drug content is considered uniform when %CV is below 6% (Kaialy, Nokhodchi, 2015). Simultaneously, mannitol content uniformity was determined as the ratio of the measured concentration of mannitol contained in the blend sample to the theoretical concentration of mannitol and expressed as a percentage. All NMR data were processed using TopSpin™ software 4.1.0 (Bruker BioSpin GmbH, Germany).

6.11. Impaction study

The aerodynamic performance of four DPI formulations (SDGLP(NaOH), SDGLP(NH₄OH), SDG10GMB, and SDGRMB) was assessed *in vitro* using a next generation impactor (NGI, Copley Scientific, UK) with the Alberta Idealised Throat 28028 (AIT, Copley Scientific, UK). The NGI was equipped with a Critical Flow Controller (TPK 2000, Copley Scientific, UK) connected to a Vacuum pump (HPC5, Copley Scientific, UK). The flow rate was set at 30 L min⁻¹ with the test airflow duration of 3 sec using the Critical Flow Controller Model TPK 2000 (Copley Scientific, UK) and a Flow Meter Model DFM2000 (Copley Scientific, UK). The critical flow (P3/P2 ratio ≤ 0.5, flow rate stability) was achieved. A leak test was performed on the NGI prior to each use. Handihaler® (Boehringer Ingelheim, Germany, a single capsule inhalation device with high resistance) was used as a DPI to deliver the content of SD GLP-1 powders filled (total fill mass per capsule: 2.0-2.3 mg for SD GLP-1 alone and 20 mg ± 1 mg for carrier-based DPI formulations) in the HPMC size 3 capsules (CAPSUGEL®, UK) during the impaction studies. In carrier-based DPI formulations the drug content was limited to 2 mg in 20 mg total mass of adhesive mixtures (drug: carrier = 1:9) per capsule. SD GLP-1 powders deposited on AIT and all NGI stages (stages 1-7 and micro orifice collector, MOC) were collected using distilled water (2 mL) and immediately quantified by the developed RP-HPLC method (Section 6.14.1 and 6.14.2). SD GLP-1 powders deposited on 7 stages in the NGI were based on the aerodynamic cut-off diameters of 0.541 µm (stage 7), 0.834 µm (stage 6), 1.357 µm (stage 5), 2.299 µm (stage 4), 3.988 µm (stage 3), 6.395 µm (stage 2), and 11.719 µm (stage 1) at flow rate of 30 L min⁻¹. All NGI studies were performed in triplicate at room temperature. The aerosolisation performance of SD GLP-1 powders was assessed using Microsoft® Excel and Copley Inhaler Testing Data Analysis Software (CITDAS) Version 3.10 Wibu (Copley Scientific, UK) to determine GLP-1 delivered dose, fine particle fraction (FPF), mass median aerodynamic diameter (MMAD) and geometric standard deviation (GSD). The delivered dose (%) was determined as the ratio of the total

SD GLP-1 deposition on AIT and all the NGI stages excluding the deposition in the inhaler device and capsules to the total SD GLP-1 dose delivered from the device including the deposition in the inhaler device and capsules (i.e., the mass of the GLP-1 powders filled into the capsule). Therefore, drug loss (%) was determined as follows: $100 - \text{delivered dose (\%)}$. The FPF defined as the mass fraction of the delivered drug dose with less than or equal to $5.0 \mu\text{m}$ aerodynamic diameter was used to characterise the aerosolisation performance of DPI formulations.

6.12. GLP-1 stability study

Preliminary stability study on SD GLP-1 powders before and after spray drying and during storage (room temperature, $22^\circ\text{C} \pm 3^\circ\text{C}$ and RH: <4% in a desiccator measured by Ebro Data logger, EBI 20-IF, Germany) for up to 7 months was performed using Fourier-transform infrared spectroscopy (FTIR) and the developed RP-HPLC method (Section 6.14.1 and 6.14.2). Structural stability of SD GLP-1 powders (SDGLP(NaOH) and SDGLP(NH₄OH)) during storage was also studied using FTIR. The FTIR spectra of raw GLP-1 and SD GLP-1 powders were acquired on a Nicolet™ iS5 FTIR spectrometer (Thermo Fisher Scientific, UK) in the range of $400\text{--}4000 \text{ cm}^{-1}$ by accumulating 16 scans with a resolution of 4 cm^{-1} at 22°C . The FTIR spectra were obtained using OMNIC™ driver version 8.2 software (Thermo Scientific, UK). The developed RP-HPLC method was used to quantify the content of GLP-1 in SD GLP-1 powders. The stability based on the GLP-1 content in SD GLP-1 powders is the ratio of GLP-1 detected content (area) at each storage time to the detected content (area) of raw GLP-1, which is the initial powder (as-received powder) used for the GLP-1 calibration curve validated based on the ICH guideline.

6.13. Statistical analysis

Statistical analysis was performed using SPSS® statistics version 26.0 (IBM, UK) along with Microsoft® Excel at significant level of $p < 0.05$. One-way ANOVA (Analysis of Variance) and t-test were used to compare the mean results for data (method development and validation, and drug content uniformity and NGI study for all DPI formulations). If the ANOVA was itself significant Post Hoc test (Tukey honestly significant difference (HSD) test) was further performed to determine which groups were different from each other (Ennos, 2012).

6.14. Results and discussion

6.14.1. Method development

The optimal chromatography conditions for GLP-1 quantification were found as follows and presented in Table 28 (Section 6.4). The mobile phase was a 41:59 (A:B, %v/v) mixture of acetonitrile with 0.1% trifluoroacetic acid (TFA) (organic phase A) and distilled water with 0.1% TFA (aqueous phase B) at a flow rate of 1.0 mL min⁻¹. To understand the role of TFA in mobile phase A, the composition of mobile phase A without the addition of 0.1% TFA was tried. Changing the composition of mobile phase A from acetonitrile with 0.1% TFA to acetonitrile alone (no 0.1% TFA) generated the same results (e.g., area and height: t-test, $p > 0.05$) with 98-100% recovery (within the acceptable range of 80-120%) and below 1.4 RSD% values (RSD%: 0.92-1.40%) (Table 31). However, mobile phase A in the absence of 0.1% TFA resulted in slightly late GLP-1 elution with fluctuated retention time and height (retention time: 4.01-4.07 min with RSD% 2.98-3.51, height RSD%: 3.90-7.09) when compared to the peak of GLP-1 in acetonitrile with 0.1% TFA (retention time: 3.84 min with RSD% 0.20-0.27, height RSD%: 0.48-0.64) (Figure 58 and Table 31). Therefore, it was found to be necessary to add 0.1% TFA in mobile phase A to aid stable GLP-1 elution.

The stationary phase selected was the C8 column. The RP-HPLC method with the use of C8 and C18 columns produced the same area of the GLP-1 peak (area: t-test, $p > 0.05$) with 100-102% recovery, however, the GLP-1 peak generated by C18 column was less symmetry (A_s : 1.14-1.18) and more tailing (T_f : 1.17-1.21) when compared to the peak with C8 column (A_s : 1.04-1.06, and T_f : 1.05-1.06) (asymmetry and tailing factors: t-test, $p < 0.05$) (Table 32). The elution mode was isocratic. A detection wavelength was set to 215 nm over 220 nm due to a better peak of GLP-1 obtained with UV 215 nm wavelength (e.g., area: 18092>15778, height: 1710>1496, Figure 59). Injection volume was 20 μ L. These conditions provided a relatively short retention time of GLP-1 (average 3.81 ± 0.004 min) with symmetry peak (A_s : 1.06 ± 0.03) and no tailing (T_f : 1.08 ± 0.04) and high efficiency of chromatography peak (N : 3061.79) (see Figure 63 for HPLC chromatograms for the GLP-1 calibration curve). The developed RP-HPLC method was used for blend homogeneity assessment (Section 6.10 and 6.14.4), impaction studies (Section 6.11 and 6.14.5) and GLP-1 stability study (Section 6.12 and 6.14.6).

Table 31: Recovery, retention time, height, and asymmetry and tailing factors for GLP-1 solutions ($80 \mu\text{g mL}^{-1}$ and $120 \mu\text{g mL}^{-1}$) using two different compositions of mobile phase A: acetonitrile with 0.1% trifluoroacetic acid (TFA) and acetonitrile alone (Data presented as mean \pm standard deviation). RSD: relative standard deviation.

Mobile phase A composition	GLP-1 concentration ($\mu\text{g mL}^{-1}$)	Recovery		Retention time		Height		Asymmetry factor	Tailing factor
		Recovery (%)	RSD (%)	Retention time (min)	RSD (%)	Height (mAU)	RSD (%)		
Acetonitrile with 0.1% TFA	120.0	99.84 ± 1.39 (n=6)	1.40	3.84 ± 0.01	0.27	193.32 ± 1.23	0.64	1.06 ± 0.005	1.06 ± 0.005
	80.0	100.33 ± 1.32 (n=6)	1.32	3.84 ± 0.01	0.20	130.62 ± 0.63	0.48	1.04 ± 0.009	1.05 ± 0.007
Acetonitrile alone (No 0.1% TFA)	120.0	98.59 ± 0.91 (n=5)	0.92	4.01 ± 0.12	2.98	177.77 ± 6.93	3.90	1.09 ± 0.01	1.10 ± 0.01
	80.0	99.56 ± 1.14 (n=4)	1.15	4.07 ± 0.14	3.51	117.78 ± 8.34	7.09	1.07 ± 0.02	1.08 ± 0.02



Figure 58: HPLC chromatograms for GLP-1 dissolved in distilled water (GLP-1 concentration A: $80 \mu\text{g mL}^{-1}$ and B: $120 \mu\text{g mL}^{-1}$) with two different compositions of mobile phase A: acetonitrile with 0.1% TFA (red) or acetonitrile alone (blue). (Area and height: t-test, $p > 0.05$). Vertical axis represents area (mAU), and horizontal axis represents retention time (min).

Table 32: Comparison of asymmetry and tailing factors for GLP-1 ($80 \mu\text{g mL}^{-1}$ and $120 \mu\text{g mL}^{-1}$) between two different columns: C8 ($4.6 \times 250 \text{ mm}$, $5 \mu\text{m}$) and C18 ($4.6 \times 250 \text{ mm}$, $4 \mu\text{m}$) (Data presented as mean \pm standard deviation). RSD: relative standard deviation.

Column	Nominal GLP-1 concentration ($\mu\text{g mL}^{-1}$)	Mean measured GLP-1 concentration ($\mu\text{g mL}^{-1}$)	Recovery (%)	RSD (%)	Asymmetry factor	Tailing factor
C8 $4.6 \times 250 \text{ mm}$, $5 \mu\text{m}$ (n=6)	120	121.87	101.56 ± 0.84	0.83	1.06 ± 0.01	1.06 ± 0.01
	80	80.36	100.45 ± 1.65	1.65	1.04 ± 0.005	1.05 ± 0.01
C18 $4.6 \times 250 \text{ mm}$, $4 \mu\text{m}$ (n=5)	120	121.45	101.21 ± 0.57	0.56	1.18 ± 0.02	1.21 ± 0.01
	80	81.03	101.29 ± 1.39	1.37	1.14 ± 0.01	1.17 ± 0.01

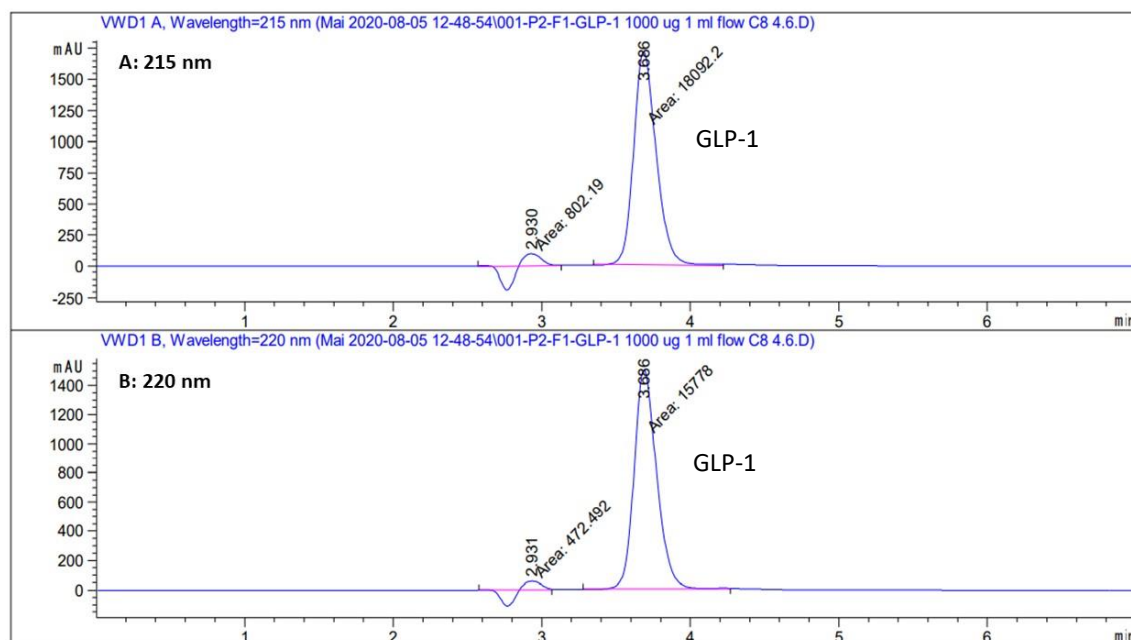


Figure 59: HPLC chromatograms for GLP-1 stock solution (GLP-1 concentration: $1020 \mu\text{g mL}^{-1}$) at a retention time of 3.7 mins with two detection wavelengths: 215 nm (A) and 220 nm (B). Vertical axis represents area (mAU), and horizontal axis represents retention time (min).

6.14.2. Method validation

6.14.2.1. Stability

GLP-1 standard stock solution

GLP-1 stock solution was tested to be stable for up to 7-9 days when stored at room temperature and for up to 18 days at least when stored at 4°C (Table 33). However, freshly made stock solutions were used for all experiments throughout the study. It was observed that GLP-1 stock solution stored at room temperature for 13 days generated few extra small peaks before and after the GLP-1 peak at a retention time of 3.8 minutes and the height of the GLP-1 peak became short (Figure 60).

Table 33: Stability study on GLP-1 standard stock solution (1 mg mL⁻¹) stored at room temperature for up to 13 days and at 4°C for up to 18 days (Data presented as mean (%) ± standard deviation, n=3).

Storage duration	Room temperature	Storage duration	4°C
1 day	100.21 ± 0.57	1 day	99.58 ± 0.27
3 days	101.11 ± 1.40	2 days	99.59 ± 0.62
4 days	100.09 ± 0.62	5 days	100.79 ± 1.05
7 days	98.54 ± 0.98	14 days	99.97 ± 0.33
9 days	90.21 ± 1.14	18 days	100.62 ± 0.70
10 days	77.10 ± 0.73	-	-
13 days	13.99 ± 0.11	-	-

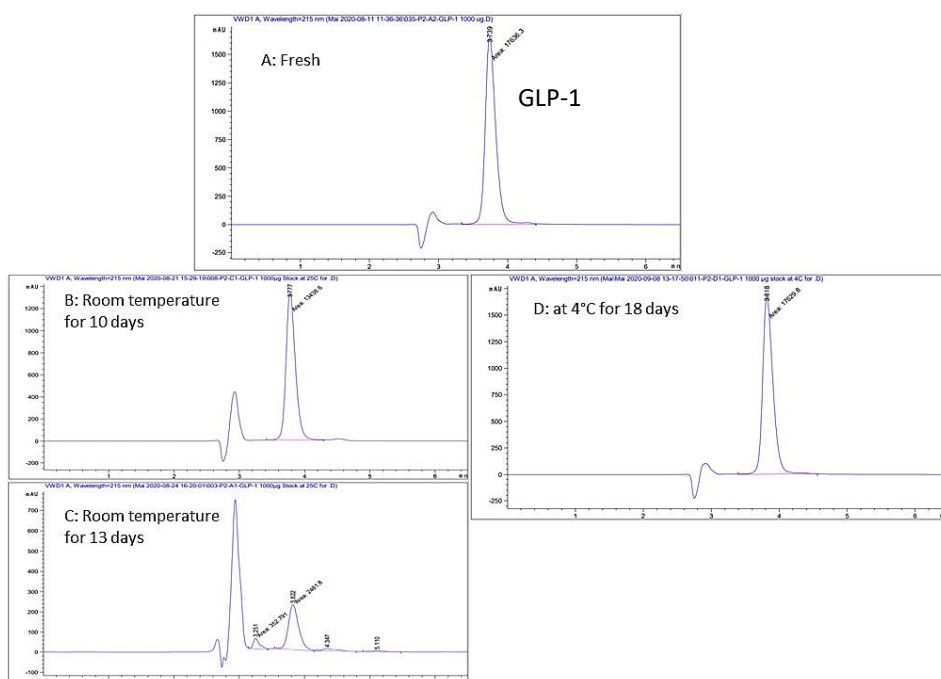


Figure 60: HPLC chromatograms for freshly prepared GLP-1 stock solution (GLP-1 concentration: 1 mg mL⁻¹) (A), GLP-1 stock solution stored at room temperature for 10 days (B) and 13 days (C) and stored at 4°C for 18 days (D). GLP-1 retention time: around 3.8 minutes.

Vertical axis represents area (mAU), and horizontal axis represents retention time (min).

GLP-1 calibration standard solutions for short-term storage

GLP-1 calibration standard solutions in the concentration range of 3.0 µg mL⁻¹ to 120.0 µg mL⁻¹ which is above LOQ (2.39 µg mL⁻¹, Table 37 in Section 6.14.2.5) were relatively stable (>80% stability) for 24 hours when stored at room temperature (Table 34). However, it is recommended that freshly made solutions should be run immediately after sample preparation (within 24 hours) due to instability of the solutions in the lower concentrations (e.g., 3.0 µg mL⁻¹).

Table 34: Stability study on short-term storage of GLP-1 calibration standard solutions stored at room temperature for 24 hours (Data presented as mean ± standard deviation, n=3).

Nominal GLP-1 concentration (µg mL ⁻¹)	Measured GLP-1 concentration (µg mL ⁻¹)	Stability (%)
120.0	120.84 ± 0.67	100.70 ± 0.56
80.0	81.02 ± 0.13	101.27 ± 0.17
40.0	39.37 ± 0.28	98.43 ± 0.70
20.0	17.73 ± 0.50	88.67 ± 2.49

10.0	9.27 ± 0.49	92.69 ± 4.91
5.0	4.49 ± 0.09	89.73 ± 1.74
3.0	2.50 ± 0.11	83.48 ± 3.67

GLP-1 acidic aqueous solutions

GLP-1 acidic aqueous solutions (0.1% acetic acid with 1M NaOH or 0.1% acetic acid with 35% NH₄OH, pH 3.5) for spray drying (Section 6.7) were tested to be stable for up to at least 7 days when stored both at room temperature and at 4°C (Table 35). However, freshly made solutions were used for spray drying.

Table 35: Stability study on GLP-1 (1 mg mL⁻¹) dissolved in acidic aqueous solution (0.1% acetic acid with 1M NaOH, pH 3.5 or 0.1% acetic acid with 35% NH₄OH, pH 3.5) stored at room temperature and at 4°C for up to 7 days (Data presented as mean (%) ± standard deviation, n=3).

GLP-1 dissolved in 0.1% acetic acid with 1M NaOH (1 mg mL ⁻¹)	Storage duration	4 hours	1 day	2 days	3 days	7 days
	Room temperature	100.68 ± 1.30	100.46 ± 0.80	100.35 ± 1.14	100.41 ± 1.15	100.26 ± 1.46
4 °C	-	100.38 ± 1.42	100.78 ± 0.96	100.80 ± 0.68	100.82 ± 1.38	
GLP-1 dissolved in 0.1% acetic acid with 35% NH ₄ OH (1 mg mL ⁻¹)	Storage duration	3 hours	1 day	2 days	3 days	7 days
	Room temperature	100.05 ± 0.64	99.80 ± 0.61	98.69 ± 0.42	98.73 ± 0.58	98.24 ± 0.87
4 °C	-	100.30 ± 0.64	99.27 ± 0.58	99.38 ± 0.49	98.77 ± 0.61	

6.14.2.2. Specificity

All the peaks of mobile phases (A: 41% v/v, acetonitrile with 0.1% TFA and B: 59% v/v, distilled water with 0.1% TFA), acidic aqueous solutions (0.1% acetic acid with 1M NaOH and 0.1% acetic acid with 35% NH₄OH, pH 3.5) and each component of GLP-1 DPI formulations (mannitol and glycine) were well separated from the peak of GLP-1 at the retention time of around 3.8 mins (Figure 61). There were no changes observed in the peak position of GLP-1 when measured GLP-1 in the presence of formulation components (mannitol and glycine) (Figure 61F). These indicate that mobile phases and the excipients used in DPI formulations did not interfere in the analysis of GLP-1 quantification.

Therefore, the developed RP-HPLC method was found to be specific to measure GLP-1 in DPI formulation samples.

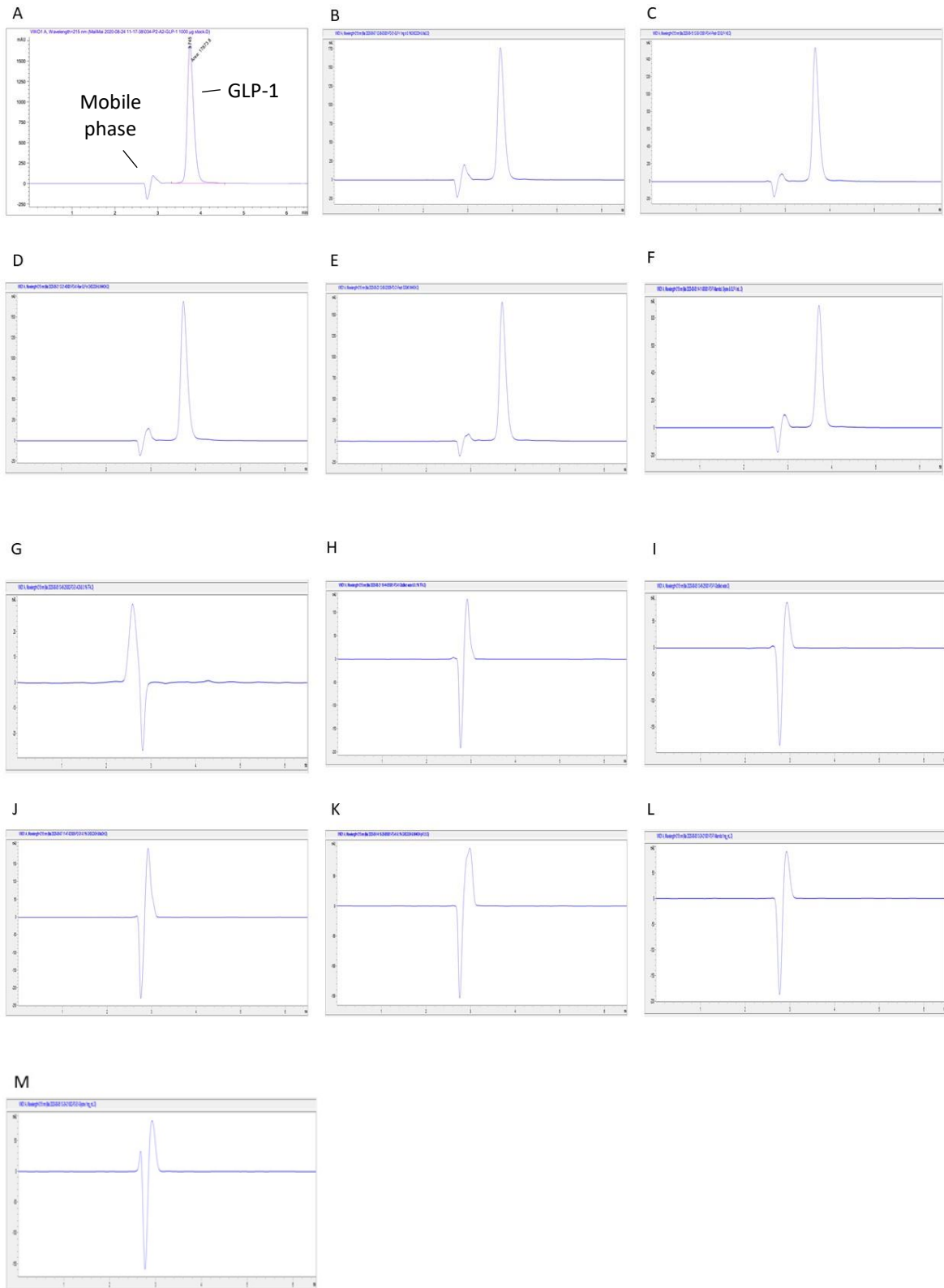


Figure 61: HPLC chromatograms for mobile phases (41:59 (%v/v) mixture of acetonitrile with 0.1% trifluoroacetic acid (TFA) and distilled water with 0.1% TFA) at a retention time of 2-3 mins and raw GLP-1 (1 mg mL^{-1}) dissolved in distilled water at a retention time of 3.8 mins (A), raw GLP-1 (1 mg mL^{-1}) dissolved in 0.1% acetic acid with 1M NaOH aqueous solution (pH 3.5) (B), spray dried (SD) GLP-1 powder prepared from 0.1% acetic acid with 1M NaOH dissolved in distilled water (0.9 mg mL^{-1}) (C), raw GLP-1 (1 mg mL^{-1}) dissolved in 0.1% acetic acid with 35% NH_4OH aqueous solution (pH 3.5) (D), SD GLP-1 powder prepared from 0.1% acetic acid with 35% NH_4OH dissolved in distilled water (1 mg mL^{-1}) (E), raw GLP-1 ($600 \text{ } \mu\text{g mL}^{-1}$) dissolved in a mixture of glycine ($300 \text{ } \mu\text{g mL}^{-1}$) and mannitol ($300 \text{ } \mu\text{g mL}^{-1}$) aqueous solution (F), mobile phase A: acetonitrile with 0.1% TFA (G), mobile phase B: distilled water with 0.1% TFA (H), distilled water (I), 0.1% acetic acid with 1M NaOH aqueous solution (pH 3.5) (J), 0.1% acetic acid with 35% NH_4OH aqueous solution (pH 3.5) (K), raw mannitol (1 mg mL^{-1}) dissolved in distilled water (L), raw glycine (1 mg mL^{-1}) dissolved in distilled water (M). Vertical axis represents area (mAU), and horizontal axis represents retention time (min).

6.14.2.3. Linearity and range

The calibration curve constructed for GLP-1 was linear with R^2 value of 0.9999 in the concentration range of $2.0 \text{ } \mu\text{g mL}^{-1}$ to $140.0 \text{ } \mu\text{g mL}^{-1}$ (Figure 62). HPLC chromatograms for GLP-1 calibration curve presented in Figure 63 show that the area of the peak is proportional to the concentration within the concentration range selected.

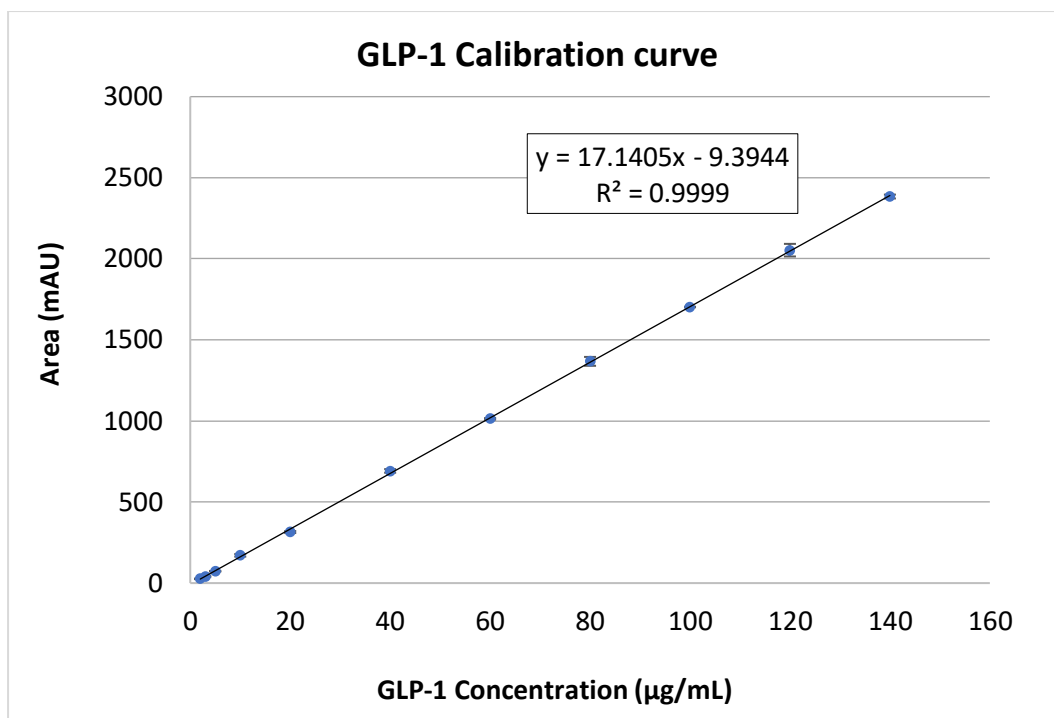


Figure 62: Calibration curve for GLP-1 in the concentration range of 2.0 µg mL⁻¹ to 140.0 µg mL⁻¹ (n=3).

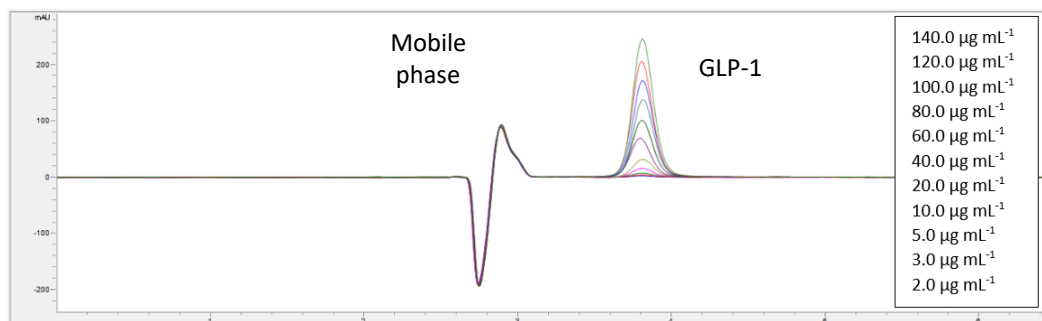


Figure 63: HPLC chromatograms for GLP-1 calibration curve in the concentration range from 2.0 µg (bottom) to 140.0 µg (top) mL⁻¹. Average retention time: 3.81 ± 0.004 min, asymmetry factor: 1.06 ± 0.03, tailing factor: 1.08 ± 0.04 and efficiency of chromatography: 3061.79. Vertical axis represents area (mAU), and horizontal axis represents retention time (min).

6.14.2.4. Accuracy and precision

The accuracy and precision of the RP-HPLC method was assessed at five different concentrations. Table 36 shows that relative error (%) at five different concentrations were all below 5.0% (0.22%-4.65%). The SDv and RSD% were all below 1.3 (SDv: 0.21-1.23) and below 4.5 (RSD%: 0.67-4.50),

respectively. These results demonstrated that the RP-HPLC method produced accurate (relative error%: <5.0) and precise data with high repeatability (RSD%: <4.5) over the concentration range used.

Table 36: Accuracy (relative error %), intra-day precision (six replicates per concentration on the same day) and inter-day precision (18 replicates per concentration over 3 days) at five different concentrations for RP-HPLC method. Data presented as mean with standard deviation (SDv). RSD: relative standard deviation.

Nominal GLP-1 concentration ($\mu\text{g mL}^{-1}$)	Intra-day precision (n=6)			Inter-day precision (n=6x3)		
	Mean measured GLP-1 concentration ($\mu\text{g mL}^{-1}$) \pm SDv	RSD (%)	Relative error (%)	Mean measured GLP-1 concentration ($\mu\text{g mL}^{-1}$) \pm SDv	RSD (%)	Relative error (%)
120.0	121.86 \pm 1.03	0.85	1.55	121.19 \pm 1.23	1.02	1.00
80.0	81.72 \pm 0.72	0.88	2.15	81.13 \pm 0.54	0.67	1.41
40.0	41.03 \pm 0.34	0.82	2.57	40.09 \pm 0.58	1.47	0.22
10.0	10.07 \pm 0.21	2.05	0.72	10.09 \pm 0.40	3.88	0.93
5.0	4.79 \pm 0.21	4.46	-4.27	4.77 \pm 0.21	4.50	-4.65

6.14.2.5. Limit of detection and limit of quantitation

The LOD and LOQ calculated for the calibration curve were $0.79 \mu\text{g mL}^{-1}$ and $2.39 \mu\text{g mL}^{-1}$, respectively (Table 37). This demonstrated that the concentration range of the calibration curve were within LOD, and GLP-1 was quantitative with suitable accuracy and precision above the LOQ level.

Table 37: Linear correlation coefficient (R^2), regression equation, limit of detection (LOD) and limit of quantitation (LOQ).

GLP-1 concentration range	Calibration curve regression equation	R^2	LOD ($\mu\text{g mL}^{-1}$)	LOQ ($\mu\text{g mL}^{-1}$)
2.0-140.0 $\mu\text{g mL}^{-1}$	$y = 17.1405x - 9.3944$	0.9999	0.7894	2.3921

6.14.2.6. Robustness

The robustness of the RP-HPLC method was assessed based on the values of recovery (%) with RSD% and the results are presented in Table 38. The change of flow rate from 1.0 mL min⁻¹ to 0.9 mL min⁻¹ resulted in slightly late GLP-1 elution (around 4.1-4.2 mins) when compared to the GLP-1 peak at flow rate of 1.0 mL min⁻¹ (Figure 64). However, the RP-HPLC method generated similar results (e.g., area and height: t-test, p>0.05) with 110% recovery (within the acceptable range of 80-120%) and RSD% value of below 1.0% (RSD%: 0.38-0.53%) (Table 38). The use of a different HPLC equipment under the optimal settings uninfluenced the measurement results (e.g., area and height: t-test, p>0.05) with 98-100% recovery (within the acceptable range of 80-120%) and RSD% of below 1.8 (Table 38 and Figure 65). This can be indicated that the RP-HPLC method is robust with changes of flow rate (from 1.0 mL min⁻¹ to 0.9 mL min⁻¹) and HPLC equipment (with the same manufacture and model).

Table 38: Results of robustness study. Data presented as mean. SDv: standard deviation, RSD: relative standard deviation.

Parameters	Nominal GLP-1 concentration (µg mL ⁻¹)	Mean measured GLP-1 concentration (µg mL ⁻¹)	Recovery (%)	SDv	RSD (%)
Flow rate: 0.9 mL min ⁻¹ (n=5)	120.0	132.11	110.10	0.42	0.38
	80.0	88.34	110.43	0.58	0.53
Different HPLC #5 equipment (n=6)	120.0	120.31	100.26	1.44	1.44
	80.0	79.67	99.59	0.97	0.98
	40.0	39.23	98.08	1.74	1.78

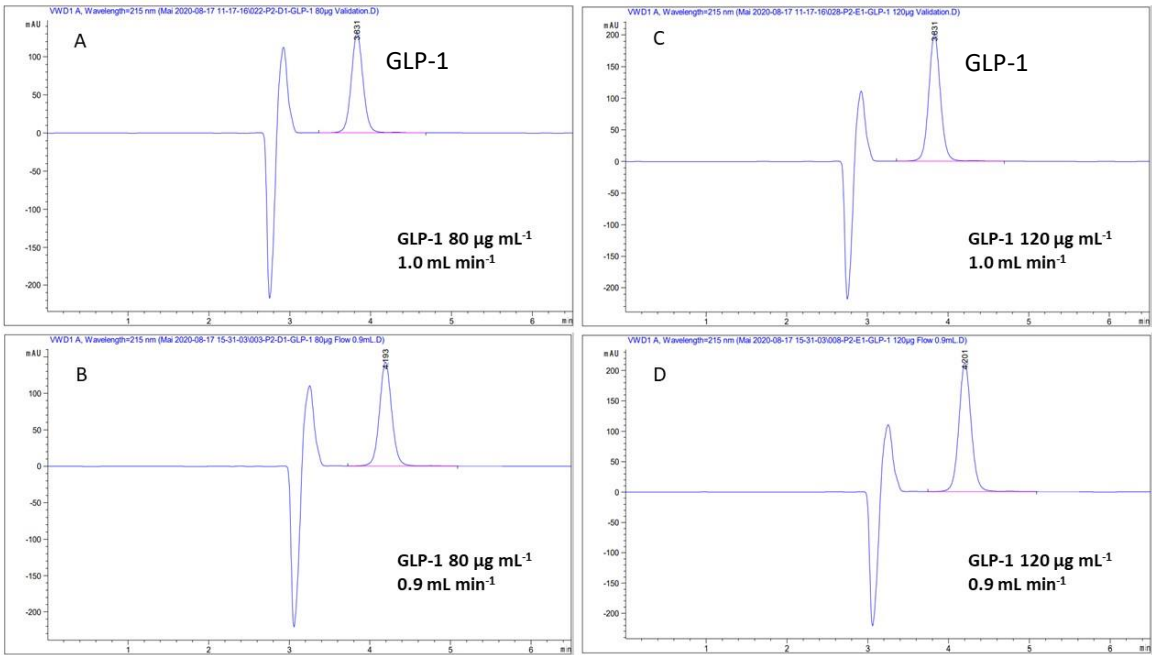


Figure 64: HPLC chromatograms for GLP-1 dissolved in distilled water (GLP-1 concentration: 80 µg mL⁻¹ and 120 µg mL⁻¹) with two different flow rates (1.0 mL min⁻¹ and 0.9 mL min⁻¹). A: 80 µg mL⁻¹ at 1.0 mL min⁻¹, B: 80 µg mL⁻¹ at 0.9 mL min⁻¹, C: 120 µg mL⁻¹ at 1.0 mL min⁻¹, and D: 120 µg mL⁻¹ at 0.9 mL min⁻¹. (Area and height: t-test, p>0.05).

Vertical axis represents area (mAU), and horizontal axis represents retention time (min).

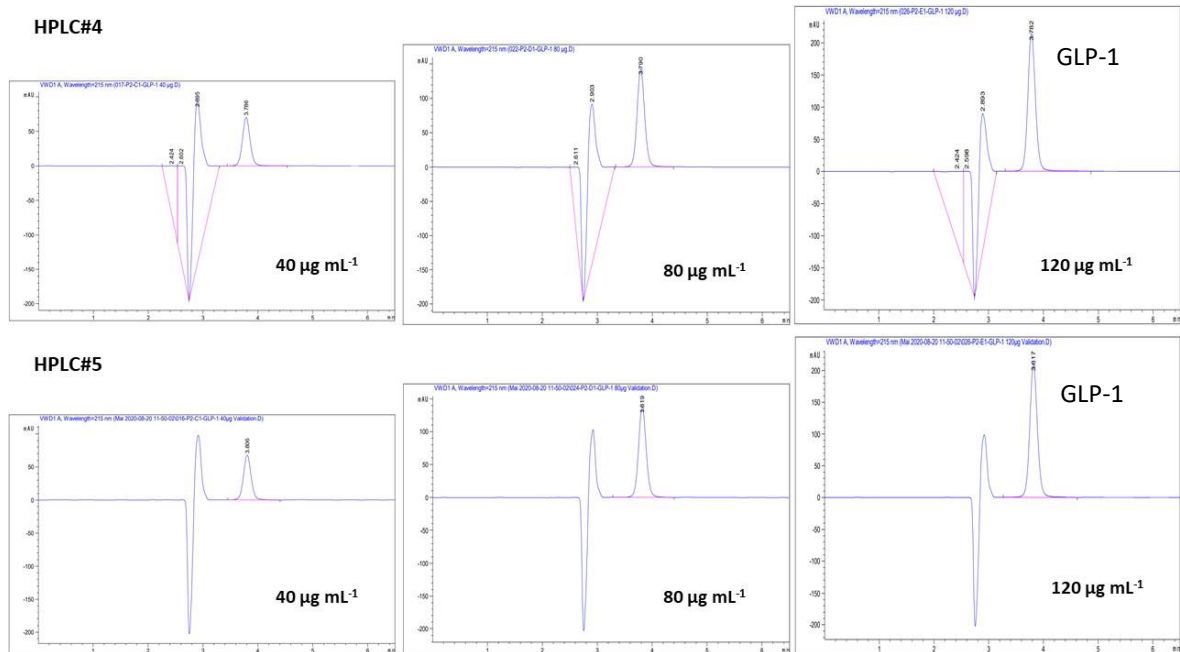


Figure 65: HPLC chromatograms for GLP-1 dissolved in distilled water (GLP-1 concentration: 40 µg mL⁻¹ (left), 80 µg mL⁻¹ (middle), 120 µg mL⁻¹ (right)) at a retention time of around 3.8 mins with two different HPLC systems (HPLC#4 and HPLC#5). (Area and height: t-test, p>0.05).

Vertical axis represents area (mAU), and horizontal axis represents retention time (min).

6.14.2.7. System suitability

All RSD% values of system suitability parameters (e.g., retention time, peak area, height, theoretical plates, asymmetry and tailing factor) were within 1.0% (RSD%: 0.08-1.01) and the efficiency of the column was above 2000 (N: 3537.71) (Table 39). The peak of GLP-1 was symmetry (As: 1.06) and not tailing (Tf: 1.07). This indicated that all the acceptable criteria for system suitability were met and all the results generated by the HPLC equipment were verified. Therefore, the developed method was suitable to use for blend homogeneity assessment (Section 6.14.4), impaction studies for GLP-1 pulmonary deposition *in vitro* (Section 6.14.5) and GLP-1 stability study (Section 6.14.6).

Table 39: Results of system suitability study (Data presented as mean, n=6). SDv: standard deviation, RSD: relative standard deviation.

GLP-1 concentration (80 µg mL ⁻¹)	System suitability parameter					
	Retention time (min)	Peak area (mAU)	Peak height (mAU)	Theoretical plates	Asymmetry factor	Tailing factor
Mean	3.78	1387.48	142.67	3537.71	1.06	1.07
SDv	0.0029	3.43	0.42	14.33	0.01	0.0097
RSD (%)	0.08	0.25	0.30	0.41	1.01	0.91

6.14.3. Physicochemical characterisation

6.14.3.1. Scanning electron microscopy

GLP-1 powders as received were lyophilised fluffy powders that exhibited the morphology of irregular particle shapes (e.g., flakes) with particle size ranging from 10 µm to 50 µm as observed under SEM (Figure 66A). Because the purchased GLP-1 powder product was not an inhalation grade (not within the suitable particle size range, aerodynamic diameter ≤ 5 µm for pulmonary delivery), spray drying was employed to reduce the particle size suitable for pulmonary drug deposition. The SEM images of SD GLP-1 powders produced from two acidic aqueous solutions; acetic acid with NaOH (Figure 66B) and acetic acid with NH₄OH (Figure 66C) both showed the particle size range of 1 µm to 5 µm, which is suitable for drug deposition in the lungs and similar morphologies of spherical

particles with dimples on the surface. Spray drying method demonstrated to reduce the particle size of GLP-1 powders in the suitable particle size range (1-5 μm) for pulmonary delivery also modified the morphology of the GLP-1 powders. The formation of the indented/dimpled surfaces could be associated with the drying process (e.g., rapid evaporation of the solvent upon drying). The observed morphologies of SD GLP-1 powders tend to be common as SD peptides/proteins (e.g., insulin, glycoprotein and immunoglobulin) reported in the literatures (Vehring, 2007, Bowey et al., 2013). It was observed that SD GLP-1 particles were agglomerated (Figure 66B,C) indicating cohesive particles. Such agglomerated particles are likely to have poor flowability (Peng et al., 2016). Therefore, SD GLP-1 powder (SDGLP(NH₄OH)) was mixed with SFD 10% glycine-mannitol carrier or raw mannitol carrier (both sieved, particle size fraction: 90-125 μm) to improve the efficiency of drug aerosolisation and drug delivery. The SEM images of SFD 10% glycine-mannitol carrier (Figure 67A) and raw mannitol carrier (Figure 68A) both showed the suitable carrier size range of 60 μm to 200 μm (50-200 μm as described in Introduction 6.2). However, different morphologies were observed between them. SFD 10% glycine-mannitol carrier (Figure 67A-B) showed spherical and highly porous particles whereas raw mannitol carrier (Figure 68A-B) showed elongated particles (non-porous). The surface properties such as roughness were also different in both carriers. SFD mannitol-based carrier had rough and wavy surface/uneven surface with small and shallow indentations and some open pores on the surfaces (Figure 67A-B yellow box). On the other hand, raw mannitol carrier exhibited rather smooth surface with larger indentations (an increase in the indentation depth and length) (Figure 68A-B). This presents that spray freeze drying method demonstrated to modify the surface properties (e.g., morphology and roughness) of raw mannitol and produced porous (and fluffy) powders compared to raw mannitol powders.

Following the blending process, the SEM images of carrier-based DPI formulations (SDG10GMB and SDGRMB) showed that SD GLP-1 particles (SDGLP(NH₄OH)) were adhered to both carriers (Figure 67C-D and Figure 68C-D). The particles of SD GLP-1 and carriers can be clearly distinguished in the SEM images of the blends (Figure 67C-D and Figure 68C-D) as SD GLP-1 particles presented dimpled particles in the small particle size range (1-5 μm) (Figure 66C) whereas SFD carrier was spherical and porous (Figure 67A-B) and raw mannitol was elongated (Figure 68A-B) and both in the larger particle size range (60-200 μm). As shown in Figure 67C-D, SDGLP(NH₄OH) particles were less agglomerated and evenly distributed on the surface of SFD 10% glycine-mannitol carrier (Figure 67C-D). This could be attributed to the rough and wavy surface of the porous and spherical SFD carrier with small and shallow indentations. Such indentations were not deep enough to hold large amounts of small drug particles on the SFD carrier, therefore more irregularities associated with larger surface areas (Kaialy, 2016, Rudén et al., 2019). This would have kept the GLP-1 particles relatively separated by

providing more contact areas available for drug-carrier adhesion. This suggests that during mixing the addition of SFD 10% glycine-mannitol carrier in the formulation demonstrated to break up SD GLP-1 cohesive particles/agglomerates (Figure 66C) followed by adhering the drug particles to the small indentations on the surface of the SFD carrier as a single adhesion layer of drug particles. However, some SD GLP-1 particles were seen between the small indentations on the surface of SFD 10% glycine-mannitol carrier (Figure 67D yellow circles) where the drug particles could fit into the void spaces (macroscale roughness, carrier surfaces with large scale asperities that are larger than the drug particle size, Chapter 2.4.3, (Nokhodchi, Martin, 2015, Shalash, Molokhia & Elsayed, 2015)). The small indentations yet slightly larger than the drug particle size could shield the drug particles from forces (e.g., drag and lift forces) during aerosolisation (Nokhodchi, Martin, 2015, Shalash, Molokhia & Elsayed, 2015). This could possibly lead to poor drug detachment from the SFD carrier and affect the aerosolisation performance of the formulations.

On the other hand, the carrier surface of raw mannitol particles was overloaded with SDGLP(NH₄OH) particles (Figure 68C-D) in comparison to the surface of SFD mannitol-based carrier particles (Figure 67C-D). It can be seen from Figure 68D that SDGLP(NH₄OH) particles were present as agglomerates between the large indentations on the surface of raw mannitol carrier. This could be attributed to fewer overall contact areas available on the surface of the non-engineered raw mannitol carrier for drug-carrier adhesion. Raw mannitol particles with large indentations therefore less irregularities would be associated with small surface areas providing a small contact area for drug-carrier adhesion. This suggests that only some GLP-1 particles could adhere to indentations/irregularities on the surface of raw mannitol carrier and start to form multi adhesion layers of drug particles (SD GLP-1 particles aggregates) (Rudén et al., 2019). Consequently these differences in particle surface properties (e.g., morphology and surface roughness) affected the GLP-1 content uniformity (Section 6.14.4) and aerosolisation performance of DPI formulations (Section 6.14.5).

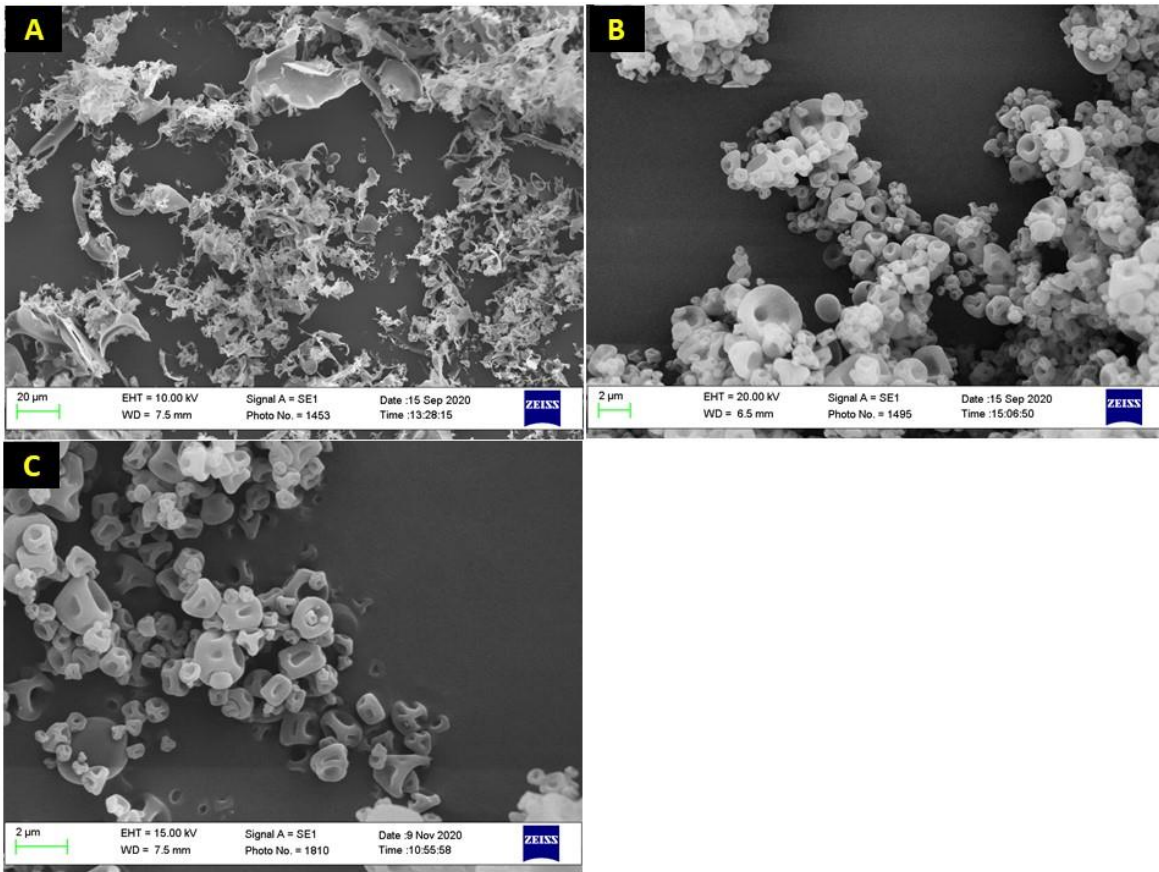


Figure 66: Scanning electron microscopy (SEM) images of raw GLP-1 powder as received (A), spray dried (SD) GLP-1 powder produced from acetic acid with 1M NaOH (B), SD GLP-1 powder produced from acetic acid with 35% NH₄OH (C).

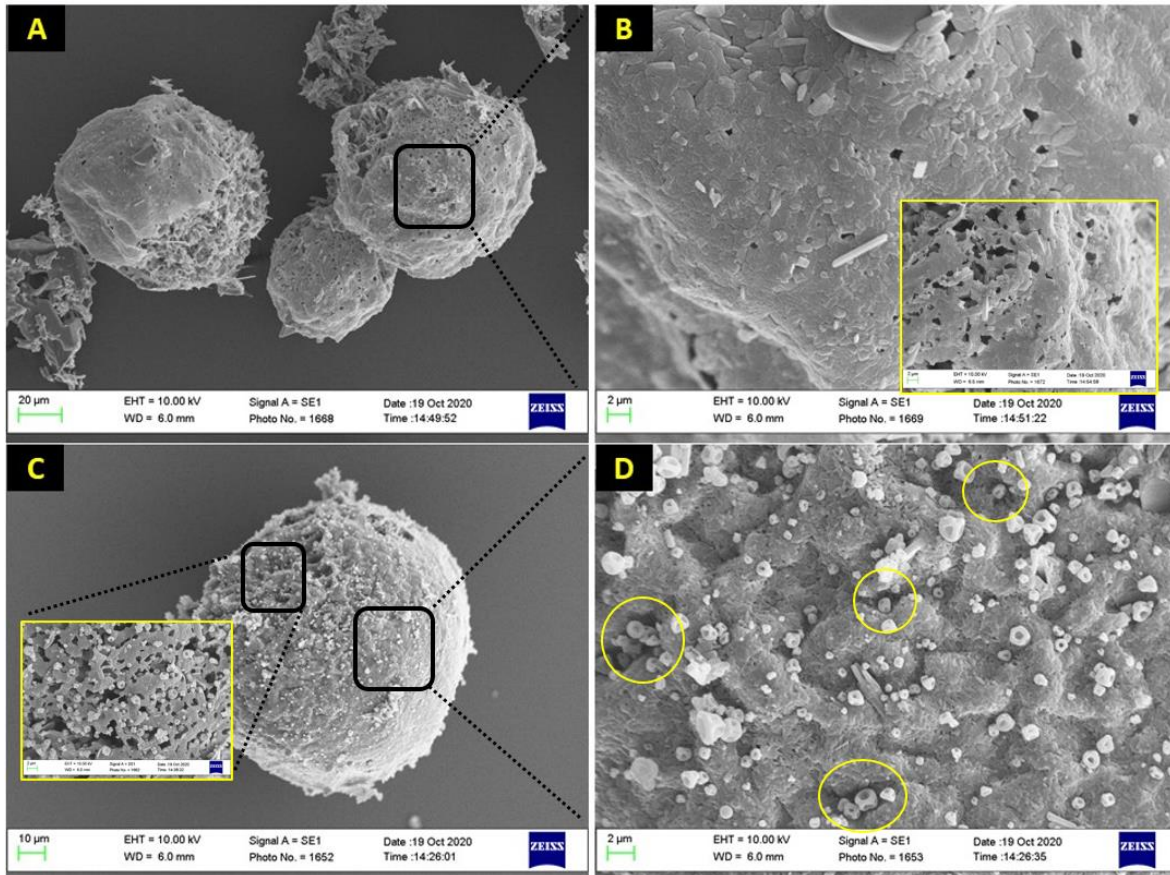


Figure 67: SEM images of spray freeze dried (SFD) 10% glycine-mannitol carrier powder (sieved 90-125 μm) (A,B) and spray dried GLP-1 powder produced from acetic acid with 35% NH_4OH blended with SFD 10% glycine-mannitol carrier powder (C,D). Yellow boxes indicate SEM images with 2 μm scale bar. Yellow circles indicate SD GLP-1 particles fitting into the void spaces between indentations.

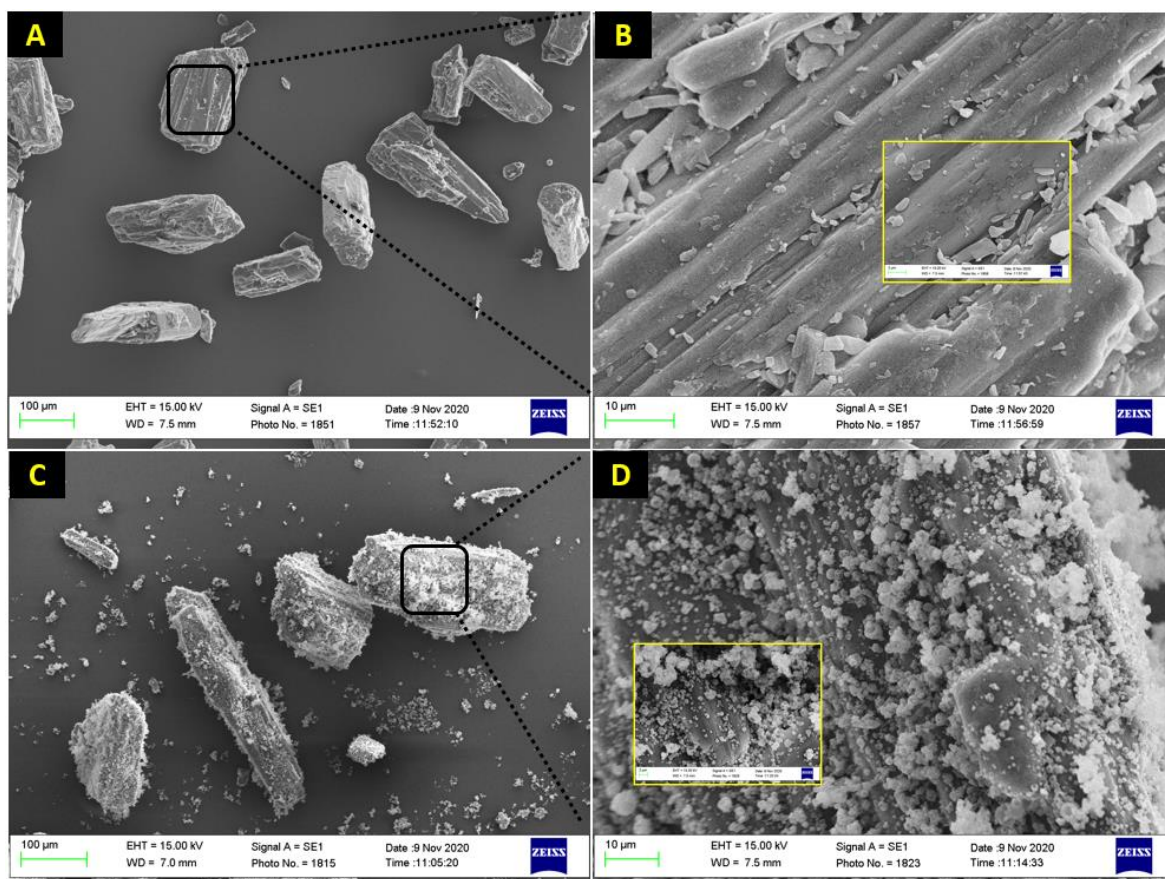


Figure 68: SEM images of raw mannitol powder (sieved 90-125 μm) (A,B) and spray dried GLP-1 powder produced from acetic acid with 35% NH₄OH blended with raw mannitol carrier powder (C,D). Yellow boxes indicate SEM images with 2 μm scale bar.

6.14.3.2. Differential scanning calorimetry

The results of DSC analysis for raw GLP-1 and two SD GLP-1 powders (SDGLP(NaOH) and SDGLP(NH₄OH)) showed no significant sharp peaks as all the peaks observed were small and broad indicating amorphous nature of GLP-1 powders (Figure 69). This suggests that spray drying maintained GLP-1 in an amorphous state. The DSC curves for all GLP-1 powders showed three endothermic peaks; a broad endothermic peak between 40°C and 100°C, a small endothermic peak between 140°C and 160°C and a broad endothermic peak started at around 180°C (Figure 69). SDGLP(NaOH) powder showed an extra small endothermic peak around 235°C followed by another broad endothermic peak at 257°C (Figure 69B), whereas SDGLP(NH₄OH) powder showed a small endothermic peak around 250°C (Figure 69C). The first broad endothermic peaks seen below 100°C were attributed to moisture loss. This indicates that spray drying did not remove all water resulting in the production of moisture-contained SD GLP-1 powders or SD GLP-1 powders may be considered

susceptible to moisture if exposed to atmosphere (i.e., during sample preparation for DSC). SD GLP-1 powders were found to be amorphous therefore easier to absorb water vapor from air relative to crystalline materials (Weers, Miller, 2015). This may affect the long-term stability of the DPI formulations (Banga, 2015). The second small endothermic peaks around 150°C would be ascribed to the onset of GLP-1 degradation. The small and broad endothermic peaks observed between 180°C and 260°C could be attributed to its decompositions induced by increasing temperature. This could indicate that there would be a series of decomposition processes involved in the thermal breakdown of GLP-1 during the temperature change. These events observed in SD GLP-1 were similar to the SD insulin thermal transition observed in DSC analysis (Figure 50B in Chapter 5.12.1.2). Therefore, this could be attributed to the degradation of GLP-1 occurred via the chemical or physical process influenced by the temperature conditions (Ansari et al., 2016).

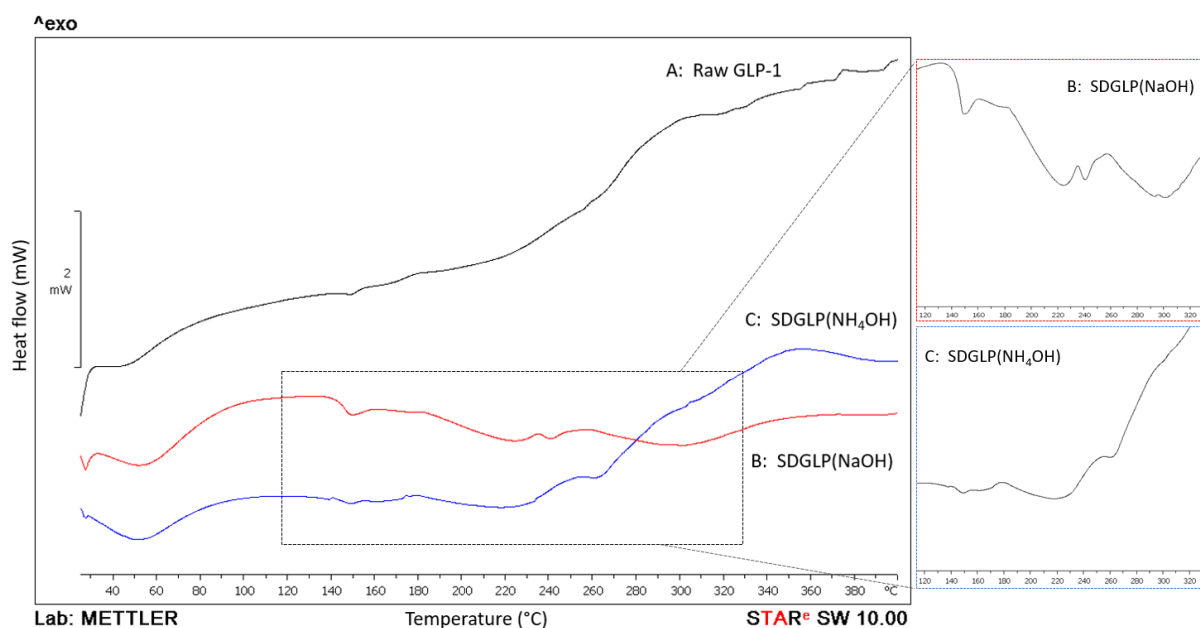


Figure 69: Combined DSC thermograms of raw GLP-1 (A), SDGLP(NaOH): spray dried (SD) GLP-1 prepared from acetic acid with 1M NaOH (B), and SDGLP(NH₄OH): SD GLP-1 prepared from acetic acid with 35% NH₄OH (C).

6.14.3.3. Thermogravimetric analysis

The combined TGA curves for raw GLP-1 and two SD GLP-1 powders (SDGLP(NaOH) and SDGLP(NH₄OH)) are shown in Figure 70. The TGA curve of all GLP-1 powders showed apparent

weight gains (4-8%, the mass was higher than the initial mass) below 40°C (Figure 70). It takes some time for the crucible to be uniformly heated in the TGA equipment, therefore, the actual temperature of the gas in the furnace atmosphere would have been higher at the beginning of the measurement than the sample temperature measured and recorded. This would have led to the drastic change of the gas density on heating of the samples influencing the sample mass (Craig, Reading, 2006, Mettler-Toledo International Inc, 2021). There are generally some delays in heat transfer from the furnace to the sample due to the thermal conductivity of the samples and the delay is generally great if samples are poorly conducting materials (Craig, Reading, 2006). Therefore, all GLP-1 powders can be considered as poorly conductive materials or non-conductive materials. Continuous weight gains were also observed for SDGLP(NaOH) and SDGLP(NH₄OH) until around 200°C (Figure 70B,C). This would have resulted from interactions with a trace of oxygen in the nitrogen purge gas or volatilised products generated during the experiments in the furnace atmosphere (Craig, Reading, 2006). The TGA curve of raw GLP-1 showed few steps of mass loss (Figure 70A). The first step (about 4% w/w) observed in the temperature range of 50°C to 100°C was associated with moisture content where water evaporation would have taken place. This supports the DSC curve for raw GLP-1 where the endothermic peak observed below 100°C (Figure 69A) was attributed to moisture loss. The mass losses observed around 150°C (about 2% w/w), 200°C (about 12% w/w), 240°C (3% w/w) and 260°C (34 % w/w) (Figure 70A) could be attributed to the multi-step thermal decompositions caused by the thermal breakdown of GLP-1 on heat stress. This also supports the DSC curve of raw GLP-1 where the small endothermic peaks observed above 140°C (Figure 69A) were attributed to its thermal decompositions.

There were no steps observed below 200°C for both SD GLP-1 powders (SDGLP(NaOH) and SDGLP(NH₄OH)) due to the continuous weight gains observed (Figure 70B,C). Steps associated with moisture content below 100°C could be hidden as the DSC curves for both SD GLP-1 powders (Figure 69B,C) showed broad endothermic peaks below 100°C attributed to moisture loss. However, above 200°C, SDGLP(NaOH) powder (Figure 70B) showed three steps of mass loss starting at around 200°C (12% w/w), 240°C (4% w/w) and 260°C (24% w/w) in the TGA curves. These mass losses can be associated with its decomposition therefore support the DSC curve where the broad endothermic peaks observed around 180°C, 240°C and 260°C (Figure 69B) were attributed to its decomposition. It was observed that raw GLP-1 and SDGLP(NaOH) showed the similar trend of the mass change above 240°C in the TGA curves (Figure 70A,B) whereas SDGLP(NH₄OH) showed a small change in mass (about 6% w/w) in the temperature range of 220°C and 340°C (Figure 70C). This could indicate that SDGLP(NH₄OH) would be more thermostatically stable (e.g., less susceptible to change in temperature) than SDGLP(NaOH).

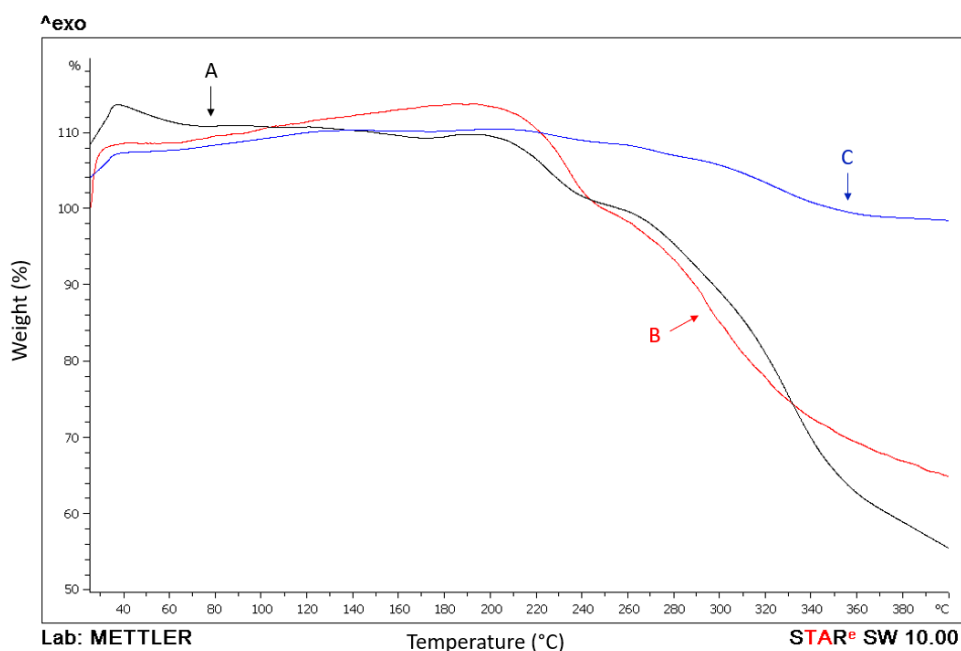


Figure 70: Combined TGA curves of raw GLP-1 (A), spray dried (SD) GLP-1 powder prepared from acetic acid with 1M NaOH (SDGLP(NaOH)) (B), and SD GLP-1 powder prepared from acetic acid with 35% NH₄OH (SDGLP(NH₄OH)) (C).

6.14.4. Blend homogeneity assessment

The GLP-1 content tested by RP-HPLC and mannitol content tested by ¹H qNMR in two carrier-based DPI formulations (SDG10GMB and SDGRMB) are presented in Table 40. Figure 71 shows ¹H NMR spectra of mannitol from three different positions of SDG10GMB and SDGRMB in the blending container. Both DPI formulations exhibited a high degree of mannitol carrier content uniformity (SDG10GMB: 99.67% ± 0.06% and SDGRMB: 104.16% ± 0.12) with good mannitol homogeneity (%CV, SDG10GMB: 0.06 and SDGRMB: 0.12) (Table 40). The intensity of all mannitol peaks observed by NMR showed comparable for both formulations presenting similar mannitol concentrations were determined (Figure 71). However, they exhibited significantly different mannitol uniformity from each other (t-test, p<0.05). DPI formulation with raw mannitol carrier (SDGRMB) showed higher mannitol content present in the formulation (104.16%, %CV: 0.12) than DPI formulation with SFD 10% glycine-mannitol carrier (SDG10GMB, 99.67%, %CV: 0.06) (t-test, p<0.05) (Table 40). Similarly, GLP-1 uniformity was significantly different between SDG10GMB and SDGRMB (t-test, p<0.05).

These findings could imply that drug (GLP-1) content influences carrier (mannitol) content or vice versa consequently affecting the overall homogeneity of the formulation blends (One-way ANOVA, $p < 0.05$). The drug content uniformity for SDGRMB (95.42%) fell within the acceptable range of 85-115% of the nominal dose (British Pharmacopoeia (Yeung et al., 2019) and FDA guidelines) with good drug content homogeneity (%CV: 1.81) whereas the drug content uniformity for SDG10GMB (79.75%) was outside the acceptable range with a higher CV (2.55%) (Table 40). This could be related to the width of the particle size distribution (i.e., span). SFD 10% glycine-mannitol carrier exhibited the wider size distribution, thus higher span value (span: 5.82 in Table 22 Chapter 4.13.3.2) than raw mannitol carrier with low span value (span: 2.25 in Table 7 Chapter 3.11.2.2) (span values determined by laser diffraction are from the previous studies in Chapter 3 and Chapter 4). Low span of particle size distribution is associated with low variation in drug content (e.g., low %CV) which is related to the uniformity of the dose (Kaialy, Nokhodchi, 2015). Carrier particles with higher span value could contain different amounts of drug particles per unit mass (Aulton, Taylor, 2013, Kaialy, Nokhodchi, 2015). Also, this could be attributed to different morphologies observed between SFD 10% glycine-mannitol carrier (Figure 67A-B) and raw mannitol carrier (Figure 68A-B). SFD 10% glycine-mannitol carrier (Figure 67A-B) showed highly porous particles that would have been associated with lower density in comparison to non-porous raw mannitol carrier (heavier) (Figure 68A-B). SFD carrier would have had lower shear forces (e.g., press-on forces) in the low shear blender used (Turbula®) resulting in poor drug-carrier adhesion forces therefore poor distribution of SD GP-1 powders on the surface of SFD carrier particles (Hertel, Birk & Scherließ, 2020). This indicates that the fraction of the drug particles available in SDG10GMB for systemic pulmonary delivery would be lower than SDGRMB as SFD carrier retained less GLP-1 particles.

Table 40: The content uniformity (%) with coefficient of variation for GLP-1 and mannitol in carrier-based dry powder inhaler (DPI) formulations (data presented as mean (%) \pm standard deviation, $n=3$ per position). SDG10GMB: Spray dried (SD) GLP-1 (SDGLP(NH₄OH)) blended with spray freeze dried 10% glycine-mannitol carrier and SDGRMB: SDGLP(NH₄OH) blended with raw mannitol carrier.

DPI formulation	GLP-1 uniformity (%) (HPLC)	Coefficient of variation (%)	Mannitol uniformity (%) (NMR)	Coefficient of variation (%)
SDG10GMB	79.75 \pm 2.00 ^a	2.55	99.67 \pm 0.06 ^b	0.06
SDGRMB	95.42 \pm 1.66 ^a	1.81	104.16 \pm 0.12 ^b	0.12

Groups denoted by the same letter (^{a-a}, ^{b-b}) are significantly different from each other (t-test, $p < 0.05$).

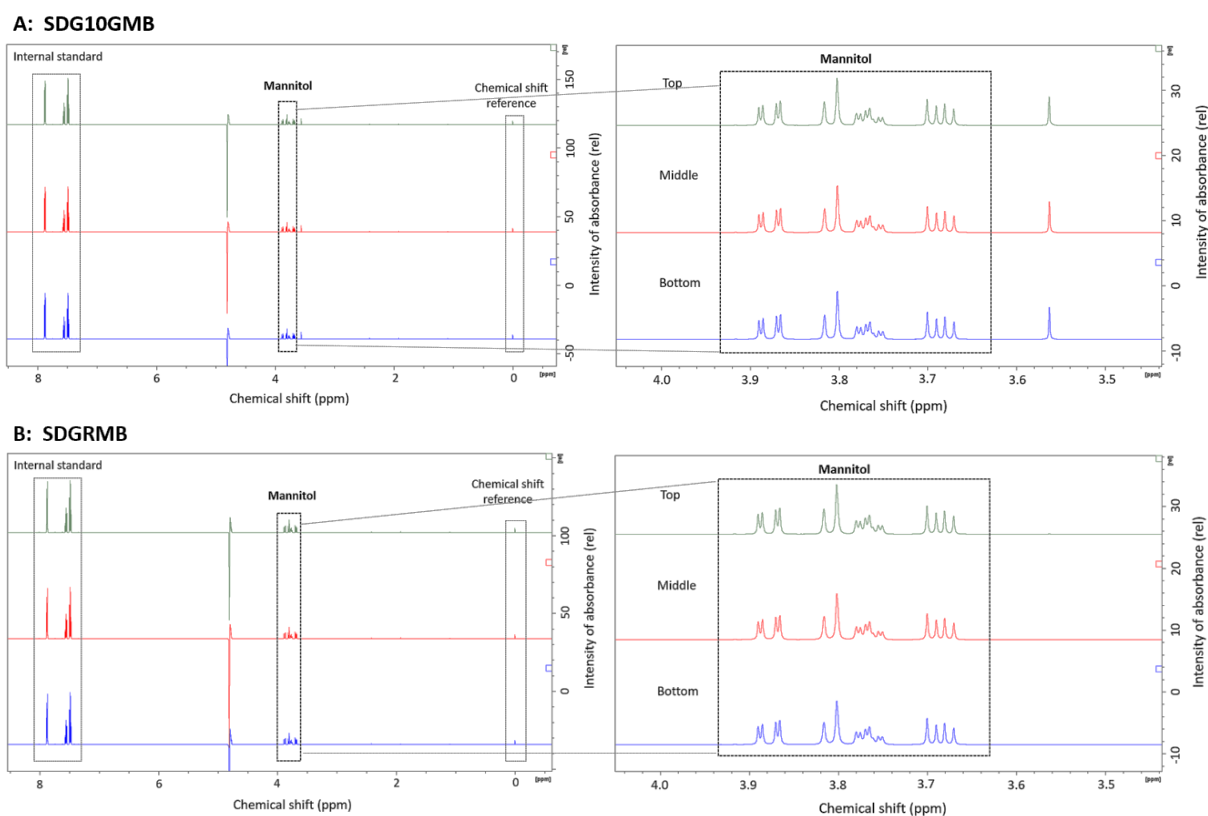


Figure 71: ^1H NMR spectra of mannitol from three different positions of carrier-based DPI formulations in the blending container. SDG10GMB: Spray dried (SD) GLP-1 (SDGLP(NH_4OH)) blended with spray freeze dried 10% glycine-mannitol carrier (A) and SDGRMB: SDGLP(NH_4OH) blended with raw mannitol carrier (B). Dashed boxes indicate peaks of the internal standard (sodium benzoate), mannitol, chemical shift reference (sodium 3-trimethylsilyl propionate-2,2,3,3- d_4 , TSP).

6.14.5. Impaction study

SD GLP-1 powders deposited on AIT and all NGI stages were quantified by RP-HPLC and the results of GLP-1 depositions within the NGI are shown in Figure 72. The flow rate and test duration for the NGI study were adjusted based on the design of the device used (Handihaler[®]) and reported studies. Handihaler[®] is a high resistance inhaler designed to generate high pressure drop and studies have shown that *in vitro* performance of Handihaler[®] was not influenced by the flow rate between at 30 L min^{-1} and 60 L min^{-1} with the inhalation volume of 1 L. 30 L min^{-1} of inspiratory flow rate was sufficient for successful inhalation for Handihaler[®] used by patients in a broad age range from children to elderly and disease states (e.g., asthma, chronic obstructive pulmonary disease (COPD)) (Lindert, Below & Breitzkreutz, 2014, Levy et al., 2019). Patients also can produce a minimum pressure drop of around 1 kPa ($\sim 10 \text{ cmH}_2\text{O}$) across DPI inhaler devices including Handihaler[®] (e.g.,

Easyhaler[®], Turbohaler[®]/Turbuhlaer[®], Diskus[®]) which are found to be sufficient for pulmonary deposition and patients should receive a necessary drug dose (Clark, Weers & Dhand, 2019). In addition, people with diabetes are associated with obesity which causes a reduction in lung volume (e.g., functional residual capacity) and lung function (e.g., forced expiratory volume in one second) due to physiological changes (increased mass of the chest wall compress the chest cavity resulting in reduced lung volume) (Lumb, Thomas, 2020). This leads to a change in breathing pattern, increased work of breathing (e.g., obese subjects with body mass index, BMI $39 \pm 6 \text{ kg/m}^2$, breathing frequency: 18 ± 2 breath per minute, ventilation: $12.26 \pm 2.27 \text{ L min}^{-1}$ and control subjects with BMI $23 \pm 3 \text{ kg/m}^2$, breathing frequency: 10 ± 2 breath per minute, ventilation: $7.84 \pm 0.99 \text{ L min}^{-1}$, $p < 0.001$ (Chlif et al., 2009)), frequent airway closure and increased risk of developing airway disease (e.g., COPD) (Chlif et al., 2009, Lumb, Thomas, 2020). The duration of time (e.g., 8 sec) to draw 4L of air (according to the European Pharmacopoeia) through Handihaler[®] during testing would be long for people with diabetes.

SD GLP-1 powder (SDGLP(NH₄OH)) produced from acidic aqueous solution (pH 3.5) composed of acetic acid and 35% NH₄OH was selected over SD GLP-1 powder (SDGLP(NaOH)) produced from acetic acid with 1M NaOH acidic aqueous solution (pH 3.5) to prepare carrier-based DPI formulations (SDG10GMB and SDGRMB). SDGLP(NH₄OH) presented better aerosolisation performance in terms of FPF and MMAD (Table 41). Carrier free DPI formulations, SDGLP(NaOH) and SDGLP(NH₄OH) both demonstrated similar GLP-1 delivered dose (SDGLP(NaOH): $33.31\% \pm 12.52\%$ and SDGLP(NH₄OH): $32.88\% \pm 7.00\%$) (Table 41) as the total GLP-1 depositions between AIT and all NGI stages (stages 1-7 and MOC) were not significantly different from each other (t-test, $p > 0.05$). This presents that using two different acidic aqueous solutions to produce SD GLP-1 powders did not affect the overall GLP-1 delivered dose. However, SDGLP(NH₄OH) showed significantly low GLP-1 deposition between AIT and stage 2 (AIT and stage 1 generally represent the oropharynx region) and significantly high GLP-1 deposition in the lower NGI stages (i.e., stages 5-6, lower NGI stages represent the desired deep lung regions for systemic pulmonary delivery) in comparison to SDGLP(NaOH) (t-test, $p < 0.05$) (Figure 72). Therefore, SDGLP(NH₄OH) generated higher FPF ($90.73\% \pm 1.76\%$) and smaller MMAD ($1.96 \mu\text{m} \pm 0.07 \mu\text{m}$) with lower GSD (1.71 ± 0.07) than SDGLP(NaOH) (FPF: $52.21\% \pm 7.30\%$, MMAD: $3.49 \mu\text{m} \pm 0.61 \mu\text{m}$ and GSD: 2.64 ± 0.31) (Table 41). This implies that using feed solution composed of acetic acid and NH₄OH to spray dry GLP-1 significantly improved the aerodynamic performance (e.g., FPF, MMAD) by decreasing drug deposition in high NGI stages (AIT and stages 1-2) in comparison to using feed solution composed of acetic acid and NaOH (t-test, $p < 0.05$). This trend is in agreement with the results of aerodynamic assessment for SD insulin powders (device used: Turbospin[®], flow rate: 60 L min^{-1}) reported by Balducci *et al.* (2014). Balducci *et al.* (2014) prepared SD insulin powders from

acetic acid (0.4N) with NH_4OH (10% v/v, pH 3.6) that showed high FPF ($83.6\% \pm 4.7\%$) and small MMAD ($1.79 \mu\text{m} \pm 0.18 \mu\text{m}$) in comparison to SD insulin powders prepared from acetic acid (0.4N) with NaOH (1N, pH 3.1) that had lower FPF ($65.5\% \pm 3.0\%$) and larger MMAD ($3.21 \mu\text{m} \pm 0.11 \mu\text{m}$) (Balducci et al., 2014). Their results were attributed to the different particle shapes of SD insulin powders produced from their two different acidic feed solutions; more volatile ammonium acetate was present in the solution than sodium acetate in the solution. This resulted in the formation of more deeply shrivelled particles of SD particles with NH_4OH and smaller particles due to the evaporation rate of solvent relative to diffusion of insulin molecule during spray drying compared to SD particles with NaOH which was wrinkled raisin-like shapes (Balducci et al., 2014).

The NGI study showed that all four DPI formulations aerosolised differently using the capsule-based inhaler device (Handihaler[®]) as they showed significantly different GLP-1 depositions in the high NGI stages (i.e., AIT and stages 1-2) and lower NGI stages (i.e., stages 3-6) (One-way ANOVA, $p < 0.05$) (Figure 72). This means that GLP-1 deposition patterns in high and lower stages were dependent on the formulations; therefore, affected the aerosolisation performance of SD GLP-1 powders. Carrier free DPI formulation of SDGLP(NH_4OH) produced the highest FPF ($90.73\% \pm 1.76\%$) with the smallest MMAD ($1.96 \mu\text{m} \pm 0.07 \mu\text{m}$) whereas carrier-based DPI formulation of SDG10GMB exhibited the lowest FPF ($29.20\% \pm 5.62\%$) with the largest MMAD ($5.85 \mu\text{m} \pm 1.25 \mu\text{m}$) (One-way ANOVA, $p < 0.05$) (Table 41). The highest FPF obtained for SDGLP(NH_4OH) could indicate that higher amount of GLP-1 (aerodynamic diameter: $\leq 5 \mu\text{m}$) would be expected to reach the deep lung regions for systemic pulmonary delivery compared to the lowest FPF value obtained for SDG10GMB ($29.20\% \pm 5.62\%$). However, despite that SDGLP(NH_4OH) carrier free DPI formulation had the highest FPF ($90.73\% \pm 1.76\%$), GLP-1 delivered dose was just over 30% ($32.88\% \pm 7.00\%$) (Table 41) representing high amount of drug (GLP-1) loss (about 70% of drug loss). In contrast, DPI formulation using SFD 10% glycine-mannitol carrier (SDG10GMB) demonstrated the highest GLP-1 delivered dose ($45.92\% \pm 5.84\%$) therefore reduced the drug loss by about 15% (70% \rightarrow 55% drug loss). This indicates that the addition of SFD 10% glycine-mannitol carrier to the DPI formulation enhanced the powder flow and powder release from the DPI (Handihaler[®]) therefore facilitated the delivery of SD GLP-1 powder (1.4-fold increase in GLP-1 delivery dose against SD GLP-1 alone, $32.88\% \pm 7.00\% \rightarrow 45.92\% \pm 5.84\%$) (Table 41). This could be due to the porous and fluffy particles of 10% glycine-mannitol carrier produced by spray freeze drying that resulted in better fluidisation and powder emission/release from the inhaler device. The engineered SFD carrier provided a means to enhance the flowability and improved the drug delivery using the DPI (Handihaler[®]). Many studies on the inhalation performance of carrier-based DPI formulations also have shown the advantages of the use of carriers/engineered carriers (e.g., increase FPF) (Kaialy, Nokhodchi, 2013, Kaialy, Nokhodchi, 2016,

Rashid et al., 2019). However, the addition of raw mannitol carrier to the DPI formulation (SDGRMB) resulted in the lowest GLP-1 delivered dose ($25.74\% \pm 8.50\%$) (Table 41) therefore the highest drug (GLP-1) loss ($>74\%$, 74.26%). Most of the drug remained on the wall of the capsule covered in a layer of white powders containing GLP-1 (the capsule retained a high fraction of drug particles). This suggests that this formulation did not fluidise efficiently with Handihaler[®] and raw mannitol carrier is not a good carrier candidate to enhance the powder flow and facilitate the drug delivery. This could be explained by the morphology of raw mannitol carrier powder that is not porous (Figure 68A-B) resulting in poor flowability and low drug delivered dose. This demonstrated the advantages of using engineered carrier-based DPI formulations. Further, SDG10GMB and SDGRMB both showed significantly different GLP-1 depositions between AIT and stage 2 (t-test, $p < 0.05$) (Figure 72). SDGRMB exhibited lower SD GLP-1 particles deposition as SD GLP-1-raw mannitol carrier mixtures in AIT and stages 1-2 therefore more SD GLP-1 particles were available for deposition in the lower NGI stages (e.g., stages 3-5) resulting in higher FPF ($60.41\% \pm 11.12\%$). On the other hand, SDG10GMB demonstrated significantly higher GLP-1 depositions as SD GLP-1-SFD carrier mixtures between AIT and stage 2 in comparison to SDGRMB (t-test, $p < 0.05$). Consequently, only small amount of the drug remained to reach the lower NGI stages resulting in the lowest FPF ($29.20\% \pm 5.62\%$) with the highest MMAD ($5.85 \mu\text{m} \pm 1.25 \mu\text{m}$) for SDG10GMB (Table 41). This suggests that SD GLP-1 particles adhered to the surface of raw mannitol carrier detached more easily than SD GLP-1 particles attached to SFD 10% glycine-mannitol carrier. This could be attributed to the agglomerates of SD GLP-1 particles (multi layers of drug particles) seen on the surface of raw mannitol particles (Figure 68C-D). These particles were associated with better dispersion as some drug particles were not attached to the raw mannitol carrier surface and freely available for aerosolisation that resulted in higher FPF values (Leung et al., 2016). However, this adversely can affect the mechanical powder stability (e.g., powder handling and dosing) and dose delivery consistency (uniform drug delivery into the lungs) as drug-carrier adhesive forces are to stabilise the drug-carrier mixtures (Chapter 2.4) (Kaialy, 2016, Sibum et al., 2018, Scherließ, Etschmann, 2018). It could be speculated that the process of drug-carrier detachment for SDGRMB would have been associated with more like drug-drug particle de-agglomeration rather than drug-carrier detachment. As shown in Figure 72 both SDGRMB and SDGLP(NH₄OH) showed similar drug deposition profiles in stages 3-6 and statistically GLP-1 depositions in stages 3-6 for SDGRMB and SDGLP(NH₄OH) were not significantly different from each other (t-test, $p > 0.05$). SDG10GMB with the lowest FPF could be due to the small indentations on the surface of SFD 10% glycine-mannitol carrier where some SD GLP-1 particles fitted into the void spaces between the small indentations (Figure 67D yellow circles). The small indentations yet slightly larger than the drug particle size observed by SEM (Figure 67) would have shielded the drug

particles from forces (e.g., drag and lift forces) during aerosolisation affecting drug dispersion/the drug-carrier detachment therefore the aerosolisation performance of the formulation. GLP-1 depositions in stages 3-6 for SDG10GMB was significantly lower than carrier free SDGLP(NH₄OH) (t-test, p<0.05). This could be interpreted that Handihaler® with high resistance (resistances to inhaled airflow/airflow resistance) can fluidise the powder blend of SD GLP-1 and the porous SFD carrier (SDG10GMB formulation) relatively well as the highest GLP-1 delivered dose (45.92 ± 5.84%) was achieved because of the porous carrier powder used. However, the device might not be designed to separate drug-SFD carrier mixtures effectively as FPF obtained was the lowest indicating the poor drug-carrier detachment. This can lead to insufficient therapeutic GLP-1 deposition in the desired deep lung regions for systemic drug absorption. Handihaler® is designed for patients with COPD who have difficulty in generating sufficient inspiratory flow through DPIs therefore less dependent on patient inspiration flow rate (inhalation effort required by the patients is low to fluidise the powders) (Altman et al., 2018). Airflow generated by high resistance DPIs (using low flow rate) might not be sufficient to disperse the drug-carrier powders efficiently when SFD carrier-based DPI formulations (drug: carrier = 1:9) were used. Handihaler® might not be the inhaler device of choice for carrier-based DPI formulations as more inspiratory flow would be required for drug-carrier detachment.

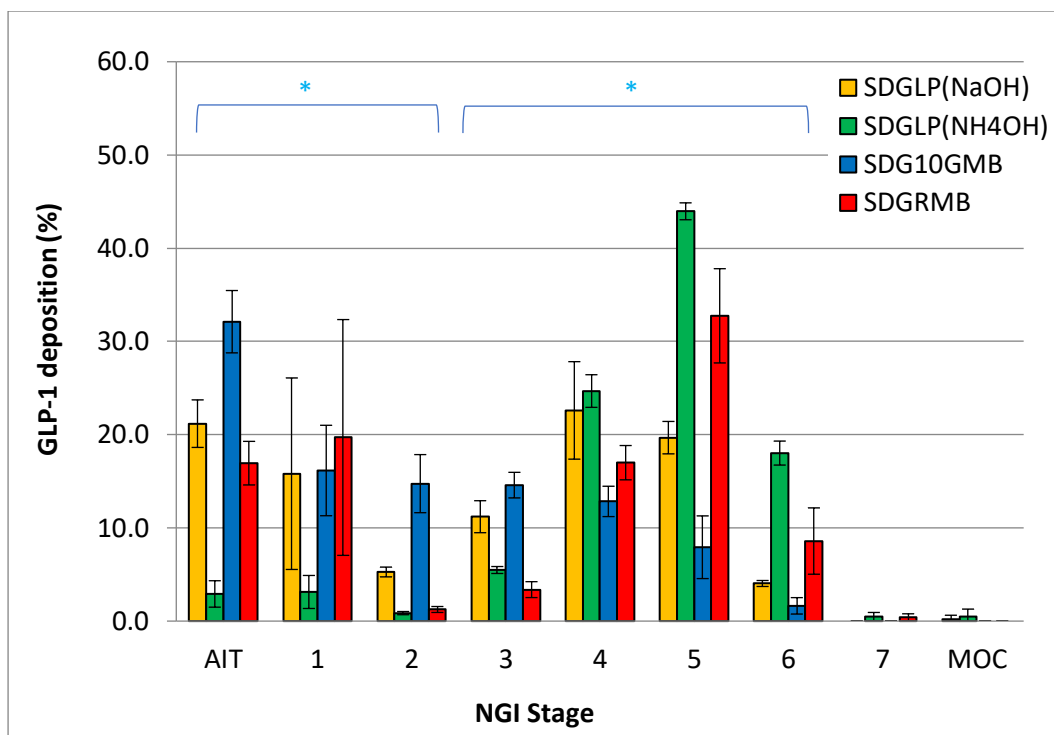


Figure 72: Next Generation Impactor (NGI) deposition profiles of SD GLP-1 in four different dry powder inhaler formulations aerosolised from Handihaler[®] at flow rate of 30 L min⁻¹. GLP-1 deposition is expressed as delivered dose (%) per NGI stage (Data presented as mean \pm standard deviation, n=3). AIT: Alberta idealised throat, MOC: Micro orifice collector. SDGLP(NaOH): spray dried (SD) GLP-1 prepared from acetic acid with 1M NaOH, SDGLP(NH₄OH): SD GLP-1 prepared from acetic acid with 35% NH₄OH, SDG10GMB: SDGLP(NH₄OH) blended with SFD 10% glycine-mannitol carrier and SDGRMB: SDGLP(NH₄OH) blended with raw mannitol carrier. Asterisks (*) indicate significantly different GLP-1 depositions in the high NGI stages (i.e., AIT and stages 1-2) and lower NGI stages (i.e., stages 3-6) between DPI formulations (One-way ANOVA, p<0.05).

Table 41: GLP-1 delivered dose (%), fine particle fraction (FPF% \leq 5.0 μ m), mass median aerodynamic diameter (MMAD) and geometric standard deviation (GSD) determined by Next Generation Impactor study with Handihaler[®] at flow rate of 30 L min⁻¹ for dry powder inhaler (DPI) formulations (Data presented as mean \pm standard deviation, n=3). SDGLP(NaOH): spray dried (SD) GLP-1 prepared from acetic acid with 1M NaOH, SDGLP(NH₄OH): SD GLP-1 prepared from acetic acid with 35% NH₄OH, SDG10GMB: SDGLP(NH₄OH) blended with SFD 10% glycine-mannitol carrier and SDGRMB: SDGLP(NH₄OH) blended with raw mannitol carrier.

DPI Formulation	Dose		Size Distribution	
	GLP-1 delivered dose (%)	FPF (%) [*]	MMAD (μ m) [*]	GSD
SDGLP(NaOH)	33.31 \pm 12.52	52.21 \pm 7.30 ^a	3.49 \pm 0.61 ^c	2.64 \pm 0.31
SDGLP(NH ₄ OH)	32.88 \pm 7.00	90.73 \pm 1.76^a	1.96 \pm 0.07^c	1.71 \pm 0.07^e
SDG10GMB	45.92 \pm 5.84	29.20 \pm 5.62 ^b	5.85 \pm 1.25 ^d	2.26 \pm 0.10 ^e
SDGRMB	25.74 \pm 8.50	60.41 \pm 11.12 ^b	2.56 \pm 0.74 ^d	2.70 \pm 0.00

Asterisks (*) denote statistically significant differences between DPI formulations (One-way ANOVA, $p < 0.05$). Groups denoted by the same letter (^{a-a}, ^{b-b}, ^{c-c}, ^{d-d}, ^{e-e}) are significantly different from each other (t-test, $p < 0.05$).

6.14.6. GLP-1 stability study

The preliminary stability study was performed to see whether SD GLP-1 powders were stable after spray drying process and could be used for the impaction studies (also to provide information for further studies such as scale-up study). In general, room temperature stable formulations are ideal for inhaled products (Sadrzadeh et al., 2010). Therefore, storage conditions used for GLP-1 stability studies were room temperature (real time/real temperature conditions (ICH, 1995)) and the final products will be protected against humidity. FTIR was used to study the structure integrity (e.g., secondary structure) of GLP-1 in SD GLP-1 powders (SDGLP(NaOH) and SDGLP(NH₄OH)) whether the process of spray drying using high temperatures (inlet temperature at 119°C and outlet temperature at 60°C ± 2°C, Section 6.7) had an adverse effect on the structure of GLP-1. The FTIR spectra in Figure 73A for raw GLP-1 powder as received (GLP-1(7-36) amide powder purchased from the Chinese supplier, see Materials in 6.3) showed few peaks including common peptide/protein characteristic absorption bands such as Amide I (1700-1600 cm⁻¹) and Amide II bands (1575-1480 cm⁻¹) (Sarmiento et al., 2006, Tiernan, Byrne & Kazarian, 2020). The absorption peaks appeared at 3291 cm⁻¹ and around 3065-2960 cm⁻¹ would be assigned to N-H stretching vibration and C-H stretching vibration, respectively. The characteristic peaks at 1655.53 cm⁻¹ would be attributed to Amide I (C=O stretching vibration) and at 1541.21 cm⁻¹ would be assigned to Amide II (N-H bending vibration and C-N stretching vibration). The peaks at 1201.01 cm⁻¹ and at 1136.43 cm⁻¹ would be assigned to C-C=O stretching vibration and C-C stretching vibration, respectively. These characteristic band positions observed for raw GLP-1 were similar to the FTIR result of exenatide (the first approved GLP-1RA, synthetic form of 39-amino acid peptide incretin for the treatment of Type 2 diabetes) reported by Zhu *et al.* (2015). Their reported peaks were as follows: N-H stretching vibration at 3303.1 cm⁻¹, C-H stretching vibration at 3065.3 cm⁻¹, C=O stretching vibration at 1657.2 cm⁻¹, N-H bending vibration and C-N stretching vibration at 1542.6 cm⁻¹, C-C=O stretching vibration peak at 1203.4 cm⁻¹, C-C stretching vibration at 1139.5 cm⁻¹ (Zhu et al., 2015).

The FTIR spectra between raw GLP-1 (Figure 73A) and two SD GLP-1 powders (SDGLP(NaOH) in Figure 73B and SDGLP(NH₄OH) in Figure 73C) produced from two different acidic solutions showed similarities as no major shift of the characteristic band positions were observed: 3292-3290 cm⁻¹ for N-H stretching vibration, 3065-2960 cm⁻¹ for C-H stretching, 1655-1651 cm⁻¹ for C=O stretching

vibration of the amide groups (Amide I), 1542-1540 cm^{-1} for C-N stretching vibration of Amide II, 1456-1453 cm^{-1} for C-H bending, 1202-1201 cm^{-1} for C-C=O stretching vibration, and 1137-1135 cm^{-1} for C-C stretching vibration (Figure 73). The similarity of the FTIR spectra between raw GLP-1 (before spray drying) and SD GLP-1 powders (after spray drying) indicates that the integrity of GLP-1 structure (e.g., secondary structure) was maintained after the process of spray drying despite the use of relatively high temperatures (inlet temperature at 119°C and outlet temperature at 60°C \pm 2°C, Section 6.7). Therefore, the employed spray drying parameters did not have an influence of thermal stress on the GLP-1 structure. In addition, dissolving GLP-1 in two different acidic aqueous solutions for spray drying did not affect the structure of GLP-1.

The FTIR spectra of raw GLP-1 powder was compared with raw human insulin powder to see whether they exhibit structural differences between them. Figure 74 shows the similarity of the FTIR spectra for raw GLP-1 (Figure 74A) and raw human insulin (Figure 74B) in the characteristic band positions of around 3290 cm^{-1} (N-H stretching), 2960 cm^{-1} (C-H stretching), 1655-1645 cm^{-1} (C=O stretching vibration, Amide I) and 1540-1515 cm^{-1} (N-H bending vibration and C-N stretching vibration, Amide II). However, some differences in characteristic band positions (cm^{-1}) were observed. There were no peaks appeared around 1386 cm^{-1} (C-H bending) for raw GLP-1 (Figure 74A) while these were observed in raw human insulin (Figure 74B also Figure 55 in Chapter 5.12.4). Raw GLP-1 showed two small peaks at 1201 cm^{-1} (C-C=O stretching vibration) and 1136 cm^{-1} (C-C stretching vibration) whereas raw human insulin showed one small and broad peak around 1235 cm^{-1} (Figure 74 also Figure 55 in Chapter 5.12.4).

The FTIR spectra of SD GLP-1 powders (SDGLP(NaOH) in Figure 75 and SDGLP(NH₄OH) in Figure 76) stored at room temperature for up to 7 months showed no major changes in the characteristic band positions (e.g., Amide I and Amide II) between raw GLP-1 and two SD GLP-1 powders. This suggests that the integrity of secondary structure of GLP-1 in SD powders stored at room temperature was retained for up 7 months.

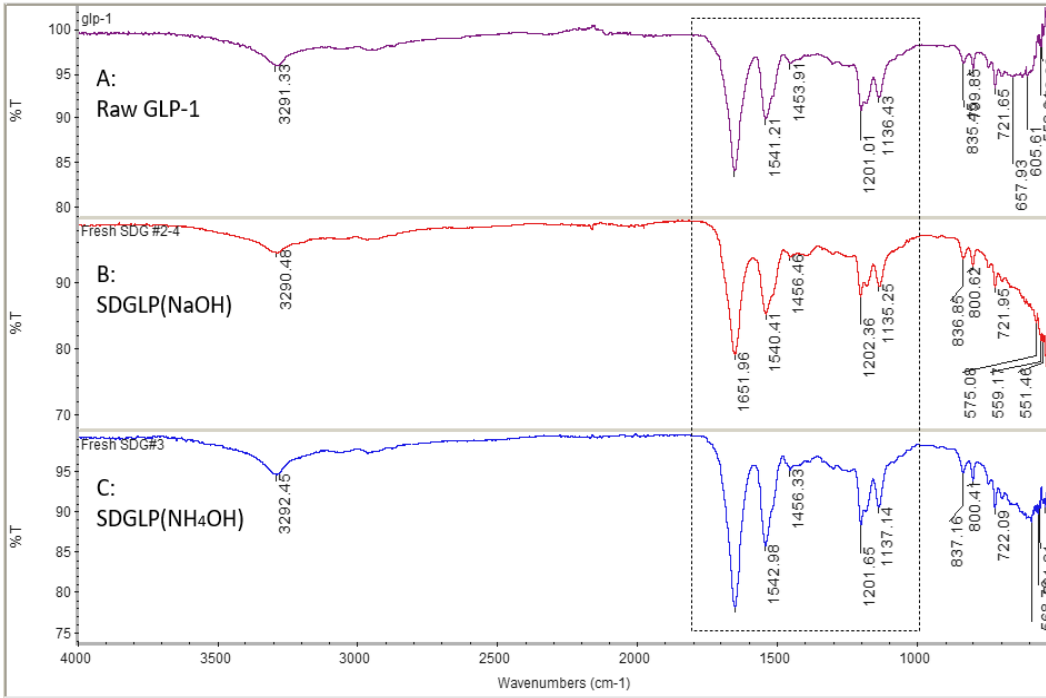


Figure 73: FTIR spectra of raw GLP-1 powder (as received) stored at 4°C (A), SDGLP(NaOH): freshly prepared spray dried (SD) GLP-1 from acetic acid with 1M NaOH (B) and SDGLP(NH₄OH): freshly prepared SD GLP-1 from 0.1% acetic acid with 35% NH₄OH (C). %T: Transmittance.

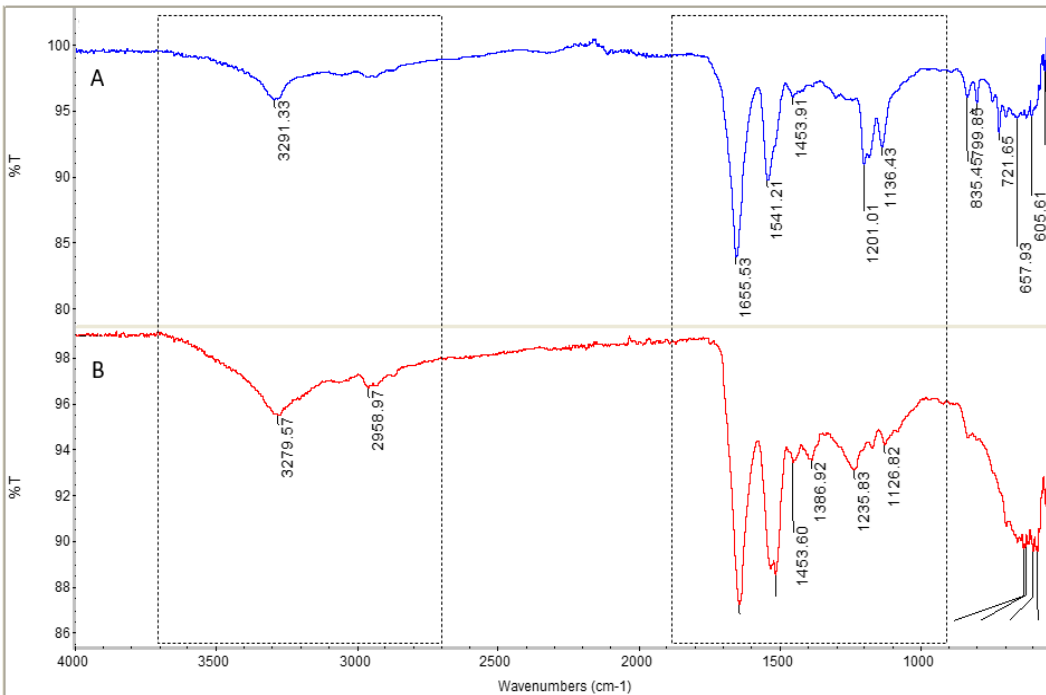


Figure 74: FTIR spectra of raw GLP-1 powder stored at 4°C (A) and raw human insulin powder stored at -20°C (B) for comparison. %T: Transmittance.

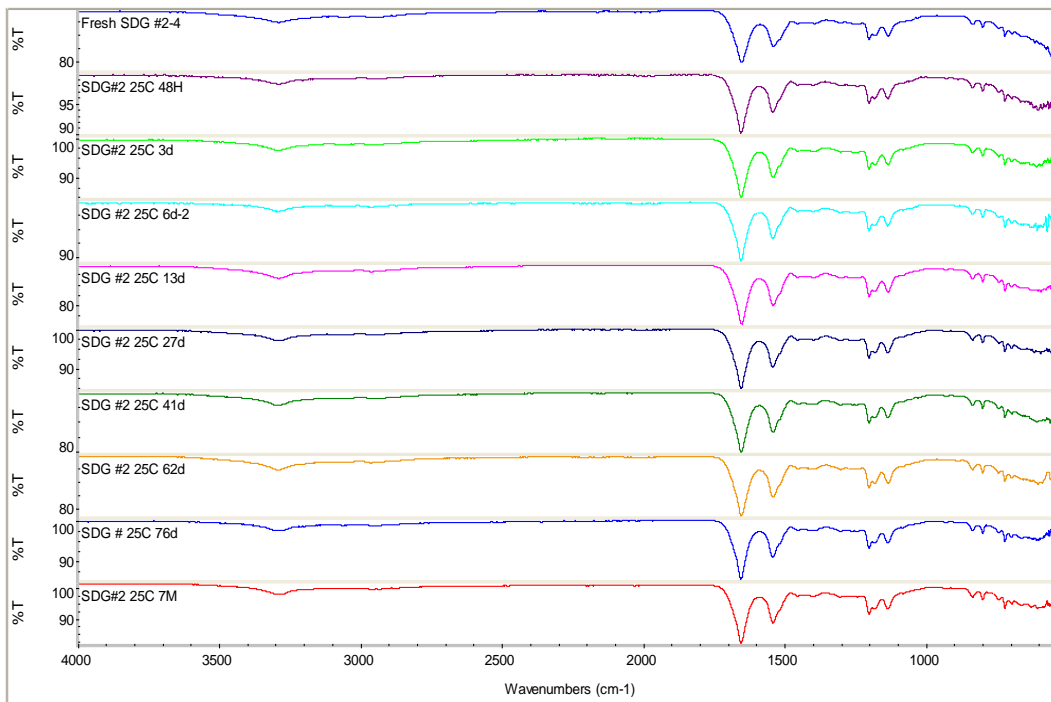


Figure 75: FTIR spectra of freshly prepared spray dried GLP-1 powder of SDGLP(NaOH) from 0.1% acetic acid with 1M NaOH (top, blue), SDGLP(NaOH) powder stored at room temperature for 48 hours, 3 days, 6 days, 13 days, 27 days, 41 days, 62 days, 76 days, and 209 days (7 months, bottom, red). %T: Transmittance.

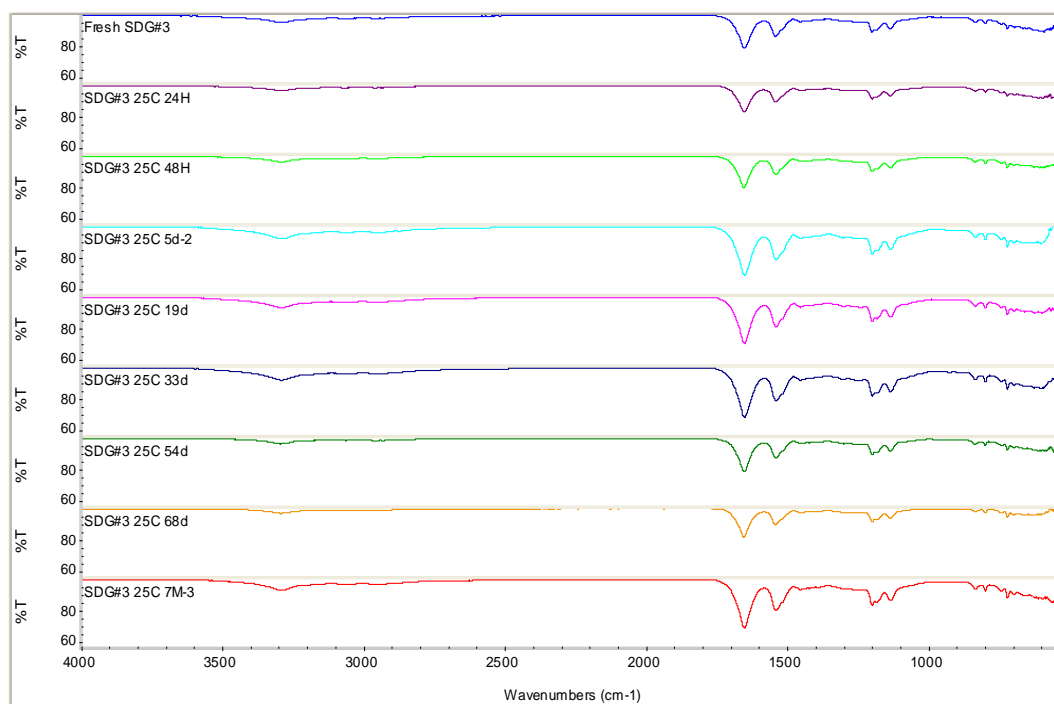


Figure 76: FTIR spectra of freshly prepared spray dried GLP-1 powder of SDGLP(NH₄OH) from 0.1% acetic acid with 35% NH₄OH (top, blue), SDGLP(NH₄OH) powder stored at room temperature for 24 hours, 48 hours, 5 days, 19 days, 33 days, 54 days, 68 days, and 203 days (7 months, bottom, red). %T: Transmittance.

The stability of GLP-1 was also assessed by RP-HPLC. No structural changes or degradation of GLP-1 molecule would have occurred during the process of spray drying as GLP-1 content determined by RP-HPLC in both SDGLP(NaOH) and SDGLP(NH₄OH) within 24-48 hours of SD powders production were 100% ± 1% (Figure 77A and Figure 77B, respectively). Further, SDGLP(NaOH) maintained their stability for up to 27 days at room temperature after the process of spray drying then dropped by over 10% within 15 days (87% at 41 days) and reached a plateau for about 6 months (84-86% at 62-209 days) (Figure 77A). In comparison, SDGLP(NH₄OH) maintained their stability for up to 7 months (GLP-1 content: 100% ± 3%) after the process of spray drying (Figure 77B).

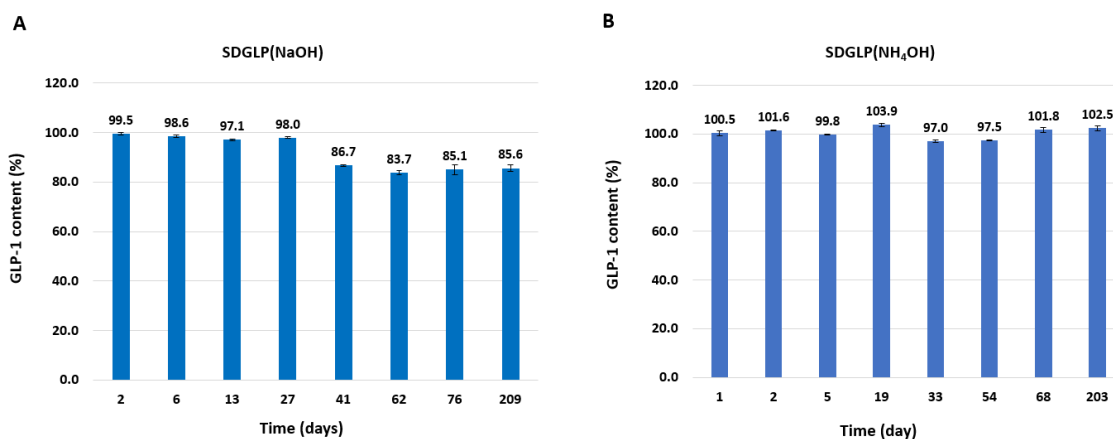


Figure 77: GLP-1 content determined by RP-HPLC. (A) SDGLP(NaOH): Spray dried (SD) GLP-1 powder produced from 0.1% acetic acid with 1M NaOH stored at room temperature for up to 209 days (7 months). (B) SDGLP(NH₄OH): SD GLP-1 powder produced from 0.1% acetic acid with 35% NH₄OH stored at room temperature for up to 203 days (7 months). (Data presented as mean \pm standard deviation, n=4).

6.15. Conclusion

Both carrier free and carrier-based DPI formulations exhibited significantly different aerosolisation performance tested from Handihaler[®], the inhaler device used. Carrier free DPI formulation which is not associated with the process of drug-carrier detachment upon inhalation demonstrated good aerosolisation performance (highest FPF and smallest MMAD) however exhibited poor powder flow. On the other hand, carrier-based DPI formulations showed more complex in drug deposition profiles as different carrier surface properties (e.g., roughness) affected drug particle detachment from the carrier surface therefore the fraction of the particles reached the lower NGI stages (i.e., FPF). Handihaler[®] aerosolised carrier-based DPI formulation better when the porous engineered SFD carrier was used compared to non-engineered carrier. In addition, low GLP-1 delivered dose obtained from carrier free DPI formulation was improved when the formulation contained SFD 10% glycine-mannitol carrier because of the porous carrier produced by spray freeze drying. This study demonstrated the advantages of using SFD carrier-based DPI formulation. Since Handihaler[®] requires low inhalation effort by the patients to fluidise and disperse the powders, the airflow generated from Handihaler[®] might be too low for drug-carrier detachment (when high concentration of drug is employed in DPI formulations, drug: carrier = 1:9). The process of drug-carrier detachment is crucial for drug delivery to the lung in carrier-based DPI formulations. Inhaler devices with high resistance might not be the inhaler device of choice for carrier-based DPI formulations. Higher inspiratory flow would be required for drug-carrier detachment. Inhaler devices

with low resistance which use higher flow rate (Chapter 2.5.4) might be more applicable for carrier-based DPI formulations. Overall, both carrier free and carrier-based DPI formulations have shown advantages with different challenges for pulmonary administration of GLP-1. The optimised DPI formulations can be achieved by using particle engineering to prepare engineered particles based on the type of DPI formulations (carrier free or carrier-based) and the optimised formulations adapt to inhaler devices suited for the intended formulations instead of formulations adapting to the already available inhalers (e.g., inhalers could be designed based on the formulations). When selecting DPIs for the development of DPI formulations type of DPI formulations should be taken into consideration. Alternatively, DPI formulations can be developed together with developing new devices. The successful inhaled GLP-1 product will provide an alternative treatment option for people with Type 2 diabetes by eliminating the use of subcutaneous injection and improve patient compliance and adherence to treatment and consequently quality of life affected by injection treatment. Therefore, pharmacokinetics and pharmacodynamics profiles of inhaled SD GLP-1 powders can be further investigated in animal models for the feasibility of systemic pulmonary delivery of GLP-1 for Type 2 diabetes therapy.

Chapter 7. Perception of patients with Type 1 diabetes on insulin inhalers: An online survey

7.1. Abstract

An online survey consisting of 28 questions was performed to assess insulin inhaler acceptability by people with Type 1 diabetes mellitus (T1DM). A total of 390 participants with T1DM completed the survey and 73.4% of participants were willing to try insulin inhalers. Insulin inhaler acceptability was significantly associated with many factors, such as age, compliance level of current insulin treatment, duration of insulin use, and the National Health Service (NHS) availability. Participants aged 19-25 (84.5%) were the most willing to try insulin inhalers, whereas participants aged over 60 (53.8%) showed resistance to trying insulin inhalers ($p=0.001$). Participants with low compliance and poor satisfaction levels towards their current insulin therapy showed willingness to try insulin inhalers ($p<0.0005$). Participants on insulin for a shorter period were more likely to request insulin inhalers on the NHS if available ($p=0.001$). Participants' interest and perception had a significant impact on their willingness to try insulin inhalers ($p<0.0005$). 94.1% of participants with positive perception would try insulin inhalers. Participants generally accepted the idea of insulin inhalers. However, many participants were not aware of insulin inhalers. 86.9% of participants had very poor or poor knowledge of insulin inhalers. 50.8% of participants reported not enough information as the main barrier to try insulin inhalers. It can be suggested that more information should be available with easy access for more awareness of the idea of delivering insulin via the lung.

Keywords: Insulin dry powder inhalers, Type 1 diabetes mellitus, Inhaler device, Pulmonary drug delivery

7.2. Introduction

So far, two inhaled insulin products; Exubera[®] approved by the U.S. Food and Drug Administration (FDA) and the European Medicines Agency in 2006 and Afrezza[®] approved by FDA in 2014 have reached the market for the therapeutic indications of both Type 1 diabetes mellitus (T1DM) and

Type 2 diabetes mellitus (T2DM) (Al-Tabakha, 2015). Afrezza® is currently available in the USA whereas Exubera® was withdrawn from the market only one year after the FDA approval due to low product sales attributed to several factors (e.g., design of the inhaler device, poor acceptability from patients and physicians, difficult dose equivalence system) (Chapter 1.1.4) (Al-Tabakha, 2015, Fleming, Fleming & Davis, 2015, Easa et al., 2019). Exubera® used the bulky design of the inhaler device (30 cm when extended for inhalation) leading to poor patient acceptability and poor sales. This resulted in the product withdrawal. The device design was not based on the patient's perspective (Chapter 1.1.4, Chapter 2.5.1 and 2.5.8)(Al-Tabakha, 2015).

In 2006, a small-scale study consisting of only four questions was conducted over the phone by Diabetes UK to find out what factors affecting the lifestyle of patients with diabetes on SC insulin therapy, whether patients switch to insulin inhalers if available and perceived potential advantage and disadvantage of insulin inhalers (Diabetes UK, 2006). The results of the phone interview revealed that injection related factors such as frequency of injection, pain, fear of needles, injection in public were affecting patient's quality of life. Concerns about the size of the device for inhaled insulin (e.g., big devices would affect transportability) were raised (Diabetes UK, 2006). Over three quarters of participants stated, they would consider using inhaled insulin as it would be easier to administer insulin compared to injection also avoiding many injections would be an advantage (Diabetes UK, 2006). However, this study involved only 26 participants with diabetes (Diabetes UK, 2006). It is important to design dry powder inhaler devices from patient's perspective for improved patient compliance and adherence to therapy which is associated with better treatment outcomes (Chapter 2.5.1) (Levy et al., 2019). Since pulmonary drug delivery is an attractive non-invasive route of drug administration alternative to injections for the management of diabetes, the aim of the study was to carry out a large-scale study to explore patient's perspective on insulin inhalers and assess insulin inhaler acceptability and see if there is a demand for the UK market. Insulin inhalers are not currently available in the UK.

7.3. Subjects, materials, and methods

7.3.1. Participants

The target population of the study was T1DM patients who reside in the UK in any age group and are on SC insulin therapy. The exclusion criteria were those living outside the UK and T2DM patients

(i.e., non T1DM patients). The sample size was calculated based on the number of people with T1DM in the UK (i.e., 400,000, 8% of 4.9 million stated in Introduction 7.2) using the sample size calculator, Raosoft® (Raosoft, US) (Raosoft, 2020). The minimum recommended sample size of the survey was 384 with a 95% confidence level and 5% margin of error. The survey study was approved by the Delegated Ethical Approval Committee of Kingston University London on the 24th January 2019.

7.3.2. Questionnaire and data collection

An online survey was created using Survey Monkey® (Momentive Inc., US) and promoted on forums (Diabetes.org.uk, Diabetes.co.uk and Facebook groups) for patients with T1DM. The online survey was made available for seven weeks between February to March 2019. The survey consisted of 28 questions divided into five sections: participant information, opinions on injecting insulin, knowledge of insulin inhalers, insulin inhalers, and patient demographics (See **Appendix 1**). Section one was related to participants' history of insulin therapy along with complications they experience/suffer and included smoking status and respiratory conditions to assess their eligibility of using insulin inhalers. Both inhaled insulin products (i.e., Exubera® and Afrezza®) are not recommended in patients who smoke or have recently stopped smoking and contraindicated in patients with chronic pulmonary diseases such as asthma and chronic obstructive pulmonary disease (COPD) due to reduced lung function and acute bronchospasm risk (Al-Tabakha, 2015, Kim, Plosker, 2015). Section two asked about participants' opinions on insulin regime and injection. Section three was related to participants' knowledge of insulin inhalers. Section four was aimed at examining participants' perception of insulin inhalers and provided pictures and brief descriptions of each seven different inhalers selected (i.e., Exubera®, Afrezza®, 3M™, Twist+, Turbohaler®, Handihaler® and Relvar® Ellipta®) that participants were asked to rate their preferences of inhalers. The brief descriptions provided in the questionnaire are as follows. Exubera® require placing a blister containing insulin powder and administered using an inhaler device with a clear holding chamber that allows seeing inside. Afrezza® is a compact and portable disposable inhaler without cleaning or maintenance necessary. Afrezza® also requires placing a cartridge (three different units; 4, 8 and 12 unit available) into the inhaler. 3M™ (3M, 2016, Life Science Integrates, 2019) and Twist+ (Yanko Design, 2014) are not yet available in the market. The features of the 3M™ device include an electronic display to provide instructions, record and store the patient's inhaled dose information. All the data recorded with every use can be accessed on a smartphone and shared with family or doctors. Twist+ can send reports on smartphone applications also remind the user if they forgot the inhaler at home. Turbohaler®, Handihaler® and Relvar® Ellipta® are all currently available inhalers for asthma and

COPD in the market. Turbohaler® has the dose indication feature that shows the number of puffs available and produces a sound when the dose is correct by twisting forward and backward. Turbohaler® requires a deep breath when it is used. Handihaler® is a portable inhaler and requires a capsule insertion with every use. Relvar® Ellipta® contain a month unit pre-filled drug formulation and has a dose counter window. Lastly, Section five was about participant demographics (gender, age, ethnic background). The survey employed various types of questions, such as multiple choice (multiple answer options, tick all that apply), contingency (i.e., “Will you be willing to try insulin inhalers?” If no move to other question), dichotomous (i.e., “Do you have any information about insulin inhalers?” Yes or No), rating scale (e.g., 1= least preferred to 10= most preferred), Likert scale with five levels (e.g., very satisfied, satisfied, neither satisfied nor unsatisfied, unsatisfied, very unsatisfied), and open ended questions (e.g., state any additional answers). Approximately 10 mins were required to complete the questionnaire. Completing the survey was considered as consenting to participate in the study. The survey was completed anonymously, and only non-identifiable information was collected.

7.3.3. Statistical analysis

Statistical analysis was performed using SPSS® version 24.0 (IBM, UK) and Microsoft® Excel. Data was reported as frequencies with percentages. To examine data for associations, the bivariate correlation analysis (Pearson correlation coefficient, r and Spearman correlation coefficient, r_s) and Chi-square tests were used. p-values less than 0.05 ($p < 0.05$) were considered statistically significant.

7.4. Results

A total of 393 participants completed the survey. Of these participants, three were excluded because they did not have Type 1 diabetes which was not the inclusion criteria. Thus, the number of responses were 390 which were included in the analysis.

7.4.1. Demographics and characteristics of participants

The demographics of participants with T1DM (309 participants provided their gender, age, and ethnic background) are presented in Table 42. Participants were predominantly females (71.8%,

n=222) and 27.2% (n=84) were males. The modal age category of participants was 41-59 (32.0%, n=99) and only 3.6% of participants were under 12 years (n=11). 60.0% (n=234/390) of participants were on insulin for over 10 years. More than half of participants were on NovoRapid® insulin type (53.8 %, n=210/390). 84.9% (n=331/390) of participants were non-smokers and 82.1% (n=320/390) did not have any pulmonary diseases. Therefore, 15.1% (n=59/390) of participants who smoke or stopped smoking within 6 months and 17.9% (n=70/390) of participants who have respiratory conditions would not be eligible to use insulin inhalers due to their smoking status and pulmonary diseases, respectively.

Table 42: Demographics of participants with Type 1 diabetes (n=309, excluded incomplete responses (n=81) for gender, age, and ethnic background questions).

Age category (years)	Male n=84 (27.2%)	Female n=222 (71.8%)	Other n=3 (1.0%)
Under 12	4 (1.3)	6 (1.9)	1 (0.3)
12-18	5 (1.6)	13 (4.2)	0
19-25	17 (5.5)	41 (13.2)	0
26-40	25 (8.1)	72 (23.3)	0
41-59	29 (9.4)	68 (22.0)	2 (0.6)
Over 60	4 (1.3)	22 (7.2)	0
Ethnic Background			
White British	42 (13.6)	149 (48.4)	1 (0.3)
White Other	22 (7.1)	47 (15.2)	2 (0.6)
Black African	4 (1.3)	3 (1.0)	0
Black Other	1 (0.3)	0	0
Chinese	5 (1.6)	0	0
Indian	2 (0.6)	5 (1.6)	0
Pakistani	3 (1.0)	1 (0.3)	0
Asian Other	1 (0.3)	0	0
Other	3 (1.0)	11 (3.6)	0
Prefer not to say	1 (0.3)	6 (1.9)	0
Duration of insulin use (years)			
<1 year	5 (1.6)	15 (4.8)	0
1-3 years	14 (4.5)	33 (10.7)	1 (0.3)
4-6 years	13 (4.2)	18 (5.8)	1 (0.3)
7-9 years	9 (2.9)	12 (3.9)	0
Over 10 years	43 (13.9)	144 (46.6)	1 (0.3)
Insulin type			
NovoRapid®	45 (14.5)	127 (41.0)	2 (0.6)
Humalog®	23 (7.4)	54 (17.4)	0
Levemir®	30 (9.7)	40 (12.9)	1 (0.3)
Lantus®	21 (6.8)	42 (13.5)	0

Humulin S®	0	5 (1.6)	0
Humulin I®	1 (0.3)	1 (0.3)	0
Novomix®	1 (0.3)	0	0
Other	20 (6.5)	77 (24.8)	1 (0.3)
Smoking status			
Smoker	19 (6.1)	24 (7.8)	1 (0.3)
Non-smokers	62 (20.1)	195 (63.1)	2 (0.6)
Stopped less than 6 months ago	3 (1.0)	3 (1.0)	0
Suffering from any respiratory conditions			
Yes	17 (5.5)	41 (13.3)	0
No	67 (21.7)	181 (58.6)	3 (1.0)

45.4% of participants (n=177/390) reported suffering from hypoglycaemia once a week followed by once a day (18.5%, n=72/390) whereas 31.8% of participants (n=124/390) were suffering from hyperglycaemia once a day followed by once a week (27.2%, n=106/390). Only 2.6% (n=10/390) and 2.3% (n=9/390) participants never suffered from hypoglycaemia and hyperglycaemia, respectively. The main drawbacks of injecting insulin stated by participants (n=382) were inconvenience (34.6%, n=132/382), weight gain (13.4%, n=51/382) and complexity of the regimen (12.6%, n=48/382). Less than 10% of participants selected pain (8.6%, n=33/382), hypoglycaemia (7.3%, n=28/382) and problems with locating the injection site (7.1%, n=27/382) as limitations of their current insulin injection treatment. Fear of needles (4.7%, n=18/382) was selected as the least disadvantage. Other responses stated by participants (11.8%, n=45/382) include “not flexible or slow response to injected insulin” (13.3%, n=6/45), “everything” (11.1%, n=5/45), and “multiple injections a day” (6.7%, n=3/45).

7.4.2. Perception towards insulin inhalers

81.2% (n=225/277) of participants had no information about insulin inhalers. 86.9% of participants had very poor or poor knowledge of insulin inhalers (n=326/375), whereas only 2.1% (n=8/375) of participants rated their knowledge as very good (Figure 78A). 73.4% of participants (n= 229/312) stated willing to try insulin inhalers (Figure 78B). Regardless of having information or not, over 70% of participants were still willing to try insulin inhalers (Figure 78C). This result showed no significant association between participants' information status and willingness of taking insulin inhalers (p=0.635) (Table 43). 50% of participants with very good knowledge and understanding of insulin

inhalers showed their willingness to try or not to try insulin inhalers (Figure 78D). Then the poorer the knowledge participants had, their willingness to try insulin inhalers increased whereas their knowledge status became higher, their willingness to use insulin inhalers declined. However, there was no significant association between participants' knowledge level about insulin inhalers and willingness to try insulin inhalers ($r_s=-0.081$, $p=0.154$) (Table 43).

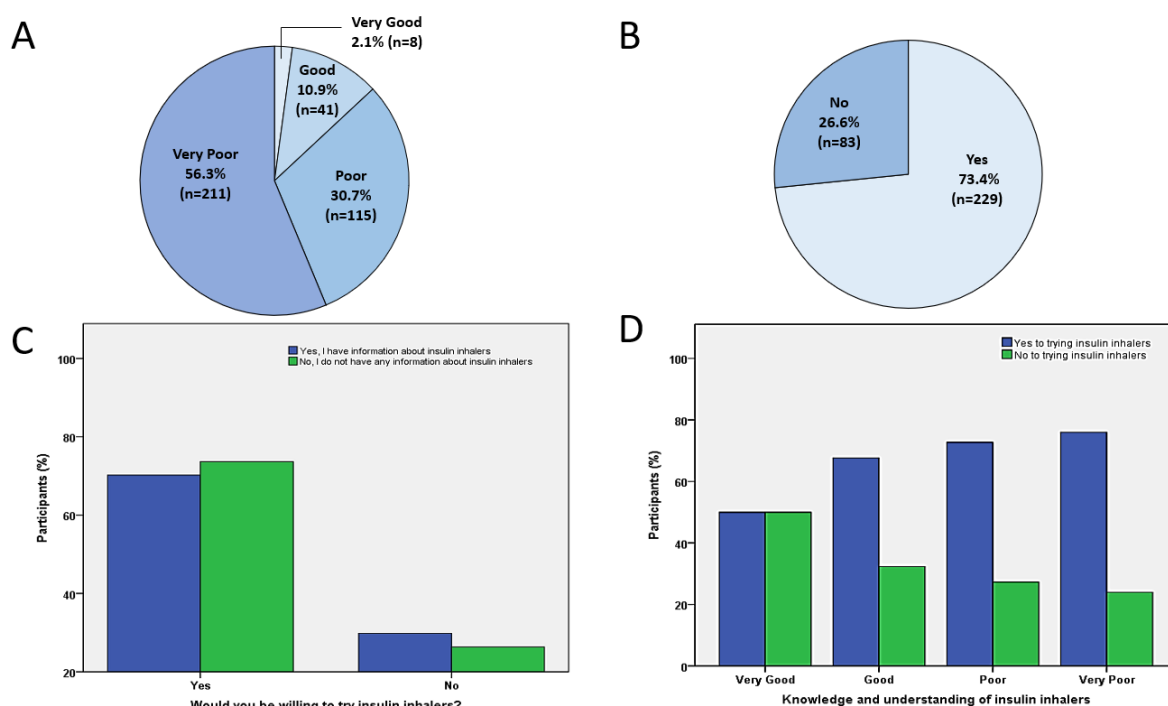


Figure 78: Participants' knowledge and understanding level of insulin inhalers (n=375) (A), participants' willingness to try insulin inhalers (n=312) (B), participants' willingness to try insulin inhalers based on information status about insulin inhalers (n=233) ($p=0.635$) (C), participants' willingness to try insulin inhalers based on their level of knowledge and understanding of insulin inhalers (n=312) ($p=0.154$) (D).

Participants were asked about reasons towards not to try insulin inhalers in a multiple-choice question. Figure 79A shows that not enough information (50.8%, $n=198/390$) was the main barrier to try insulin inhalers followed by undesirable side effects associated with insulin inhalers such as cough and throat irritation (39.2%, $n=153/390$) which were stated in the questionnaire. Only 9.7% of participants ($n=38/390$) selected lung capacity test requirement as a barrier. Some of other responses (17.7%, $n=69/390$) were "accuracy issues and concerns about small dose availability or

dose flexibility” (43.5%, n=30) and “safety concerns and long-term impact on the lungs” (13.0%, n=9). Important features of insulin inhalers were rated by participants who were interested in insulin inhalers, from 1 (not important) to 10 (very important) in a rating scale question (Figure 79B). 69.0% of participants (n=191/277) rated effectiveness as a very important feature of inhalers followed by easy to use (47.1%, n=130/276) and convenience (44.4%, n=123/277) while style (colour/design) (39.8%, n=109/274) and personalise (34.1%, n=93/273) were found to be not important (Figure 79B). There was a significant association between all the features of insulin inhalers and participants' willingness to try insulin inhalers ($p < 0.001$) (Table 43). Participants also rated each of seven selected inhalers from 1 (least preferred) to 10 (most preferred) based on the pictures and information provided in the questionnaire (Section 7.3.2). Figure 79C shows that the non-marketed inhaler, 3M™ was selected as the most preferred inhaler (33.1%, n=93/281) followed by Relvar® Ellipta® (15.3%, n=31/202) and Afrezza® (11.7%, n=32/273) while Exubera® was selected as the least preferred inhaler (49.1%, n=134/273)(Figure 79C). Overall, Handihaler®, Turbohaler® and another non-marketed inhaler, Twist+ seemed to be the neutral design as participants rated these inhalers as '5' the most (mode responses) (Figure 79C). In addition, the most and least preferred inhalers based on gender (male and female) were identified. For data analysis purposes, the rating scale between 7 and 10 were regarded as preferred and most preferred whereas 1-3 were regarded as least preferred. It was found that the non-marketed 3M™ inhaler was the most preferred inhaler in both males (52.6%, n=40/76) and females (67.0%, n=134/200) (Figure 79D). However, there was a significant association observed between 3M™ and gender ($r_s = 0.126$, $p = 0.035$) presenting that female were more likely to select 3M™ than males. The second most preferred inhaler was Afrezza® for males (46.5%, n=33/71) and Relvar® Ellipta® for females (46.4%, n=65/140) followed by Relvar® Ellipta® for males (32.2%, n=19/59) and Twist+ for females (34.9%, n=68/195). The choice of Afrezza® and Relvar® Ellipta® was significantly associated with gender ($r_s = -0.192$, $p = 0.002$ and $r_s = 0.161$, $p = 0.023$, respectively), but no statistical significance was observed between Twist+ and gender ($r_s = -0.020$, $p = 0.739$). Afrezza® was more likely male choice, whereas Relvar® Ellipta® was more likely female choice. Afrezza® was selected as the second least preferred inhaler for females (39.1%, n=77/197). There was no significant correlation observed between the rest of the inhalers and gender ($p > 0.05$). Exubera® was the least choice of inhaler in both males (67.1%, n=49/73) and females (69.2%, n=135/195) ($r_s = -0.016$, $p = 0.795$).

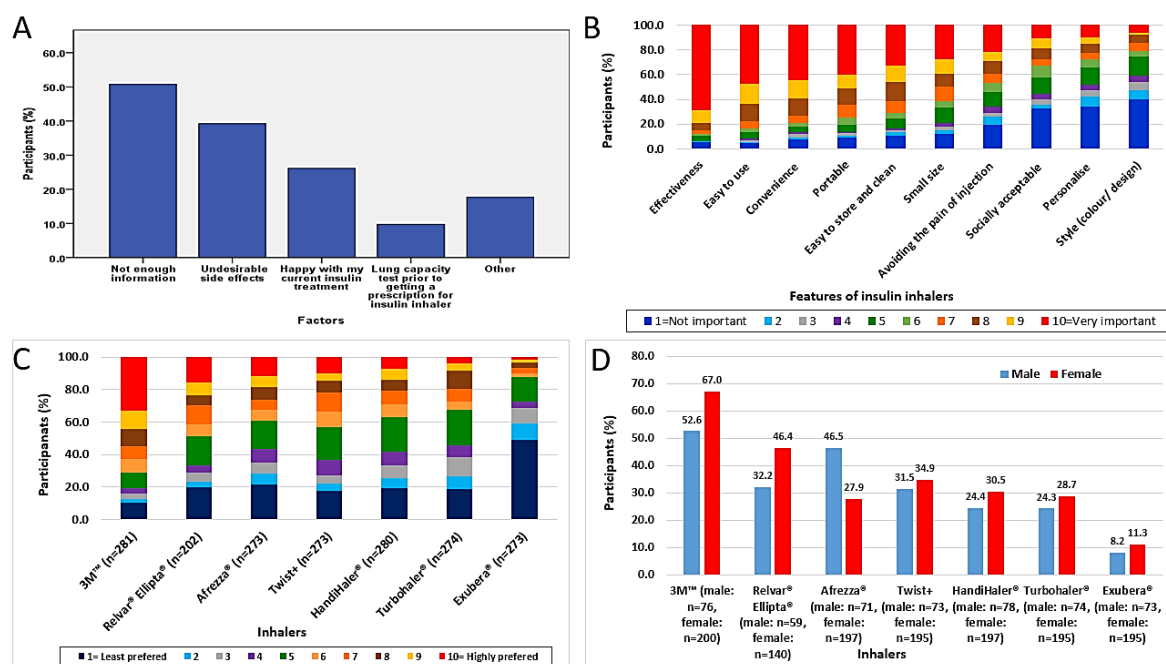


Figure 79: Reasons not to use insulin inhalers (n=390) (A), features of insulin inhalers rated on a scale from 1 (not important) to 10 (very important) (B), participants' preferences for different inhalers rated on a scale from 1 (least preferred) to 10 (highly preferred) (C), male and female preferred inhalers based on a scale between 7 (preferred) and 10 (highly preferred) (D).

7.4.3. Factors that affect insulin inhaler acceptability

In order to investigate what factors affect participants' willingness to try insulin inhalers, participants were asked about their compliance and satisfaction level of current insulin regimen, duration of insulin use, interest in insulin inhalers, perception towards insulin inhalers over injections, and previous experience of using any inhalers. In addition, insulin inhaler acceptability was assessed if it were to be available on the NHS. Possible factors affecting insulin inhaler acceptability are presented in Table 43. In this survey, no significant association was observed between gender and participants' willingness to try insulin inhalers ($p=0.304$), however, there was a significant association between age and their willingness ($r_s=0.186$, $p=0.001$). Participants aged 19-25 (84.5%, $n=49$) showed the highest willingness to try insulin inhalers followed by participants aged 26-40 (78.4%, $n=76$), 12-18 (77.8%, $n=14$), under 12 (72.7%, $n=8$) and then 41-59 (68.7%, $n=68$) (Figure 80A). The age group over 60 was least likely to try insulin inhalers (53.8%, $n=14$) (Figure 80A). Participants aged under 60 were more willing to try insulin inhalers than the ones aged over 60. There was also a significant association between NHS availability and participants' willingness to try insulin inhalers ($r_s=0.569$, $p<0.0005$) (Table 43). Although the modal response was 'unsure' (36.2%, $n=113/312$) for questions related to NHS availability (Figure 80B-D). 74.6% of participants ($n=291/390$) had high self-rated

compliance towards their current insulin therapy and their compliance was significantly associated with age ($r_s=0.180$, $p=0.001$). Participants aged 19-25 showed low compliance whereas participants aged over 26 showed higher compliance. Participants' compliance level was significantly associated with their insulin inhaler acceptability on the NHS ($r=0.244$, $p<0.0005$). Participants with low compliance were more likely to request insulin inhalers if available on the NHS, while participants with higher compliance were less likely to request insulin inhalers on the NHS (Figure 80B). Participants' insulin inhaler acceptability on the NHS was also significantly influenced by their satisfaction level with their current insulin treatment ($r=-0.367$, $p<0.0005$). Participants unsatisfied with their current insulin treatment were likely to request insulin inhalers if available on the NHS, while participants satisfied with their current insulin treatment were less likely to request insulin inhalers on the NHS (Figure 80C). However, 33.3% of participants who were very unsatisfied with their current insulin treatment were still highly unlikely to request insulin inhalers on the NHS (Figure 80C).

Participants' insulin inhaler acceptability if available on the NHS was significantly associated with the duration of insulin therapy ($r_s=0.185$, $p=0.001$). Figure 80D shows that 50.0% of participants on insulin for less than a year were highly likely or likely to request insulin inhalers if available on the NHS. This was followed by participants who were on insulin for 1-3 years (49.0%), for 4-6 years (37.5%), 7-9 years (33.3%) and for over 10 years (30.0%) (Figure 80D). Participants on insulin for a shorter period were more likely to request insulin inhalers on the NHS and participants on insulin for over 10 years were highly unlikely or unlikely (32.6%) to request insulin inhalers on the NHS (Figure 80D). Regardless of satisfaction level of their current insulin treatment, participants who were on insulin for over 10 years showed resistance to changing their regimes to insulin inhalers. Also, it was found that participants' interest in insulin inhalers had a significant impact on their willingness to try insulin inhalers ($p<0.0005$) (Table 43). 90.4% ($n=189/209$) of participants who would like to know more about insulin inhalers would be willing to try insulin inhalers while 61.2% of participants who had no interest would not try insulin inhalers ($n=63/103$). Further, participants' interest in insulin inhalers was significantly associated with the duration of insulin use ($r_s=0.134$, $p=0.01$). Participants on insulin for 4-6 years showed the highest interest in finding out more about insulin inhalers (76.3%, $n=29/38$) whereas participants on insulin for over 10 years showed the least interest in insulin inhalers (60.8%, $n=138/227$) (Figure 80E). Participants' perception towards insulin inhalers over injections showed a significant impact on their willingness to try insulin inhalers ($p<0.0005$). Over 60% of participants (61.9%, $n=192/310$) corresponded that insulin inhalers were not appropriate method of taking insulin. However, 60.4% of those participants ($n=116/192$) still considered trying it (Figure 80F). For participants who considered inhaling insulin as appropriate

method (38.1%, n=118/310), 94.1% of these participants (n=111/118) showed their willingness to try insulin inhalers (Figure 80F). It was found that participants' perception towards insulin inhalers were not dependent on the duration of insulin use (p=0.078) or insulin inhaler's information status (p=0.455). Generally, participants on insulin for over 10 years (65.6% n=124/189) had the most negative perception about insulin inhalers (i.e., not appropriate method). Previous experience of using any type of inhalers (p=0.869) and brand of participants' current insulin treatment (p=0.403) had no significant impact on participants' willingness to try insulin inhalers (Table 43).

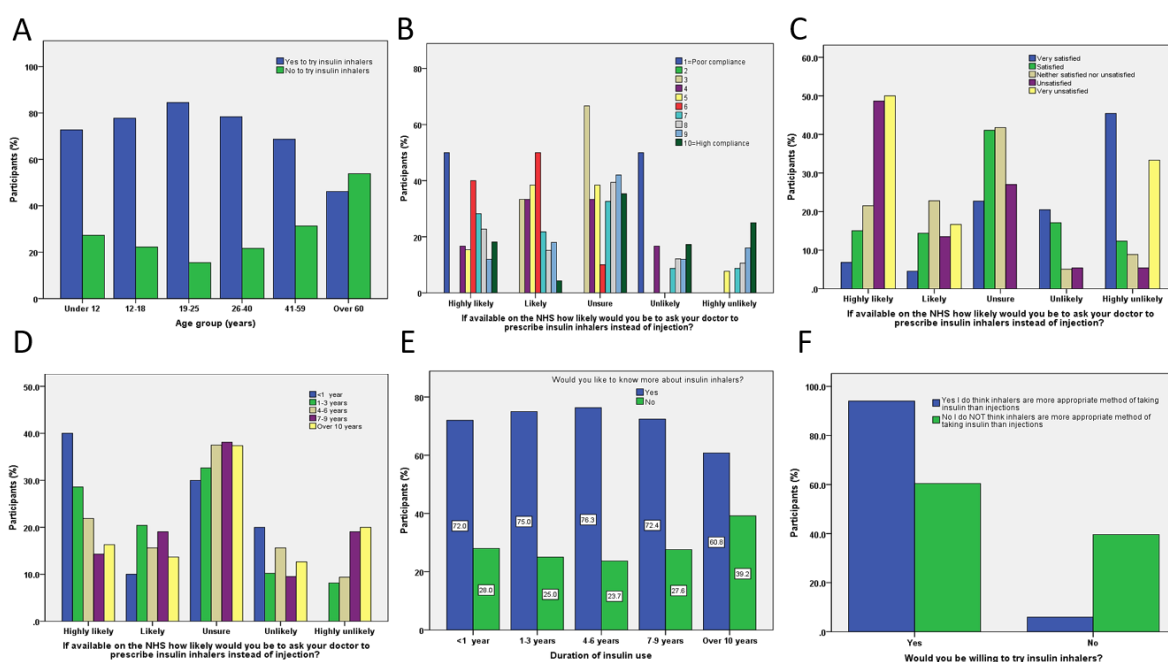


Figure 80: Participants' willingness to try insulin inhalers in accordance to age group (n=309) (p=0.001) (A), participants' insulin inhaler acceptability if available on the NHS based on their self-rated compliance level towards current insulin treatment (n=312) (p<0.0005) (B), participants' insulin inhaler acceptability if available on the NHS based on their current insulin treatment satisfaction level (n=312) (p<0.0005) (C), participants' insulin inhaler acceptability if available on the NHS based on the duration of insulin use (n=312) (p=0.001) (D), participants' interest in insulin inhalers based on the duration of insulin use (n=375) (p=0.01) (E), participants' willingness to try insulin inhalers based on participants' perception (inhalers versus injections) (n=310) (p<0.0005) (F).

Table 43: Factors affecting and not affecting insulin inhaler acceptability.

Factors affecting insulin inhaler acceptability	P value	Factors NOT affecting insulin inhaler acceptability	P value

Features of insulin inhalers	P<0.001	Having information about insulin inhalers	P=0.635
Age	p=0.001	Level of knowledge and understanding of insulin inhalers	P=0.154
NHS availability	P<0.0005	Gender	p=0.304
Compliance level of current insulin treatment	P<0.0005	Previous experience of inhaler use	P=0.869
Satisfaction level of current insulin treatment	P<0.0005	Brand of participants' current insulin treatment	P=0.403
Duration of insulin therapy if available on NHS	p=0.001		
Participants' interest in insulin inhalers	P<0.0005		
Participants' perception towards insulin inhalers over injections	P<0.0005		

7.5. Discussion

This study showed limitations of injecting insulin that participants faced with their current insulin therapy and participants' perception towards insulin inhalers. Participants' insulin inhaler acceptability was assessed by identifying factors affecting their willingness to try insulin inhalers. In addition, participants' preferences for different inhaler devices were presented. Participants found their current insulin therapy inconvenient (34.6%) and complex (12.6%). This reflected the importance of insulin inhaler's features and supported the reasons behind Exubera®'s withdrawal. The main important features of insulin inhalers stated by participants were found to be effectiveness (69.0%), ease of use (47.1%) and convenience (44.4%). Dekhuijzen *et al.* (2016) also reported that simplicity, ease of use and convenience, which implies size, portability, and ease of cleaning, were important factors for any inhaler devices to maintain patient's treatment. Complexity of inhaler devices could lead to poor patient adherence to treatment (Dekhuijzen, Lavorini & Usmani, 2016). Therefore, the features of insulin inhalers should be taken into consideration for improved patient acceptability which can lead to improved patient's compliance and adherence to therapy. Participants who took part in the survey considered that injection related factors such as pain (8.6%), problems with locating the site (7.1%) and fear of needles (4.7%) were less disadvantageous. This could be attributed that 60.0% of participants were on insulin for long (over 10 years). In terms of adverse event related factors, 13.4% of participants were concerned about weight gain and only 7.3% of participants reported hypoglycaemia as a drawback of injecting insulin. However,

participants declared suffering from hypoglycaemia once a week (45.4%) or once a day (18.5%) and some participants experienced hypoglycaemia 2-4 times a week. According to a study conducted by Farsaei *et al.* (2014) to assess the barriers to insulin injection in patients with T1DM, factors influencing patient adherence to insulin injection therapy were mainly related to the injection itself such as time consuming for administration (92.8%), difficulty of injection (90.8%), syringe based regimen (90.8%), and injection site pain (70.1%) (Chapter 1.1.4) (Farsaei *et al.*, 2014). Adverse event related factors included fear of hypoglycaemia (78.9%); however, weight gain was not a concern (0.8%) (Farsaei *et al.*, 2014). On the other hand, Santos and Edelman (2014) and Kim and Plosker (2015) reported that patients would be reluctant to start insulin therapy due to injection related limitations (inconvenience, anticipated pain and injection phobia) and insulin adverse events (fear of hypoglycaemia and weight gain) (Santos Cavaiola, Edelman, 2014, Kim, Plosker, 2015). These findings were slightly different from study to study; however, disadvantages associated with SC insulin therapy were generally consistent. Participants facing limitations of SC insulin therapy would benefit from inhalation route of drug administration. Slow response to injected insulin was also reported as a disadvantage by some participants. Exubera[®] exhibited rapid absorption (onset time: 10-20 min, t_{max} : 38-78 min) comparable to SC rapid acting insulin lispro (onset time: 15-30 min, t_{max} : 30-90 min) and faster than regular human insulin (onset time: 30 min, t_{max} : 48-120 min) in patients with T1DM and T2DM (Al-Tabakha, 2015). Afrezza[®] demonstrated faster absorption (t_{max} : 12-15 mins) than SC insulin lispro in T1DM patients (Chapter 1.1.4) (Sang M. Chung, Manoj Khurana, 2013, Al-Tabakha, 2015, Kim, Plosker, 2015). Afrezza[®] demonstrated less severe hypoglycaemia incidence (18.4% vs 29.2%; $p=0.0156$) and lost body weight (average of 0.4 kg weight **loss**) when compared to T1DM patients on SC insulin aspart (average of 0.9 kg weight **gain**, $p=0.0102$) (Kim, Plosker, 2015). In this study, 73.4% of participants showed their willingness to try insulin inhalers which is consistent with the results of the small telephone survey ($n=26$) conducted by Diabetes UK in 2006 (Introduction 7.2)(Diabetes UK, 2006). Not enough information (50.8%) and undesirable side effects (39.2%) associated with inhaled insulin were found to be the main barriers to try insulin inhalers. Cough was reported as the most common adverse event associated with Afrezza[®]; however, it was mild and diminished over time (Kim, Plosker, 2015). The requirement of spirometry tests for pulmonary function prior to the initiation of inhaled insulin is usually considered as a burden for patients and healthcare professionals (Heinemann, 2018). However, this survey result showed that it was not the main concern (9.7%) for participants to try insulin inhalers. Participants raised dosing related concerns such as accuracy, small dose availability or dose flexibility (43.5%) and safety concerns such as long-term impact on the lungs (13.0%) as barriers to try insulin inhalers. In contrast to insulin injections with 0.5-unit adjustment possible, insulin inhalers might face a limitation of

dosing flexibility as Afrezza® offers the unit starting with 4 units (Oleck, Kassam & Goldman, 2016). There were two cases of lung cancer reported for patients with a history of smoking during two clinical trials with Afrezza®, which was a small incidence rate and smoking history could be the risk factor (Afrezza® are not recommended in patients who smoke stated in Section 7.3.2) (Al-Tabakha, 2015). However, due to no sufficient data available yet a post-marketing clinical trial recommended by the FDA would be required in order to evaluate the potential risk of lung cancer associated with Afrezza® (Al-Tabakha, 2015).

This study identified participants' inhaler device preferences. The non-marketed inhaler, 3M™ which is not available for commercial sale (Life Science Integrates, 2019) and will be developed in partnership with a pharmaceutical company (3M, 2016) was the most preferred inhaler in both males (52.6%) and females (67.0%). However, females selected 3M™ more than males ($p=0.035$). The second most preferred inhalers, Afrezza® selected by males (46.5%) and Relvar® Ellipta® selected by females (46.4%) were also significantly associated with gender. This could indicate that females would like to have the feature of 'display' in their insulin inhaler to check the dose status. However, incorporating electronic features with dose recoding systems will lead to high cost of manufacturing (Dekhuijzen, Lavorini & Usmani, 2016). Like 3M™ in terms of having a display in the inhaler device, Relvar® Ellipta® has a dose counter window that displays starting number (GlaxoSmithKline, 2021) whereas Afrezza® does not have such a display window. Afrezza® requires placing a cartridge (MannKind Corporation, 2021) as well as Handihaler® requires placing a capsule with every use (Boehringer Ingelheim International GmbH, 2018). Females selected Handihaler® (30.5%) as a more preferred inhaler over Afrezza® (27.5%) and selected Afrezza® as the second least preferred choice (39.1%). This could be suggested that the design of Afrezza® was not favoured by females.

The online survey revealed that insulin inhaler acceptability was significantly associated with many factors; age, compliance and satisfaction level of current insulin treatment, duration of insulin use, NHS availability, participant's interest in insulin inhalers and perception towards insulin inhalers over injection (Table 43). Participants generally showed high compliance towards their current insulin therapy (74.6 %) and their compliance was dependent on age ($p=0.001$). These results are in line with the study conducted by Farsaei *et al.* (2014) indicating that patients with T1DM (85.7%) were adherent to insulin therapy as patients with T1DM would be aware that insulin therapy is necessary due to insulin secretion deficiency (Farsaei *et al.*, 2014). It was also reported that young patients with T1DM had poor adherence to insulin therapy (Farsaei *et al.*, 2014). These findings reflected participants' willingness to try insulin inhalers and insulin inhaler acceptability on the NHS.

Participants aged 19-25 (84.5%) were the most willing to try insulin inhalers, whereas participants

aged over 60 (53.8%) showed resistance to trying insulin inhalers ($p=0.001$). Further, the likelihood of requesting insulin inhalers if available on the NHS was higher amongst participants who had lower self-rated compliance and poor satisfaction levels towards their current insulin therapy ($p<0.0005$). The duration of participants' insulin use also had a significant influence on their insulin inhaler acceptability on the NHS ($p=0.001$). Participants' willingness to try insulin inhalers was dependent on participants' interest ($p<0.0005$) which was based on the duration of insulin use ($p=0.01$) and perception towards insulin inhalers over injections ($p<0.0005$). Insulin users for a shorter period were more likely to request insulin inhalers on the NHS if available ($p=0.001$). Participants on insulin for over 10 years and aged over 60 were not interested in switching to a new treatment regimen as they showed resistance to trying or requesting insulin inhalers on the NHS due to no interest or having negative perception about them. When participants had high interest and positive perception towards insulin inhalers, over 90% of participants showed willingness to try insulin inhalers. However, over one-third of participants (36.2%) were generally unsure whether to request insulin inhalers if available on the NHS. Majority of participants were not aware of insulin inhalers (81.2%) and had very poor or poor knowledge of insulin inhalers (86.9%). If participants had enough information, the results might have been different. Insulin inhalers might be of benefit to those participants who are not satisfied with their current SC insulin treatment. According to the phase 3 clinical trial (NCT00309244) for the assessment of patient reported outcomes in adults with T2DM using Afrezza[®] and basal insulin (insulin glargine) or premixed aspart insulin 70/30, treatment with Afrezza[®] did not have a negative impact on health-related quality of life and resulted in improved treatment satisfaction and perceptions of insulin therapy therefore reduced their worries towards diabetes (Peyrot, Rubin, 2011, Kim, Plosker, 2015).

7.6. Conclusion

This study showed that participants generally accepted the idea of insulin inhalers. Participants' willingness to try insulin inhalers was dependent on their interest in insulin inhalers and perception towards insulin inhalers over injections. Since majority of participants were not aware of insulin inhalers, more information should be available with easy access for more awareness of the idea of delivering insulin via the lung. The features of insulin inhalers preferred by participants such as effectiveness and ease of use should be incorporated to improve patient acceptability which would lead to high market acceptability. Participants (both male and female) favoured an inhaler that has the advanced design and features (electronic features). The development of insulin inhalers should

consider incorporating the features favoured by both genders however should be cost effective. NHS availability will be an important factor as participants' willingness to try insulin inhalers was significantly associated with NHS availability. Administering insulin by inhalation will improve patient compliance and adherence to therapy by reducing the burden of injection related barriers therefore improve patient's quality of life. The outcomes of this study can be used to reflect on the design of insulin inhalers for improved patient acceptability.

Chapter 8. Conclusion

This thesis has worked on the development of insulin and GLP-1 inhalation systems as an alternative treatment option to injectable antidiabetic medications for people with diabetes to improve patient compliance and adherence to treatment. Particle engineering was employed as a formulation strategy to improve the aerosolisation performance of DPI formulations containing insulin or GLP-1 and two different type of DPI formulations; carrier free and carrier-based DPI formulations were studied. This particle engineering approach focused on minimising cohesive forces naturally existing between drug particles by modifying particle morphology via spray drying. Spray freeze drying was used to produce porous carrier powders to aid and/or reduce interaction between drug and carrier particles therefore improve/facilitate flowability of drug particles and drug particle detachment from the carrier surface (drug-carrier detachment). In addition, SD drug particles were prepared in the absence of excipients to minimise the lung safety concern. The conclusions from this thesis are summarised as follows.

The study has demonstrated that both carrier free and carrier-based DPI formulations exhibited different aerosolisation performance (different *in vitro* lung drug deposition profiles, FPF). When carrier free DPI formulations were studied, FPF was higher than carrier-based DPI formulations as carrier free formulations skip the process of drug-carrier detachment upon inhalation. However, this type of formulation was associated with poor drug delivery efficiency (high drug loss) from the inhaler device (Handihaler®) compared to carrier-based DPI formulations. Drug particles in the aerodynamic diameter range of 1 μm to 5 μm were naturally cohesive (high degree of drug-drug agglomeration) associated with high inter-particulate forces between drug particles (drug-drug cohesive forces) therefore exhibited poor powder flow and low drug delivery efficiency. The studies within the thesis demonstrated that the addition of engineered SFD mannitol-based carrier to the formulations is a good formulation approach to improve the aerosolisation performance of drug particles and reduce drug loss. For carrier-based DPI formulations, only detached drug particles during inhalation reach the lungs and carrier is cleared by swallowing as carrier particles are designed not to reach the lungs. In Chapter 4, using the developed ^1H qNMR method (Chapter 3), higher SFD mannitol carrier deposition was retrieved from the AIT and stage 1 (above 11.719 μm cut-off diameter) compared to SD insulin powder deposition, while SD insulin deposition in stages 3-5 (below 3.988 μm cut-off diameter) was higher in comparison to SFD mannitol carrier deposition. SFD mannitol carrier exhibited a more marked oropharyngeal deposition pattern and successfully facilitated insulin deposition into the lower NGI stages (below stage 3). This suggests that the use of porous SFD mannitol carrier is feasible to enhance the aerosolisation performance of insulin and insulin delivery from DPI formulations. Further study in Chapter 6 demonstrated the advantages of

using SFD amino acid-mannitol carrier (SFD 10% glycine-mannitol) over non-engineered raw mannitol carrier. When the porous SFD 10% glycine-mannitol carrier was used, carrier-based DPI formulation containing SD GLP-1 aerosolised better from Handihaler® and exhibited higher GLP-1 delivered dose compared to DPI formulation with non-engineered raw mannitol carrier that resulted in low GLP-1 delivered dose with high drug loss (>74%) (Chapter 6). Chapter 5 and Chapter 6 both demonstrated that drug delivered dose was improved by the addition of engineered SFD 10% glycine-mannitol carrier to the DPI formulation when compared to carrier free DPI formulations. Overall, both carrier free and carrier-based DPI formulations have shown advantages with different challenges for pulmonary administration of insulin and GLP-1. The optimised DPI formulations can be achieved by using particle engineering to prepare engineered particles based on the type of DPI formulations, carrier free or carrier-based DPI formulations. However, carrier-based DPI formulations showed more complex *in vitro* pulmonary drug deposition performance as different carrier properties (e.g., morphology, surface roughness) affected drug-carrier detachment (*in vitro* drug deposition profiles) therefore the FPF (Chapters 4-6). The challenge for carrier-based DPI formulations is the effect of carrier properties on aerosolisation performance of drug particles thus the drug detachment from the carrier. In addition, changing a drug from insulin to GLP-1 influenced the drug aerosolisation performance (i.e., drug carrier detachment, FPF) while using the same carrier (SFD 10% glycine-mannitol carrier). In Chapter 5, SD insulin was used while SD GLP-1 was used in Chapter 6. Both SD drug particles exhibited similar particle size range of 1 µm to 5 µm suitable for pulmonary delivery with slightly different morphologies: the deformed/wrinkled raisin-like particles for SD insulin compared to dimpled particles for SD GLP-1. This resulted in different aerosolisation performance of carrier-based DPI formulations. Chapter 5 studied the aerosolisation performance of SD insulin DPI formulations where SFD 10% glycine-mannitol carrier facilitated SD insulin dry powder delivery from Handihaler® and drug-carrier detachment leading to optimum aerosolisation performance of SD insulin in terms of delivered dose, FPF and MMAD. The use of SFD 10% glycine-mannitol carrier improved the aerosolisation performance of DPI formulations containing SD insulin therefore could lead to higher insulin bioavailability (Chapter 5). Chapter 6 also showed improved SD GLP-1 dry powder delivery from Handihaler® when SFD 10% glycine-mannitol carrier was added to the formulation. However, using SFD 10% glycine-mannitol carrier exhibited poor drug carrier detachment (low FPF and large MMAD) (Chapter 6). The airflow generated by Handihaler® was found to be too low for sufficient drug-carrier detachment when SFD 10% glycine-mannitol carrier was used for SD GLP-1 DPI formulation (Chapter 6). These both studies in Chapter 5 and Chapter 6 suggest that the aerosolisation performance of carrier-based DPI formulations were dependent on both properties of drug and carrier powders as changing a drug while using the same carrier (SFD

10% glycine-mannitol carrier) changed the drug inhalation performance. This consequently affected the efficiency of pulmonary drug delivery (i.e., FPF) and overall aerosolisation performance of DPI formulations. Using a different drug with similar properties (i.e., particle size) can affect aerosolisation performance of DPI formulations.

Therefore, to further understand the mechanisms of drug particle detachment from the carrier surface, future studies should focus on the investigation of the surface properties (roughness) of both drug and carrier powders in addition to the use of SEM images. Such surface morphology can be examined by Atomic Force Microscopy (AFM). AFM is used to measure inter-particulate forces (cohesive and adhesive forces) based on the particle morphology/the surface roughness that can be used to characterise the aerosolisation performance (Shetty et al., 2020). The process of drug-carrier detachment is crucial for drug delivery to the lung in carrier-based DPI formulations. The efficiency of drug delivery via the lungs depends not only on the properties of DPI formulations but also on the choice of DPI device (design) together with patient factors (e.g., lung anatomy and physiology, health condition, disease states) and patients' inhalation profiles (e.g., inspiratory flow rate). Inhaler devices with high resistance such as Handihaler® might not be the ideal inhaler device of choice for carrier-based DPI formulations. Higher inspiratory flow would be required for drug-carrier detachment. Therefore, inhaler devices with low resistance (use higher flow rate) can be tried for future studies as they might be more applicable for the process of drug-carrier detachment in carrier-based DPI formulations. In addition, future studies should include scale-up studies in the preparation of drug-carrier mixtures (e.g., larger scale blends of drug and carrier) for carrier-based DPI formulations as all the studies performed within this thesis were based on the small-scale powder mixtures (micrograms) due to the use of expensive materials (i.e., insulin and GLP-1). The scale-up process might affect the homogeneity of the powder mixtures therefore alter the balance of inter-particulate forces between drug and carrier within powder mixtures. Pharmacokinetics and pharmacodynamics profiles of inhaled SD insulin and SD GLP-1 powders can be investigated to see if they exhibit fast absorption rate and high bioavailability and are effective in glycaemic control in animals (e.g., rats).

Pulmonary delivery will offer feasible solutions to overcome barriers to injection treatment for people with diabetes who would like to avoid injections as it is non-invasive that minimises the limitations associated with subcutaneous injection. The long-term therapy can become more comfortable and convenient. This can lead to improved patient compliance and adherence to therapy which in turn achieve better control of blood glucose levels and reduce the risk of development of complications of diabetes. Consequently, this will result in improved patient's

quality of life. For patients with Type 2 diabetes which is more common than Type 1 diabetes, the risk of hypoglycaemia and weight gain could be reduced with inhaled GLP-1.

According to an online survey conducted in 2019, patients with diabetes (Type 1) generally accepted the idea of insulin delivery via inhalers as 73.4% of participants were willing to try insulin inhalers. However, many participants were not aware of insulin inhalers. It can be suggested that more information should be available with easy access for more awareness of the idea of delivering antidiabetic drugs (insulin and GLP-1) via the lung. NHS availability will have a significant influence on participants' willingness to try insulin inhalers for the management of diabetes. The successful inhaled insulin and GLP-1 products will provide an alternative treatment option for people with diabetes by reducing the burden of injection related barriers therefore improve patient compliance and adherence to antidiabetic therapy and consequently quality of life affected by injection treatment.

References

- 3M, I.R.D. 2016, 19 April-last update, *3M Unveils Intelligent Inhaler Designed to Help Control Spiraling Costs of Respiratory Disease*. Available: <https://investors.3m.com/news/news-details/2016/3M-Unveils-Intelligent-Inhaler-Designed-to-Help-Control-Spiraling-Costs-of-Respiratory-Disease/default.aspx> [2021, 18 August].
- Adali, M., Barresi, A., Boccardo, G. & Pisano, R. 2020, "Spray Freeze-Drying as a Solution to Continuous Manufacturing of Pharmaceutical Products in Bulk", *Processes*, vol. 8, no. 6, pp. 709.
- Agrawal, G.R., Wakte, P. & Shelke, S. 2017, "Formulation, physicochemical characterization and in vitro evaluation of human insulin-loaded microspheres as potential oral carrier", *Progress in biomaterials*, vol. 6, no. 3, pp. 125-136.
- Al-Hashimi, N., Babenko, M., Saeed, M., Kargar, N. & ElShaer, A. 2020, "The impact of natural and synthetic polymers in formulating micro and nanoparticles for antidiabetic drugs", *Current Drug Delivery*, vol. 18, no. 3, pp. 271-288.
- Al-Tabakha, M.M. & Arida, A.I. 2008, "Recent Challenges in Insulin Delivery Systems: A Review", *Indian Journal of Pharmaceutical Sciences*, vol. 70, no. 3, pp. 278-286.
- Al-Tabakha, M. 2015, "Future prospect of insulin inhalation for diabetic patients: The case of Afrezza versus Exubera", *Journal of Controlled Release*, vol. 215, pp. 25-38.
- Altman, P., Wehbe, L., Dederichs, J., Guerin, T., Ament, B., Moronta, M.C., Pino, A.V. & Goyal, P. 2018, "Comparison of peak inspiratory flow rate via the Breezhaler®, Ellipta® and HandiHaler® dry powder inhalers in patients with moderate to very severe COPD: a randomized cross-over trial", *BMC pulmonary medicine*, vol. 18, no. 1, pp. 100.
- Ambrus, R., Benke, E., Farkas, Á, Balásházy, I. & Szabó-Révész, P. 2018, "Novel dry powder inhaler formulation containing antibiotic using combined technology to improve aerodynamic properties", *European Journal of Pharmaceutical Sciences*, vol. 123, pp. 20-27.
- Amorij, J., Saluja, V., Petersen, A.H., Hinrichs, W.L.J., Huckriede, A. & Frijlink, H.W. 2007, "Pulmonary delivery of an inulin-stabilized influenza subunit vaccine prepared by spray-freeze drying induces systemic, mucosal humoral as well as cell-mediated immune responses in BALB/c mice", *Vaccine*, vol. 25, no. 52, pp. 8707-8717.
- Anderson, S.L., Beutel, T.R. & Trujillo, J.M. 2020, "Oral semaglutide in type 2 diabetes", *Journal of diabetes and its complications*, vol. 34, no. 4, pp. 107520.
- Ansari, M.J., Anwer, M.K., Jamil, S., Al-Shdefat, R., Ali, B.E., Ahmad, M.M. & Ansari, M.N. 2016, "Enhanced oral bioavailability of insulin-loaded solid lipid nanoparticles: pharmacokinetic bioavailability of insulin-loaded solid lipid nanoparticles in diabetic rats", *Drug delivery*, vol. 23, no. 6, pp. 1972-1979.
- Aulton, M.E. & Taylor, K.M.G. 2013, *Aulton's pharmaceuticals: the design and manufacture of medicines*, 4th edn, Churchill Livingstone/Elsevier, Edinburgh.

- Babenko, M., Peron, J.R., Kaialy, W., Calabrese, G., Alany, R.G. & Elshaer, A. 2019, "1H NMR quantification of spray dried and spray freeze-dried saccharide carriers in dry powder inhaler formulations", *International journal of pharmaceutics*, vol. 564, pp. 318-328.
- Balducci, A.G., Cagnani, S., Sonvico, F., Rossi, A., Barata, P., Colombo, G., Colombo, P. & Buttini, F. 2014, "Pure insulin highly respirable powders for inhalation", *European Journal of Pharmaceutical Sciences*, vol. 51, pp. 110-117.
- Banga, A.K. 2015, *Therapeutic Peptides and Proteins: Formulation, Processing, and Delivery Systems*, Third edn, Taylor & Francis Group, Baton Rouge, United States.
- Berkenfeld, K., Lamprecht, A. & McConville, J. 2015, "Devices for Dry Powder Drug Delivery to the Lung", *AAPS PharmSciTech*, vol. 16, no. 3, pp. 479-490.
- Bharti, S.K. & Roy, R. 2012, "Quantitative 1H NMR spectroscopy", *Trends in Analytical Chemistry*, vol. 35, pp. 5-26.
- Bi, R., Shao, W., Wang, Q. & Zhang, N. 2008, "Spray-freeze-dried dry powder inhalation of insulin-loaded liposomes for enhanced pulmonary delivery", *Journal of drug targeting*, vol. 16, no. 9, pp. 639-648.
- BNF 2021a, *COLISTIMETHATE SODIUM - Colobreathe inhalation powder capsules (Teva UK Ltd)*, NICE: National Institute for Health and Care Excellence.
- BNF 2021b, *FLUTICASONE WITH VILANTEROL*, NICE: National Institute for Health and Care Excellence.
- BNF 2021c, *INSULIN*, NICE: National Institute for Health and Care Excellence.
- BNF 2021d, *MANNITOL*, NICE: National Institute for Health and Care Excellence.
- BNF 2021e, *SALBUTAMOL*, NICE: National Institute for Health and Care Excellence.
- BNF 2021f, *SEMAGLUTIDE*, NICE: National Institute for Health and Care Excellence.
- BNF 2021g, *TIOTROPIUM*, NICE: National Institute for Health and Care Excellence.
- BNF 2021h, *TOBRAMYCIN*, NICE: National Institute for Health and Care Excellence.
- BNF 2021i, *Type 2 diabetes*, NICE: National Institute for Health and Care Excellence.
- Boehringer Ingelheim International GmbH 2018, February-last update, *SPIRIVA® HANDIHALER® (tiotropium bromide inhalation powder), for oral inhalation use*. Available: <https://docs.boehringer-ingelheim.com/Prescribing%20Information/PIs/Spiriva/Spiriva.pdf#page=15> [2021, 19 August].
- Bowey, K., Swift, B.E., Flynn, L.E. & Neufeld, R.J. 2013, "Characterization of biologically active insulin-loaded alginate microparticles prepared by spray drying", *Drug development and industrial pharmacy*, vol. 39, no. 3, pp. 457-465.

- Brayden, D.J., Hill, T.A., Fairlie, D.P., Maher, S. & Mrsny, R.J. 2020, "Systemic delivery of peptides by the oral route: Formulation and medicinal chemistry approaches", *Advanced Drug Delivery Reviews*, vol. 157, pp. 2-36.
- Brunaugh, A.D. & Smyth, H.D.C. 2018, "Formulation techniques for high dose dry powders", *International journal of pharmaceuticals*, vol. 547, no. 1-2, pp. 489-498.
- Büchi 2021, , *Büchi Mini Spray Dryer B-290*. Available: <https://www.buchi.com/us-en/products/spray-drying-and-encapsulation/mini-spray-dryer-b-290> [2021, 23 July].
- Chen, L., Okuda, T., Lu, X. & Chan, H. 2016, "Amorphous powders for inhalation drug delivery", *Advanced Drug Delivery Reviews*, vol. 100, pp. 102-115.
- Chen, Y., Mehok, A.R., Mant, C.T. & Hodges, R.S. 2004, "Optimum concentration of trifluoroacetic acid for reversed-phase liquid chromatography of peptides revisited", *Journal of Chromatography A*, vol. 1043, no. 1, pp. 9-18.
- Chiara Pietrogrande, M., Barbaro, E., Bove, M.C., Clauser, G., Colombi, C., Corbella, L., Cuccia, E., Dalla Torre, S., Decesari, S., Fermo, P., Gambaro, A., Gianelle, V., Ielpo, P., Larcher, R., Lazzeri, P., Massabò, D., Melchionna, G., Nardin, T., Paglione, M., Perrino, C., Prati, P., Visentin, M., Zanca, N. & Zangrando, R. 2017, "Results of an interlaboratory comparison of analytical methods for quantification of anhydrosugars and biosugars in atmospheric aerosol", *Chemosphere*, vol. 184, pp. 269-277.
- Chlif, M., Keochkerian, D., Choquet, D., Vaidie, A. & Ahmaidi, S. 2009, "Effects of obesity on breathing pattern, ventilatory neural drive and mechanics", *Respiratory physiology & neurobiology; Respir Physiol Neurobiol*, vol. 168, no. 3, pp. 198-202.
- Clark, A.R., Weers, J.G. & Dhand, R. 2019, "The Confusing World of Dry Powder Inhalers: It Is All About Inspiratory Pressures, Not Inspiratory Flow Rates", *Journal of Aerosol Medicine and Pulmonary Drug Delivery*, vol. 33, no. 1, pp. 1-11.
- Clipper F, Y., Joy, D., Hui, Y.K., Sumera, A. & Jay H, S. 2019, "Insulin Therapy for Type 2 Diabetes: Social, Psychological, and Clinical Factors", *Primary Care Reports*, vol. 25, no. 1, pp. n/a.
- Coombes, S.R., Hughes, L.P., Phillips, A.R. & Wren, S.A.C. 2014, "Proton NMR: a new tool for understanding dissolution", *Analytical Chemistry*, vol. 86, no. 5, pp. 2474.
- Cowart, K. 2020, "Oral Semaglutide: First-in-Class Oral GLP-1 Receptor Agonist for the Treatment of Type 2 Diabetes Mellitus", *Annals of Pharmacotherapy*, vol. 54, no. 5, pp. 478-485.
- CPEX Pharmaceuticals Inc. 2016, 15 February-last update, *Intranasal Insulin (Nasulin™) and Its Effect on Postprandial Glucose Metabolism in Comparison to Subcutaneous Insulin*. Available: <https://clinicaltrials.gov/ct2/show/study/NCT00850161> [2021, 3 April].
- Craig, D.Q.M. & Reading, M. 2006, *Thermal analysis of pharmaceuticals*, CRC Press, Taylor & Francis Group, New York: London.
- D'Addio, S., Chan, J., Kwok, P., Benson, B., Prud'homme, R. & Chan, H. 2013, "Aerosol Delivery of Nanoparticles in Uniform Mannitol Carriers Formulated by Ultrasonic Spray Freeze Drying", *Pharmaceutical research*, vol. 30, no. 11, pp. 2891-2901.

- Das, S.C., Stewart, P.J. & Tucker, I.G. 2018, "The respiratory delivery of high dose dry powders", *International journal of pharmaceuticals*, vol. 550, no. 1-2, pp. 486-487.
- Dekhuijzen, P.N.R., Lavorini, F. & Usmani, O.S. 2016, "Patients' perspectives and preferences in the choice of inhalers: the case for Respimat® or HandiHaler®", *Patient Preference and Adherence*, vol. 10, pp. 1561.
- Department of Health and Social Care 2020, 27 July-last update, *New obesity strategy unveiled as country urged to lose weight to beat coronavirus (COVID-19) and protect the NHS*. Available: <https://www.gov.uk/government/news/new-obesity-strategy-unveiled-as-country-urged-to-lose-weight-to-beat-coronavirus-covid-19-and-protect-the-nhs> [2021, 23 August].
- Depreter, F., Pilcer, G. & Amighi, K. 2013, "Inhaled proteins: Challenges and perspectives", *International journal of pharmaceuticals*, vol. 447, no. 1-2, pp. 251-280.
- Diabetes UK, N. 2006, , *NICE TECHNOLOGY APPRAISAL: INHALED INSULIN-DIABETES UK RESPONSE*. Available: <https://www.nice.org.uk/guidance/TA113/documents/diabetes-uk6> [2021, 18 August].
- Diabetes, U.K. 2021a, , *Diagnostic criteria for diabetes*. Available: <https://www.diabetes.org.uk/professionals/position-statements-reports/diagnosis-ongoing-management-monitoring/new-diagnostic-criteria-for-diabetes> [2021, 29 October].
- Diabetes, U.K. 2021b, , *GLP-1 analogues*. Available: <https://www.diabetes.org.uk/guide-to-diabetes/managing-your-diabetes/treating-your-diabetes/tablets-and-medication/incretin-mimetics> [2022, 4 February].
- Diabetes, U.K. 2020a, 7 January-last update, *Certain Insuman® products set to be discontinued in spring 2020*. Available: <https://www.diabetes.org.uk/about-us/news/insuman-discontinuation-sanofi> [2021, 26 March].
- Diabetes, U.K. 2020b, , *Diabetes Statistics, Diabetes facts & figures*. Available: <https://www.diabetes.org.uk/professionals/position-statements-reports/statistics> [2021, 10 December].
- Diabetes, U.K. 2019, 14 November-last update, *Number of people with obesity almost doubles in 20 years*. Available: <https://www.diabetes.org.uk/about-us/news/number-obesity-doubles-twenty-years> [2021, 27 March].
- Diabetes, U.K. 2017, 7 August-last update, *Withdrawal of bovine insulin in the UK*. Available: <https://www.diabetes.org.uk/about-us/news/withdrawal-of-bovine-insulin-in-the-uk> [2021, 24 March].
- Duddu, S. & Dal Monte, P. 1997, "Effect of Glass Transition Temperature on the Stability of Lyophilized Formulations Containing a Chimeric Therapeutic Monoclonal Antibody", *Pharmaceutical research*, vol. 14, no. 5, pp. 591-595.
- Duru, C., Swann, C., Dunleavy, U., Mulloy, B. & Matejtschuk, P. 2015, "The importance of formulation in the successful lyophilization of influenza reference materials", *Biologicals*, vol. 43, no. 2, pp. 110-116.

- Easa, N., Alany, R.G., Carew, M. & Vangala, A. 2019, "A review of non-invasive insulin delivery systems for diabetes therapy in clinical trials over the past decade", *Drug discovery today*, vol. 24, no. 2, pp. 440-451.
- Eli Lilly 2008, 7 March-last update, *Lilly Announces Termination of AIR Insulin Program | Eli Lilly and Company*. Available: <https://investor.lilly.com/news-releases/news-release-details/lilly-announces-termination-air-insulin-program> [2021, 2 July].
- Elliott, W.H. & Elliott, D.C. 2001, *Biochemistry and molecular biology*, 2nd edn, Oxford: Oxford University Press, Oxford.
- Elsayed, M.M.A. & Shalash, A.O. 2018, "Modeling the performance of carrier-based dry powder inhalation formulations: Where are we, and how to get there?", *Journal of Controlled Release*, vol. 279, pp. 251-261.
- Emami, F., Vatanara, A., Najafabadi, A.R., Kim, Y., Park, E.J., Sardari, S. & Na, D.H. 2018, "Effect of amino acids on the stability of spray freeze-dried immunoglobulin G in sugar-based matrices", *European Journal of Pharmaceutical Sciences*, vol. 119, pp. 39-48.
- Emami, F., Vatanara, A., Park, E.J. & Na, D.H. 2018, "Drying Technologies for the Stability and Bioavailability of Biopharmaceuticals", *Pharmaceutics MDPI*, vol. 10, no. 131, pp. 1-22.
- emc 2021, 11 May-last update, *Colobreathe inhalation powder, hard capsules*. Available: <https://www.medicines.org.uk/emc/medicine/27647#DOCREVISION> [2021, 28 July].
- emc 2020a, 23 July-last update, *Abasaglar®*. Available: https://www.medicines.org.uk/emc/product/8190/smpc#PHARMACOLOGICAL_PROPS [2021, 25 March].
- emc 2020b, 03 September-last update, *Humalog® Mix 25*. Available: <https://www.medicines.org.uk/emc/product/3829/smpc> [2021, 26 March].
- emc 2020c, 13 August-last update, *Humulin® M3 (Mixture 3)*. Available: <https://www.medicines.org.uk/emc/product/8193/smpc> [2021, 25 March].
- emc 2020d, 13 August-last update, *Humulin® I (Isophane)*. Available: <https://www.medicines.org.uk/emc/product/8196/smpc> [2021, 25 March].
- emc 2020e, 13 August-last update, *Humulin® S (Soluble)*. Available: <https://www.medicines.org.uk/emc/product/8198/smpc> [2021, 25 March].
- emc 2020f, 20 August-last update, *Hypurin® Porcine 30/70 Mix*. Available: https://www.medicines.org.uk/emc/product/1675/smpc#PHARMACOLOGICAL_PROPS [2021, 26 March].
- emc 2020g, 20 August-last update, *Hypurin® Porcine Isophane*. Available: <https://www.medicines.org.uk/emc/product/1670/smpc> [2021, 25 March].
- emc 2020h, 20 August-last update, *Hypurin® Porcine Neutral*. Available: <https://www.medicines.org.uk/emc/product/1673/smpc> [2021, 25 March].

- emc 2020i, September-last update, *Insulatard*[®]. Available:
<https://www.medicines.org.uk/emc/product/3848/smpc> [2021, 25 March].
- emc 2020j, 10 August-last update, *Insuman*[®] *Basal*. Available:
<https://www.medicines.org.uk/emc/product/4099/smpc> [2021, 25 March].
- emc 2020k, 10 August-last update, *Insuman*[®] *Comb 25*. Available:
<https://www.medicines.org.uk/emc/product/4102/smpc> [2021, 25 March].
- emc 2020l, 10 August-last update, *Insuman*[®] *Comb 50*. Available:
<https://www.medicines.org.uk/emc/product/4107#> [2021, 25 March].
- emc 2020m, 10 August-last update, *Insuman*[®] *Rapid*. Available:
<https://www.medicines.org.uk/emc/product/3854> [2021, 25 March].
- emc 2020n, 10 August-last update, *Lantus*[®]. Available:
<https://www.medicines.org.uk/emc/product/8097/smpc> [2021, 26 March].
- emc 2020o, September-last update, *Levemir*[®]. Available:
https://www.medicines.org.uk/emc/product/7890/smpc#PHARMACOLOGICAL_PROPS [2021, 25 March].
- emc 2020p, September-last update, *NovoMix*[®] *30*. Available:
<https://www.medicines.org.uk/emc/product/7915/smpc> [2021, 26 March].
- emc 2020q, November-last update, *Rybelsus*[®]. Available:
<https://www.medicines.org.uk/emc/product/11507#> [2021, 29 October].
- emc 2020r, 10 August-last update, *Toujeo*[®]. Available:
https://www.medicines.org.uk/emc/product/10277/smpc#PHARMACOLOGICAL_PROPS [2021, 26 March].
- emc 2020s, November-last update, *Tresiba*[®]. Available:
<https://www.medicines.org.uk/emc/product/2944/smpc> [2021, 26 March].
- emc 2019a, 25 February-last update, *Bronchitol 40 mg inhalation powder, hard capsules*. Available:
<https://www.medicines.org.uk/emc/product/4085/smpc> [2021, 10 August].
- emc 2019b, 1 March-last update, *Osmohale Inhalation Powder, Hard Capsule*. Available:
<https://www.medicines.org.uk/emc/product/4809/smpc> [2021, 10 August].
- emc 2019c, 18 November-last update, *Relenza 5mg/dose inhalation powder*. Available:
<https://www.medicines.org.uk/emc/product/3809/smpc>.
- emc 2019d, January-last update, *Spiriva 18 microgram inhalation powder, hard capsule*. Available:
https://www.medicines.org.uk/emc/product/1693/smpc#PHARMACOLOGICAL_PROPS [2021, 17 April].
- emc 2019e, 3 May-last update, *Tobi Podhaler 28 mg inhalation powder*. Available:
<https://www.medicines.org.uk/emc/product/4757/smpc#PRODUCTINFO> [2021, 5 April].

Ennos, R. 2012, *Statistical and data handling skills in biology*, 3rd edn, Pearson, Harlow, England.

Escalada, J., Orozco-Beltran, D., Morillas, C., Alvarez-Guisasola, F., Gomez-Peralta, F., Mata-Cases, M., Palomares, R., Iglesias, R. & Carratalá-Munuera, C. 2016, "Attitudes towards insulin initiation in type 2 diabetes patients among healthcare providers: A survey research", *Diabetes research and clinical practice*, vol. 122, pp. 46-53.

European Medicines Agency 2022, 3 February-last update, *Bronchitol*. Available: <https://www.ema.europa.eu/en/medicines/human/EPAR/bronchitol> [2022, 4 February].

European Medicines Agency 2021a, 1 March-last update, *Bydureon SUMMARY OF PRODUCT CHARACTERISTICS*. Available: <https://www.ema.europa.eu/en/medicines/human/EPAR/bydureon> [2022, 4 February].

European Medicines Agency 2021b, 1 March-last update, *Byetta SUMMARY OF PRODUCT CHARACTERISTICS*. Available: <https://www.ema.europa.eu/en/medicines/human/EPAR/byetta#product-information-section> [2021, 12 March].

European Medicines Agency 2021c, 11 March-last update, *Lyxumia SUMMARY OF PRODUCT CHARACTERISTICS*. Available: <https://www.ema.europa.eu/en/medicines/human/EPAR/lyxumia> [2021, 11 March].

European Medicines Agency 2021d, 11 January-last update, *Ozempic SUMMARY OF PRODUCT CHARACTERISTICS*. Available: <https://www.ema.europa.eu/en/medicines/human/EPAR/ozempic> [2021, 12 March].

European Medicines Agency 2021e, 1 February-last update, *Trulicity SUMMARY OF PRODUCT CHARACTERISTICS*. Available: <https://www.ema.europa.eu/en/medicines/human/EPAR/trulicity> [2021, 12 March].

European Medicines Agency 2021f, 12 February-last update, *Victoza SUMMARY OF PRODUCT CHARACTERISTICS*. Available: <https://www.ema.europa.eu/en/medicines/human/EPAR/victoza> [2021, 12 March].

European Medicines Agency 2020a, 24 September-last update, *Actrapid*[®]. Available: <https://www.ema.europa.eu/en/medicines/human/EPAR/actrapid> [2021, 25 March].

European Medicines Agency 2020b, 5 November-last update, *Apidra*[®]. Available: <https://www.ema.europa.eu/en/medicines/human/EPAR/apidra> [2021, 25 March].

European Medicines Agency 2020c, 24 September-last update, *Fiasp*[®]. Available: <https://www.ema.europa.eu/en/medicines/human/EPAR/fiasp> [2021, 25 March].

European Medicines Agency 2020d, 4 September-last update, *Humalog*[®]. Available: <https://www.ema.europa.eu/en/medicines/human/EPAR/humalog> [2022, 4 February].

European Medicines Agency 2020e, November 23-last update, *NovoRapid*[®]. Available: <https://www.ema.europa.eu/en/medicines/human/EPAR/novorapid> [2022, 4 February].

- European Medicines Agency 2020f, 26 November-last update, *Suliqua SUMMARY OF PRODUCT CHARACTERISTICS*. Available: <https://www.ema.europa.eu/en/medicines/human/EPAR/suliqua> [2021, 12 March].
- European Medicines Agency 2020g, 13 October-last update, *Xultophy SUMMARY OF PRODUCT CHARACTERISTICS*. Available: <https://www.ema.europa.eu/en/medicines/human/EPAR/xultophy> [2021, 12 March].
- Farsaei, S., Radfar, M., Heydari, Z., Abbasi, F. & Qorbani, M. 2014, "Insulin adherence in patients with diabetes: Risk factors for injection omission", *Primary Care Diabetes*, vol. 8, no. 4, pp. 338-345.
- Faulhammer, E., Zellnitz, S., Wutscher, T., Stranzinger, S., Zimmer, A. & Paudel, A. 2018, "Performance indicators for carrier-based DPIs: Carrier surface properties for capsule filling and API properties for in vitro aerosolisation", *International journal of pharmaceuticals*, vol. 536, no. 1, pp. 326-335.
- Ferdynand, M.S. & Nokhodchi, A. 2020, "Co-spraying of carriers (mannitol-lactose) as a method to improve aerosolization performance of salbutamol sulfate dry powder inhaler", *Drug delivery and translational research*, vol. 10, no. 5, pp. 1418–1427.
- Ferrati, S., Wu, T., Kanapuram, S.R. & Smyth, H.D.C. 2018, "Dosing considerations for inhaled biologics", *International journal of pharmaceuticals*, vol. 549, no. 1-2, pp. 58-66.
- Fleming, L., Fleming, J.W. & Davis, C.S. 2015, *Afrezza: An inhaled approach to insulin delivery*.
- Fonte, P., Soares, S., Sousa, F., Costa, A., Seabra, V., Reis, S. & Sarmiento, B. 2014, "Stability study perspective of the effect of freeze-drying using cryoprotectants on the structure of insulin loaded into PLGA nanoparticles", *Biomacromolecules*, vol. 15, no. 10, pp. 3753.
- Gatto, N.M., Koralek, D.O., Bracken, M.B., Duggan, W.T., Lem, J., Klioze, S., Koch, G.G., Wise, R.A., Cohen, R.B. & Jackson, N.C. 2019, "Lung Cancer-Related Mortality With Inhaled Insulin or a Comparator: Follow-Up Study of patients previously enrolled in Exubera Controlled Clinical Trials (FUSE) Final Results", *Diabetes Care*, vol. 42, no. 9, pp. 1708-1715.
- Geller, D.E., Weers, J. & Heurding, S. 2011, "Development of an inhaled dry-powder formulation of tobramycin using PulmoSphere™ technology", *Journal of Aerosol Medicine and Pulmonary Drug Delivery*, vol. 24, no. 4, pp. 175-182.
- Giraudeau, P., Silvestre, V. & Akoka, S. 2015, *Optimizing water suppression for quantitative NMR-based metabolomics: a tutorial review*.
- GlaxoSmithKline 2021, March-last update, *Ellipta inhaler products*. Available: <https://gskpro.com/en-gb/products/ellipta-inhaler/> [2021, 19 August].
- Goldberg, T. & Wong, E. 2015, "Afrezza (Insulin Human) Inhalation Powder: A New Inhaled Insulin for the Management Of Type-1 or Type-2 Diabetes Mellitus", *P & T: a peer-reviewed journal for formulary management*, vol. 40, no. 11, pp. 735-741.
- Guerci, B., Chanan, N., Kaur, S., Jasso-Mosqueda, J. & Lew, E. 2019, "Lack of Treatment Persistence and Treatment Nonadherence as Barriers to Glycaemic Control in Patients with Type 2 Diabetes", *Diabetes therapy*, vol. 10, no. 2, pp. 437-449.

- Günther, H. 2013, *NMR spectroscopy: basic principles, concepts, and applications in chemistry*, Siegen, Wiley-VCH.
- Haidl, P., Heindl, S., Siemon, K., Bernacka, M. & Cloes, R.M. 2016, "Inhalation device requirements for patients' inhalation maneuvers", *Respiratory medicine*, vol. 118, pp. 65-75.
- Haj-Ahmad, R., Elkordy, A.A., Chaw, C.S. & Moore, A. 2013, "Compare and contrast the effects of surfactants (Pluronic®F-127 and Cremophor®EL) and sugars (β -cyclodextrin and inulin) on properties of spray dried and crystallised lysozyme", *European journal of pharmaceutical sciences*, vol. 49, no. 4, pp. 519-534.
- Healy, A.M., Amaro, M.I., Paluch, K.J. & Tajber, L. 2014, "Dry powders for oral inhalation free of lactose carrier particles", *Advanced Drug Delivery Reviews*, vol. 75, pp. 32-52.
- Heinemann, L. 2018, "Inhaled Insulin: Dead Horse or Rising Phoenix?", *Journal of Diabetes Science and Technology*, vol. 12, no. 2, pp. 239-242.
- Heinemann, L., Braune, K., Carter, A., Zayani, A. & Krämer, L.,A. 2021, "Insulin Storage: A Critical Reappraisal", *Journal of Diabetes Science and Technology*, vol. 15, no. 1, pp. 147-159.
- Heinemann, L. & Jacques, Y. 2009, "Oral Insulin and Buccal Insulin: A Critical Reappraisal", *Journal of Diabetes Science and Technology*, vol. 3, no. 3, pp. 568-584.
- Heinemann, L. & Parkin, C.G. 2018, "Rethinking the Viability and Utility of Inhaled Insulin in Clinical Practice", *Journal of Diabetes Research*, vol. 2018.
- Hertel, N., Birk, G. & Scherließ, R. 2020, "Particle engineered mannitol for carrier-based inhalation – A serious alternative?", *International journal of pharmaceutics*, vol. 577.
- Holman, N., Knighton, P., Kar, P., O'Keefe, J., Curley, M., Weaver, A., Barron, E., Bakhai, C., Khunti, K., Wareham, N.J., Sattar, N., Young, B. & Valabhji, J. 2020, "Risk factors for COVID-19-related mortality in people with type 1 and type 2 diabetes in England: a population-based cohort study", *The lancet. Diabetes & endocrinology*, vol. 8, no. 10, pp. 823-833.
- Holt, T. & Kumar, S. 2015, *ABC of diabetes*, Seventh edition edn, Chichester, West Sussex, United Kingdom; Hoboken, New Jersey: John Wiley & Sons.
- Holzgrabe, U. 2010, "Quantitative NMR spectroscopy in pharmaceutical applications", *Progress in Nuclear Magnetic Resonance Spectroscopy*, vol. 57, no. 2, pp. 229-240.
- Hoppentocht, M., Hagedoorn, P., Frijlink, H.W. & de Boer, A.H. 2014, "Technological and practical challenges of dry powder inhalers and formulations", *Advanced Drug Delivery Reviews*, vol. 75, pp. 18-31.
- Hou, Z., Liang, X., Du, L., Su, F. & Su, W. 2014, "Quantitative determination and validation of avermectin B 1a in commercial products using quantitative nuclear magnetic resonance spectroscopy", *Magnetic Resonance in Chemistry*, vol. 52, no. 9, pp. 480-485.
- Hu, C. & Jia, W. 2019, "Therapeutic medications against diabetes: What we have and what we expect", *Advanced Drug Delivery Reviews*, vol. 139, pp. 3-15.

- ICH 2005, *VALIDATION OF ANALYTICAL PROCEDURES: TEXT AND METHODOLOGY Q2(R1)*, The International Council for Harmonisation of Technical Requirements for Pharmaceuticals for Human Use (ICH).
- ICH 1995, *QUALITY OF BIOTECHNOLOGICAL PRODUCTS: STABILITY TESTING OF BIOTECHNOLOGICAL/BIOLOGICAL PRODUCTS Q5C*, The International Council for Harmonisation of Technical Requirements for Pharmaceuticals for Human Use (ICH).
- Ishwarya, S.P., Anandharamakrishnan, C. & Stapley, A.G.F. 2015, "Spray-freeze-drying: A novel process for the drying of foods and bioproducts", *Trends in Food Science & Technology*, vol. 41, no. 2, pp. 161-181.
- Islam, N. & Cleary, M.J. 2012, "Developing an efficient and reliable dry powder inhaler for pulmonary drug delivery – A review for multidisciplinary researchers", *Medical engineering & physics; Med Eng Phys*, vol. 34, no. 4, pp. 409-427.
- Islam, N. & Gladki, E. 2008, "Dry powder inhalers (DPIs)—A review of device reliability and innovation", *International journal of pharmaceutics; Int J Pharm*, vol. 360, no. 1, pp. 1-11.
- Ismail, R. & Csóka, I. 2017, "Novel strategies in the oral delivery of antidiabetic peptide drugs – Insulin, GLP 1 and its analogs", *European journal of pharmaceutics and biopharmaceutics*, vol. 115, pp. 257-267.
- Kadota, K., Yanagawa, Y., Tachikawa, T., Deki, Y., Uchiyama, H., Shirakawa, Y. & Tozuka, Y. 2019, "Development of porous particles using dextran as an excipient for enhanced deep lung delivery of rifampicin", *International journal of pharmaceutics*, vol. 555, pp. 280-290.
- Kadoya, S., Fujii, K., Izutsu, K., Yonemochi, E., Terada, K., Yomota, C. & Kawanishi, T. 2010, "Freeze-drying of proteins with glass-forming oligosaccharide-derived sugar alcohols", *International journal of pharmaceutics*, vol. 389, no. 1, pp. 107-113.
- Kaialy, W. 2016, *On the effects of blending, physicochemical properties, and their interactions on the performance of carrier-based dry powders for inhalation — A review*.
- Kaialy, W. 2016, "A review of factors affecting electrostatic charging of pharmaceuticals and adhesive mixtures for inhalation", *International journal of pharmaceutics*, vol. 503, no. 1-2, pp. 262-276.
- Kaialy, W., Momin, M.N., Ticehurst, M.D., Murphy, J. & Nokhodchi, A. 2010, "Engineered mannitol as an alternative carrier to enhance deep lung penetration of salbutamol sulphate from dry powder inhaler", *Colloids and Surfaces B: Biointerfaces*, vol. 79, no. 2, pp. 345-356.
- Kaialy, W. & Nokhodchi, A. 2016, "The use of freeze-dried mannitol to enhance the in vitro aerosolization behaviour of budesonide from the Aerolizer[®]", *Powder Technology*, vol. 288, pp. 291-302.
- Kaialy, W. & Nokhodchi, A. 2015, "Dry powder inhalers: Physicochemical and aerosolization properties of several size-fractions of a promising alternative carrier, freeze-dried mannitol", *European Journal of Pharmaceutical Sciences*, vol. 68, pp. 56-67.

- Kaialy, W. & Nokhodchi, A. 2013, "Freeze-Dried Mannitol for Superior Pulmonary Drug Delivery via Dry Powder Inhaler", *Pharmaceutical research*, vol. 30, no. 2, pp. 458-477.
- Kim, A.I., Akers, M.J. & Nail, S.L. 1998, "The Physical State of Mannitol after Freeze-Drying: Effects of Mannitol Concentration, Freezing Rate, and a Noncrystallizing Cosolute", *Journal of Pharmaceutical Sciences*, vol. 87, no. 8, pp. 931-935.
- Kim, E. & Plosker, G. 2015, "AFREZZA® (insulin human) Inhalation Powder: A Review in Diabetes Mellitus", *Drugs*, vol. 75, no. 14, pp. 1679-1686.
- Kim, H., Park, H., Lee, J., Kim, T.H., Lee, E.S., Oh, K.T., Lee, K.C. & Youn, Y.S. 2011, "Highly porous large poly(lactic-co-glycolic acid) microspheres adsorbed with palmityl-acylated exendin-4 as a long-acting inhalation system for treating diabetes", *Biomaterials*, vol. 32, no. 6, pp. 1685-1693.
- Kuehl, P., Cherrington, A., Dobry, D., Edgerton, D., Friesen, D., Hobbs, C., Leach, C., Murri, B., Neal, D., Lyon, D., Vodak, D. & Reed, M. 2014, "Biologic Comparison of Inhaled Insulin Formulations: Exubera™ and Novel Spray-Dried Engineered Particles of Dextran-10", *AAPS PharmSciTech*, vol. 15, no. 6, pp. 1545-1550.
- Kukut Hatipoglu, M., Hickey, A.J. & Garcia-Contreras, L. 2018, "Pharmacokinetics and pharmacodynamics of high doses of inhaled dry powder drugs", *International journal of pharmaceutics*, vol. 549, no. 1-2, pp. 306-316.
- Lau, M., Young, P.M. & Traini, D. 2017, *A review of co-milling techniques for the production of high dose dry powder inhaler formulation*.
- Lavorini, F., Pistolesi, M. & Usmani, O.S. 2017, "Recent advances in capsule-based dry powder inhaler technology", *Multidisciplinary respiratory medicine*, vol. 12, no. 1, pp. 1-7.
- Leary, A.C., Dowling, M., Cussen, K., O'Brien, J. & Stote, R.M. 2008, "Pharmacokinetics and Pharmacodynamics of Intranasal Insulin Spray (Nasulin™) Administered to Healthy Male Volunteers: Influence of the Nasal Cycle", *Journal of Diabetes Science and Technology*, vol. 2, no. 6, pp. 1054-1060.
- Lechanteur, A. & Evrard, B. 2020, "Influence of Composition and Spray-Drying Process Parameters on Carrier-Free DPI Properties and Behaviors in the Lung: A review", *Pharmaceutics*, vol. 12, no. 1, pp. 55.
- Lee, H., Kim, D. & Park, C. 2018, "Dry powder inhaler for pulmonary drug delivery: human respiratory system, approved products and therapeutic equivalence guideline", *Journal of Pharmaceutical Investigation*, vol. 48, no. 6, pp. 603-616.
- Leung, C.M.S., Tong, Z., Zhou, Q.T., Chan, J.G.Y., Tang, P., Sun, S., Yang, R. & Chan, H. 2016, "Understanding the Different Effects of Inhaler Design on the Aerosol Performance of Drug-Only and Carrier-Based DPI Formulations. Part 1: Grid Structure", *The AAPS journal; AAPS J*, vol. 18, no. 5, pp. 1159-1167.
- Levy, M.L., Carroll, W., Izquierdo Alonso, J., L., Keller, C., Lavorini, F. & Lehtimäki, L. 2019, "Understanding Dry Powder Inhalers: Key Technical and Patient Preference Attributes", *Advances in Therapy; Adv Ther*, vol. 36, no. 10, pp. 2547-2557.

- Li, L., Sun, S., Parumasivam, T., Denman, J.A., Gengenbach, T., Tang, P., Mao, S. & Chan, H. 2016, "L-Leucine as an excipient against moisture on in vitro aerosolization performances of highly hygroscopic spray-dried powders", *European Journal of Pharmaceutics and Biopharmaceutics*, vol. 102, pp. 132-141.
- Lian, L. & Roberts, G. 2011, *Protein NMR Spectroscopy: Practical Techniques and Applications*, Chichester: Wiley, Chichester; Hoboken.
- Liang, W., Pan, H.W., Vllasaliu, D. & Lam, J.K.W. 2020, "Pulmonary delivery of biological drugs", *Pharmaceutics*, vol. 12, no. 11, pp. 1-28.
- Life Science Integrates 2019, 9 January-last update, *3M: How connected technology is helping to put patients at the centre of drug delivery*. Available: <https://www.lifescienceintegrates.com/3m-how-connected-technology-is-helping-to-put-patients-at-the-centre-of-drug-delivery/> [2021, 18 August].
- Lin, Y., Mi, F., Lin, P., Miao, Y., Huang, T., Chen, K., Chen, C., Chang, Y. & Sung, H. 2019, "Strategies for improving diabetic therapy via alternative administration routes that involve stimuli-responsive insulin-delivering systems", *Advanced Drug Delivery Reviews*, vol. 139, pp. 71-82.
- Lindert, S., Below, A. & Breitzkreutz, J. 2014, "Performance of dry powder inhalers with single dosed capsules in preschool children and adults using improved upper airway models", *Pharmaceutics; Pharmaceutics*, vol. 6, no. 1, pp. 36-51.
- Lumb, A.B. & Thomas, C.R. 2020, *Nunn and Lumb's Applied Respiratory Physiology*, 9th edn, Elsevier.
- Lyu, F., Liu, J.J., Zhang, Y. & Wang, X.Z. 2017, "Combined control of morphology and polymorph in spray drying of mannitol for dry powder inhalation", *Journal of Crystal Growth*, vol. 467, pp. 155-161.
- Maltesen, M.J., Bjerregaard, S., Hovgaard, L., Havelund, S. & van de Weert, M. 2008, "Quality by design – Spray drying of insulin intended for inhalation", *European Journal of Pharmaceutics and Biopharmaceutics*, vol. 70, no. 3, pp. 828-838.
- MannKind Corporation 2021, , *What is Afrezza?*. Available: <https://afrezza.com/about-afrezza/> [2021, 19 August].
- Mannkind Corporation 2020, 27 July-last update, *Afrezza Efficacy & Safety* . Available: <https://www.afrezzahcp.com/efficacy-and-safety> [2021, 21 July].
- MannKind Corporation 2015, *AFREZZA®*, FDA.
- McCarty, D., Olenik, A. & McCarty, B.P. 2019, "Efficacy and Safety of Basal Insulin/GLP-1 Receptor Agonist Used in Combination for Type 2 Diabetes Management", *Journal of Pharmacy Practice*, vol. 32, no. 6, pp. 671-678.
- McGill, J.B., Peters, A., Buse, J.B., Steiner, S., Tran, T., Pompilio, F.M. & Kendall, D.M. 2020, "Comprehensive Pulmonary Safety Review of Inhaled Technosphere® Insulin in Patients with Diabetes Mellitus", *Clinical drug investigation; Clin Drug Investig*, vol. 40, no. 10, pp. 973-983.

- Mehta, P. 2018, "Imagine the Superiority of Dry Powder Inhalers from Carrier Engineering", *Journal of Drug Delivery*, vol. 2018.
- Mensink, M.A., Frijlink, H.W., van Der Voort Maarschalk, Kees & Hinrichs, W.L.J. 2017, "How sugars protect proteins in the solid state and during drying (review): Mechanisms of stabilization in relation to stress conditions", *European Journal of Pharmaceutics and Biopharmaceutics*, vol. 114, pp. 288-295.
- Merck KGaA 2021, , *Factors Affecting Resolution in HPLC*. Available: <https://www.sigmaaldrich.com/technical-documents/articles/analytical/factors-affecting-resolution-in-hplc.html#peak-symmetry> [2021, 15 October].
- Mettler-Toledo International Inc 2021, , *Interpreting TGA Curves*. Available: https://www.mt.com/us/en/home/supportive_content/matchar_apps/MatChar_UC131.html [2021, 5 February].
- Molina, C., Kaialy, W. & Nokhodchi, A. 2019, "The crucial role of leucine concentration on spray dried mannitol-leucine as a single carrier to enhance the aerosolization performance of Albuterol sulfate", *Journal of drug delivery science and technology*, vol. 49, pp. 97-106.
- Mutukuri, T.T., Wilson, N.E., Taylor, L.S., Topp, E.M. & Zhou, Q.T. 2021, "Effects of drying method and excipient on the structure and physical stability of protein solids: Freeze drying vs. spray freeze drying", *International journal of pharmaceutics*, vol. 594, pp. 120169.
- Nahar, K., Gupta, N., Gauvin, R., Absar, S., Patel, B., Gupta, V., Khademhosseini, A. & Ahsan, F. 2013, "In vitro, in vivo and ex vivo models for studying particle deposition and drug absorption of inhaled pharmaceuticals", *European Journal of Pharmaceutical Sciences*, vol. 49, no. 5, pp. 805-818.
- Nezzal, A., Aerts, L., Verspaille, M., Henderickx, G. & Redl, A. 2009, "Polymorphism of sorbitol", *Journal of Crystal Growth*, vol. 311, no. 15, pp. 3863-3870.
- Nokhodchi, A. & Martin, G.P. 2015, *Pulmonary Drug Delivery: Advances and Challenges*, 1st edn, United Kingdom: John Wiley & Sons, Ltd Inc.
- Novo Nordisk, A. 2021, January-last update, *RYBELSUS® Semaglutide Tablets 7mg/14mg*. Available: <https://www.rybelsus.com/content/rybelsus/en/why-rybelsus/rybelsus-results.html> [2021, 29 March].
- Novo Nordisk, A. 2020, 2 March-last update, *PIONEER 4 Efficacy and Safety of Oral Semaglutide Versus Liraglutide and Versus Placebo in Subjects With Type 2 Diabetes Mellitus* [Homepage of Novo Nordisk A/S], [Online]. Available: <https://clinicaltrials.gov/ct2/show/NCT02863419> https://clinicaltrials.gov/ProvidedDocs/19/NCT02863419/SAP_001.pdf [2021, 31 March].
- Nuffer, W., Guesnier, A. & Trujillo, J.M. 2018, "A review of the new GLP-1 receptor agonist/basal insulin fixed-ratio combination products", *Therapeutic Advances in Endocrinology and Metabolism*, vol. 9, no. 3, pp. 69-79.
- Nuffer, W., Trujillo, J.M. & Ellis, S.L. 2015, "Technosphere Insulin (Afrezza): A New, Inhaled Prandial Insulin", *Annals of Pharmacotherapy*, vol. 49, no. 1, pp. 99-106.

- Ogienko, A.G., Bogdanova, E.G., Trofimov, N.A., Myz, S.A., Ogienko, A.A., Kolesov, B.A., Yunoshev, A.S., Zubikov, N.V., Manakov, A.Y., Boldyrev, V.V. & Boldyreva, E.V. 2017, "Large porous particles for respiratory drug delivery. Glycine-based formulations", *European Journal of Pharmaceutical Sciences*, vol. 110, pp. 148-156.
- Okuda, T., Suzuki, Y., Kobayashi, Y., Ishii, T., Uchida, S., Itaka, K., Kataoka, K. & Okamoto, H. 2015, "Development of biodegradable polycation-based inhalable dry gene powders by spray freeze drying", *Pharmaceutics*, vol. 7, no. 3, pp. 233-254.
- Okumura, K., Iwakawa, S., Yoshida, T., Seki, T. & Komada, F. 1992, "Intratracheal delivery of insulin Absorption from solution and aerosol by rat lung", *International journal of pharmaceutics*, vol. 88, no. 1, pp. 63-73.
- Oleck, J., Kassam, S. & Goldman, J.D. 2016, "Commentary: Why Was Inhaled Insulin a Failure in the Market?", *Diabetes spectrum : a publication of the American Diabetes Association*, vol. 29, no. 3, pp. 180.
- Oliva, A., Fariña, J. & Llabrés, M. 2000, "Development of two high-performance liquid chromatographic methods for the analysis and characterization of insulin and its degradation products in pharmaceutical preparations", *Journal of chromatography.B, Biomedical sciences and applications*, vol. 749, no. 1, pp. 25-34.
- Otake, H., Okuda, T., Hira, D., Kojima, H., Shimada, Y. & Okamoto, H. 2016, "Inhalable Spray-Freeze-Dried Powder with L-Leucine that Delivers Particles Independent of Inspiratory Flow Pattern and Inhalation Device", *Pharmaceutical research*, vol. 33, no. 4, pp. 922-931.
- Pansare, S. & Patel, S. 2016, "Practical Considerations for Determination of Glass Transition Temperature of a Maximally Freeze Concentrated Solution", *AAPS PharmSciTech*, vol. 17, no. 4, pp. 805-819.
- Patton, J.S., Bukar, J.G. & Eldon, M.A. 2004, "Clinical Pharmacokinetics and Pharmacodynamics of Inhaled Insulin", *Clinical pharmacokinetics; Clin Pharmacokinet*, vol. 43, no. 12, pp. 781-801.
- Patton, J.S. & Byron, P.R. 2007, "Inhaling medicines: delivering drugs to the body through the lungs", *Nature Reviews Drug Discovery*, vol. 6, no. 1, pp. 67-74.
- Patwa, A. & Shah, A. 2015, "Anatomy and physiology of respiratory system relevant to anaesthesia", *Indian Journal of Anaesthesia*, vol. 59, no. 9, pp. 533-541.
- Pauli, G., Godecke, T., Jaki, B. & Lankin, D.C. 2012, *Quantitative H-1 NMR. Development and Potential of an Analytical Method: An Update*.
- Peng, T., Lin, S., Niu, B., Wang, X., Huang, Y., Zhang, X., Li, G., Pan, X. & Wu, C. 2016, "Influence of physical properties of carrier on the performance of dry powder inhalers", *Acta Pharmaceutica Sinica B*, vol. 6, no. 4, pp. 308-318.
- Peng, T., Zhang, X., Huang, Y., Zhao, Z., Liao, Q., Xu, J., Huang, Z., Zhang, J., Wu, C., Pan, X. & Wu, C. 2017, "Nanoporous mannitol carrier prepared by non-organic solvent spray drying technique to enhance the aerosolization performance for dry powder inhalation", *Scientific Reports*, vol. 7.

- Peyrot, M. & Rubin, R.R. 2011, "Patient-Reported Outcomes in Adults with Type 2 Diabetes Using Mealtime Inhaled Technosphere Insulin and Basal Insulin Versus Premixed Insulin", *Diabetes technology & therapeutics; Diabetes Technol Ther*, vol. 13, no. 12, pp. 121-1206.
- Pfizer 2012, 23 October-last update, *An Observational Follow-Up Study Of Patients Previously Enrolled In Exubera Controlled Clinical Trials*. Available: <https://clinicaltrials.gov/ct2/show/NCT00734591> [2021, 20 July].
- Piccirilli, F., Mangialardo, S., Postorino, P., Lupi, S. & Perucchi, A. 2013, "FTIR analysis of the high pressure response of native insulin assemblies", *Journal of Molecular Structure*, vol. 1050, pp. 159-165.
- Pilcer, G. & Amighi, K. 2010, "Formulation strategy and use of excipients in pulmonary drug delivery", *International journal of pharmaceuticals*, vol. 392, no. 1, pp. 1-19.
- Pinho, A.R., Fortuna, A., Falcão, A., Santos, A.C., Seïça, R., Estevens, C., Veiga, F. & Ribeiro, A.J. 2019, "Comparison of ELISA and HPLC-MS methods for the determination of exenatide in biological and biotechnology-based formulation matrices", *Journal of Pharmaceutical Analysis*, vol. 9, no. 3, pp. 143-155.
- Powell, J., Piszczatoski, C. & Taylor, J.R. 2020, "Oral Semaglutide: The First-available Noninjectable Glucagon-like Peptide 1 Receptor Agonist", *Clinical therapeutics*, vol. 42, no. 10, pp. 2100-2116.
- Public Health England 2020, 25 July-last update, *Excess weight can increase risk of serious illness and death from COVID-19*. Available: <https://www.gov.uk/government/news/excess-weight-can-increase-risk-of-serious-illness-and-death-from-covid-19> [2021, 23 August].
- Pyne, A., Chatterjee, K. & Suryanarayanan, R. 2003, "Solute Crystallization in Mannitol–Glycine Systems—Implications on Protein Stabilization in Freeze-Dried Formulations", *Journal of pharmaceutical sciences; J.Pharm.Sci*, vol. 92, no. 11, pp. 2272-2283.
- Qian, F., Mathias, N., Moench, P., Chi, C., Desikan, S., Hussain, M. & Smith, R.L. 2009, "Pulmonary delivery of a GLP-1 receptor agonist, BMS-686117", *International journal of pharmaceuticals*, vol. 366, no. 1, pp. 218-220.
- Quarta, E., Chierici, V., Flammini, L., Tognolini, M., Barocelli, E., Cantoni, A.M., Dujovny, G., Ecenarro Probst, S., Sonvico, F., Colombo, G., Rossi, A., Bettini, R., Colombo, P. & Buttini, F. 2020, "Excipient-free pulmonary insulin dry powder: Pharmacokinetic and pharmacodynamics profiles in rats", *Journal of Controlled Release*, vol. 323, pp. 412-420.
- Rahimpour, Y., Kouhsoltani, M. & Hamishehkar, H. 2014, "Alternative carriers in dry powder inhaler formulations", *Drug discovery today*, vol. 19, no. 5, pp. 618-626.
- Raosoft, I. 2020, , *Sample size calculator*. Available: <http://www.raosoft.com/samplesize.html> [2021, 17 August].
- Rashid, M.A., Elgied, A.A., Alhamhoom, Y., Chan, E., Rintoul, L., Allahham, A. & Islam, N. 2019, "Excipient interactions in glucagon dry powder inhaler formulation for pulmonary delivery", *Pharmaceuticals*, vol. 11, no. 5.

- Razavi Rohani, S.S., Abnous, K. & Tafaghodi, M. 2014, "Preparation and characterization of spray-dried powders intended for pulmonary delivery of Insulin with regard to the selection of excipients", *International journal of pharmaceuticals*, vol. 465, no. 1-2, pp. 464-478.
- Richards, S.A. & Hollerton, J.C. 2011, *Essential practical NMR for organic chemistry*, Chichester, West Sussex, U.K. : John Wiley, Chichester, West Sussex, U.K.
- Rosenstock, J., Muchmore, D., Swanson, D. & Schmitke, J. 2007, "AIR Inhaled Insulin System: a novel insulin-delivery system for patients with diabetes", *Expert Review of Medical Devices*, vol. 4, no. 5, pp. 683-692.
- Rudén, J., Frenning, G., Bramer, T., Thalberg, K., An, J. & Alderborn, G. 2019, "Linking carrier morphology to the powder mechanics of adhesive mixtures for dry powder inhalers via a blend-state model", *International journal of pharmaceuticals*, vol. 561, pp. 148-160.
- Sadrzadeh, N., Glembourtt, M.J. & Stevenson, C.L. 2007, *Peptide drug delivery strategies for the treatment of diabetes*, Hoboken.
- Sadrzadeh, N., Miller, D.P., Lechuga-Ballesteros, D., Harper, N.J., Stevenson, C.L. & Bennett, D.B. 2010, "Solid-state stability of spray-dried insulin powder for inhalation: Chemical kinetics and structural relaxation modeling of Exubera above and below the glass transition temperature", *Journal of pharmaceutical sciences*, vol. 99, no. 9, pp. 3698-3710.
- Sandow, J., Landgraf, W., Becker, R. & Seipke, G. 2015, "Equivalent Recombinant Human Insulin Preparations and their Place in Therapy", *European endocrinology*, vol. 11, no. 1, pp. 10-16.
- Sang M. Chung & Manoj Khurana 2013, *Afrezza FDA CLINICAL PHARMACOLOGY AND BIOPHARMACEUTICS REVIEW(S)*, U.S. Food and Drug Administration (FDA).
- Sanketkumar, P. & Amit, M. December 2015, "Inhalable Glucagon-like Peptide 1 Porous Particles Prepared by Spray Freeze Drying Technique", *Drug Delivery to the Lungs (DDL26)*The Aerosol Society, , 9th December - 11th December 2015.
- Santos Cavaiola, T. & Edelman, S. 2014, "Inhaled Insulin: A Breath of Fresh Air? A Review of Inhaled Insulin", *Clinical therapeutics*, vol. 36, no. 8, pp. 1275-1289.
- Sarmiento, B., Ferreira, D., Veiga, F. & Ribeiro, A. 2006, "Characterization of insulin-loaded alginate nanoparticles produced by ionotropic pre-gelation through DSC and FTIR studies", *Carbohydrate Polymers*, vol. 66, no. 1, pp. 1-7.
- Scherließ, R. & Etschmann, C. 2018, "DPI formulations for high dose applications – Challenges and opportunities", *International journal of pharmaceuticals*, vol. 548, no. 1, pp. 49-53.
- Schievano, E., Tonoli, M. & Rastrelli, F. 2017, "NMR Quantification of Carbohydrates in Complex Mixtures. A Challenge on Honey", *Analytical Chemistry (Washington)*, vol. 89, no. 24, pp. 13405-13414.
- Schmid, T., Baumann, B., Himmelsbach, M., Klampfl, C. & Buchberger, W. 2016, "Analysis of saccharides in beverages by HPLC with direct UV detection", *Analytical and Bioanalytical Chemistry*, vol. 408, no. 7, pp. 1871-1878.

- Shalash, A.O., Molokhia, A.M. & Elsayed, M.M.A. 2015, "Insights into the roles of carrier microstructure in adhesive/carrier-based dry powder inhalation mixtures: Carrier porosity and fine particle content", *European Journal of Pharmaceutics and Biopharmaceutics*, vol. 96, pp. 291-303.
- Shetty, N., Cipolla, D., Park, H. & Zhou, Q.T. 2020, "Physical stability of dry powder inhaler formulations", *Expert opinion on drug delivery*, vol. 17, no. 1, pp. 77-96.
- Sibum, I., Hagedoorn, P., de Boer, A.H., Frijlink, H.W. & Grasmeijer, F. 2018, "Challenges for pulmonary delivery of high powder doses", *International journal of pharmaceutics*, vol. 548, no. 1, pp. 325-336.
- Simmler, C., Napolitano, J.G., Mcalpine, J.B., Chen, S. & Pauli, G.F. 2014, "Universal quantitative NMR analysis of complex natural samples", *Current opinion in biotechnology*, vol. 25, pp. 51-59.
- Son, Y. & McConville, J.T. 2008, "Advancements in Dry Powder Delivery to the Lung", *Drug development and industrial pharmacy; Drug Dev Ind Pharm*, vol. 34, no. 9, pp. 948-959.
- Sou, T., Forbes, R.T., Gray, J., Prankerd, R.J., Kaminskas, L.M., McIntosh, M.P. & Morton, D.A.V. 2016, "Designing a multi-component spray-dried formulation platform for pulmonary delivery of biopharmaceuticals: The use of polyol, disaccharide, polysaccharide and synthetic polymer to modify solid-state properties for glassy stabilisation", *Powder Technology*, vol. 287, pp. 248-255.
- Sou, T., Orlando, L., McIntosh, M.P., Kaminskas, L.M. & Morton, D.A.V. 2011, "Investigating the interactions of amino acid components on a mannitol-based spray-dried powder formulation for pulmonary delivery: A design of experiment approach", *International journal of pharmaceutics*, vol. 421, no. 2, pp. 220-229.
- Ståhl, K., Claesson, M., Lilliehorn, P., Lindén, H. & Bäckström, K. 2002, "The effect of process variables on the degradation and physical properties of spray dried insulin intended for inhalation", *International journal of pharmaceutics*, vol. 233, no. 1-2, pp. 227-237.
- Sterling, C., Crouch, R., Russell, D. & Calderon, A.I. 2013, "H-1-NMR Quantification of Major Saccharides in Acai Raw Materials: a Comparison of the Internal Standard Methodology with the Absolute Intensity qNMR Method", *Phytochemical Analysis*, vol. 24, no. 6, pp. 631-637.
- Strickley, R.G. & Anderson, B.D. 1997, "Solid-state stability of human insulin II. Effect of water on reactive intermediate partitioning in lyophiles from pH 2–5 solutions: Stabilization against covalent dimer formation", *Journal of Pharmaceutical Sciences*, vol. 86, no. 6, pp. 645-653.
- Tiernan, H., Byrne, B. & Kazarian, S.G. 2020, "ATR-FTIR spectroscopy and spectroscopic imaging for the analysis of biopharmaceuticals", *Spectrochimica acta. Part A, Molecular and biomolecular spectroscopy*, vol. 241, pp. 118636.
- Tosoh Bioscience, G. 2021, , *System Suitability Calculations* . Available: <https://separations.eu.tosohbioscience.com/technical-support/technical-resources/chromatographic-calculations/system-suitability-calculations> [2021, 9 August].
- U.S. Food & Drug Administration 2020, 31 July-last update, *Generally Recognized As Safe (GRAS) Substances*. Available:

<https://www.cfsanappsexternal.fda.gov/scripts/fdcc/index.cfm?set=SCOGS&sort=Sortsubstance&order=ASC&startrow=1&type=basic&search=mannitol> [2021, 10 August].

- Ung, K.T., Rao, N., Weers, J.G., Clark, A.R. & Chan, H. 2014, "In Vitro Assessment of Dose Delivery Performance of Dry Powders for Inhalation", *Aerosol Science and Technology*, vol. 48, no. 10, pp. 1099–1110.
- Ung, K.T., Rao, N., Weers, J.G., Huang, D. & Chan, H. 2016, "Design of spray dried insulin microparticles to bypass deposition in the extrathoracic region and maximize total lung dose", *International journal of pharmaceutics*, vol. 511, no. 2, pp. 1070-1079.
- Vahl, T.P., Paty, B.W., Fuller, B.D., Prigeon, R.L. & D'Alessio, D.A. 2003, "Effects of GLP-1-(7–36)NH₂, GLP-1-(7–37), and GLP-1-(9–36)NH₂ on Intravenous Glucose Tolerance and Glucose-Induced Insulin Secretion in Healthy Humans", *The Journal of Clinical Endocrinology & Metabolism*, vol. 88, no. 4, pp. 1772-1779.
- Vanea, E., Moraru, C., Vulpoi, A., Cavalu, S. & Simon, V. 2014, "Freeze-dried and spray-dried zinc-containing silica microparticles entrapping insulin", *Journal of Biomaterials Applications*, vol. 28, no. 8, pp. 1190-1199.
- Vehring, R. 2007, "Pharmaceutical Particle Engineering via Spray Drying", *Pharmaceutical research*, vol. 25, no. 5, pp. 999-1022.
- Vishali, D.A., Monisha, J., Sivakamasundari, S.K., Moses, J.A. & Anandharamakrishnan, C. 2019, "Spray freeze drying: Emerging applications in drug delivery", *Journal of Controlled Release*, vol. 300, pp. 93-101.
- Wallmeier, J., Samol, C., Ellmann, L., Zacharias, H.U., Vogl, F.C., Garcia, M., Dettmer, K., Oefner, P.J. & Gronwald, W. 2017, "Quantification of Metabolites by NMR Spectroscopy in the Presence of Protein", *Journal of Proteome Research*, vol. 16, no. 4, pp. 1784-1796.
- Walters, R.H., Bhatnagar, B., Tchessalov, S., Izutsu, K., Tsumoto, K. & Ohtake, S. 2014, "Next Generation Drying Technologies for Pharmaceutical Applications", *Journal of pharmaceutical sciences*, vol. 103, no. 9, pp. 2673-2695.
- Wanning, S., Süverkrüp, R. & Lamprecht, A. 2015, "Pharmaceutical spray freeze drying", *International journal of pharmaceutics*, vol. 488, no. 1-2, pp. 136-153.
- Weers, J.G. & Miller, D.P. 2015, "Formulation Design of Dry Powders for Inhalation", *Journal of pharmaceutical sciences*, vol. 104, no. 10, pp. 3259-3288.
- Weiss, M., Steiner, D.F. & Philipson, L.H. 2014, "Insulin Biosynthesis, Secretion, Structure, and Structure-Activity Relationships" in *Endotext*, eds. K.R. Feingold, B. Anawalt, A. Boyce, et al, MDTText.com, Inc., South Dartmouth (MA).
- Wilson, E.M., Luft, J.C. & DeSimone, J.M. 2018, "Formulation of High-Performance Dry Powder Aerosols for Pulmonary Protein Delivery", *Pharmaceutical research; Pharm Res*, vol. 35, no. 10, pp. 1-11.
- World Health Organization 2021a, , *Coronavirus*. Available: https://www.who.int/health-topics/coronavirus#tab=tab_1 [2021, 27 March].

- World Health Organization 2021b, , *Diabetes*. Available: https://www.who.int/health-topics/diabetes#tab=tab_1, <https://www.who.int/news-room/fact-sheets/detail/diabetes> [2021, 29 October].
- World Health Organization 2019, *Classification of Diabetes Mellitus*, World Health Organization, Switzerland.
- Yamazaki, T. & Takatsu, A. 2014, "Quantitative NMR spectroscopy for accurate purity determination of amino acids, and uncertainty evaluation for different signals", *Accreditation and Quality Assurance*, vol. 19, no. 4, pp. 275-282.
- Yang, M.Y., Chan, J.G.Y. & Chan, H. 2014, "Pulmonary drug delivery by powder aerosols", *Journal of Controlled Release*, vol. 193, pp. 228-240.
- Yanko Design 2014, 25 February-last update, *Asthma Inhaler for Proactive Healthcare*. Available: <https://www.yankodesign.com/2014/02/25/asthma-inhaler-for-proactive-healthcare/> [2021, 18 August].
- Yeung, S., Traini, D., Lewis, D. & Young, P.M. 2018, "Dosing challenges in respiratory therapies", *International journal of pharmaceuticals*, vol. 548, no. 1, pp. 659-671.
- Yeung, S., Traini, D., Tweedie, A., Lewis, D., Church, T. & Young, P.M. 2019, "Effect of Dosing Cup Size on the Aerosol Performance of High-Dose Carrier-Based Formulations in a Novel Dry Powder Inhaler", *Journal of pharmaceutical sciences*, vol. 108, no. 2, pp. 949-959.
- Yu, M., Benjamin, M.M., Srinivasan, S., Morin, E.E., Shishatskaya, E.I., Schwendeman, S.P. & Schwendeman, A. 2018, "Battle of GLP-1 delivery technologies", *Advanced Drug Delivery Reviews*, vol. 130, pp. 113-130.
- Zhang, X., Yue, X., Cui, Y., Zhao, Z., Huang, Y., Cai, S., Wang, G., Wang, W., Hugh, S., Pan, X., Wu, C. & Tan, W. 2020, "A Systematic Safety Evaluation of Nanoporous Mannitol Material as a Dry-Powder Inhalation Carrier System", *Journal of pharmaceutical sciences*, vol. 109, no. 5, pp. 1692-1702.
- Zhang, X., Zhao, Z., Cui, Y., Liu, F., Huang, Z., Huang, Y., Zhang, R., Freeman, T., Lu, X., Pan, X., Tan, W. & Wu, C. 2018, "Effect of powder properties on the aerosolization performance of nanoporous mannitol particles as dry powder inhalation carriers", *Powder Technology*, vol. 358, pp. 46-54.
- Zheng, X., Li, Y., Li, X., Tang, L., Xu, W. & Gong, M. 2011, "Peptide complex containing GLP-1 exhibited long-acting properties in the treatment of type 2 diabetes", *Diabetes research and clinical practice*, vol. 93, no. 3, pp. 410-420.
- Zhu, C., Huang, Y., Zhang, X., Mei, L., Pan, X., Li, G. & Wu, C. 2015, "Comparative studies on exenatide-loaded poly (d,l-lactic-co-glycolic acid) microparticles prepared by a novel ultra-fine particle processing system and spray drying", *Colloids and Surfaces B: Biointerfaces*, vol. 132, pp. 103-110.
- Ziaee, A., Albadarin, A.B., Padrela, L., Femmer, T., O'Apos, Reilly, E. & Walker, G. 2019, *Spray drying of pharmaceuticals and biopharmaceuticals: Critical parameters and experimental process optimization approaches*.

K1455177

Appendix 1

Questionnaire

SECTION ONE: PARTICIPANT INFORMATION

1) Do you have type 1 diabetes?

- Yes
- No

2) How long have you been using insulin for?

- < 1 year
- 1-3 years
- 4-6 years
- 7-9 years
- Over 10 years

3) What type of insulin are you currently using? (Tick ALL that applies)

- Humalog®
- Humulin S®
- Humulin I®
- Novomix®
- Novorapid®
- Levemir®
- Lantus®
- Other (please specify)

4) How compliant are you with your current insulin regimen?

(Poor compliance) 1 2 3 4 5 6 7 8 9 10 (High compliance)

5) How often do you suffer from hyperglycaemia (high blood sugar levels above 11mmol/L)?

- Once a month
- Once a week
- Once a day
- More than once a day
- Other (Please specify)

6) How often do you suffer from hypoglycaemia (low blood sugar below 3.5mmol/L)?

- Once a month
- Once a week
- Once a day
- More than once a day
- Other (Please specify)

7) How often you been hospitalised over the last year due to diabetes?

- Once
- Twice
- Thrice

Other (Please specify)

8) Do you suffer from any of the following diabetic complications?

- High blood pressure
- High cholesterol
- Heart failure
- Nerve disease
- Kidney disease
- Eye disease
- Foot conditions
- Skin conditions
- Hearing impairment
- None
- Others (Please specify)

9) Do you smoke?

- Yes
- No
- Stopped less than 6 months ago

10) Do you currently suffer from any respiratory conditions? (Such as Asthma, Chronic obstruction pulmonary disease: COPD)

- No
- Yes (Please specify)

11) Have you ever used any type of inhalers?

- Yes
- No

SECTION TWO: OPINIONS ON INJECTING INSULIN

12) How satisfied are you with your current insulin regimen?

- Very satisfied
- Satisfied
- Neither satisfied nor unsatisfied
- Unsatisfied
- Very unsatisfied

13) According to your experience what is the main drawback of injecting insulin?

- Pain
- Inconvenience
- Hypoglycaemia
- Complexity of the regimen
- Problems with locating the site
- Weight gain
- Fear of needles
- Other (Please specify)

SECTION THREE: KNOWELEDGE OF INSULIN INHALERS

14) Do you have any information about insulin inhalers?

- Yes
- No

15) How would you describe your current knowledge and understanding of insulin inhalers?

- Very Good
- Good
- Poor
- Very Poor

16) What is the source of your information about insulin inhalers?

- Social media
- Online forums
- News
- Medical websites
- Journals
- Through friends and family
- Other (Please specify)

17) Would you like to know more about the insulin inhalers?

- Yes (please specify what in particular)
- No

SECTION FOUR: INSULIN INHALERS



18) Would you be willing to try insulin inhalers?

- Yes
- No (Move to question 20)

19) What factors will you towards using insulin inhalers? (1 = least likely, 10= most likely)

	1	2	3	4	5	6	7	8	9	10
Avoiding the pain of injection										
Convenience of inhaled insulin										
Small size										
Style (colour/ design)										
Socially acceptable										
Effectiveness										
Easy to store and clean										
Portable										
Personalise										
Easy to use										

20) Please read the description of the following inhalers and answer the question below.

<p>Exubera®</p>  <p>Withdrawn from the market</p>	<ul style="list-style-type: none"> • A clear holding chamber that allows visualisation • Repeated dosing available • Need to insert a blister that contains the powder insulin • Acts rapidly • Bulky size
<p>Afrezza®</p>  <p>Currently available in the US market</p>	<ul style="list-style-type: none"> • Disposable inhaler • Does not require cleaning or maintenance • Available in cartridges of 4,8 and 12 units to use as prescribed • Compact and discreet sizing, design based on the feedback received by bulky Exubera® inhalers. • Easily portable • Need to place a cartridge into the inhaler
<p>3M™</p>	<ul style="list-style-type: none"> • Contains an electronic display to provide instructions • Records every time the patient has inhaled the dose • Provides a steady, measured dose regardless of the patient's inhalation profile • Stores all the data which can be accessed on a smartphone and shared with family or doctors



Just a design of an inhaler that is not yet available in the market

Twist+





Just a design of an inhaler that is not yet available in the market

- Dry powder inhaler
- Detects the quality of the air and sends reports on smartphone applications, which can warn the patients about the presence of volatile organic compounds (gases released from certain solids or liquids which can have adverse health effects).
- The application linked to the inhaler can also remind the user if they forget their inhaler at home

Turbohaler®



- Twisting forward and backward as far as it goes will produce a sound which indicates when the dose is correct
- Counter indicates the number of puffs that is available
- Need to inhale deeply and strongly when using it

<p>A type of inhaler that is currently available in the market for Asthma and COPD</p>	
<p>HandiHaler®</p>  <p>A type of inhaler that is currently available in the market for Asthma and COPD</p>	<ul style="list-style-type: none"> • Single dose capsule based dry powder inhaler • Portable inhaler • Need to insert a capsule into the inhaler with every use
<p>Relvar Ellipta®</p>  <p>A type of inhaler that is currently available in the market for Asthma and COPD</p>	<ul style="list-style-type: none"> • Inhaler pre-loaded with a month's pre-filled drug formulation • Has a dose counter window that displays starting number • The blister strip present in the inhaler protects the drug from contaminants

Based on the design, which of the following inhalers would you prefer to use? (1= least preferred, 10= most preferred)

	1	2	3	4	5	6	7	8	9	10
Exubera®										
Afrezza®										
3M™										
Twist+										
Turbohaler®										
HandiHaler®										
Relvar Ellipta®										

21) **What is the reason you would NOT use insulin inhalers as part of your diabetes management?**
(Tick ALL appropriate)

- Not enough information
- Undesirable side effects (such as cough, throat irritation)
- Happy with my current insulin treatment
- Taking a lung capacity test prior to getting a prescription for insulin inhaler
- Other (Please specify)

22) **Do you think inhalers are a more appropriate method of taking insulin?**

- Yes (Please explain why)
- No (Please explain why)

23) **If available on the NHS would you ask your doctor to prescribe insulin inhalers instead of injection?**

- Highly likely
- Likely
- Unsure
- Unlikely
- Highly unlikely

24) **Are there any additional features that you would like an insulin inhaler to have?**

.....
.....

25) **What do you think are the potential challenges of using insulin inhalers?**

.....
.....

SECTION FIVE: PATIENT DEMOGRAPHICS

26) **What is your gender?**

- Male
- Female
- Other

27) **Which of the following categories describes your age?**

- Under 12
- 12 -18
- 19-25
- 26-40
- 41- 59
- Over 60

28) **What is your ethnic background?**

- Prefer not to say
- Black African
- Chinese

Bangladeshi

White British

Black Caribbean

Indian

Pakistani

White Other (*please Specify*): _____

Black Other (*please Specify*): _____

Asian Other (*please Specify*): _____

Other (*please Specify*): _____